Springer Protocols

Methods in Molecular Biology 623

RNA Interference

From Biology to Clinical Applications

Edited by

Wei-Ping Min
Thomas Ichim

Humana Press

METHODS IN MOLECULAR BIOLOGY™

Series Editor
John M. Walker
School of Life Sciences
University of Hertfordshire
Hatfield, Hertfordshire, AL10 9AB, UK

For other titles published in this series, go to
www.springer.com/series/7651

RNA Interference

From Biology to Clinical Applications

Edited by

Wei-Ping Min

Departments of Surgery, Microbiology and Immunology, and Pathology, University of Western Ontario, London, ON, Canada

Thomas Ichim

MediStem Laboratories Inc., San Diego, CA, USA

Humana Press

Editors
Wei-Ping Min, MD, Ph.D.
Departments of Surgery
Microbiology and Immunology, and Pathology
University of Western Ontario
London, ON
Canada
mweiping@uwo.ca

Thomas Ichim, Ph.D.
MediStem Laboratories Inc.
San Diego, CA
USA
thomas.ichim@gmail.com

ISSN 1064-3745 e-ISSN 1940-6029
ISBN 978-1-60761-587-3 e-ISBN 978-1-60761-588-0
DOI 10.1007/978-1-60761-588-0
Springer New York Dordrecht Heidelberg London

Library of Congress Control Number: 2010920843

Humana Press is a part of Springer Science+Business Media (www.springer.com)

Preface

There are a few moments, defining the research path of one's career that remain crystal clear and as memorable as yesterday. For both of us, one such moment was our learning of the process of RNA interference and the stunning realization of its implications in our discipline. Being immunologists by training, we have been interested in exploring how to either activate this T cell more toward one direction or manipulate this dendritic cell in another. We have been used to doing this through different tissue culture conditions, or addition of chemical inhibitors: these having the drawbacks of unscalability and unspecificity, respectively.

It was a cold Canadian night in the winter of 2001. We were having coffee at the Hospital Cafeteria waiting for some data coming out of the laboratory, and both of us were talking about the future of immunology. The need for specific ways of modulating genes so that we would be spared of the need for impractical approaches was discussed. "How exciting would it be just to use antisense oligonucleotides to silence immune stimulatory genes in the dendritic cell?" "It must have been performed already." "If it has, then why don't we know about it?" "It's much easier to evoke a therapeutic effect by modulating immunological genes, in that, unlike viral or oncogenes, even a 20% gene inhibition will cause a biological response." "Someone must have done that with antisense already." As this was before the time everyone had a Blackberry and an iPhone, we would have to wait until we got upstairs to check Pubmed. But we continued the conversation: "Is there anything better than antisense? What about ribozymes?" And this led to the discussion regarding RNA interference.

At that time, the concept of RNA interference was still restricted mainly to the world of molecular biologists. We remembered a dear friend telling us about this bizarre phenomena, whereby introduction of a double strand of RNA would induce cleavage not only of the introduced nucleic acids but also any other nucleic acids that resembled it. He told us about this being the "next antisense" since it is part of the body's endogenous defenses against viruses and therefore theoretically should be more potent for silencing. "It's easier to take away a gene than add one." "Yes, but the double strands would activate interferon responses – The paper our friend told us about was in worms." "But imagine if there was a way to get around that? Plus if you use it to suppress immune suppressive cytokines in cancer then the interferon alpha response is actually beneficial."

We left our coffees and hurriedly went to the computers upstairs to see what has and has not been done in this field. We printed out everything that had the words "RNA interference" the 1998 Nature paper that described RNA interference in worms (which subsequently won Fire and Mello the Nobel Prize), the paper by Elbashir et al. showing that the interferon alpha response can be avoided in mammals, the work describing use of siRNA for studying mammalian genes. That night, neither of us had much sleep thinking about the possibility of specifically silencing immunological genes. We had a perfect model, the dendritic cells, which reside at the center of the "immunological universe," and are relatively simple cells to transfect and manipulate, Wei-Ping having already induced them to express various immune regulatory genes such as FasL

Initial silencing of the interleukin-12 p35 gene was performed. The degree of knock-down was phenomenal. These data led us into a journey that continues today, having silenced both immune suppressive and immune stimulatory genes ranging from cytokines, to membrane proteins, to oncogenes, to transcription factors. This journey has taken us personally from ex vivo cell manipulation to current cell-targeting immunoliposomes that deliver siRNA to dendritic cells only, thus alleviating the need for hydrodynamic injection. Disease models treated have included rheumatoid arthritis, allergy, transplant rejection, and cancer.

When we were contacted by Humana with the possibility of being editors for this volume, we gladly accepted it. In the same way that we described our personal journey, we aimed in this book to represent the journey of our field. From those early days where RNA interference was a strange artifact in worms, to the 2006 Noble Prize to Fire and Mello, to the current clinical trials and the $1 billion purchase of a siRNA company by Merck, the field of RNA interference has grown at a breakneck pace.

In this volume, we will overview the science and the Protocols at present that span the biological disciplines from detailed nucleic acid chemistry, to pharmacology, to manipulation of signal transduction pathways. By compiling an overview of the different ongoing areas of scientific investigation of RNAi, we hope to do two things: stimulate new questions and provide you with the tools to start addressing those questions. The book is divided into three main segments. The first deals with the Physiology of RNA Interference, in which we try to overview the biological relevance of this process and provide a context for the next sections. The second section, entitled "RNA interference in the laboratory and siRNA delivery" outlines practical uses of RNAi either as research tools or as components in the development of therapeutics. Finally, the last part of the book deals with actual preclinical and clinical issues associated with the use of RNAi-inducing agents as drugs. Through this clustering of chapters in segments, we hoped to provide a logical context for the current state of the art.

Starting the first section, Drs. Abubaker and Wilkie from University of Guelph, Canada provide a comparative biology examination of the relevance of RNAi processes to viral defense. They overview commonalities and differences between gene silencing effector mechanisms and host–parasite interactions in forms of life ranging from fungi, to worms, to insects, to mammals. Subsequent to establishing an overall framework for understanding the various biological pathways associated with RNA interference as a gene-specific mechanism of defense, they move into a discussion on innate defense mechanisms, namely the ability of double-stranded RNA molecules to activate the interferon alpha response through activation of toll like receptors (TLR) 7/8 and the acid inducible gene I (RIG-I). In the subsequent chapter, Drs. Gantier and Williams from Monash University in Clayton, Australia review the relevance of this "danger-associated" TLR pathway as a method of immune activation and provide methodology for assessment, in both mouse and man, of its activation. RNAi-induction by microRNA (miRNA) also plays a role of fundamental innate protection mechanisms against pathogens. The miRNA can be pre-existing in the host cell or can be transcribed by the invading virus. Drs. Ouellet and Provost from Laval University in Canada, go into considerable detail across the major viruses to discuss the impact of host and viral miRNA in the battle for survival. Of particular interest are the analytical methods for detection of even transiently expressed miRNAs.

The exquisite sensitivity and selectivity of RNAi induction allows for knock-down of specific alleles of a gene. Dr. Hohjoh from the National Institute of Neuroscience in Tokyo, Japan, provides protocols for silencing of the Photinus and *Renilla luciferase* genes

in mammalian cells. The same selectivity that allows for allele-specific silencing by siRNA also requires great care in designing siRNAs, in that numerous factors contribute to silencing efficacy. The issue of siRNA-designing algorithms is reviewed by Dr. Kim from the University of Science & Technology in Daejeon, Korea who presents the AsiDesigner, a web-based siRNA design program that takes into consideration alternative splicing in designing optimum siRNAs. Drs. Muhonen and Holthöfer from Dublin City University, Dublin, Ireland, continue on the theme of optimizing siRNA design by discussing issues of target messenger accessibility and provide various bioinformatics approaches for identifying active and specific sites on the mRNA for silencing. Dr. Ishigaki's group from the Kanazawa Medical University, Kanazawa, Japan, describes another method of increasing potency of siRNA. In their chapter, shRNAs are expressed on a single plasmid, so that by concurrently targeting different areas of the same transcript, increased silencing may be achieved. They proved a detailed protocol for generating dual shRNA expressing plasmids and describe various methodological peculiarities of this approach. Of particular relevance to therapeutic development, the authors detail possible adverse effects by overconsumption of cellular transcription machinery when various promoters of shRNA transcription are used. Practical application of multi-shRNA derived from a single plasmid could include suppression of HIV. Drs. Rossi and Zhang from the Beckman Research Institute, City of Hope, CA, address this possible therapeutic approach through disclosing their technique involving a new combinatorial anti-HIV gene expression system that allows for simultaneous expression of multiple RNAi effector units from a single Pol II polycistronic transcript. In their system, they avoid the cell toxicity associated with expressing numerous shRNAs from Pol III promoters by using endogenous RNAi transcripts and miRNAs for expression of multiple RNAi effector units off a single Pol II polycistronic transcript. University of Vienna's Dr. Hofacker, subsequently discusses in silico tools that consider only siRNA-specific design criteria and those that integrate mRNA structure features as well as basic siRNA features for selection of shRNA and siRNAs. The final chapter of the First Section is by Dr. Engels et al. from J.W. Goethe-Universität in which protocols for synthesis of various siRNAs are provided.

In the Second Section, we transition from the biology of RNA interference to issues related to implementation, both in the laboratory setting as a basic research reagent and as a potent tool useful for the development of therapeutics for diseases. Dr. Zheng et al. from University of Western Ontario, Canada, begin the section by describing methodology for producing cell-targeting siRNA-bearing immunoliposomes. Through the ability of immunoliposomes to selectively bind to antigen-expressing cells corresponding to the antibody on the immunoliposome, the investigators provide a delivery platform that is relatively simple to generate and has widespread applications. The original method of in vivo siRNA delivery, hydrodynamic injection, is reviewed in the next chapter by Drs. Evers and Rychahou from the University of Texas. This method involves a rapid administration of high volume siRNA intravenously, which temporarily causes micropores and loosening of tight junctions in the endothelium, causing siRNA entry across the plasma membrane into intracellular compartments. To date, this method has been used to deliver siRNA to the liver, lungs, and brain.

In the same way that DNA array technologies have allowed for en masse identification of gene expression patterns in various cells and biological conditions, the knock-down of genes using high throughput siRNA technologies has allowed for the understanding of cellular phenotypes after a gene is suppressed. Fujita et al. from the Research Institute for Cell Engineering (RICE) and the National Institute of Advanced Industrial Science and

Technology (AIST), Tokyo, Japan, describe two protocols for reserve transfection of siRNA molecules on solid surfaces, the first for microarrays and the second for microtiter plates.

Moving from general to specific, the use of siRNA in specific pathologies is examined in greater detail. Prakash et al. from McGill University, Canada, are focused on neurodegenerative diseases and the means of traversing the blood brain barrier. They provide a detailed review of the state of the art regarding neurological uses of siRNA and subsequently describe the generation of optimized siRNA sequences and delivery methods for in vivo targeting using cationic nanoparticles. Huang et al. from the Chang Gung Memorial Hospital-Kaohsiung Medical Center in Taiwan used a bioinformatics approach to selectively identify genes in lung cancer through random knock-down and assessment of phenotype. Using this approach, they identified FLJ10540, a target associated with cancer invasion and migration. In their chapter, they describe upstream and downstream control of this tumor-associated factor. Delivery of siRNA and shRNA, of particular interest to cancer models, is described in the Chapter of Drs. Jere and Cho (Seoul National University, Korea) who provide protocols for generation of biodegradable cationic polymers. Methods of tracking cellular update and intracellular trafficking as well as protocols for the evaluation of the impact on cancer cells are provided. While selective delivery of RNAi-inducing molecules has been performed with immunoliposomes or affinity-targeting agents, an interesting approach is described by Ohtsuki's group from Okayama University in Okayama, Japan, who used HIV-tat conjugation of siRNA to allow intracellular delivery and could activate the gene silencing process using photons. This novel method, termed CPP-linked RBP-mediated RNA internalization and photoinduced RNAi (CLIP-RNAi), could have many applications in therapeutic scenarios where localized silencing is desirable.

The issue of siRNA degradation is examined by Aigner et al. who utilize various polyethylenimines to increase protection from nucleases, both extracellular and intracellular. In their chapter, the authors provide a comparison of the different polyethylenimines in respect to cationic charge, ability to form noncovalent interactions with siRNA, and compaction of the siRNA into complexes that allow for internalization by endocytosis. On the same topic of crossing the plasma membrane, Brito et al. from King's College, London, England provide a rather interesting transfection methodology: temporary permeabilization with streptolysin-O. They provide protocols that have been optimized for gene silencing of multiple myeloma cell lines, which have great importance for therapeutics development.

The third section of the book covers the issue of clinical implementation of RNAi. A look at www.clinicaltrials.gov , the NIH registry for ongoing clinical trials, reveals seven ongoing clinical investigations using RNAi induction for conditions such as wet macular degeneration, infectious diseases, and cancer. The current chapter will address some of the issues that need to be addressed in the translation of this new class of therapeutic approaches. Dr. Akaneya from the Osaka University Graduate School of Medicine, Japan, begins by describing the advantages and disadvantages of using RNAi-inducing approaches for neurological conditions. Specific diseases discussed include ALS and inflammatory conditions. Issues such as immunogenicity, interferon response, and localization are discussed. Drs. Mao and Wu from Johns Hopkins School of Medicine, Baltimore, describe specifics of using RNAi-based approaches in cancer immunotherapy. They discuss various important immunological targets starting with specific effector molecules, and then moving on to more general upstream transcription factors such as STATs and other global regulators of numerous immune response genes. The issue of endogenous miRNA controlling of the immune response, both natural and stimulated, is also overviewed.

The authors conclude by evaluating various RNAi-inducing approaches for the most rapid clinical translation in immunotherapy of cancer.

Tissue injury prevention by RNAi strategies is discussed by Zhang et al. from University of Western Ontario, Canada. They provide details of assays used to assess renal injury in an ischemia/reperfusion model and prevention by suppression of caspase transcription. From the same Institute, Drs. Zhang and Li present protocols for the in vitro silencing of dendritic cells with siRNA and subsequent use of these cells to modulate and/or suppress transplant rejection. The advantage of this approach is the potent immune stimulatory/immune suppressive ability of DC dependent on expression of costimulatory molecules. Targeting of RelB, an NF-kB family member, is demonstrated in the protocols, which causes suppression of various cytokine and costimulatory molecules on the dendritic cell, this suppression associated with inhibited immunogenicity.

Continuing on the theme of immune modulation, Ritprajak et al. from Tokyo Medical and Dental University, Tokyo, Japan utilize siRNA to enter across the stratum corneum and into dermal dendritic cells. By modulating these cells, the authors describe suppression of costimulatory molecules and possible use for treatment of allergic disease. Sarret et al. from University of Sherbrooke, Canada, use RNAi to tackle the problem of pain in a nonpharmacological manner. They discuss protocols for siRNA administration, targets, and behavioral systems used in researching this unique approach to pain management, with particular reference to G protein-coupled receptors. Seth et al. from MDRNA Inc, Bothell, USA, describe the use of RNAi in treatment of respiratory viruses, with emphasis on influenza. They describe various viral targets, animal models, and methods of delivery for maximum antiviral activity. An interesting subject is the interaction between siRNA that stimulates interferon alpha responses and the overall antiviral activity of these molecules. Drs. Malek and Tchernitsa from the Institute of Pathology, Charité – Universitätsmedizin Berlin, Germany and Oncology Institute of Southern Switzerland provide detailed protocols for silencing of ovarian cancer cells in vitro and in vivo. Of particular interest is the clinically relevant human xenograft ascites model that is described.

As you may see, the progress of RNA interference research has been significant. The question of whether it will deliver on its promise is still open; however, we hope this volume will provide to you, our reader, the same amount of excitement we've had in seeing the field progress to where it is today.

2009 ***Wei-Ping Min and Thomas Ichim***

Contents

Contributors

Achim Aigner • *Department of Pharmacology and Toxicology, School of Medicine, Philipps-University, Marburg, Germany*

Yukio Akaneya • *Division of Neurophysiology, Department of Neuroscience, Osaka University Graduate School of Medicine, Osaka, Japan*

Miyuki Azuma • *Department of Molecular Immunology, Graduate School, Tokyo Medical and Dental University, Tokyo, Japan*

Oleksandr Baturevych • *Department of Pharmacology, Toxicology and Virology, MDRNA Inc., Bothell, WA, USA*

Nicolas Beaudet • *Department of Physiology and Biophysics, Faculty of Medicine and Health Sciences, Université de Sherbrooke, Sherbrooke, QC, Canada*

Marianne E. Beduhn • *Departments of Surgery, Microbiology and Immunology, and Pathology, University of Western Ontario, London, ON, Canada*

Jose L. R. Brito • *Section of Haemato-Oncology, Institute for Cancer Research, London, UK*

Nicola Brown • *Division of Genetics and Molecular Medicine, Department of Medical and Molecular Genetics, School of Medicine, King's College London, London, UK*

Chang-Han Chen • *Department of Otolaryngology, Chang Gung Memorial Hospital-Kaohsiung Medical Center, Chang Gung University College of Medicine, Kaohsiung, Taiwan; Kaohsiung Chang Gung Head and Neck Oncology Group, Chang Gung Memorial Hospital-Kaohsiung Medical Center, Chang Gung University College of Medicine, Kaohsiung, Taiwan*

Chong-Su Cho • *Department of Agricultural Biotechnology, College of Agriculture and Life Sciences, Seoul National University, Seoul, South Korea*

Louis Doré-Savard • *Department of Physiology and Biophysics, Faculty of Medicine and Health Sciences, Université de Sherbrooke, Sherbrooke, QC, Canada*

Tamaki Endoh • *Department of Bioscience and Biotechnology, Okayama University, Okayama, Japan*

Joachim W. Engels • *Institute of Organic Chemistry and Chemical Biology, J.W. Goethe-Universität, Frankfurt am Main, Germany*

B. Mark Evers • *Department of Surgery, Sealy Center for Cancer Cell Biology, The University of Texas Medical Branch, Galveston, TX, USA*

Satoshi Fujita • *Research Institute for Cell Engineering (RICE), National Institute of Advanced Industrial Science and Technology (AIST), Tokyo, Japan*

Michael P. Gantier • *Monash Institute of Medical Research, Monash University, Clayton, VIC, Australia*

Jens Haas • *BioNTech AG c/o Department of Internal Medicine III, Experimental and Translational Oncology, Johannes Gutenberg University, Mainz, Germany*

Masaaki Hashiguchi • *Department of Molecular Immunology, Graduate School, Tokyo Medical and Dental University, Tokyo, Japan*
Sabrina Höbel • *Department of Pharmacology and Toxicology, School of Medicine, Philipps-University, Marburg, Germany*
Ivo L. Hofacker • *Institute for Theoretical Chemistry, University Vienna, Vienna, Austria*
Hirohiko Hohjoh • *National Institute of Neuroscience, NCNP, Tokyo, Japan*
Harry Holthofer • *Centre for BioAnalytical Sciences, Dublin City University, Dublin, Ireland*
Chi-Ying F. Huang • *Institute of Clinical Medicine, National Yang-Ming University, Taipei, Taiwan*
Yasuhito Ishigaki • *Division of Core Facility, Medical Research Institute, Kanazawa Medical University, Kahoku-gun, Japan*
Dhananjay J. Jere • *Department of Agricultural Biotechnology, College of Agriculture and Life Sciences, Seoul National University, Seoul, South Korea*
Anthony M. Jevnikar • *Departments of Surgery, Microbiology and Immunology, and Pathology, University of Western Ontario, London, ON, Canada; The Multi-Organ Transplant Program, London Health Sciences Centre, London, ON, Canada; Transplantation, Immunity and Regenerative Medicine, Lawson Health Research Institute, London, ON, Canada*
Young J. Kim • *Department of Functional Genomics, University of Science & Technology (UST), Daejeon, Korea; Medical Genomics Research Center, Korea Research Institute of Bioscience and Biotechnology (KRIBB), Daejeon, Korea*
Jin-Mei Lai • *Department of Life Science, Fu-Jen Catholic University, Taipei, Taiwan*
Mu Li • *Applied Biosystems/Ambion, Austin, TX, USA*
Anastasia Malek • *Laboratory of Experimental Oncology, Oncology Institute of Southern Switzerland, Bellinzona, Switzerland*
Meenakshi Malhotra • *Biomedical Technology and Cell Therapy Research Laboratory, Departments of Biomedical Engineering and Physiology, Faculty of Medicine, Artificial Cells and Organs Research Center, McGill University, Montreal, QC, Canada*
Chih-Ping Mao • *Department of Pathology, Johns Hopkins School of Medicine, Baltimore, MD, USA*
Tsukasa Matsunaga • *Laboratory of Human Molecular Genetics, Graduate School of Natural Science and Technology, Kanazawa University, Kanazawa, Japan*
Wei-Ping Min • *Departments of Surgery, Microbiology and Immunology, and Pathology, University of Western Ontario, London, ON, Canada; The Multi-Organ Transplant Program, London Health Sciences Centre, London, ON, Canada; Transplantation, Immunity and Regenerative Medicine, Lawson Health Research Institute, London, ON, Canada*
Jun Miyake • *Research Institute for Cell Engineering (RICE), National Institute of Advanced Industrial Science and Technology (AIST), Tokyo, Japan; Department of Bioengineering, School of Engineering, University of Tokyo, Tokyo, Japan*
Masato Miyake • *Research Institute for Cell Engineering (RICE), National Institute of Advanced Industrial Science and Technology (AIST), Tokyo, Japan*

Gareth J. Morgan • *Section of Haemato-Oncology, Institute for Cancer Research, London, UK*
Pirkko Muhonen • *Centre for BioAnalytical Sciences, Dublin City University, Dublin, Ireland*
Akihiro Nagao • *Division of Core Facility, Medical Research Institute, Kanazawa Medical University, Kahoku-gun, Japan*
Dalibor Odadzic • *Institute of Organic Chemistry and Chemical Biology, J.W. Goethe-Universität, Frankfurt am Main, Germany*
Takashi Ohtsuki • *Department of Bioscience and Biotechnology, Okayama University, Okayama, Japan*
Eiji Ota • *Research Institute for Cell Engineering (RICE), National Institute of Advanced Industrial Science and Technology (AIST), Tokyo, Japan*
Dominique L. Ouellet • *Centre de Recherche en Rhumatologie et Immunologie, CHUL Research Center/CHUQ, Quebec, QC, Canada; Faculty of Medicine, Université Laval, Quebec, QC, Canada*
Satya Prakash • *Biomedical Technology and Cell Therapy Research Laboratory, Departments of Biomedical Engineering and Physiology, Faculty of Medicine, Artificial Cells and Organs Research Center, McGill University, Montreal, QC, Canada*
Patrick Provost • *Centre de Recherche en Rhumatologie et Immunologie, CHUL Research Center/CHUQ, Quebec, QC, Canada; Faculty of Medicine, Université Laval, Quebec, QC, Canada*
Venkatesh Rengaswamy • *Advance Microscopy and Imaging Facility, Molecular Virology and Cell Biology Lab, Indian Institute of Technology (IIT), Chennai, India*
Patcharee Ritprajak • *Department of Microbiology and Immunology, Faculty of Dentistry, Chulalongkorn University, Bangkok, Thailand*
John J. Rossi • *Division of Molecular Biology, Graduate School of Biological Sciences, Beckman Research Institute of City of Hope, Duarte, CA, USA*
Piotr G. Rychahou • *Department of Surgery, The University of Texas Medical Branch, Galveston, TX, USA*
Takuma Sano • *Research Institute for Cell Engineering (RICE), National Institute of Advanced Industrial Science and Technology (AIST), Tokyo, Japan*
Philippe Sarret • *Department of Physiology and Biophysics, Faculty of Medicine and Health Sciences, Université de Sherbrooke, Sherbrooke, QC, Canada*
Shaguna Seth • *Department of Pharmacology, Toxicology and Virology, MDRNA Inc., Bothell, WA, USA*
Gregory Severson • *Department of Pharmacology, Toxicology and Virology, MDRNA Inc., Bothell, WA, USA*
Aminah Shunner • *Departments of Surgery, Microbiology and Immunology, and Pathology, University of Western Ontario, London, ON, Canada*
Abubaker M. E. Sidahmed • *Department of Experimental Therapeutics, Toronto General Hospital, Toronto, ON, Canada; Institute of Medical Science, University of Toronto, Toronto, ON, Canada*
Romualdas Smicius • *Biotherapeutics and Bioinnovation Center, Coley Pharmaceutical GmbH (a Pfizer Company), Düsseldorf, Germany*

Hakim Tafer • *Institute for Theoretical Chemistry, University Vienna, Vienna, Austria*
Kota Takano • *Research Institute for Cell Engineering (RICE), National Institute of Advanced Industrial Science and Technology (AIST), Tokyo, Japan*
Oleg Tchernitsa • *Laboratory of Molecular Tumor Pathology, Institute of Pathology, Charité – Universitätsmedizin, Berlin, Germany*
Michael V. Templin • *Department of Pharmacology, Toxicology and Virology, MDRNA Inc., Bothell, WA, USA*
Costin Vladau • *Departments of Surgery, Microbiology and Immunology, and Pathology, University of Western Ontario, London, ON, Canada*
Bruce Wilkie • *Department of Pathobiology, University of Guelph, Guelph, ON, Canada*
Bryan R. G. Williams • *Monash Institute of Medical Research, Monash University, Clayton, VIC, Australia*
T-C Wu • *Departments of Pathology, Oncology, Obstetrics, and Gynecology, and Molecular Microbiology and Immunology, Johns Hopkins School of Medicine, Baltimore, MD, USA*
Tomohiro Yoshikawa • *Research Institute for Cell Engineering (RICE), National Institute of Advanced Industrial Science and Technology (AIST), Tokyo, Japan*
Jane Zhang • *City of Hope Graduate School of Biological Sciences, Beckman Research Institute of City of Hope, Duarte, CA, USA*
Xusheng Zhang • *Departments of Surgery and Pathology, University of Western Ontario, London, ON, Canada*
Zhu-Xu Zhang • *Departments of Surgery, Microbiology and Immunology, and Pathology, University of Western Ontario, London, ON, Canada; The Multi-Organ Transplant Program, London Health Sciences Centre, London, ON, Canada; Transplantation, Immunity and Regenerative Medicine, Lawson Health Research Institute, London, ON, Canada*
Xiufen Zheng • *Departments of Surgery, Microbiology and Immunology, and Pathology, University of Western Ontario, London, ON, Canada*

Part I

Physiology of RNA Interference

Chapter 1

Endogenous Antiviral Mechanisms of RNA Interference: A Comparative Biology Perspective

Abubaker M.E. Sidahmed and Bruce Wilkie

Abstract

RNA interference (RNAi) is a natural process that occurs in many organisms ranging from plants to mammals. In this process, double-stranded RNA or hairpin RNA is cleaved by a RNaseIII-type enzyme called Dicer into small interfering RNA duplex. This then directs sequence-specific, homology-dependent, posttranscriptional gene silencing by binding to its complementary RNA and triggering its elimination through degradation or by inducing translational inhibition. In plants, worms, and insects, RNAi is a strong antiviral defense mechanism. Although, at present, it is unclear whether RNA silencing naturally restricts viral infection in vertebrates, there are signs that this is certainly the case. In a relatively short period, RNAi has progressed to become an important experimental tool both in vitro and in vivo for the analysis of gene function and target validation in mammalian systems. In addition, RNA silencing has subsequently been found to be involved in translational repression, transcriptional inhibition, and DNA degradation. In this article we review the literature in this field, which may open doors to the many uses to which this important technology is being put, including the potential of RNAi as a therapeutic strategy for gene regulation to modulate host–pathogen interactions.

Key words: RNA interference, Dicer, Transposons, siRNA, miRNA, Antiviral, Silencing, Suppressors, Quelling

1. Discovery and Historical Overview

RNA silencing is a broad term that has been used to describe RNA interference (RNAi) in animals, posttranscriptional gene silencing in plants, and quelling in fungi, which are all phenotypically different but mechanistically similar forms of RNAi (1).RNAi is a natural process in which double-stranded RNA (dsRNA) or hairpin RNA is cleaved by RNaseIII-type enzyme called Dicer into small interfering RNA (siRNA) duplex of 21–26 nucleotides, which then direct sequence-specific, homology-dependent, posttranscriptional

Wei-Ping Min and Thomas Ichim (eds.), *RNA Interference*, Methods in Molecular Biology, vol. 623,
DOI 10.1007/978-1-60761-588-0_1, © Springer Science+Business Media, LLC 2010

gene silencing by binding to its complementary RNA and triggering its elimination through degradation or by inducing translational inhibition (2, 3). RNA silencing is an evolutionarily ancient RNA surveillance mechanism, conserved among eukaryotes as a natural defense mechanism to protect the genome against invasion by mobile genetic elements, such as viruses, transposons, and possibly other highly repetitive genomic sequence and also to orchestrate the function of developmental programs in eukaryotic organisms (1, 2). Declaration of RNAi in 2002 as a "breakthrough" by the journal *Science* (4) encouraged scientists to revise their vision of cell biology and cell evolution, and the discovery of RNAi resulted in the Nobel Prize for Physiology or Medicine, being awarded to Andrew Fire and Craig Mello in 2006.

The discovery of RNAi followed observations in the late 1980s of transcriptional inhibition by antisense RNA expressed in transgenic plants (5), during a search for transgenic petunia flowers that were expected to be a more intense color of purple. In an attempt to alter flower colors in petunias, Jorgensen and colleagues (6) sought to upregulate the activity of the chalcone sythase (*chsA*) enzyme, which is involved in the production of anthocyanin pigments. They introduced additional copies of this gene. The overexpressed gene was expected to result in darker flowers in transgenic petunia, but instead it produced less pigmented, fully or partially white flowers, demonstrating that the activity of *chsA* had been significantly decreased. Actually, both the endogenous genes and the transgenes were downregulated in the white flowers. Surprisingly, the loss of cytosolic *chsA* mRNA was not linked with reduced transcription as tested by run-on transcription assays in isolated nuclei. Further investigation of the phenomenon in plants indicated that the downregulation was due to posttranscriptional inhibition of gene expression by an increased rate of mRNA degradation (6). Jorgensen invented the term "co-suppression of gene expression" to describe the elimination of mRNA of both the endogenous gene and the transgene, but the molecular mechanism remained unclear (6).

Other laboratories around the same time reported that the introduction of the transcribing sense gene could downregulate the expression of homologous endogenous genes (6, 7). A homology-dependent gene silencing phenomenon termed "quelling" was noted in the fungus *Neurospora crassa* (8). Quelling was recognized during attempts to increase the production of orange pigment expressed by the gene *al1* of *N. crassa* (8). Wild-type *N. crassa* was transformed with a plasmid containing a 1.5 kb fragment of the coding region of the *al1* gene. Some transformants were stably quelled and showed albino phenotypes. In these *al1*-quelled fungi, the amount of native mRNA was highly reduced while that of unspliced al1 mRNA was similar to the wild-type fungi. This indicated that quelling, but not the

rate of transcription, affected the level of mature mRNA in a homology-dependent manner.

Shortly thereafter, plant virologists conducting experiments to improve plant resistance to viral infection made a similar, unexpected observation. While it was documented that plants produced proteins that mediated virus-specific enhancement of tolerance or resistance to viral infection, a surprising finding was that short, noncoding regions of viral RNA sequences carried by plants provided the same degree of protection. It was concluded that viral RNA produced by transgenes could also inhibit viral accumulation (9). Homology-dependent RNA elimination was also noticed to occur during an increase in viral genome of infected plants (10). Ratcliff et al. (11) described a reverse experiment, in which short sequences of plant genes were introduced into viruses and the targeted gene was suppressed in an infected plant. Viruses can be the source, the target, or both for silencing. This phenomenon was named "virus-induced gene silencing" (VIGS), and the whole set of similar phenomena was collectively named posttranscriptional gene silencing (11).

Not long after these observations in plants, investigators searched for homology-dependent RNA elimination phenomena in other organisms (12, 13). The phenomenon of RNAi first came to light after the discovery by Andrew Fire et al. in 1998 of a potent gene silencing effect, which occurred after injecting purified dsRNA directly into adult *Caenorhabditis elegans* (2). The injected dsRNA corresponded to a 742 nucleotide segment of the *unc22* gene. This gene encodes nonessential but abundant myofilament muscle protein. The investigators observed that neither mRNA nor antisense RNA injections had an effect on production of this protein, but dsRNA successfully silenced the targeted gene. A decrease in *unc22* activity is associated with severe twitching phenotype, and the injected animal as expected showed a very weak twitching phenotype, whereas the progeny nematodes showed strong twitching. The investigators then showed similar loss-of-function knockouts could be generated in a sequence-specific manner, using dsRNA corresponding to four other *C. elegans* genes, and they coined the term RNAi.

The Fire et al. discovery was particularly important because it was the first recognition of the causative agent of what was until then an unexplained phenomenon. RNAi can be initiated in *C. elegans* by injecting dsRNA into the nematodes (2), soaking them in a solution of dsRNA (14), feeding the worms bacteria that express dsRNA (15), and using transgenes that express dsRNA in vivo (16). This very potent method for knocking out genes required only catalytic amounts of dsRNA to silence gene expression. The silencing was not only in gut and other somatic cells, but also spread through the germ line to several subsequent generations (14). Similar silencing was soon confirmed in plants (17),

trypanosomes (18), flies (19) and many other invertebrates and vertebrates. In parallel, it was determined that dsRNA molecules could specifically downregulate gene expression in *C. elegans* (2).

Subsequent genome screening lead to identification of small temporal RNA (stRNA) molecules that were similar to the siRNA in size, but in contrast to the siRNAs, stRNA were single-stranded and paired with genetically defined target mRNA sequences that were only partly complementary to the stRNA (20). Particularly, stRNAs lin-4 and let-7 were determined to bind with the 3′ noncoding regions of target lin-14 and lin-41 mRNAs, respectively, leading to reduction in mRNA-encoded protein accumulation. These observations encouraged investigators to look for stRNA-like molecules in different organisms, leading to the identification of hundreds of highly conserved RNA molecules with stRNA-like structural properties (21). These small RNAs are termed micro RNAs (miRNAs). They are produced from transcript that folds to stem-loop precursor molecules first in the nucleus by the RNA III enzyme Dorsha and then in the cytosol by Dicer, and they are present in almost every tissue of every animal investigated (22). Thus, the RNAi pathway guides two distinct RNA classes, double-stranded siRNA and single-stranded miRNA, to the cytosolic RISC complex, which brings them to their target molecules.

2. The Molecular Mechanism of RNA Interference

RNAi is a natural process of gene silencing that occurs in many organisms ranging from plants to mammals. RNAi was observed first by a plant scientist in the late 1980s, but the molecular basis of its mechanism remained unknown until the late 1990s, when research using the *C. elegans* nematode showed that RNAi is an evolutionarily conserved gene-silencing mechanism (2). Sequence-specific posttranscriptional RNAi gene silencing by double-stranded RNA is conserved in a wide range of organisms: plants (*Neurospora*), insect (*Drosophila*), nematodes (*C. elegans*), and mammals. This process is part of the normal defense mechanism against viruses and the mobilization of transposable genetic elements (2, 3). Although first discovered as a response to experimentally introduced RNA initiator, it is now known that RNAi and related pathways regulate gene expression at both transcriptional and posttranscriptional levels. The key steps in RNAi underlie several gene regulatory mechanisms that include downregulation of the expression of endogenous genes, direct transcriptional gene silencing and alteration of chromatin structure to promote kinetochore function, and chromosome segregation and direct elimination of DNA from somatic nuclei in tetrahymena (23).

The dsRNAs, generated by replicating viruses, integrated transposons, or one of the recently discovered classes of regulatory noncoding miRNAs, are processed into short dsRNAs (20). These short RNAs generate a flow of molecular and biochemical events involving a cytoplasmic ribonuclease III (RNase III)-like enzyme, known as Dicer, and a multi-subunit ribonucleoprotein complex called RNA-induced silencing complex (RISC). The antisense (guide) strand of the dsRNA directs the endonuclease activity of RISC to the homologous (target) site on the mRNAs, leading to its degradation and posttranscriptional gene silencing. The naturally occurring miRNAs are synthesized in large precursor forms in the nucleus. An RNA III enzyme called Drosha mediates the processing of the primary miRNA transcripts into pre-miRNA (70–80 mers), which are then exported via the exportin-5 receptor to the cytoplasm (24). In the cytoplasm, Dicer cleaves dsRNA, whether derived from endogenous miRNA or from replicating viruses, into small RNA duplexes of 19–25 base pairs (bp). These have characteristic 3′-dinucleotide overhangs that allow them to be recognized by RNAi enzymatic machinery, leading to degradation of target mRNA (25). Dicer works with a small dsRNA-binding protein, R2D2, to pass off the siRNA to the RISC, which has the splicing protein Argonaute 2 (Ago2). Argonaute cleaves the target mRNA between bases 10 and 11 in relation to the 5′-end of the antisense siRNA strand (26). The siRNA duplex is loaded into the RISC, whereupon an ATP-dependent helicase (Ago2) unwinds the duplex, allowing the release of "passenger" strand and leading to an activated form of RISC with a single-stranded "guide" RNA molecule (27, 28). The extent of complementarities between the guide RNA strand and the target mRNA decides whether mRNA silencing is achieved by site-specific cleavage of the mRNA in the region of the siRNA–mRNA duplex (29) or through an miRNA-like mechanism of translational repression (30). For siRNA-mediated silencing, the cleavage products are released and degraded, leaving the disengaged RISC complex to further survey the mRNA pool.

3. Intrinsic Antiviral Defense Mechanism of RNAi

3.1. Antiviral RNA Silencing in Mammals

To protect themselves from viral infections, cells have evolved several mechanisms. In plants, worms, and insects, RNAi is a strong antiviral defense mechanism. The interferon (IFN) response of innate immunity is a well-known and defined antiviral mechanism in mammals. In mammalian cells, virus-specific dsRNA induce the IFN pathway via the Toll-like receptor family or via a replication-dependent pathway involving the

cytoplasmic dsRNA sensors retinoic-acid-inducible protein-1/melanoma–differentiation-associated gene 5 (RIG-1/MD5) (31, 32). Antiviral proteins that are induced by dsRNA also include the 2′-5′ oligoadenylate cyclase (2′-5′OAS)/RNAseL/PKR (33, 34). As RNAi, IFN responses, and 2′-5′OAS)/RNAseL/PKR are initiated by dsRNA, it is most likely these pathways work together in the antiviral innate immune response. Because the helicase RIG-1/MDA5 pathway can be stimulated by siRNA, these proteins could link antiviral RNAi and IFN responses (34, 35). Initiation of RNAi in mammalian cells by endogenous expression of short hairpin RNAs (shRNAs) is a potent, novel antiviral mechanism (36).

In most cases of viral infection of mammalian cells, however, virus-specific siRNA could not be detected (37). Pfeffer et al. have analyzed siRNA expressed in the cells infected by a variety of viruses including DNA viruses, such as human cytomegalovirus (CMV), Kaposi sarcoma-associated herpes virus (KSHV), murine herpes virus and Epstein–Bar virus (EBV), as well as the human retrovirus HIV-1 and the RNA viruses, such as yellow fever virus and hepatitis C virus (HCV). Although they failed to identify antiviral siRNA, they were able to identify several virally encoded miRNA, particularly in DNA virus-infected cells, which clearly suggested that viruses use host cellular RNAi machinery for their own benefit (37).

To date, virus-specific siRNA have only been detected in human cells for immunodeficiency virus type one (HIV-1) and the LINE-1 retrotransposon (38–40). Virus-specific siRNA accumulation in mammalian cells is low in comparison with plants, insects, and nematodes. The reasons for this remain unclear. One explanation could be the lack of RNA-dependent RNA polymerase enzyme (RdRp) function in mammals. In insects and plants this enzyme is responsible for amplification of RNAi signals. The absence of RdRp enzyme activity, in combination with viral RNA silencing suppressors (RSS) activity, could also explain the low siRNA in mammalian cells. Another explanation is that antiviral RNAi in mammalian cells is initiated by cellular miRNA rather than production of completely new siRNA (41). This was suggested for the retrovirus primate foamy type 1 (PFV-1) in which the endogenous cellular miR-32 was found to target sequences of PFV-1. PFV-1 overcomes this micro-RNA-mediated defense mechanism by expressing and producing RSS Tas protein (41).

Recently, it has been reported that virus replication was enhanced in cells with defective RNAi machinery. HIV-1 replication is increased in human cells in which Dicer and Dorsha expression is knocked out (42). This is another indication that RNAi plays an important role in the anti-HIV-1 defense mechanism in human cells. The antiviral activity of RNAi was confirmed in a

report showing enhanced accumulation of the mammalian vesicular stomatitis virus in *C. elegans* with defective RNAi machinery (43). A good indication for the role of RNAi-mediated antiviral activity in mammalian cells came from evidence that many mammalian viruses express strong RSS activity (39).

Endogenous cellular miRNA are important for regulation of cellular genes, but recent evidence indicates that miRNA can also provide antiviral defense. miRNA impinges on the viral life cycle, viral tropism, and pathogenesis of viral diseases. Human miR-32 contributes to the repression of replication of retrovirus PFV-1 in human cells by partial complementary binding to the 3′UTR sites of five different mRNAs produced by PFV-1. The downregulation of these five genes by miR-32 repressed the replication of PFV-1 (41). This study highlighted the antiviral activity of miRNA and suggested a possibly broad effect of these molecules on viral infection. In support of this, other investigators recently reported that the IFN pathway, which has a central role in defense against viral infection in mammalian cells, works in coordination with miRNA to control viral infection (44). In this study, Pedersen et al. showed that IFN-β can induce the expression of several cellular miRNAs, including miR-1, miR-30, miR-128, miR-196, miR-296, miR-351, miR-431, and miR-448, that form almost perfect nucleotide base pair matches with the HCV genome, and some of these have predicted targets in the virus (44). In support of their antiviral role, when these miRNA are experimentally introduced they reproduce the antiviral effects of IFN-β on HCV, and the IFN defense is lost when they are experimentally removed. These host-encoded miRNA may contribute to the antiviral defense mechanism of IFN-β against HCV (44). Surprisingly, IFN-β was also reported to downregulate the expression of miR-122, a miRNA that has been reported to be essential for HCV replication in hepatic cells (45). It becomes clear that host miRNA can also modulate cellular genes involved in the IFN response, as reported for mir-146 The expression of mir-146 is stimulated by the EBV-encoded latent membrane protein (LMP1) (46), which suggests an intricate role of miRNA in viral–host interactions. These results provided proof that cellular miRNA is part of the innate immune system, and they revealed a component of innate defense based on direct reaction between host-produced miRNA and viral-encoded nucleic acid.

Many viruses encode miRNA to exploit this gene regulatory mechanism and to facilitate infection. Viral-encoded miRNA regulates both viral and host genes (47). The list of viruses that encode these miRNA includes EBV, KSHV, and CMV (37, 48–50). Different miRNA are expressed at different stages in cells latently infected with EBV, indicating that viral miRNA are involved in the regulation and maintenance of viral latency (37, 48). Herpes simplex virus-1 (HSV-1) encodes miR-LAT to maintain the host

cells' latency and to inhibit apoptosis of the cells by decreasing expression of transforming growth factor-β (TGF-β) and mothers against decapentaplegic homologue 3 (SMAD-3) in host cells, which interferes with TGF-β-dependent signaling pathways and prevents host cell apoptosis (51). Human CMV-encoded miR-UL112 represses the expression of MHC-class-1-polypeptide-related sequence B (MICB). MICB is a natural killer cell (NK)-activating receptor group-2, member D (NKG2D) stress-induced ligand. NKG2D is required for NK cell-mediated killing of infected cells (52). These findings indicate that CMV escapes host immune surveillance by encoding viral miRNA, which attacks cellular mRNA. This suggests that viruses use miRNA not only to regulate their own life cycles, but also to evade the host immune system and facilitate infection. Specifically, hepatic-cell-produced miR-122 has been reported to facilitate the replication of HCV by interacting with 5′UTR of HCV RNA (45). As animal miRNA are so far only reported to work at the posttranscriptional level to downregulate gene expression, this experiment shows that HCV evolved to develop miRNA-mediated gene regulation to escape host immune surveillance and to facilitate viral replication by yet-to-be-determined mechanisms. Surprisingly, most of the viral miRNAs discovered so far lack extensive homology to each other or to animal miRNA. It is also interesting that miRNA is only detected in DNA viruses and not in RNA or retroviruses (48). It is also noteworthy that no virus-encoded siRNA have been detected in virus-infected cells (37, 48). In addition to virus-encoded miRNA that allow viruses to regulate their genes and host genes, some viruses were found to produce silencing suppressor proteins that counteract miRNA or siRNA-mediated immune defense response. A good example of such a mechanism was found in PFV-1, which encodes the silencing suppressor Tas that can interfere with the miR-32-mediated downregulation of its mRNA and allow the PFV-1 to infect and replicate in infected cells (41). In the same way HIV-1 uses one of its own transcriptional activators, Tat as a miRNA-silencing suppressor that interferes with RNAi machinery enzyme, Dicer functions to prevent processing of dsRNA into siRNA (39, 42). In agreement with these results, an HIV-1 strain that is deficient in Tat does not spread effectively in human cells, perhaps due to its inability to suppress RNAi in host cells.

3.2. Antiviral RNA Silencing in Insects

Like all other organisms, insects are susceptible to viral infections, and some viruses threaten insects that are useful to humans, such as honeybees or silkworms. Some of these, especially arthropod-borne viruses, such as dengue virus and West Nile virus, can be transmitted by blood-sucking insects to vertebrate hosts and these viruses are of growing importance. Several species of arthropod, including fruit flies and mosquitoes, have been found to possess

an ability to induce RNA silencing (19, 53). The contribution of RNA silencing to antiviral defense mechanisms in these species was first reported in 2002 by Li et al. (54) who reported the accumulation of virus-derived siRNA in flock house virus (FHV)-infected Drosophila S2 cells. FHV is a member of the nodaviridae family, which are small nonenveloped riboviruses with a two single-stranded, positive-sense RNA genome. The viral accumulation was further found to be enhanced in S2 cells by a knockout Ago2 gene, which is an important component of the RISC machinery as reported earlier (54). Indeed, increased viral loads have also been shown in *Anopheles gambiae* mosquitoes with downregulation of the Ago2 gene, which functions together with Dicer-2 in the RNAi pathway (24, 54).To counter this, FHV encodes RSS named B2 (12-kilodalton protein), which is functional in insects and plants, indicating that the silencing components that are suppressed by B2 are shared by insects and plants and that RNAi mechanisms are conserved from plants to insects (54). Further studies indeed showed that B2 silencing suppressor binds to dsRNA, regardless of their length, and inhibits the Dicer-mediated cleavage of dsRNA (55). Furthermore, the Dicer-2 mutant flies were also more susceptible to infection with two other RNA viruses, Drosophila C virus (DCV) and Sindbis virus (SINV) (56). Virus-induced gene silencing, similar to plants, was also reported in the silkmoth *Bombyx mori* in which Broad-complex transcription factor was silenced by infection with a recombinant sindbis alpha virus expressing a Broad-complex antisense RNA (57).

These results confirmed that insect cells can mount antiviral response based on the activation of RNAi silencing pathways. Although no member of the RdRp gene family can be identified in the Drosophila genome, RdRp activity has been reported in Drosophila embryonic extracts (58). It has been conclusively demonstrated that transitive RNA silencing or transport of silencing information does not exist in adult Drosophila where RNAi, triggered by transgenes that express dsRNA, remains strictly confined within the cells where it generated (59). In contrast to *C. elegans* and plants, Drosophila lack RdPd that can amplify silencing signals. Such amplification of small amounts of transported dsRNA might be necessary for efficient RNAi silencing and its subsequent exportation (59). This difference may explain the need for a cytokine-mediated signaling mechanism that alerts noninfected cells to the infection in flies (59).

The question still remains to be answered as to whether RNAi is an efficient component of insect antiviral response. However, an indirect sign of natural RNAi directed against invading viruses in insects may be given by the mechanism that has been elaborated by the Drosophila genome to domesticate endogenous and mobile genetic elements. Jensen et al. (60) reported that a

transposional activity of transposon, similar to mammalian LINE elements, called I element can be suppressed by transfection with transgenes expressing a small internal region of I element (60). This regulatory mechanism has features similar to co-suppression originally described in plants, and this repression does not require any translatable sequence (60). It was also reported by Sarot et al. (61) that Gypsy, an endogenous retrovirus, is silenced by the action of one Ago protein in fly ovaries, and that ovary cells naturally accumulate gypsy-derived small RNA (61). RNAi directed against endogenous and invasive sequences is therefore analogous to those directed against invading exogenous pathogens. Nonetheless, the production of an RSS by an endogenous element has not been reported to date. Transposon calming is also reported in plants that possess clearly efficient RNAi silencing against exogenous viruses (62).

3.3. Antiviral RNA Silencing in Nematodes

In *C. elegans*, transposable elements were also reported to be controlled by an RNAi silencing-related mechanism. The informative findings about potential implication of RNAi in the nematode antiviral defense mechanism were reported by Sejen et al. (63). They detected dsRNA and siRNA derived from various regions of Tc1 transposon, and also reported that, when a stretch of the Tc1 sequence was fused to germline-expressed reporter, it is silenced in a manner dependent on essential silencing components (63). Other indirect evidence of involvement of RNAi in the antiviral defense mechanism is that, in contrast to Drosophila, RNAi is systemic in worms, spreading from tissue to tissue (63). Fire et al. (2) reported that dsRNA is the key initiator of RNA silencing, and they also showed that introduction of dsRNA into the body cavity or gonad of young adult worms generated gene-specific interference in somatic tissues. The *C. elegans* genome has 2RdRp genes called ego-1 and rrf-1, which are required for RNAi in germline and somatic tissues, respectively (63). The obligate and mandatory requirement of RdRp activity for RNAi in nematodes makes it difficult to determine whether it is required for signal amplification, as in plants. However, Alder et al. demonstrated that mRNA, targeted by RNAi, functions as template for 5′ to 3′ synthesis of new RNA (64). This effect was not cell-confined and autonomous as dsRNA, targeted to a gene expressed in a specific cell type, can lead to transitive RNAi-mediated silencing of a second gene expressed in a different cell type. A better understanding of the molecular basis of transitive silencing in worms came from studies by two groups, which genetically screened and isolated defective mutants called systemic RNAi defective (sid) (65) and RNA spreading defective (rsd) (66). These groups identified a specific gene, sid-1/rsd-8, which encodes a multispan transmembrane protein necessary for systemic, but not cell autonomous, RNAi (65, 66). Feinberg et al. using Drosophila S2 cells

showed that SID-1 facilitated passive cellular uptake, especially of long dsRNA (67). Surprisingly, SID-1, localized in cell membrane, enhanced passive transportation of siRNA resulting in increased efficacy of siRNA-mediated gene silencing in human cells (68).

The mechanism of trasposon taming and RNA silencing movement suggest that RNAi plays a central role in antiviral defense mechanisms in nematodes. However, the involvement of RNAi in worm antiviral mechanisms is complicated by absence of worm-specific viruses, although worms are used by some plant viruses as transmission vectors (69). Lately, it has been reported that two nonnatural viruses efficiently initiate antiviral RNAi in *C. elegans* (43, 55). Wilkins et al. demonstrated that nematode N2 cells can support the replication of mammalian vesicular stomatitis virus (VSV) (43). These studies showed that worms with mutations in *rde-1* (which encodes a member of the Argo family) or *rde-4* (which encodes a dsRNA-binding protein facilitating the loading of siRNA onto the RISC machinery) enhance viral replication and contain higher viral loads after infection with VSV or FHV (43). In contrast, the replication of VSV is inhibited in the worms with mutations in two of the silencing negative regulators, RFF-3 and ERI-1. It is known that ERI-1 is a member of the DEDDh nuclease family, which cleaves dsRNA in a preferential manner. siRNA are more stable and accumulate in ERI-1 mutants, resulting in enhanced gene inhibition (70). RRF-3, a member of the RdRp gene family in *C. elegans*, inhibits RdRp-directed siRNA amplification, and RRF-3mutant worms are more sensitive and susceptible to RNAi induced by dsRNA (71). Wilkins et al. reported for the first time virus-specific, 20–30 nucleotides long siRNA (43). Similarly, other investigators reported complete replication of the FHV bipartite, plus-strand RNA genome in *C. elegans*. Furthermore, they showed that FHV replication in *C. elegans* induces a potent antiviral response that requires RDE-1, an Argo protein essential for RNAi mediated by siRNA, but not by miRNA (55). This antiviral response could be inhibited by the FHV-encoded B2 silencing suppressor (55). The presence of four Dicers in *Arabidopsis thaliana*, two in Drosophila, and one in nematode as well as the ability of *C. elegans* to mount virus-derived siRNA antiviral response to viral infection indicate the complexity of siRNA silencing pathways. These also indicate that the variable number of Dicers does not control the expression of antiviral silencing. This is especially relevant to antiviral roles of silencing in mammals which, like worms, have only one Dicer. Very recently, RNAi has also been identified as an important antiviral defense in fungi (72).

3.4. Antiviral RNA Silencing in Plants

The possibility that RNAi might have an antiviral function was first suggested from plant-based research when experimentally

induced gene silencing was found to provide resistance to viruses carrying an identical sequence (73). For example, replication of Tobacco mosaic virus (TMV), harboring partial cDNA of phytoene desaturase (PDS), easily silenced PDS mRNA (74). This study led to the development of virus-induced gene silencing, a reverse genetic tool now widely used by plant biologists. The fact that plant viruses are targeted by RNA silencing has been further demonstrated in studies in which transgenic plants, expressing the coat protein of Tobacco etch virus (TEV), were infected with TEV. Signs of infection clearly appeared on inoculated leaves but gradually disappeared in new growth. New growth became resistant to superimposed infection with TEV and this was termed "recovery phenomenon" (73). This resistance was due to complete degradation of both TEV and coat protein mRNA. The recovery phenomenon was later discovered to be naturally initiated by some plant viruses when infecting wild-type plants (9, 11). RNA silencing helps to explain this cross-protection phenomenon in which attenuated strains of specific virus are used to immunize plants against a strongly virulent strain of the same virus (75). This is demonstrated by plants, carrying a GFP insert, that become resistant to TMV after being infected with a recombinant potato virus X (PVX) that carries the same insert (76). The ultimate proof of the plant-virus-initiated RNAi silencing was provided by the fact that virus-derived siRNA highly accumulate in plants during viral infection (77).

The vast majority of plant viruses are RNA viruses. The dsRNA replication intermediates of RNA viruses and high secondary structures of single-stranded RNA (for DNA plant viruses) are considered to make up the substrate of at least one of the plant Dicer homologs. In the plant genetic model *A. thaliana*, the two Dicer-like (DCL) enzymes, DCL4 and DCL2, mediate the generation of siRNA from dsRNA and are involved in antiviral responses (78). The DCL-2 was shown to generate the siRNA derived from the turnip crinkle virus (TCV), but not those from the cucumber mosaic virus strain (CMV-Y) or the turnip mosaic virus (TMV). Furthermore, Xie et al. (79) have demonstrated that replication of CMV-Y and TMV were not affected by impairment of DCL-1 and DCL-3 functions in plants, and they concluded that DCL-4 functions as a component of the anti-TMV and anti-CMV silencing (79). It has been reported that plant cells naturally produced numerous subclasses of small RNA involved in epigenetic modification and biogenesis of other small RNA, but these are not yet identified in mammalian cells (80, 81).

Other than the fact that *A. thaliana* devotes two Dicer genes to the control of viral infections, the main difference between plants and flies is that RNAi is systemic in plants, spreading from tissue to tissue. This systemic RNAi response involves cell-to-cell signaling that is mediated by DCL4-generated siRNA of 21 mers

in length, coupled to the generation of dsRNA in noninfected tissues by host RdRp. Thus, siRNA can be propagated and act systemically over long distances to mediate a protective antiviral state in non-infected cells (82). The discovery of virus-encoded suppressors of silencing also provided indirect proof that RNA silencing has efficient antiviral effects in plants (82). The observation of synergism, a phenomenon in which augmentation of signs induced by one virus by co-infection with another unrelated virus, provides the first clue for virus-mediated silencing suppressors (83). The Potyvirus Y (PVY) dramatically increases the replication of PVX when co-infected, indicating that PVY-encoded RNAi silencing suppressor against host defense recapitulates the molecular effects and disease signs of this viral infection (83). Following several similar observations, it was demonstrated that silencing suppressors are a common feature of most, if not all, plant viruses (84).

Surprisingly, these RNAi silencing suppressors are diverse in their sequence and structure, encoded by both DNA and RNA plants viruses and are thought to affect all levels of RNAi silencing (84). From these studies, it is concluded that antiviral RNAi silencing requires observation of the presence of siRNA, production of virus-encoded RNAi silencing suppressor and the movement of silencing in the infected host.

4. Conclusions

RNA interference is a natural process of gene silencing that occurs in many organisms, ranging from plants to mammals. An interesting question for the future is whether RNAi mechanisms also exist for counteracting bacterial and fungal infections in animals, and whether RNAi plays a more general role in innate immune defense of higher animals, including mammals. Although, at present, it is unclear whether RNA silencing naturally restricts viral infection in vertebrates, there are signs that this is certainly the case. Many suppressors of the RNAi pathway were reported to be encoded by mammalian viruses, and host-encoded miRNA have been shown to both repress and enhance intracellular amounts of viral RNA. Given the fast and exciting progress in this field, one can only expect that future research will be able to reveal if RNAi plays a central role in host defense immune response against microbial infections in general.

In a relatively short period, RNAi has progressed to become an important experimental tool both in vitro and in vivo for the analysis of gene function and target validation in mammalian systems. In addition, RNA silencing has subsequently been found to

be involved in translational repression, transcriptional inhibition, and DNA degradation. As a result, it has only been possible to review here a small portion of the hundreds of papers that have already been published in this area. However, this may open doors to the many uses to which this important technology is being put and to the potential of RNAi as a therapeutic strategy. RNAi-based gene therapy has great potential in cancer and infectious diseases, as well as in genetic diseases that are due to a dominant genetic effect. Finally, the discovery that virus and host both use RNAi for their own benefit and advantage introduces a new level of gene regulation that modulates pathogen–host interactions.

References

1. Fritz, J.H., Girardin, S.E. and Philpott, D.J. (2006) Innate immune defense through RNA interference. *Sci. STKE* **339**, pe27.
2. Fire, A., Xu, S., Montgomery, M.K., Kostas, S.A., Driver, S.E. and Mello, C.C. (1998) Potent and specific genetic interference by double-stranded RNA in *Caenorhabditis elegans*. *Nature* **391**, 806–801.
3. Meister, G. and Tuschl, T. (2004) Mechanisms of gene silencing by double-stranded RNA. *Nature* **431**, 343–349.
4. Couzin, J. (2002) Breakthrough of the year: small RNAs make big splash. *Science* **298**, 2296–2297.
5. Ecker, J.R. and Davis, R.W. (1986) Inhibition of gene expression in plant cells by expression of antisense RNA. *Proc. Natl. Acad. Sci. U.S.A.* **83**, 5372–5376.
6. Van Blokland, R., Van der Geest, N., Mol, J.N.M. and Kooter, J.M. (1994) Transgene-mediated suppression of chalcone synthase expression in *Petunia hybrida* results from an increase in RNA turnover. *Plant J.* **6**, 861–877.
7. Napoli, C., Lemieux, C. and Jorgensen, R. (1990) Introduction of a Chimeric Chalcone Synthase Gene into Petunia Results in Reversible Co-Suppression of Homologous Genes in trans. *Plant Cell* **2**, 279–289.
8. Romano, N. and Macino, G. (1992) Quelling: transient inactivation of gene expression in *Neurospora crassa* by transformation with homologous sequences. *Mol. Microbiol.* **6**, 3343–3453.
9. Covey, S., Al-Kaff, N., Lángara, A. and Turner, D. (1997) Plants combat infection by gene silencing. *Nature* **385**, 781–782.
10. Fagard, M. and Vaucheret, H. (2000) (Trans) gene silencing in plants: how many mechanisms? *Annu. Rev. Plant Physiol. Plant Mol. Biol.* **51**, 167–194.
11. Ratcliff, F., Harrison, B. and Baulcombe, D. (1997) A similarity between viral defense and gene silencing in plants. *Science* **276**, 1558–1560.
12. Guo, S. and Kemphues, K. (1995) par-1, a gene required for establishing polarity in *C. elegans* embryos, encodes a putative Ser/Thr kinase that is asymmetrically distributed. *Cell* **81**, 611–620.
13. Pal-Bhadra, M., Bhadra, U. and Birchler, J. (1997) Cosuppression in *Drosophila*: gene silencing of Alcohol dehydrogenase by white-Adh transgenes is Polycomb dependent. *Cell* **90**, 479–490.
14. Tabara, H., Grishok, A. and Mello, C.C. (1998) RNAi in *C. elegans*: soaking in the genome. *Science* **282**, 430–431.
15. Timmons, L. and Fire, A. (1998) Specific interference by ingested dsRNA. *Nature* **395**, 854.
16. Tavernarakis, N., Wang, S.L., Dorovkov, M., Ryazanov, A. and Driscoll, M. (2000) Heritable and inducible genetic interference by double-stranded RNA encoded by transgenes. *Nat. Genet.* **24**, 180–183.
17. Waterhouse, P.M., Graham, M.W. and Wang, M.B. (1998) Virus resistance and gene silencing in plants can be induced by simultaneous expression of sense and antisense RNA. *Proc. Natl. Acad. Sci. U.S.A.* **95**, 13959–13964.
18. Ngo, H., Tschudi, C., Gull, K. and Ullu, E. (1998) Double-stranded RNA induces mRNA degradation in *Trypanosoma brucei*. *Proc. Natl. Acad. Sci. U.S.A.* **95**, 14687–14692.
19. Kennerdell, J.R. and Carthew, R.W. (1998) Use of dsRNA-mediated genetic interference to demonstrate that frizzled and frizzled

2 act in the wingless pathway. *Cell* **95**, 1017–1026.

20. Bartel, D.P. (2004) MicroRNAs: genomics, biogenesis, mechanism, and function. *Cell* **116**, 281–297.
21. Lewis, B.P., Shih, I.H., Jones-Rhoades, M.W., Bartel, D.P. and Burge, C.B. (2003) Prediction of mammalian microRNA targets. *Cell* **115**, 787–798.
22. Lagos-Quintana, M., Rauhut, R., Yalcin, A., Meyer, J., Lendeckel, W. and Tuschl, T. (2002) Identification of tissue-specific microRNAs from mouse. *Curr. Biol.* **12**, 735–739.
23. Yao, M.C. and Chao, J.L. (2005) RNA-guided DNA deletion in *Tetrahymena*: an RNAi-based mechanism for programmed genome rearrangements. *Annu. Rev. Genet.* **39**, 537–559.
24. Lee, Y., Ahn, C., Han, J., Choi, H., Kim, J., Yim, J., et al. (2003). The nuclear RNase III drosha initiates MicroRNA processing. *Nature* **425**, 415–419.
25. Bernstein, E., Caudy, A.A., Hammond, S.M. and Hannon, G.J. (2001) Role for a bidentate ribonuclease in the initiation step of RNA interference. *Nature* **409**, 363–366.
26. Meister, G., Lndthaler, M., Pathaniowska, A., Dorsett, Y., Teng, G. and Tuschl, T. (2004) Human Argonaute2 mediates RNA cleavage targeted by miRNAs and siRNAs. *Mol. Cell* **15**, 185–197.
27. Kisielow, M., Kleiner, S., Nagasawa, M., Faisal, A. and Nagamine, Y. (2002) Isoform-specific knockdown and expression of adaptor protein ShcA using small interfering RNA. *Biochem. J.* **363**, 1–5.
28. Tang, G. (2005) siRNA and miRNA: an insight into RISCs. *Trends Biochem. Sci.* **30**, 106–114.
29. Caudy, A.A., Ketting, R.F., Hammond, S.M., Denli, A.M., Bathoorn, A.M., Tops, B.B., et al. (2003) A micrococcal nuclease homologue in RNAi effector complexes. *Nature* **425**, 411–414.
30. Doench, J.G., Petersen, C.P. and Sharp, P.A. (2003) SiRNAs can function as MIRNAS. *Genes Dev.* **17**, 438–442.
31. Kato, H., Takeuchi, O., Sato, S., Yoneyama, M., Yamamoto, M., Matsui, K., et al. (2006) Differential roles of MDA5 and RIG-I helicases in the recognition of RNA viruses. *Nature* **441**, 101–105.
32. Marques, J.T., Devosse, T., Wang, D., Zamanian-Daryoush, M., Serbinowski, P., Hartmann, R., et al. (2006) A structural basis for discriminating between self and nonself double-stranded RNAs in mammalian cells. *Nat. Biotechnol.* **24**, 559–565.
33. Stark, G.R., Kerr, I.M., Williams, B.R., Silverman, R.H. and Schreiber, R.D. (1998) How cells respond to interferons. *Annu. Rev. Biochem.* **67**, 227–264.
34. Zhou, A., Paranjape, J., Brown, T.L., Nie, H., Naik, S., Dong, B., et al. (1997) Interferon action and apoptosis are defective in mice devoid of 2′,5′-oligoadenylate-dependent RNase L. *EMBO J.* **16**, 6355–6363.
35. Hilleman, M.R. (2004) Strategies and mechanisms for host and pathogen survival in acute and persistent viral infections. *Proc. Natl. Acad. Sci. U.S.A.* **101** (Suppl. 2), 14560–14566.
36. Haasnoot, P.C.J. and Berkhout, B. (2006) RNA interference: use as antiviral therapy. Handbook of experimental pharmacology. *Heidelberg: Springer-Verlag.* pp. 117–150.
37. Pfeffer, S., Zavolan, M., Grasser, F.A., Chien, M., Russo, J.J., Ju, J., et al. (2004) Identification of virus-encoded microRNAs. *Science* **304**, 734–736.
38. Soifer, H.S., Zaragoza, A., Peyvan, M., Behlke, M.A. and Rossi, J.J. (2005) A potential role for RNA interference in controlling the activity of the human LINE-1 retrotransposon. *Nucleic Acids Res.* **33**, 846–856.
39. Bennasser, Y., Le, S.Y., Benkirane, M. and Jeang, K.T. (2005) Evidence that HIV-1 encodes an siRNA and a suppressor of RNA silencing. *Immunity* **22**, 607–619.
40. Yang, N., Kazazian, H.H. Jr. (2006) L1 retrotransposition is suppressed by endogenously encoded small interfering RNAs in human cultured cells. *Nat. Struct. Mol. Biol.* **13**, 763–771.
41. Lecellier, C.H., Dunoyer, P., Arar, K., Lehmann-Che, J., Eyquem, S., Himber, C., Saib, A., Voinnet, O. (2005) A cellular microRNA mediates antiviral defense in human cells. *Science* **308**, 557–560.
42. Triboulet, R., Mari, B., Lin, Y.L., Chable-Bessia, C., Bennasser, Y., Lebrigand, K., et al. (2007) Suppression of microRNA-silencing pathway by HIV-1 during virus replication. *Science* **315**, 1579–1582.
43. Wilkins, C., Dishongh, R., Moore, S.C., Whitt, M.A., Chow, M. and Machaca, K. (2005) RNA interference is an antiviral defence mechanism in *Caenorhabditis elegans. Nature* **436**, 1044–1047.
44. Pedersen, I. M., Cheng, G., Wieland, S., Volinia, S., Croce, C.M., Chisari, F.V. and David, M. (2007) Interferon modulation of cellular microRNAs as an antiviral mechanism. *Nature* **449**, 919–921.

45. Jopling, C. L., Yi, M., Lancaster, A. M., Lemon, S. M. and Sarnow, P. (2005) Modulation of hepatitis C virus RNA abundance by a liver-specific microRNA. *Science* **309**, 1577–1581.
46. Cameron, J.E., Yin, Q.Y., Fewell, C., Lacey, M., McBride, J. and Wang, X. (2008) Epstein–Barr virus latent membrane protein 1 induces cellular microRNA miR-146a, a modulator of lymphocyte signaling pathways. *J. Virol.* **83**, 1946–1958.
47. Sarnow, P., Jopling, C. L., Norman, K. L., Schutz, S. and Wehner, K. A. (2006) MicroRNAs: expression, avoidance and subversion by vertebrate viruses. *Nat. Rev. Microbiol.* **4**, 651–659.
48. Pfeffer, S., Sewer, A., Lagos-Quintana, M., Sheridan, R., Sander, C., Grässer, F.A., et al. (2005) Identification of microRNAs of the herpesvirus family. *Nat. Methods* **2**, 269–276.
49. Sullivan, C.S., Grundhoff, A.T., Tevethia, S., Pipas, J.M. and Ganem, D. (2005) SV40-encoded microRNAs regulate viral gene expression and reduce susceptibility to cytotoxic T cells. *Nature* **435**, 682–686.
50. Cai, X., Lu, S., Zhang, Z., Gonzalez, C.M., Damania, B. and Cullen, B.R. (2005) Kaposi's sarcoma-associated herpesvirus expresses an array of viral microRNAs in latently infected cells. *Proc. Natl. Acad. Sci. U.S.A.* **102**, 5570–5575.
51. Gupta, A., Gartner, J.J., Sethupathy, P., Hatzigeorgiou, A.G. and Fraser, N.W. (2006) Anti-apoptotic function of a microRNA encoded by the HSV-1 latency-associated transcript. *Nature* **442**, 82–85.
52. Stern-Ginossar, N., Elefant, N., Zimmermann, A., Wolf, D.G., Saleh, N., Biton, M., et al. (2007) Host immune system gene targeting by a viral miRNA. *Science* **317**, 376–381.
53. Levashina, E.A., Moita, L.F., Blandin, S., Vriend, G., Lagueux, M. and Kafatos, F.C. (2001) Conserved role of a complement-like protein in phagocytosis revealed by dsRNA knockout in cultured cells of the mosquito, *Anopheles gambiae*. *Cell* **104**, 709–718.
54. Li, H., Li, W.X. and Ding, S.W. (2002) Induction and suppression of RNA silencing by an animal virus. *Science* **296**, 1319–1321.
55. Lu, R., Maduro, M., Li, F., Li, H.W., Broitman-Maduro, G., Li, W.X. and Ding, S.W. (2005) Animal virus replication and RNAi-mediated antiviral silencing in *Caenorhabditis elegans*. *Nature* **436**, 1040–1043.
56. Galiana-Arnoux, D., Dostert, C., Schneemann, A., Hoffmann, J.A. and Imler, J.L. (2006) Essential function in vivo for Dicer-2 in host defense against RNA viruses in drosophila. *Nat. Immunol.* **7**, 590–597.
57. Uhlirova, M., Foy, B.D., Beaty, B.J., Olson, K.E., Riddiford, L.M. and Jindra, M. (2003) Use of Sindbis virus-mediated RNA interference to demonstrate a conserved role of Broad-Complex in insect metamorphosis. *Proc. Natl. Acad. Sci. U.S.A.* **100**, 15607–15612.
58. Lipardi, C., Wei, Q. and Paterson, B.M. (2001) RNAi as random degradative PCR: siRNA primers convert mRNA into dsRNAs that are degraded to generate new siRNAs. *Cell* **107**, 297–307.
59. Roignant, J.Y., Carre, C., Mugat, B., Szymczak, D., Lepesant, J.A. and Antoniewski, C. (2003) Absence of transitive and systemic pathways allows cell-specific and isoform-specific RNAi in *Drosophila*. *RNA* **9**, 299–308.
60. Jensen, S., Gassama, M.P. and Heidmann, T. (1999) Taming of transposable elements by homology-dependent gene silencing. *Nat. Genet.* **21**, 209–212.
61. Sarot, E., Payen-Groschene, G., Bucheton, A. and Pelisson, A. (2004) Evidence for a piwi-dependent RNA silencing of the gypsy endogenous retrovirus by the *Drosophila melanogaster* flamenco gene. *Genetics* **166**, 1313–1321.
62. Hamilton, A., Voinnet, O., Chappell, L. and Baulcombe, D. (2002) Two classes of short interfering RNA in RNA silencing. *EMBO J.* **21**, 4671–4679.
63. Sijen, T. and Plasterk, R.H. (2003) Transposon silencing in the *Caenorhabditis elegans* germ line by natural RNAi. *Nature* **426**, 310–314.
64. Alder, M.N., Dames, S., Gaudet, J. and Mango, S.E. (2003) Gene silencing in *Caenorhabditis elegans* by transitive RNA interference. *RNA* **9**, 25–32.
65. Winston, W.M., Molodowitch, C. and Hunter, C.P. (2002) Systemic RNAi in *C. elegans* requires the putative transmembrane protein SID-1. *Science* **295**, 2456–2459
66. Tijsterman, M., May, R.C., Simmer, F., Okihara, K.L. and Plasterk, R.H. (2004) Genes required for systemic RNA interference in *Caenorhabditis elegans*. *Curr. Biol.* **14**, 111–116.
67. Feinberg, E.H. and Hunter, C.P. (2003) Transport of dsRNA into cells by the transmembrane protein SID-1. *Science* **301**, 1545–1547.
68. Duxbury, M.S., Ashley, S.W. and Whang, E.E. (2005) RNA interference: a mammalian SID-1 homologue enhances siRNA uptake and gene silencing efficacy in human

cells. *Biochem. Biophys. Res. Commun.* **331**, 459–463.

69. Gray, S.M. (1996) Plant virus proteins involved in natural vector transmission. *Trends Microbiol.* **4**, 259–264.
70. Kennedy, S., Wang, D. and Ruvkun, G.A. (2004) Conserved siRNA-degrading RNase negatively regulates RNA interference in *C. elegans*. *Nature* **427**, 645–649.
71. Simmer, F., Tijsterman, M., Parrish, S., Koushika, S.P., Nonet, M.L., Fire, A., Ahringer, J., Plasterk, R.H. (2002) Loss of the putative RNA-directed RNA polymerase RRF-3 makes *C. elegans* hypersensitive to RNAi. *Curr. Biol.* **12**, 1317–1319.
72. Hammond, T.M., Andrewski, M.D., Roossinck, M.J. and Keller, N.P. (2008) *Aspergillus* mycoviruses are targets and suppressors of RNA silencing Eukaryot. *Cell* 7, 350–357.
73. Lindbo, J.A., Silvarosales, L., Proebsting, W.M. and Dougherty, W.G. (1993) Induction of a highly specific antiviral state in transgenic plants – implications for regulation of gene-expression and virus-resistance. *Plant Cell* **5**, 1749–1759.
74. Kumagai, M.H., Donson, J., della-Cioppa, G., Harvey, D., Hanley, K. and Grill, L.K. (1995) Cytoplasmic inhibition of carotenoid biosynthesis with virus-derived RNA. *Proc. Natl. Acad. Sci. U.S.A.* **92**, 1679–1683.
75. Valle, R.P., Skrzeczkowski, J., Morch, M.D., Joshi, R.L., Gargouri, R., Drugeon, G., et al. (1988) Plant viruses and new perspectives in cross-protection. *Biochimie* **70**, 695–703.
76. Ratcliff, F.G., MacFarlane, S.A. and Baulcombe, D.C. (1999) Gene silencing without DNA: RNA-mediated cross-protection between viruses. *Plant Cell* **11**, 1207–1216.
77. Hamilton, A.J. and Baulcombe, D.C. (1999) A species of small antisense RNA in posttranscriptional gene silencing in plants. *Science* **286**, 950–952.
78. Deleris, A., Gallego-Bartolome, J., Bao, J., Kasschau, K.D., Carrington, J.C. and Voinnet, O. (2006) Hierarchical action and inhibition of plant Dicer-like proteins in antiviral defense. *Science* **313**, 68–71
79. Xie, Z., Johansen, L.K., Gustafson, A.M., Kasschau, K.D., Lellis, A.D., Zilberman, D., Jacobsen, S.E. and Carrington, J.C. (2004) Genetic and functional diversification of small RNA pathways in plants. *PLoS Biol.* **2**, E104.
80. Carrington, J.C. (2005) Small RNAs and Arabidopsis. A fast forward look. *Plant Physiol.* **138**, 565–566.
81. Baulcombe, D. (2005) RNA silencing. *Trends Biochem. Sci.* **30**, 290–293.
82. Dunoyer, P., Himber, C. and Voinnet, O. (2005) DICER-LIKE 4 is required for RNA interference and produces the 21-nucleotide small interfering RNA component of the plant cell-to-cell silencing signal. *Nat. Genet.* **37**, 1356–1360.
83. Vance, V.B., Berger, P.H., Carrington, J.C., Hunt, A.G. and Shi, X.M. (1995) 5′ proximal potyviral sequences mediate potato virus X/potyviral synergistic disease in transgenic tobacco. *Virology* **206**, 583–590.
84. Voinnet, O., Pinto, Y.M. and Baulcombe, D.C. (1999) Suppression of gene silencing: a general strategy used by diverse DNA and RNA viruses of plants. *Proc. Natl. Acad. Sci. U.S.A.* **96**, 14147–14152.

Chapter 2

Monitoring Innate Immune Recruitment by siRNAs in Mammalian Cells

Michael P. Gantier and Bryan R.G. Williams

Abstract

The use of small interfering RNAs (siRNAs) in human therapy may be hindered by the recruitment of nonspecific effects such as the activation of innate immune responses. Recently, several innate immune receptors have been implicated in the detection of siRNAs. This chapter provides a brief overview of the current knowledge of siRNA-induced innate immunity, as well as protocols for the rapid identification of siRNAs with innate immune stimulatory activity.

Key words: Innate immunity, RNA interference, siRNA, RIG-I, TLR7, TLR8

1. Introduction

During viral infection, mammals rely on an early detection of foreign ribonucleic acids to mount a rapid antiviral response. While this phenomenon has been known for more than four decades, insights into the molecular identity of components of the response have been gained only recently (1). Two detection pathways have been identified in blood immune cells as directly involved in innate immune activation by exogenous RNAs. The cells orchestrating the initiation of this antiviral response sense viral RNAs through Toll-like receptors (TLRs) or retinoic acid inducible gene I (RIG-I)-like receptors (1).

Originally thought to be too small to be recognized by the sensors of the innate immune system, small interfering RNA (siRNA) activation of a strong innate immune response is now well established (2). To date, four main characteristics of siRNAs have been associated with the recruitment of innate

Wei-Ping Min and Thomas Ichim (eds.), *RNA Interference*, Methods in Molecular Biology, vol. 623,
DOI 10.1007/978-1-60761-588-0_2,

immunity and subsequent cytokine production: a) Secondary structure, which is detected by TLR3; b) uridine content, detected by TLR 7/8; c) end terminal structure of blunt-end siRNA from 21-27 nt detected by RIG-1; and 25 nt duplexes bearing a 5' or 3' monophosphate, also detected by RIG-1 (3–11).

We have established different protocols that allow for rapid discrimination among different siRNAs for their capacity to recruit TLR7/8 and RIG-I (12, 13). Whether or not the ability of an siRNA to induce immunostimulation through these receptors is the desired outcome (14), these systems are a useful starting point prior to further validation in peripheral blood mononuclear cells (PBMCs) from animal models.

In this chapter, we describe two protocols allowing for the evaluation of mouse TLR7 (and per se, also human TLR7) and human TLR8 recruitment by siRNAs. We also describe a simple real-time Reverse Transcription-Polymerase Chain Reaction (RT-PCR) protocol, based on human T98G cells (adapted from Marques et al. (8)).

2. Materials

2.1. Cell Culture

1. RAW 264.7: ATCC reference TIB-71. T98G cells: ATCC reference CRL-1690.
2. Ficoll-Paque Plus (GE Healthcare)
3. Lithium-heparin sterile tubes (Sarstedt, Nümbrecht, Germany).
4. Dulbecco's Modified Eagle's Medium (DMEM) (Invitrogen Corporation) supplemented with 10% sterile fetal bovine serum (FBS; ICPBio Ltd, Auckland, New Zealand) and 1× antibiotic/antimycotic (Invitrogen Corporation) (referred to as complete DMEM medium).
5. Roswell Park Memorial Institute medium (RPMI) 1640 plus L-glutamine medium (Invitrogen Corporation) complemented with 1× antibiotic/antimycotic and 10% FBS (referred to as complete RPMI 1640).
6. Dulbecco's Phosphate-Buffered Saline (PBS, Invitrogen Corporation).
7. TrypLE™ Express Stable Trypsin (Invitrogen Corporation).
8. Sterile tissue culture-treated microtest™ 96-well plates (Falcon)
9. Sterile, tissue culture-treated 48-well plates (JET BIOFIL, Guangzhou, China).

10. Human TLR8 and mouse TLR7 agonist: CL75 (Invivogen, San Diego, USA).
11. *N*-[1-(2,3-Dioleoyloxy)propyl]-*N*,*N*,*N*-trimethylammonium methylsulfate (DOTAP) (Roche).
12. Opti-MEM® (Invitrogen Corporation).
13. Lipofectamine 2000 (Invitrogen Corporation).
14. siRNAs: synthesized by Integrated DNA Technologies (IDT) as single-stranded RNAs; resuspended in filter-sterilized duplex buffer (100 mM potassium acetate, 30 mM HEPES, pH 7.5) in UltraPure™ DNase/RNase-Free Distilled Water (referred to as RNase-free H_2O, Invitrogen Corporation) to a concentration of 80 µM. Each duplex is annealed at 92°C for 2 min and left for 30 min at room temperature before being aliquoted and frozen at –80°C. siControl is a nontargeting 21 nucleotide siRNA (siControl 1, Ambion).

2.2. Tumor Necrosis Factor α (TNF-α) Enzyme-Linked ImmunoSorbent Assay (ELISA)

1. OptEIA ELISA sets (BD Biosciences).
2. PBS 10×: NaCl 8% (w/v), KCl 0.2% (w/v), Na_2HPO_4 1.22% (w/v), KH_2PO_4 0.2% (w/v) in ddH_2O – pH 7.4 (all reagents are from Sigma-Aldrich).
3. PBS-tween (PBST): 1× PBS diluted in H_2O complemented with 0.05% tween 20 (Sigma-Aldrich).
4. Pharmingen Assay Diluent (BD Biosciences Pharmingen).
5. F96 maxisorp plates (nunc, Roskilde, Denmark).
6. Tetramethyl benzidine substrate (TMB, Sigma-Aldrich)
7. Sulfuric acid 2 N (Sigma-Aldrich).
8. Plate reader with 450 nm absorbance filter.

2.3. RNA Extraction/ cDNA Synthesis/Real Time

1. NucleoSpin RNA II kit (MACHEREY-NAGEL, Düren, Germany). Supplement RA1 buffer with 1% v/v 2-mercaptoethanol (Bme) (Sigma-Aldrich) immediately before adding to the cells.
2. Superscript III Reverse Transcriptase – includes 5× first strand buffer and 0.1 M dithiothreitol (DTT), 10 mM deoxy-nucleotides triphosphate (dNTPs), $Oligo(dT)_{20}$ Primer, and RNaseOUT™ (all from Invitrogen Corporation).
3. SYBR GreenER™ qPCR SuperMix for iCycler® instrument (Invitrogen Corporation).
4. IQ5 Multicolor Biorad i-cycler.
5. Optical Tape (Bio-Rad).
6. Multiplate 96-well clear (Bio-Rad).

3. Methods

3.1. Sequence-Specific Recruitment of TLR7 and 8

First and foremost, the ability of siRNAs to recruit the innate immune system is highly dependent on the cell type considered. Plasmacytoid dendritic cells and macrophages/monocytes are the main detectors of TLR7/8 agonists amongst other immune blood cells (1). Because the route of siRNA delivery in vivo is intrinsically related to a potential recruitment of immune blood cells, it is important to assess the detection of siRNAs by TLR7/8 when selecting appropriate siRNA candidates for in vivo delivery. Although uridine-based motifs within small RNA sequences have been found to be important for TLR7/8 activation (4–7), *in silico* prediction of the overall immunostimulatory potency of an siRNA remains highly inaccurate. We and others have found that single-stranded RNAs bearing uridine motifs that induce strong immunostimulation in human PBMCs can be completely masked when present in a double-stranded siRNA structure (6, 13). For this reason, direct measurement of the immunogenicity of a novel siRNA sequence is currently the most accurate method of evaluating recruitment of TLR7/8 by siRNAs.

While both human TLR7 and TLR8 (hTLR7/8) have been implicated in sequence-specific sensing of small RNAs, the murine homolog of TLR8 is not able to detect RNA on its own (12, 15, 16). Rather, sequence-specific sensing of RNAs relies exclusively on TLR7 in the mouse (12, 15). It has recently been shown by us and others that hTLR7 and hTLR8 recognize different RNA sequences, thus the immunogenicity of some sequences preferentially recognized by hTLR8 is not conserved between human and mouse (12, 15, 16). Nevertheless, our observations based on a large panel of oligoribonucleotides have led us to the conclusion that sequence-specific sensing of small RNAs by TLR7 is conserved between human and mouse (12) (see Fig. 1). Here, we describe two protocols allowing for the evaluation of mouse TLR7 (and per se, also human TLR7) and human TLR8 recruitment by siRNAs. For mouse TLR7 recruitment, we rely on the induction of mouse TNF-α (mTNF-α) by a macrophage-like cell line (RAW 264.7) (5, 12). Making use of the conservation of TLR7 sensing between human and mouse avoids using a costly human interferon-α (IFN-α) ELISA and yet captures most of the hTLR7-driven IFN-α response observed in human PBMCs (see Fig. 1). It is noteworthy that when a sequence is found not to trigger TNF-α induction in RAW 264.7 cells, no conclusion can be drawn regarding its innate immune activating potential in human blood without further validation of hTLR8 activity via human TNF-α (hTNF-α) production in human PBMCs (see Fig. 1).

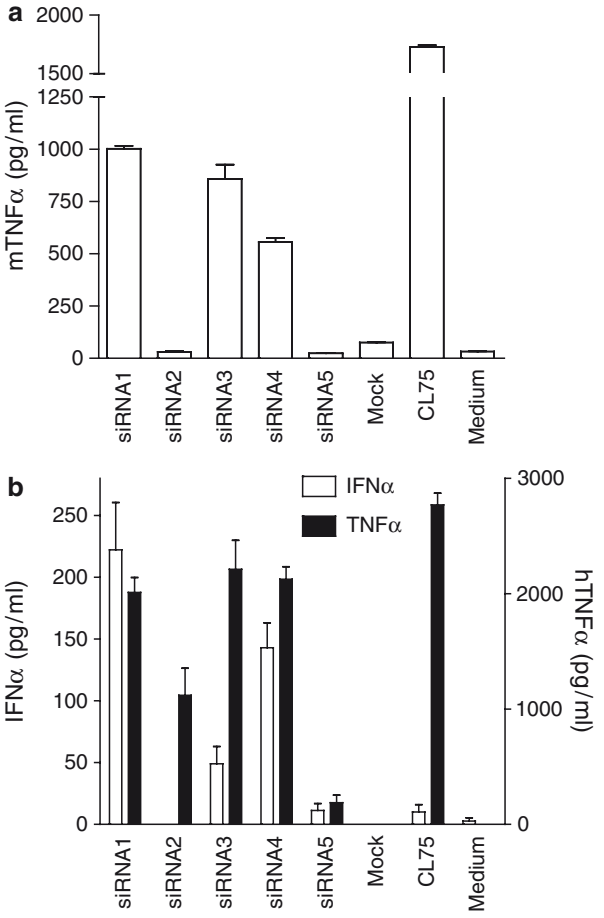

Fig. 1. siRNA-induced TNF-α in human and mouse macrophages. (**a**) Mouse RAW 264.7 cells and (**b**) human PBMCs were treated as presented in Subheading 3.1 with 750 nM of siRNAs complexed with DOTAP for 18 h. Each treatment was carried out in biological triplicate and the data is from one representative experiment for both (**a**) and (**b**). The error bars represent the standard error of the mean (SEM). In this example, the mouse macrophage cell line data (**a**) indicates that siRNA1, 3 and 4 are immunostimulatory (through mouse TLR7), whereas siRNA2 and 5 are not. While a similar observation can be made in human PBMCs (**b**) when looking at IFN-α (indicative of human TLR7 recruitment), we find that siRNA2 is a good inducer of TNF-α (indicative of human TLR8 recruitment) but not IFN-α. However, siRNA5 appears to be a very low inducer of both IFN-α and TNF-α in PBMCs and would therefore be considered here as very poorly immunostimulatory

3.1.1. Preparation of Mouse RAW Cells for TLR7 Activation

Plate RAW 264.7 cells passaged on surface-treated plasticware to a confluency of ~80,000 cells per well of a 96-well plate in 150 μL complete RPMI medium in the morning of the TLR stimulation (see Note 1). Incubate the cells at 37°C in 5% CO_2 for a minimum of 4 h prior to treatment with the TLR agonists.

3.1.2. Preparation of Human PBMCs for hTLR8 Activation

1. Collect blood from healthy volunteers in heparin-treated tubes (see Note 2) and mix with pure RPMI medium (no FBS, no antibiotics) in a 1:1 (v/v) ratio. Very gently, deposit the resulting RPMI-blood solution onto the surface of a Ficoll-Paque Plus layer in a 50 mL sterile tube, while avoiding any perturbation of the Ficoll-Paque Plus. A 1:1.2 ratio of Ficoll-Paque Plus to RPMI-blood volume is used. Centrifuge the 50-mL tubes at 1,000×*g* for 22 min at 4°C, using reduced break if possible. Following this gradient separation, discard the upper phase by gentle suction until the "white" interphase is reached. Transfer the PBMC-containing interphase to a new 15 mL sterile tube, taking care not to disturb the underlying Ficoll phase. Add RPMI medium to the collected interphase, up to a final volume of 10–12 mL, before spinning at 600×*g* for 7 min at 4°C. Following centrifugation, a pellet of cells should be visible. Discard the supernatant, wash the cell pellet with 10 mL of RPMI medium, and pellet again at 350×*g* for 7 min. Resuspend the cell pellet in 2 mL of complete RPMI and count using a hemacytometer.
2. Seed an average of 130,000–200,000 PBMCs in 150 μL of complete RPMI medium in each well of a 96-well plate (see Note 3). Rest the cells for a minimum of 1 h at 37°C in 5% CO_2 prior to stimulation.

3.1.3. TLR Stimulation of Human PBMCs and Mouse RAW Cells

Both cell types are treated the same way. Perform each treatment in biological triplicate: the amounts of the reagents given here are sufficient for three wells of a 96-well plate.

1. In sterile microcentrifuge tubes, aliquot 63.8 μL of pure RPMI. Dilute 11.2 μL of 40 μM siRNA into each tube (resulting in 75 μL per tube).
2. In a separate tube, mix 21 μl DOTAP with 54 μl pure RPMI (a mastermix conserving this ratio can be made). Mix the tube by gentle tapping, then incubate at room temperature for 5 min.
3. Add 75 μL of DOTAP/RPMI mix to each diluted siRNA, mix gently, then incubate the tubes for a further 10 min at room temperature.
4. Add 50 μL of the DOTAP-siRNA mixture to each well of plated cells (three wells per condition) to give a final volume of 200 μL and a final siRNA-DOTAP concentration of 750 nM (see Note 4). Incubate the plate overnight at 37°C for 14–18 h.
5. The following morning, inspect the cells using inverted microscopy. In all conditions using DOTAP + RNA complexes, some small cell debris/dots should be visible between the cells. Collect 100 μL of supernatant and dilute 1:2 with

OPti-EA buffer if the cells are PBMCs (there is no need to dilute the RAW cell supernatants). Freeze the supernatants at –80°C and keep until cytokine analysis by ELISA.

3.1.4. Cytokine Production Analysis by ELISA

A TNF-α ELISA is performed to assess the sequence-specific recruitment of mouse/human TLR7 and human TLR8. The same procedure is used for both the human and mouse TNF-α ELISA, with the exception of step 3.

1. The day before the assay (or a few days before), coat a maxisorp 96-well plate with 100 µL of capture antibody diluted 1:500 in coating buffer, and leave sealed with tape at 4°C. The morning of the assay, rinse the plate three times with PBST and block for 1 h at room temperature with 130 µL Assay Diluent per well, with rocking.
2. Following blocking, wash the plate three times with PBST. Prepare the TNF-α standard curve following the Analysis Certificate leaflet from the kit, to give a concentration range from 1,000 to 15.6 pg/mL (7 points). Add 75–100 µL of diluted/neat supernatant to each well of the ELISA plate, and incubate for 2 h at room temperature, with rocking.
3. Wash the plate four times with PBST and prepare the diluted capture antibody.
   (a) For human TNF-α, dilute both detection antibody and streptavidin-horseradish peroxidase (SAv-HRP) to 1:500 in Assay Diluent. Incubate for 10 min before adding 100 µL per well, and further incubate for 1 h at room temperature.
   (b) For mouse TNF-α, first dilute the detection antibody 1:500 in Assay Diluent. Apply 100 µL per well and incubate for 1 h at room temperature, with rocking. After four PBST washes, add 100 µL of 1:500 diluted SAv-HRP and incubate for 30 min at room temperature.
4. Following five to seven PBST washes, perform the enzymatic assay. Add 100 µL of prewarmed TMB (at 25–37°C) per well and stop the reaction with 50 µL sulfuric acid (see Note 5). Read the absorbance in a plate reader within 30 min at 450 nm (correction using absorbance at 570 nm can be applied) (see Note 6).

3.2. RIG-I Recognition of siRNAs

Originally thought to be exclusive to blunt-end siRNAs (8), recent insights into the mechanisms of RIG-I activation have led to the conclusion that other structural features of siRNAs permit innate immune recruitment. First, it was discovered that the presence of a 5′-triphosphate motif on single-stranded RNAs was a trigger for RIG-I activation of innate immunity (10, 17).

In accordance with previous claims for a role of 5′-triphosphate from bacteriophage synthesis of siRNA duplexes in the activation of the IFN pathway (9), these reports imply that all in vitro transcribed siRNAs have the potential to recruit and activate RIG-I. A recent study by Poeck et al. made use of RIG-I activation by 5′-triphosphate siRNA to synergize with the silencing efficacy of a pro-apoptotic siRNA to provoke increased apoptosis in tumor cells (14). Second, a recent publication from Takahasi et al. demonstrated that all synthetic double-stranded RNAs (blunt or with 2 nt overhangs) as short as 25 nt could bind RIG-I and activate it, provided they possess at least a 5′ or 3′ monophosphate (11). With the growing number of siRNA synthesis options/scaffolds in the past 5 years, an increase in siRNAs found to activate RIG-I should be anticipated.

Whether it is to avoid or intentionally recruit RIG-I activation, siRNAs for use in animal work should be validated in a cell model responsive to RIG-I. Here, we describe a simple real-time Reverse Transcription-Polymerase Chain Reaction (RT-PCR) protocol based on human T98G cells (adapted from Marques et al. (8)).

3.2.1. Treatment of T98G Cells with siRNA

This protocol relies on reverse transfection of the T98G cells – meaning that the cells are passaged and plated when the siRNAs are to be transfected. Using the volumes indicated here, each transfection mix will give three biological replicates in a 48-well plate format (see Note 7).

1. Prepare a mix of transfection reagent by adding 1.5 µL of Lipofectamine 2000 to 75 µl of Opti-MEM and incubate for 5 min at room temperature.
2. In a separate tube, dilute 1.875 µl of 4 µM siRNA in 75 µL of Opti-MEM. Slowly add the transfection mix to the diluted siRNA, gently agitate, then incubate at room temperature for 20–30 min.
3. While incubating the siRNA/Lipofectamine 2000 mix, trypsinize an 80% confluent flask of T98G cells with TryplE-Express and neutralize with pure DMEM (no FBS, no antibiotics). Count the cells using a hemacytometer, and dilute the volume required to obtain 90,000 cells in a final 600 µL of pure DMEM.
4. When ready, add 50 µL of siRNA/Lipofectamine 2000 mix to the bottom of the wells of a 48-well plate (using three wells for the same siRNA mix). Gently swirl the plate to cover most of the well surface. Then add 200 µL of cells in pure DMEM to each well (giving 250 µL at 10 nM), avoiding agitation (to keep the cells well dispersed). Incubate the 48-well plate at 37°C, in 5% CO_2.

5. After 4 h of incubation, aspirate the transfection mix and rinse each well in 200 µL of fresh DMEM complete. Some cells will detach, but most cells should remain stuck at the bottom of the wells. Incubate the 48-well plate for another 16–20 h at 37°C, in 5% CO_2.
6. Following incubation, the cells should be ~50% confluent, with the majority stuck at the bottom of the wells. Discard the medium (do not wash the cells with PBS) and add 100 µL of RA1-Bme solution directly to each well. Store the plate at −80°C for further RNA purification, or process directly.

3.2.2. RNA Extraction Using Nucleospin RNA II Columns

Purify the RNA following the manufacturer's protocol, with the following modifications.

1. Slowly thaw the samples, if frozen, at room temperature for ~20 min.
2. Use 100 µL of 75% EtOH in combination with 100 µL of filtered lysates before applying the samples to Nucleospin columns.
3. Extend the DNase 1 treatment to 30 min to minimize genomic DNA contamination.
4. Perform the elution with 40 µL of RNase-free H_2O only. Place the samples on ice for direct processing or keep at −80°C.

3.2.3. cDNA Synthesis Using Superscript III

For each RNA sample, synthesize cDNA using the following procedure.

1. Add 1 µL of 10 mM dNTP mix and 0.5 µL of $Oligo(dT)_{20}$ to 8.5 µL of RNA. Incubate at 65°C for 5 min, then place on ice for 2 min.
2. Add 4 µL of 5× first strand buffer, 1 µL of DTT, 0.5 µL of RNase OUT, and 0.2 µL Superscript III to each sample with RNase-free H_2O up to 20 µL. Incubate for 50 min at 50°C and denature for 5 min at 85°C. Store the resulting 20 µL of cDNA at −80°C until real-time PCR analysis.

3.2.4. Real-Time PCR of Human Interferon-Induced Protein 56 (P56): IFIT1

We have been using SYBR-GreenER on an IQ5 Multicolor i-cycler using GAPDH as a housekeeping gene with the primer pairs specified in Table 1. However, any other chemistry can be applied here (such as Taqman gene assay for IFIT1: Hs00356631_g1 – Applied Biosystems). Any significant induction of P56 between the sample and the control siRNA denotes an upstream activation of RIG-I (8) (see Fig. 2).

Prepare a mastermix with 10 µL of SYBR-GreenER and 8.2 µL of RNase-free H_2O per sample. Add 0.4 µL of both forward and reverse primers at 5 µM per sample. Aliquot this mix

Table 1
The sequences of DNA primers and siRNA

DNA primer sequence name (human)	5′-3′ sequence
GAPDH-FWD	CATCTTCCAGGAGCGAGATCCC
GAPDH-REV	TTCACACCCATGACGAACAT
P56-FWD	TCACCAGATAGGGCTTTGCT
P56-REV	CACCTCAAATGTGGGCTTTT
RNA duplex name	5′----------3′ 3′----------5′
siGFP27+0[a]	5′-AAGCUGACCCUGAAGUUCAUCUGCACC-3′ 3′-UUCGACUGGGACUUCAAGUAGACGUGG-5′
siGFP27+2[a]	5′-GCUGACCCUGAAGUUCAUCUGCACCACUU-3′ 3′-UUCGACUGGGACUUCAAGUAGACGUGGUG-5′

[a]The single-stranded RNAs used to create these duplexes do not bear any 5′ or 3′ monophosphate groups

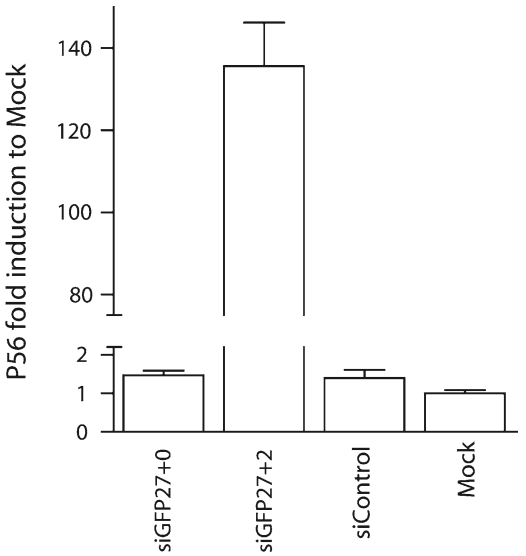

Fig. 2. siRNA-induced P56 mRNA in human T98G cells. 10 nM of each indicated siRNA was transfected into human T98G cells following the procedure presented in Subheading 3.2 and incubated for 20 h. The expression of P56 and GAPDH was measured by real-time RT-PCR using a standard curve for each target gene. P56 expression was normalized to GAPDH levels for each sample, and the values were further reported to the average P56 expression of the Mock (Lipofectamine 2000 only) condition. The data is from one experiment, which is representative of three independent experiments, in biological triplicate. The error bars represent the SEM. While the siGFP27+0 blunt siRNA is a very strong inducer of P56, its variant siGFP27+2 and the 19 + 2 control siRNA (siControl) appear not to affect the RIG-I pathway

into a 96-well Multiplate and add 1 μL of cDNA. Seal the plate with optical tape, centrifuge briefly at 300×*g* to pellet the reaction mix, and run the PCR cycle (using Tm of 58°C) – 2 min at 50°C, 10 min at 95°C, 40 cycles of: 95°C 15 s, 58°C 15 s, 60°C 45 s (Acquire). Perform the melting curve analysis cycle following the manufacturer's guidelines.

4. Notes

1. The RAW cells can be cultured on surface-treated plasticware – enhancing adherence – or in nontreated flasks/dishes. If using surface-treated plasticware, collect the cells with TryplE-Express for 5 min at 37°C. If using RAW cells on surface-treated plastics, keep the passage number of the cells under 15 from the time they are defrosted to avoid differentiation.
2. As a guide, 18 mL of blood will provide enough PBMCs to plate 60 wells of a 96-well plate – however, there are important variations among blood donors.
3. The number of cells plated is not critical for the assay, although the more cells the higher the cytokine levels produced. The cell confluency should be greater than 50% – however, even 30–40% cell confluency will give good cytokine production.
4. Positive and negative controls should be included for each experiment. CL75 (1 μg/mL) is a strong activator of mouse TLR7 and human TLR8, and therefore conveniently suits both assays (12). CL75 TNF-α induction levels should be at the higher end of the standard curve (and possibly above the linear range of the standard curve), i.e., ~1,000–2,000 pg/mL. A Mock control, with DOTAP and 11.2 μL of duplex buffer only, together with a Medium-only (50 μL of pure RPMI per well) control should be used. The concentration of TNF-α, obtained for both Mock and Medium controls, gives an idea of the baseline production of TNF-α by the cells. While it should be relatively low for the assay to be relevant, in most cases it averages between 0 and 50 ng/mL.
5. The reaction should be stopped when a blue coloration for each standard of the standard curve is visible or when the intensity of the blue coloration of the samples is more intense than the 1,000 ng/mL control of the standard curve. Importantly, if saturation is reached for some standards, they should be discarded as they will not be within the linear range of the enzymatic reaction.

6. When an siRNA sequence induction of TNF-α is significantly higher than the baseline level over a minimum of two independent experiments in duplicate, it can be concluded that it is immunostimulatory through both mouse and human TLR7 if RAW cells are used, and through hTLR8 only or both hTLR7 and hTLR8 together if human PBMCs are used (see Fig. 1). However, it should be noted that the concentration of siRNAs used here, even if very high, might not be sufficient to activate TLR7 and 8 in vitro. It is possible that a sequence that does not induce any significant TNF-α production in either assay will still promote a low immunostimulation in vivo. Ultimately, this should be assessed in vivo by measuring cytokine production in the blood of the animal treated.
7. The assay should always include one positive control (such as the blunt siRNA siGFP27+0) and one negative control (such as siGFP27+2, with 2 nt overhangs and no monophosphate), in addition to the treated samples. An alternative positive control is to use an in vitro synthesized single-stranded RNA. Of note, it is preferable to use synthetic RNAs from the same source (such as Integrated DNA Technology).

Acknowledgments

This work was supported by NIH grant P01 CA062220 and NHMRC grant 491106.

References

1. Gantier, M. P., and Williams, B. R. (2007) The response of mammalian cells to double-stranded RNA. *Cytokine Growth Factor Rev.* **18**, 363–371.
2. Marques, J. T., and Williams, B. R. G. (2005) Activation of the mammalian immune system by siRNAs. *Nat. Biotechnol.* **23**, 1399–1405.
3. Kleinman, M. E., Yamada, K., Takeda, A., Chandrasekaran, V., Nozaki, M., Baffi, J. Z., et al. (2008) Sequence- and target-independent angiogenesis suppression by siRNA via TLR3. *Nature* **452**, 591–597.
4. Hornung, V., Biller, M. G., Bourquin, C., Ablasser, A., Schlee, M., Uematsu, S., et al. (2005) Sequence-specific potent induction of IFN-alpha by short interfering RNA in plasmacytoid dendritic cells through TLR7. *Nat. Med.* **11**, 263–270.
5. Judge, A. D., Sood, V., Shaw, J. R., Fang, D., McClintock, K., and MacLachlan, I. (2005) Sequence-dependent stimulation of the mammalian innate immune response by synthetic siRNA. *Nat. Biotechnol.* **23**, 457–462.
6. Sioud, M. (2006) Single-stranded small interfering RNA are more immunostimulatory than their double-stranded counterparts: A central role for 2′-hydroxyl uridines in immune responses. *Eur. J. Immunol.* **36**, 1222–1230.
7. Diebold, S. S., Massacrier, C., Akira, S., Paturel, C., Morel, Y., and Sousa, C. R. (2006) Nucleic acid agonists for Toll-like receptor 7 are defined by the presence of uridine ribonucleotides. *Eur. J. Immunol.* **36**, 3256–3267.
8. Marques, J. T., Devosse, T., Wang, D., Daryoush, M. Z., Serbinowski, P., Hartmann, R., et al. (2006) A structural basis for discriminating between self and

nonself double-stranded RNAs in mammalian cells. *Nat. Biotechnol.* **24**, 559–565.

9. Kim, D. H., Longo, M., Han, Y., Lundberg, P., Cantin, E., and Rossi, J. J. (2004) Interferon induction by siRNAs and ssRNAs synthesized by phage polymerase. *Nat. Biotechnol.* **22**, 321–325.
10. Hornung, V., Ellegast, J., Kim, S., Brzozka, K., Jung, A., Kato, H., et al. (2006) 5′-Triphosphate RNA is the ligand for RIG-I. *Science* **314**, 994–997.
11. Takahasi, K., Yoneyama, M., Nishihori, T., Hirai, R., Kumeta, H., Narita, R., et al. (2008) Nonself RNA-sensing mechanism of RIG-I helicase and activation of antiviral immune responses. *Mol. Cell* **29**, 428–440.
12. Gantier, M. P., Tong, S., Behlke, M. A., Xu, D., Phipps, S., Foster, P. S., and Williams, B. R. (2008) TLR7 is involved in sequence-specific sensing of single-stranded RNAs in human macrophages. *J. Immunol.* **180**, 2117–2124.
13. Zamanian-Daryoush, M., Marques, J. T., Gantier, M. P., Behlke, M. A., John, M., Rayman, P., Finke, J., and Williams, B. R. (2008) Determinants of cytokine induction by small interfering RNA in human peripheral blood mononuclear cells. *J. Interferon Cytokine Res.* **28**, 221–233.
14. Poeck, H., Besch, R., Maihoefer, C., Renn, M., Tormo, D., Morskaya, S. S., et al. (2008) 5′-Triphosphate-siRNA: turning gene silencing and Rig-I activation against melanoma. *Nat. Med.* **14**, 1256–1263.
15. Heil, F., Hemmi, H., Hochrein, H., Ampenberger, F., Kirschning, C., Akira, S., et al. (2004) Species-specific recognition of single-stranded RNA via toll-like receptor 7 and 8. *Science* **303**, 1526–1529.
16. Forsbach, A., Nemorin, J. G., Montino, C., Muller, C., Samulowitz, U., Vicari, A. P., et al. (2008) Identification of RNA sequence motifs stimulating sequence-specific TLR8-dependent immune responses. *J. Immunol.* **180**, 3729–3738.
17. Pichlmair, A., Schulz, O., Tan, C. P., Naslund, T. I., Liljestrom, P., Weber, F., and Reis e Sousa, C. (2006) RIG-I-mediated antiviral responses to single-stranded RNA bearing 5′-phosphates. *Science* **314**, 997–1001.

Chapter 3

Current Knowledge of MicroRNAs and Noncoding RNAs in Virus-Infected Cells

Dominique L. Ouellet and Patrick Provost

Abstract

Within the past few years, microRNAs (miRNAs) and other noncoding RNAs (ncRNAs) have emerged as elements with critically high importance in posttranscriptional control of cellular and, more recently, viral processes. Endogenously produced by a component of the miRNA-guided RNA silencing machinery known as Dicer, miRNAs are known to control messenger RNA (mRNA) translation through recognition of specific binding sites usually located in their 3′ untranslated region. Recent evidences indicate that the host miRNA pathway may represent an adapted antiviral defense mechanism that can act either by direct miRNA-mediated modulation of viral gene expression or through recognition and inactivation of structured viral RNA species by the protein components of the RNA silencing machinery such as Dicer. This latter process, however, is a double-edge sword, as it may yield viral miRNAs exerting gene regulatory properties on both host and viral mRNAs. Our knowledge of the interaction between viruses and host RNA silencing machineries, and how this influences the course of infection, is becoming increasingly complex. This chapter aims to summarize our current knowledge about viral miRNAs/ncRNAs and their targets, as well as cellular miRNAs that are modulated by viruses upon infection.

Key words: Virus, MicroRNA, Noncoding RNA, RNA interference, Posttranscriptional regulation

1. Introduction

1.1. Description of MicroRNAs

Over the past few years, microRNAs (miRNAs) have established themselves as important posttranscriptional regulators of gene expression. These short ~21 to 24-nucleotides (nt) noncoding RNA (ncRNA) species are expressed in most eukaryotes and by several viruses. They are known to mediate their action through imperfect base-pairing with their target RNA, mainly with the 3′ untranslated region (3′UTR) of messenger RNA (mRNA), to repress translation, thereby inhibiting protein expression. MiRNAs can also bind to mRNA through perfect complementarity to induce

Wei-Ping Min and Thomas Ichim (eds.), *RNA Interference*, Methods in Molecular Biology, vol. 623,
DOI 10.1007/978-1-60761-588-0_3,

cleavage of the mRNA (1, 2). A recent study has reported that miRNAs could also enhance protein expression during the cell cycle (3); this aspect remains under active investigation. According to the latest release of miRBase (release 14,0, September 2009), the repository of miRNA data on the web, over 721 different miRNAs have been identified in humans as well as more than 175 miRNAs originating from mammalian viruses (4, 5). The number of deposited miRNA sequences continues to increase quasi-exponentially since the creation of miRBase in 2004, suggesting that the number of miRNAs may be estimated to reach thousands. Moreover, this repository does not include a panoply of recently discovered, small ncRNAs found in living organisms and forming additional classes of gene regulatory RNAs distinct from miRNAs such as the repeat-associated small interfering RNAs (rasiRNAs) (6), the tiny noncoding RNAs (tncRNAs) (7), and the Piwi-interacting RNAs (piRNAs) (6). Some ncRNAs produced by viruses are hundreds to thousands of nucleotides in length and represent potential regulators of gene expression (8–12).

1.2. MicroRNA Biogenesis and Function

As illustrated in Fig. 1, miRNA genes are transcribed in the nucleus mainly by RNA polymerase (pol) II into stem-loop structured primary miRNAs (pri-miRNAs). Harboring a 5′ m7G cap and a 3′ poly(A) tail (13, 14), these pri-miRNAs are then trimmed into ~60 to 70-nt miRNA precursors (pre-miRNAs) by the nuclear ribonuclease (RNase) III Drosha (15), acting in concert with the DiGeorge syndrome critical region 8 (DGCR8) protein within the microprocessor complex (16–19). A noncanonical generation of pre-miRNAs, in which certain debranched small introns mimic the structural features of pre-miRNAs to enter the miRNA-processing pathway without Drosha-mediated cleavage, named “mirtrons”, has been described initially in *Drosophila* (20), but are also present in mammals (21). To date, no viral “mirtrons” have been reported. The canonical and noncanonical pre-miRNAs are subsequently exported to the cytoplasm via Exportin-5 (22–25), and the base of their stem is recognized by the PAZ domain of Dicer (26). Acting as an intramolecular dimer, Dicer RNase IIIa and IIIb domains cleave the stem at the base of the loop to generate a miRNA:miRNA* duplex (26–29). The transactivating response RNA-binding protein (TRBP) (30) has been shown to operate with Dicer within a pre-miRNA processing complex (31, 32), although their precise mechanistic interaction remains elusive. Following a strand selection and separation step, which is based on the thermodynamic stability of the RNA duplex (33), the miRNA strand (~21 to 24-nt) with the least stable 5′ end pairing (called the guide strand) is incorporated into effector miRNA-containing ribonucleoprotein (miRNP) complexes containing Argonaute 2 (Ago2), TRBP and Dicer (32), guiding them toward specific messenger RNAs (mRNAs).

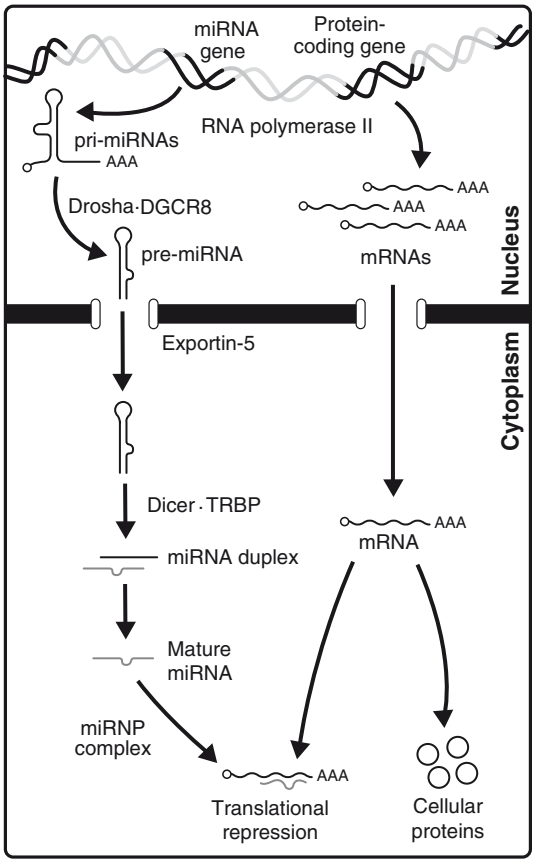

Fig. 1. Schematic representation of the miRNA-guided RNA silencing pathway in mammalian cells. miRNA genes are transcribed mainly by RNA polymerase II into primary miRNAs (pri-miRNAs). These RNA species are then trimmed into miRNA precursors (pre-miRNAs) in the nucleus by the microprocessor complex, which is composed of the ribonuclease Drosha and its cofactor DGCR8. Pre-miRNAs are then exported by Exportin-5 to the cytoplasm, where they are cleaved by the pre-miRNA processing complex formed of Dicer and TRBP, to generate miRNA:miRNA* duplexes. Following a strand selection and separation step, the mature miRNA is incorporated into an Ago2-containing miRNA ribonucleoprotein complex (miRNP) (or effector complex) to mediate recognition and translational repression of specific cellular mRNAs

The opposite miRNA* strand (also called passenger strand) is encountered much less frequently and is presumably degraded (34). miRNA assembly on specific mRNA sequences may be facilitated by the fragile X mental retardation protein, which can accept and use miRNAs derived from Dicer (35). The targeted mRNA will be primarily subjected to translational repression, although mRNAs containing partial miRNA complementary sites may also be targeted for degradation in vivo (36). These regulatory events may occur at specific cytoplasmic foci referred to as processing bodies (P-bodies) (37, 38) or GW182-containing bodies (GW-bodies) (39), which are formed as a consequence of

the presence of miRNAs (40). P-bodies are enriched in proteins involved in RNA-mediated gene silencing such as Ago2 (37), mRNA degradation (41), and nonsense-mediated mRNA decay (42, 43).

Cellular miRNAs have been shown to control various processes such as cell proliferation, apoptosis and hematopoietic cell differentiation (44). As for viral miRNAs, which is the subject of this chapter, they can regulate expression of viral as well as host proteins by directing repression or cleavage of mRNA transcripts, thereby inhibiting key cellular processes involved in the response to viral infection. At the molecular level, recognition of mRNAs by miRNAs is based mainly on imperfect sequence complementarity and the identification of their physiological mRNA targets remains difficult to predict and is rather arduous. Characterization of a few experimentally validated miRNA:mRNA interactions (45), however, is allowed to establish a context in which this interaction is favored. The critical miRNA:mRNA pairing region, referred to as the "miRNA seed", involves nt 2–8 of the miRNA in the 5′ to 3′ orientation. Because a miRNA can affect a large number of mRNAs, bioinformatic approaches are used in combination with large-scale micro-array-based analyses of regulated mRNAs and/or proteomic analyses of differentially expressed proteins in order to validate miRNA-regulated mRNAs. Whether they originate from the host-infected cells or the viruses themselves, it has become a priority to improve our understanding of the mechanisms by which miRNAs or other ncRNAs mediate their action, to identify the mRNA targets they regulate, and to determine how they can modulate the host response to viral infection and the intrinsic replication of the virus. This chapter will present and discuss some examples in which miRNAs and ncRNAs can act as key regulators of cellular and viral gene expression in virus-infected cells.

1.3. Techniques for miRNA/ncRNA Detection

Over the last several years, many different techniques have been used to predict and identify miRNAs derived from viruses and their host cells. As part of the effort to better understand the interaction between miRNAs and their targets, computational algorithms have been developed, based on well-defined rules for various molecular features. These *in silico* approaches provide important tools for miRNA target detection and, together with more elaborate experimental validation strategies, help reveal mRNA targets that are functionally regulated by miRNAs.

Standard Northern blot hybridization, which may be adapted for specific applications, is the most commonly used technique to detect miRNAs and other small ncRNAs, as described recently (46, 47). A method of choice to visualize specific miRNAs under various conditions, Northern blotting requires the design and synthesis of many sequence-specific, complementary DNA probes, which hampers its use in large-scale miRNA detection strategies.

RNase protection assay (RPA) is another indirect technique used to detect unique miRNAs in aqueous solutions. This approach consists in the annealing of our RNA species of interest with a complementary, radiolabeled RNA probe in a test tube, followed by RNAse A/T1 digestion of single-stranded RNA species. Protected upon annealing of the RNA species of interest, the radiolabeled probe is then revealed by denaturing PAGE and autoradiography. Although both methodologies demand that the sequence of the RNA species of interest to be known, which makes them unsuitable for discovering miRNAs of unknown sequences, RPA requires lower amounts of RNA than Northern blot hybridization. Furthermore, whereas both techniques allow discrimination between pre-miRNA and mature miRNA species, RPA may represent a suitable and more sensitive detection method than Northern blot hybridization for miRNAs that are expressed at very low levels such as those originating from the human immunodeficiency virus type 1 (HIV-1) transactivating responsive (TAR) element (48).

As for the sequence determination of miRNAs of low abundance, primer extension may prove to be more useful and informative than miRNA cloning strategies. It consists in the reverse transcriptase (RT)-driven elongation of a DNA probe designed to be complementary to the 3′ end of the miRNA. Visualized by denaturing PAGE and autoradiography, the length of the elongated product determines the 5′ end of the miRNA under study.

In situ detection approaches of miRNA expression also offers several advantages. Using paraffin-embedded and formalin-fixed tissues, this method may provide access to large repositories of archived biological materials, thereby allowing retrospective studies to be conducted. The Plasterk laboratory, among others, has performed a lot of work in animal embryos by using Locked Nucleic Acid™ (LNA)-modified oligonucleotide probes that contain nucleic acid analogues in which the ribose ring is locked by a methylene bridge connecting the 2′-O atom with the 4′-C atom. This molecular conformation allows higher sensitivity and thermal stability. Specific in situ detection of miRNA is also applicable to whole mounts, thin sections, single cells, and frozen samples. LNA™ probes can also find applications in Northern blot hybridization. As for colorimetric assays using digoxigenin-labeled or biotin-labeled probes, or fluorescence microscopy using fluorescein-labeled probes, it may help visualize the expression profile of specific miRNAs.

The detection and identification of miRNAs and ncRNAs, which may be used as biomarkers, may be clinically relevant and provide critical information for diagnostic purposes. Significant progresses have been made in that area with the development of quantitative bioanalytical methods for the rapid and multiplexed detection of all miRNAs present in a particular cell or tissue sample.

Common research laboratory techniques, such as reverse transcription and real-time polymerase chain reaction (RT-PCR), are now being used in combination with microarrays for the identification of pri-miRNAs, pre-miRNAs, and mature forms of miRNAs. These techniques, however, often require several cloning steps as well as the need for expensive devices and pieces of equipment to compute and analyze data. High throughput, deep sequencing technologies have been developed recently and have been shown to deliver several orders of magnitude more sequences than is possible with the traditional Sanger method. This advanced technology has already been used to identify conserved and nonconserved miRNAs. Concomitantly, new algorithms have been developed in order to analyze and make sense of the huge amounts of sequencing data that can be generated. Such a bioinformatic tool, miRDeep, uses a probabilistic model of miRNA biogenesis to score compatibility of the position and frequency of sequenced RNA with the predicted secondary structure of the miRNA precursor (49). Sequences obtained by deep sequencing are aligned to the genome and miRDeep computes their secondary RNA structure. Potential pre-miRNA sequences are then identified and, according to miRDeep algorithm, scored for their likelihood to represent real pre-miRNAs. The output is a list of known and putative pre-miRNAs and mature miRNAs, as well as the probabilities of being false positives.

The increasing importance of endogenous miRNAs and ncRNAs in health and diseases, as well as their potential clinical use, will further encourage the improvement of current methods and stimulate the development of new technologies and strategies that will enhance the chances of successful knowledge transfer from the laboratory to the bedside of patients.

2. Viral miRNAs and ncRNAs in Viral-Infected Cells

2.1. Herpesviridae

The family of Herpesviridae is represented by three virus subgroups (alpha, beta, and gamma) that contain large double-stranded DNA (dsDNA) genomes as long as ~125– 230 kilobases (kb) (50). Typically, herpes viruses cause lytic infections or generate latent infections where only a few specialized viral genes are used by the virus to establish lifelong persistence in the human host. Some herpes viruses have been found to express miRNAs (51, 52). For instance, a mouse herpesvirus, known as mouse cytomegalovirus (mCMV), contains more than 18 validated miRNAs, all of which are related to the lytic phase of infection

Table 1
MicroRNAs and noncoding RNAs expressed by human viruses

Virus family	Virus name	miRNAs/ncRNAs Predicted	Validated	Identification of validated miRNAs/ncRNAs	References
Herpesvirus	Herpes simplex virus type 1 (HSV-1, HHV-1)	(mi) 24	(mi) 8	hsv-miR-H1, miR-H2-3p, miR-H4-3p, miR-H2-5p, miR-H3 , miR-H5, miR-H6, miR-I	(51, 52, 61, 64)
		0	(nc) 2	~38 and ~110 nt from the LAT transcript	(55)
	Herpes simplex virus type 2 (HSV-2, HHV-2)	(mi) 10	0	–	(51, 55)
	Varicella zoster virus (VZV, HHV-3)	0	0	–	–
	Epstein–Barr virus (EBV, HHV-4)	(mi) 7	(mi) 23	miR-BHRF1-1 to BHRF1-3, miR-BART-1 to miR-BART-20	(51, 52, 66) (70, 73)
			(nc) 2	EBER1, EBER2	(8, 125, 126)
	Human cytomegalovirus (HCMV, HHV-5)	(mi) 11	(mi) 11	miR-UL22A, miR-UL36, mir-UL70, miR-UL112, miR-UL148D, miR-US4, miR-US5-1,miR-US5-2, miR-US25-1, miR-US25-2, miR-US33	(50, 80, 81)
			(nc) 1	β2.7	(127)
	Roseolo virus (HHV-6)	0	0	–	–
	HHV-7	0	0	–	–
	Kaposi's sarcoma-associated herpesvirus (KSHV, HHV-8)	(mi) 8	(mi) 12	miR-K12-1 to miR-K12-12	(51, 66, 91, 92)
Poliomavirus	Simian virus 40 (SV40)	(mi) 1	(mi) 2	sv40-miR-S1-5p, sv40-miR-S1-3p	(51,101)
	Simian virus 12 (SV12)	ND	(mi) 2	unnamed	(102)
	Jamestown Canyon virus (JCK)	(mi) 1	(mi) 2	unnamed	(103)
	BKV	(mi) 1	(mi) 2	unnamed	(103)
Adenovirus	Adenovirus type 2 and 5	0	(nc) 2	VAI, VAII	(12, 104)
		(mi) 1	(mi) 3	mivaRI-137, mivaRI-138 (or 3'svaRNA), mivaRII-138	(47, 104–107)

(continued)

Table 1 (continued)

Virus family	Virus name	miRNAs/ncRNAs Predicted	Validated	Identification of validated miRNAs/ncRNAs	References
Retrovirus	Human immunodeficiency virus type 1	0	(mi) 3	miR-N367, miR-TAR-5p, miR-TAR-3p	(48, 113, 116)
	Human immunodeficiency virus type 2	(mi) 2	0	–	(118)
	HTLV-1	0	0	–	(119)

(53, 54). In this section, we will discuss and provide more details about miRNAs generated by herpes viruses as well as their potential gene targets in infected human cells.

2.1.1. Herpes Simplex Virus 1 (HSV-1) and 2 (HSV-2)

The first group to study and report the computational predictions and identification of miRNAs derived from viruses was led by Thomas Tuschl (51, 52). Using mainly miRNA cloning strategies as their experimental miRNA discovery tool, they were unable either to validate some of their predictions or to confirm the existence of some viral miRNAs discovered later by other groups using means other than miRNA cloning.

For example, Cui et al. (55) have predicted the existence of 13 pre-miRNAs and 24 mature miRNA candidates from 11 genomic loci in HSV-1 (or human herpesvirus type 1, HHV-1), 30% of which are predicted to be conserved in HSV-2 (or human herpesvirus type 2, HHV-2). The authors used Northern blot hybridization to validate the first miRNA in HSV-1, which is encoded upstream of the transcription start site of the latency-associated transcript (LAT); this miRNA was named hsv1-miR-H1. LAT is an ~8.3 kb capped and polyadenylated RNA transcript, not coding for a protein, which is spliced to give a ~2.0 kb stable intron and an unstable exonic RNA of ~6.3 kb (56). Additional small ncRNA species of ~38 and ~110 nt were also identified, although whether they play a role in HSV-1 biology remains unclear.

Although its role and importance in HSV-1 biology remains elusive, hsv1-miR-H1 is expected to act upon and regulate cellular and viral RNA transcripts. Among the predicted pre-miRNAs that could derive from HSV-1, two of them may target U_L15, $U_L15.5$ and the intron-containing *HSV-1 infected-cell protein 0 (ICP0)* transcripts. The latter transcript encodes for an immediate-early

polypeptide with transcriptional activation properties found to exert antiproliferative action in infected cells (57) and to favor viral RNA transcription (58). While hsv1-miR-HI targets remain under investigation, two independent groups recently published the identification of novel miRNA candidates and their putative targets for HSV-1 and HSV-2 (Table 2). Umbach et al. (59) used the 454 sequencing technology to analyze 293T cells transfected with a LAT-expressing plasmid as well as the trigeminal ganglia of mice latently infected with HSV-1. They were able to obtain more than 200,000 sequence reads, of which more than half represented cellular miRNAs. The authors found 651 HSV-1-derived miRNAs in 293T cells and more than 815 HSV-1 miRNAs in mouse trigeminal ganglia. Six mature miRNA candidates were identified in both cell types: miR-H2-3p (359 reads), miR-H4-3p (266 reads), miR-H2-5p (10 reads), miR-H4-5p (61 reads), miR-H3 (23 reads), miR-H5 (41 reads). Three of these miRNAs had been computationally predicted (51, 55), whereas four derived from exon 2 of the spliced ~6.3 kb *LAT* transcript, which may explain its characteristic instability and provide a rationale for

Table 2
The viral and cellular messenger RNA targets of viral microRNAs

Viral miRNA	Target	Targeted mRNA	References
HSV-1 miR-H1	Viral mRNA	HSV-1 ICP0	(55)
HSV-1 miR-H2-3p		HSV-1 ICP0	(59)
HSV-1 miR-H6		HSV-1 ICP4	(59)
HSV-1 miR-I		HSV-1 ICP34.5	(62)
EBV miR-BART-2		EBV BALF5	(52)
EBV miR-BART-1-5p, miR-BART-16, miR-BART-17-5p		EBV LMP1	(73)
HCMV miR-UL112-1		HCMV IE72/IE1	(82, 83)
SV40 sv40-miR-S1-5p, sv40-miR-S1-3p		SV40 T-antigen	(101)
HIV-1 miR-N367[a]		HIV-1 Nef	(114)
HIV-1 TAR miRNA		HIV-1 LTR	(116)
EBV miR-BART-5	Cellular mRNA	PUMA	(76)
EBV BHRF1-3		CXCL11/I-TAC	(77)
HCMV miR-UL112-1		MICB	(84)
KSHV miR-K12–1, miR-K12-3-3p, miR-K12-6-3p and miR-K12–11		Thrombospondin 1	(93)
KSHV miR-K12-11		BACH-1	(97, 98)

[a] Please note that, according to the miRBase registry, this sequence should be considered at risk of deletion from future releases

the existence of spliced *LAT* transcript, according to Umbach et al. (59). These authors also described that miR-H2-3p and miR-H6 may target *ICP0* and *ICP4*, respectively, which are two transcription factors implicated in HSV-1 replication. If ICP0 and ICP4 proteins can promote exit from latency (60), the regulation of their mRNAs by HSV-1 miRNAs could contribute to maintaining the latent state of herpes viral infections.

The existence of viral miRNAs suggests that they may play an important role in viral pathogenesis. For instance, it has been known for some time that the herpesvirus ICP34.5 protein promotes replication of the virus in neuronal cells in vivo (61). Tang et al. (62) recently found a miRNA derived from HSV-1, namely miR-I, which has been shown to reduce the protein expression level of ICP34.5 in transfected or HSV-1-infected cells. These results prompted the authors to hypothesize that the control of ICP34.5 expression in individual infected neurons by these LAT-encoded miRNAs may affect the outcome of viral infection, i.e., productive infection versus latency, leading either to viral spreading to other neurons or establishment of latency, respectively.

2.1.2. Epstein–Barr Virus (EBV)

Epstein–Barr virus (EBV), or human herpesvirus type 4 (HHV-4), is a gammaherpesvirus, which is maintained in the nucleus of the infected cell as an extrachromosomal circular episome. Found to be widespread in all human populations, EBV is known to persist in the vast majority of individuals as a lifelong, asymptomatic infection of the B-lymphocyte pool (63, 64). In fact, EBV has the capacity to immortalize B cells in culture. This virus has been identified as the causative agent of infectious mononucleosis, Hodgkin's lymphoma (HL), Burkitt's lymphoma (BL), and nasopharyngeal carcinoma (NPC) (65). A study of Pfeffer et al. (52) reported the cloning of miRNAs from BL cell lines infected with EBV B95-8 strain, where 4% of the total miRNA content obtained by cloning originated from the EBV genome. They found five miRNAs originating from two different clusters, i.e., either located within the *BHRF1* (Bam HI fragment H rightward open readingframe 1) gene or in the intronic regions of the *BART* (Bam HI-A region rightward transcript) gene. The existence of miRNAs derived from these clusters in EB has been confirmed by an independent group (66). It is now known that EBV miRNAs originate from three clusters; two of the three clusters of miRNAs are made from the BART gene, a set of alternatively spliced transcripts that are highly abundant in NPC, but have not been shown to produce detectable levels of proteins (67). Therefore, whereas three pre-miRNAs are encoded in the BHRF cluster, more than 20 pre-miRNAs are found within the introns of the BART transcript.

The life cycle of EBV, as with other herpesvirus, is biphasic. Upon primary infection, EBV replication is associated with the expression of more than 50 viral proteins that helps the virus establish a latent infection in these cells (68). EBV infection is characterized by three different stages of latency (I, II, and III), which are each associated with the expression of various subsets of latent genes. Latency I, which is related to BL, is characterized by the expression of latency-associated membrane protein 2a (LMP2A) and EBV-associated nuclear antigen 1 (EBNA1), which is responsible for EBV viral replication. Some lytic events may occur in latency I. Latency II is an intermediate state and is followed by latency III, where all 12 latency genes are expressed, including six nuclear proteins (EBNA-1–6), three membrane proteins (LMP-1, LMP-2A and LMP-2B), BART and two small nontranslated RNAs (EBER 1 and 2; see Fig. 2). This stage of infection is observed in B cells transformed in vitro by EBV or in lymphoproliferative disorders arising in the presence of immunosuppression. Latent EBV gene expression may exhibit cell type-specific patterns in cultured cells, as observed following infection of primary resting human B cells (latency III, the growth program) or in cell lines derived from EBV-associated cancers (latency I or II) (68, 69).

The expression pattern of the various EBV miRNAs appears to be fairly complex and depends on both the cell type and on the overall expression pattern of the EBV genes (8). For example, the BART miRNA cluster is well expressed during the lytic process and in cells lines derived from NPC, whereas it is less abundant in B cells transformed in vitro or derived from BL (70). On the other hand, the BHRF cluster is expressed in BL cells, but not detected in NPC cell lines (70, 71). Thus, expression of EBV miRNAs at different stages of infection may underlie their specific role and importance in viral pathogenesis progression.

Several reports have described cellular and viral targets for EBV miRNAs. One of the first targets to be reported was for miR-BART-2 (Table 2). This miRNA was found to target, through perfect complementary, the 3′UTR of the viral polymerase BALF5 mRNA, which is transcribed antisense to miR-BART-2 (52). Evidence for this regulation came from the following observation made after induction of the lytic viral replication cycle in the EBV B95.2 cell line: the decrease in BALF5 3′UTR cleavage was concomitant with that of the level of miR-BART-2 (72). Expressed at very low levels in latently infected cells, miR-BART-2 could downregulate the levels of aberrant BALF5 mRNA transcripts in order to prevent viral replication during latency.

Other BART miRNAs were recently shown to target an EBV viral gene. MiR-BART-1-5p, miR-BART-16 and miR-BART-17-5p were shown to downregulate EBV latent membrane protein 1 (LMP1) through recognition of the 3′UTR of its mRNA (Table 2) (73). LMP1 has oncogenic properties and is a signaling protein that acts as an active tumor necrosis factor receptor (TNFR) through its resemblance to CD40, thereby activating a number of

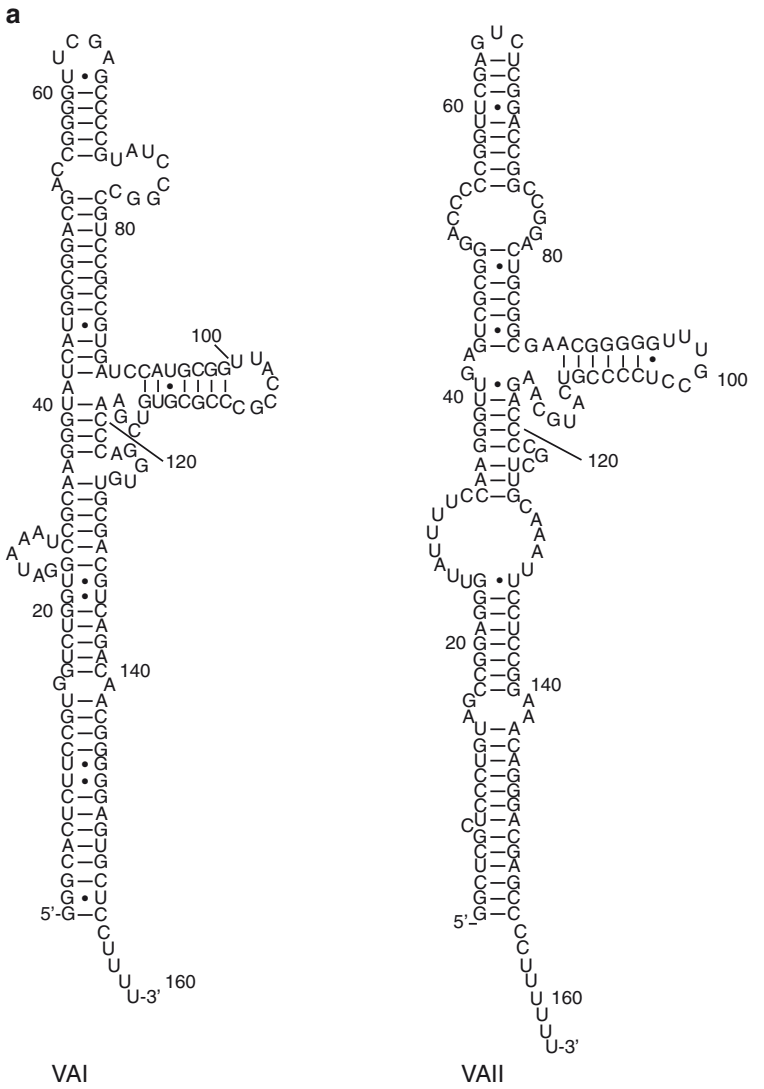

Fig. 2. Representation of noncoding RNAs from Adenovirus and Epstein–Barr virus. (**a**) VAI and VAII RNAs from Adenovirus 5 (Ad5). Adapted from Xu et al. (109)

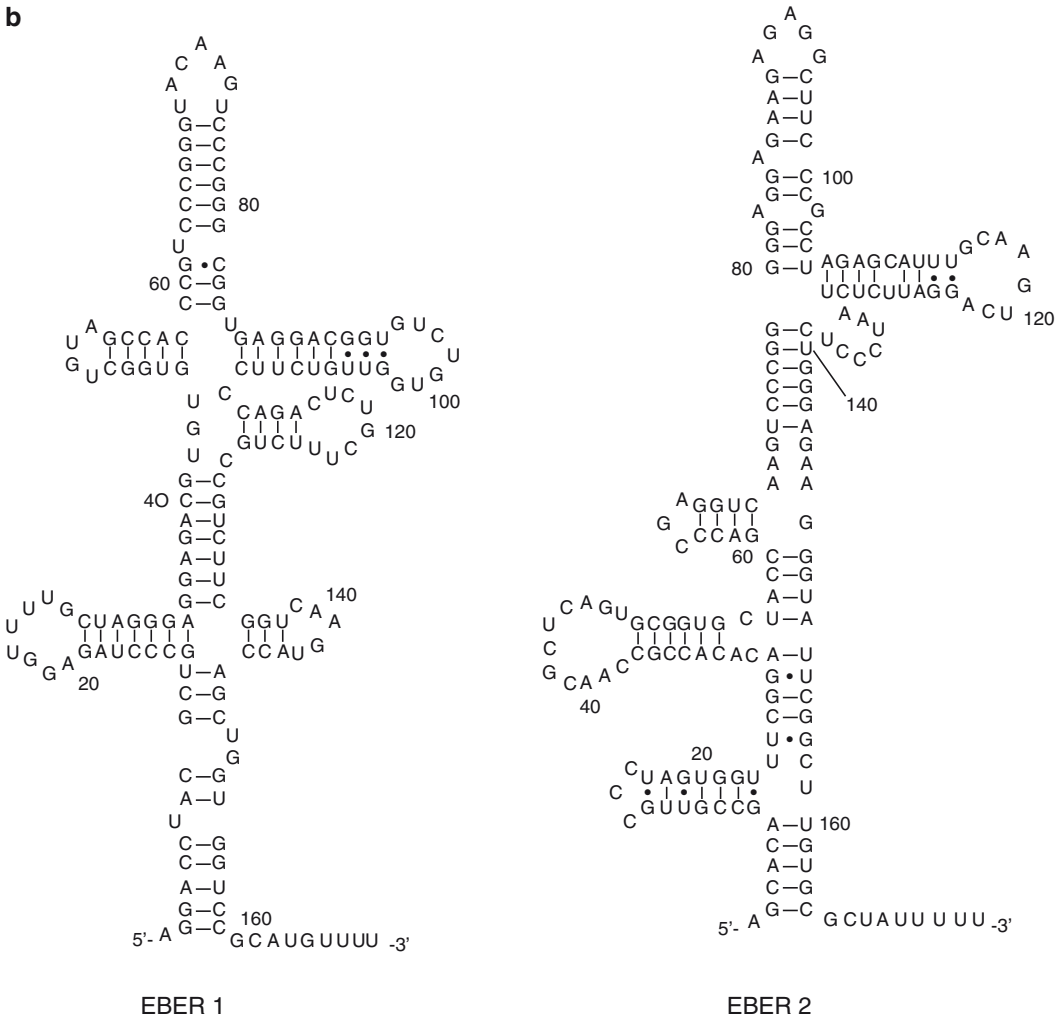

Fig. 2 (continued) (**b**) EBER1 and EBER2 RNAs from Epstein–Barr virus. Adapted from Rosa et al. (123)

signalling pathways in a ligand-independent manner (74, 75). Another BART miRNA was recently described to target the cellular PUMA mRNA, which encodes for a protein known to upregulate p53-mediated apoptosis (Table 2) (76). By targeting PUMA mRNA, miR-BART-5 could render NPC and EBV gastric carcinoma cells less sensitive to proapoptotic agents. In that context, apoptosis could be triggered either by depleting miR-BART-5 levels or by enhancing PUMA expression. These findings support a role for miRNAs in the establishment of latent infection through promotion of host cell survival.

Whereas the BART miRNAs may act mainly during the replicative period of EBV infection, BHRF1 miRNAs are produced in latently infected cells. A cellular target has been validated for one of the three BHRF1 miRNAs that are produced by EBV. The BHRF1-3 miRNA has been found to target, through perfect complementary, the 3′UTR of IFN-inducible T-cell attractive chemokine CXCL11/I-TAC (Table 3.2) (77). Downregulation of CXCL11/I-TAC levels by miR-BHRF1-3 could lead to the immunomodulation of EBV-infected tumor cells by interfering with the IFN-responding pathway. EBV may also interfere with other immune processes of the host cells through the regulation of cellular miRNAs, as discussed in Subheading 3.

Interestingly, the authors also observed high expression levels of miR-BHRF1-3 in latency type III EBV-infected cells and in primary EBV-associated AIDS-related diffuse large B-cell lymphomas (DLBCL) (77). This pattern differs from that of miR-BART-2, which exhibits low expression levels in latency type III EBV-infected cells but high expression, as BHRF1-3, in AIDS-related DLBCL. These observations raise the possibility that EBV miRNA expression may be modulated by HIV-1 or others viruses, and influence the course of EBV infection, which adds to the complexity of co-infection cases.

2.1.3. Human Cytomegalovirus (HCMV)

Human cytomegalovirus (HCMV), or human herpesvirus type 5 (HHV-5), was first identified in 1904 as a betaherpesvirus with high prevalence in human adults (50–80%) and mainly asymptomatic, except for immunocompromised individuals such as very young children, organ transplant recipients, HIV-1-infected persons, and those with leukemia. Far from being harmless, this virus has emerged in recent years as the most important cause of congenital infection in the developed world, commonly leading to mental retardation and developmental disability. In healthy people, however, shedding of the virus can occur intermittently, without any detectable signs or symptoms in the long term. The latent form of the virus may persist in T lymphocytes ($CD8^+$) and some hematopoietic cells (78, 79).

Pfeffer et al. (51) initially predicted the presence of miRNA precursors in the genome of HCMV, of which nine of them have been cloned from small RNA libraries isolated from primary infected human fibroblasts. Additional HCMV miRNAs were subsequently reported (80, 81). To date, miR-UL112-1 is the only HCMV miRNA for which an mRNA target has been identified. In fact, miR-UL112-1 has been proposed to regulate the immediate-early protein IE72/IE1 of HCMV (82, 83) as well as the major histocompatibility complex class I polypeptide-related sequence B, or MICB, of the host (Table 2) (84). HCMV IE72/IE1 is a multifunctional protein involved in many cellular processes including cell cycle regulation, apoptosis, nuclear architecture, and gene

expression (85). The observations that miR-UL112-1 is expressed early and is accumulating during HCMV infection led Grey and colleagues to suggest that the regulation of IE72/IE1 protein at later stages of viral replication may attenuate the acute phase of replication (80, 86). The biological significance of the IE72/IE1 suppression, however, remains unclear. The other target of miR-UL112-1, MICB, has been postulated to help the HCMV-infected cells evade killing by activated natural killer (NK) cells (84). MICB, a stress-induced ligand of the NK cell activating receptor NKG2D, is critical for the NK cell killing of tumor and virus-infected cells (Table 2). Suppression of MICB expression by miR-UL112-1 would prevent recognition by NK cells, a function shared by six other HCMV genes encoding proteins UL16, UL18, UL40, UL83, UL141 and UL142, (87). HCMV UL16 protein, like miR-UL112-1, targets MICB (88) and may further contribute to HCMV persistence in its host cells.

Although it remains unclear as to how miR-UL112-1 may influence HCMV pathogenesis through its regulatory effects on a viral and a cellular target, these findings argue for the persistence of HCMV in infected cells through reduction of the viral load and promotion of immune evasion mechanisms.

2.1.4. Kaposi's Sarcoma-Associated Herpesvirus (KSHV)

This recently known virus, also referred to as human herpesvirus type 8 (HHV-8), is less common among healthy individuals (<2% of the population of developed countries), and is rather unique in that it acquires numerous genes from host cells and incorporates them into its own genome. Some of these genes encode for complement-binding protein, IL-6, Bcl-2, cyclin D, a G protein-coupled receptor, interferon regulatory factor, Fas-ligand inhibitory protein (FLIP) and DNA synthesis proteins, such as dihydrofolate reductase, thymidine kinase, thymidylate synthetase, DNA polymerase, and several others (89). The gammaherpesvirus KSHV-induced skin lesion manifestations were visualized on KSHV- and HIV-1-infected patients who are immunocompromised. Additional symptoms associated with KSHV infection are primary effusion lymphoma (PEL) and Castleman's disease (89), which exhibit KSHV-positive tumors hypersecreting IL-6 in response to viral protein vIL-6 (90).

Reported by Pfeffer and collaborators (51), miRNAs are abundant in the KSHV genome. All ten KSHV miRNA stem-loops identified are located in one short segment in the ~141-kb KSHV genome, and are all oriented in the same direction suggesting that they may all derive from a single pri-miRNA transcript (91). So far, 12 miRNAs derived from the KSHV genome have been identified from four independent teams of investigators (see Table 1) (51, 66, 91, 92).

As other herpes viruses, KSHV latency occurs following primary infection through the expression of latency genes, which are restricted to a few viral genes, most of which are located in, or nearby, the region comprising ORF71 to K12 (Kaposin gene), which encodes more than 10 miRNAs (91). This region of the KSHV genome presents polycistronic latency-associated transcripts encoding the latency-associated nuclear antigen (LANA or open reading frame 73; ORF73), v-cyclin (ORF72), and v-Flip (ORF71). MiRNAs and KSHV-associated latency genes are expressed coordinately in latent cells.

Microarray analysis of cell lines stably expressing the KSHV miRNA cluster revealed decreasing levels of several mRNAs, all of which may represent potential cellular targets of KSHV miRNA (93). Using luciferase derepression assays involving cotransfection of 3′UTR-coupled reporter genes and specific 2′OMe antisense RNAs, Samols et al. (93) found that the 2,095 bp-long thrombospondin 1 (THBS1) mRNA 3′UTR is targeted by multiple KSHV miRNAs, in particular miR-K12–1, miR-K12-3-3p, miR-K12-6-3p, and miR-K12–11 (Table 2). This cellular protein (which possesses antiproliferative, angiogenic, and immunostimulatory functions) has been reported to be downregulated in several types of cancer, including Kaposi sarcoma (KS) (94–96). Cellular proteins exerting a role similar to THBS1 in proliferation, immune modulation, angiogenesis and apoptosis, such as osteopontin (SPP1), the S100 calcium-binding protein A2 (S100A2), the plasticity-related gene 1 (SRGN or PRG1), and the integral membrane protein 2A (ITM2A), are all downregulated by >4 fold upon expression of the KSHV miRNA cluster. Again, these findings are supportive of a viral miRNA-based escape mechanism from the immune system for KSHV in KS.

Interestingly, miR-K12-11 derived from KSHV contains a seed sequence identical to the oncogenic cellular miR-155, as reported recently (97, 98). In fact, these two independent groups described the downregulation of 20 and 14 cellular genes by both miRK12-11 and miR-155, respectively. A single gene, however, was identified by both teams: BACH-1 (Tables 2 and 3). This gene is known to encode a transcription factor that negatively regulates transcription of some stress-responding factors in cells (99). Among the other genes identified in these studies are members of cell signaling pathways, cell division, apoptosis, T-cell activation as well as transcription factors. The discrepancies between these studies may be explained by the differences in the cell types and models that were used. Skalsky et al. (98) used PEL-derived cell lines (BC-1, JSC-1, VG-1, BCBL-1, and BCB-1) and overexpression of miR-K12-11 and miR-155 in Hek 293 cells, whereas Gottwein et al. (97) expressed physiological levels of miR-K12-11 and miR-155 from lentivirus in BJAB cells.

Table 3
The viral and messenger RNA targets of cellular microRNAs upon viral infection

Cellular miRNA	Target	Targeted mRNA	References
hsa-miR-122	Viral mRNA	HCV 5'UTR (upon HCV infection)	(131)
hsa-miR-196, miR-296, miR-351, miR-431, miR-448		HCV genome (upon IFN response)	(139)
hsa-miR-155 (KSHV miR-K12-11 ortholog)	Cellular mRNA	BACH-1 (upon KSHV infection)	(97, 98)
hsa-miR-17-5p and miR-20		PCAF (upon HIV-1 infection)	(134)
hsa-miR-128		SNAP25 (upon HIV-1 infection)	(138)

2.1.5. Other Herpes Viruses

To date, no miRNAs have been either predicted or identified for the alphaherpesvirus Varicella zoster or for the human herpesvirus type 3 (HHV-3) (51), which is the causative agent of chickenpox and zona, in which symptoms take the form of red papules in the body of the infected host. The same applies for Roseolovirus, or human herpesvirus type 6 (HHV-6), as well as HHV-7, which is genetically closely related to HHV-6. In contrast to previously described herpes viruses, the calculated probability to find an miRNA within their genomes is inferior to 50% in HHV-3 and HHV-7. The probability that HHV-6 encodes for an miRNA is high at 84%, although no miRNA has been identified yet. Possibly expressed at very low levels, miRNAs derived from HHV-6 may have escaped detection so far.

2.2. Other DNA Viruses (Polyomaviruses and Adenoviruses)

Several DNA viruses, in contrast to herpes viruses, contain small genomes of a few thousands bp that encode a small number of proteins. Three polyomavirus have been isolated in humans: Jamestown Canyon virus (JCV), BK virus (BKV), and the simian virus 40 (SV40). Both JCV and BKV can infect humans and cause serious diseases, such as progressive multifocal leukoencephalopathy (PML) upon JCV infection in AIDS-immunocompromised patients and tubulointerstitial nephritis upon BKV infection in kidney transplant patients. Both JCV and BKV may have their importance in cancer (100). As for the monkey SV40 virus, it has contaminated the human population when poliovirus vaccination was used 50 years ago.

Two miRNAs, originating from the same pre-miRNA and produced from the SV40 genome, were computationally predicted and experimentally validated by Sullivan et al. (101) in 2005. By using Northern blot and RNase protection assay (RPA), the group mapped the production of sv40-miR-S1-5p and sv40-miR-S1-3p from TC-7/Db cells infected with SV40 (Table 2). They explored the function of these miRNAs by using a mutant that was constructed by mutagenizing selected bases in the region of the predicted pre-miRNA to disrupt the hairpin structure of the pre-miRNA on the late strand, while leaving intact the amino acid coding potential of the T antigen on the early strand. It came to light that SV40 miRNAs, expressed late in the infection, can direct cleavage of early mRNAs that occur for small- and large-T antigens. Without affecting the infectivity or replication of the virus, downregulation of the T antigens seemed to decrease the susceptibility to cytotoxic T lymphocytes (CTL) and cytokine release, again suggesting a role for viral miRNAs in escape mechanisms from the host immune system. The same year, another group published the identification of miRNAs from the simian virus 12 (SV12) with intriguing sequence complementarities with the SV40 antigen (102).

Three years later, new miRNA sequences from polyomavirus genome were identified using similar experimental approaches. JCV, BKV, and SV40 were reported to share homologous pre-miRNA hairpins, both arms of which are processed into mature miRNAs (103). Despite being only ~65% identical (5p miRNAs are ~55% identical, and 3p miRNAs are ~75% identical), all three pre-miRNAs share several atypical properties in terms of processing and abundance (103). Interestingly, the authors have reported that both arms of the precursor hairpin can be active on the same target, in this case viral early RNAs. They reported the same directed cleavage of these mRNAs by JCV and BKV miRNAs, as for those from SV40, by using 5′RACE to map the early mRNA cleavage products. Finally, detection of JCV miRNAs in the brain tissues of PML patients may help create therapies based on interference with existing miRNAs.

Bigger than polyomavirus, adenoviruses are medium-size dsDNA viruses known to infect mammalian cells (104). Most infections with adenovirus result in problems with the upper respiratory tract of the infected host. Other pathologies were also assigned to adenoviruses, such as ear infection, gastroenteritis, cough and, rarely, viral encephalitis. Some miRNAs have been predicted for a few species of adenoviruses (51) but, until recently, no miRNA function has been described. A particular aspect of the adenovirus 2 biology is worth noting and it pertains to the production of two noncoding RNAs, named VAI and VAII (See Fig. 2a) (105). The ~160-nt long VAI RNA accumulates in large amounts during adenovirus infection. As discussed later,

VAI RNA has the ability to interfere with the interferon-related cellular defense mechanism and, thus, with protein synthesis by blocking the activity of protein kinase R (PKR) and leading to the inhibition of eukaryotic initiation factor 2α (eIF2α) phosphorylation (10, 106).

VAI RNA also exhibits a secondary structure formed of two short imperfectly base-paired stems, referred to as the terminal and apical stems, respectively, and a structurally complex domain, known as the central domain (See Fig. 2a) (11). Although the ability of the VAI RNA to interfere with the cellular components of the miRNA pathway of the host will be discussed later (see Subheading 2.4), its processing by components of the miRNA pathway, such as Dicer, is a recent concept supported by two independent groups (107, 108). Sano et al. (108) found that VAI RNA is processed by Dicer in the cytoplasm and identified by Northern blot hybridization one miRNA originating from the right strand of the 3′ terminal stem region. They determined the cleavage sites by S1 nuclease mapping, which consists in the degradation by S1 nuclease of single-stranded RNA (ssRNA) (or ssDNA), while preserving dsRNA hybrids (108). Although the authors have shown that the small RNA derived from VAI is functional and can downregulate a reporter gene in cultured cells, whether it influences expression of any cellular genes remains to be determined.

Other groups have reported the identification of one to three different miRNAs generated from VAI and VAII RNAs of the adenovirus type 5, and originating from the 3′stem region (107, 109, 110). VAII RNA represented a more potent substrate for Dicer and ~2-fold more VAII RNA-derived small RNAs were present in the total pool of small RNAs. Approximately 1.5% of VAII RNA is cleaved by Dicer, resulting in the production of ~75,000 copies of mivaRII-138 miRNA in late-infected cells. This huge amount of mivaRII-138 miRNA may exert potent gene regulatory effects and influence the outcome of adenoviral infections. Whether the effects of VAI RNA on host cells relate to the biogenesis of small regulatory RNAs derived from VAI or to the inhibitory interference of VAI RNA with Dicer remains unclear.

These issues warrant further investigations, considering that adenoviral vectors are among the most commonly used vectors for gene therapy, aimed at delivering small interfering RNAs (siRNAs) and short hairpin RNAs (shRNAs) to target cells, second only to retroviruses (111).

2.3. Retroviruses

In contrast to DNA viruses, members of the retrovirus family possess an RNA genome. Replication of retroviruses occurs via a DNA intermediate and involves the viral RT enzyme, which converts RNA into DNA. The viral DNA is then integrated into the

host genome for subsequent viral gene transcription and virus production. Retroviral genomes commonly contain three open reading frames that encode for structural proteins (e.g., *gag*), for an RT, for an integrase and protease (*pol*), and for retroviral coat proteins (*env*). Among the subfamilies of retroviruses, the group of lentiviruses is represented by many well-known members, including human immunodeficiency viruses 1 and 2 (HIV-1 and HIV-2) and simian immunodeficiency virus (SIV), whereas the deltaretrovirus subfamily is represented by human T-cell leukemia/lymphoma virus type 1 (HTLV-1).

After cell entry, RNA decapsidation occurs in the cytoplasm and likely exposes some RNA structures to cellular components of the miRNA pathway, such as Dicer. Transcription of viral mRNAs in the nucleus may also expose the viral RNA structures that may be recognized and processed by the microprocessor complex containing Drosha. However, initial studies have failed to identify miRNAs originating from HIV-1 or other retroviruses in virus-infected cells. Using better adapted and more sensitive approaches, other groups were able to detect miRNAs derived from the RNA of retroviruses, such as HIV-1.

Using a bioinformatic tool designed to uncover well-ordered folding patterns in nucleotide sequences, five candidate pre-miRNAs encoded by different regions of the HIV-1 genome were initially flagged (112). Omoto and colleagues (113) then reported an miRNA, named miR-N367, derived from the *nef* region, an accessory gene partially overlapping with the 3′ long terminal repeat (LTR). This HIV-1 miRNA has been detected by Northern blot hybridization in MT-4 T cells persistently infected with HIV-1 IIIB strain and cloned from a ~25-nt RNA subpopulation. Overexpression of miR-N367, which shows perfect complementarity with *nef*, seemed to suppress HIV-1 LTR-driven transcription in reporter gene assays (114), suggesting that this *nef*-derived miRNA could act as a negative regulator of HIV-1 transcription. The biogenesis and function of this viral miRNA requires further investigation (Table 2).

Another study reported that the HIV-1 RNA genome also encodes an siRNA derived from the *env* gene (115). The authors observed that an RNA strand forming a perfect 19-bp duplex, joined by an extended 198-nt loop, could be converted into an siRNA upon incubation with recombinant Dicer in vitro. A probe specific to this viral siRNA detected a ~24-nt signal not seen in mock-infected cells by Northern blot analysis (115). Overexpression of this viral siRNA effectively reduced *env* mRNA levels and viral replication, whereas its neutralization with complementary 2~O-methyl oligonucleotides led to a dose-dependent increase in HIV-1 replication in human cells (115). These results suggest that an HIV-1-derived siRNA can modulate virus production.

Another HIV-1 RNA structure, the TAR element, was reported to be cleaved by Dicer into miRNAs (48, 116). Klase et al. (116) suggested that HIV-1 TAR-derived miRNAs may act by recruiting the histone deacetylase HDAC-1 to the HIV-1 LTR promoter in the nucleus in order to silence transcription by chromatin remodeling, a concept that has been proposed previously (Table 2) (117). The authors hypothesize that this sequence of events may suppress transcription of viral as well as cellular genes, thereby influencing particular steps of HIV-1 pathogenesis, such as latency.

More recently, our group demonstrated that the TAR element of HIV-1 could release two miRNAs, namely miR-TAR-5p and miR-TAR-3p, through an asymmetrical processing reaction involving Dicer (48). This reaction led to the preferential release and accumulation of miR-TAR-3p from the right arm of the TAR element, which may explain, at least in part, the superior potency of miR-TAR-3p in mediating gene silencing in vivo. Although HIV-1 can generate two miRNAs from the same hairpin, i.e., TAR element, like JCV, BK, and SV40 viruses, it remains unclear as to whether miR-TAR-5p and miR-TAR-3p could regulate the same transcript(s). Computational analysis of the TAR element of HIV-2, which is larger (~123 bp) than that of HIV-1, suggests that it may also be a source of two miRNAs (118), whose existence remains to be validated experimentally.

A recent study by Lin and Cullen (119) is challenging the existence of miRNAs derived from primate retroviruses such as HIV-1 and HTLV-1. We cannot exclude the possibility that the identification of some miRNAs may be restricted to specific viral strains or that miRNAs may have escaped detection by standard small RNA cloning strategies, since methylation of the 2′ hydroxyl of the terminal ribose significantly reduces the cloning efficiency of silencing-associated small RNAs (120). This would explain some of the discrepancies observed between laboratories using different techniques to identify viral miRNAs. Related to that issue, the recent report on the presence of highly homologous and/or larger numbers of miRNAs resulting from retroviruses that have been integrated into the human genome, such as human endogenous retrovirus L (HERV-L), simian foamy viruses, and human foamy viruses and HTLV-1, is intriguing and suggests that this may be a mechanism by which the retrovirus-infected host is more or less susceptible to subsequent viral infections (121).

2.4. Noncoding RNAs Expressed by Viruses

Several DNA viruses have been shown to generate ncRNAs. The first ncRNA to be described is VAI RNA from adenovirus 2. As previously mentioned, VAI RNA was found to interfere with the PKR response of virus-infected cells, although it may also take part in the strategy that adenoviruses have evolved to counteract

cellular antiviral defense systems based on the miRNA pathway. Transcribed by RNA polymerase III, VAI RNA (see Fig. 2a) has been shown to inhibit the nuclear export of pre-miRNAs by competition with Exportin-5 nuclear export factor as well as Dicer activity through direct binding to the enzyme (12). Another group observed the direct binding of VAI and VAII RNAs to Dicer as well as to the RNA-induced silencing complex (RISC) or miRNP (107). These observations are counterbalanced by the fact that, in contrast to two similar noncoding RNAs, i.e., EBER-1 from EBV (122, 123) and hY1 from human cells (124), they are refractory to processing by Dicer (108), VAI and VAII RNAs may be processed by Dicer into miRNAs (107–110), which may exert gene regulatory functions in adenovirus-infected cells. Nevertheless, the VAI/VAII RNA-mediated attenuation of the cellular miRNA pathway may confer an advantage to the virus through a decreased level in cellular antiviral miRNAs.

Epstein–Barr virus-encoded small RNAs (EBERs) have also been proposed, like VAI RNA, to bind PKR (9). EBER1 (167 nt) and EBER2 (172 nt) (see Fig. 2b) are generally the most abundant RNAs in EBV-infected cells (8, 122). Structural similarities were observed between EBERs and VAI/VAII ncRNAs and, interestingly, the generation of adenoviral mutants, in which VA RNAs were replaced by EBERs, showed that EBERs could substitute for VA RNA function (125, 126). Several roles have been attributed to EBERs such as cell transformation and regulation of gene expression, whereas nuclear EBER1 and EBER2 ncRNAs may act as transcriptional regulators for cytokines and growth factors expression, and inhibit apoptosis via binding to PKR. More recently, it has been speculated that EBER RNAs could be involved in the rescue of EBV from cytoprotective transcriptional repression under particular stress conditions in vivo (for a review of EBER RNA function, see (8)). VA and EBER ncRNAs may thus counteract the activation of host defenses in virus-infected cells.

Additional viral ncRNAs have been found in the genome of HCMV. One of them, a ~2.7 kb transcript called β2.7 RNA, is particularly abundant during the early time of infection (127). Reeves et al. (128) reported the ability of the β2.7 RNA transcript to interact with a subunit of the mitochondrial enzyme complex I (reduced nicotinamide adenine dinucleotide–ubiquinone oxidoreductase), suggesting a role for β2.7 RNA in protecting cells from apoptosis induced via that complex. It is now clear that viruses have developed refined strategies based on ncRNAs in order to circumvent key cellular processes that allow them to persist in their hosts.

Recently, a hepatitis delta virus (HDV) small RNA of ~24 to 25 nt was reported to be expressed from the bottom strand of the antigenomic pode of the viral RNA genome (129) (pode and

antipode refer to both extremities of the HDV RNA hairpin ends, excluded from the coding region of hepatitis delta antigen (HDAg)). HDV is a subviral satellite that encodes for a single protein, the HDAg, and can propagate solely in the presence of hepatitis B virus (HBV) or in cells previously infected with HBV. After cell entry, HDV circular genomic RNA becomes a template for rolling-circle replication in the nucleus to produce antigenomic RNA multimers, which are further cleaved into monomers by the intrinsic ribozyme activity of the antigenomic strand. Characterizing the extremities of the HDV RNA hairpin, Haussecker et al. (129) found a 5′ capped, 2′-3′-hydroxylated small RNA from HDV. Position of the small RNA within the HDV sequence led the authors to suggest that it could be involved in HDV transcription initiation. They identified and cloned additional small RNAs from both HDV genomic and antigenomic polarities that may function as small priming RNA (spRNAs) to help transcription initiation and, consequently, the success of the HDV infection.

Together, the discovery, role, and importance of viral ncRNAs raise several important issues: How many small or large ncRNAs are produced from viral genomes? How do they contribute either to facilitate the infectious process or to assist in immune evasion mechanisms? What is their impact in viral pathogenesis? In cell biology? Answers to these questions will help us better understand viral infections and, perhaps, create new therapeutic opportunities to fight viruses.

3. Cellular miRNAs in Virus-Infected Cells

3.1. Effects of Cellular miRNAs on Virus Biology

In noninfected cells, miRNAs have been proposed to regulate up to 90% of the genes (130). A case of intricate relationship between cellular miRNAs and viruses came from the observation that replication of hepatitis C virus (HCV) was dependent on cellular miR-122 expression (131). They demonstrated that HCV RNA can replicate in miR-122-expressing Huh-7 cells, but not in HepG2 cells lacking miR-122. A binding site for miR-122 was predicted to reside close to the 5′ end of the viral genome, and creation of a loss-of-function mutation led to reduced levels of intracellular viral RNA. MiR-122 is expressed at high levels in human hepatocellular carcinoma (HHC), a well-known consequence of the HCV chronic infection (132). Increased miR-122 expression may lead to the regulation of anti-apoptotic genes (133) and enhance viral replication to promote cell proliferation. The exact mechanism by which miR-122 favors HCV replication in hepatocytes, however, remains the subject of speculations (Table 3) (134).

More recent studies have explored the importance of the cellular miRNA pathway in the control of HIV-1 replication (135, 136). Using siRNAs against Drosha and Dicer in peripheral blood mononuclear cells (PBMCs) isolated from HIV-1-infected patients, Triboulet et al. (135) observed faster virus replication kinetics in Drosha- or Dicer-depleted cells, as compared to cells treated with a control siRNA. The authors also confirmed a role for Drosha and Dicer in the suppression of HIV-1 replication in latently infected U1 cells.

Huang et al. (136) showed that the 3′ UTR of almost all HIV-1 mRNAs produced in resting primary $CD4^+$ T lymphocytes during latency contain a 1.2-kb fragment that can be recognized by cellular miRNAs, with a negative impact on viral protein production. Combined with the relatively inefficient synthesis of Tat and Rev, miRNAs expressed by resting $CD4^+$ T cells may participate in the posttranscriptional regulation of HIV-1 mRNA and contribute to keep the virus in its latent phase, as observed in patients with suppressive highly active antiretroviral therapy (HAART) (136). These new elements contribute to our understanding of the molecular basis of viral latency and may help us design therapeutic strategies aimed at purging HIV-1-infected patients of the quiescent virus.

3.2. Role of Cellular miRNAs in Host Defenses Against Viruses

As discussed above, ncRNAs derived from some viruses are able to interact with PKR, an effector of the interferon (IFN) pathway, which is activated upon viral infection. It is relevant to note here that IFN may be linked to the generation of miRNAs. Pedersen et al. (137) recently reported the modulation of miRNAs upon IFNβ induction. Interestingly, 8 of these IFNβ-induced miRNAs have sequence-predicted targets within the HCV genomic RNA. Individual transfection experiments revealed that miR-196, miR-296, miR-351, miR-431, and miR-448 were able to substantially attenuate HCV replication, whereas miRNAs miR-1, miR-30, and miR-128 had no effect alone. The anti-HCV properties of IFNβ may also be mediated through downregulation of miR-122 expression, which appears to be important for HCV replication (131). These results suggest that the IFNβ-induced expression of endogenous miRNAs may confer and help establish anti-viral properties to human cells (Table 3).

Another example of the complex interaction between viruses and cellular components is the miRNA miR-K12-11 derived from KSHV that functions as an ortholog of miR-155, an oncogenic miRNA upregulated in lymphomas (137). The sequence identity between miR-K12-11 and miR-155, which implies a common set of regulated genes, suggests that KSHV may thwart its host through an miRNA mimicking strategy.

A few years ago, some HIV-1 gene candidates were predicted to be controlled by host miRNAs in view of thermodynamically

favorable miRNA:RNA target base pairing (138). In addition, changes in miRNA expression profiles, more specifically the downregulation of a large pool of cellular miRNAs, have been observed in human HeLa cells transfected with the infectious molecular HIV-1 clone pNL4-3 (139). Similar observations were reported recently, in which HIV-1 infection was associated with either up- or downregulation of specific miRNA clusters located within the host genome. For example, expression of the miR-17/92 cluster, which encodes seven miRNAs, among which miR-17-5p and miR-20 may target the histone acetyltransferase and HIV-1 Tat cofactor p300/CBP-associated factor (PCAF), was substantially downregulated (135). The authors proposed that this gene regulatory axis may help us understand how latent virus reservoirs could be activated (Table 3).

The presence of miRNAs has been documented in mature neuronal dendrites, suggesting that they may be involved in controlling local protein translation and synaptic function. A rare clinical manifestation of HIV-1 infection, HIV-1 encephalopathy (HIVE), results in neuronal damage and dysfunction. If neurons are rarely infected by HIV-1, they are nevertheless exposed to the viral components of HIV-1, including its transactivating protein Tat. Eletto et al. (140) recently showed that Tat deregulates expression of selected miRNAs in primary cortical neurons, including the neuronal miR-128, which has been shown to normally inhibit expression of the pre-synaptic protein SNAP25. This is yet another mechanism by which HIV-1 and its components can perturb normal cellular activities and compromise health of the infected individuals.

4. Concluding Remarks

Whereas some viruses may take advantage of the cellular and viral miRNAs for their own replication, others may be targeted by cellular miRNAs that function as part of the host defenses against viruses. Similarly, while some viral RNAs may be processed by components of the host miRNA pathway, such as Dicer, others have evolved countermeasures in the form of various inhibitors of RNA silencing. Elucidation of the complex relationship between viruses and their hosts involving miRNAs and ncRNAs is mandatory for the development of antiviral gene therapies based on the neutralization and/or promotion of miRNA/ncRNA expression.

Acknowledgments

We are grateful to the CHUQ Research Center Computer Graphics Department for the graphic illustrations. P. P. is a Senior Scholar from the Fonds de la Recherche en Santé du Québec. This work was supported by grant HOP-83069 from Health Canada/Canadian Institutes of Health Research (CIHR) to P.P.

References

1. Yekta, S., Shih, I.H. and Bartel, D.P. (2004) MicroRNA-directed cleavage of HOXB8 mRNA. *Science* **304**, 594–596.
2. Mansfield, J.H., Harfe, B.D., Nissen, R., Obenauer, J., Srineel, J., Chaudhuri, A., *et al.* (2004) MicroRNA-responsive 'sensor' transgenes uncover Hox-like and other developmentally regulated patterns of vertebrate microRNA expression. *Nat. Genet.* **36**, 1079–1083.
3. Vasudevan, S., Tong, Y. and Steitz, J.A. (2007) Switching from repression to activation: microRNAs can up-regulate translation. *Science* **318**, 1931–1934.
4. Griffiths-Jones, S., Grocock, R.J., van Dongen, S., Bateman, A. and Enright, A.J. (2006) miRBase: microRNA sequences, targets and gene nomenclature. *Nucleic Acids Res.* **34**, D140–144.
5. Griffiths-Jones, S., Saini, H.K., van Dongen, S. and Enright, A.J. (2008) miRBase: tools for microRNA genomics. *Nucleic Acids Res.* **36**, D154–158.
6. Aravin, A.A., Lagos-Quintana, M., Yalcin, A., Zavolan, M., Marks, D., Snyder, B., et al. (2003) The small RNA profile during *Drosophila melanogaster* development. *Dev. Cell* **5**, 337–350.
7. Ambros, V., Lee, R.C., Lavanway, A., Williams, P.T. and Jewell, D. (2003) MicroRNAs and other tiny endogenous RNAs in C. elegans. *Curr. Biol.* **13**, 807–818.
8. Swaminathan, S. (2008) Noncoding RNAs produced by oncogenic human herpesviruses. *J. Cell Physiol.* **216**, 321–326.
9. Clemens, M.J., Laing, K.G., Jeffrey, I.W., Schofield, A., Sharp, T.V., Elia, A., et al. (1994) Regulation of the interferon-inducible eIF-2 alpha protein kinase by small RNAs. *Biochimie* **76**, 770–778.
10. Kitajewski, J., Schneider, R.J., Safer, B., Munemitsu, S.M., Samuel, C.E., Thimmappaya, B. and Shenk, T. (1986) Adenovirus VAI RNA antagonizes the antiviral action of interferon by preventing activation of the interferon-induced eIF-2 alpha kinase. *Cell* **45**, 195–200.
11. Furtado, M.R., Subramanian, S., Bhat, R.A., Fowlkes, D.M., Safer, B. and Thimmappaya, B. (1989) Functional dissection of adenovirus VAI RNA. *J. Virol.* **63**, 3423–3434.
12. Lu, S. and Cullen, B.R. (2004) Adenovirus VA1 noncoding RNA can inhibit small interfering RNA and microRNA biogenesis. *J. Virol.* **78**, 12868–12876.
13. Cai, X., Hagedorn, C.H. and Cullen, B.R. (2004) Human microRNAs are processed from capped, polyadenylated transcripts that can also function as mRNAs. *RNA* **10**, 1957–1966.
14. Lee, Y., Kim, M., Han, J., Yeom, K.H., Lee, S., Baek, S.H. and Kim, V.N. (2004) MicroRNA genes are transcribed by RNA polymerase II. *EMBO J.* **23**, 4051–4060.
15. Lee, Y., Ahn, C., Han, J., Choi, H., Kim, J., Yim, J., *et al.* (2003) The nuclear RNase III Drosha initiates microRNA processing. *Nature* **425**, 415–419.
16. Denli, A.M., Tops, B.B., Plasterk, R.H., Ketting, R.F. and Hannon, G.J. (2004) Processing of primary microRNAs by the Microprocessor complex. *Nature* **432**, 231–235.
17. Gregory, R.I., Yan, K.P., Amuthan, G., Chendrimada, T., Doratotaj, B., Cooch, N. and Shiekhattar, R. (2004) The Microprocessor complex mediates the genesis of microRNAs. *Nature* **432**, 235–240.
18. Han, J., Lee, Y., Yeom, K.H., Kim, Y.K., Jin, H. and Kim, V.N. (2004) The Drosha-DGCR8 complex in primary microRNA processing. *Genes Dev.* **18**, 3016–3027.
19. Landthaler, M., Yalcin, A. and Tuschl, T. (2004) The human DiGeorge syndrome critical region gene 8 and its D. melanogaster homolog are required for miRNA biogenesis. *Curr. Biol.* **14**, 2162–2167.

20. Ruby, J.G., Jan, C.H. and Bartel, D.P. (2007) Intronic microRNA precursors that bypass Drosha processing. *Nature* **448**, 83–86.
21. Berezikov, E., Chung, W.J., Willis, J., Cuppen, E. and Lai, E.C. (2007) Mammalian mirtron genes. *Mol. Cell* **28**, 328–336.
22. Bohnsack, M.T., Czaplinski, K. and Gorlich, D. (2004) Exportin 5 is a RanGTP-dependent dsRNA-binding protein that mediates nuclear export of pre-miRNAs. *RNA* **10**, 185–191.
23. Brownawell, A.M. and Macara, I.G. (2002) Exportin-5, a novel karyopherin, mediates nuclear export of double-stranded RNA binding proteins. *J. Cell Biol.* **156**, 53–64.
24. Lund, E., Guttinger, S., Calado, A., Dahlberg, J.E. and Kutay, U. (2004) Nuclear export of microRNA precursors. *Science* **303**, 95–98.
25. Yi, R., Qin, Y., Macara, I.G. and Cullen, B.R. (2003) Exportin-5 mediates the nuclear export of pre-microRNAs and short hairpin RNAs. *Genes Dev.* **17**, 3011–3016.
26. Zhang, H., Kolb, F.A., Jaskiewicz, L., Westhof, E. and Filipowicz, W. (2004) Single processing center models for human Dicer and bacterial RNase III. *Cell* **118**, 57–68.
27. Bernstein, E., Caudy, A.A., Hammond, S.M. and Hannon, G.J. (2001) Role for a bidentate ribonuclease in the initiation step of RNA interference. *Nature*, **409**, 363–366.
28. Provost, P., Dishart, D., Doucet, J., Frendewey, D., Samuelsson, B. and Radmark, O. (2002) Ribonuclease activity and RNA binding of recombinant human Dicer. *EMBO J.* **21**, 5864–5874.
29. Zhang, H., Kolb, F.A., Brondani, V., Billy, E. and Filipowicz, W. (2002) Human Dicer preferentially cleaves dsRNAs at their termini without a requirement for ATP. *EMBO J.* **21**, 5875–5885.
30. Gatignol, A., Buckler-White, A., Berkhout, B. and Jeang, K.T. (1991) Characterization of a human TAR RNA-binding protein that activates the HIV-1 LTR. *Science* **251**, 1597–1600.
31. Haase, A.D., Jaskiewicz, L., Zhang, H., Laine, S., Sack, R., Gatignol, A. and Filipowicz, W. (2005) TRBP, a regulator of cellular PKR and HIV-1 virus expression, interacts with Dicer and functions in RNA silencing. *EMBO Rep.* **6**, 961–967.
32. Chendrimada, T.P., Gregory, R.I., Kumaraswamy, E., Norman, J., Cooch, N., Nishikura, K. and Shiekhattar, R. (2005) TRBP recruits the Dicer complex to Ago2 for microRNA processing and gene silencing. *Nature* **436**, 740–744.
33. Schwarz, D.S., Hutvagner, G., Du, T., Xu, Z., Aronin, N. and Zamore, P.D. (2003) Asymmetry in the assembly of the RNAi enzyme complex. *Cell* **115**, 199–208.
34. Matranga, C., Tomari, Y., Shin, C., Bartel, D.P. and Zamore, P.D. (2005) Passenger-strand cleavage facilitates assembly of siRNA into Ago2-containing RNAi enzyme complexes. *Cell* **123**, 607–620.
35. Plante, I., Davidovic, L., Ouellet, D.L., Gobeil, L.A., Tremblay, S., Khandjian, E.W. and Provost, P. (2006) Dicer-derived microRNAs are utilized by the fragile X mental retardation protein for assembly on target RNAs. *J. Biomed. Biotechnol.* **2006**, 64347.
36. Bagga, S., Bracht, J., Hunter, S., Massirer, K., Holtz, J., Eachus, R. and Pasquinelli, A.E. (2005) Regulation by let-7 and lin-4 miRNAs results in target mRNA degradation. *Cell* **122**, 553–563.
37. Liu, J., Valencia-Sanchez, M.A., Hannon, G.J. and Parker, R. (2005) MicroRNA-dependent localization of targeted mRNAs to mammalian P-bodies. *Nat. Cell Biol.* **7**, 719–723.
38. Teixeira, D., Sheth, U., Valencia-Sanchez, M.A., Brengues, M. and Parker, R. (2005) Processing bodies require RNA for assembly and contain nontranslating mRNAs. *RNA* **11**, 371–382.
39. Eystathioy, T., Chan, E.K., Tenenbaum, S.A., Keene, J.D., Griffith, K. and Fritzler, M.J. (2002) A phosphorylated cytoplasmic autoantigen, GW182, associates with a unique population of human mRNAs within novel cytoplasmic speckles. *Mol. Biol. Cell* **13**, 1338–1351.
40. Eulalio, A., Behm-Ansmant, I., Schweizer, D. and Izaurralde, E. (2007) P-body formation is a consequence, not the cause, of RNA-mediated gene silencing. *Mol. Cell Biol.* **27**, 3970–3981.
41. Eystathioy, T., Jakymiw, A., Chan, E.K., Seraphin, B., Cougot, N. and Fritzler, M.J. (2003) The GW182 protein colocalizes with mRNA degradation associated proteins hDcp1 and hLSm4 in cytoplasmic GW bodies. *RNA* **9**, 1171–1173.
42. Fukuhara, N., Ebert, J., Unterholzner, L., Lindner, D., Izaurralde, E. and Conti, E. (2005) SMG7 is a 14-3-3-like adaptor in the nonsense-mediated mRNA decay pathway. *Mol. Cell* **17**, 537–547.
43. Unterholzner, L. and Izaurralde, E. (2004) SMG7 acts as a molecular link between mRNA surveillance and mRNA decay. *Mol. Cell* **16**, 587–596.

44. Bartel, D.P. (2004) MicroRNAs: genomics, biogenesis, mechanism, and function. *Cell* **116**, 281–297.
45. Vella, M.C., Reinert, K. and Slack, F.J. (2004) Architecture of a validated microRNA:target interaction. *Chem. Biol.* **11**, 1619–1623.
46. Pall, G.S., Codony-Servat, C., Byrne, J., Ritchie, L. and Hamilton, A. (2007) Carbodiimide-mediated cross-linking of RNA to nylon membranes improves the detection of siRNA, miRNA and piRNA by northern blot. *Nucleic Acids Res.* **35**, e60.
47. Pall, G.S. and Hamilton, A.J. (2008) Improved Northern blot method for enhanced detection of small RNA. *Nat. Protoc.* **3**, 1077–1084.
48. Ouellet, D.L., Plante, I., Landry, P., Barat, C., Janelle, M.E., Flamand, L., Tremblay, M.J. and Provost, P. (2008) Identification of functional microRNAs released through asymmetrical processing of HIV-1 TAR element. *Nucleic Acids Res.* **36**, 2353–2365.
49. Friedlander, M.R., Chen, W., Adamidi, C., Maaskola, J., Einspanier, R., Knespel, S. and Rajewsky, N. (2008) Discovering microRNAs from deep sequencing data using miRDeep. *Nat. Biotechnol.* **26**, 407–415.
50. Heldwein, E.E. and Krummenacher, C. (2008) Entry of herpesviruses into mammalian cells. *Cell Mol. Life Sci.* **65**, 1653–1668.
51. Pfeffer, S., Sewer, A., Lagos-Quintana, M., Sheridan, R., Sander, C., Grasser, F.A., *et al.* (2005) Identification of microRNAs of the herpesvirus family. *Nat. Methods* **2**, 269–276.
52. Pfeffer, S., Zavolan, M., Grasser, F.A., Chien, M., Russo, J.J., Ju, J., *et al.* (2004) Identification of virus-encoded microRNAs. *Science* **304**, 734–736.
53. Buck, A.H., Santoyo-Lopez, J., Robertson, K.A., Kumar, D.S., Reczko, M. and Ghazal, P. (2007) Discrete clusters of virus-encoded micrornas are associated with complementary strands of the genome and the 7.2-kilobase stable intron in murine cytomegalovirus. *J. Virol.* **81**, 13761–13770.
54. Dolken, L., Perot, J., Cognat, V., Alioua, A., John, M., Soutschek, J., et al. (2007) Mouse cytomegalovirus microRNAs dominate the cellular small RNA profile during lytic infection and show features of posttranscriptional regulation. *J. Virol.* **81**, 13771–13782.
55. Cui, C., Griffiths, A., Li, G., Silva, L.M., Kramer, M.F., Gaasterland, T., Wang, X.J. and Coen, D.M. (2006) Prediction and identification of herpes simplex virus 1-encoded microRNAs. *J. Virol.* **80**, 5499–5508.
56. Bloom, D.C. (2004) HSV LAT and neuronal survival. *Int. Rev. Immunol.* **23**, 187–198.
57. Cuchet, D., Ferrera, R., Lomonte, P. and Epstein, A.L. (2005) Characterization of antiproliferative and cytotoxic properties of the HSV-1 immediate-early ICPo protein. *J. Gene Med.* **7**, 1187–1199.
58. La Frazia, S., Amici, C. and Santoro, M.G. (2006) Antiviral activity of proteasome inhibitors in herpes simplex virus-1 infection: role of nuclear factor-kappaB. *Antivir. Ther.* **11**, 995–1004.
59. Umbach, J.L., Kramer, M.F., Jurak, I., Karnowski, H.W., Coen, D.M. and Cullen, B.R. (2008) MicroRNAs expressed by herpes simplex virus 1 during latent infection regulate viral mRNAs. *Nature* **454**, 780–783.
60. Halford, W.P., Kemp, C.D., Isler, J.A., Davido, D.J. and Schaffer, P.A. (2001) ICP0, ICP4, or VP16 expressed from adenovirus vectors induces reactivation of latent herpes simplex virus type 1 in primary cultures of latently infected trigeminal ganglion cells. *J. Virol.* **75**, 6143–6153.
61. Thompson, R.L. and Stevens, J.G. (1983) Biological characterization of a herpes simplex virus intertypic recombinant which is completely and specifically non-neurovirulent. *Virology* **131**, 171–179.
62. Tang, S., Bertke, A.S., Patel, A., Wang, K., Cohen, J.I. and Krause, P.R. (2008) An acutely and latently expressed herpes simplex virus 2 viral microRNA inhibits expression of ICP34.5, a viral neurovirulence factor. *Proc. Natl. Acad. Sci. U S A* **105**, 10931-10936.
63. Brady, G., MacArthur, G.J. and Farrell, P.J. (2007) Epstein-Barr virus and Burkitt lymphoma. *J. Clin. Pathol.* **60**, 1397–1402.
64. Tao, Q., Young, L.S., Woodman, C.B. and Murray, P.G. (2006) Epstein-Barr virus (EBV) and its associated human cancers--genetics, epigenetics, pathobiology and novel therapeutics. *Front. Biosci.* **11**, 2672–2713.
65. Young, L.S. and Rickinson, A.B. (2004) Epstein-Barr virus: 40 years on. *Nat. Rev. Cancer* **4**, 757–768.
66. Grundhoff, A., Sullivan, C.S. and Ganem, D. (2006) A combined computational and microarray-based approach identifies novel microRNAs encoded by human gamma-herpesviruses. *RNA* **12**, 733–750.
67. Edwards, R.H., Marquitz, A.R. and Raab-Traub, N. (2008) Epstein-Barr virus BART microRNAs are produced from a large intron prior to splicing. *J. Virol.* **82**, 9094–9106.

68. Amon, W. and Farrell, P.J. (2005) Reactivation of Epstein-Barr virus from latency. *Rev. Med. Virol.* **15**, 149–156.
69. Rickinson, A.B., Lee, S.P. and Steven, N.M. (1996) Cytotoxic T lymphocyte responses to Epstein-Barr virus. *Curr. Opin. Immunol.* **8**, 492–497.
70. Cai, X., Schafer, A., Lu, S., Bilello, J.P., Desrosiers, R.C., Edwards, R., Raab-Traub, N. and Cullen, B.R. (2006) Epstein-Barr virus microRNAs are evolutionarily conserved and differentially expressed. *PLoS Pathog* **2**, e23.
71. Xing, L. and Kieff, E. (2007) Epstein-Barr virus BHRF1 micro- and stable RNAs during latency III and after induction of replication. *J. Virol.* **81**, 9967–9975.
72. Barth, S., Pfuhl, T., Mamiani, A., Ehses, C., Roemer, K., Kremmer, E., et al. (2008) Epstein-Barr virus-encoded microRNA miR-BART2 down-regulates the viral DNA polymerase BALF5. *Nucleic Acids Res.* **36**, 666–675.
73. Lo, A.K., To, K.F., Lo, K.W., Lung, R.W., Hui, J.W., Liao, G. and Hayward, S.D. (2007) Modulation of LMP1 protein expression by EBV-encoded microRNAs. *Proc. Natl. Acad. Sci. U S A* **104**, 16164–16169.
74. Zheng, H., Li, L.L., Hu, D.S., Deng, X.Y. and Cao, Y. (2007) Role of Epstein-Barr virus encoded latent membrane protein 1 in the carcinogenesis of nasopharyngeal carcinoma. *Cell. Mol. Immunol.* **4**, 185–196.
75. Mosialos, G., Birkenbach, M., Yalamanchili, R., VanArsdale, T., Ware, C. and Kieff, E. (1995) The Epstein-Barr virus transforming protein LMP1 engages signaling proteins for the tumor necrosis factor receptor family. *Cell* **80**, 389–399.
76. Choy, E.Y., Siu, K.L., Kok, K.H., Lung, R.W., Tsang, C.M., To, K.F., et al. (2008) An Epstein-Barr virus-encoded microRNA targets PUMA to promote host cell survival. *J. Exp. Med.* **205**, 2551–2560.
77. Xia, T., O'Hara, A., Araujo, I., Barreto, J., Carvalho, E., Sapucaia, J.B., et al. (2008) EBV microRNAs in primary lymphomas and targeting of CXCL-11 by ebv-mir-BHRF1-3. *Cancer Res.* **68**, 1436–1442.
78. Reeves, M. and Sinclair, J. (2008) Aspects of human cytomegalovirus latency and reactivation. *Curr. Top. Microbiol. Immunol.* **325**, 297–313.
79. Britt, W. (2008) Manifestations of human cytomegalovirus infection: proposed mechanisms of acute and chronic disease. *Curr. Top. Microbiol. Immunol.* **325**, 417–470.
80. Grey, F., Antoniewicz, A., Allen, E., Saugstad, J., McShea, A., Carrington, J.C. and Nelson, J. (2005) Identification and characterization of human cytomegalovirus-encoded microRNAs. *J. Virol*,. **79**, 12095–12099.
81. Dunn, W., Trang, P., Zhong, Q., Yang, E., van Belle, C. and Liu, F. (2005) Human cytomegalovirus expresses novel microRNAs during productive viral infection. *Cell. Microbiol.* **7**, 1684–1695.
82. Grey, F., Meyers, H., White, E.A., Spector, D.H. and Nelson, J. (2007) A human cytomegalovirus-encoded microRNA regulates expression of multiple viral genes involved in replication. *PLoS Pathog.* **3**, e163.
83. Murphy, E., Vanicek, J., Robins, H., Shenk, T. and Levine, A.J. (2008) Suppression of immediate-early viral gene expression by herpesvirus-coded microRNAs: implications for latency. *Proc. Natl. Acad. Sci. U S A* **105**, 5453–5458.
84. Stern-Ginossar, N., Elefant, N., Zimmermann, A., Wolf, D.G., Saleh, N., Biton, M., Horwitz, E., et al. (2007) Host immune system gene targeting by a viral miRNA. *Science* **317**, 376–381.
85. Spengler, M.L., Kurapatwinski, K., Black, A.R. and Azizkhan-Clifford, J. (2002) SUMO-1 modification of human cytomegalovirus IE1/IE72. *J. Virol.* **76**, 2990–2996.
86. Grey, F. and Nelson, J. (2008) Identification and function of human cytomegalovirus microRNAs. *J. Clin. Virol.* **41**, 186–191.
87. Wilkinson, G.W., Tomasec, P., Stanton, R.J., Armstrong, M., Prod'homme, V., Aicheler, R., et al. (2008) Modulation of natural killer cells by human cytomegalovirus. *J. Clin. Virol.* **41**, 206–212.
88. Dunn, C., Chalupny, N.J., Sutherland, C.L., Dosch, S., Sivakumar, P.V., Johnson, D.C. and Cosman, D. (2003) Human cytomegalovirus glycoprotein UL16 causes intracellular sequestration of NKG2D ligands, protecting against natural killer cell cytotoxicity. *J. Exp. Med.* **197**, 1427–1439.
89. Antman, K. and Chang, Y. (2000) Kaposi's sarcoma. *N. Engl. J. Med.* **342**, 1027–1038.
90. Aoki, Y., Yarchoan, R., Wyvill, K., Okamoto, S., Little, R.F. and Tosato, G. (2001) Detection of viral interleukin-6 in Kaposi sarcoma-associated herpesvirus-linked disorders. *Blood* **97**, 2173–2176.
91. Cai, X., Lu, S., Zhang, Z., Gonzalez, C.M., Damania, B. and Cullen, B.R. (2005) Kaposi's sarcoma-associated herpesvirus expresses an array of viral microRNAs in latently infected cells. *Proc. Natl. Acad. Sci. U S A* **102**, 5570–5575.

92. Samols, M.A., Hu, J., Skalsky, R.L. and Renne, R. (2005) Cloning and identification of a microRNA cluster within the latency-associated region of Kaposi's sarcoma-associated herpesvirus. *J. Virol.* **79**, 9301–9305.
93. Samols, M.A., Skalsky, R.L., Maldonado, A.M., Riva, A., Lopez, M.C., Baker, H.V. and Renne, R. (2007) Identification of cellular genes targeted by KSHV-encoded microRNAs. *PLoS Pathog.* **3**, e65.
94. de Fraipont, F., Nicholson, A.C., Feige, J.J. and Van Meir, E.G. (2001) Thrombospondins and tumor angiogenesis. *Trends Mol. Med.* **7**, 401–407.
95. Lawler, J. (2002) Thrombospondin-1 as an endogenous inhibitor of angiogenesis and tumor growth. *J. Cell. Mol. Med.* **6**, 1–12.
96. Narizhneva, N.V., Razorenova, O.V., Podrez, E.A., Chen, J., Chandrasekharan, U.M., DiCorleto,P.E.,etal.(2005)Thrombospondin-1 up-regulates expression of cell adhesion molecules and promotes monocyte binding to endothelium. *FASEB J.* **19**, 1158–1160.
97. Gottwein, E., Mukherjee, N., Sachse, C., Frenzel, C., Majoros, W.H., Chi, J.T., et al. (2007) A viral microRNA functions as an orthologue of cellular miR-155. *Nature* **450**, 1096–1099.
98. Skalsky, R.L., Samols, M.A., Plaisance, K.B., Boss, I.W., Riva, A., Lopez, M.C., Baker, H.V. and Renne, R. (2007) Kaposi's sarcoma-associated herpesvirus encodes an ortholog of miR-155. *J. Virol.* **81**, 12836–12845.
99. Ochiai, S., Mizuno, T., Deie, M., Igarashi, K., Hamada, Y. and Ochi, M. (2008) Oxidative stress reaction in the meniscus of Bach 1 deficient mice: potential prevention of meniscal degeneration. *J. Orthop. Res.* **26**, 894–898.
100. Randhawa, P., Vats, A. and Shapiro, R. (2006) The pathobiology of polyomavirus infection in man. *Adv. Exp. Med. Biol.* **577**, 148–159.
101. Sullivan, C.S., Grundhoff, A.T., Tevethia, S., Pipas, J.M. and Ganem, D. (2005) SV40-encoded microRNAs regulate viral gene expression and reduce susceptibility to cytotoxic T cells. *Nature* **435**, 682–686.
102. Cantalupo, P., Doering, A., Sullivan, C.S., Pal, A., Peden, K.W., Lewis, A.M. and Pipas, J.M. (2005) Complete nucleotide sequence of polyomavirus SA12. *J. Virol.* **79**, 13094–13104.
103. Seo, G.J., Fink, L.H., O'Hara, B., Atwood, W.J. and Sullivan, C.S. (2008) Evolutionarily conserved function of a viral microRNA. *J. Virol.* **82**, 9823–9828.
104. Mathews, M.B. and Shenk, T. (1991) Adenovirus virus-associated RNA and translation control. *J. Virol.* **65**, 5657–5662.
105. Reich, P.R., Forget, B.G. and Weissman, S.M. (1966) RNA of low molecular weight in KB cells infected with adenovirus type 2. *J. Mol. Biol.* **17**, 428–439.
106. Maran, A. and Mathews, M.B. (1988) Characterization of the double-stranded RNA implicated in the inhibition of protein synthesis in cells infected with a mutant adenovirus defective for VA RNA. *Virology* **164**, 106–113.
107. Andersson, M.G., Haasnoot, P.C., Xu, N., Berenjian, S., Berkhout, B. and Akusjarvi, G. (2005) Suppression of RNA interference by adenovirus virus-associated RNA. *J. Virol.* **79**, 9556–9565.
108. Sano, M., Kato, Y. and Taira, K. (2006) Sequence-specific interference by small RNAs derived from adenovirus VAI RNA. *FEBS Lett.* **580**, 1553–1564.
109. Xu, N., Segerman, B., Zhou, X. and Akusjarvi, G. (2007) Adenovirus virus-associated RNAII-derived small RNAs are efficiently incorporated into the rna-induced silencing complex and associate with polyribosomes. *J. Virol.* **81**, 10540–10549.
110. Aparicio, O., Razquin, N., Zaratiegui, M., Narvaiza, I. and Fortes, P. (2006) Adenovirus virus-associated RNA is processed to functional interfering RNAs involved in virus production. *J. Virol.* **80**, 1376–1384.
111. Ghosh, S.S., Gopinath, P. and Ramesh, A. (2006) Adenoviral vectors: a promising tool for gene therapy. *Appl. Biochem. Biotechnol.* **133**, 9–29.
112. Bennasser, Y., Le, S.Y., Yeung, M.L. and Jeang, K.T. (2004) HIV-1 encoded candidate micro-RNAs and their cellular targets. *Retrovirology* **1**, 43.
113. Omoto, S., Ito, M., Tsutsumi, Y., Ichikawa, Y., Okuyama, H., Brisibe, E.A., Saksena, N.K. and Fujii, Y.R. (2004) HIV-1 nef suppression by virally encoded microRNA. *Retrovirology* **1**, 44.
114. Omoto, S. and Fujii, Y.R. (2005) Regulation of human immunodeficiency virus 1 transcription by nef microRNA. *J. Gen. Virol.* **86**, 751–755.
115. Bennasser, Y., Le, S.Y., Benkirane, M. and Jeang, K.T. (2005) Evidence that HIV-1 encodes an siRNA and a suppressor of RNA silencing. *Immunity* **22**, 607–619.
116. Klase, Z., Kale, P., Winograd, R., Gupta, M.V., Heydarian, M., Berro, R., McCaffrey, T. and Kashanchi, F. (2007) HIV-1 TAR element is processed by Dicer to yield a viral micro-RNA involved in chromatin remodeling of the viral LTR. *BMC Mol. Biol.* **8**, 63.
117. Weinberg, M.S. and Morris, K.V. (2006) Are viral-encoded microRNAs mediating latent HIV-1 infection? *DNA Cell Biol.* **25**, 223–231.

118. Purzycka, K.J. and Adamiak, R.W. (2008) The HIV-2 TAR RNA domain as a potential source of viral-encoded miRNA. A reconnaissance study. *Nucleic Acids Symp. Ser. (Oxf.)*, 511–512.
119. Lin, J. and Cullen, B.R. (2007) Analysis of the interaction of primate retroviruses with the human RNA interference machinery. *J. Virol.* **81**, 12218–12226.
120. Ebhardt, H.A., Thi, E.P., Wang, M.B. and Unrau, P.J. (2005) Extensive 3′ modification of plant small RNAs is modulated by helper component-proteinase expression. *Proc. Natl. Acad. Sci. U S A* **102**, 13398–13403.
121. Hakim, S.T., Alsayari, M., McLean, D.C., Saleem, S., Addanki, K.C., Aggarwal, M., Mahalingam, K. and Bagasra, O. (2008) A large number of the human microRNAs target lentiviruses, retroviruses, and endogenous retroviruses. *Biochem. Biophys. Res. Commun.* **369**, 357–362.
122. Lerner, M.R., Andrews, N.C., Miller, G. and Steitz, J.A. (1981) Two small RNAs encoded by Epstein-Barr virus and complexed with protein are precipitated by antibodies from patients with systemic lupus erythematosus. *Proc. Natl. Acad. Sci. U S A* **78**, 805–809.
123. Rosa, M.D., Gottlieb, E., Lerner, M.R. and Steitz, J.A. (1981) Striking similarities are exhibited by two small Epstein-Barr virus-encoded ribonucleic acids and the adenovirus-associated ribonucleic acids VAI and VAII. *Mol. Cell. Biol.* **1**, 785–796.
124. Wolin, S.L. and Steitz, J.A. (1983) Genes for two small cytoplasmic Ro RNAs are adjacent and appear to be single-copy in the human genome. *Cell* **32**, 735–744.
125. Bhat, R.A. and Thimmappaya, B. (1983) Two small RNAs encoded by Epstein-Barr virus can functionally substitute for the virus-associated RNAs in the lytic growth of adenovirus 5. *Proc. Natl. Acad. Sci. U S A* **80**, 4789–4793.
126. Bhat, R.A. and Thimmappaya, B. (1985) Construction and analysis of additional adenovirus substitution mutants confirm the complementation of VAI RNA function by two small RNAs encoded by Epstein-Barr virus. *J. Virol.* **56**, 750–756.
127. Spector, D.H. (1996) Activation and regulation of human cytomegalovirus early genes. *Intervirology* **39**, 361–377.
128. Reeves, M.B., Davies, A.A., McSharry, B.P., Wilkinson, G.W. and Sinclair, J.H. (2007) Complex I binding by a virally encoded RNA regulates mitochondria-induced cell death. *Science* **316**, 1345–1348.
129. Haussecker, D., Cao, D., Huang, Y., Parameswaran, P., Fire, A.Z. and Kay, M.A. (2008) Capped small RNAs and MOV10 in human hepatitis delta virus replication. *Nat. Struct. Mol. Biol.* **15**, 714–721.
130. Miranda, K.C., Huynh, T., Tay, Y., Ang, Y.S., Tam, W.L., Thomson, A.M., Lim, B. and Rigoutsos, I. (2006) A pattern-based method for the identification of microRNA binding sites and their corresponding heteroduplexes. *Cell* **126**, 1203–1217.
131. Jopling, C.L., Yi, M., Lancaster, A.M., Lemon, S.M. and Sarnow, P. (2005) Modulation of hepatitis C virus RNA abundance by a liver-specific microRNA. *Science* **309**, 1577–1581.
132. Varnholt, H., Drebber, U., Schulze, F., Wedemeyer, I., Schirmacher, P., Dienes, H.P. and Odenthal, M. (2008) MicroRNA gene expression profile of hepatitis C virus-associated hepatocellular carcinoma. *Hepatology* **47**, 1223–1232.
133. Lin, C.J., Gong, H.Y., Tseng, H.C., Wang, W.L. and Wu, J.L. (2008) miR-122 targets an anti-apoptotic gene, Bcl-w, in human hepatocellular carcinoma cell lines. *Biochem. Biophys. Res. Commun.* **375**, 315–320.
134. Gottwein, E. and Cullen, B.R. (2008) Viral and cellular microRNAs as determinants of viral pathogenesis and immunity. *Cell Host Microbe* **3**, 375–387.
135. Triboulet, R., Mari, B., Lin, Y.L., Chable-Bessia, C., Bennasser, Y., Lebrigand, K., et al. (2007) Suppression of microRNA-silencing pathway by HIV-1 during virus replication. *Science* **315**, 1579–1582.
136. Huang, J., Wang, F., Argyris, E., Chen, K., Liang, Z., Tian, H., et al. (2007) Cellular microRNAs contribute to HIV-1 latency in resting primary CD4+ T lymphocytes. *Nat. Med.* **13**, 1241–1247.
137. Tam, W. and Dahlberg, J.E. (2006) miR-155/BIC as an oncogenic microRNA. *Genes Chromosomes Cancer* **45**, 211–212.
138. Hariharan, M., Scaria, V., Pillai, B. and Brahmachari, S.K. (2005) Targets for human encoded microRNAs in HIV genes. *Biochem. Biophys. Res. Commun.* **337**, 1214–1218.
139. Yeung, M.L., Bennasser, Y., Myers, T.G., Jiang, G., Benkirane, M. and Jeang, K.T. (2005) Changes in microRNA expression profiles in HIV-1-transfected human cells. *Retrovirology* **2**, 81.
140. Eletto, D., Russo, G., Passiatore, G., Del Valle, L., Giordano, A., Khalili, K., Gualco, E. and Peruzzi, F. (2008) Inhibition of SNAP25 expression by HIV-1 Tat involves the activity of mir-128a. *J. Cell. Physiol.* **216**, 764–770.

Chapter 4

Allele-Specific Silencing by RNA Interference

Hirohiko Hohjoh

Abstract

Allele-specific gene silencing by RNA interference (RNAi) is therapeutically useful for specifically inhibiting the expression of disease-associated alleles without suppressing the expression of corresponding wild-type alleles. To realize such allele-specific RNAi (ASP-RNAi), the design and assessment of small interfering RNA (siRNA) duplexes conferring ASP-RNAi is vital; however, it is also difficult. We have developed an assay system with reporter alleles that encode the *Photinus* and *Renilla luciferase* genes carrying mutant and wild-type allelic sequences in their 3′-untranslated regions. The assay system allows us to evaluate designed siRNAs and also short hairpin RNAs for allele-specific silencing against target mutant alleles as well as off-target silencing against corresponding wild-type alleles simultaneously in a qualitative and quantitative manner.

Key words: Allele-specific RNAi (ASP-RNAi), Reporter alleles, *Photinus* and *Renilla* luciferase genes, *β-Galactosidase* gene

1. Introduction

RNA interference (RNAi) is a powerful tool for suppressing the expression of a gene of interest (1, 2), and its application is expanding to various fields of science. Allele-specific gene silencing by RNAi (allele-specific RNAi: ASP-RNAi) is an advanced application of RNAi techniques, by which the expression of an allele of interest can be inhibited without suppressing the expression of its corresponding allele (3). Thus, ASP-RNAi would be therapeutically very useful, as it can specifically inhibit the expression of disease-associated alleles without suppressing the expression of corresponding wild-type alleles (4–12). To realize and control such allele-specific silencing by RNAi, it is necessary to design competent small interfering RNAs (siRNAs) that confer strong allele-specific silencing; thus, siRNAs must be designed such that

Wei-Ping Min and Thomas Ichim (eds.), *RNA Interference*, Methods in Molecular Biology, vol. 623,
DOI 10.1007/978-1-60761-588-0_4,

they are able to carry nucleotide variations characterizing target disease alleles and to discriminate the target alleles from corresponding wild-type alleles. In addition, qualitative and quantitative assessment of such designed siRNAs for allele-specific silencing is also necessary. We have developed an assay system to evaluate ASP-RNAi with mutant and wild-type reporter alleles encoding the *Photinus* and *Renilla luciferase* genes (7, 9). The system allows us to determine the effects of designed siRNAs and short-hairpin RNAs (shRNAs) against mutant (target) alleles in allele-specific silencing, as well as off-target silencing against corresponding wild-type (non-target) alleles simultaneously.

2. Materials

2.1. Chemically Synthesized Oligonucleotides and Annealing

1. Synthetic DNA oligonucleotides (Invitrogen Corporation, Carlsbad, CA, USA).
2. Synthetic siRNAs (TAKARA BIO INC, Shiga, Japan).
3. DNA annealing buffer (10×): 100 mM Tris–HCl (pH 8.0), 10 mM EDTA, 1 M NaCl. Store at 4°C.
4. siRNA annealing buffer (5×): 250 mM Tris–HCl (pH 7.5), 0.5 M NaCl. Store at 4°C.
5. Control siRNA (nonsilencing siRNA) (QIAGEN, Hilden, Germany).
6. TE: 10 mM Tris–HCl (pH 8.0), 1 mM EDTA.
7. RNase-free H_2O: Distilled Water, DNase RNase Free [Invitrogen (Gibco)].

2.2. Construction of Reporter Alleles

1. Plasmids:
   (a) pGL3-Control, phRL-TK, pSV-β-Galactosidase Control vectors (Promega, Madison, WI, USA)
   (b) p β gal-Control vector (TAKARA BIO).
   (c) pGL3-TK (Fig. 1) (see Note 1).
2. Restriction enzymes:
   (a) *Xba*I, *Not*I, *Sph*I, *Nhe*I (NIPPON GENE, Toyama, Japan).
   (b) Restriction enzyme H buffer (10×): 1 M NaCl, 500 mM Tris-HCl (pH 7.5), 100 mM $MgCl_2$, 10 mM DTT.
3. Ligation:
   Ligation-Convenience Kit (NIPPON GENE).
4. Purification of DNA:
   Wizard SV Gel and PCR Clean-Up System (Promega).

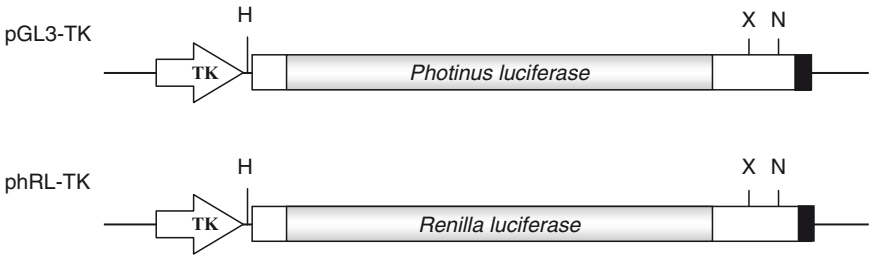

Fig. 1. Schematic drawing of luciferase reporter genes used for the construction of reporter alleles. Plasmids, encoding the reporter genes, are indicated (pGL3-TK, phRL-TK). The herpes simplex virus thymidine kinase promoter (TK) and reporter genes are represented by arrows and boxes, respectively. The amino acid coding region and the SV40 late poly (A) region are indicated by gray and solid boxes, respectively. The *Hin*dIII (H), *Xbal* (X), and *Notl* (N) restriction enzyme sites are indicated

5. Competent cells:
   JM109 Competent cells (Promega).
6. S.O.C. Medium (Invitrogen)

2.3. Isolation of Plasmid DNA

1. STET solution: 8% (w/v) sucrose, 5% (w/v) TritonX-100 (or NP-40), 50 mM Tris–HCl (pH 8.0), 50 mM EDTA. Store at 4°C.
2. TAE buffer (10×): 48.4 g Tris base, 11.42 mL glacial acetic acid, 20 mL of 0.5 M EDTA per liter of deionized H_2O. Store at room temperature.
3. Ribonuclease Mix solution (NIPPON GENE).
4. PEG solution: 20% (w/v) Polyethylene Glycol 6000, 2.5 M NaCl. Sterilize by autoclaving. Store at room temperature.
5. HiSpeed Plasmid kit (Qiagen) for large-scale isolation and purification of plasmid DNA.

2.4. Cell Culture and Transfection

1. Dulbecco's Modified Eagle's Medium (DMEM) (Wako Pure Chemical Industries, Osaka, Japan) supplemented with 10% fetal bovine serum (Invitrogen), 100 U/mL penicillin, and 100 μg/mL streptomycin (Wako).
2. Trypsin-EDTA: 0.25% Trypsin, 1 mM EDTA·4Na (1×)
3. Lipofectamine 2000 Transfection Reagent (Invitrogen).
4. Opti-MEM I Reduced-Serum Medium from (Invitrogen).
5. Dulbecco's Phosphate Buffered Saline [D-PBS(–)] (SIGMA-ALDRICH).

2.5. Luciferase and β-Galactosidase Assay

1. Dual-Luciferase Reporter Assay System (Promega)
2. Beta-Glo Assay System (Promega)
3. Luminometer (see Note 2)

3. Methods

The assay process is schematically shown in Figs. 2 and 3. (1) The *Photinus* and *Renilla luciferase* genes, driven by the same herpes simplex virus thymidine kinase (HSV-TK) promoter, are prepared (Fig. 1) (see Note 3) (13). (2) Reporter alleles are constructed by inserting synthetic oligonucleotides of mutant (target) and wild-type (non-target) allelic sequences into the 3′-untranslated regions (UTRs) of the reporter genes (Fig. 2) (see Note 4), i.e., the resultant reporter alleles encode *luciferase* reporter genes carrying artificially inserted allelic sequences of interest. (3) Various siRNA duplexes targeting alleles of interest (the mutant allele in this protocol) are designed and chemically synthesized (Fig. 2); the important point is that the designed siRNAs must contain nucleotide variation(s) characterizing target alleles. (4) The synthetic siRNA duplexes, reporter alleles, and the *β-galactosidase* gene as

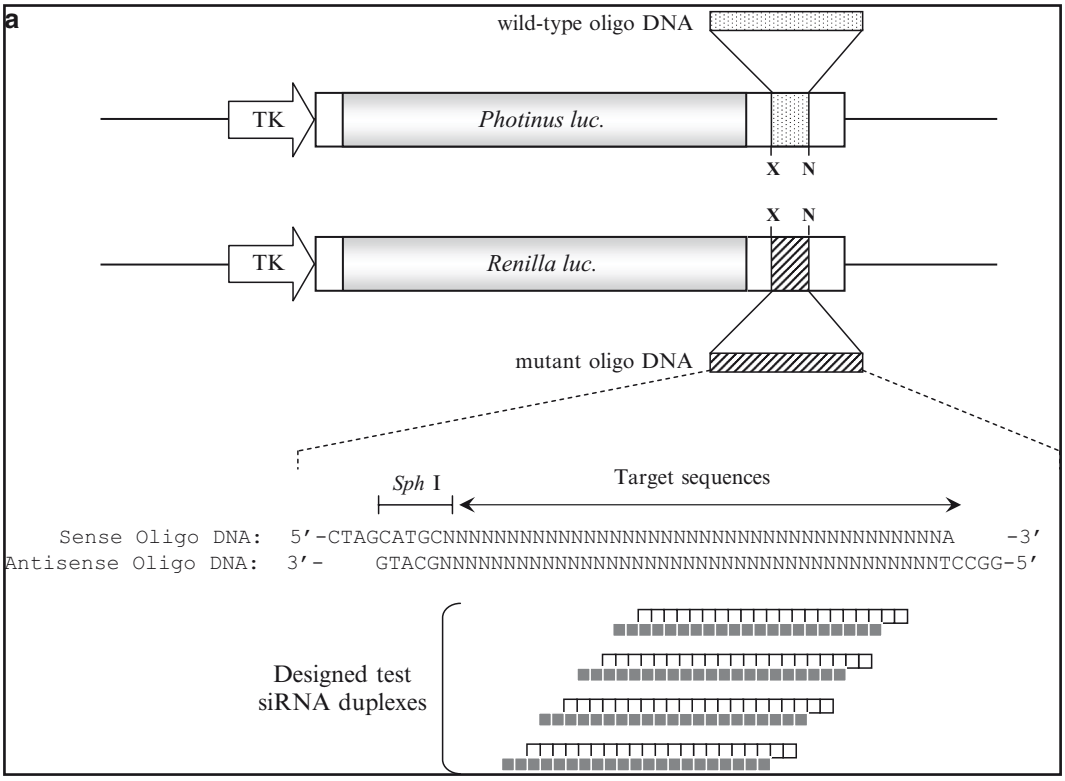

Fig. 2. Schematic drawing of reporter alleles. (**a**) The *Photinus* and *Renilla* luciferase reporter genes are indicated as in Fig. 1. Reporter alleles are constructed by inserting synthetic oligonucleotide duplexes of wild-type (*indicated by dotted box*) and mutant (*indicated by hatched box*) allelic sequences into the 3′-untranslated regions of reporter genes. The inserted oligonucleotide sequences carry the *Sph*I restriction enzyme site for the judgment of proper clones, and possess cohesive ends matched to the *Xba*I (X) and *Not*I (N) digested ends. Various siRNA duplexes targeting the mutant allele (indicated) are designed and assessed.

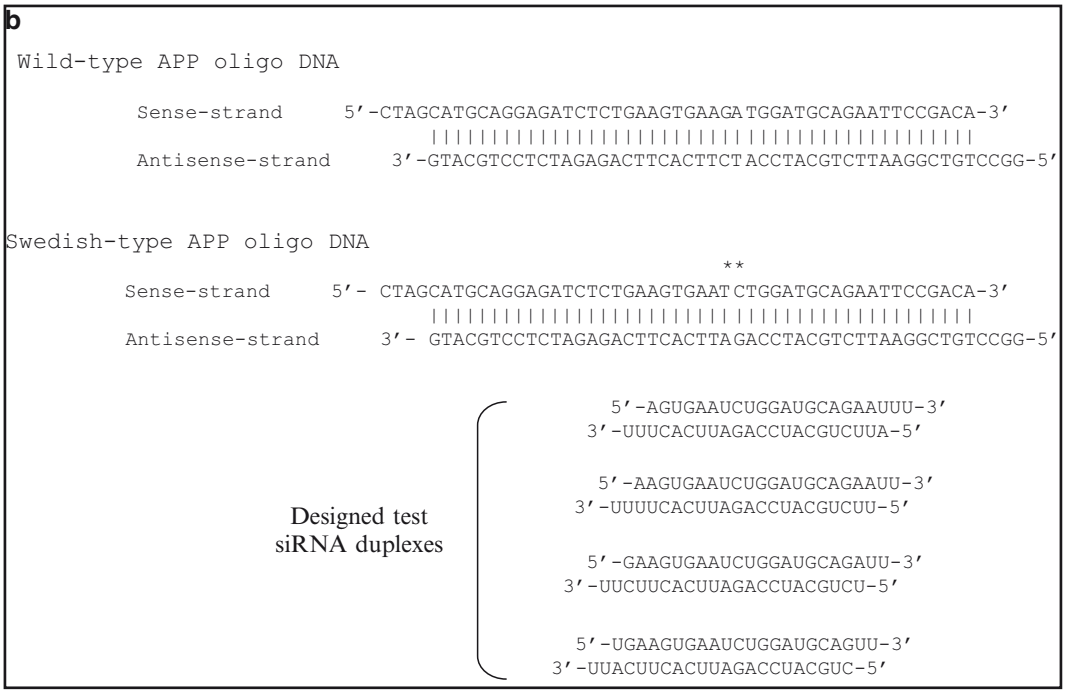

Fig. 2. (continued) (**b**) Designed oligo DNA and siRNA duplexes for ASP-RNAi against the Swedish-type amyloid precursor protein (APP) mutant. As an example, designed oligonucleotide sequences of the wild-type and Swedish-type APP alleles and siRNA duplexes targeting the Swedish-type APP mutant are indicated (7). *Asterisks* indicate the nucleotide variations in the Swedish-type APP mutant

a control (see Note 5) are cotransfected into cultured mammalian cells (Fig. 3). (5) Twenty-four hours after transfection, expression levels of the reporter genes are examined. The level of either target (mutant) allele or non-target (wild-type) allele luciferase activity is normalized against the level of β-galactosidase activity, and the ratios of mutant and wild-type luciferase activities in the presence of test siRNA duplexes are normalized against the control ratios obtained in the presence of siControl duplex (non-silencing siRNA duplex). Because the *Photinus* and *Renilla* luciferases possess distinct substrate preferences to each other and since their expression levels can be represented by their catalytic activities, the assay system enables us to perform qualitative and quantitative assessment for allele-specific silencing.

3.1. Preparation of Allelic Oligonucleotide Sequences

1. Allelic oligonucleotide sequences (sense and anti sense strand sequences) are designed such that nucleotide variation(s) is (are) located at the central position of the sequences, in which the *Sph*I restriction enzyme site is also present (Fig. 2) (see Note 6), and chemically synthesized.
2. Synthetic oligonucleotides are dissolved in TE (final concentration of 100 μM).

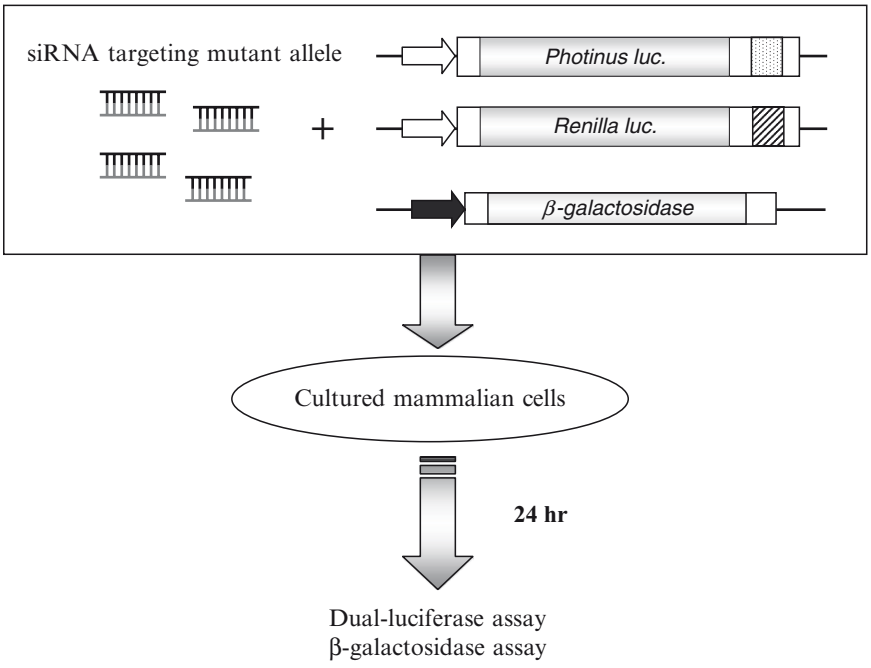

Fig. 3. Schematic drawing of the assay system for allele-specific gene silencing. Wild-type and mutant reporter alleles, synthetic siRNA duplex targeting the mutant allele, and the *β-galactosidase* gene as a control are cotransfected into cultured mammalian cells. Twenty-four hours after transfection, cell lysate is prepared, and expression levels of luciferase and β-galactosidase are examined by means of dual-luciferase and β-galactosidase assay systems

3. Mix the following reagents in a 0.5 mL tube:
   (a) 1 μL of DNA annealing buffer (10×)
   (b) 1 μL of sense strand oligonucleotide (100 μM)
   (c) 1 μL of antisense-strand oligonucleotide (100 μM)
   (d) 7 μL of H_2O
4. Heat-denature at 80°C for 5 min, and let stand at room temperature over 30 min for annealing. Store at 4°C.

3.2. Preparation of Reporter Plasmids

1. Prepare 50 μL of reaction mix as follows:
   (a) 5 μL of 10× Restriction enzyme H buffer
   (b) 1 μL of Reporter plasmid (pGL3-TK and phRL-TK) (1 μg/μL)
   (c) 42 μL of H_2O
   (d) 1 μL of *Not*I (5–20 units/μL)
   (e) 1 μL of *Xba*I (5–20 units/μL)
2. Incubate the reaction at 37°C for 6 h ~ overnight (see Note 7).
3. Purify digested reporter plasmid by a Wizard SV Gel and PCR Clean-Up System according to the manufacturer's instructions (see Note 8).

4. Measure concentration of the purified reporter plasmid fragment. Store at 4°C.

3.3. Ligation and Transformation

1. Prepare 6 μL of ligation reaction mix as follows:
   (a) 2 μL of the purified reporter plasmid fragment (10 μg/mL)
   (b) 1 μL of the annealed oligonucleotide duplex (see Subheading 3.1)
   (c) 3 μL of 2× Ligation Mix
2. Incubate the reaction at 16°C for 30 min.
3. Add the whole reaction to 20 μL of JM109 competent cells on ice.
4. Incubate the cells on ice for 30 min.
5. Heat shock at 42°C for 1 min, and immediately chill on ice.
6. Incubate on ice for 2 min.
7. Add 100 μL of S.O.C. medium (see Note 9) and transfer the transformed competent cells onto agar LB medium containing ampicillin (20 μg/mL).
8. Incubate at 37°C overnight.

3.4. Isolation of Plasmid DNA (easy mini prep.) and Check for Inserted Fragments

1. Culture transformants (bacteria) in 3 of LB medium containing ampicillin (60 μg/mL) at 37°C overnight with vigorous shaking.
2. Pour 1 mL of the culture into a 1.5 mL tube.
3. Centrifuge at 12,000×*g* for 1 min and remove the medium.
4. Add 300 μL of STET, resuspend the bacteria by vortexing, and place on ice for 30 s to 10 min.
5. Place the tube in a boiling water bath for 1 min, and immediately transfer it into iced water.
6. Incubate in iced water for 5 min (see Note 10).
7. Centrifuge at 20,000×*g* for 10 min at 4°C.
8. Collect 200 μL of the supernatant (see Note 11) and transfer it into a 1.5-mL tube.
9. Add 600 μL of ethanol and mix well.
10. Centrifuge at 20,000×*g* for 10 min at 4°C (see Note 12).
11. Remove the supernatant and dry the precipitated pellet.
12. Resuspend the pellet in 50 μL of TE.
13. Prepare 15 μL of restriction enzyme reaction mix as follows:
    (a) 1.5 μL of 10× restriction enzyme H buffer
    (b) 3 μL of plasmid solution
    (c) 9.9 μL of H_2O
    (d) 0.2 μL of *Sph*I (1–2 units)

(e) 0.2 μL of *Eco*RI (1–2 units)

(f) 0.2 μL of Ribonuclease Mix solution 14. Incubate the reaction at 37°C for 5 h

14. Examine 8 μL of the reaction by gel electrophoresis with a 1% agarose gel in 1× TAE buffer, followed by ethidium bromide staining.
15. See Fig. 4 for a judgment of positive clones.
16. Treat the plasmid solution before sequence determination as follows:

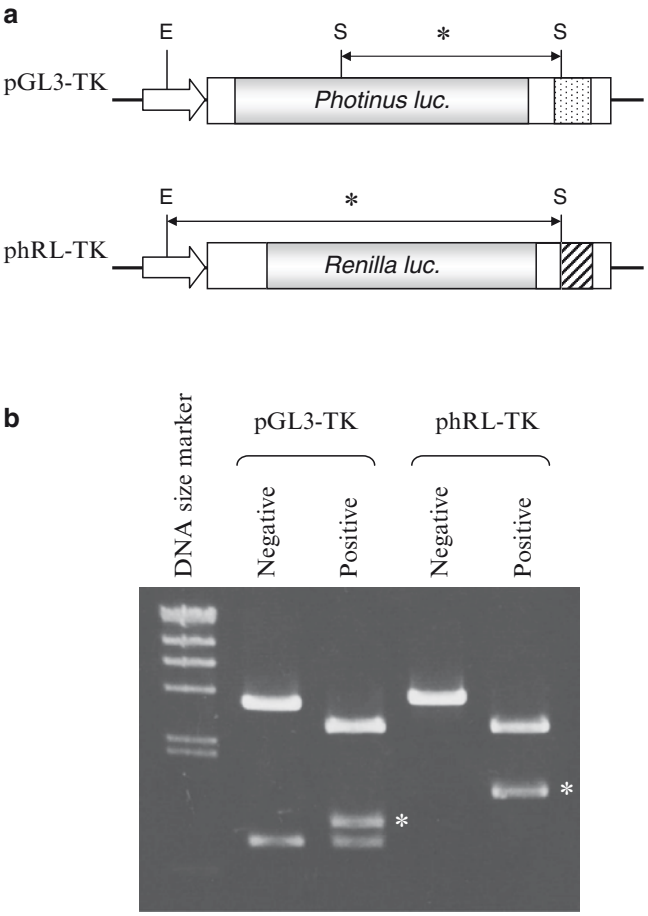

Fig. 4. Positive clone selection. (**a**) Schematic drawing of proper reporter alleles. Reporter alleles are represented as in Fig. 4.2. The *Sph*I (S) and *Eco*RI (E) restriction enzyme sites are indicated. The expected DNA fragments derived from positive report alleles are indicated by asterisks. (**b**) Agarose gel electrophoresis profiles of reporter plasmids. Plasmid DNAs were digested with *Sph*I and *Eco*RI and electrophoretically separated in 1% agarose gels. Positive and negative clone examples in each of the reporter plasmids are shown. The DNA fragments derived from the positive reporter alleles are indicated by asterisks as in A. DNA size marker is *Hin*dIII-digested λDNA

(a) Add 1 μL of Ribonuclease Mix solution
(b) Incubate at 37°C for 30 min
(c) Add 30 μL of PEG solution
(d) Incubate on ice for 1 h
(e) Centrifuge at 20,000×*g* for 10 min at 4°C
(f) Rinse the pellet with 75% ethanol, and air dry
(g) Dissolve the pellet in 20 μL of TE

17. Sequence determination by a conventional dye terminator cycle sequencing with following sequence primers:

    Primer for pGL3-TK backbone plasmids:5′-TGTGGACGAA GTACCGAAAG-3′

    Sequence primer for phRL-TK backbone plasmids:

    5′-CTAACACCGAGTTCGTGAAG-3′

3.5. Preparation of siRNA Duplexes (20 μM)

1. Mix the following reagents in a 0.5-mL tube:
   (a) 20 μL of siRNA annealing buffer (5×)
   (b) 2 μL of sense stranded oligonucleotide (1 mM)
   (c) 2 μL of antisense stranded oligonucleotide (1 mM)
   (d) 76 μL of RNase-free H_2O
2. Heat-denature at 80°C for 5 min, and stand at 37°C over 30 min for annealing. Store at –20°C (see Note 13).

3.6. Transfection

1. Prepare cells for transfection as follows:

   The day before transfection, cultured cells are trypsinized, diluted with fresh medium without antibiotics, and seeded onto 24-well culture plates (approximately 0.5×10^5 cells/well).
2. Mix together the plasmid DNA solutions (see Note 14) (for 10 tests):
   (a) 10 μL of pGL3-TK backbone plasmid (0.2 μg/μL)
   (b) 10 μL of phRL-TK backbone plasmid (0.05 μg/μL)
   (c) 10 μL of pβgal-Control vector (0.1 μg/μL)
3. Prepare each transfection sample as follows (see Note 15):
   (a) Dilute 3 μL of the plasmid mixture and 1 μL of each siRNA duplex in 50 μL of Opti-MEM I (see Note 16)
   (b) Dilute 1 μL of Lipofectamine 2000 in 50 μL of Opti-MEM I, mix gently and incubate for 5 min at room temperature
   (c) Combine the diluted plasmids and siRNA (a) with the diluted Lipofectamine 2000 (b), and mix gently (total volume is 100 μL)
   (d) Incubate for 20 min at room temperature
4. During the incubation, replace the culture medium with 0.5 mL of fresh medium without antibiotics.

5. After 20 min incubation, add the 100 μL of the transfection mixture to each well containing cells and medium.
6. Incubate the cells at 37°C in 5% CO_2 humidified chamber for 24 h.

3.7. Determination of the Expression Levels of Reporter Alleles

1. Rinse the transfected cells twice with D-PBS(−).
2. Add 100 μL of Passive Lysis buffer (1×) (contained in the Dual-Luciferase Reporter Assay System) to each well.
3. Gently shake for 15 min at room temperature.
4. Determine the *Photinus* and *Renilla* luciferase activities by the Dual-Luciferase Reporter Assay System with 10 μL of each cell lysate according to the manufacturer's instructions. (see Note 17)
5. Determine the β-galactosidase activity as a control by Beta-Glo Assay System with 10 μL of each cell lysate according to the manufacturer's instructions. (see Note 17)
6. Calculate the expression levels of reporter alleles as follows (see Table 1):
   (a) Normalized wild-type allele expression in the presence of test siRNA:
   Pho_luc(siTest)/Gal(siTest)
   (b) Normalized mutant allele expression in the presence of test siRNA:
   Re_luc(siTest)/Gal(siTest)
   (c) Normalized wild-type allele expression in the presence of control siRNA:
   Pho_luc(siCont)/Gal(siCont)
   (d) Normalized mutant allele expression in the presence of control siRNA:
   Re_luc(siCont)/Gal(siCont)

Table 1
Data obtained by the reporter gene expression assays

	Test siRNA (siTest)	Control siRNA (siCont)
Photinus luciferase (wild-type allele)	Pho_luc(siTest)(540)	Pho_luc(siCont)(500)
Renilla luciferase (mutant allele)	Re_luc(siTest)(420)	Re_luc(siCont)(2,500)
β-Galactosidase	Gal(siTest)(6,000)	Gal(siCont)(5,000)

Figures in parentheses are examples of assay data given in arbitrary units, and used for plotting graphs in Fig. 5

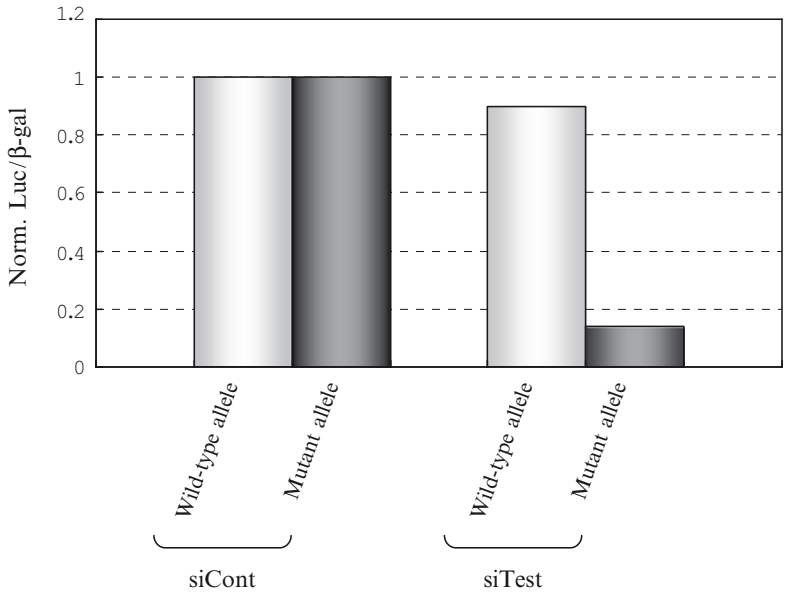

Fig. 5. Example of assessment of ASP-RNAi with reporter alleles. Examples of luciferase and β-galactosidase activity data are indicated in Table 1. Levels of either mutant (*dark gray boxes*) or wild-type (*light gray boxes*) allele luciferase activity are normalized against the levels of β-galactosidase activity (**step 6a–d** of Subheading 3.7), and the ratios of mutant and wild-type luciferase activities in the presence of test siRNAs (siTest) are normalized against the control ratios obtained in the presence of control siRNA (siCont) (**step 6e and f** of Subheading 3.7)

(e) Suppression level of untargeted wild-type allele by the test siRNA:

[Pho_luc(siTest)/Gal(siTest)]/[Pho_luc(siCont)/Gal(siCont)]

(f) Suppression level of targeted mutant allele by the test siRNA:

[Re_luc(siTest)/Gal(siTest)]/[Re_luc(siCont)/Gal(siCont)]

4. Notes

1. pGL3-TK is constructed by substitution of the *Hin*dIII-*Xba*I region encoding the *Photinus luciferase* gene from the pGL3-Control vector, for the *Hin*dIII-*Xba*I region containing the *Renilla luciferase* gene in the phRL-TK vector: the resultant pGL3-TK plasmid contains the *Photinus luciferase* gene linked with the TK promoter (Fig. 1) (13).
2. TD-20/20 (Promega) is used in our assay.
3. This is done to avoid a bias derived from transcriptional activities. Accordingly, if the *Photinus* and *Renilla luciferase* genes are expressed by a common promoter, any promoters may be acceptable.

4. Because synthetic allelic sequences are inserted into the 3′-UTR of the reporter genes, there is no need to worry about any in-frame insertion of the allelic sequences into the reporter genes.
5. The expression of the *β-galactosidase* gene is examined as a non-silencing control because both target and non-target reporter alleles more or less undergo gene silencing.
6. The *Sph*I restriction enzyme site is used for the judgment of proper reporter alleles in plasmid screening.
7. I recommend using an air incubator to avoid water droplet condensation in long duration incubations.
8. The short DNA fragment generated by restriction enzyme digestion can be eliminated by purification.
9. If necessary, after adding S.O.C. medium, the transformed competent cells can be incubated at 37°C for 1 h, as with conventional methods.
10. This incubation is important for the aggregation of denatured proteins and bacterial chromosomal DNA.
11. In the case of inadequate aggregation, collect the supernatant carefully so as not to take bacterial chromosomal DNA.
12. No incubation before centrifugation is necessary because contaminating bacterial RNAs can function as a carrier and help ethanol-precipitation of plasmid DNAs.
13. Divide the annealed siRNA solution into several aliquots and store them. This is done to avoid degradation of siRNA from repeated freezing and thawing.
14. Plasmid DNAs for transfection are prepared by a HiSpeed Plasmid kit (Qiagen).
15. This transfection procedure almost follows the instructions of the manufacturer.
16. Preparation of plasmid DNAs and siRNA is separately carried out: dilute plasmid DNAs and siRNA each in Opti-MEM I, and combine each with the diluted Lipofectamine 2000 transfection reagent.
17. Prepare enough master assay reagents for testing all the samples and extra ones (2–3 samples) before transferring the reagents into test tubes. Do not use or add a different vial of reagents during the assays. This is very important in order to carry out all the assays under the same condition.

Acknowledgments

The author would like to thank Yusuke Ohnishi and Mariko Yoshida for their helpful assistance. This work was supported by a research grant from the Ministry of Health, Labor, and Welfare of Japan and by a Grant-in-Aid from the Japan Society for the Promotion of Science.

References

1. Dykxhoorn, D.M., Novina, C.D. and Sharp, P.A. (2003) Killing the messenger: short RNAs that silence gene expression. *Nat. Rev. Mol. Cell Biol.* **4**, 457–467.
2. Meister, G. and Tuschl, T. (2004) Mechanisms of gene silencing by double-stranded RNA. *Nature* **431**, 343–349.
3. Victor, M., Bei, Y., Gay, F., Calvo, D., Mello, C. and Shi, Y. (2002) HAT activity is essential for CBP-1-dependent transcription and differentiation in *Caenorhabditis elegans*. *EMBO Rep.* **3**, 50–55.
4. Wood, M., Yin, H. and McClorey, G. (2007) Modulating the expression of disease genes with RNA-based therapy. *PLoS Genet.* **3**, e109.
5. Miller, V.M., Gouvion, C.M., Davidson, B.L. and Paulson, H.L. (2004) Targeting Alzheimer's disease genes with RNA interference: an efficient strategy for silencing mutant alleles. *Nucleic Acids Res.* **32**, 661–668.
6. Miller, V.M., Xia, H., Marrs, G.L., Gouvion, C.M., Lee, G., Davidson, B.L. and Paulson, H.L. (2003) Allele-specific silencing of dominant disease genes. *Proc. Natl. Acad. Sci. U.S.A.* **100**, 7195–7200.
7. Ohnishi, Y., Tokunaga, K., Kaneko, K. and Hohjoh, H. (2006) Assessment of allele-specific gene silencing by RNA interference with mutant and wild-type reporter alleles. *J. RNAi Gene Silencing*, **2**, 154–160.
8. Xia, H., Mao, Q., Eliason, S.L., Harper, S.Q., Martins, I.H., Orr, H.T., et al. (2004) RNAi suppresses polyglutamine-induced neurodegeneration in a model of spinocerebellar ataxia. *Nat. Med.* **10**, 816–820.
9. Ohnishi, Y., Tamura, Y., Yoshida, M., Tokunaga, K. and Hohjoh, H. (2008) Enhancement of allele discrimination by introduction of nucleotide mismatches into siRNA in allele-specific gene silencing by RNAi. *PLoS ONE* **3**, e2248.
10. Rodriguez-Lebron, E. and Paulson, H.L. (2006) Allele-specific RNA interference for neurological disease. *Gene Ther.* **13**, 576–581.
11. Maxwell, M.M., Pasinelli, P., Kazantsev, A.G. and Brown, R.H., Jr. (2004) RNA interference-mediated silencing of mutant superoxide dismutase rescues cyclosporin A-induced death in cultured neuroblastoma cells. *Proc. Natl. Acad. Sci. U.S.A.* **101**, 3178–3183.
12. Denovan-Wright, E.M. and Davidson, B.L. (2006) RNAi: a potential therapy for the dominantly inherited nucleotide repeat diseases. *Gene Ther.* **13**, 525–531.
13. Ohnishi, Y., Tokunaga, K. and Hohjoh, H. (2005) Influence of assembly of siRNA elements into RNA-induced silencing complex by fork-siRNA duplex carrying nucleotide mismatches at the 3′- or 5′-end of the sense-stranded siRNA element. *Biochem. Biophys. Res. Commun.* **329**, 516–521.

Chapter 5

Computational siRNA Design Considering Alternative Splicing

Young J. Kim

Abstract

RNA interference (RNAi) with small interfering RNA (siRNA) has become a powerful tool in functional and medical genomic research through directed post-transcriptional gene silencing. In order to apply RNAi technique to eukaryotic organisms, where frequent alternative splicing results in diversification of mRNAs and finally of proteins, we need spliced mRNA isoform silencing to study the function of individual proteins.

AsiDesigner is a web-based siRNA design software system, which provides siRNA design capability to account for alternative splicing in mRNA level gene silencing. It provides numerous novel functions, including designing common siRNAs for the silencing of more than two mRNAs simultaneously, a scoring scheme to evaluate the performance of designed siRNAs by adopting state-of-the-art design factors, stepwise off-target searching with BLAST and FASTA algorithms, as well as checking the folding secondary structure energy of siRNAs.

To do this, we developed a novel algorithm to evaluate the common target region where siRNAs can be designed to knockdown a specific mRNA isoform or more than two mRNA isoforms from a target gene simultaneously. The developed algorithm and the AsiDesigner were tested and validated as being very effective throughout widely performed gene silencing experiments. It is expected that AsiDesigner will play an important role in functional genomics, drug discovery, and other molecular biological research. AsiDesigner is freely accessible at http://sysbio.kribb.re.kr/AsiDesigner.

Key words: siRNA, RNAi, Design, AsiDesigner, Alternative splicing

1. Introduction

Short interfering RNAs (siRNAs) degrade specific target mRNAs, the transcription products of genes through the RNA interference (RNAi) mechanism. The importance of siRNAs has been widely recognized, and a series of studies on siRNA applications have been conducted in diverse research fields, including functional genomics and drug discovery (1, 2).

Wei-Ping Min and Thomas Ichim (eds.), *RNA Interference*, Methods in Molecular Biology, vol. 623,
DOI 10.1007/978-1-60761-588-0_5, © Springer Science+Business Media, LLC 2010

To date, various siRNA design algorithms and programs have been developed and serviced to provide good performance in siRNA design for biologists (3). These include many design servers provided by both enterprises engaged in siRNA-related business (4–8) and open source society (9–11). Traditionally, these siRNA design algorithms have considered certain rules, such as Tuschl's rules (12) that contain several parameters: 3′overhangs, GC contents, absence of internal repeats, homology to other mRNAs, absence of SNPs, and RNA secondary structure, etc. In recent years, the binding energy factors of double stranded region were considered important; as Khvorova suggested, the thermodynamic properties of siRNA play a critical role in determining the functions (13). Reynold's algorithm and Choi's algorithm also considered relative binding energy profiles for rational siRNA design (14, 15). These algorithms are known to be efficient for siRNA selection; however, the algorithms are limited to gene-level silencing. Restated, their knockdown capacity is limited to a specific mRNA or to all the isoforms from a target gene.

For eukaryotic organisms, alternative splicing contributes to the diversity of gene functions, resulting in the production of multiple proteins from a gene (16). Thus, it is necessary to control an individual spliced mRNA isoform producing a specific protein to thoroughly study the functions of alternatively splicing genes (17). Moreover, it is feasible to knockdown a specific combination of more than two mRNA isoforms from a gene simultaneously. In this case, the possible combination of targets, dependent on the purpose of research, and the number of combinations, will be too numerous to prepare siRNA libraries for all the occasions. Thus, considering alternative splicing a new algorithm and tool to design common siRNAs for a given combination of targets is urgently needed.

We developed a novel algorithm to evaluate a common target region where siRNAs can be designed to knockdown a specific mRNA isoform or multiple mRNA isoforms from a target gene (18). AsiDesigner is a web-based siRNA design software system, providing siRNA design capability to take into account alternative splicing for mRNA level gene silencing. It provides many useful functions, which include designing common siRNAs for silencing more than two mRNAs simultaneously, a scoring scheme to evaluate the performance of designed siRNAs by adopting state-of-the-art design factors, a two-step off-target searching with sequence alignment algorithms, and checking the folding secondary structure energy of siRNAs.

2. Materials

AsiDesigner was developed on a Linux machine (kernel release 2.6.9–67.0.7.ELsmp) that had eight Intel dual quad processors, 16 GB of memory and software programs (Apache 2.0.48, MySQL 5.0.45, Bioperl 1.52, and Perl 5.8.8).

3. Methods

3.1. Evaluation of a Common Target Region

AsiDesigner uses a novel and effective algorithm for selecting siRNA target regions that consider alternative splicing. The purpose of this algorithm is to evaluate a region to design siRNAs targeting one or more mRNAs selectively from an available mRNA isoform set of a target gene. To design siRNAs, a target region must be selected from common exons of the targeted mRNA isoforms, and any exons of non-target mRNA isoforms should be excluded from this target region. Therefore, as shown in Fig. 1a, the final target region will be equivalent to the subtraction of the union of non-target isoform mRNA exons from the intersection of target isoform mRNA exons. There could be two methods to achieve this purpose: the first may use the result of multiple sequence alignment of all the available mRNA isoforms, and the second may use the result of mapping all the available isoform mRNAs on the genome. In this algorithm, we applied the latter method and the mapping information of mRNAs on the genome of UCSC Genome Bioinformatics (http://genome.ucsc.edu/) was utilized.

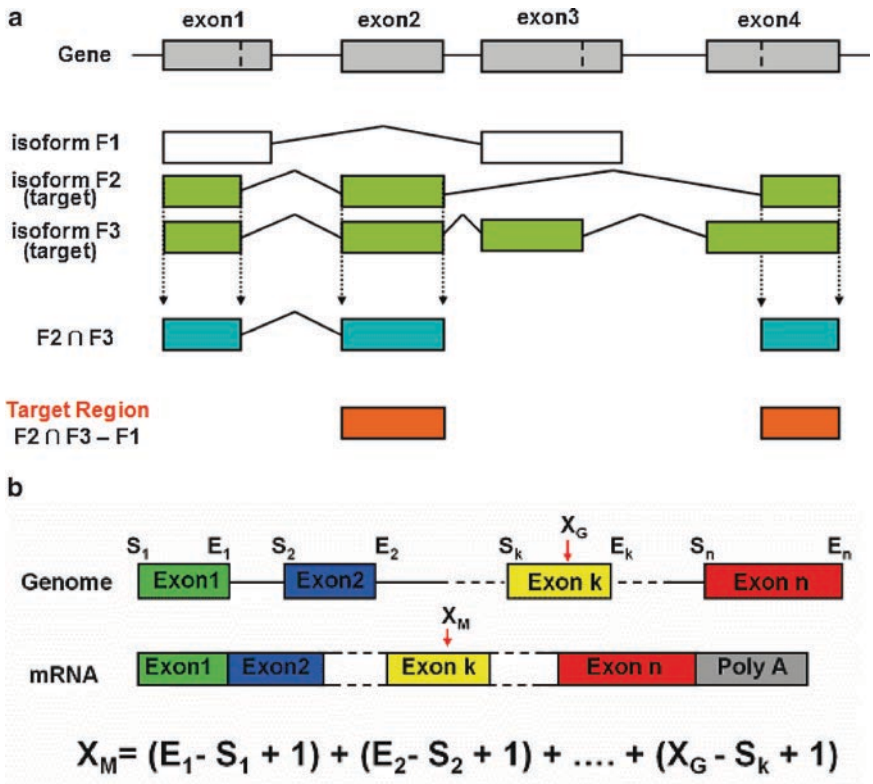

Fig. 1. Schematic diagrams for evaluating a target region to design siRNAs for specific alternative spliced isoforms (**a**) and conversion process of a siRNA position on the genome to the mRNA-based coordinate (**b**)

In an actual evaluation of target region, this process is carried out with the information of both target and non-target exon positions. First, common target exon region is evaluated as follows:

- Select a target isoform mRNA as the main target and other mRNA isoforms as the co-targets,
- Evaluate common exon region(s) of the main target and one of the co-targets by comparing their positions on the genome,
- Evaluate common exon region(s) of previously evaluated common exon region and one of the other co-targets,
- Repeat this processing until all co-targets are processed.

Next, the final target region evaluation is the same as the preceding method. It is accomplished by the repeated exclusion of the overlapping regions of common target exon regions with the non-target exon regions.

The target template sequence for siRNA design can be extracted from genome or mRNA sequence corresponding to the target region. However, the actual target of siRNA is mRNA, and there may be a little difference between the genome and mRNA sequences by post-transcriptional processing such as RNA editing. Since we need to use a mRNA sequence to extract templates, the position information of target region on the genome was converted to that on the main target mRNA by Eq. 1 for a sense strand coded gene on the genome as shown in Fig. 1b.

$$X_{M+} = (X_G - S_k + 1) + \sum_{i=1}^{k-1} (E_i - S_i + 1) \quad (1)$$

Here, XM_+ is the position on the main target mRNA corresponding to XG, the position on the genome, for a gene made of n exons. Si is the starting position of i-th exon and Ei is the end position of i-th exon. If a gene is coded in an antisense strand on the genome, Eq. 2 may be used.

$$X_{M-} = (S_k - X_G) + \sum_{i=k}^{n} (E_i - S_i + 1) \quad (2)$$

3.2. Rules for siRNA Selection and Efficiency Scoring

After evaluating the common target region and sequence, actual siRNA design is performed by the optimized siRNA design algorithm, implementing the relative binding energy profile discrimination method published previously (15). The algorithm includes consideration of state-of-the-art design factors and efficiency of each candidate siRNA sequence generated from a template sequence of the target region, which is assessed by applying the following siRNA selection and performance scoring rules.

3.2.1. siRNA Selection Rules

Candidate siRNA sequences are screened and selected based on the following selection rules:

- G/C content: users set up allowable range of GC content (default: 30–62%),
- Maximum consecutive bases (default: maximum 5 for A or T, maximum 3 for G or C, and maximum 7 for G/C mixed),
- Existence of single nucleotide polymorphism (SNP) in the siRNA target region,
- Self-alignment energy of siRNA ($\Delta G < -4$ kcal/mol by Mfold),
- Maximum identical bases to the non-target mRNAs for off-target filtering (default: equal to or less than 15/19).

3.2.2. Scoring Rules for siRNA Efficiency

AsiDesigner uses an optimized scoring scheme to assess the performance of designed siRNAs. This performance scoring system assigns individual scores (*Zi*) for five main design parameters affecting the performance of siRNAs and combines them linearly with the statistically evaluated weighting factors (*Wi*) for each design parameter to get the final performance score (*Zt*) (15).

$$Z_t = \frac{\sum_i W_i \frac{Z_i}{M_i}}{\sum_i W_i} \times 100 \tag{3}$$

Where *Mi* is the maximum score for each design parameter, *i* is an index for each design parameter: 36–53% GC content, 3 or more A/U existence at 15–19th bases from 5′ sense position, G/C existence at the 1st 5′ sense position, A/U existence at the 19th base from 5′ sense position, and the relative binding energy profile respectively, and $W_1 = 0.11$, $W_2 = 0.07$, $W_3 = 0.5$, $W_4 = 0.19$, and $W_5 = 0.90$. A schematic diagram for a siRNA design process in AsiDesigner is shown in Fig. 2.

3.3. Implementation

AsiDesigner was developed as a web application program based on Java, JSP/JSF technologies and MySQL relational database. Users may access and interactively use AsiDesigner under the user-friendly GUI environment through the internet.

3.3.1. Input and Options

With a step-by-step input interface (Fig. 3), users can design siRNAs by AsiDesigner with ease. After searching and selecting target mRNA(s) or submitting a target mRNA sequence, AsiDesigner (with a number of design options) designs and provides a sequential list of optimized siRNAs by using the internal algorithm and scoring scheme.

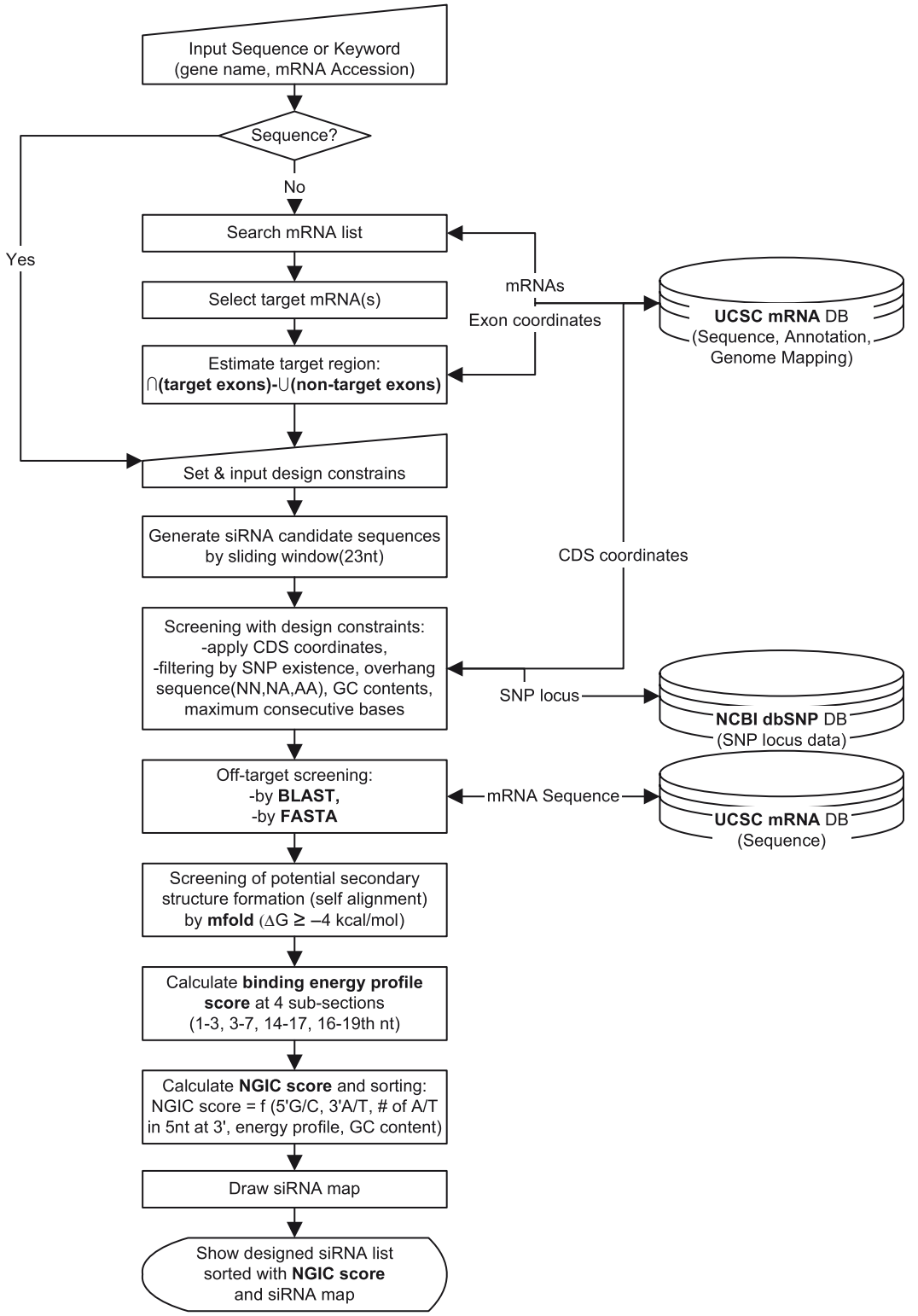

Fig. 2. Schematic diagram of a data processing flow for siRNAs design in AsiDesigner

Fig. 3. Screenshots for siRNA design procedure in AsiDesigner: step 1 for submitting target information in terms of gene symbol or GenBank accession number of mRNA or protein (**a**), step 2 for target mRNA selection and available isoform search (**b**), step 3 for co-target isoform selection (**c**), step 4 for setting siRNA design options (**d**), and step 5 for the output of designed siRNA list (**e**)

To search and select target mRNA(s), users undertake the following steps (Fig. 3a–c):

1. Selection of organism and retrieving target gene (mRNAs),
2. Selection of main target mRNA from the retrieved mRNA list and searching available mRNA isoforms from the target gene, and
3. Selection of co-target mRNA(s) from the retrieved available mRNA isoforms.

In the input window (Fig. 3a), an organism list box for human, mouse, and rat is provided as choices. The organism information chosen is then used for searching genes or mRNAs, off-target filtering and SNP checking for the selected organism. In the next step, in order to search for the target gene or mRNA information, users may use keywords, i.e. gene symbols (for example "BCL2l1" or "BRCA2") or GenBank accession numbers of mRNAs or proteins (for example "NM_138578" or "NP_612815"), which is the keyword-based input mode. Alternatively, if users have only partial sequence of target mRNA, it is possible to use DNA or RNA sequence in the sequence-based input mode in FASTA format.

After submitting target gene information in the keyword-based input mode, AsiDesigner retrieves gene information from the mRNA database corresponding to the given keyword and prints out a matched mRNA list (Fig. 3b). Users check whether the mRNA from the target exists in the list and select one of them as a main target, then all the available mRNA isoforms of the main target mRNA are retrieved and listed in a table with a map (Fig. 3c). After checking co-target mRNAs in the available mRNA isoform list, a window for setting up design options appears (Fig. 3d). In the design option window, users can set options such as types of overhang (AA, NA, or NN), sub-target region, range of GC content, identify limit for off-target filtering, SNP-based filtering, secondary structure-based filtering, and the number of siRNAs to be shown. Detailed information with respect to siRNA design with AsiDesigner is provided on the web page.

In the sequence-based input mode, once a user submits a sequence after selecting an organism, a design option window appears and the following processes will be identical to the keyword-based input mode. Input target sequence should be in FASTA format and should include a string of unmodified RNA/DNA bases i.e., A, U/T, G, and C only. Any other characters in the sequence will be edited and removed. Multiple FASTA format sequences are not supported; only the first sequence will be processed. The maximum length of the input sequence is 5 kbps.

3.3.2. Output

After setting and submitting the design options, AsiDesigner designs optimized siRNA candidates using the internal algorithm and performance scoring scheme. AsiDesigner provides a sequential list of the designed siRNAs by their evaluated performance scores. The output includes the position on the main target mRNA,

siRNA sequence, GC content, existence of SNP site in the region, identity from off-target search, energy-profile score, and estimated melting temperature. Users may check and compare the position of the designed siRNAs in the output map that shows the exon structure of the target gene and non-target mRNA isoforms (Fig. 3e). Sequences of designed siRNAs are provided as the form of 23 bp RNA sequences: the left 1–2nd bases lower cased are the overhang of the antisense siRNA, the next 3–21st bases upper cased are the double stranded region, and the last 22–23rd bases lower cased are the overhang of the sense siRNA.

3.3.3. Data and Used Tools

For the keyword-based gene search, genic annotation and genome map (physical position) data of mRNAs (hg18, Mar. 2006; mm8, Mar. 2006; rn4, Nov. 2004) from UCSC Genome Bioinformatics were retrieved and stored in MySQL relational database (RDBMS). To perform off-target search, NCBI BLAST (19) and FASTA (20) programs were utilized with RefSeq mRNA sequence set (Release 22, Mar. 2007) from UCSC Genome Bioinformatics. Mfold (21) program was used for evaluating the folding energies in the secondary structures of designed siRNAs. To test the existence of SNP sites in designed siRNAs, SNP data from NCBI dbSNP (Build 127, Mar. 2007) were used with MySQL RDBMS.

3.4. Performance of Designed siRNAS

siRNAs targeted for the alternatively spliced forms of a gene are illustrated in Fig. 4. In this case, BCLX (BCL2L1) gene, which has two isoform mRNAs, Bcl-xL (NM_138578) and Bcl-xS (NM_001191), was selected as an example. The siRNAs targeted on both BCL-xL and BCL-xS (Fig. 4a) are located differently from those targeted on BCL-xL only (Fig. 4b). When BCL-xL was targeted alone, the exon region that belongs to only BCL-xL was considered for siRNA design. To verify designed siRNA performance, silencing experiments were conducted as shown in Fig. 5. Three siRNAs to knockdown both mRNAs (siRNA set 1: 719, 1632, and 644) and four siRNAs to knockdown Bcl-xL alone (siRNA set 2: 830, 819, 899, and 820) were designed and transfected into the human cell line (HeLa). Northern blotting analysis was conducted after RT-PCR. Lipofectamine 2000 was used as transfection reagent and 100 nM siRNAs were applied. Knockdown rates were analyzed using the TotalLab software program (Phoretix Co., Newcastle Upon Tyne, United Kingdom). In case of siRNA set 1, the average knockdown rates for Bcl-xL and Bcl-xS were 73% and 100%, respectively, and 71% and 2%, respectively, for siRNA set 2. Consequently, we verified that the siRNA set 2 targeting Bcl-xL alone silenced Bcl-xL properly, while siRNA set 1 targeting both isoforms knocked down both Bcl-xL and Bcl-xS as expected.

Besides this result, the performance of AsiDesigner was validated through numerous gene silencing experiments, a total of over 300 siRNAs from 12 genes (survivin, NFKB, VEGF, HCCR1, PP2A-a, PP2A-b, STE kinase, Caspase, TK kinase, and CUT).

a

Gene	siRNA pos.	Sequence	GC cont.	SNP exist	Identity	EP Score	Tm
BCL2L1	2248	ugCUGUACAUAUUUGAGACUAgu	0.32	NO	14	100.0	48.25
BCL2L1	1958	gcCCUGAGGUGAAAGGGAGCUau	0.58	NO	14	100.0	63.52
BCL2L1	717	gaCAGCAUAUCAGAGCUUUGAac	0.42	NO	15	80.9	53.9
BCL2L1	28	uuCCUGAGCUUCGCAAUUCCUgu	0.53	NO	13	80.9	59.06
BCL2L1	1819	auGACCAUACUGAGGGACCAAcu	0.53	NO	13	80.9	61.02
BCL2L1	172	acCUGUGAUACAAAAGAUCUUcc	0.32	NO	15	90.4	46.84
BCL2L1	642	ggCAGGCGACGAGUUUGAACUgc	0.53	NO	13	77.5	58.33
BCL2L1	2241	ggCUCUCUGCUGUACAUAUUUga	0.37	NO	15	72.5	51.13
BCL2L1	1777	gcAGUUCAGCACCACCCUAGUcc	0.53	NO	14	90.4	62.83
BCL2L1	714	agGGACAGCAUAUCAGAGCUUug	0.47	NO	15	72.5	57.31

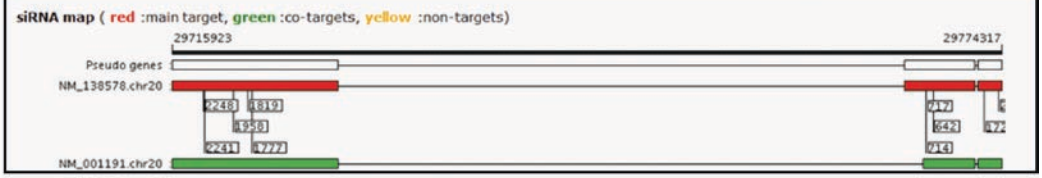

b

Gene	siRNA pos.	Sequence	GC cont.	SNP exist	Identity	EP Score	Tm
BCL2L1	830	uaGACAAGGAGAUGCAGGUAUug	0.47	NO	15	62.9	57.42
BCL2L1	819	cgUGGAAAGCGUAGACAAGGAga	0.47	NO	13	77.5	58.5
BCL2L1	836	agGAGAUGCAGGUAUUGGUGAgu	0.47	NO	15	59.6	57.48
BCL2L1	831	agACAAGGAGAUGCAGGUAUUgg	0.42	NO	14	72.5	55.71
BCL2L1	876	ggCCACUUACCUGAAUGACCAcc	0.47	NO	13	58.4	57.78
BCL2L1	899	uaGAGCCUUGGAUCCAGGAGAac	0.58	NO	15	69.1	63.15
BCL2L1	820	guGGAAAGCGUAGACAAGGAGau	0.53	NO	13	77.5	58.48
BCL2L1	880	acUUACCUGAAUGACCACCUAga	0.42	NO	15	69.1	56.77
BCL2L1	779	guCGCAUUGUGGCCUUUUUCUcc	0.47	NO	14	50.0	55.97
BCL2L1	817	ugCGUGGAAAGCGUAGACAAGga	0.53	NO	13	72.5	57.38

Fig. 4. Designed siRNAs of human BCLX (BCL2L1) gene that has two isoform mRNAs, Bcl-xL (NM_138578) and Bcl-xS (NM_001191). (**a**) 10 siRNAs targeted on both BCL-xL and BCL-xS. (**b**) 10 siRNAs targeted on only BCL-xL

Also, it was used to design 67 siRNAs from seven genes (EGFP, MAPT, SNCA, SNCB, ACTB, HSP22, and GARS) with our collaborative researchers and also to build pre-designed human kinase and phosphatase siRNA libraries.

4. Notes

At least two siRNAs should be tried in an experiment to rule out a successful knockdown by chance. When two or more siRNAs need to be selected, consider highly performance-scored siRNAs that are located away from each other, for example, 100 bps.

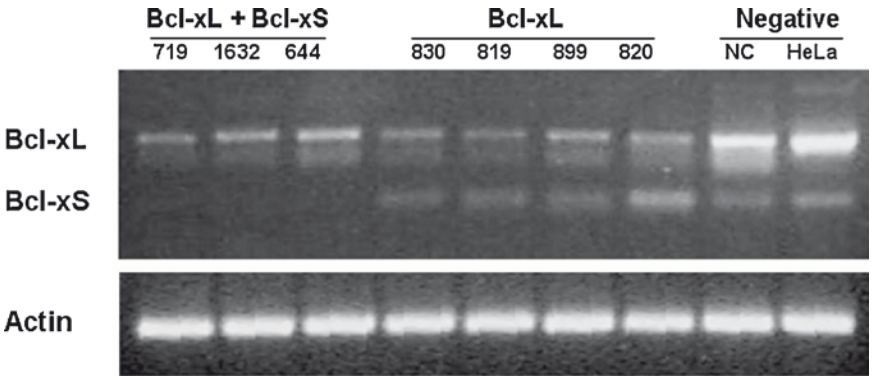

Fig. 5. Results of gene silencing experiments for two alternative isoforms, Bcl-xL (NM_138578) and Bcl-xS (NM_001191) of human BCLX (BCL2L1) gene. siRNA transfection was performed into the human cell line (HeLa) for three siRNAs to knockdown both mRNAs (siRNA set 1: 719, 1632, and 644) and four siRNAs to knockdown Bcl-xL mRNA alone (siRNA set 2: 830, 819, 899, and 820). The average knockdown rates for Bcl-xL and Bcl-xS were 73% and 100 %, respectively, by siRNA set 1 and 71% and 2%, respectively, by siRNA set 2

Even though siRNAs that were designed by AsiDesigner performed more than 79% of the time in our experiments, we found that some siRNAs for particular genes tend not to function well. We found that the performance scores of the siRNAs for those genes were generally low. In those cases, try to generate as many siRNAs for the gene as possible, for example, 100 siRNAs, and select highly scored siRNAs that are located away from the experimented siRNAs.

References

1. Couzin, J. (2002) Breakthrough of the year: small RNAs make big splash. *Science* **298**, 2296–2297.
2. Dorsett, Y., and Tuschl, T. (2004) siRNAs: applications in functional genomics and potential as therapeutics. *Nat. Rev. Drug Discov.* **3**, 318–329.
3. Birmingham, A., Anderson, E., Sullivan, K., Reynolds, A., Boese, Q., Leake, D., Karpilow, J., and Khvorova, A. (2007) A protocol for designing siRNAs with high functionality and specificity. *Nat. Protoc.* **2**, 2068–2078.
4. Ambion, siRNA target finder, http://www.ambion.com/techlib/misc/siRNA_finder.html.
5. Dharmacon, siDESIGN® center – Custom siRNA design tool, http://www.dharmacon.com/DesignCenter/DesignCenterPage.aspx.
6. Invitrogen, BLOCK-iT™ RNAi Designer, https://rnaidesigner.invitrogen.com/rnaiexpress/.
7. Novartis, BIOPREDsi, http://www.biopredsi.org/.
8. Qiagen, siRNA design tool, http://www1.qiagen.com/Products/GeneSilencing/CustomSiRna/SiRnaDesigner.aspx.
9. Chalk, A.M., Wahlestedt, C., and Sonnhammer, E.L. (2004) Improved and automated prediction of effective siRNA. *Biochem. Biophys. Res. Commun.* **319**, 264–274.
10. Yuan, B., Latek, R., Hossbach, M., Tuschl, T., and Lewitter, F. (2004) siRNA Selection Server: an automated siRNA oligonucleotide prediction server. *Nucleic Acids Res.* **32**, W130–W134.
11. Holen, T. (2006) Efficient prediction of siRNAs with siRNA rules 1.0: An open-source JAVA approach to siRNA algorithms. *RNA* **12**, 1620–1625.
12. Elbashir, S.M., Harborth, J., Lendeckel, W., Yalcin, A., Weber, K., and Tuschl, T. (2001) Duplexes of 21-nucleotide RNAs mediate RNA interference in mammalian cell culture. *Nature* **411**, 494–498.
13. Khvorova A., Reynolds A., and Jayasena S.D. (2003) Functional siRNAs and miRNAs exhibit strand bias. *Cell* **115**, 209–216.
14. Reynolds, A., Leake, D., Boese, Q., Scaringe, S., Marshall, W.S., and Khvorova, A. (2004) Rational siRNA design for RNA interference. *Nat. Biotechnol.* **22**, 326–330.

15. Choi,Y., Park, H., Choung, S., Kim, Y.J., Kim, S., Park, S., et al. (2005) Method of inhibiting expression of target mRNA using siRNA consisting of nucleotide sequence complementary to said target mRNA. *Patent* PCT/KR2005/004207 (WO 2006/062369).
16. Graveley, B.R. (2001) Alternative splicing: increasing diversity in the proteomic world. *Trends Genet.* **17**, 100–107.
17. Celotto, A.M., and Graveley, B.R. (2002) Exon-specific RNAi: a tool for dissecting the functional relevance of alternative splicing. *RNA* **8**, 718–724.
18. Park Y.K., Park S.M., Choi Y.C., Lee D., Won M., and Kim Y.J. (2008) AsiDesigner: exon-based siRNA design server considering alternative splicing. *Nucleic Acids Res.* **36**, w97–w103.
19. Altschul, S.F., Gish, W., Miller, W., Myers, E.W., and Lipman, D.J. (1990) Basic local alignment search tool. *J. Mol. Biol.* **215**, 403–410.
20. Pearson, W.R. and Lipman, D.J. (1998) Improved tools for biological sequence comparison. *Proc. Natl. Acad. Sci. U.S.A.* **85**, 2444–2448.
21. Mathews, D.H., Sabina, J., Zuker, M., and Turner, D.H. (1999) Expanded sequence dependence of thermodynamic parameters improves prediction of RNA secondary structure. *J. Mol. Biol.* **288**, 911–940.

Chapter 6

Bioinformatic Approaches to siRNA Selection and Optimization

Pirkko Muhonen and Harry Holthofer

Abstract

RNA interference mediated by short interfering RNA (siRNA) molecules represents a powerful genetic tool with an increasing interest as potential therapeutics. Current bioinformatic approaches to design functional siRNA molecules take into account both empirical and rational approaches to identify selectable characteristics of *active* and *specific* siRNA molecules and focusing the downstream events in the RNAi pathway, such as *target messenger RNA accessibility*. The design of effective siRNA molecules is the key to successful experimentation with RNAi. Here, we show advanced siRNA design parameters and options for highly efficient siRNA candidate search.

Key words: siRNA design, Specificity, Off-target effects, Stability, GC content

1. Introduction

1.1. siRNA Description

Short double-stranded RNA (dsRNA) molecules induce sequence-specific posttranscriptional gene silencing in many organisms by a process named RNA interference (RNAi). Elbashir et al. first demonstrated that the respective RNAi mediators are 21–22 nucleotides long RNA fragments with 2 nucleotide 3-overhangs (1). These short interfering RNA (siRNA) molecules are generated by RNase III-like enzyme and later activate RNA-induced silencing complex (RISC). The molecular features and characteristics of target mRNA regions have been shown to be critical for proficient gene silencing. The biogenesis of siRNA and the downstream gene silencing effects have been covered by several excellent recent review articles (2–4).

Wei-Ping Min and Thomas Ichim (eds.), *RNA Interference*, Methods in Molecular Biology, vol. 623,
DOI 10.1007/978-1-60761-588-0_6,

1.2. Challenges in siRNA Design

The use of siRNA molecules, designed to match perfectly with distinct target messenger RNA for silencing, is based on the assumption of their high target sequence specificity. However, several studies using DNA microarrays and computational approaches have conclusively shown that siRNA molecules may induce non-target mRNA degradation or translation arrest (5–9). The mechanism of siRNA off-targeting appears to be similar to that of miRNA on-targeting and requires pairing between a distinct seed sequence on a guide strand (5, 10). In addition, siRNA targeting may induce interferon responses and, eventually, cytotoxic effects (11, 12).

1.3. Recent Bioinformatic Progress in siRNA Candidate Search

Design of siRNAs with high specificity and efficacy is a critical step in all RNAi experimentations. Many of the siRNA design algorithms are based on parameters that originated from comparison of functional and nonfunctional siRNA sequences. First, siRNA design guidance includes the so-called Tuschl rules (accessible at the web page http://www.rockefeller.edu/labheads/tuschl/sirna.html). These rules were based on the results of systematic analysis of siRNA molecules in Drosophila cell lysates (1, 13–15). The latest existing approaches, instead, utilize artificial neural networks (ANNs) training with large data sets to extend earlier efforts based on experimental parameters only; ANNs can successfully process complex sequence motifs and synergistic relations between more than two factors (16, 17). Current bioinformatic approaches for siRNA design use the essential sequence characteristics of siRNA molecules as well as the secondary structures of the target messenger RNA. A wide variety of up-to-date parameters and siRNA candidate search tools for highly efficient siRNA design have become available, including, for example, siRNA nucleotide preferences, thermodynamics, and mRNA/siRNA secondary structure.

2. Web-Based siRNA Design Tools Needed

There are several web-based algorithms providing efficient siRNA candidate search and design. Table 1 lists various published siRNA design programs and their main features. In addition, Table 1 summarizes other servers helpful for confirming siRNA specificity and optimal secondary structure. This table certainly does not list all available siRNA design programs; however, it aims to show siRNA design programs with different design parameters and other additional tools to optimize siRNA candidates.

It has been shown that many of the siRNA design programs tend to select very different siRNA candidates with a range of siRNA efficacies, even the programs that operate with

Table 1

Tools and servers for siRNA design	Main features	Refs
siRNA design programs		
siRNA_profile http://bonebiology.utu.fi/pimaki/main.html	Thermodynamics and off-target	(18)
siDirect http://genomics.jp/sidirect/	Off-target search	(46, 50)
OligoWalk http://rna.urmc.rochester.edu/cgi-bin/server_exe/oligowalk/oligowalk_form.cgi	Thermodynamics and siRNA/mRNA structure	(55)
AsiDesigner	Alternative splicing	(22)
EMBOSS http://emboss.bioinformatics.nl/cgi-bin/emboss/sirna	Positional	(56)
dsCheck http://dscheck.rnai.jp/	Off-target effects	(49)
BIOPRED*si* http://www.biopredsi.org/start.html	Artificial neural network	(16)
siRNA Target Designer http://www.promega.com/siRNADesigner/program/	si/shRNA design program	Promega Corporation
RNAi explorer http://www.genelink.com/sirna/shRNAi.asp	si/shRNA design program	Gene Link™
siRNA specificity optimizing tools		
Specificity Server http://informatics-eskitis.griffith.edu.au/SpecificityServer	Off-target	(51)
BLAST (http://blast.ncbi.nlm.nih.gov/Blast.cgi)	Off-target	(45)
Target accessibility and secondary structures		
Sfold (http://sfold.wadsworth.org)	Target secondary structure	(38, 39)
GeneBee – Molecular Biology Server (http://www.genebee.msu.su/services/rna2_reduced.html)	Target secondary structure	(36)
Oligo Primer Analysis Software (http://www.oligo.net/)	siRNA hairpin structure, CG content	Molecular Biology Insights, Inc.

closely-related selection parameters for the same target regions (18). This reveals the dilemma of the bioinformatic approach to select functional siRNA sequences with the currently available algorithms. Therefore, it is advisable to test several siRNA design algorithms to search for the optimal siRNA candidates (see Note 1). Here, we demonstrate siRNA candidate search by using the *siRNA_profile* program (http://bonebiology.utu.fi/pimaki/main.html), and give additional hints for siRNA sequence optimization using other bioinformatic tools (see Note 2).

3. General Instructions for Biologically Active siRNA Selection

3.1. Targeting Specific Messenger RNA

It has been noticed that not all positions of siRNA duplexes contribute equally to target recognition and degradation (19). An open reading frame of target gene sequence should be selected, avoiding the 5′- or 3′-untranslated regions (UTRs) or regions close to the start/stop codon, as these regions may be occupied by regulatory proteins and thus interfere with the RISC binding (20). Elbashir et al. showed that siRNAs with 3′ overhanging, especially with UU dinucleotides, are most effective (14). Therefore, it was first suggested that the gene of interest should be scanned for each 5′- AA and the adjacent 19 nucleotides as potential siRNA targets. In subsequent publications, siRNAs with other 3′ terminal dinucleotide overhangs have also been shown to induce RNAi effectively.

Existence of single nucleotide polymorphism (SNP) in the siRNA target region is generally not recommended, and thus the design algorithm should take these sites into consideration. However, sometimes it is necessary to control an individually spliced mRNA isoform producing a specific protein to study the function of splicing variants (21). Therefore, an algorithm to design siRNAs considering alternative splicing has recently been developed (22).

3.1.1. Guidelines for Positional siRNA Design

1. The gene sequence of interest can be obtained from NCBI GenBank (http://www.ncbi.nlm.nih.gov/Genbank/) and pasted into the input sequence *siRNA_profile* sequence window in FASTA format or as plain text. GenBank database is a collection of publicly available annotated nucleotide sequences and has no limits to species.
2. Input sequence can be determined as mRNA, DNA, sense siRNA or antisense siRNA, depending on the user's requirements.
3. Conventional siRNA search is focused on the target with motifs 5′-AA(N19)UU-3′, where N is any nucleotide, in the mRNA, because siRNA molecules having 3′UU overhangs

appear most efficient (14, 23). The presence of 5′AA motif is necessary when siRNA synthesis is done by in vitro translation where the overhanging UU protects against single-strand-specific nuclease. The *siRNA_profile* program will give the locations of the AA motifs in the target sequence, and the program can search siRNA sequences at the AA positions of the target mRNA or without the AA requirement.

4. The ideal lengths of the siRNAs have been reported to be around 21 nucleotides. siRNA search parameters in the *siRNA_profile* algorithm are based on 19 nt siRNAs with 2 nt overhang, and this is recommended as a default. If longer siRNAs are designed, the profile is calculated for up to 27 nt long siRNAs, and scores are calculated starting from 5′terminus of the antisense strand to the 19th nucleotide.
5. Select siRNA target region from a given sequence beginning 50–100 nt downstream/upstream of the start/termination codon (20). It is advisable to avoid 5′ and 3′ untranslated regions (UTRs) as well as the close regions of the start and stop codons. These regions are rich in regulatory motifs, therefore, UTR-binding proteins and translation initiation complexes could interfere with siRNA binding.
6. Avoid single nucleotide polymorphism (SNP) sites. This may be necessary if the gene is suspected of being polymorphic. The RefSNP database (available at http://www.ncbi.nlm.nih.gov/projects/SNP/) is recommended to be used to exclude siRNA sequences that span SNP sites. siRNA sequence spanning an SNP region may directly affect its effectiveness due to mismatches.
7. Avoiding exon–intron boundaries reduces the possibility of mispairing siRNA molecule. This might be useful if alternative splicing can take place in the gene. If you are interested in mapping different mRNA isoforms, select the siRNA target region with extra care and use a program suitable for it, such as AsiDesigner (22).

3.2. Nucleotide Content of Functional siRNA Sequences

Reynolds et al. first showed the eight sequence characteristics associated with proper siRNA functionality (19), and these were accepted as "Reynolds' rational rules" in several siRNA design algorithms. Table 2 lists the nucleotide preferences obtained with five different databases of different sizes and origin (17–19, 24, 25). The nucleotide distribution along the functional siRNA molecule shows the bias towards internal stability at the 3′ terminus.

The GC content of siRNA molecule has been acknowledged as an important parameter, which correlates with siRNA end-product functionality. Too high CG content (>60%) may inhibit secondary structure of the target mRNA, whereas too low CG content (<30%) may reduce the efficacy of the mRNA recognition

and siRNA–mRNA hybridization. Consensus for the acceptable CG content in functional siRNA sequence has been established between 30 and 53% (19). Ui-Tei et al. have shown that the average GC content of highly efficient siRNA molecules in the region 2–7 nucleotides (antisense strand) was 19%, while that of the region 8–18 nucleotides was 52% (26). Also, siRNAs with long stretches of G/C residues were shown to be inefficient (26).

3.2.1. Guidelines for siRNA Design Based on Nucleotide Content

1. Statistical nucleotide content preferences of functional siRNA sequences are listed in Table 2. Primarily, there should be A/U-richness in the 5′-end and G/C in the

Table 2
Nucleotide preferences in functional siRNA sequence

		Nucleotide positions 5′–3′ of the antisense strand																	
Reference	**nt**	**1**	**2**	**3**	**4**	**5**	**6**	**7**	**8**	**9**	**10**	**11**	**12**	**13**	**14**	**15**	**16**	**17**	**18**	**19**
Reynolds (19)	A	more than 3 A or U									+									
	U	+																+		
	C	–						–												
	G	–																		
Amarzguioui (25)	A	+						+			–									–
	U	+													+					
	C	–																		+
	G				+															+
Shabalina (17)	A	+				–		+			+	–			+			–		–
	U	+	+	+		+		+						+	+					–
	C	–						–							–			+	+	+
	G	–	–				–	–						–	–		–			
Jagla (24)	A	+									+									
	U	+									+									
	C																			+
	G																			+
Muhonen (18)	A	+	+	+		–									+				–	–
	U	+	+			+									+					–
	C	–					+													
	G									+							+			
	Py						+								+					
	Pu											+					+			

3′-end of the antisense strand. The more comprehensive nucleotide requirements along the siRNA sequence contribute to the low stability region called "energy valley", described in Subheading 3.3.

2. The *siRNA_profile* program uses heuristic scoring method that is adjusted to hCyclophilin functional siRNA sequences exhibiting asymmetric energy profile (18, 19). This novel scoring system gives points or penalty scores to the thermodynamically favorable siRNA sequences in proportion to the nucleotide or purine/pyrimidine positions along the known functional siRNA sequences. After the thermodynamical selection and scoring, the siRNA sequences are sorted in order of highest scores. siRNA sequences gaining four or less points should not be selected for RNAi experiments.
3. Avoid siRNA target regions with GC content <30% or >53%. The ***siRNA_profile*** program calculates GC% in the output of each siRNA sequence. If CG content is not automatically calculated by other siRNA design programs, you may manually count the CG% by following way: $(nC + nG/N) \times 100\%$ (n = number of C or G in the siRNA strand; N = number of nucleotides in the siRNA strand, recommended 21 nt).
4. Eliminate sequences containing four repeating nucleotides. Long stretches of C and G repeats have a tendency to form quartet structures and Watson–Crick hairpin forms (27). Four A and U in a row containing sequences are also suggested to be eliminated due to the tendency of RNA polymerase III to terminate transcription at poly U sequences (28).

3.3. Thermodynamic Requirements

Basic siRNA design criteria regarding GC- and nucleotide content of the siRNA molecule have been used to search specific and efficient siRNA molecules. However, a drastic variation of silencing efficacy has been apparent when only nucleotide characteristics were used to guide siRNA design. Significant progress in siRNA design was achieved when thermodynamic factors of siRNA molecule were revealed. The two strands of siRNA duplexes are not equally eligible for assembly into the RISC. Thermodynamic parameters were discovered by distinguishing functional and nonfunctional siRNA sequences based on their internal stabilities and asymmetric properties (29, 30). Internal stabilities of dsRNA molecules were calculated by using the nearest neighbor method (31). It was suggested by Khvorova et al. that the average internal stability of the 5′-end of the antisense strand is lower than of the 3′-terminus in a functional siRNA. Functional siRNAs exhibit low overall internal stability region called "energy valley" between 9 and 14 nucleotides counted

from 5′-end of the antisense strand. Nonfunctional siRNAs lack this feature (30). Recently, it has been shown that low general stability is an additional guideline for designing highly functional siRNA molecules, see Fig. 1 (18).

3.3.1. Guidelines for siRNA Design Based on Thermodynamic Parameters

1. The *siRNA_profile* program specifies an energy difference that is the difference of calculated free energy values between the 5′-terminus and the 3′-terminus. In the *siRNA_profile* program, 1 kcal/mol is used as a default energy difference to ensure selection of strongly asymmetric siRNA (see Note 3).
2. The *siRNA_profile* user can define the exact "energy valley" location; the region between 9 and 14 nucleotides is suggested. The energy profile output of the *siRNA_profile* program blots the selected "energy valley" region in red.
3. Confirm lack of internal repeats and stable hairpin structures in the siRNA sequence. The melting temperature (*T*m) of the internal secondary structures should be less than 20°C by

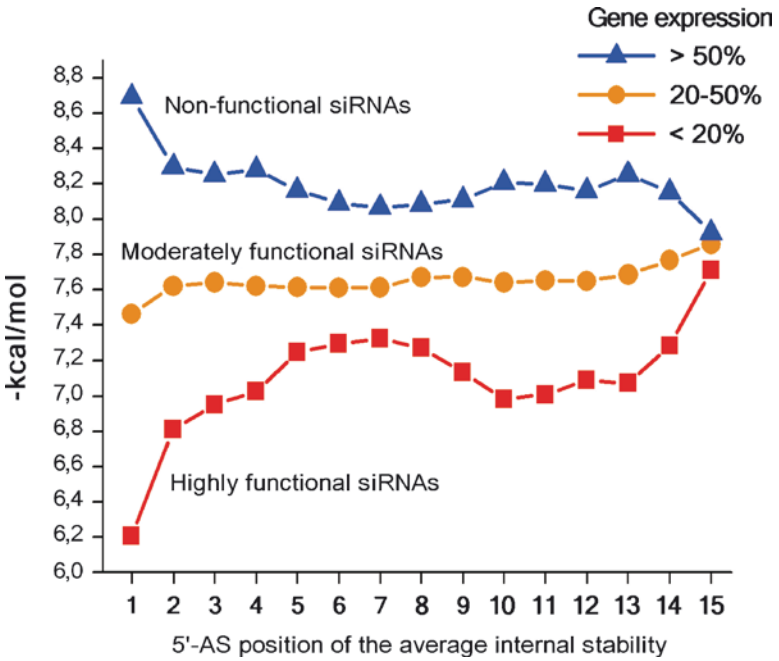

Fig. 1. Internal stability profiles of siRNA molecules determines siRNA efficacy. The internal stabilities of functional and nonfunctional siRNAs were calculated with the help of the large siRNA data set of over 2,400 individual siRNA sequences published by Huesken et al. (16). 2431 siRNA sequences were fed into the *siRNA_profile* program and siRNA profiles were divided into categories based on gene expression (GE) levels after siRNA silencing (GE level categories: ≤20%, $n=280$; 20.1–50% $n=1305$ and >50.1% $n=846$). Muhonen et al. have recently shown that siRNA efficiency display siRNA instability dependency (18). Highly functional siRNA molecules (GE level ≤ 20%) illustrated lower overall stability in addition to asymmetric average energy profile than moderately (GE level 20.1–50%) or nonfunctional (GE level > 50.1%) siRNA molecules. These results show that the siRNA sequences exhibiting both favourable asymmetric properties *and* low overall stabilities recommended for gene knock down experiments

using, for example, Oligo Primer Analysis Software (http://www.oligo.net/index.html).

3.4. mRNA Secondary Structure and Accessibility

There are contradictory reports in the literature concerning the importance of the nucleotide composition or/and thermodynamic features of siRNA molecule *or* the structure of the target mRNA to be the major determinant of the effectiveness in the RNAi pathway. Latest bioinformatic analyses have displayed the importance of the secondary RNA structure for the efficiency. A target region incorporated in various hairpin structures within the target region will dramatically affect the potency of gene silencing by siRNA (32, 33). There appears to be a linear correlation between siRNA silencing of the target gene and the local free energy (ΔG_{loc}) of the target region. A low negative ΔG_{loc}, which correlates to an open region with many unpaired nucleotides, results in improved siRNA potency (Examples are shown in Fig. 2). Based on these results, Kurreck has proposed a model in which efficiency of an siRNA is determined at two points of the RNAi pathway (34). First step, asymmetric strand incorporation into RISC is controlled by thermodynamic properties of siRNA molecule. Second, the accessibility of the target site may further modulate the efficacy of siRNA molecule.

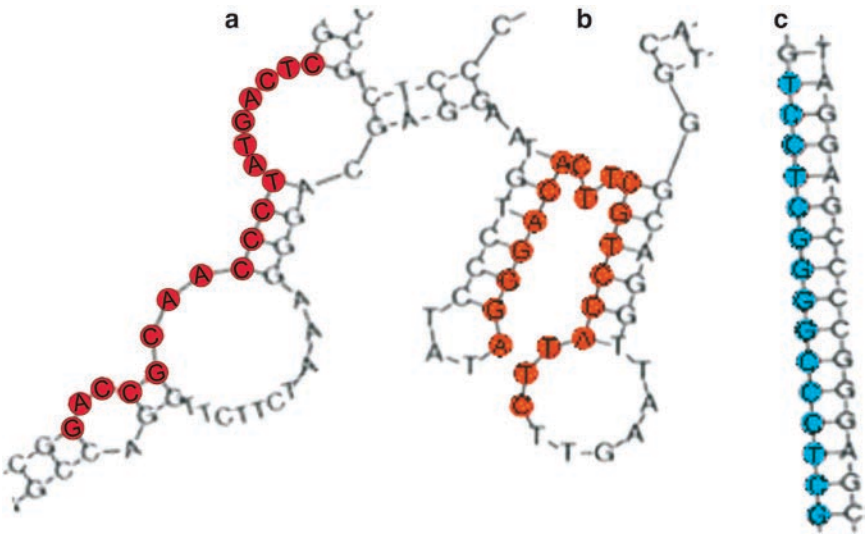

Fig. 2. Influence of target mRNA accessibility on silencing efficiency as an optional guideline for siRNA design. Local free energies ΔG_{loc} of target mRNA can be calculated by several algorithms. Even the computed local free energies can be expected to give only a rough estimation of the actual RNA stability, and it has been suggested that siRNA efficacy may correlate with ΔG_{loc} of the target structure (32). Schematic target RNA illustrates that open RNA structure with low negative ΔG_{loc} ((**a**) siRNA target region is highlighted) is more susceptible for gene silencing by siRNA than inaccessible ((**b**) siRNA target region is highlighted) and more stable internal structures ((**c**) siRNA target region is highlighted). The negative ΔG_{loc} values of schematic RNA structure are the following: **a** < **b** < **c**

Many computational methods have been developed for predicting RNA structures (35–37). These algorithms mainly represent probabilistic models to predict RNA secondary structures, while environmental factors ultimately contribute to RNA folding pathways and siRNA–RISC accessibility.

3.4.1. Guidelines for siRNA Design Based on Target mRNA Accessibility (Optional)

1. Check the target RNA accessibility by, e.g., sFold (http://sfold.wadsworth.org/), mFold (http://bioinfo.hku.hk/Pise/mfold.html), or GeneBee – Molecular Biology Server for RNA secondary structure prediction (http://www.genebee.msu.su/services/rna2_reduced.html) (32, 36, 38–40). Avoid highly stable and complex target sequence regions (high negative ΔG_{loc}) and prefer open loop regions with low negative ΔG_{loc} (see Fig. 2 and Note 4).

3.5. Off-Target Effects

Once siRNA sequences meeting criteria of optimal nucleotide content are found, siRNA sequences containing potential immunostimulatory motifs should be rejected (see **Note 5**). siRNA transfection into cells exposes siRNA molecule to endosomal and cytoplasmic RNA-sensing receptors of the innate immune system; therefore, it is understandable that an exogenous RNA molecule can posses the same molecular signatures as viral RNA. Therefore, it is not surprising that, in addition to target gene suppression by siRNAs, several publications have reported nonspecific target gene effects, mainly due to activation of the immunological defense. These siRNA molecules are named as immunostimulatory RNAs (isRNAs) (41).

dsRNA, a potent inducer of type I interferon (IFN) synthesis, is the activator of two classes of IFN-induced enzymes: RNA-binding protein kinase (PKR) and 2′,5′-oligoadenylate synthetases (OAS), whose products activate the latent ribonuclease RNaseL (42, 43). The induction of PKR activation was reduced by chemical modification of the siRNA molecule (44) (see Note 6).

Basic Local Alignment Search Tool (BLAST) – search (available at http://blast.ncbi.nlm.nih.gov/Blast.cgi) of the selected siRNA sequence against EST libraries has been recommended to ensure that only one gene is targeted (45). BLAST is incorporated in several siRNA design programs; however, it has recently been acknowledged that BLAST may not be the best software for identifying off-targets. With at least three mismatches, there are typically four or five contiguous matches, and BLAST search frequently overlooks these off-target candidates (46). Since both BLAST and Smith–Waterman algorithms are not sufficient to enhance siRNA specificity, novel bioinformatic approaches to enhance siRNA specificity are needed (5).

siRNA duplexes with GU rich sequences appear highly immunostimulatory (47). The 5′-UGUGU-3′ and 5′-GUCCUUCAA-3′

elements incorporated in a siRNA sequence has especially been shown to have immunostimulatory potential (41, 47). 5′-UGU-3 motif is recognized by TLR7/8 (41, 47). In addition, CpG motifs in RNA molecules have been shown to induce immune responses TLR7/8 and 9 independently via so far unknown mechanisms (48).

Molecular mechanisms for the off-target effects – and how to avoid them – are still poorly understood. There are only a few bioinformatics approaches that recognize possible immunostimulatory motifs and number of mismatches to avoid of siRNA candidates causing possible off-target effects (18, 49–51), whereas it may easily lead to situations in which biologically most active siRNA sequences are ultimately not selected for RNAi experiments.

3.5.1. Guidelines for siRNA Optimization Avoiding Off-Target Effects

1. Check both strands of the siRNA sequence for possible immunostimulatory motifs; e.g., repeated GU, AU, and CpG motifs (18, 48, 52). The *siRNA_profile* output has a recommendation not to use immunostimulatory sequences: siRNA candidates having CG motifs are marked in red and UGUGU-motifs are marked in blue. Discard the siRNA sequences containing immunostimulatory motifs or see Note 6.
2. Perform meticulous BLAST (http://blast.ncbi.nlm.nih.gov/Blast.cgi) and Specificity search (http://informatics-eskitis.griffith.edu.au/SpecificityServer) to avoid off-target effects on other genes or sequences (51). Discard sequences that have high homology with unwanted genes in the seed region (5′-region of the antisense strand).

4. Notes

1. Use two or more siRNA design algorithms to compare the obtained siRNA candidate sequences. A variety of siRNA design programs tend to select very different siRNA candidates with a range of siRNA efficacies, even the programs operating with related selection parameters and the same target region have been used (18).
2. If designing shRNA constructs, look at the validated shRNAs suggested from the RNAi Consortium (http://www.broad.mit.edu/rnai/trc) or from RNAi Codex (http://codex.cshl.edu/scripts/newmain.pl) if there are any available for your gene of interest. There are several shRNA design programs and services available (e.g., Invitrogen BLOCK-iT™ http://www.genelink.com/sirna/shRNAi.asp; RNAi Designer https://rnaidesigner.invitrogen.com/rnaiexpress/; and Promega siRNA

Target Designer http://www.promega.com/siRNADesigner/program/). A comparison of several siRNA design applications has revealed that algorithms that predict functional siRNA sequences may significantly differ in their capacity to predict functional shRNA sequences. For this purpose, Taxman et al. recommended the modified Ui-Tei et al. algorithm due to lowest high false positive fraction (50, 53).

3. If ready-designed siRNAs are used, you can check for the optimal thermodynamic characteristics of siRNA sequence, for example, by *siRNA_profile* and ensure siRNA specificity by using the Specificity Server. When profiling already existing siRNA sequence (19–23 nt), choose "1" for both first and last position due to the calculation method of the *siRNA_profile* algorithm.
4. There are contradictory data concerning the impact of RNA secondary structure on the siRNA efficacy. Current models to predict RNA secondary structures are very sophisticated, but may not represent the natural milieu wherein RNAi machinery is operating. Therefore, a predicted secondary structure of target RNA should be used more as an optional guideline than as a strict rule during siRNA sequence optimization.
5. Test for several siRNA duplexes targeting the same gene of interest to control the specificity of knockdown experiments; functional siRNA sequences should produce exactly the same phenotype. Use identical design parameters for each set of siRNAs.

   Note for negative controls: Always design negative controls by scrambling the targeted siRNA sequence. The negative control RNA should have the same length and nucleotide composition as the siRNA, but have at least 4–5 bases mismatched to the siRNA. Make sure the scrambling will not create new homology to other genes or immunostimulatory motifs.
6. The outcome of siRNA candidate search may result in only a short number of siRNA sequences due to rejection of immunostimulatory motifs containing siRNA sequences. This may also lead to a situation in which biologically most active siRNA sequences may be overlooked. However, chemical modifications have been shown to abrogate the immunostimulatory activity of siRNA molecule holding immunostimulatory features, thereby facilitating also these sequences for RNAi experiments, especially partial 2′-*O*-methyl modification focused on the seed region in guide strand, and it has been shown to reduce off-target silencing while the siRNA efficacy remains high (54).

References

1. Elbashir, S. M., Lendeckel, W. and Tuschl, T. (2001) RNA interference is mediated by 21- and 22-nucleotide RNAs. *Genes Dev.* **15**, 188–200.
2. Scherr, M. and Eder, M. (2007) Gene silencing by small regulatory RNAs in mammalian cells. *Cell Cycle* **6**, 444–449.
3. Farazi, T. A., Juranek, S. A. and Tuschl, T. (2008) The growing catalog of small RNAs and their association with distinct Argonaute/Piwi family members. *Development* **135**, 1201–1214.
4. Wu, L. and Belasco, J. G. (2008) Let me count the ways: mechanisms of gene regulation by miRNAs and siRNAs. *Mol. Cell.* **29**, 1–7.
5. Birmingham, A., Anderson, E. M., Reynolds, A., Ilsley-Tyree, D., Leake, D., Fedorov, Y., *et al.* (2006) 3′ UTR seed matches, but not overall identity, are associated with RNAi off-targets. *Nat. Methods* **3**, 199–204.
6. Jackson, A. L., Bartz, S. R., Schelter, J., Kobayashi, S. V., Burchard, J., Mao, M., *et al.* (2003) Expression profiling reveals off-target gene regulation by RNAi. *Nat. Biotechnol.* **21**, 635–637.
7. Vankoningsloo, S., de Longueville, F., Evrard, S., Rahier, P., Houbion, A., Fattaccioli, A., *et al.* (2008) Gene expression silencing with 'specific' small interfering RNA goes beyond specificity – a study of key parameters to take into account in the onset of small interfering RNA off-target effects. *FEBS J.* **275**, 2738–2753.
8. Anderson, E. M., Birmingham, A., Baskerville, S., Reynolds, A., Maksimova, E., Leake, D., *et al.* (2008) Experimental validation of the importance of seed complement frequency to siRNA specificity. *RNA* **14**, 853–861.
9. Jackson, A. L., Burchard, J., Schelter, J., Chau, B. N., Cleary, M., Lim, L., *et al.* (2006) Widespread siRNA "off-target" transcript silencing mediated by seed region sequence complementarity. *RNA* **12**, 1179–1187.
10. Zeng, Y., Yi, R., Cullen, B. R. (2003) MicroRNAs and small interfering RNAs can inhibit mRNA expression by similar mechanisms. *Proc. Natl. Acad. Sci. U. S. A.* **100**, 9779–9784.
11. de Veer, M. J., Sledz, C. A. and Williams, B. R. (2005) Detection of foreign RNA: implications for RNAi. *Immunol. Cell Biol.* **83**, 224–228.
12. Klatt, A. R., Klinger, G., Zech, D., Paul-Klausch, B., Renno, J. H., Schmidt, J., *et al.* (2007) RNAi in primary human chondrocytes: efficiencies, kinetics, and non-specific effects of siRNA-mediated gene suppression. *Biologicals* **35**, 321–328.
13. Elbashir, S. M., Harborth, J., Lendeckel, W., Yalcin, A., Weber, K. and Tuschl, T. (2001) Duplexes of 21-nucleotide RNAs mediate RNA interference in cultured mammalian cells. *Nature* **411**, 494–498.
14. Elbashir, S. M., Martinez, J., Patkaniowska, A., Lendeckel, W. and Tuschl, T. (2001) Functional anatomy of siRNAs for mediating efficient RNAi in *Drosophila melanogaster* embryo lysate. *EMBO J.* **20**, 6877–6888.
15. Tuschl, T., Zamore, P. D., Lehmann, R., Bartel, D. P. and Sharp, P. A. (1999) Targeted mRNA degradation by double-stranded RNA in vitro. *Genes Dev.* **13**, 3191–3197.
16. Huesken, D., Lange, J., Mickanin, C., Weiler, J., Asselbergs, F., Warner, J., *et al.* (2005) Design of a genome-wide siRNA library using an artificial neural network. *Nat. Biotechnol.* **23**, 995–1001.
17. Shabalina, S. A., Spiridonov, A. N. and Ogurtsov, A. Y. (2006) Computational models with thermodynamic and composition features improve siRNA design. *BMC Bioinformatics* **7**, 65.
18. Muhonen, P., Parthasarathy, R. N., Janckila, A. J., Buki, K. G. and Vaananen, H. K. (2008) Analysis by siRNA_profile program displays novel thermodynamic characteristics of highly functional siRNA molecules. *Source Code Biol. Med.* **3**, 8.
19. Reynolds, A., Leake, D., Boese, Q., Scaringe, S., Marshall, W. S. and Khvorova, A. (2004) Rational siRNA design for RNA interference. *Nat. Biotechnol.* **22**, 326–330.
20. Elbashir, S. M., Harborth, J., Weber, K. and Tuschl, T. (2002) Analysis of gene function in somatic mammalian cells using small interfering RNAs. *Methods* **26**, 199–213.
21. Celotto, A. M. and Graveley, B. R. (2002) Exon-specific RNAi: a tool for dissecting the functional relevance of alternative splicing. *RNA* **8**, 718–724.
22. Park, Y. K., Park, S. M., Choi, Y. C., Lee, D., Won, M. and Kim, Y. J. (2008) AsiDesigner: exon-based siRNA design server considering alternative splicing. *Nucleic Acids Res.* **36**, W97–W103.
23. Lee, H. S., Lee, S. N., Joo, C. H., Lee, H., Lee, H. S., Yoon, S. Y., *et al.* (2007) Contributions

of 3′-overhang to the dissociation of small interfering RNAs from the PAZ domain: molecular dynamics simulation study. *J. Mol. Graph Model* **25**, 784–793.

24. Jagla, B., Aulner, N., Kelly, P. D., Song, D., Volchuk, A., Zatorski, A., *et al.* (2005) Sequence characteristics of functional siRNAs. *RNA* **11**, 864–872.
25. Amarzguioui, M. and Prydz, H. (2004) An algorithm for selection of functional siRNA sequences. *Biochem. Biophys. Res. Commun.* **316**, 1050–1058.
26. Ui-Tei, K., Naito, Y. and Saigo, K. (2007) Guidelines for the selection of effective short-interfering RNA sequences for functional genomics. *Methods Mol. Biol.* **361**, 201–216.
27. Hardin, C. C., Watson, T., Corregan, M. and Bailey, C. (1992) Cation-dependent transition between the quadruplex and Watson–Crick hairpin forms of d(CGCG3GCG). *Biochemistry* **31**, 833–841.
28. Geiduschek, E. P. and Kassavetis, G. A. (2001) The RNA polymerase III transcription apparatus. *J. Mol. Biol.* **310**, 1–26.
29. Schwarz, D. S., Hutvagner, G., Du, T., Xu, Z., Aronin, N. and Zamore, P. D. (2003) Asymmetry in the assembly of the RNAi enzyme complex. *Cell* **115**, 199–208.
30. Khvorova, A., Reynolds, A. and Jayasena, S. D. (2003) Functional siRNAs and miRNAs exhibit strand bias. *Cell* **115**, 209–216.
31. Freier, S. M., Kierzek, R., Jaeger, J. A., Sugimoto, N., Caruthers, M. H., Neilson, T., *et al.* (1986) Improved free-energy parameters for predictions of RNA duplex stability. *Proc. Natl. Acad. Sci. U. S. A.* **83**, 9373–9377.
32. Schubert, S., Grunweller, A., Erdmann, V. A. and Kurreck, J. (2005) Local RNA target structure influences siRNA efficacy: systematic analysis of intentionally designed binding regions. *J. Mol. Biol.* **348**, 883–893.
33. Luo, K. Q. and Chang, D. C. (2004) The gene-silencing efficiency of siRNA is strongly dependent on the local structure of mRNA at the targeted region. *Biochem. Biophys. Res. Commun.* **318**, 303–310.
34. Kurreck, J. (2006) siRNA efficiency: structure or sequence-that is the question. *J. Biomed. Biotechnol.* **2006**, 83757.
35. Ding, Y., Chan, C. Y. and Lawrence, C. E. (2004) Sfold web server for statistical folding and rational design of nucleic acids. *Nucleic Acids Res.* **32**, W135–W141.
36. Brodskii, L. I., Ivanov, V. V., Kalaidzidis Ia, L., Leontovich, A. M., Nikolaev, V. K., Feranchuk, S. I., *et al.* (1995) [GeneBee-NET: an Internet based server for biopolymer structure analysis]. *Biokhimiia* **60**, 1221–1230.
37. Zuker, M. (2003) Mfold web server for nucleic acid folding and hybridization prediction. *Nucleic Acids Res.* **31**, 3406–3415.
38. Ding, Y., Chan, C. Y. and Lawrence, C. E. (2005) RNA secondary structure prediction by centroids in a Boltzmann weighted ensemble. *RNA* **11**, 1157–1166.
39. Ding, Y. and Lawrence, C. E. (2003) A statistical sampling algorithm for RNA secondary structure prediction. *Nucleic Acids Res.* **31**, 7280–7301.
40. Walter, A. E., Turner, D. H., Kim, J., Lyttle, M. H., Muller, P., Mathews, D. H., *et al.* (1994) Coaxial stacking of helixes enhances binding of oligoribonucleotides and improves predictions of RNA folding. *Proc. Natl. Acad. Sci. U. S. A.* **91**, 9218–9222.
41. Hornung, V., Guenthner-Biller, M., Bourquin, C., Ablasser, A., Schlee, M., Uematsu, S., *et al.* (2005) Sequence-specific potent induction of IFN-alpha by short interfering RNA in plasmacytoid dendritic cells through TLR7. *Nat. Med.* **11**, 263–270.
42. Clemens, M. J. (1997) PKR – a protein kinase regulated by double-stranded RNA. *Int. J. Biochem. Cell Biol.* **29**, 945–949.
43. Liang, S. L., Quirk, D. and Zhou, A. (2006) RNase L: its biological roles and regulation. *IUBMB Life* **58**, 508–514.
44. Puthenveetil, S., Whitby, L., Ren, J., Kelnar, K., Krebs, J. F. and Beal, P. A. (2006) Controlling activation of the RNA-dependent protein kinase by siRNAs using site-specific chemical modification. *Nucleic Acids Res.* **34**, 4900–4911.
45. Altschul, S. F. and Lipman, D. J. (1990) Protein database searches for multiple alignments. *Proc. Natl. Acad. Sci. U. S. A.* **87**, 5509–5513.
46. Yamada, T. and Morishita, S. (2005) Accelerated off-target search algorithm for siRNA. *Bioinformatics* **21**, 1316–1324.
47. Judge, A. D., Sood, V., Shaw, J. R., Fang, D., McClintock, K. and MacLachlan, I. (2005) Sequence-dependent stimulation of the mammalian innate immune response by synthetic siRNA. *Nat. Biotechnol.* **23**, 457–462.
48. Sugiyama, T., Gursel, M., Takeshita, F., Coban, C., Conover, J., Kaisho, T., *et al.* (2005) CpG RNA: identification of novel single-stranded RNA that stimulates human CD14+CD11c+ monocytes. *J. Immunol.* **174**, 2273–2279.
49. Naito, Y., Yamada, T., Matsumiya, T., Ui-Tei, K., Saigo, K. and Morishita, S. (2005) dsCheck:

highly sensitive off-target search software for double-stranded RNA-mediated RNA interference. *Nucleic Acids Res.* **33**, W589–W591.

50. Naito, Y., Yamada, T., Ui-Tei, K., Morishita, S. and Saigo, K. (2004) siDirect: highly effective, target-specific siRNA design software for mammalian RNA interference. *Nucleic Acids Res.* **32**, W124–W129.
51. Chalk, A. M. and Sonnhammer, E. L. (2008) siRNA specificity searching incorporating mismatch tolerance data. *Bioinformatics* **24**, 1316–1317.
52. Forsbach, A., Nemorin, J. G., Montino, C., Muller, C., Samulowitz, U., Vicari, A. P., *et al.* (2008) Identification of RNA sequence motifs stimulating sequence-specific TLR8-dependent immune responses. *J. Immunol.* **180**, 3729–3738.
53. Taxman, D. J., Livingstone, L. R., Zhang, J., Conti, B. J., Iocca, H. A., Williams, K. L., *et al.* (2006) Criteria for effective design, construction, and gene knockdown by shRNA vectors. *BMC Biotechnol.* **6**, 7.
54. Jackson, A. L., Burchard, J., Leake, D., Reynolds, A., Schelter, J., Guo, J., *et al.* (2006) Position-specific chemical modification of siRNAs reduces "off-target" transcript silencing. *RNA* **12**, 1197–1205.
55. Lu, Z. J. and Mathews, D. H. (2008) OligoWalk: an online siRNA design tool utilizing hybridization thermodynamics. *Nucleic Acids Res.* **36**, W104–W108.
56. Rice, P., Longden, I. and Bleasby, A. (2000) EMBOSS: the European Molecular Biology Open Software Suite. *Trends Genet.* **16,** 276–277.

Chapter 7

Optimized Gene Silencing by Co-expression of Multiple shRNAs in a Single Vector

Yasuhito Ishigaki, Akihiro Nagao, and Tsukasa Matsunaga

Abstract

Currently, RNA interference technology is one of the most powerful tools in molecular biology and has been widely used in genetic manipulation. In addition to chemically synthesized small interfering RNA (siRNA), vector-based methods have been developed for stable gene silencing by the expression of a single short-hairpin RNA (shRNA). The artificially expressed RNA molecules are processed to form a silencing complex that causes the specific degradation of its target mRNA. However, silencing vectors containing a single shRNA-expressing sequence sometimes induce only poor knockdown. In order to improve the knockdown efficiency using shRNA, the multiple shRNA-expressing sequences were introduced into a single plasmid vector. Compared with the conventional single shRNA-expression vector, the multiple shRNA-expression vectors confer higher yields of stable clones with efficient knockdown and better correlations between knockdown level and the expression level of second marker gene, enhanced green fluorescent protein, in the vector. These features are very helpful for establishing stable knockdown clones and the detailed procedure is described in this chapter.

Key words: RNA interference, Knockdown, shRNA, Plasmid vector, *XPA*

1. Introduction

RNA interference (RNAi) is one of the most useful techniques for gene silencing and is achieved by the introduction of double-stranded (ds) RNA molecules into cells (1). In mammalian cells, long dsRNA is known to induce the so-called "interferon response," including the augmentation of 2′,5′-*oligoadenylate synthetase 1* (*OAS1*) gene family expression and the activation of protein kinase R (2), finally causing the cell death. To avoid this unfavorable effect, short dsRNA (short interference RNA, siRNA) has been broadly used for RNAi induction (3, 4).

Wei-Ping Min and Thomas Ichim (eds.), *RNA Interference*, Methods in Molecular Biology, vol. 623,
DOI 10.1007/978-1-60761-588-0_7, © Springer Science+Business Media, LLC 2010

The knockdown effect of siRNA molecules is basically transient due to the gradual reduction of cellular siRNA concentration by cell divisions, which sometimes leads to inefficient gene silencing, especially in long-life proteins. In addition, the optimization of transfection conditions is essentially required for the sufficient introduction of siRNA molecules into cells.

After the discovery of successful induction of RNAi in mammalian cells, many groups have developed a vector-based siRNA expression system, in which short-hairpin RNA (shRNA) is expressed by RNA polymerase III promoters, such as U6 or H1 (5–7), although RNA polymerase II promoter has also been utilized (8). The vector contains a replication origin for mammalian cells and can be maintained even after multiple cell divisions, enabling one to obtain stable knockdown clones. Moreover, the vector-based RNAi has an advantage in its application to virus vector systems. The knockdown efficiency in the stable transfectants is often low (9). In our experiments, a conventional shRNA vector gave us only a few clones with efficient knockdown of target gene expression (10).

In order to overcome this problem, we constructed triple shRNA-expression vectors containing three identical or different shRNA-expression units to elevate the expression levels of shRNA or target regions within an mRNA molecule, respectively (10). Both new vectors also contain a neomycin (Neo) resistance gene and an enhanced green fluorescent protein (EGFP) gene for the selection of transfectants. As a result, the two vectors similarly and successfully improved the overall knockdown efficiency as well as the yield of the stable clones with sufficient silencing. Furthermore, EGFP expression levels were well-correlated with the knockdown level, which is possibly applicable to prescreening of knockdown clones by EGFP fluorescence intensity. In this chapter, we describe the detailed procedure for the highly efficient vector-based RNAi using triple shRNA-expression vectors.

2. Materials

2.1. Plasmid Constructions

1. pSilencer 1.0-U6 siRNA expression vector (Ambion, Applied Biosystems, Austin, TX)
2. Synthesized oligos for the gene-specific shRNA-expression sequence

   For designing target sequences, various web-based or commercial services are available and several candidate sequences should be picked up at this point. In the prescreening by semi-quantitative RT-PCR following plasmid construction and transient transfection, most effective shRNA sequences are finally selected (see below). All synthesized oligos were purified by cartridge chromatography and the 5′ ends were phosphorylated.

As an example, the sequences of oligos for shRNA-expression against luciferase or XPA are shown as follows: sense and antisense sequences are underlined; the loop is shown in bold; the sequences in italics are the linkers for cloning into the vector.

(1) sh *Luciferase* (*Luci*): the target is 5′-CGTACGCGGAA TACTTCGA-3′,
5′-CGTACGCGGAATACTTCGA TTCAAGAGATCGAAGTATTCCGCGTACG*TTT TTT*-**3′**, **3′**-*CCGG*GCATGCGCCTTATGAAGC TAAGTTCTCTAGCTTCATAAGGCGCATGC *AAAAAATTAA*-**5′**

(2) sh *XPA* vector 284: the target is 5′-GACCTGTTATGG AATTTGA-3′,
5′-GACCTGTTATGGAATTT GATTCAAGAGATCAAATTCCATAA CAGGTC*TTTTTT*-**3′**,**3′**-*CCGG*CTGGACAATA CCTTAAACTAAGTTCTCTAGTTTAAGG TATTGTCCAG*AAAAAATTAA*-**5′**

(3) sh *XPA* vector **526:** the target is 5′-GGTGATATGAAA CTCTACT-3′,
5′-GGTGATATGAAACTCTAC T**TTCAAGAGA**AGTAGAGTTTCATATCACC *TTTTTT*-**3′**,**3′**-*CCGG*CCACTATACTTTGA GATGA**AAGTTCTC**TCATCTCAAAGTATA GTGG*AAAAAATTAA*-**5′**

(4) sh *XPA* vector **582**: the target is 5′-GGGTAGT CAAGAAGCATTA-3′,
5′-GGGTAGTCAAGAAGCATTA **TTCAAGAGA** TAATGCTTC TTGACTACCC*TTTTTT*-**3′**,**3′**-*CCGG*CCCATCA GTTCTTCGTAAT **AAGTTCTCT** ATTACGAAGAACTGATGGG *AAA AAATTAA*-**5′**

3. Annealing buffer: 30 mM Hepes-KOH (pH 7.4), 100 mM potassium acetate, 2 mM magnesium acetate.
4. Restriction enzymes and other enzymes for cloning: *Apa*I, *Eco*RI, *Hin*dIII, *Sac*I, *Dra*III, *Pst*I, *Kpn*I, T4 DNA polymerase, and calf intestinal alkaline phosphatase (CIP) (New England Biolabs, Ipswich, MA).
5. A QIAquick Gel Extraction Kit and QIAprep Spin Miniprep Kit (Qiagen Inc., Valencia, CA) were used for DNA extraction from gel slice after agarose electrophoresis and for plasmid purification from *Escherichia coli*, respectively.
6. Highly purified DNA oligos were used as sequencing primers for the plasmids constructed.

   U6PROM-F-SEQ: 5′-CTATAGAGGCTTAATGTGCG-3′
   EGFP-74-54-R: 5′-AGTTATGTAACGCGGAACTC-3′

pSilencer 299-R: 5′-TCCCTTTAGGGTTCCGATTT-3′
pSilencer 4275-R: 5′-TGTGGAATTGTGAGCGGATA-3′

7. Precipitation of plasmid DNA: 3 M sodium acetate (Wako Pure Chemicals, Osaka, Japan), 99.9% ethanol (Wako) and 70% ethanol.
8. LB Broth, Lennox (Difco) for LB solution: After dissolving in water, autoclave and store at 4°C.
9. LB Agar, Lennox (Difco) for LB plates: After dissolving in water, autoclave and then cool to approximately 50°C. Add ampicillin (final concentration 50 μg/ml) and pour into 10-cm dishes. Store at 4°C until use.
10. Ampicillin (Sigma, St Louis, MO): Prepare 5 mg/mL stock solution with pure water and aliquots are stored in freezer.
11. Competent *E. coli* cells: DH5α (Toyobo Co. Ltd., Osaka, Japan).
12. TAKARA DNA Ligation Kit I (Takara Bio Inc., Otsu, Japan)
13. Mupid submarine electrophoresis system (Advance Co, Ltd., Tokyo, Japan)
14. UltraPure™ agarose (Invitrogen., Carlsbad, CA)
15. Ethidium bromide (Aldrich) for agarose gel electrophoresis
16. TBE Buffer (Invitrogen) for the preparation of gels and running buffer.
17. 1-kb DNA Ladder (New England Biolabs). Store at 4°C.
18. Loading dye: 50% glycerol (Wako), 0.2% bromophenol blue (Nacalai Tesque), and 0.2% xylen cyanol FF (Wako). Filtration with filter paper is necessary. Keep at 4°C.
19. Gel-Doc system (Bio-Rad Laboratories Inc., Hercules, CA)

2.2. Cell Culture and Transfection

1. Dulbecco's modified Eagle's medium (Sigma) supplemented with 10% fetal bovine serum (Sigma), penicillin and streptomycin mixture (Gibco/BRL, Bethesda, MD).
2. Dulbecco's PBS [D-PBS(−)] (Wako).
3. 0.5 g/L trypsin containing 0.53 mol/L EDTA and phenol red (Nacalai Tesque Inc., Kyoto, Japan).
4. Effectene (Qiagen) for the transfection of plasmids into mammalian cells.
5. G418 disulfate salt solution (Sigma), added directly to the culture medium.
6. Autoclave penicillin cups (a short tube, 10 mm in length and with a 5-mm inner diameter, is convenient) and silicon grease.

2.3. Semiquantitative RT-PCR

1. An RNeasy Kit (Qiagen) for total RNA extraction from cultured cells.
2. Cell scraper (Nalge Nunc)
3. For the first strand synthesis of cDNA from RNA, a Superscript II preamplification system (Invitrogen) was used.
4. Amplifications were performed with EX-Taq DNA polymerase (Takara)
5. TaKaRa TP600 PCR Thermal Cycler Dice (TaKaRa)
6. The primers used for PCR are as follows:

   XPA
   forward: 5′-AACCACTTTGATTTGCCAAC-3′
   reverse: 5′-CAGTTCATGGCCACACATAG-3′
   β-Actin

   forward: 5′-CAAGGAGATGGCCACGGCTGCT-3′
   reverse: 5′-TCCTTCTGCATCCTGTCGGCA-3′
7. Mupid submarine electrophoresis system (Advance)
8. UltraPure™ agarose (Invitrogen), ethidium bromide (Aldrich) and TBE Buffer (Invitrogen) are described in Subheading 2.1
9. 100-bp DNA Ladder (New England Biolabs)
10. The loading dye as described in Subheading 2.1
11. Gel-Doc system (Bio-Rad).

2.4. Western Blot Analysis

1. Refrigerated centrifugation: For example, 5415R Centrifuge (Eppendorf, Hamburg, Germany)
2. Heating block: ALB-220 Thermo Alumi Bath (Asahi Glass Co., Ltd., Chiba, Japan) or equivalent heater.
3. Cell scraper (Nalge Nunc).
4. Dulbecco's PBS (−) [D-PBS(−)] (Wako).
5. 5. RIPA Buffer: 50 mM Tris-HCl (pH 7.5) (Wako), 0.15 M NaCl (Wako), and 1% Nonidet P-40 (Nacalai Tesque)
6. 10 mg/mL phenylmethylsulfonyl fluoride (PMSF; Sigma), dissolved in 2-propanol (Wako). Store in a −20°C freezer. See Note 1.
7. Bio-Rad Protein Standard I (Bio-Rad)
8. Bio-Rad Protein assay (Bio-Rad)
9. Laemmli sample buffer (Bio-Rad). Add 2-mercaptoethanol (Sigma) in a fume hood before use.
10. Prestained SDS-PAGE Standards (Bio-Rad)
11. Mini-PROTEAN3 electrophoresis system (Bio-Rad)
12. Ready Gels J (Bio-Rad)

13. SDS Running Buffer: 10× Tris/glycine/SDS buffer (Bio-Rad), diluted with pure water.
14. Absorbent Blotting Paper (Atto Corp., Tokyo, Japan)
15. Immobilon-P transfer membrane (Millipore Corp., Billerica, MA)
16. Semidry-type blotting apparatus: HorizBlot (Atto)
17. 99% methanol (Wako)
18. Transfer Buffer: 24.22 g of Tris-base (Wako) and 5.86 g of glycine (Wako), dissolved in 1.6 L of water followed by the addition of 0.4 L of methanol (Wako).
19. 10 mM phosphate-buffered saline (PBS): 0.2964 g of NaH_2PO_4 (Wako), 1.1499 g of Na_2HPO_4 (Wako), and 8.1816 g of NaCl (Wako), dissolved in 1 L of water. The pH should be adjusted to 7.4.
20. PBS-T: Add 1 mL of Tween 20 to 2 L of 10 mM PBS and mix.
21. Blocking solution: 3 g of skim milk, dissolved in 60 mL of PBS-T.
22. Washing buffer: dilute Blocking solution 10 times with PBS-T.
23. Anti-GFP antibody (Clontech Laboratories, Inc., Mountain View, CA). Monoclonal antibodies against XPA and GAPDH were raised by immunizing mice with bacterially expressed XPA and purified GAPDH, respectively.
24. HRP-conjugated secondary antibodies and SuperSignal West Femto Maximum Sensitivity Substrate (Pierce, Rockford, IL)
25. Las-1000 Image Analyzer (Fujifilm Corp., Tokyo, Japan)
26. Hybridization bag (Cosmo Bio Co. Ltd., Tokyo, Japan)

3. Methods

Human *XPA* was selected as a target gene in this study. The XPA protein is a component of the nucleotide excision repair machinery that repairs bulky DNA damage caused by various damaging agents, such as ultraviolet-light (11). This gene is mutated in xeroderma pigmentosum group A (XP-A) patients, an autosomal recessive disorder characterized by hyper UV-sensitivity and high incidence of skin cancer. Nonsense mutation of this gene causes a complete loss of XPA protein via a system of nonsense-mediated mRNA decay (12, 13) and a defect in nucleotide excision repair. Consequently, the cells derived from XP-A patients contain no detectable XPA protein and mRNA, and can be used as a XPA-null control.

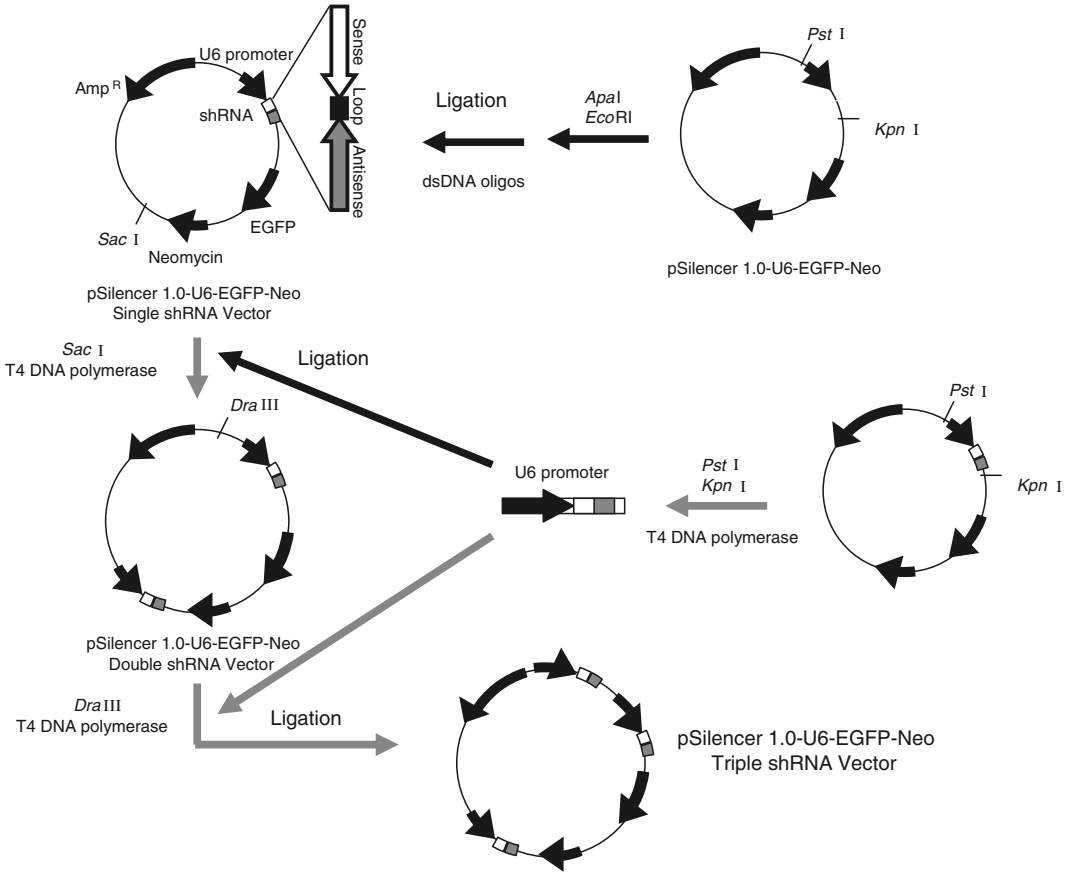

Fig. 1. Construction of triple shRNA-expression vector. The pSilencer 1.0-U6 siRNA expression vector (Ambion) was used as a parental vector. In addition to the insertion of the *Neo* and *EGFP* genes, a shRNA-expression sequence against human *XPA* gene was introduced into the vector. Anti *Luciferase* (*Luc*) shRNA-expression vector was also constructed as a control. For preparing triple expression constructs with anti-*XPA* (sh*XPA*) or anti-*Luc* (sh*Luc*) shRNA, a *Pst*I-*Kpn*I fragment carrying a shRNA-expression cassette was excised from the single shRNA-expression vector and introduced into the same vector using the *Sac*I and *Dra*III sites after treatment with T4 DNA polymerase for blunt-ending

An overview of plasmid construction is schematically shown in Fig. 1. The pSilencer 1.0-U6-EGFP-Neo vector was generated from the Ambion's pSilencer plasmid by inserting the Neo and EGFP genes to enable the efficient screening of shRNA-expressing cells. To date, however, various shRNA-expression plasmids containing such marker genes have been commercially available and the experimental procedure of this step is excluded in this chapter.

3.1. Plasmid Construction

1. pSilencer-EGFP-Neo was completely digested with *Apa*I and *Eco*RI and run on a 1% agarose gel. Linearized vector DNA was recovered from the gel using a QIAquick Gel Extraction Kit.
2. Treat the vector DNA with CIP according to the protocol from New England Biolabs, and purify using a QIAquick Gel Extraction Kit.

3. Dissolve insert DNA oligos in pure water at 100 pmol/μL and store at −20°C until use.
4. Mix 5 μL of the DNA oligo solution with 115 μL of annealing buffer and heat at 95°C for 5 min. Turn off the heater and leave until cooled to room temperature.
5. Mix 0.3 pmol of the annealed DNA oligo (step 4) with 0.03 pmol of the linearlized vector (step 2) and ligate using a DNA ligation kit. An overnight reaction is recommended.
6. Add 10 μL of the ligation mixture to 40 μL of competent *E. coli* cells and leave on ice for 30 min. After heating at 42°C for 45 s and chilling on ice for 2 min, add 200 μL of LB solution and shake at 37°C for 30–60 min. Streak onto LB plates and culture at 37°C overnight.
7. Pick up and transfer individual colonies into 2 mL of LB solution and incubate with shaking overnight. The LB should be cloudy on the following day.
8. Extract plasmid DNA using a QIAprep Spin Miniprep Kit.
9. Check the insert by appropriate restriction enzyme (*Hin*dIII etc) digestion, followed by agarose gel separation.
10. A positive clone is verified by sequencing and designated as a single shRNA-expression vector. See Note 2.
11. To construct a double shRNA-expression vector, a *Pst*I-*Kpn*I fragment was excised from the single shRNA-expression vector, removed 3′ overhangs by T4 DNA polymerase and introduced into the *Sac*I site of a single shRNA-expression vector (Fig. 1). The *Sac*I-digested vector must be treated with CIP after digestion. A triple shRNA-expression vector was similarly constructed from the double shRNA-expression vector by repeating the insertion step of the *Pst*I-*Kpn*I fragment using a *Dra*III site.

3.2. Transfection and Cloning of Resistant Colonies

1. The human cervix cancer cell line HeLa and Japanese XP-A patient-derived XP2OSSV cells were maintained in Dulbecco's modified Eagle's medium, supplemented with 10% fetal bovine serum (FBS) and antibiotics. One day before transfection, 2×10^5 cells were inoculated into 6-cm dishes.
2. Add 1/10 volume of 3 M sodium acetate to the plasmid solution and precipitate with 2.5 volume of 99.9% ethanol. After centrifugation, wash the pellet with 70% ethanol, dry, and redissolve in sterilized TE buffer or water. In order to avoid contamination, this step should be performed under sterile conditions. Determine DNA concentration by measuring OD260 nm using photometer.
3. The transfection complexes were prepared using plasmids and Effectene reagent according to the manufacturer's

instructions, and were delivered to the subconfluent cell culture prepared in step 1.

4. An anti-*luciferase* shRNA-expression vector was used as a negative control.
5. For transient experiments, cells were harvested 2 days after transfection.
6. In order to establish stable clones, spread cells from one 6-cm dish into ten 10-cm dishes containing 1500–750 μg/mL G418 1 day after transfection. After ~1-week incubation, almost all cells die suddenly. Continue the incubation for further 10–14 days until resistant colonies appear. Colonies of ~2 mm diameter are visible macroscopically and ready for harvest and expansion.
7. Wash the dish with PBS(−) and place a penicillin cup on an isolated single colony. Beforehand, smear a small amount of silicon grease evenly on the bottom edge of the cup, to fix the cup on the wet dish. Add trypsin solution into the cup and remove it immediately. After checking the cells being detached from the dish under a microscope, collect cells with medium by pipetting.
8. Inoculate cells into a 3.5-cm dish and culture in G418-containing medium. Expand confluent cells in the 3.5-cm dish to new two 6-cm dishes and use one of them for screening.

3.3. Semiquantitative RT-PCR

1. The cells cultured in a 6-cm dish were harvested, and cellular RNA was isolated using an RNeasy Kit (Qiagen) according to the manufacturer's instruction.
2. Determine RNA concentration by measuring OD at 260 nm and 280 nm using a photometer. Comprehensive instructions for handling of RNA sample are provided in the manual from Qiagen.
3. Run 1 and 0.5 μg of total RNA side by side on a 1% agarose gel containing ethidium bromide. If the RNA is successfully isolated without degradation, the two major bands of 28S and 18S ribosomal RNA will be observed and their relative band intensity should be 2:1.
4. Total RNA was reverse-transcribed using random hexamers and the Superscript II pre-amplification system according to the manufacturer's protocol.
5. Amplify the target DNA sequences of interest by PCR with specific primers and EX-Taq DNA polymerase. The best conditions for semiquantitative PCR must be determined in preliminary tests. See Note 3.
6. Run the PCR products on 2% agarose gels containing ethidium bromide and analyze using the Gel-Doc imaging system. Representative results are shown in Fig. 2.

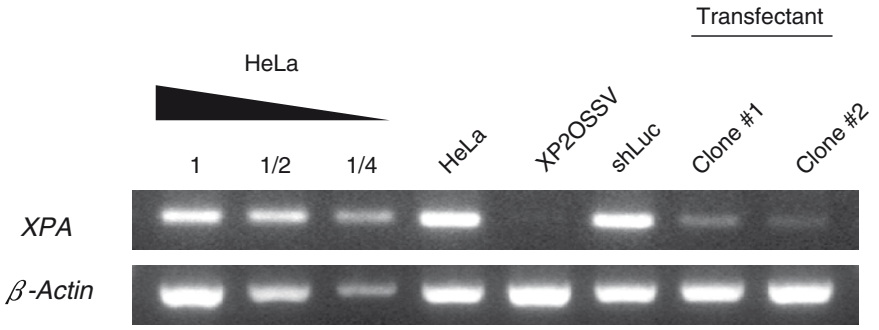

Fig. 2. Evaluation of gene silencing in stable transfectants introduced with the triple shRNA-expression vector (582). Total RNA was isolated from two clones (#1 and #2) and the amount of target *XPA* transcripts was analyzed by semiquantitative RT-PCR. *β-Actin* expression was also examined as reference. The two clones of shXPA transfectants exhibit efficient downregulation of XPA transcripts, whereas the expression level of a shLuc transfectant is not affected

3.4. Preparation of Cell Lysates

1. Keep PBS(−), RIPA buffer and tubes on ice. Do not forget to turn on a refrigerated microcentrifuge (4°C) before use.
2. Aspirate the medium from a 6-cm dish and wash 3 times with PBS(−).
3. After addition of 500 µL of PBS(−), collect cells using a cell scraper and pipetman, and transfer the cell suspension to a microtube on ice.
4. Centrifuge at maximum speed for 15 s and discard the supernatant.
5. Add 30–100 µL of RIPA buffer containing a protease inhibitor and suspend using a pipetman.
6. Keep on ice for 30 min.
7. Centrifuge at maximum speed for 20–30 min.
8. Transfer supernatant (cell lysate) to a fresh microtube.
9. Measure protein concentration using a Bio-Rad Protein assay with Protein Standard I.
10. To avoid repeated freezing and thawing, make aliquots and store at −80°C.

3.5. SDS-PAGE and Western Blotting

1. Adjust the protein concentration of each sample using RIPA buffer.
2. Add the same volume of Laemmli sample buffer containing 2-mercaptethanol and heat at 95°C for 5 min. To avoid bump-up of lid of microtube, tube with craw is useful.
3. Keep on ice for 10 min.
4. During **step 3**, set up Mini-PROTEAN apparatus and wash the slots of the gel by pipetting.
5. Apply the sample to the gel. Run for 1 h at a constant voltage of 100 V.

6. After electrophoresis, remove the gel from the apparatus and put it into transfer buffer.
7. Soak 8 sheets of 6 cm × 8 cm absorbent paper in transfer buffer.
8. Briefly soak a 6 cm × 8 cm sheet of Immobilon-P transfer membrane in methanol and put into transfer buffer. When cutting the membrane, use a clean cutter.
9. Overlay in order: 4 sheets of absorbent paper, the membrane, the gel, and again 4 sheets of absorbent paper onto the electrode plate of the HrizBlot apparatus.
10. Run at a constant current of 2 mA/cm^2 membrane for 1 h.
11. After successful transfer, the clear colors of the Prestained standards will be visible on the membrane.
12. Wash the membrane in pure water for 3 min. Do not dry the membrane during the following procedures to avoid dirty backgrounds on immunoblots.
13. Treat the membrane with blocking solution for 1 h.
14. Wash once with washing buffer for 5 min.
15. Treat with diluted first antibody for 1–16 h. Use a cold room in the case of overnight incubation.
16. Wash 3 times (5 min each) with washing buffer.
17. Treat with diluted HRP-conjugated secondary antibody for 1 h.
18. Wash once with PBS-T and twice with 10 mM PBS.
19. Transfer the membrane onto saran wrap and rapidly add SuperSignal West Femto reagent.
20. Transfer the membrane to a hybridization bag and analyze using the Las-1000 analyzer. Obtain several images for various exposure times.
21. Representative results are shown in Fig. 3. Efficient knockdown is observed in the transfectants of the triple shRNA-expression vector compared with those of the single shRNA-expression vector. See Notes 4 and 5.

4. Notes

1. A cocktail-type protease inhibitor is also commercially available and exhibited satisfactory results (e.g., Complete Mini from Gibco).
2. After the cloning of oligo DNA into the shRNA-expression plasmid, DNA sequencing of the insert and cloning sites is

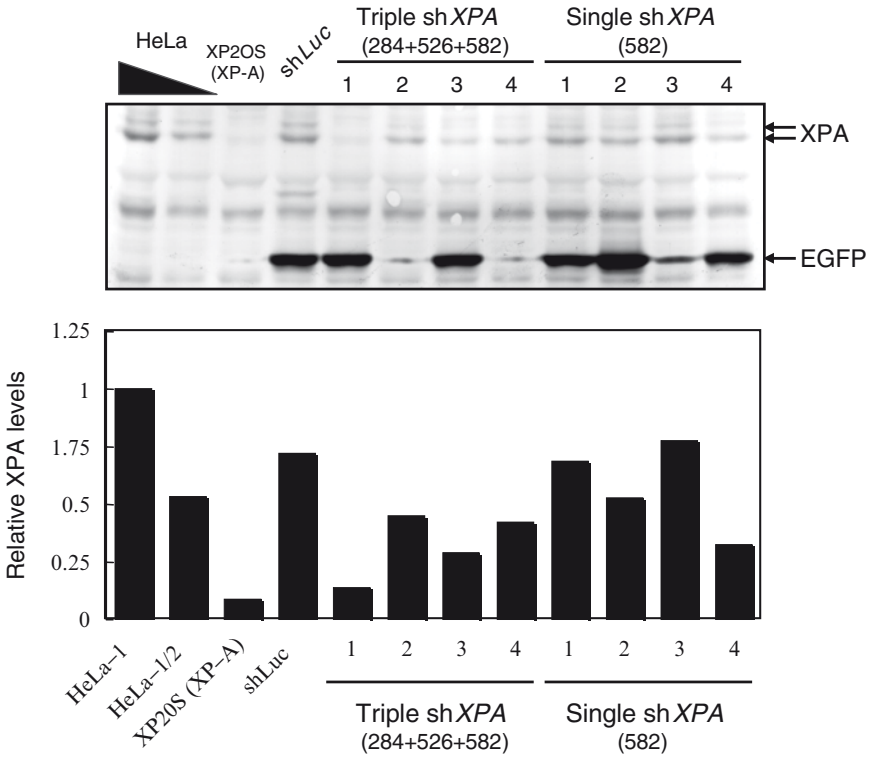

Fig. 3. Western blot analysis of target protein levels in stable transfectants. The data from the transfectants of the XPA triple shRNA-expression vector with different target sequences (284 + 526 + 582) or single shRNA-expression vector is represented here. Cell lysates, were prepared from stable transfectants and the cellular levels of XPA and EGFP proteins were analyzed by Western blotting using specific antibodies. Representative Western blot image is shown in the top panel. Band intensities of XPA were measured by an image analyzer and expressed as relative XPA levels to parental HeLa cells (*bottom panel*). Compared with the transfectants of the single XPA shRNA expression-vector, the transfectants of the triple shRNA-expression vector show more efficient knockdown of XPA and better correlation between the levels of XPA knockdown and EGFP expression

recommended. A standard sequencing reaction is applicable, even though the insert possibly forms a stem-loop structure.

3. It is very important to determine the condition of quantitative RT-PCR. Use two different dilutions of template solution (e.g., 1:1 and 1:5) and try a series of PCR cycles to obtain the most prominent difference of band intensities between the two samples. A real-time PCR system or Northern blotting are alternative choices and preferable for more accurate measurement of gene expression.
4. The transcriptome analysis was carried out using an Affymetrix GeneChip human U133 plus 2.0 DNA microarray system (Affymetrix Inc., Santa Clara, CA). In the positive clones, target *XPA* gene expression was reduced to less than 10% of the control. The expression of other repair-related genes exhibited neither downregulation nor upregulation (data not shown).

Furthermore, no significant upregulation of interferon response-related genes was observed.

5. Two transfectant clones with >90% reduction of cellular XPA level were functionally characterized and were demonstrated to exhibit a higher UV-sensitivity and reduced repair efficiency compared to control cells (10).

Acknowledgments

The authors thank Dr. Xia Zhao and Prof. H. Nakagawa of Kanazawa Medical University for his kind support. This work was also supported by KAKENHI, Kanazawa Medical University (S2007-3) and Kanazawa University.

References

1. Fire, A., Xu, S., Montgomery, M.K., Kostas, S.A., Driver, S.E. and Mello, C.C. (1998) Potent and specific genetic interference by double-stranded RNA in *Caenorhabditis elegans*. *Nature* **391**, 806–811.
2. Williams, B.R. (1999) PKR; a sentinel kinase for cellular stress. *Oncogene* **18**, 6112–6120.
3. Elbashir, S.M., Harborth, J., Lendeckel, W., Yalcin, A., Weber, K. and Tuschl, T. (2001) Duplexes of 21-nucleotide RNAs mediate RNA interference in cultured mammalian cells. *Nature* **411**, 494–498.
4. Elbashir, S.M., Lendeckel, W. and Tuschl, T. (2001) RNA interference is mediated by 21- and 22-nucleotide RNAs. *Genes Dev.* **15**, 188–200.
5. Yu, J.Y., DeRuiter, S.L. and Turner, D.L. (2002) RNA interference by expression of short-interfering RNAs and hairpin RNAs in mammalian cells. *Proc. Natl. Acad. Sci. U.S.A.* **99**, 6047–6052.
6. Brummelkamp, T.R., Bernards, R. and Agami, R. (2002) A system for stable expression of short interfering RNAs in mammalian cells. *Science* **296**, 550–553.
7. Paddison, P.J., Caudy, A.A., Bernstein, E., Hannon, G.J. and Conklin, D.S. (2002) Short hairpin RNAs (shRNAs) induce sequence-specific silencing in mammalian cells. *Genes Dev.* **16**, 948–958.
8. Zhou, H., Xia, X.G. and Xu, Z. (2005) An RNA polymerase II construct synthesizes short-hairpin RNA with a quantitative indicator and mediates highly efficient RNAi. *Nucleic Acids Res.* **33**, e62.
9. Tang, G. (2004) siRNA and miRNA:an insight into RISCs. *Trends Biochem. Sci.* **30**,106–114.
10. Nagao, A., Zhao, X., Takegami, T., Nakagawa, H., Matsu, S., Matsunaga, T., et al. (2008) Multiple shRNA expressions in a single plasmid vector improve RNAi against the XPA gene. *Biochem. Biophys. Res. Commun.* **370**, 301–305.
11. Kobayashi, T., Takeuchi, S., Saijo, M., Nakatsu, Morioka, Y.H., Otsuka, E., et al. (1998) Mutational analysis of a function of xeroderma pigmentosum group A (XPA) protein in strand-specific DNA repair. *Nucleic Acids Res.* **26**, 4662–4668.
12. Satotaka, I., Tanaka, K., Miura, N., Miyamoto, I., Satoh, Y., Kondo, S., et al. (1990) Characterization of a splicing mutation in group A xeroderma pigmentosum. *Proc. Natl. Acad. Sci. U.S.A.* **87**, 9908–9912.
13. Chang, Y.F., Imam, J.S. and Wilkinson, M.F. (2007) The nonsense-mediated decay RNA surveillance pathway. *Annu. Rev. Biochem.* **76**, 51–74.

Chapter 8

Strategies in Designing Multigene Expression Units to Downregulate HIV-1

Jane Zhang and John J. Rossi

Abstract

The treatment of viral diseases such as HIV and HCV is limited by the genetic diversity of the viruses, especially when they are under the selective pressure of drugs. This problem holds true for gene-based therapies using RNAi in which there is evolution of drug-resistant strains under the discriminating pressure of treatment (1, 2). In a gene therapy setting for treatment of HIV, the incorporation of multiple effector molecules, targeting different viral and cellular sequences, can improve viral inhibition by substantially delaying the emergence of escape mutants (3–8). However, for short hairpin RNA triggers of RNAi, high levels of expression by strong Pol III promoters has led to cell toxicity, and even death in experimental animals (9, 10). Here, we describe a new combinatorial anti-HIV gene expression system allowing simultaneous expression of multiple RNAi effector units from a single Pol II polycistronic transcript. Our platform is suitable for the inclusion of any shRNA sequence and can be combined with other types of small RNA antiviral inhibitors.

Key words: RNAi, HIV-1, miRNAs, siRNAs, Polycistron

1. Introduction

RNAi remains an attractive tool for gene silencing and is achieved by either transfection of synthetic, small, interfering RNAs (siRNAs) (11), by expression of short hairpin RNAs (shRNA) (12, 13), or by miRNA mimics (14, 15). RNAi-mediated knockdown has been successfully used to target a wide range of viral diseases, and stable expression systems can be efficiently used for the delivery of shRNA encoding genes to mammalian cells via viral vectors, resulting in long-term silencing of target genes (16–18).

Wei-Ping Min and Thomas Ichim (eds.), *RNA Interference*, Methods in Molecular Biology, vol. 623,
DOI 10.1007/978-1-60761-588-0_8,

The emergence of escape mutants has remained a limitation to the use of RNAi for gene therapy of HIV infection. Various groups have tested expression of combinations of anti-HIV shRNAs to achieve a more pronounced and longer lasting siRNA-mediated protection against HIV infection (1, 2, 19). In one study of siRNAs targeting HIV, an expression plasmid was generated that combined two or three siRNA candidates as separate Pol III expression cassettes (7). Markedly improved inhibition of HIV replication and a delayed emergence of escape mutants were observed in this study. Nevertheless, when shRNAs are ectopically expressed from strong Pol III promoters, there is clearly the potential for cell toxicity as a consequence of competition for endogenous microRNA pathway components (9, 10). To avoid this problem, we take advantage of endogenous RNAi transcripts and miRNAs (20–22) to express multiple RNAi effector units from a single Pol II polycistronic transcript.

We have shown that the incorporation and delivery of multiple miRNA mimics from a single RNA Pol II-promoted transcript, results in a marked inhibition of HIV-1 activity (23). Our miRNA-based siRNA expression system can be used for a variety of applications in both basic experimentation and in therapeutic applications where multiple siRNA or miRNA expression is required.

2. Materials

2.1. Cell Culture and Lysis

1. HEK293, 293T, and HT1080 cells: maintained in high glucose (4.5 g/l) Dulbecco's Modified Eagles Medium (DMEM) (Mediatech, Herndon, VA), supplemented with 10% fetal bovine serum (FBS) (Gibco, Grand Island, NY), 2 mM l-glutamine (Irvine Scientific, Santa Ana, CA), and 2 mM Penicillin/Streptomycin (Gibco, Grand Island, NY).
2. Human T-cell line CEM cells: maintained in RPMI 1640 medium (Mediatech, Herndon, VA) supplemented with 5 mM Sodium Pyruvate (Irvine Scientific, Santa Ana, CA), 10% FBS, 2 mM l-glutamine, and 2 mM Penicillin/Streptomycin.
3. Solution of Trypsin EDTA 1× in HBSS (Irvine Scientific, Santa Ana, CA).

2.2. Denaturing Urea-PAGE Gel

1. Tris Borate (TBE) Buffer 10×: 0.089 M Tris Borate pH 8.3, 2 mM Na_2EDTA (National Diagnostics, Atlanta, GA). Store at room temperature.
2. Urea (Biorad, Hercules, CA).
3. Ammonium Persulfate (APS) (Sigma, St. Louis, MO): prepare 10% solution in water, freeze in single use (200 µl) aliquots, and store at −20°C.

4. Tetramethylethylenediamine (TEMED) (Sigma, St. Louis, MO).
5. Bis-acrylamide solution: Accu-gel 19:1 Acrylamide 40% (w/v) (National Diagnostics, Atlanta, GA).
6. Loading dye: 10% sodium dodecyl sulfate (SDS) (Sigma-Aldrich, St. Louis, MO), 0.5 M EDTA (Sigma-Aldrich, St. Louis, MO), 1% bromophenol blue (Sigma-Aldrich, St. Louis, MO), 1% xylene cyanol (Fisher Biotech, Houston, TX).

2.3. Northern Blot

1. Running buffer (1×): 0.089 M Tris Borate pH 8.3, 2 mM Na_2EDTA. Store at room temperature.
2. Electrophoresis power supply (Dan-Kar Corp, Woburn, MA).
3. Vertical Gel Electrophoresis Apparatus, model V16 (Gibco-BRL Life Technologies, Gaithersburg, MD).
4. Transfer Power Supply: Electrophoresis Power Supply, model EC-150 (EC Apparatus Corporation, St. Petersburg, FL). Store at 4°C.
5. Genie electrophoretic transfer system (IDEA Scientific Company, Minneapolis, MN)
6. Hybond-N+ Nitrocellulose membrane (Amersham Biosciences, Piscataway, NJ).
7. 3MM chr chromatography paper (Whatmann, Maidstone, UK)
8. Molecular weight marker: Decade Marker (Applied Biosciences, Austin, TX). Store at –20°C.
9. Autoradiography cassette: Kodak BioMax cassette (Kodak, Rochester, NY).
10. BioMax MS film, 8×10 in. (Kodak, Rochester, NY).
11. G25 Microspin columns (GE Healthcare, Piscataway, NJ).
12. Large Hybrigene glass tube (Techne, Burlington, NJ).
13. Hybridization Incubator (Techne, Burlington, NJ).
14. 2× Wash Buffer: 2% SSC (Sigma-Aldrich, St. Louis, MO) and 0.1% SDS (Sigma-Aldrich, St. Louis, MO).
15. 0.5× Wash Buffer: 0.5% SSC (Sigma-Aldrich, St. Louis, MO) and 0.1% SDS (Sigma-Aldrich, St. Louis, MO).

2.4. p24 Assay

1. Hanks balanced salt solution (HBSS) (Irvine Scientific, Santa Ana, CA).
2. Alliance HIV-1 p24 antigen ELISA kit (Perkin Elmer, Wellesley, MA).
3. Microplate washer: MRW, model AM60 (Dynex Technologies, Chantilly, VA).
4. Microplate reader: Victor^3 1420 Multilabel Plate Reader (Perkin Elmer, Wellesley, MA).

3. Methods

The following describes the design and selection criteria necessary for the creation of shRNAs for insertion into a multi-shRNA expression platform. Once the construct is complete, it is expressed stably within the target cell (6) in which expression patterns and inhibitory function can be monitored. The levels of expression can be detected through Northern blotting of the RNAs, while the functional inhibition of HIV can be monitored by using a p24 ELISA assay.

3.1. Design of Multigene Expression Unit for Easy Insertion of shRNAs

1. These instructions are adapted from (23), with permission from Nature Publishing Group.
2. In generating a siRNA multiplexing expression system within a single transcript, choose a naturally occurring polycistronic miRNA as a scaffold. This miRNA expression unit should endogenously express two or more miRNAs from a single promoter. If the platform is in an intron, ensure that the cluster includes the flanking exons within the cluster for efficient heterologous miRNA processing and expression.
3. For easy insertion of shRNAs, clone into the scaffold unique restriction sites on both sides and as close as possible to the pre-miRNA sequences while using a minimal number of nucleotide substitutions. See Fig. 1 for an example of the constructs generated.
4. The heterologous hairpins should be designed to contain the natural pri-miR sequences at the base of the stems up to the final closing base pair, proximal to the mature miRNA (see Note 1). The upper part of the structure will then be replaced with an artificial, fully paired 23 bp stem, with an artificial 5-base loop that targets somewhere within the HIV-1 mRNA transcript. The upper part of this structure should closely resemble a classical Pol III-promoted shRNA construct.
5. For the majority of miRNAs, one strand is asymmetrically loaded into RISC to function as the guide strand to direct silencing of the target mRNA (21, 24–26). To ensure correct strand selectivity, the passenger strand sequence should be revised to closely mimic the secondary structure of the natural miRNA, while the guide strand should retain the original sequence. By maintaining the general secondary structures of the premiRNA leader sequences and heterologous stems, the efficacy and specificity of the miRNAs are greatly improved.
6. To further suppress HIV-1 replication and any escape mutants that may arise, another inhibitory agent may be added onto the construct. In particular, we have inserted a RNA TAR decoy that is processed via the snoRNA processing mechanism,

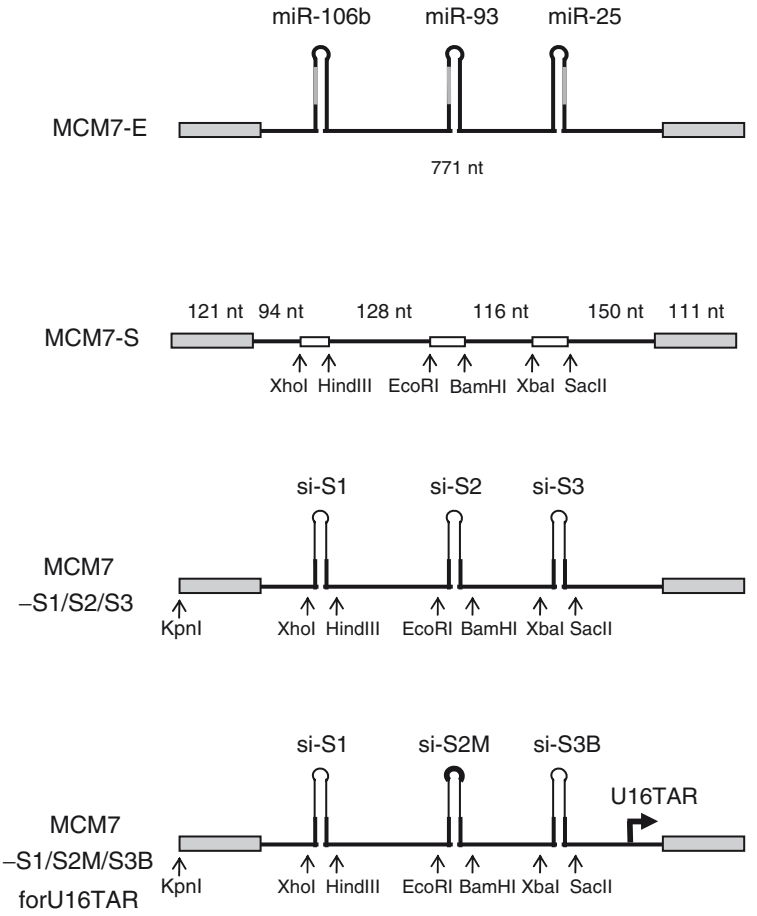

Fig. 1. Overview of mir-106b polycistron based expression plasmids. (**a**) Schematic diagram of the mir-106b polycistronic miRNA expression plasmids and the derived siRNA expression plasmid. The "MCM7" name was used to indicate that the mir-106b cluster is located in intron 13 of the protein encoding gene MCM7 on chromosome 7q22.1. MCM7-E and –S, refers to exon and scaffold, respectively. MCM7-S1/S2/S3 refers to targeting of three independent targets sites, S1–S3, in the viral HIV-1 genome. U16TAR decoy refers to the nucleolar RNA TAR decoy. (Reproduced from (23) with permission from Nature Publishing Group)

downstream of the last miRNA hairpin. We have shown that the addition of this TAR decoy greatly adds to the inhibitory effect of the cluster upon viral replication (23). Any other modality other than RNAi (such as snoRNAs) may be used to increase the effectiveness of the cluster (see Fig. 1).

3.2. Preparation of Samples for Detection of RNA Expression by Northern Blotting

1. Stably transduced CEM cells are maintained in RPMI media and split at 1:6 when approaching confluency (see Note 2).
2. Isolate approximately $5–10 \times 10^6$ cells and extract RNA using your method of choice (see Note 3).
3. Resuspend the RNA pellet in 30 µl of RNAse-free H_2O and measure sample concentration.

4. Add one volume of loading dye to 20 µg of RNA (see Note 4).
5. Incubate at 90°C for 5 min and place on ice until needed. Store the remainder of your RNA sample at –80°C (see Note 5).

3.3. Urea-PAGE

1. These instructions pertain to the use of a vertical gel electrophoresis apparatus, model V16 (Gibco-BRL Life Technologies, Gaithersburg, MD) with an electrophoresis power supply from Dan-Kar Corp, Woburn, MA. Glass plates should be washed extensively in distilled water with a rinsable detergent (e.g. Bacti-Stat by Ecolab, St. Paul, MN), cleaned with 70% EtOH, and air dried.
2. Prepare an 8% Urea-PAGE gel (see Note 6) by adding 10.5 ml of dH_2O, 3 ml of 10× TBE, 14.4 g of urea, and 6 ml of 19:1 acrylamide.
3. Allow the urea to go into solution by heating the sample in a 50°C water bath for 5 min, inverting every minute to speed up the process.
4. Add 250 µl of 10% APS and 25 µl of TEMED to the warm urea mixture (see Note 7), invert quickly to mix, and pour the solution into the glass plate cast while avoiding the formation of bubbles. Lay the cast flat on the table and insert the comb. The gel should polymerize in about 15 min.
5. Set up the vertical gel apparatus by placing the gel plate cast in front of the apparatus; secure it by using large binder clips on either side to connect the gel to the apparatus. Pour 1× TBE running buffer into the bottom and top chambers, respectively. Ensure there are no leaks (see Note 8).
6. Slowly remove the comb from the gel and wash each well extensively by using a 20 gauge needle attached to a 50 ml syringe filled with 1× TBE.
7. Prerun the gel at 400 V for 20 min.
8. Again, flush the wells with 1× TBE and begin loading RNA samples (see Note 9).
9. Run the gel at 250 V for 2 h or until the bromophenol blue dye migrates 1–2 in. above the bottom of the gel (see Note 10).

3.4. Northern Blotting for RNA Expression

1. Samples that have been separated in the aforementioned steps are transferred to nitrocellulose membranes electrophoretically. We use the Genie electrophoretic transfer system (IDEA Scientific Company, Minneapolis, MN) with the use of a transfer power supply model EC-150 (EC Apparatus Corporation, St. Petersburg, FL). The entire transfer procedure should take place at 4°C.
2. Prepare the transfer apparatus by presoaking the four green Scotch-Brite pads in 1× TBE.

3. Cut out six pieces of Whatman paper and one piece of Hybond-N+ membrane that are similar in size to the gel, and soak the membrane and five pieces of the Whatman paper in 1× TBE.
4. Remove the Urea-PAGE gel from the glass plates by separating the glass plates from one another, placing the dry Whatman paper onto the gel, flipping the glass plate over so that it is now facing upward, and carefully peeling the gel/paper downward and away from the glass plate.
5. Assemble the transfer apparatus "sandwich" by placing the following in this specific order: the lower electrode (usually the [−] cathode) onto the plastic tray, then the two bubble screens with ribs facing down, two Scotch-Brite pads, two pieces of pre-soaked Whatman paper, the dry Whatman paper with gel in place, the pre-soaked membrane, the remaining three Whatman papers, two Scotch-Brite pads, two bubble screens with ribs facing up, the upper electrode (usually the [+] anode), and lastly the plastic electrode cover. See Fig. 2.
6. Slide the entire tray into the transfer apparatus holder and pour 1× TBE into the system until the entire sandwich is covered when the apparatus is stood upright.
7. Transfer the RNA at 0.65 milliAmps for 1.5 h at 4°C (see Note 11).
8. Remove the membrane from the transfer apparatus and mark the membrane with a lead pencil to ensure which side contains the RNA.
9. UV cross-link the RNA to the membrane two times with an exposure of 2,000 millijoules/cm^2 each.
10. Place the membrane into a Hybrigene glass tube, add 10 ml of hybridization buffer, and hybridize at 42°C for 2 h in the hybridization incubator.
11. Prepare a labeled probe for the RNA by adding 15 μl of distilled H_2O, 1 μl of 10 mM oligo (see Note 12), 2 μl of 10× PNK Buffer, 1 μl of T4 PNK, and 1 μl of γ-ATP (see Note 13). Incubate the sample at 37°C for 30 min.
12. Add 30 μl of distilled H_2O to the probe and purify in the G25 microspin column by spinning the entire sample at 1,073×*g* for 4 min at room temperature.
13. Add 20 μl of the purified probe directly to the hybridization buffer in the glass tube and allow to hybridize overnight at 42°C in the hybridization incubator.
14. The following morning, wash the membrane by discarding the labeled probe buffer into an appropriate trash receptacle, and pour in approximately 25 ml of 2× wash buffer. Place back into the 42°C incubator for 10 min. Repeat a second time.

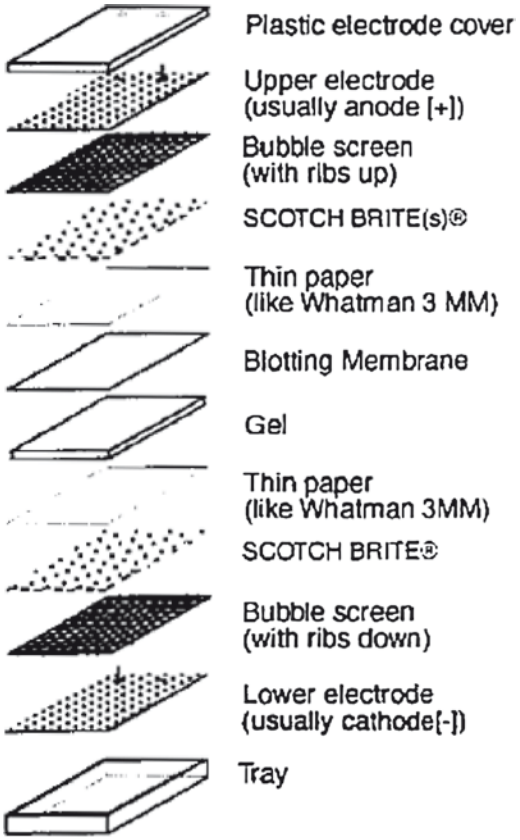

Fig. 2. Loading the Genie Blotter. Assembly of the Genie Blotter transfer apparatus tray. (Reproduced with permission from Idea Scientific Company.)

15. Pour out the 2× wash buffer, replace with 25 ml 0.5× wash buffer (see Note 14) and incubate for another 10 min.
16. Remove the membrane from the glass tube and wrap with one layer of plastic wrap, taking care to smooth out any wrinkles.
17. Place wrapped membrane into the autoradiography cassette and while in a dark room, place one piece of film directly on top of the membrane and incubate at −80°C for approximately 7 h (see Note 15) before developing. An example of the results produced is shown in Fig. 3.

3.5. Stripping and Reprobing the Blot

1. Once the desired bands are detected, the membrane can then be stripped and reprobed with a different probe. Strip the membrane by incubating at 80°C for 10 min in the hybridization incubator. Determine the strength of probe left by measuring levels of radioactivity using a Geiger counter.
2. Once the blot is stripped, it can then be reprobed with a second probe following the same steps as previously mentioned (see Note 16).

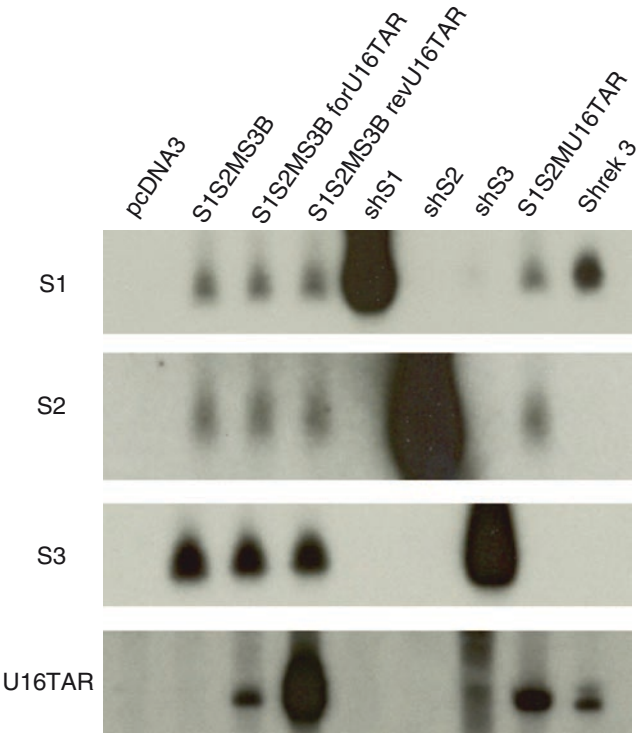

Fig. 3. Expression of the RNAs in the optimized MCM7 constructs. HEK293 cells were transiently transfected with each of the optimized MCM7 constructs and controls. Forty-eight hours following transfection, total RNA was collected, electrophoresed in an 8% polyacrylamide gel with 8M urea, blotted onto a nylon membrane, and hybridized with the corresponding 32P-labeled probes. Hybridization to U6-driven short hairpin siRNAs S1, S2, S3, and the U16TAR decoy expressed from Shrek 368 were used as positive controls. RNA prepared from an empty vector (pcDNA) transfected cell line was used as a negative control. S1, S2, and S3 siRNAs are approximately 21 nucleotides. The U16TAR decoy is 132 nucleotides. (Reproduced from (23) with permission from Nature Publishing Group.)

3.6. HIV-IIIB Infection of Cells

1. Collect 1×106 stably transduced CEM cells in 1 ml RPMI medium (see Note 17).
2. Add an appropriate amount of HIV-IIIB virus for an MOI of 0.01 (see Note 18).
3. Incubate overnight at 37°C.
4. Spin cells at 131×*g* for 10 min at 4°C.
5. To wash the cells, remove supernatant and resuspend the pellet in 3 ml of HBSS.
6. Repeat steps 4–5 of Subheading 3.5 for a total of three HBSS washes.
7. Resuspend each pellet in 1 ml medium, place in an individual well of a 24-well tissue culture plate, and incubate at 37°C.
8. After 3–4 days of incubation, resuspend cells carefully and split the cells by discarding 500 µl of sample.
9. Replace with 600 µl of fresh RPMI medium.

10. On day 7 following the viral challenge, collect 500 µl of sample and spin for 5 min at 2,415×*g* at room temperature.
11. While avoiding the cell pellet, carefully transfer 400 µl of supernatant to a newly labeled tube and store supernatant at –20°C until needed.
12. Continue to split the cells at every 3–4 days and collect samples every week (see Note 19).

3.7. p24 Assay for Measure of HIV-1 Replication

1. These directions pertain to the use of Perkin Elmer's Alliance HIV-1 p24 ELISA Assay kit. Plate washes will be performed with the MRW (AM60) by Dynex Technologies. The assay should be performed in a room designated for work with biohazard materials.
2. Equilibrate kit reagents and frozen samples to room temperature for 30 min.
3. Dilute Plate Wash Concentrate 20× to 1× by mixing 50 ml of 20× Concentrate with 950 ml H_2O and pour into Bottle A.
4. Pour fresh H_2O into Bottle B and empty waste Bottles C and D.
5. Prepare p24 Standards using the Positive control reagent (provided in kit) (see Note 20).
6. Add 20 µl Triton ×-100 to all wells except the substrate blank (see Note 21).
7. Add 200 µl of standards, negative control (sample media), and diluted samples to appropriate wells (see Note 22).
8. Seal plate with sealer tape (provided in kit) and incubate for 2 h at 37°C.
9. Wash plate in cell washer.
10. Add 100 µl Detector Antibody to all wells except for the substrate blank.
11. Seal plate and incubate for 1 h at 37°C.
12. Make the SA-HRP 1:100 Working Dilution Mix by adding 12 ml of Streptavidin-HRP Diluent to 120 µl of Streptavidin-HRP concentrate. Keep sample in the dark (see Note 23).
13. Wash plate in cell washer.
14. Add 100 µl SA-HRP Working Dilution Mix to all wells except for the substrate blank.
15. Seal plate and incubate for 30 min at room temperature, cover with foil, and store in a drawer.
16. Add 1 OPD tablet to 11 ml of Substrate Diluent and store away from light.
17. Wash plate in cell washer.
18. Add 100 µl OPD Mix to all wells, including the substrate blank.

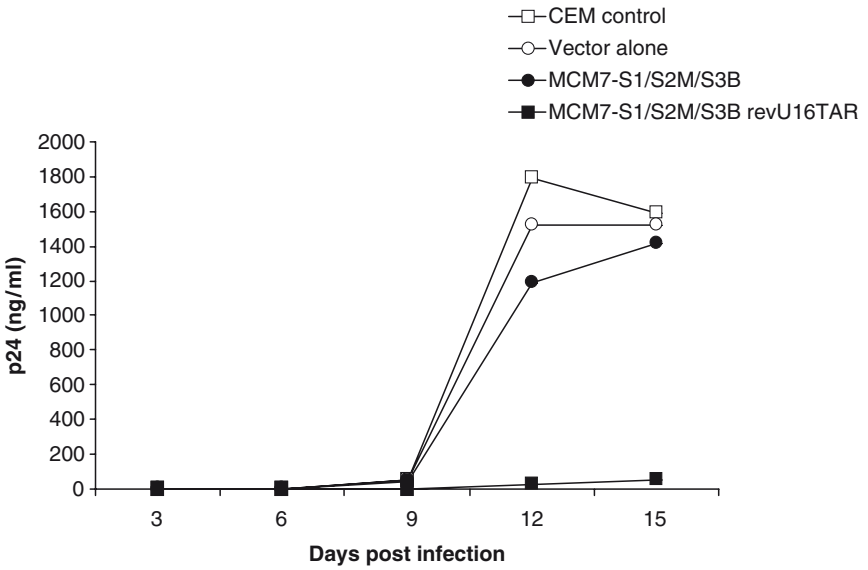

Fig. 4. Addition of the U16TAR decoy confers greater anti-HIV-1 activity. Stably transduced CEM-T cells (**a**) expressing the indicated vectors were challenged with HIV-IIIB. Culture supernatants were collected at various time points and analyzed by a p24 ELISA assay. Data points are reported as means ± standard deviation. Standard deviation calculations for each data point were <1.3. The addition of the U16TAR decoy in the MCM7-S1/S2M/S3B revU16TAR (*closed square*) confers long-term viral inhibition as compared to the MCM7-S1/S2M/S3B construct (*closed circle*). (Reproduced from (23) with permission from Nature Publishing Group.)

19. Seal plate and cover in foil. Incubate at room temperature for 10–15 min or until the samples turn bright orange.
20. Stop the reaction by adding 100 µl of stop solution to all wells.
21. Read the plate using the Victor 1420 Multilabel Plate Reader from Perkin Elmer at an absorbance of 450 nm and 490 nm with a read time of 1 s each. An example of the results is shown in Fig. 4.

4. Notes

1. Removal of the flanking pri-miRNA sequences abolishes siRNA functionality (23).
2. Confluency can usually be assumed when the media has changed from a red to a yellow/orange color.
3. We use RNA STAT-60 for our RNA extractions (Tel-Test, Friendswood, TX).
4. For example, if your RNA concentration is 1 µg/µl, you would need 20 µl of RNA to have a concentration of 20 µg.

You would then add 20 μl (1 gel volume) of loading dye to your sample.

5. RNA samples stored at −80°C can be used for up to a year.
6. The percentage of acrylamide used is dependent upon the size of your RNA. The larger your molecular weight, the less percentage of acrylamide is needed.
7. Step 4 of Subheading 3.3 must be completed as quickly as possible. The addition of APS and TEMED will cause the solution to polymerize within a minute or two.
8. If a radioactive-labeled marker is to be used on the gel, perform the following steps in an appropriate room designated for radioactivity work.
9. A decade marker may be loaded onto the gel if the size of the RNA sample is needed to differentiate from other RNA bands.
10. Alternatively, the gel may be run at 300 V for 1–1.5 h, if in a rush. However, a slower voltage is preferred for better separation and visualization of the RNA sample.
11. If in a rush, the transfer can be completed in just 1 h. However, to ensure proper transferring of the RNA to membrane, 1.5 h is optimal.
12. The oligo should be designed to contain at least 20 nt of the RNA.
13. Extreme care should be taken when handling radioactive material.
14. A more stringent wash is necessary to remove any residual unspecific background probe.
15. The length of time and number of washes are dependent on the strength of your probe and the γ-ATP used. If the RNA sample does not appear after 7 h, incubate the membrane with a fresh piece of film for a longer period of time until a satisfactory exposure has been obtained.
16. A single membrane can be stripped and reprobed multiple times. We have done so with five separate probes on the same membrane.
17. If duplicates or triplicates are required for each sample, adjust the amount of cells and virus accordingly.
18. The amount of virus will change according to the titer of the stock. Handle the virus and the cells with care; the entire procedure should take place in a room specialized for working with biohazard materials.
19. The collection of weekly time points are described in this method, and thus, cells need to be split to avoid over-confluency.

If time points are taken every 3 or 4 days instead, cells do not need to be split.

20. Follow the manufacturer's protocol to make the p24 standards.
21. When working with such a large sample size, it's easier to use a multi-channel pipetman. Pour the reagent into a plastic trough for ease of access. The first well of the plate must be left empty and is considered the "substrate blank."
22. Each sample must be diluted appropriately in order to record values within the range of the standards.
23. Streptavidin-HRP is light sensitive and must be kept away from light. We normally store our sample in a drawer until needed.

References

1. Dykxhoorn, D.M. and Lieberman, J. (2006) Silencing viral infection. *PLoS Med* **3**(7):e242.
2. Grimm, D. and Kay, M.A. (2007) Combinatorial RNAi: A Winning Strategy for the Race Against Evolving Targets? *Mol. Ther.* **15**(5): 878–888.
3. Andersson, M.G., Haasnoot, P.C., Xu, N., Berenjian, S., Berkhout, B. and Akusjarvi, G. (2005) Suppression of RNA interference by adenovirus virus-associated RNA. *J. Virol.* **79**(15):9556–9565.
4. Chang, L.J., Liu, X. and He, J. (2005) Lentiviral siRNAs targeting multiple highly conserved RNA sequences of human immunodeficiency virus type 1. *Gene Ther.* **12**(14):1133–1144.
5. Henry, S.D., van der Wegen, P., Metselaar, H.J., Tilanus, H.W., Scholte, B.J. and van der Laan, L.J. (2006) Simultaneous targeting of HCV replication and viral binding with a single lentiviral vector containing multiple RNA interference expression cassettes. *Mol. Ther.* **14**(4):485–493.
6. Li, M. and Rossi, J.J. (2005) Lentiviral vector delivery of siRNA and shRNA encoding genes into cultured and primary hematopoietic cells. *Methods Mol. Biol.* **309**:261–272.
7. ter Brake, O., Konstantinova, P., Ceylan, M. and Berkhout, B. (2006) Silencing of HIV-1 with RNA interference: a multiple shRNA approach. *Mol. Ther.* **14**(6):883–892.
8. ter Brake, O., t Hooft, K., Liu, Y.P., Centlivre, M., von Eije, K.J. and Berkhout, B. (2008) Lentiviral vector design for multiple shRNA expression and durable HIV-1 inhibition. *Mol. Ther.* **16**(3):557–564.
9. An, D.S., Qin, F.X., Auyeung, V.C., et al. (2006) Optimization and functional effects of stable short hairpin RNA expression in primary human lymphocytes via lentiviral vectors. *Mol. Ther.* **14**(4):494–504.
10. Grimm, D., Streetz, K.L., Jopling, C.L., et al. (2006) Fatality in mice due to oversaturation of cellular microRNA/short hairpin RNA pathways. *Nature* **441**(7092):537–541.
11. Elbashir, S.M., Harborth, J., Lendeckel, W., Yalcin, A., Weber, K., and Tuschl T. (2001) Duplexes of 21-nucleotide RNAs mediate RNA interference in cultured mammalian cells. *Nature* **411**(6836):494–498.
12. Brummelkamp, T.R., Bernards, R., and Agami, R. (2002) A system for stable expression of short interfering RNAs in mammalian cells. *Science* **296**(5567):550–553.
13. Paddison, P.J., Caudy, A.A., Bernstein, E., Hannon, G.J., and Conklin, D.S. (2002) Short hairpin RNAs (shRNAs) induce sequence-specific silencing in mammalian cells. *Genes Dev.* **16**(8):948–958.
14. Bartel, D.P. and Chen, C.Z. (2004) Micromanagers of gene expression: the potentially widespread influence of metazoan microRNAs. *Nat. Rev. Genet.* **5**(5):396–400.
15. Zeng, Y., Wagner, E.J. and Cullen, B.R. (2002) Both natural and designed micro RNAs can inhibit the expression of cognate mRNAs when expressed in human cells. *Mol. Cell* **9**(6):1327–1333.
16. Li, M.J., Bauer, G., Michienzi, A., et al. (2003) Inhibition of HIV-1 infection by lentiviral vectors expressing Pol III-promoted anti-HIV RNAs. *Mol. Ther.* **8**(2):196–206.
17. Rubinson, D.A., Dillon, C.P., Kwiatkowski, A.V., et al. (2003) A lentivirus-based system to functionally silence genes in primary mamma-

lian cells, stem cells and transgenic mice by RNA interference. *Nat. Genet.* **33**(3): 401–406.

18. Snove, O., Jr. and Rossi, J.J. (2006) Expressing short hairpin RNAs in vivo. *Nat. Methods* **3**(9):689–695.
19. Song, E., Lee, S.K., Dykxhoorn, D.M., et al. (2003) Sustained small interfering RNA-mediated human immunodeficiency virus type 1 inhibition in primary macrophages. *J. Virol.* **77**(13):7174–1781.
20. Bartel, D.P. (2004) MicroRNAs: genomics, biogenesis, mechanism, and function. *Cell* **116**(2):281–297.
21. Kim, V.N. (2005) MicroRNA biogenesis: coordinated cropping and dicing. *Nat. Rev. Mol. Cell Biol.* **6**(5):376–385.
22. Kim, V.N. (2005) Small RNAs: classification, biogenesis, and function. *Mol. Cells* **19** (1):1–15.
23. Aagaard, L.A., Zhang, J., von Eije, K.J., et al. (2008) Engineering and optimization of the miR-106b cluster for ectopic expression of multiplexed anti-HIV RNAs. *Gene Ther.* **15**(23):1536–1549.
24. Chendrimada, T.P., Gregory, R.I., Kumaraswamy, E., et al. (2005) TRBP recruits the Dicer complex to Ago2 for microRNA processing and gene silencing. *Nature* **436**(7051):740–744
25. Gregory, R.I., Chendrimada, T.P., Cooch, N. and Shiekhattar, R. (2005) Human RISC couples microRNA biogenesis and posttranscriptional gene silencing. *Cell* **123**(4): 631–640.
26. Lee, Y., Jeon, K., Lee, J.T., Kim, S. and Kim, V.N. (2002) MicroRNA maturation: stepwise processing and subcellular localization. *EMBO J.* **21**(17):4663–4670.

Chapter 9

Designing Optimal siRNA Based on Target Site Accessibility

Ivo L. Hofacker and Hakim Tafer

Abstract

RNA interference, mediated by small interfering RNAs (siRNAs), is a powerful tool for investigation of gene functions and it is increasingly being used as a therapeutic agent. However, not all siRNAs are equally potent – although simple rules for the selection of good siRNAs were proposed early on, siRNAs are still plagued with widely fluctuating efficiency. Recently, new design tools that incorporate both the structural features of the targeted RNAs and the sequence features of the siRNAs have substantially improved the efficacy of siRNAs. In this chapter, we present the algorithms behind these accessibility-aided tools and show how to design efficient siRNAs with their help.

Key words: RNA interference, mRNA structure, Target accessibility, siRNA design tools, Tutorial

1. Introduction

RNA interference (RNAi) describes the posttranscriptional gene silencing process triggered by endogenous or exogenous double-stranded RNAs (dsRNAs). After being processed by Dicer, the dsRNAs are transferred to the RNA-Induced Silencing Complex (RISC), where one of the strands (the guide strand) is introduced while the other strand is degraded (the passenger strand). Target recognition happens through hybridization of the guide RNA with its target gene, which causes the cleavage and the subsequent degradation of the target strand.

The successful utilization of artificial dsRNAs to knockdown specific genes was first reported by Fire et al. (1). In 2001, Elbashir et al. (2) showed that siRNA-mediated gene knockdown could also be applied in mammalian cells. Initial expectations that there was no need to search for optimal siRNA sequences (3), rapidly proved to be unfounded, as strong variations in silencing efficiency were reported for different siRNAs directed against the same target

Wei-Ping Min and Thomas Ichim (eds.), *RNA Interference*, Methods in Molecular Biology, vol. 623,
DOI 10.1007/978-1-60761-588-0_9,

(4). Nevertheless, the potential of RNAi to transiently knockdown genes motivated the scientific community to improve the siRNA design rules (for a review see (5)). Elbashir et al. (6) published the first protocol for designing active siRNAs. They encouraged the use of 21 nucleotides long siRNAs with a G/C content of about 50% and two nucleotides 3′overhangs.

In 2003, Khvorova et al. (7) and Schwarz et al. (8) proved that even though both strands of the dsRNA could serve as a guide strand (2, 6), the strand with the lower 5′ stability was preferentially incorporated into the RISC complex. Subsequent studies concentrated on finding sequence patterns on the guide strand that correlated with the repression efficacy (9–14). The majority of those studies confirmed that the relative stability of the siRNA ends was a major determinant of the functionality of siRNAs. Further improvements in the design of siRNA came from the study published by Patzel et al. (15), who showed that siRNA efficiency directly correlates with the siRNA structure.

The small number of siRNAs used in those early studies led to little agreement on the sequence patterns and parameter overfitting (16). The use of heterogeneous data, gathered either from previous work or from siRNA databases (for example, siRecords (17)), did not resolve this issue, as the oligonucleotide activity is highly sensitive to biological and experimental parameters (transfection efficiency, cell type, siRNA concentration, target concentration, efficiency measure). To overcome those problems, Huesken et al. (18) generated a set of 2,431 randomly selected siRNAs targeted against 34 mRNAs, which were used to train an artificial neural network for designing siRNAs. Statistical analysis of this data set confirmed some of the previously published features of siRNAs (duplex asymmetry) and also revealed new, highly significant sequence motives.

A long-debated topic in the field of siRNA design is the influence of the target structure on siRNA efficiency. While target site structure has been recognized as an important feature in the design of antisense oligonucleotides and ribozymes (19–24), data arguing both for (25–39) and against (14, 15, 40) the influence of target site accessibility on siRNA efficiency has been reported. From a thermodynamic point of view, the interaction of two RNAs can be decomposed into two stages: binding can only occur at positions not already involved in intramolecular base pairs. Thus, base pairs within the target site have to be opened to make the site *accessible*. The energy necessary to do this is termed “the disruption” or “breaking energy”. Once the binding site is devoid of structure, intermolecular helices can be formed, yielding a stabilizing interaction energy. The total binding energy is then computed as the sum of the hybridization energy and the breaking energy.

In principle, such a model could directly predict the fraction of mRNAs that will be bound by siRNAs. This, however, requires

knowledge of siRNA and mRNA concentrations, which are generally not available. Furthermore, the model implicitly assumes that reactants are free solutes, thus neglecting possible influences of mRNA binding proteins, active translation by the ribosome, and the RISC complex on the siRNA binding. Still, the application of this approach on siRNA data published by Schubert et al. (34), in which siRNA was targeted to a gradually less accessible target site, showed that siRNA efficiency is directly correlated to target site accessibility (41, 42). Those findings were corroborated by five further studies (29, 30, 37–39), which looked specifically at the effect of local target secondary structure on RNAi efficiency based on large (100 siRNAs against three genes) to very large (3,084 siRNAs against 82 genes) homogeneous data sets.

The majority of the siRNA design rules mentioned above can be mapped to key events of the silencing pathways (see Fig. 1). The limited length of the siRNA duplex, as well as the presence of 3′ end dangles, allows the siRNA to evade immunorecognition (43–45). The rules promoting the sequence/energy asymmetry (7, 8) reflect the ability of Dicer to sense the thermodynamic asymmetry between the two ends of the duplex. The negative effect of the guide strand's structure on the repression efficiency may be explained by a reduced ability of the siRNA to bind to its target and/or a hindered interaction of the siRNA with RISC components (15). Finally, the influence of the target site accessibility on the siRNA efficiency derives from (1) the ability of RISC to bind to single-stranded region only and (2) the inability of RISC to unfold structured RNA (36).

In the following section, we discuss the three siRNA design tools (*Si*rna (29, 46), OligoWalk (37, 38), and RNAxs (39)) that perform siRNA design aided by target accessibility criteria. We further explain in detail how siRNAs can be efficiently designed with their help.

2. Accessibility-Aided siRNA Design

2.1. *Sirna*

Ding et al. (29) presented the first attempt to design siRNAs by considering target site accessibility in 2004. Their algorithm called *Si*rna selects siRNAs based on sequence and accessibility criteria. In their algorithm, accessible regions are identified with the help of *S*fold. *S*fold computes the accessibility along the target sequence by generating a statistically representative sample of 1,000 structures from the Boltzmann-weighted ensemble of secondary structures. The equilibrium probability of nucleotide i in the target sequence to be unbound (the accessibility of nucleotide i) is estimated by counting how often the nucleotide is unbound in the sampled structures (24). A siRNA target site is

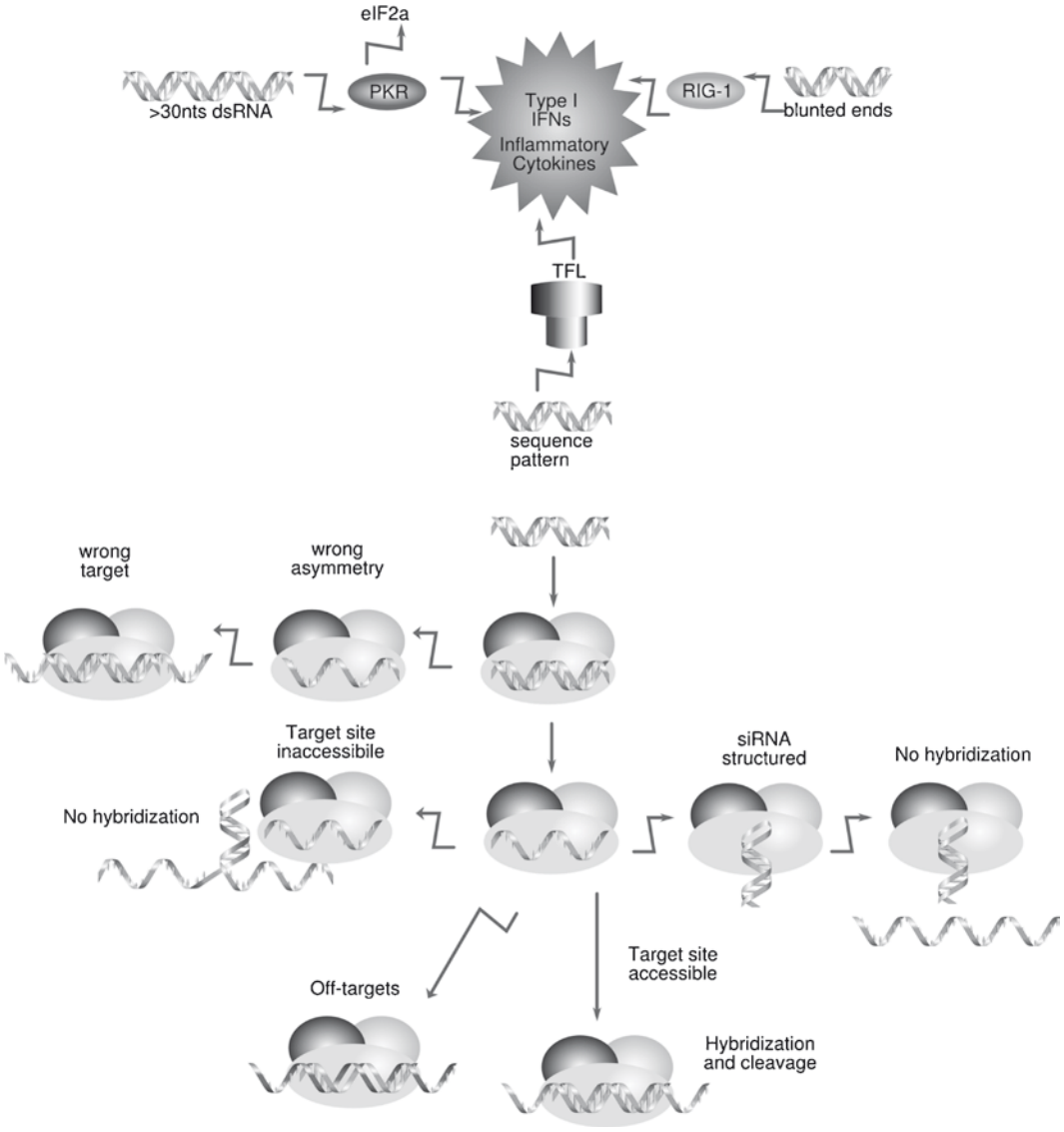

Fig. 1. Impact of siRNA characteristics along the silencing pathway. The innate immune system may be activated by dsRNAs. dsRNAs with specific sequence patterns or high "U" contents are recognized by Toll-Like Receptors (TLRs), inducing inflammatory cytokines and interferon of type I (IFN–α, IFN–β). Large dsRNAs (>30nts) are sensed by PKR (double-stranded RNA-activated protein kinase), which can induce interferon response, expression of inflammatory cytokines and cell death. dsRNAs with 2nts overhangs escape the RIG-1 triggered cytokines and interferon response. Once into RISC, the passenger strand is separated from the guide strand. The strand with the lower 5′–end stability is incorporated into RISC, while the other strand is degraded. A wrong asymmetry results in the selection of the bad siRNA strand, leading to no on-target effect. siRNAs that are highly structured are not able to hybridize to their target. Reciprocally, siRNAs targeting a highly structured region can not bind to their target. Finally, sequence-specific off-target effects make it more difficult to gain information from RNAi experiments

then considered accessible if the single nucleotide accessibility averaged over the binding site is higher than 0.5. For each such site, *S*irna selects siRNAs that further meet requirements of empirical sequence-based rules, including Reynolds rules (14), a

G/C content of 30–70%, the cleavage site instability rules of Khvorova et al. (7), and the asymmetry rules (7, 8). For each of the siRNAs that passed the previous filters, a further measure of accessibility is computed. This feature, termed "accessibility weighted interaction energy," is calculated by weighing each stacked base pair in the siRNA-mRNA interaction by the probability of the dinucleotide that is involved in the stack to be unpaired. siRNAs having a weighted interaction energy ≤ –10 kcal/mol are selected.

In a further study (30), Shao et al. extended *S*irna by using a slightly different accessibility measure. Shao defined the accessibility as the energy cost for breaking intramolecular base pairs located at the binding site. This disruption energy is the energy difference between the free energy of the original mRNA structure and the energy of the altered structure, where the siRNA target site is devoid of intramolecular base pairs. Again, this disruption energy is determined using a sample of 1,000 mRNA structures as computed by *S*fold (24, 29, 47). For each sampled structure, the breaking energy is computed by removing pairs in the target site and re-evaluating the energy of this modified structure. The resulting energy difference is averaged over the 1,000 structures in the sample. Note that this procedure differs somewhat from the thermodynamic model mentioned before, in that it does not allow for any refolding. Thus, it assumes that there is no time for the mRNA structure to adapt in response to siRNA binding, except for opening a few base pairs within the target site.

Based on a dataset of 100 published siRNAs directed against three mRNAs (PTEN (28), CD54 (28) and Lamin A (48)), Shao et al. showed that their new measure of accessibility can improve the siRNA selection efficiency over a random selection process by nearly 40%, 2.5 times more than the asymmetry criterion (16%), and significantly more than the degree of improvement using the sequence-based design rules (see for example, (14)). They advised designing siRNA against regions with disruption energies > –10 kcal/mol, with G/C content between 30% and 70% and without AAAA, UUUU, GGGG, or CCCC repeats.

2.1.1. Usage of Sirna

The user is faced with a sequence input form where sequence can be pasted or uploaded. All parameters and thresholds are preset and cannot be modified by the user. After processing, two result files sirna_f.out and sirna_de.out are available, containing the siRNAs designed using the Ding et al. or the Shao et al. rules, respectively (see Fig. 2 for a sample output). Currently, there is no way to select siRNAs that passes both the Ding and Shao filters. *S*irna can be found at http://sfold.wadsworth.org/sirna.pl.

2.2. OligoWalk

As in Shao et al. (30), the accessibility in OligoWalk is defined as the energy cost for removing all base pairs at the siRNA target site (37, 38). Here, however, this cost is defined as the difference in free energy of the mRNA in the native state and for the mRNA with the

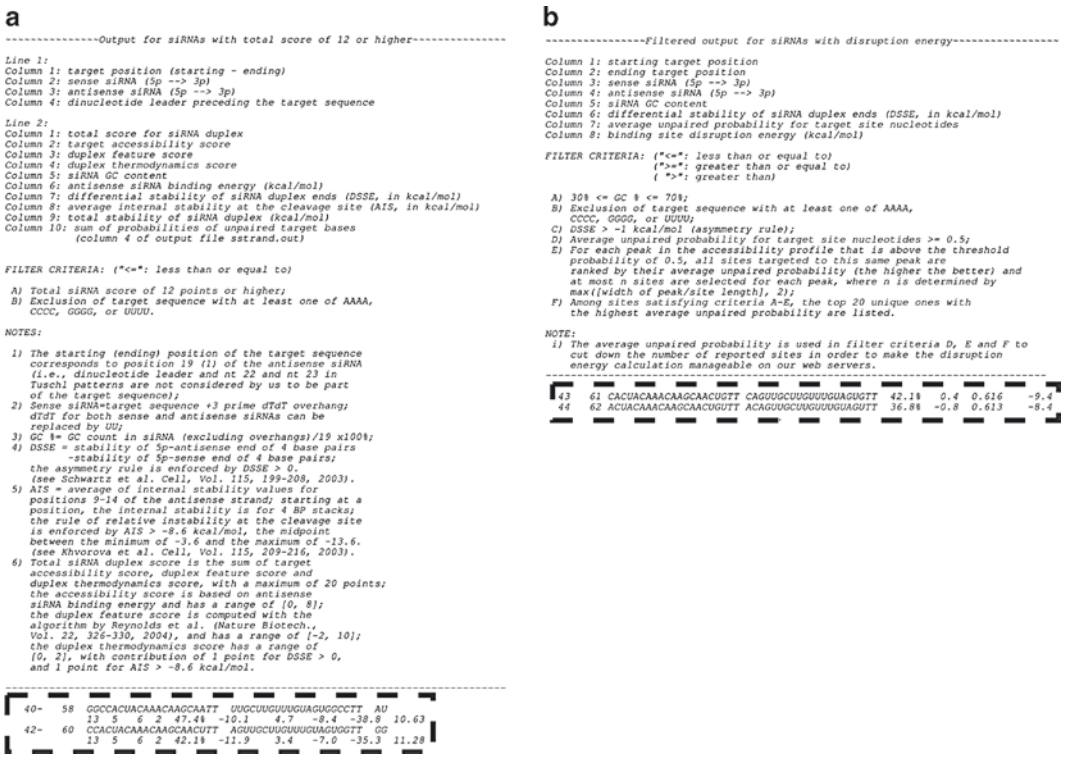

Fig. 2. Output generated by *S*irna. (**a**) siRNA designed based on the Ding design rules (29). (**b**) siRNA designed based on the Shao design rules (46). Both files contain a header describing the results as well as the set of features and the threshold applied. The siRNAs (*dotted rectangle*) are ordered by the position of the target site in the mRNA sequence

hybridization site single-stranded. The latter is computed by folding the mRNA under the constraint that bases within the target site are not allowed to pair. In contrast to Shao et al. (30), this allows the mRNA structure to assume different structures in the bound and unbound case. Moreover, rather than rely on a stochastic sample, free energies are computed exactly via the partition function over all possible secondary structures.

OligoWalk also uses the folding energy of the siRNA alone, as a measure of its propensity to form self-structure that may interfere with mRNA binding. In addition, it uses a larger number of sequence-based rules than most other methods. In total, the designs process considers 28 features (38) (five thermodynamics features, 23 sequence features from Launga et al. (49)). The selection of the siRNAs is carried out by a support vector machine (SVM) trained on the Huesken dataset by considering all 28 features. On their test dataset (653 siRNAs targeting 52 mRNAs), 78% of the siRNAs predicted by OligoWalk downregulated their target by more than 70%, an improvement of 33% over a random selection process.

2.2.1. Usage of OligoWalk (Fig. 3)

The web interface to OligoWalk can be found at: http://rna.urmc.rochester.edu/cgi-bin/server_exe/oligowalk/oligowalk_form.cgi.

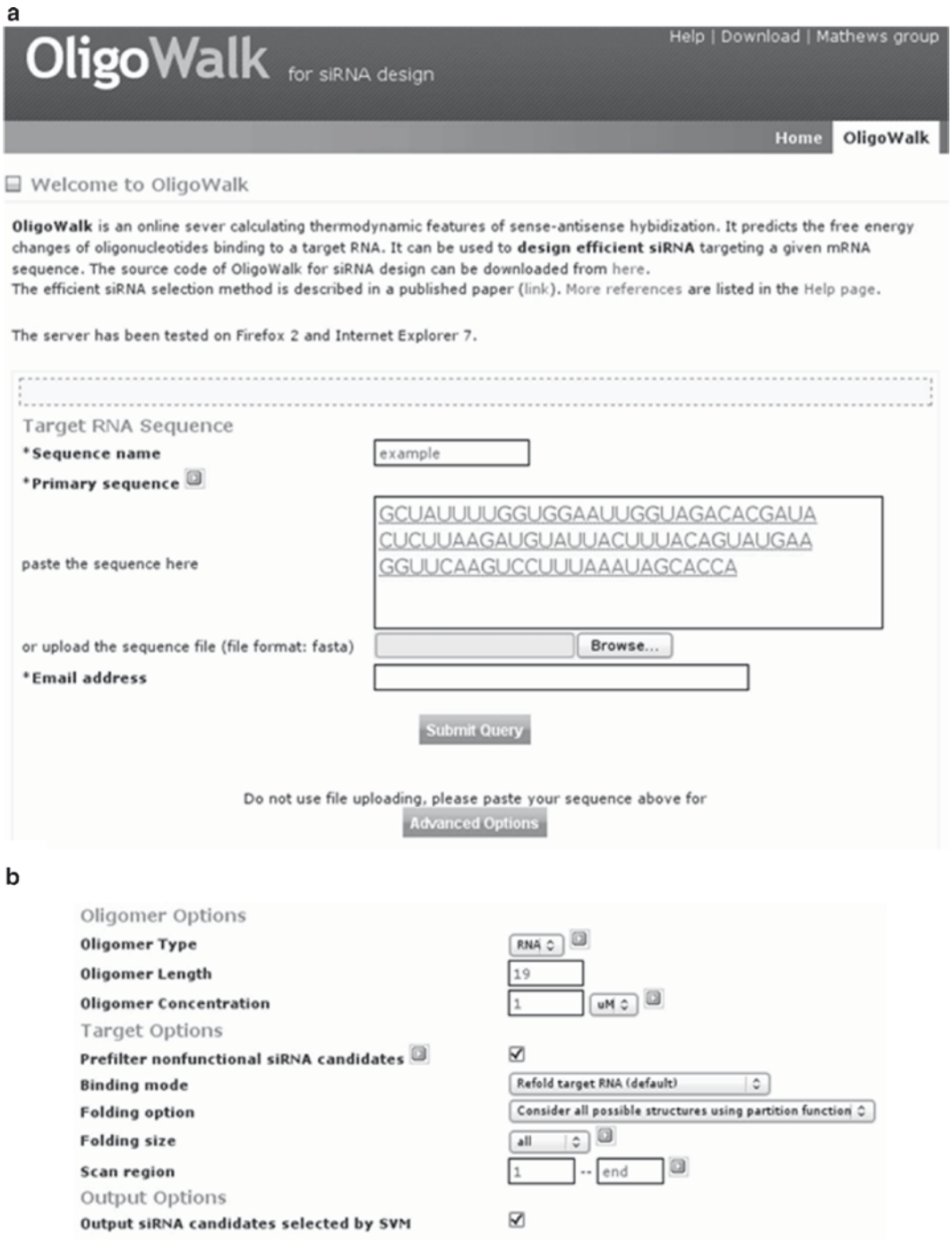

Fig. 3. Input forms of OligoWalk. (**a**) Default form. It allows the user to enter the sequence and its name as well as the email address. (**b**) Advanced form. The user can define the length of the siRNA, whether the siRNA should be filtered based on the Reynolds rules, and how the accessibility of the target should be computed. The default design options are shown

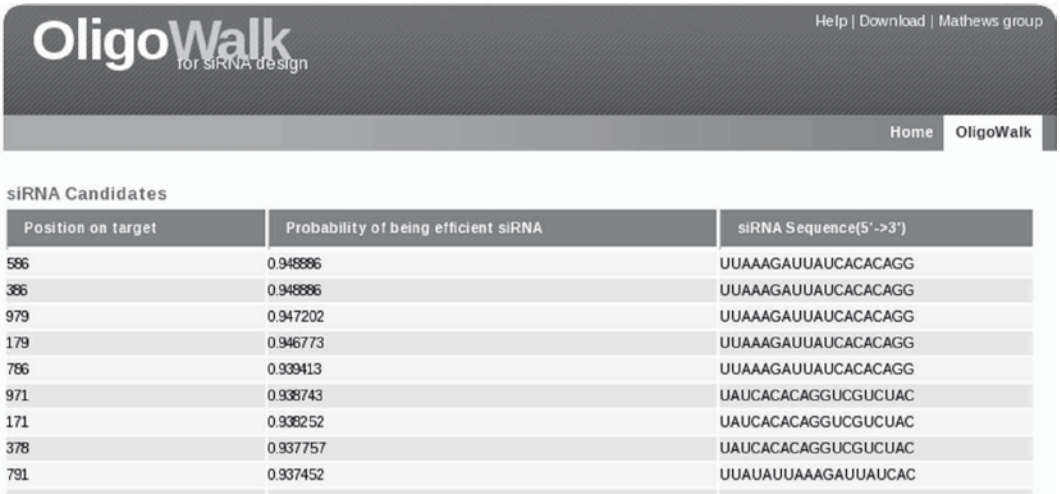

Fig. 4. Output generated by OligoWalk. The siRNAs are ranked based on their predicted repression efficiency

- Paste an mRNA sequence into the text field or upload a FASTA file.
- Give an email address in the email address form as it is mandatory.
- Click on the "Advanced Options"
- We recommend selecting "Prefilter nonfunctional siRNA candidates", as this significantly reduces the overall runtime of OligoWalk by computing the target accessibility only for those siRNAs that pass the Reynolds rules (14).
- Choose "Refold Target RNA" as the binding mode and "Consider all possible structures using partition function" as the folding options to guarantee the most precise accessibility computation.
- Click on "Submit Query" and wait for the results.

The selected siRNAs are ranked based on their predicted repression efficiency as computed by the SVM. A sample output of OligoWalk is shown in Fig. 4.

2.3. RNAxs

Tafer et al. (39) analyzed the effect of the target mRNA structure on RISC function *in silico*, and compared the potential of target site accessibility as an siRNA design criterion to a broad range of sequence-based design rules. Their definition of siRNA target site accessibility is the same as in OligoWalk, although the manner of computation is different. Accessibilities are computed using a local folding algorithm as implemented in RNAplfold (50, 51). In short, the program works by sliding a window of length *W*

over the sequence and computing for each window the partition function under the constraint that only *local* base pairs (where the two pairing partners are separated by at most L nucleotides) are allowed (see Fig. 5). From this, RNAplfold computes the accessibilities for all regions of length u as the probability that this stretch is unpaired in thermodynamic equilibrium. Furthermore, the accessibility for a region is averaged over all sequence windows of length W containing this region. The main advantage of this method is speed– as it considers only structures of size L, runtime is reduced from $O(n^3)$ to $O(n^2L)$, where n is the length of the mRNA. Most importantly, while OligoWalk needs to perform a separate RNA folding for each potential target site, RNAplfold computes the accessibilities of all possible target sites in a single pass.

In order to verify if the target site accessibility, as computed by RNAplfold, can be used to discriminate between functional and nonfunctional siRNAs, and to determine the optimal parameters for W, L, and u, two independent siRNA data sets of measured siRNA efficacies were used (18, 39). From both data sets, highly functional and poorly functional siRNAs were selected and the accessibility of their target sites was assessed with RNAplfold for different W, L, and u. Silencing efficiency correlated significantly with target site accessibility, with the most significant separation resulting from 80 nucleotides and 40 nucleotides for W and L, respectively.

When varying the length u of the unpaired region, two parameter ranges with especially good separation were observed. The first peak measures the accessibility of the 6–8 nucleotides starting at the 3′ end of the target site and therefore, corresponds to the so-called seed region. This is in agreement with previous observations that the 5′-seed region of both siRNAs and microRNAs is the major determinant for RISC-mediated target recognition (36, 52, 53). Furthermore, a second peak was observed for u values of 12–16, reminiscent of biochemical data showing that accessibility of the first 16 nucleotides within the target site is required for highly efficient RISC-mediated cleavage (36) (see Fig. 5).

Accessibility was further compared to a number of additional sequence and structure features (7, 8, 14, 15). The best two design criteria were asymmetry of the siRNA and target site accessibility. The overall best predictions resulted from the combination of accessibility, asymmetry, self-folding (folding energy of the siRNA (15)), and free-end (folding structure of the siRNA (15)) criteria.

In addition to the filtering, RNAxs uses a ranking of the siRNAs according to their overall performance in all four criteria. Because different selection criteria are crucial for distinct stages in

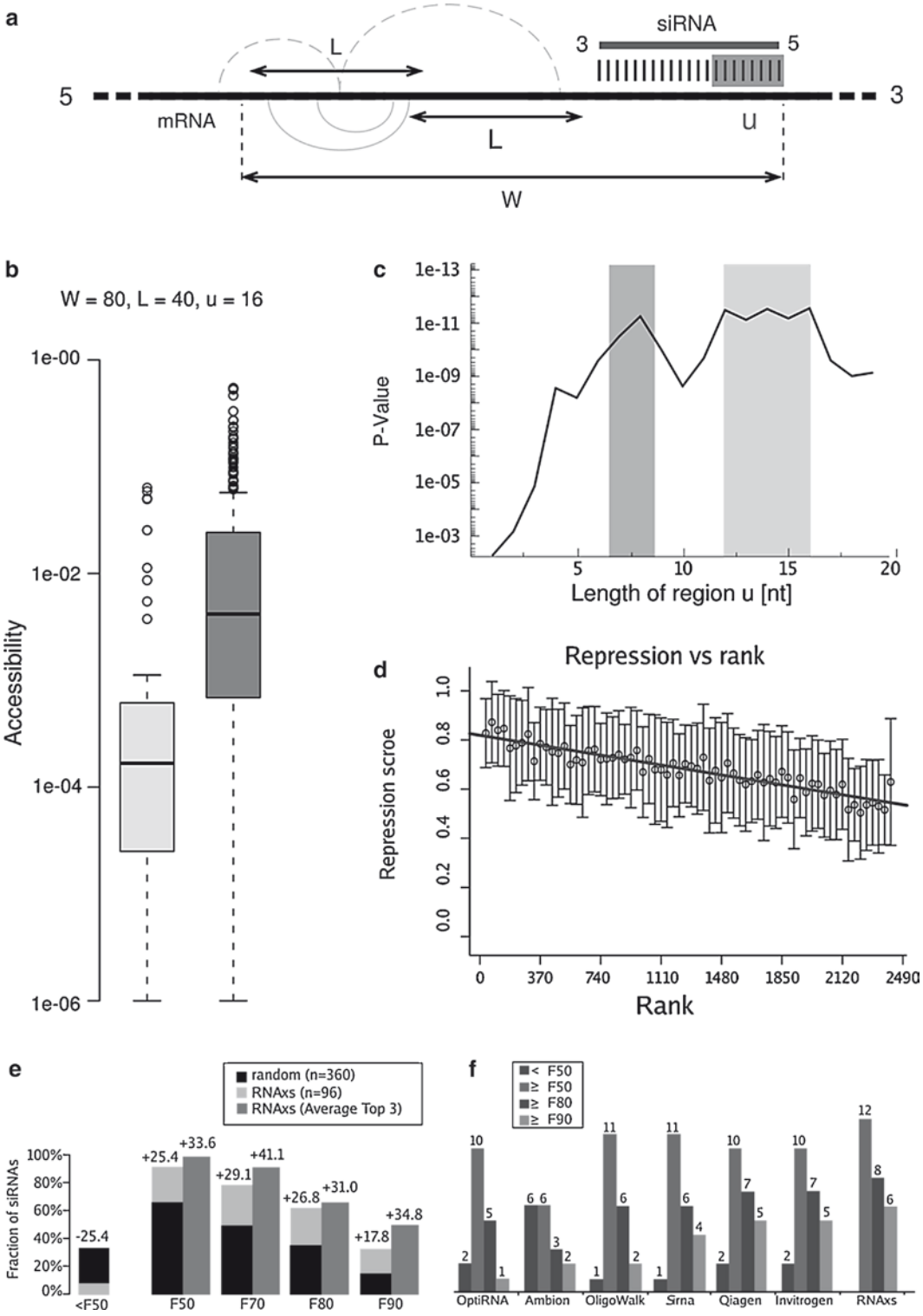
a
siRNA
3
5
L
5
3
mRNA
L
u
W
b
W = 80, L = 40, u = 16
Accessibility
1e-00
1e-02
1e-04
1e-06
c
P-Value
1e-13
1e-11
1e-09
1e-07
1e-05
1e-03
5
10
15
20
Length of region u [nt]
d
Repression vs rank
Repression scroe
0.0
0.2
0.4
0.6
0.8
1.0
0
370
740
1110
1480
1850
2120
2490
Rank
e
random (n=360)
RNAxs (n=96)
RNAxs (Average Top 3)
Fraction of siRNAs
100%
80%
60%
40%
20%
0%
-25.4
+25.4
+33.6
+29.1
+41.1
+26.8
+31.0
+17.8
+34.8
<F50
F50
F70
F80
F90
f
< F50
≥ F50
≥ F80
≥ F90
OptiRNA
Ambion
OligoWalk
Srna
Qiagen
Invitrogen
RNAxs

the RNAi pathway, poor performance in one descriptor cannot presumably be compensated by good values in another. Therefore, a hierarchical sorting was devised that emphasizes the least favorable criterion for each siRNA, rather than constructing a combined score (see Fig. 5).

The algorithm was tested on an independent dataset of 360 siRNAs, targeting every other position of four genes. On average, over 75% of the rationally selected siRNAs had a repression efficiency >70% (+30% improvement over randomly selected siRNAs), and almost every third siRNA reduced gene expression by more than 90% (+18%). When considering the three top-ranked siRNAs for all four genes, half of them silenced the targeted gene by more than 90% (+35%) (see Fig. 5).

Prediction efficiency of RNAxs was compared to OligoWalk and *S*irna, as well as three commercial siRNA selection tools (Invitrogen, Ambion, Qiagen) and a machine-learning method, which does not use accessibility to design siRNA (OptiRNA). The comparison was carried out by sorting the designed siRNAs into different functionality classes (less than 50% (<F50), more than 50% (≥F50), more than 80% (≥F80), and more than 90% (≥F90). RNAxs was the only tool where all predicted siRNA had measured repression efficiency ≥F50. It was also the only tool to predict 50% of the siRNAs in the best functional category (16% for OligoWalk, 33% for *S*irna).

2.3.1. Design of siRNAs with the RNAxs Webserver

RNAxs (see Fig. 6) is available as a web service at: http://rna.tbi.univie.ac.at/cgi-bin/RNAxs.

- Paste a FASTA-formatted sequence into the sequence form. A sample sequence can be used by clicking on the "sample sequence" link.
- Thresholds in the design options might be used to limit the number of siRNAs. Each threshold can be set between 0 and 1, where 0 means no threshold is applied and 1 means the highest possible threshold is applied. The default thresholds should perform well for the majority of mRNAs.

Fig. 5. (**a**) The RNA is folded locally in a sliding window approach (window size W). Within W, base pairing is restricted to a maximum distance L. u represents the stretch of consecutive nucleotides within a siRNA target site starting at its 3′ end for which the accessibility is computed. Allowed and forbidden base pairs are shown in plain and dotted curved lines, respectively. (**b**) Box-plot diagram comparing the accessibility of functional (*dark box*) and non-functional (*light box*) siRNAs. The quartiles are represented by the edges of the rectangles; *black* horizontal lines within the boxes depict medians. The *circles* represent outliers and *dotted lines* show the standard deviation. (**c**) Accessibility distributions of functional and non-functional siRNAs are best differentiated for a length of 8 and/or 16 nucleotides (according to *p*-values). (**d**) Plot of the ranking of the siRNAs as defined in RNAxs and the measured repression efficiency. (**e**) Performance of RNAxs on a set of 360 siRNAs. siRNAs were grouped into five functionality classes: repression efficiency <50% (<F50), ≥50% (F50), ≥70% (F70), ≥80% (F80) or ≥90% (F90). (**f**) Performance of RNAxs compared to six other design tools. All tools were used with default parameters using the available web servers to design siRNAs against four genes. For each tool and each gene, the repression efficiency of the three best-ranked siRNAs was assessed

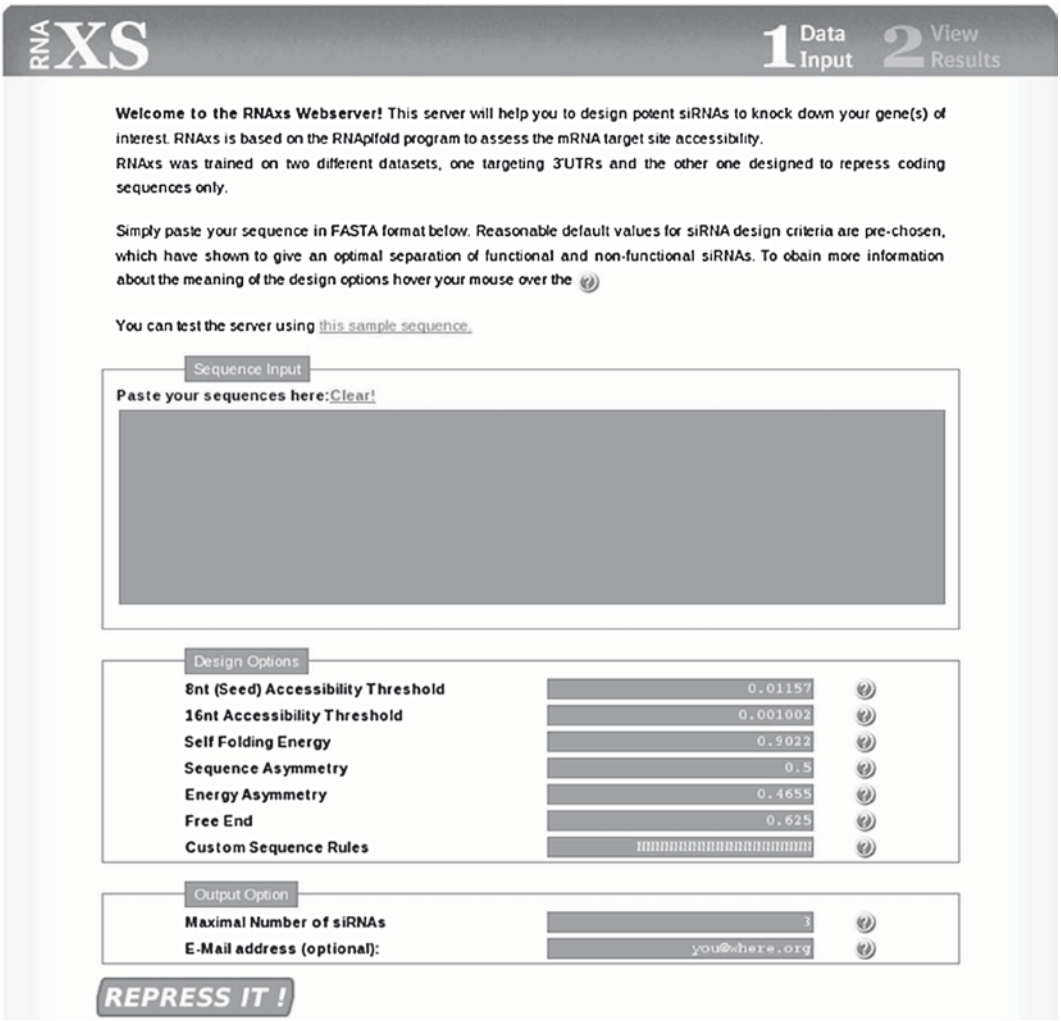

Fig. 6. Design form of RNAxs. The form is divided in three areas: a sequence input area, where a FASTA formatted sequence is pasted. A design area where thresholds on different parameters as well as base preferences can be set, and the output area which allows to set the number of siRNAs candidates. For each of them a plot of the accessibility is generated

- siRNAs can be filtered based on user-specified sequence rules. The pattern ANNNNGNNNNNNNNNNNN would force RNAxs to select only siRNAs containing a A at position 1 and a G at position 5. It should be noted that pattern must be exactly 19nts long.
- The "Maximal Number of siRNAs" option allows the user to choose the number of top-ranked siRNAs for which a detailed graphical output is desired. As this drastically increases the computation time, we do not recommend values higher than 10.

The results page contains the user-specified number of ranked siRNAs with their features scores, rank, and a graphical representation

of the accessibility profile around the target site (see Fig. 7). For each siRNA, a link to the NCBI BLAST program allows the user to check for putative off-targets. A tab-separated file, which contains the features scores and rank information for all siRNAs that passed the filters, can be downloaded.

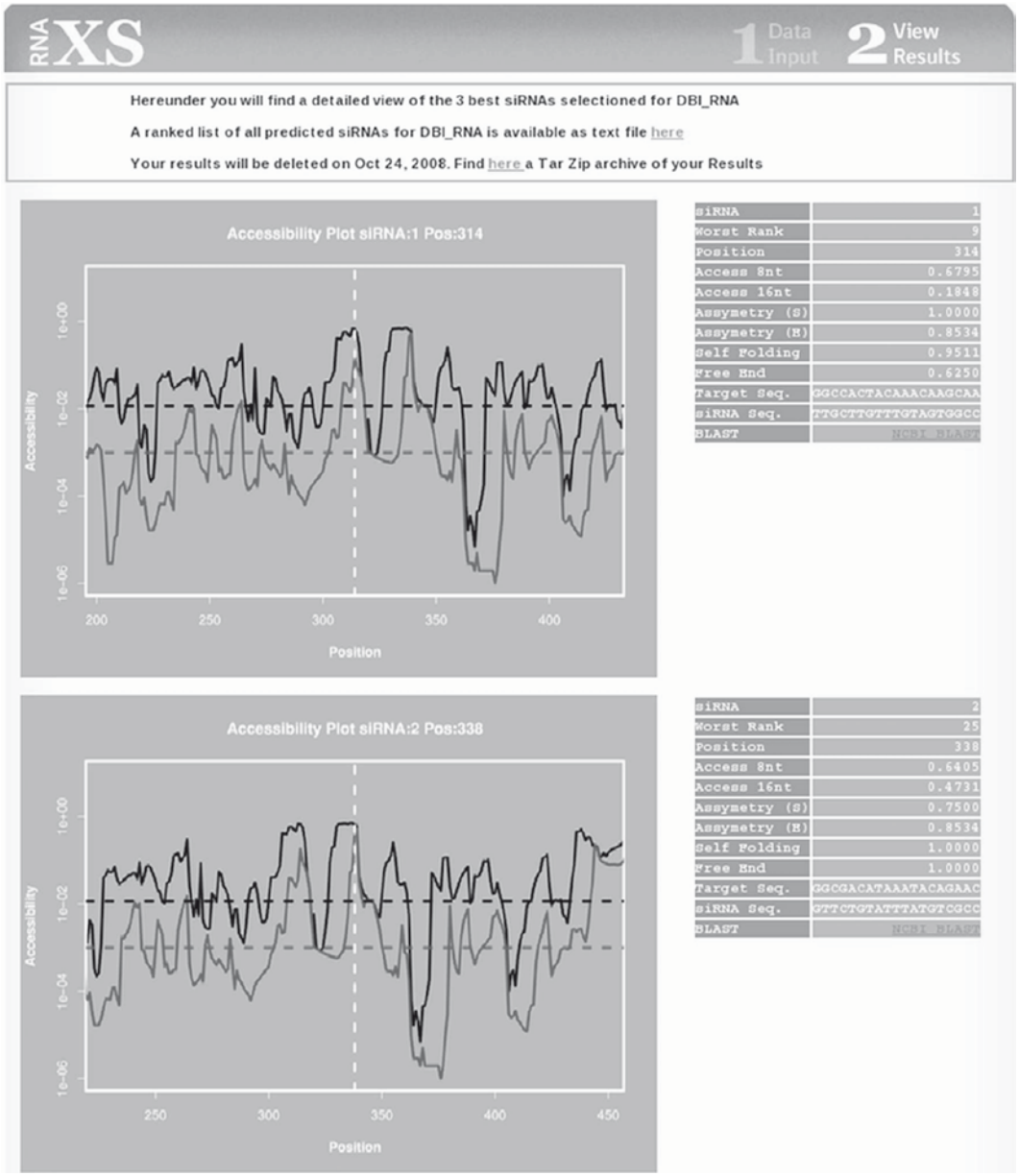

Fig. 7. Typical output of a RNAxs session. A user-defined number of siRNA are shown with their features scores as well as a plot of the accessibility profile around the target site. For each siRNA, a link to NCBI blast allows a search for putative off-targeted genes

2.3.2. Design of siRNAs with the RNAxs Standalone Version

RNAxs also exists as a standalone perl script available from http://www.tbi.univie.ac.at/~htafer/RNAxs/RNAxs.pl. The standalone version depends on RNAplfold (part of the ViennaRNA package) and the "Algorithm:Diff" perl module. In contrast to the web-server, the perl script does not produce a graphical output of the accessibility profile around siRNAs target sites; however, it has a number of additional features, such as the ability to design siRNAs against more than one target at a time. The design of siRNAs with the perl script is achieved by entering the following command: RNAxs.pl -s Sequence_file.seq where Sequence_file.seq is a FASTA-formatted file containing one or more mRNA sequences. For each sequence, a directory named after the sequence header is created. Each directory contains the accessibility profile for 8 and 16 nucleotides (8_unp, 16_unp), as well as the siRNAs ranked list (output.csv). An example output can be found in Table 1.

Furthermore, the perl script can design siRNAs that target several sequences at once. This is useful when homolog genes in different species should be downregulated by the same siRNA, or when all splice variants of a gene should be simultaneously knocked down. This is accomplished by specifying the -d option on the command-line, as in RNAxs.pl -s Sequence_file.seq -d 1.

The designed siRNAs are ranked by the overall worst_rank (worst rank of the siRNA for all targeted genes). A sample output file for all splice variants of HYAL1 can be found online at http://www.tbi.univie.ac.at/htafer/RNAxs/HYAL1_COMMON.xls.

Conversely, RNAxs can design siRNAs that target specific sequences within a set of similar genes, such as when only a particular splice variant should be downregulated or when paralogous genes have to be targeted individually. The command line is: RNAxs.pl -s Sequence_file.seq -x 1.

For each gene in the sequence file, a list of specific siRNAs is returned. An output file for all splice variants of HYAL1 can be found online at: http://www.tbi.univie.ac.at/htafer/RNAxs/HYAL1_SPECIFIC.xls.

RNAxs can further rank a user-specified list of siRNAs (e.g., from another design tool) based on its own design criteria. The corresponding command is:RNAxs.pl -s sequence_file.seq -c siRNA_files.seq.

The output is formatted in the same way as the output.csv files.

3. Notes

Currently, siRNA design tools can be split into two groups – tools that consider only siRNA-specific design criteria and tools that integrate mRNA structure features as well as basic siRNA features.

Table 1
Format of the output.csv file. The siRNAs are ranked by their worst rank (RANK), (the worst rank over all six design criteria). Pos stands for the position in the target sequence. Acc. 8 represents the accessibility of the seed on the target site. Acc. 16 represents the accessibility of the first 16 nucleotides on the 3′ end of the target site. Asy E stands for the energy asymmetry. Asy S stands for the sequence asymmetry. SelfFld represents the minimal free folding-energy and FreeEnd represents the number of paired nucleotides among the first four nucleotides at the 5′- and 3′-end. For all criteria, the scores are mapped to the interval [0..1], where 0 is the worst possible and 1 the best possible score

RANK	Pos	Target sequence	siRNA sequence	Acc. 8	Acc. 16	Asy E	Asy S	SelfFld	FreeEnd
21	1807	CCTTTATTCTCTTCTTAAT	ATTAAGAAGAGAATAAAGG	0.545	0.243	0.836	1.000	1.000	1.000
47	1207	CCCAGTACGCTAAAACAAT	ATTGTTTTAGCGTACTGGG	0.596	0.077	0.982	1.000	1.000	1.000

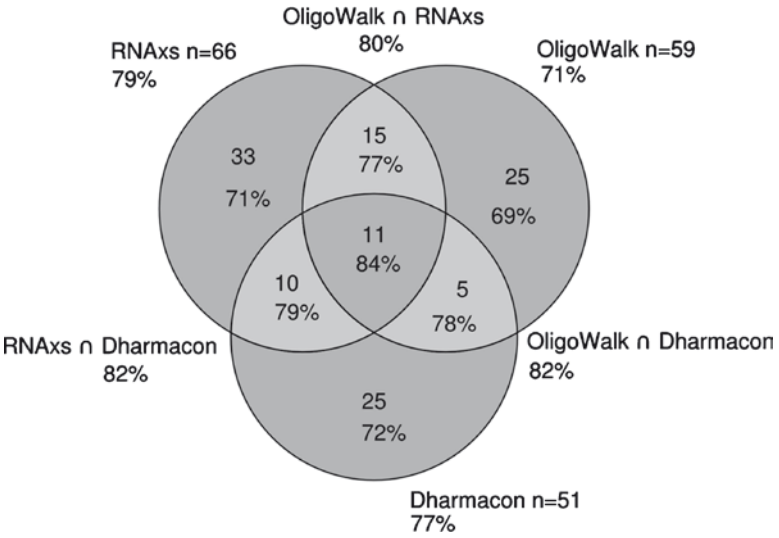

Fig. 8 Venn diagram of the siRNA predicted by three design tools (RNAxs, OligoWalk, Dharmacon) against the 4 genes of the test set of Tafer et al. (39). Average siRNA efficiency and number of siRNA is indicated. siRNAs predicted exclusively by one tool have a smaller average efficiency than siRNAs predicted by two or all three tools. Owing to their similar approaches, OligoWalk and RNAxs have more siRNAs in common than, for example, RNAxs and Dharmacon

Both approaches have their shortcomings: the negligence of the target site accessibility increases the number of predictions with low efficiency, while the negligence of sequence patterns hinders the selection of siRNAs with very high efficiency. The limitations of the current design approaches can be bypassed by selecting siRNAs that are highly scored by both types of tools (see Fig. 8).

References

1. Fire, A., Xu, S., Montgomery, M.K., Kostas, S.A., Driver, S.E., and Mello, C.C. (1998) Potent and specific genetic interference by double-stranded RNA in Caenorhabditis elegans. *Nature* **391,** 806–811
2. Elbashir, S.M., Harborth, J., Lendeckel, W., Yalcin, A., Weber, K. and Tuschl, T. (2001) Duplexes of 21-nucleotide RNAs mediate RNA interference in cultured mammalian cells. *Nature* **411,** 494–498
3. Stein, C. A. (2001) Antisense that comes naturally. *Nat. Biotechnol.* **19,** 737–738.
4. Holen, T., Amarzguioui, M., Wiiger, M.T., Babaie, E. and Prydz, H. (2002) Positional effects of short interfering RNAs targeting the human coagulation trigger Tissue Factor. *Nucleic Acids Res.* **30,** 1757–1766.
5. Patzel, V. (2007) In silico selection of active siRNA. *Drug Discov. Today* **12,** 139–148.
6. Elbashir, S.M., Martinez, J., Patkaniowska, A., Lendeckel, W. and Tuschl, T. (2001) Functional anatomy of siRNAs for mediating efficient RNAi in Drosophila melanogaster embryo lysate. *EMBO J.* **20,** 6877–6888.
7. Khvorova, A., Reynolds, A. and Jayasena, S.D. (2003) Functional siRNAs and miRNAs exhibit strand bias. *Cell* **115,** 209–216.
8. Schwarz, D. S., Hutvágner, G., Du, T., Xu, Z., Aronin, N. and Zamore, P.D. (2003) Asymmetry in the assembly of the RNAi enzyme complex. *Cell* **115,** 199–208.
9. Amarzguioui, M. and Prydz, H. (2004) An algorithm for selection of functional siRNA sequences. *Biochem. Biophys. Res. Commun.* **316,** 1050–1058.
10. Hohjoh, H. (2004) Enhancement of RNAi activity by improved siRNA duplexes. *FEBS Lett.* **557,** 193–198.

11. Hsieh, A.C., Bo, R., Manola, J., Vazquez, F., Bare, O., Khvorova, A., Scaringe, S. and Sellers, W.R. (2004) A library of siRNA duplexes targeting the phosphoinositide 3-kinase pathway: determinants of gene silencing for use in cell-based screens. *Nucleic Acids Res.* **32,** 893–901.
12. Takasaki, S., Kotani, S. and Konagaya, A. (2004) An effective method for selecting siRNA target sequences in mammalian cells. *Cell Cycle* **3,** 790–795.
13. Ui-Tei, K., Naito, Y., Takahashi, F. , Haraguchi, T., Ohki-Hamazaki, H., Juni, A., Ueda, R. and Saigo, K. (2004) Guidelines for the selection of highly effective siRNA sequences for mammalian and chick RNA interference. *Nucleic Acids Res.* **32,** 936–948.
14. Reynolds, A., Leake, D., Boese, Q., Scaringe, S., Marshall, W.S. and Khvorova, A. (2004) Rational siRNA design for RNA interference. *Nat. Biotechnol.* **22,** 326–330.
15. Patzel, V., Rutz S., Dietrich, I., Köberle, C., Scheffold, A. and Kaufmann, S.H.E. (2005) Design of siRNAs producing unstructured guide-RNAs results in improved RNA interference efficiency. *Nat. Biotechnol.* **23,** 1440–1444.
16. Saetrom, P. (2004) Predicting the efficacy of short oligonucleotides in antisense and RNAi experiments with boosted genetic programming. *Bioinformatics* **20,** 3055–3063.
17. Ren, Y., Gong, W., Xu, Q., Zheng, X., Lin, D., Wang, Y., and Li, T. (2006) siRecords: an extensive database of mammalian siRNAs with efficacy ratings. *Bioinformatics* **22,** 1027–1028.
18. Huesken, D., Lange, J., Mickanin, C., Weiler, J., Asselbergs, F., Warner, J. et al. (2005) Design of a genome-wide siRNA library using an artificial neural network. *Nat. Biotechnol.* **23,** 995–1001.
19. Lima, W. F., Monia, B. P., Ecker, D. J. and Freier, S. M. (1992) Implication of RNA structure on antisense oligonucleotide hybridization kinetics. *Biochemistry* **31,** 12055–12061.
20. Vickers, T.A., Wyatt, J.R. and Freier, S.M. (2000) Effects of RNA secondary structure on cellular antisense activity. *Nucleic Acids Res.* **28,** 1340–1347.
21. Mir, K.U. and Southern E.M. (1999) Determining the influence of structure on hybridization using oligonucleotide arrays. *Nat. Biotechnol.* **17,** 788–792.
22. Milner, N., Mir, K.U., and Southern, E.M. (1997) Selecting effective antisense reagents on combinatorial oligonucleotide arrays. *Nat. Biotechnol.* **15,** 537–541.
23. Zhao, J. J., and Lemke, G. (1998) Rules for ribozymes. *Mol. Cell Neurosci.* **11,** 92–97.
24. Ding, Y., and Lawrence, C.E. (2001) Statistical prediction of single-stranded regions in RNA secondary structure and application to predicting effective antisense target sites and beyond. *Nucleic Acids Res.* **29**, 1034–1046.
25. Bohula, E.A., Salisbury, A.J., Sohail, M., Playford, M.P., Riedemann, J., Southern, E.M. and Macaulay, V.M. (2003) The efficacy of small interfering RNAs targeted to the type 1 insulin-like growth factor receptor (IGF1R) is influenced by secondary structure in the IGF1R transcript. *J. Biol. Chem.* **278**, 15991–15997.
26. Kretschmer-Kazemi Far R. and Sczakiel, G. (2003) The activity of siRNA in mammalian cells is related to structural target accessibility: a comparison with antisense oligonucleotides. *Nucleic Acids Res.* **31**, 4417–4424.
27. Xu, Y., Zhang, H-Y., Thormeyer, D., Larsson, O., Du, Q., Elmén, J., Wahlestedt, C. and Liang, Z. (2003) Effective small interfering RNAs and phosphorothioate antisense DNAs have different preferences for target sites in the luciferase mRNAs. *Biochem. Biophys. Res. Commun.* **306**, 712–717.
28. Vickers, T.A., Koo, S., Bennett, C.F., Crooke, S.T., Dean, N.M. and Baker, B.F. (2003) Efficient reduction of target RNAs by small interfering RNA and RNase H-dependent antisense agents. A comparative analysis. *J. Biol. Chem.* **278,** 7108–7118.
29. Ding, Y., Chan, C. Y. and Lawrence, C. E. (2004) Sfold web server for statistical folding and rational design of nucleic acids. *Nucleic Acids Res.* **32** (Web Server issue), W135–W141.
30. Shao, Y., Chan, C.Y., Maliyekkel, A., Lawrence, C.E., Roninson, I. B. and Ding, Y. (2007) Effect of target secondary structure on RNAi efficiency. *RNA* **13,** 1631–1640.
31. Luo, K.Q. and Chang, D.C. (2004) The gene-silencing efficiency of siRNA is strongly dependent on the local structure of mRNA at the targeted region. *Biochem. Biophys. Res. Commun.* **318,** 303–310.
32. Yoshinari, K., Miyagishi, M. and Taira ,K. (2004) Effects on RNAi of the tight structure, sequence and position of the targeted region. *Nucleic Acids Res.* **32**, 691–699.
33. Overhoff, M., Alken, M., Far, R.K., Lemaitre, M., Lebleu, B., Sczakiel, G. and Robbins, I. (2005) Local RNA target structure influences siRNA efficacy: a systematic global analysis. *J. Mol. Biol.* **348**, 871–881.

34. Schubert, S., Grünweller, A., Erdmann, V.A. and Kurreck, J. (2005) Local RNA target structure influences siRNA efficacy: systematic analysis of intentionally designed binding regions. *J. Mol. Biol.* **348**, 883–893.
35. Brown, J.R. and Sanseau, P. (2005) A computational view of microRNAs and their targets. *Drug Discov. Today* **10**, 595–601.
36. Ameres, S. L., Martinez, J. and Schroeder, R. (2007) Molecular basis for target RNA recognition and cleavage by human RISC. *Cell* **130,** 101–112.
37. Lu, Z.J., and Mathews, D.H. (2008) OligoWalk: an online siRNA design tool utilizing hybridization thermodynamics. *Nucleic Acids Res.* **36** (Web Server issue), W104–W108.
38. Lu, Z.J. and Mathews, D. H. (2008) Efficient siRNA selection using hybridization thermodynamics. *Nucleic Acids Res.* **36**, 640–647
39. Tafer, H., Ameres, S. L., Obernosterer, G., Gebeshuber, C.A., Schroeder, R., Martinez, J. and Hofacker, I.L. (2008) The impact of target site accessibility on the design of effective siRNAs. *Nat. Biotechnol.* **26**, 578–583.
40. Boese, Q., Leake, D., Reynolds, A., Read, S., Scaringe, S.A., Marshall, W.S .and Khvorova, A. (2005) Mechanistic insights aid computational short interfering RNA design. *Methods Enzymol.* **392**, 73–96.
41. Mückstein, U., Tafer, H., Hackermüller, J., Bernhart, S. H., Stadler, P. F. and Hofacker, I. L. (2006) Thermodynamics of RNA-RNA binding. *Bioinformatics* **22**, 1177–1182.
42. Mückstein, U., Tafer, H., Bernhart, S. H., Hernandez-Rosales, M., Vogel, J., Stadler, P. F. and Hofacker, I. L. (2008) Translational control by RNA–RNA interaction: Improved computation of RNA–RNA binding thermodynamics, In: Bioinformatics research and development (vol. 13), Communications in computer and information science (Elloumi, M., Kung. J., Linial, M., Murphy, R., Schneider, K., and Toma, C., eds.). Springer, pp. 114–127.
43. Hornung, V., Guenthner-Biller, M., Bourquin, C., a Ablasser, A., Schlee, M., Uematsu, S. et al. (2005) Sequence-specific potent induction of IFN-alpha by short interfering RNA in plasmacytoid dendritic cells through TLR7. *Nat. Med.* **11,** 263–270.
44. de Haro, C., Méndez, R. and Santoyo, J. (1996) The eIF-2alpha kinases and the control of protein synthesis. *FASEB J.* **10,** 1378–1387.
45. Marques, J.T, and Williams, B. R. G. (2005) Activation of the mammalian immune system by siRNAs. *Nat. Biotechnol.* 23, 1399–1405.
46. Shao, X-D., Wu, K-C., Guo, X-Z., Xie, M-J., Zhang, J. and Fan, D-M. (2008) Expression and significance of HERG protein in gastric cancer. *Cancer Biol. Ther.* 7, 45–50.
47. Ding, Y. and Lawrence, C. E. (2003) A statistical sampling algorithm for RNA secondary structure prediction. *Nucleic Acids Res.* **31**, 7280–7301.
48. Harborth, J., Elbashir, S.M., Vandenburgh, K., Manninga, H., Scaringe, S.A., Weber, K. and Tuschl, T. (2003) Sequence, chemical, and structural variation of small interfering RNAs and short hairpin RNAs and the effect on mammalian gene silencing. *Antisense Nucleic Acid Drug Dev.* **13**, 83–105.
49. Ladunga, I. (2007) More complete gene silencing by fewer siRNAs: transparent optimized design and biophysical signature. *Nucleic Acids Res.* **35**, 433–440.
50. Bernhart, S.H., Tafer, H., Mückstein, U., Flamm, C., Stadler, P.F. and Hofacker , I.L. (2006) Partition function and base pairing probabilities of RNA heterodimers. *Algorithms Mol. Biol.* 1, 3
51. Bompfünewerer, A. F., Backofen, R., Bernhart, S.H., Hertel, J., Hofacker, I. L., Stadler, P. F. and Will, S. (2008) Variations on RNA folding and alignment: Lessons from Benasque. *J. Math. Biol.* **56,** 119–144.
52. Haley, B., and Zamore, P.D. (2004) Kinetic analysis of the RNAi enzyme complex. *Nat. Struct. Mol. Biol.* **11**, 599–606.
53. Jackson, A.L., Bartz, S.R., Schelter, J., Kobayashi, S.V., Burchard, J., Mao, M., et al. (2003) Expression profiling reveals off-target gene regulation by RNAi. *Nat. Biotechnol.* **21**, 635–637.

Chapter 10

Chemical Synthesis of 2′-O-Alkylated siRNAs

Joachim W. Engels, Dalibor Odadzic, Romualdas Smicius, and Jens Haas

Abstract

Chemical synthesis has been a major endeavor to create active siRNAs. The downregulation of mRNA by 21-mer double-stranded siRNAs can be improved by using modified nucleotides, especially *2′-O*-alkylated ones. Besides the commercially available *2′-O*-methyl ribosides, 2′-alkyl groups bearing positive charges are especially promising candidates. We have shown that in a proper formulation they are superior to unmodified siRNAs. This may be due to enhanced stability and most probably to a better uptake into the cells.

Key words: siRNA, High pressure liquid chromatography, Mass spectrometry, Alkylation

1. Introduction

The use of 21-mer siRNAs was introduced (1) shortly after the pioneering work of Fire (2) and Mello (3) on the mechanism of RNAi. In these constructions, Tuschl and co-workers recommended using 21-mer double-stranded RNA-oligonucleotides with 3′-end TT overhangs to mimic the cuts resulting from Dicer (Fig. 1). Early on, studies showed the possibility of using modified synthetic oligonucleotides with improved pharmacokinetic and pharmacodynamic properties for in vivo application (4–6) (Fig. 2). From earlier work on antisense oligonucleotides, it was shown that phosphorothioates and *2′-O*-alkylation are well-accepted. 2′-O-methyl sugar modification preserves the RNA type A-helix conformation, which is necessary for the RNAi mechanism and additionally increases nuclease stability (7, 8). Based on our present understanding of the RISC mechanism, the proper choice of strand to be selected by Ago2 determines the silencing event (9).

Wei-Ping Min and Thomas Ichim (eds.), *RNA Interference*, Methods in Molecular Biology, vol. 623,
DOI 10.1007/978-1-60761-588-0_10,

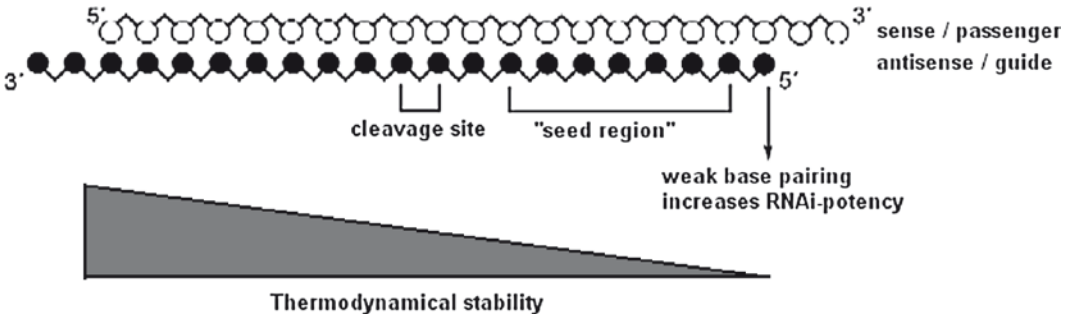

Fig. 1. siRNA design according to the Tuschl design (1, 4)

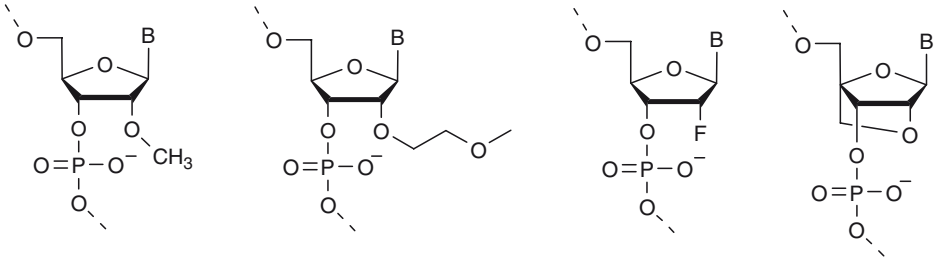

Fig. 2. Representative RNA derivatives for siRNA use, 2′-OMe, 2′-MOE, 2′-F and LNA

Cationic or better zwitterionic oligonucleotides (10) described here are expected to have an improved affinity to negatively charged RNA. Thus, the now easily accessible *2′-O*-aminoethyl-ribooligonucleotides (11, 12) or *2′-O*-aminopropyl-ribooligonucleotides (13, 14) are good candidates for siRNA silencing. Nuclease resistance has been generally obtained by modifying the phosphate backbone to phosphorothioates, and blocking the 2′-hydroxy group mainly by alkylation (15–17) 2′-O-modified oligonucleotides can be considered as analogs of oligoribonucleotides. *2′-O*-methyl ether can be found in naturally occurring RNA; for example, at certain positions in tRNAs, rRNAs, and snRNAs. The stability of (RNA)·(*2′-O*-alkyl-RNA) heteroduplexes (18) clearly depends on the nature of the 2′-O-alkyl group and increases in the order *2′-O*-dimethylallyl < *2′-O*-butyl < 2′-OH < *2′-O*-allyl < *2′-O*-methoxyethoxy. As early as 1987, it was reported that *2′-O*-methyl RNA forms a more stable duplex with a complementary RNA strand, than either unmodified DNA or even RNA (19).

The 2′-O-alkylribonucleotides prefer the C(3′)-endo conformation in a duplex with RNA. This sugar pucker has been found as a key structural element in RNA–RNA duplexes, which are generally more stable than DNA–DNA duplexes of the same sequence. It is worthwhile mentioning that the *2′-O*-methoxyethoxy modification does not only result in enhanced binding affinity to

RNA, but at the same time, it renders the oligomer more stable toward nuclease degradation as is also the case for most of the *2′-O*-alkyl derivatives, such as guanidinoethyl (11).

2. Materials

2.1. Synthesis

1. Triethylamine (NEt_3) (Fluka).
2. Dicyanoimidazole (DCI) (Acros Organics) chloro-N,N-diisopropylamino-2-cyanoethoxyphosphine (Fluka) bis-(N,N-diisopropylamino)-2-cyanoethoxyphosphine (Digital Speciality Chemicals Ltd.).
3. Dichloromethane (CH_2Cl_2) (Fluka).
4. Magnesium sulphate ($MgSO_4$) (Grüssing).
5. Sodium chloride (NaCl) (Grüssing).
6. Silica gel for preparative chromatography (Roth).
7. Tlc silica gel F_{254} (Merck).

2.2. RNA Synthesis Cycle

1. The ribonucleoside phosphoramidites can be synthesized as described in Subheading 3.1 or can be obtained commercially. The following ribophosphoramidites are available from Chem Genes:

   N-Bz-5′-O-DMTr-2′-O-TBDMS-adenosine-3′-O-N,N′-diisopropyl(2-cyanoethyl)phosphoramidite

   N-iBu-5′-O-DMTr-2′-O-TBDMS-guanosine-3′-O-N,N′-diisopropyl(2-cyanoethyl)phosphoramidite

   N-Bz-5′-O-DMTr-2′-O-TBDMS-cytidine-3′-O-N,N′-diisopropyl(2-cyanoethyl)phosphoramidite

   5′-O-DMTr-2′-O-TBDMS-uridine-3′-O-N,N’-diisopropyl(2-cyanoethyl)phosphoramidite.
2. Ribonucleoside functionalized solid support (LCAA-CPG) can be obtained commercially. The following solid supports are available from Chem Genes:

   N-Bz-5′-DMTr-2′(3′)-Ac-A-LCAA-CPG

   2.N-ibu-5′-DMTr-2′(3′)-Ac-G-LCAA-CPG

   N-Bz-5′-DMTr-2′(3′)-Ac-C-LCAA-CPG

   5′-DMTr-2′(3′)-Ac-U-LCAA-CPG.
3. The following reagents, which can be obtained from Sigma-Proligo or Applied Biosystems, are the same as those used for DNA synthesis.

   (a) *Anhydrous acetonitrile:* Dry acetonitrile redestilled from phosphorus pentoxide. We use the anhydrous acetonitrile, on the one hand, for amidite dissolution and, on the other hand, for the intermediate washing steps.

(b) *Detritylation*: 3% TCA/Dichloromethane for deblocking the DMTr group.

(c) *Activation*: 0.5 M tetrazole in acetonitrile.

(d) *Capping*: 10% acetic anhydride/10% 2,6-lutidine/THF and 16% N-methylimidazole/THF.

(e) *Oxidation*: 0.1 M iodine in THF:pyridine:water (75:20:2 v/v/v).

2.3. Workup and Purification of Oligonucleotides

1. Oligomer cleavage: For the cleavage of the solid support/cyanoethyl group and the exocyclic amino protecting groups of the base, we use NH_3/EtOH (3:1).
2. Desilylation: N-Methlypyrrolidone/NEt_3/NEt_3·3HF (3 eq/1.5 eq/2 eq).
3. Deionized sterile water: Sterilize distilled water by treatment with DEPC (diethylpyrocarbonate) as a 1% solution, followed by autoclaving at 120°C for 20 min. After cooling down, the water is buffered with LiOH to a pH of 8 (see Note 1).
4. HPLC buffer: Phosphate buffer, water, NaCl, acetonitrile (chromatography grade).
   Apparatus: HPLC-System, RP-18, or preferred anion exchange column, (e.g., DIONEX DNA Pac PA-100).
   Chemicals: Triethylamine, acetic acid, water, acetonitrile (chromatography grade).
   Hexafluoroisopropanol (HFIP) (Aldrich), Lithium chloride, DEPC-water.

2.4. Analysis

1. Dissolved in DEPC water for UV-measurement.
2. Analytical HPLC ion exchange MeCN buffer.
3. MALDI-MS: Matrix = ATT 6-Aza-2-Thiothymine/Ammoniumhydrogencitrate (*see* Note 2).

2.5. Strand Preparation for Biological Testing

Determine concentration by UV or perhaps use MALDI-MS analysis for exact match.

3. Methods

The RNA synthesis, according to the phosphoramidite method, relies on properly protected building blocks. These are either commercially available or have to be prepared. Here, we only concentrate on the final step of introducing the phosphoramidite moiety to the modified nucleoside. *2′-O*-alkylated nucleosides have been synthesized (14), mostly by direct alkylation of suitably protected nucleosides where the *2′-O*-OH is free. For the standard

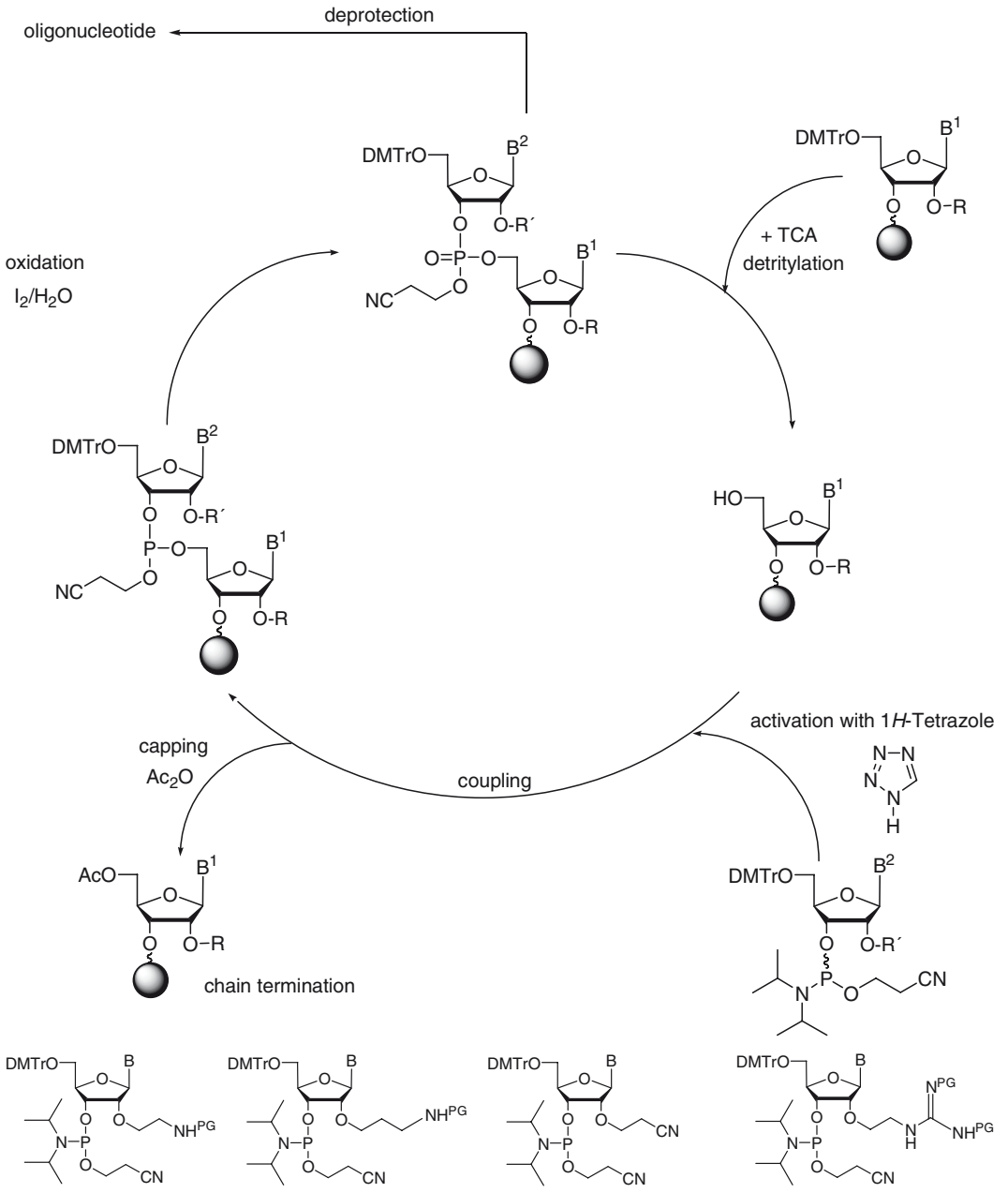

Fig. 3. Caruthers oligonucleotide synthesis cycle and phosphoramidites for siRNA synthesis

phosphoramidite solid-phase synthesis (Fig. 3), the prepared alkylated phosphoramidites are added in the cycle.

3.1. Preparation of Phosphoramidites

1. As was described earlier, incorporation of 2′-O-alkyl nucleosides into siRNAs improves their pharmacokinetic and pharmacodynamic properties. For the synthesis of siRNA oligomers,

the most popular and commercially developed phosphoramidite approach is used (20). Only a few phosphoramidites of 2′-O-alkyl modified nucleosides are available from commercial sources, and to test desired modification in RNAi very often it is inevitable to synthesize the corresponding nucleoside and convert it to phosphoramidite, suitable for solid-phase synthesis (11–13).

2. The synthesis of 3′-O-phosphoramidites of 2′-O-alkyl nucleosides represents simple nucleophilic substitution of chloro or diisopropylamine residues at P(III) atom by alcohol (3′-OH group of nucleoside). To avoid any side reactions, 3′-O-phosphoramidites of 2′-O-modified nucleosides are synthesized from corresponding nucleosidic precursors, which are protected at the 5′-hydroxyl of the sugar moiety and the amino groups of the nucleobases. These protecting groups should meet the following requirements – they should be stable during synthesis and purification of phosphoramidites and be compatible with the solid-phase synthesis conditions, cleavage from solid support and final deprotection steps (20). The 4,4′-dimethoxytrityl (DMTr) group is widely used for the protection of 5′-OH. For the exocyclic amino groups of heterocyclic bases, mostly acyl residues like acetyl-, isobutyryl-, or benzoyl- are used. Uridine usually does not have any protection on the nucleobase. The additional advantage of 2′-O-modified nucleosides is their missing necessity to protect 2′-hydroxy group on the sugar moiety.
3. Phosphitylation can be carried out with chloro-N,N-diisopropylamino- or bis-(N,N-diisopropylamino)-2-cyanoethoxyphosphines (Fig. 4, *P1* and *P2*) in the appropriate solvents. The *P1* derivative represents very reactive

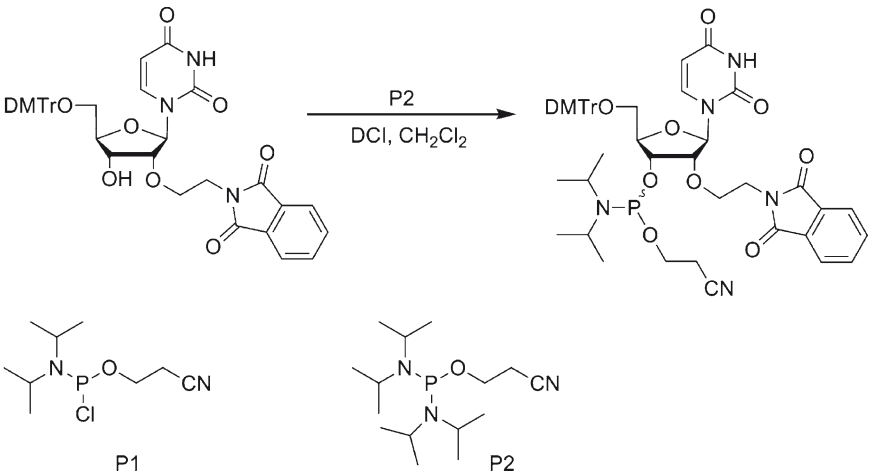

Fig. 4. Phosphitylation

phosphoryl chloride species. It reacts with 3′-OH group of nucleoside already at 0°C, and in this case a base, such as tertiary amine (e.g., triethylamine, N,N-diisopropylethylamine) or pyridine derivative (e.g., *sym*. Collidine), is used for neutralization of HCl, released during the reaction. In contrast to P1, bis-(N,N-diisopropylamino)-2-cyanoethoxyphosphine (*P2*) does not take part in reaction without activation by a mild acid. For those purposes, 4,5-dicyanoimidazole (DCI) or 1*H*-tetrazole are used. Although the reactions using chloro phosphine are much faster (0.5–1 h) than with bisaminophosphine 2 (3–5 h), the usage of bisamino phosphine *P2* is more advantageous due its ease of handling.

4. The phosphitylation reaction can be performed using a wide range of organic solvents, the most widely used include dichloromethane, acetonitrile and tetrahydrofurane (see Note 3). One of the general requirements for this synthesis and its components is that it must be performed under inert atmosphere (to avoid hydrolysis and/or oxidation of P(III) derivatives). For this purpose, usually nitrogen or argon gas is used (see Note 4).

3.1.1. Synthetic Procedure to Phosphoramidites of 2′-O-Alkyl-Modified Nucleosides

1. The protected nucleoside is dissolved in dichloromethane under inert gas (usually 10–15 ml of dichloromethane for 1 mmol of nucleoside) and 1.1–1.5 eq. of triethylamine is added. The mixture is cooled to 0°C using ice-water bath, and slowly (dropwise) 1.1–1.5 eq. of chloro-N,N-diisopropylamino-2-cyanoethoxyphosphine (*P1*) is added (the amount of *P1* should be equal or lower than triethylamine!). Then, the reaction mixture is allowed slowly to warm to room temperature and further stirred at room temperature while monitoring the reaction with TLC.

   The reaction with bis-(N,N-diisopropylamino)-2-cyanoethoxyphosphine (P2) is performed a similar way as described above. To a solution of nucleoside (at room temperature), 1.1–1.2 eq. of DCI is added, followed by addition of 1.1–1.5 eq. of phosphine *P2*. The reaction mixture is stirred at room temperature, monitoring the reaction with TLC.

   Once the reaction is completed (see Note 5), 40–60 ml of dichloromethane is added to the mixture. The solution is washed with saturated sodium hydrogencarbonate (2 × 100 ml) and then with saturated sodium chloride (100 ml). After workup, the organic layer is dried with sodium or magnesium sulfate, filtered and evaporated until dry. The crude phosphoramidite is purified by silica-gel column chromatography using methanol-dichloromethane or another appropriate mixture of solvents (e.g., hexane-ethyl acetate, dichlormethane-ethyl acetate), containing 0.05–0.1%

of triethylamine as eluants and collecting the fractions with both diastereomers. The fractions are united and evaporated to dryness. To remove (if any) traces of water and/or inclusion of silica-gel, the product is dissolved in ~30 ml of dichloromethane (see Note 6), dried with magnesium sulfate, filtered and, after removing the solvent, dried in vacuo for at least 12 h.

2. For characterization of newly synthesized phosphoramidites, ^{31}P-NMR and mass-spectrometry should be used. The ^{31}P-NMR of synthesized phosphoramidite should reveal one or two peaks (two diastereomers) in the 145–155 ppm area (see Note 7). The peaks in the area of 5–15 ppm represent undesirable impurities of H-phosphonates. The molecular mass of phosphoramidite should be confirmed by mass-spectrometry (ESI or MALDI).

3.1.2. Phosphitylation of 2′-O-alkyl Nucleoside as an Example

1. Synthesis of 5′-*O*-(4,4′-dimethoxytrityl)-2′-*O*-(2-phthalimidoethyl) uridine-3′-*O*-(cyanoethyl-*N*,*N*-diisopropyl)phosphoramidite (9).

To a solution of 5′-*O*-(4,4′-dimethoxytrityl)-2′-*O*-(2-phthalimidoethyl)uridine (0.36 g, 0.5 mmol) in 6 ml of CH_2Cl_2, add bis-(N,N-diisopropylamino)-2-cyanoethoxyphosphine (0.24 ml, 0.226 g, 0.75 mmol) and 4,5-dicyanoimidazole (DCI) (0.068 g, 0.575 mmol). The reaction mixture is stirred for 3 h at room temperature. Then the mixture is diluted with 60 ml of CH_2Cl_2, washed with saturated $NaHCO_3$ (2 × 150 ml), and then washed with saturated NaCl (1 × 150 ml), dried over Na_2SO_4, and evaporated until dry. The mixture of diastereomers is purified by column chromatography using 20–100% AcOEt in CH_2Cl_2 (with 0.1% Et_3N) as eluant, and collecting fractions with Rf = 0.6 and 0.7 (1/1 AcOEt/CH_2Cl_2) to produce 0.372 g (81%) of 5′-*O*-(4,4′-dimethoxytrityl)-2′-*O*-(2-phthalimidoethyl)uridine-3′-*O*-(cyanoethyl-*N*,*N*-diisopropyl)phosphoramidite as a white foam.

^{31}P NMR (400 MHz, $CDCl_3$): δ 149.3 and 149.8.

ESI-MS: *m/z* calcd for $C_{49}H_{54}N_5O_{11}P$ 920.4 [M + H]+, found 920.5.

3.2. RNA Synthesis

The most important method for synthesizing oligonucleotides, using automatic solid phase synthesis, is the phosphoramidite method. The synthesis cycles of the phosphoramidite-solid phase method according to M. Caruthers (21) is given below.

Steps of the oligonucleotide synthesis are as follows:

1. Deprotection of the 5′-DMTr group (and the boc groups of the modifications) with 3% TCA in dichloromethane
2. Activation of the amidite with 1H-tetrazole in acetonitrile

3. Coupling (sometimes we use double couple for our modifications)
4. Protection of the unreacted 5′-OH group with acetic anhydride/2,6-lutidine/THF and 1-methylimidazole in THF, known as capping
5. Oxidation with iodine in water/pyridine/THF.

Our solid phase syntheses are all carried out on an Expedite Perseptive Biosystems or ABI392 DNA/RNA Synthesizer in 0.2 or 1.0 μmol scale.

The ribonucleosides–phosphoramidites are dissolved in dry acetonitrile (10 mg in 0.1 ml acetonitrile), filtered and then transferred into 1 g bottles. The solid support for the 1 μmol scale has to be transferred into empty Teflon synthesis columns (Applied Biosystem) and closed with filters (see Note 8). In our 1 μmol scale synthesis, the support is first treated with TCA to deblock the 5′-DMTr group. Use the protocol for RNA synthesis, according to the vendor of your synthesizer, for the exact times and washing steps.

Each synthesis cycle takes about 15 min to complete. Quantitation of the trityl cation released during each cycle from the 5′ terminus of the growing oligonucleotide chain is used as a primary monitor of the synthesis performance. Therefore, the absorbance at 504 nm of each TCA eluate is measured with an inline detector. The value obtained for each TCA eluate is compared as a percentage to that of the previous TCA eluate (see Note 9).

The deprotection of the synthesized RNA oligomers is straightforward.

1. The first step is treatment with ammonia/ethanol (3:1) for 24 h at 35°C (“normal”) or 2 h at 65°C (“fast”), which cleaves the oligonucleotide from the solid support and removes the exocyclic amino-protecting groups for the phtalimido protecting group the ammonia treatment should be 48h at 50 C.
2. Therefore, one should decant the solid support in a 4 ml tube, treated with the ammonia/ethanol solution and incubate at 35°C for 24 h.
3. Afterward, the solution is lyophilized on a speed vac until dry, washed with 0.3 ml DEPC Water, and lyophilized again.
4. The white residue is treated with 0.3 ml of 1-Methylpyrrolidone/Triethlyamine/Triethylamine·3 HF(3 eq/1.5 eq/2 eq) and incubated at 65°C for 1.5 h to cleave the 2′-O-TBDMS protecting groups.
5. The precipitation is performed with 1.2 ml butanol. The solution is cooled down at –78°C for 0.5–1 h. After centrifugation, the supernatant is removed and the RNA pellet dissolved in 0.15 ml 1-Methylpyrrolidone and 0.15 ml DEPC-water and then purified by HPLC.

3.3. Purification

High performance liquid chromatography (HPLC) is the most widespread tool in the analysis of oligos – it is fast and the chromatogram can be monitored online, quantified, and stored. The retention times are reproducible and a scale for the preparative purification of synthetic oligos is possible. Among HPLC techniques, two main forms are distinguished according to the separation principle applied: reversed-phase (RP) and anion-exchange chromatography. In RP-HPLC, the oligo is bound by hydrophobic interaction to a nonpolar matrix and eluted with a gradient of increasing organic solvent content. For anion exchange HPLC, a positively charged ion exchange material is used as the stationary phase. The oligo binds to this material with the negatively charged phosphorodiester backbone. The elution is accomplished by a gradient of increasing ionic strength.

Reversed-phase HPLC is frequently used for the analysis of crude oligo synthesis mixtures. Because the separation is based on the hydrophobic interactions with the column material, it is advisable to leave the terminal dimethoxytrityl (DMTr) protection group still attached to the oligo. This nonpolar group retards the migration and allows a good separation of the full length product from truncated sequences, which do not carry a DMTr group. With preparative HPLC separations, the DMTr group is cleaved from the oligo after purification by acidic treatment and removed by extraction with diethylether. In every case, care should be taken to prevent undesired detritylation of the oligo during chromatography. Analysis of trityl bearing oligos occasionally reveals splitting into two product peaks. Short oligos (<10 nts) can also be analyzed with the DMTr group off but the resolution quickly decreases with increasing length of the molecule. For analytical HPLC chromatogram, approximated 0.1–0.2 OD_{260} units corresponding to 0.5–1.0 nmol of a 20-mer oligo are required. The sample solution must not contain any particles that may cause a blockade of the column.

3.3.1. Protocol 2: RP-HPLC Analysis of Oligonucleotides (Optional)

1. Prepare a 1 M stock solution of triethylammonium acetate, by carefully mixing on ice, 140 ml triethylamine and 58 ml acetic acid. Make up to 1 l < solution?> with distilled water and adjust the pH to 7.0 with triethylamine or acetic acid. Dilute this solution with a ninefold volume of water and check the pH value to obtain solvent A. This solution should be filtered through a 0.45 μm membrane filter before use.
2. Use chromatography grade acetronitrile as eluent B.
3. Use a RP C18 (5 μm, 250×4 mm) or equivalent column with a flow rate of 1.0 ml/min. For analytical separations, the analysis should be performed at ambient temperature with detection of the oligo at 254 nm.

4. Dissolve 0.2 OD_{260} units DMTr-On oligo (corresponding to approximately 1 nmol of a 21-mer) in 100 µl water, and filter this solution through a 0.45-µm membrane filter, if necessary.
5. Inject the sample at 5% B and run a linear gradient to 45% B for 40 min. Increase to 100% B within 10 min., hold for 10 min and return to start conditions.

The crude RNA oligomer can be purified with reversed-phase or ion-exchange HPLC. Here we present the general procedure for purification of RNA oligomers using ion-exchange HPLC. Before preparative purification, it is very useful to perform an analytical HPLC-MS to identify the fraction (and retention time) of desired oligomer (usually it is represented by the highest peak on the chromatogram). Also, it shows how many impurities are in the crude product and helps with choosing the conditions (e.g., gradient of eluants, temperature) for preparative HPLC (see Note 10).

1. The RNA pellet (from 1 µmol synthesis) is dissolved in 200 µl-N-methypyrrolidone and 200 µl DEPC-water (pH 8.0) and purified by ion-exchange HPLC using DIONEX DNA Pac PA-100 (9×250 mm).
2. For the elution, two buffer systems are used – A: DEPC water (pH 8.0) and 1 M LiCl/DEPC water (pH 8.0) as elution buffer, flow rate at 5 ml/min.
3. The fraction of desired RNA oligomer is collected, lyophilized, and the residue is dissolved in 1 ml DEPC-water (pH 8.0).
4. Finally, the residue is desalted with Sephadex™ G-25M (PD-10 column) (GE Healthcare). Desalted RNA oligomer is lyophilized on a speed vac and can be stored at –20°C.

3.3.2. Protocol 3: Analytical Anion-Exchange HPLC of Oligonucleotides

1. Either, follow the same procedure as above, but use an analytical column DIONEX DNA Pac PA-100, 4×250 mm.

   Or *follow this* better procedure:
2. Use an analytical HPLC-MS with RP (reversed-phase) Water Acquity UPLC OST C18 1.7 µm, 2.1×80 mm column and system of eluants HFIP/TEA and methanol.
3. Amount of analyzed sample of RNA – 2 µl (0.25 µg/µl)
   Buffer A – Hexafluoroisopropanol (HFIP)/triethylamine (TEA) = 20/1 v/v
   Buffer B – Methanol.
4. The elution starts with the mixture of 95% buffer A and 5% buffer B, increasing concentration of B to 35% in 11.5 min; then increasing to 100% in 0.5 min.

3.4. Analysis

Analytical methods for checking the identity and purity of oligonucleotides (oligos) have improved in parallel with methods of synthesis. A variety of sophisticated analytical methods, employing classical electrophoresis, chromatographic techniques, or mass spectrometry, are now available.

During chemical synthesis, the growing oligo chain is treated with several reagents. Although the synthesis conditions are optimized, each of the four reactions of the synthesis cycle may lead to formation of small amounts of side products. In addition, incomplete coupling results in contamination of the full length oligo with $n - 1$ failure sequences. The problems can be monitored by chromatography or electrophoresis. Furthermore, the protecting groups applied in the synthesis have to be separated from the oligo product after cleavage. In these cases, HPLC is a good method to verify the purity of the product.

UV-spectroscopy, an easy and sensitive technique, is the first method employed in the analysis of nucleic acids. A typical UV spectrum of an RNA-oligo has an absorbance maximum at approximately 260 nm and a minimum at 230 nm.

Since no separation of the molecules in the sample is accomplished by spectroscopy, the measured signal is the sum of the individual absorbance spectra of all compounds present in the sample solution. UV spectra of nucleic acids show pronounced hypochromicity. The absorbance of a native DNA duplex is 20–30% lower than the absorbance of single strands in random coil conformation. This phenomenon is employed to measure the melting behavior of oligos.

UV-spectrophotometry is the main technique for quantification of nucleic acids because the ionic character of these molecules results in an extensive hydration in the solid state. This, and the possibility of salt contamination, complicates the direct weighing of dry DNA samples. The determination of the absorbance or optical density (OD) is a good way to measure oligo amounts when the extinction coefficient (ε) of the molecule is known. The concentration (c) of the oligo solution is correlated with the absorbance reading (OD) according to Beer's law: $\mathrm{OD} = \varepsilon \times c \times 1$ (1 = path length of the cuvette).

The concentration of an oligo solution can be determined by hydrolysis of the oligo into mononucleotides, thereby minimizing stacking interactions between the bases. Provided that its base composition is known, this is the most accurate way to determine the concentration, but hydrolysis, especially of modified oligos, is not always possible. For duplexes or self-complementary sequences, the OD measurement has to be performed above the melting point otherwise the results will be imprecise. The extinction coefficient is almost independent from the nature of the phosphate group so that these calculations are applicable for backbone-modified oligos without correction.

The measurement is routinely performed in 1-cm cuvettes with a volume of 1 ml. The absorbance at 260 nm is then referred to as OD_{260} unit.

The extinction coefficient at 260 nm is calculated as follows:

$$\varepsilon(260) = (a \times 15.34 + g \times 12.16 + u \times 8.70 + c \times 7.60) \times 0.9 \times 10^3 [M/cm^2]$$

a, u, g, c correspond to the number of the respective bases in the oligo sequence.

The concentration of an oligo solution is: $c = OD_{260}/\varepsilon \times 1$

Calculate the molecular mass (M) of an oligo as follows:

$$(M) = a \times 249.230 + u \times 242.188 \times g \times 265.229 + c225.204 + 2.016 + (n-1) \times 62.972 + (n-1) \times 1.008$$

in which:

1. a, u, g, c correspond to the number of the respective bases in the oligo sequence and n is total number of nucleotides.
2. The summand 2.016 represents the two hydrogen atoms at the strand ends.
3. 62.972 is the mass of the phosphorodiester group. Replace this factor with 79.039 for each phosphorothioate linkage.
4. 1.008 is the mass of the proton as counter-ion to the negatively charged phosphate backbone; calculate with 22.990 to obtain the mass of the sodium salt and 18.039 for the NH_4^+ salt of the oligo.
5. Example: The molecular mass of the free acid of a 22-mer oligo with the base composition A6, G2, U7, and C7 calculates to:
6. $(M) = 6 \times 249.230 + 7 \times 242.188 + 2 \times 265.229 + 7 \times 225.204 + 2.016 + 21 \times 79.039 + 21 \times 1.008$
7. $(M) = 6{,}883.18$
8. Now, we have to add the modifications so 2×44.02
9. $(M) = 6{,}971.2$.

The purity and identity of newly synthesized siRNA oligomer must be confirmed by analytical HPLC and mass-spectrometry (MALDI or ES). Figures 5 and 6 show analytical HPLC-MS of crude (48% purity) and purified (83% purity) AAUCCAUCCACAUAGGCUCUUU, where U is *2′-O*-aminoethyluridine. These analytical HPLC-MS were performed with Agilent 1200 Rapid Resolution HPLC using RP Water Acquity UPLC OST C18 1.7 µm, 2.1 × 80 mm column and system of eluants HFIP/TEA and methanol.

3.5. siRNA Preparation for Biological Testing

The quality of synthetic siRNA depends on the percentage of full-length siRNA present in the preparation. Synthesis of an RNA strand starts at the 3′-end. Less than 100% coupling efficiency

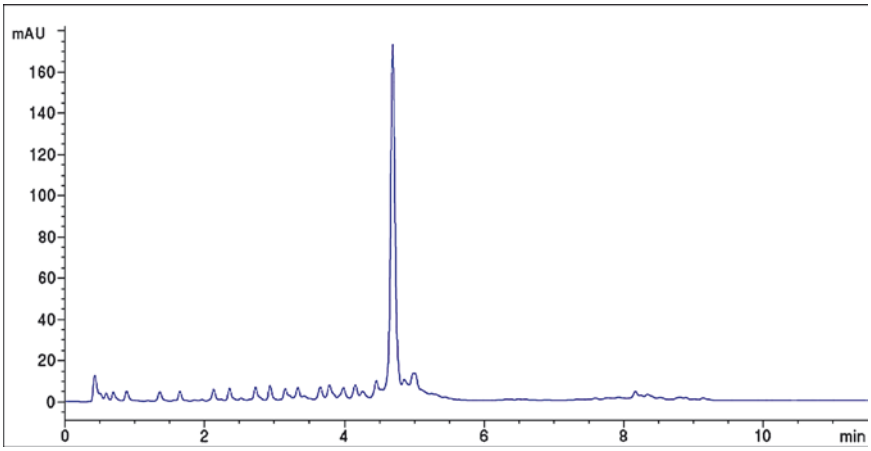

Fig. 5. Analytical HPLC-MS of crude (50% purity) ss siRNA (AAUCCAUCCACAUAGGCUCUUU, whereas U is *2′-O*-aminoethyluridine) Found *M* = 6,970.1, calcd. 6,971.2

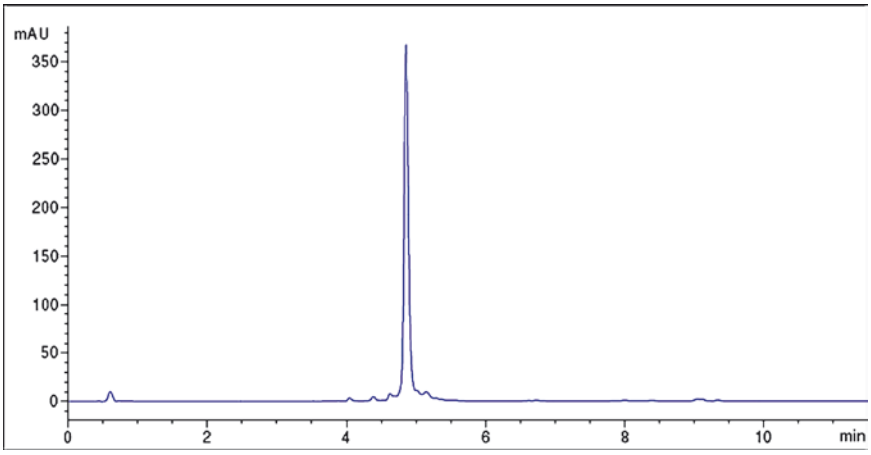

Fig. 6. Analytical HPLC-MS of purified (85% purity) ss siRNA (AAUCCAUCCACAUAGGCUCUUU, whereas U is *2′-O*-aminoethyluridine) found *M* = 6,970.1, calcd. 6,971.2

results in truncated products. After QC is complete, the molar concentration of the sense and antisense strands are normalized, and the strands are annealed to form duplexes. For stability during delivery, siRNA duplexes are shipped as a lyophilized pellet. The annealed siRNA duplexes are vacuum dried in 96-well plates or in individual tubes. In the case of fluorophore-labeled siRNA, it is wrapped in foil to protect the fluorophore from exposure to light.

3.5.1. Duplex Analysis

To start the experiment, both oligonucleotides ((+)-siRNA and (–)-siRNA) are diluted in sterile, deionized water and mixed, if necessary. The use of a buffer is not recommended. Precipitation is not necessary. Hybridization is done in a HEPES-KOH pH 7.4 buffer

system: 100 mM potassium acetate, 30 mM HEPES-KOH pH 7.4, and 2 mM magnesium acetate. First, the hybridization solution is heated to 80°C and then incubated at 37°C for at least 5 min. For very accurate quantification, the specific extinction coefficient of each individual base and the interaction between neighboring bases has to be known. Experimental results have shown that errors can be up to 14%, thus alternative methods are recommended, such as mass spectrometry and a recent protocol that suggests MALDI (22). The solution is now ready for transfection. There are a number of transfection helper agents: most commonly, Lipofectamin and Oligofectamin are used.

4. Notes

1. After treatment, the pH (usually around 6) is adjusted with LiOH to 8.
2. The oligonucleotides, which attract a large number of cations such as sodium or potassium, and have to be desalted thoroughly.
3. A very important requirement for the solvents – they must not contain any traces of water or other protic solvents.
4. The equipment – the flasks, magnetic stirrer, syringes and needles – used for the reaction must be pre-dried before the reaction.
5. Ensure no starting material is visible on TLC.
6. Always add 0.1% of triethylamine when using dichloromethane or silica.
7. Sometimes, the peaks are not well-separated.
8. Ensure the filter is tight and no silica enters the system.
9. It should be noted that evaluation of the synthesis performance by HPLC and UV measurement is more accurate than the trityl assay.
10. Important notice – for all operations DNase, RNase-free water should be used (e.g., GIBCO® ultra pure, DNase, RNase-free).

Acknowledgments

The authors would like to thank S. Bernhardt and H. Brill for technical assistance and the EU Right project (LSHB-CT-2004-005476) for financial support.

References

1. Elbashir, S. M., Harborth, J., Lendeckel, W., Yalcin, A., Weber, K. and Tuschl, T. (2001) Duplexes of 21-nucleotide RNAs mediate RNA interference in cultured mammalian cells. *Nature* 411, 494–498.
2. Fire, A. Z. (2007) Gene silencing by double-stranded RNA (Nobel lecture). *Angew. Chem. Int. Ed.* 46, 6966–6984.
3. Mello, C. C. (2007) Return to the RNAi world: rethinking gene expression and evolution (Nobel lecture). *Angew. Chem., Int. Ed.* 46, 6985–6994.
4. Dorsett, Y. and Tuschl, T. (2004) siRNAs: applications in functional genomics and potentials as therapeutics. *Nat. Rev. Drug. Discov.* 3, 318–329.
5. Bumcrot, D., Manoharan, M., Koteliansky, V. and Sah, W. Y. D. (2006) RNAi therapeutics: a potential new class of pharmaceutical drugs. *Nat. Chem. Biol.* 12, 711.
6. Behlke, M. A. (2008) Chemical modification of siRNAs for *in vivo* use. *Oligonucleotides* 18, 305–320.
7. Allerson C. R., Sioufi, N., Jarres, R., Prakash T. P., Naik, N., Berdeja, A., et al. (2005) Fully 2′-modified oligonucleotide duplexes with improved *in vitro* potency and stability compared to unmodified small interfering RNA. *J. Med. Chem.* 48, 901–904.
8. Koller, E., Propp, S., Murray, H., Lima, W., Bhat B., Prakash T.P., et al. (2006) Competition for RISC binding predicts *in vitro* potency of siRNA. *Nucleic Acids Res.* 16, 4467–4476.
9. Wang, Y., Juranek, S., Li, H., Sheng, G., Tuschl, T. and Patel, D. J. (2008) Structure of the guide-strand-containing argonaute silencing complex. *Nature* 456, 209-213. doi:10.1038/nature07315.
10. Griffey, R. H., Monia, B.P., Cummins, L. L., Freier, S., Greig, M. J., Guinosso, C. J., et al. (1996) 2′-*O*-aminopropyl ribonucleotides: a zwitterionic modification that enhances the exonuclease resistance and biological activity of antisense Oligonucleotides. *J. Med. Chem.* 39, 5100–5109.
11. Odadzic, D., Bramsen, J. B., Smicius, R., Bus, C., Kjems J., Engels, J. W. (2008) Synthesis of 2′-*O*-modified adenosine building blocks and application for RNA interference. *Bioorg. Med. Ch em.* 16 (1), 518–529.
12. Smicius, R. and Engels, J. W. (2008) Preparation of zwitterionic ribonucleoside phosphoramidites for solid-phase siRNA synthesis. *J. Org. Chem.* 73, 4994–5002.
13. Haas, J. and Engels, J. W. (2007) A novel entry to 2′-*O*-aminopropyl modified nucleosides amenable for further modifications. *Tetrahedron Lett.* 48 (50), 8891–8894.
14. Bramsen, J. B., Laursen, M. B., Bus, C., Hansen, T. B., Langkjær, N., Babu, B. R., et al. (2009) A large-scale chemical modification screen identifies design rules to generate siRNAs with high activity, high stability and low toxicity. *Nucleic Acids Res.* 37, 2867–2881. doi:10.1093/nar/gkp106
15. Sproat, B. S. (1993) Synthesis of 2′-*O*-alkylribonucleotides, in *Protocols for Oligonucleotides and Analogs, Methods in Molecular Biology* (Agrawal, S., ed.), Humana Press, Totowa, New Jersey 20, pp. 115–141.
16. Czauderna, F., Fechtner, M., Dames, S., Aygün, H., Klippel, A., Pronk G. J., Giese, K., Kaufmann, J. (2003) Structural variations and stabillising modifications of synthectic siRNAs in mammalian cells. *Nucleic Acids Res.* 11, 2705–2716.
17. Kraynack, B. A. and Baker, B. F. (2006) Small interfering RNAs containing full 2 ′-*O*- methylribonucleotide-modified sense strands display Argonaute 2/elF2C2-dependent activity. *RNA* 12, 163–176.
18. Freier, S. M. and Altmann K. H. (1997) The ups and downs of nucleic acid duplex stability: structure-stability studies on chemically-modified DNA:RNA duplexes *Nucleic Acids Res.* 22, 4429–4443.
19. Inoue, H., Hayase, Y., Imura, A., Iwai, S., Miura, K., Ohtsuka, E. (1987) Synthesis and hybridization studies on two complementary nona(2'-O-methyl)ribonucleotides. *Nucleic Acids Res.* 15, 6131–6148.
20. Beaucage, S.L. and Iyer, R.P. (1992) Advances in the synthesis of oligonucleotides by the phosphoramidite approach. *Tetrahedron* 48, 2223-2311.
21. Caruthers, M. H. (1985) Gene synthesis machines: DNA chemistry and its uses. *Science* 230, 281–285.
22. Bahr, U., Aygün H., and Karas, M. (2008) Detection and relative quantification of siRNA double strands by MALDI Mass Spectrometry. *Anal. Chem.*16, 6280–6285.

Part II

RNA Interference in the Laboratory and siRNA Delivery

Chapter 11

siRNA Specific Delivery System for Targeting Dendritic Cells

Xiufen Zheng, Costin Vladau, Aminah Shunner, and Wei-Ping Min

Abstract

siRNA therapy offers immense potential for clinical application. Under physiological conditions, however, siRNA was demonstrated to have a short half-life. Additionally, it may also cause ubiquitous gene silencing as it does not possess a tissue-specific homing mechanism. Thus, the rate-limiting step in the emergence of siRNA as a potential therapeutic agent is the current lack of a safe and tissue- or cell-specific in vivo delivery system. Herein, we propose a novel, cell-specific method for the in vivo delivery of siRNA to dendritic cells (DCs) with the purpose of inducing immune modulation. CD40 siRNA was incorporated within the interior of 86 nm liposomes, which were decorated with surface-bound mAb NLDC-145 as a targeting mechanism. The siRNA encapsulation efficiency was determined to be approximately 7%. CD40 siRNA immunoliposomes (CD40 siILs) were able to specifically bind to DCs and silence CD40 expression in vitro. Furthermore, in vitro CD40-silenced DCs significantly inhibited the proliferation of alloreactive T cells in an MLR. Upon in vivo administration, siIL-encapsulated, Cy3-labeled siRNA exhibited moderate uptake by the liver at an early time point following administration with greater accumulation in the spleen at a later time point. In contrast, naked siRNA primarily accumulated in the kidney immediately after administration and circulated out in a short time period. To address in vivo gene silencing and immune modulation, mice were simultaneously immunized with KLH and subcutaneously injected with DC-specific CD40 siILs, siILs containing negative control siRNA, naked CD40 siRNA, or PBS. A second injection of CD40 siILs, or control treatments, followed 24 h later. Flow cytometry, reverse transcriptase PCR, and quantitative real-time PCR analysis of $CD11c^+$ DCs from mice treated with CD40 siILs demonstrated reduced expression of CD40, in comparison with control groups. $CD11c^-$ cells were also analyzed by flow cytometry, but no differences were observed between treatment groups. Furthermore, CD40 siIL-treated mice were found to have an increased proportion of Treg cells ($CD4^+CD25^+$ $FoxP3^+$), and DCs cells from these mice were able to inhibit T cell proliferation in an antigen-specific recall response. In summary, CD40 siILs were shown to specifically target and deliver CD40 siRNA to DCs, significantly reducing CD40 expression and resulting in DC-mediated immune modulation as well as generation of Treg cells. These findings highlight the therapeutic potential for siRNA-based and DC-mediated immunotherapy in the clinic. To the best of our knowledge, this is the first study to use siILs for targeted delivery of siRNA to DCs and for immune modulation.

Key words: RNAi, siRNA, Specifically target, Delivery, Immunoliposome, DC, $CD11c^+$

Wei-Ping Min and Thomas Ichim (eds.), *RNA Interference*, Methods in Molecular Biology, vol. 623,
DOI 10.1007/978-1-60761-588-0_11, © Springer Science+Business Media, LLC 2010

1. Introduction

Dendritic cells (DCs) are the most potent stimulators of T cell activation (1). Paradoxically, DCs also possess immune regulatory properties that play an essential role in preventing autoimmune disease by inducing antigen-specific tolerance to self-antigens. We have previously generated tolerogenic DCs (tol-DCs) by silencing immune-related genes ex vivo using short interfering RNA (siRNA) (2, 3). However, the necessity of manipulating DCs ex vivo on an individual basis represents a major hurdle for large-scale clinical use of DC-mediated immunotherapy. Additionally, there is also the associated risk of activating DCs during ex vivo handling, rendering them immunogenic rather than tolerogenic. Therefore, DC-based immunotherapy would be much more feasible if immunosuppressive agents, such as siRNA, could be selectively targeted to DCs in vivo for the generation of tol-DCs.

siRNA is a powerful gene silencing tool and a revolutionary discovery in the field of functional genomics (4). These double-stranded RNA molecules are approximately 19–21 base pairs in length and exert their gene silencing function through seeking out and cleaving complementary mRNA (5). Upon gaining entry into the cytoplasm, the RNA duplex associates with the RNA-induced silencing complex (RISC), guiding this endonucleolytic complex to its target mRNA sequence (6, 7). mRNA complementary to the antisense strand of siRNA is rapidly degraded, resulting in decreased expression of a given gene – a process also referred to as "gene silencing." The gene blocking efficiency of siRNA exceeds that of other functionally similar molecules, such as antisense oligodeoxynucleotides (ODN) (8, 9). siRNA-mediated gene silencing is also more powerful, more specific, and much less toxic than low molecular weight chemical inhibitors or blocking mAbs (10, 11). Therefore, the potency and safety record of siRNA make this molecule a valuable candidate as a novel therapeutic agent that could potentially treat a myriad of diseases, such as cancers, viral infections, autoimmune disorders, and transplant-related complications, in which silencing certain gene products can be beneficial (10).

Despite growing interest in using siRNA in vivo systems, the most challenging hurdle in the development of siRNA as a clinical therapy is in vivo delivery (12). Over the past several years, multiple strategies, which can be categorized into viral and nonviral methods, have been employed for in vivo delivery of siRNA (4, 13). Despite the high transfection efficiency exhibited by viral systems, this strategy was demonstrated to be unsafe for human use because of the associated inflammatory and oncogenic potential (14, 15). Thus, to circumvent such side effects, many groups are

now using nonviral systems, such as (1) systemic intravenous injection or local administration of naked, unmodified siRNA; (2) complex of siRNA with various cationic molecules including lipids (lipoplex), liposomes, and peptides (polyplex); and (3) conjugation of siRNA to natural ligands, such as cholesterol (4).

Most strategies of non-viral targeting, however, are considered to be passive and non-specific in nature as they lack the ability to target any particular cell or tissue type (16). Unfortunately, systemic distribution of non-specifically targeted siRNA reduces gene silencing efficiency through allowing siRNA to be taken up indiscriminately by multiple cell and tissues types, and consequently, it can result in global gene silencing. Another issue is the short half-life of siRNA under physiological conditions (17). When administered using the aforementioned non-viral methods, siRNA can be directly exposed to harmful endogenous nucleases in the blood and/or body fluids (17, 18). In addition, in vivo administered siRNA is rapidly eliminated from the circulation (16). To address the problem of specific siRNA delivery, herein, we describe a cell-targeted siRNA delivery system using immunolipsomes that contain siRNA within their aqueous interior and are conjugated to surface-bound, dendritic cell-specific antibodies.

2. Materials

2.1. Animals

Male C57/B6 mice and BALB/c mice were purchased from Jackson Laboratories (Bar Harbor, ME) and housed in filter-top cages (4 mice per cage) at the Animal Facility, University of Western Ontario according to the Canadian Council for Animal Guidelines. Mice were fed food and water ad libitum, and were allowed to settle for 2 weeks before the initiation of experimentation, which had ethical approval from the university board.

2.2. siRNA Immunoliposome

1. 1-Palmitoyl-2-oleoyl-*sn*-glycerol-3-phosphocholine (POPC)
2. dimethyldioctadecylammonium bromide (DDAB)
3. distearoylphosphatidylethanolamine-PEG^{2000}(DSPE-PEG^{2000}) from Avanti Polar Lipids (Alabaster, AL).
4. PEG^{2000} is 2000 Dalton polyethylene glycol.
5. Cy3-labeled siRNA: Dharmacom Company
6. ShortCut RNase buffer (10% v/v), $MnCl_2$ (10% v/v)
7. ShortCut RNase III (New England Biolabs, Ipswich, MA)
8. Millipore Ultra-centrifugal Devices (Millipore) with a molecular weight cut off (MWCO) of 100 kDa.

9. Sepharose CL-4B gel matrix (Amersham Biosciences, Uppsala, Sweden)
10. Sepharose CL-4B beads conjugated to recombinant streptococcal protein G (Amersham Biosciences).
11. Hybridomas that produce the NLDC-145 mAb were a kind gift from Dr. Georg Kraal (19).
12. 1.5 x 10 cm Bio-Rad Econo chromatography column
13. Zetasizer Nano particle sizer (Malvern Instruments, Worcestershire)
14. Cary Eclipse mass spectrofluorometer (Varian Inc, Palo Alto, CA)
15. 2-iminothiolane (Traut's reagent): (Sigma-Aldrich, Oakville, ON)
16. Polycarbonate membranes: pore size 400 nm, 200 nm, 100 nm, and 50 nm (all from Avestin, Ottawa, Canada)
17. Beckman Coulter DU800 spectrophotometer (Beckman Coulter, Mississauga, ON)

2.3. Culture Medium and Cytokines for Cells and Cell Lines

1. L929 cell line: from ATCC
2. Cytokines: mouse recombinant IL-4, GM-CSF (growth factor of cloning)
3. PRIM-1640 (Invitrogen Life Technologies, Ontario, Canada)
4. FBS (Invitrogen Life Technologies, Ontario, Canada)
5. L-glutamine (Invitrogen Life Technologies, Ontario, Canada)
6. Penicillin (Invitrogen Life Technologies, Ontario, Canada)
7. Streptomycin (Invitrogen Life Technologies, Ontario, Canada)
8. 2-Mercaptoethanol (Invitrogen Life Technologies, Ontario, Canada)
9. GM-CSF (10 ng/ml; PeproTech, Rocky Hill, NJ)
10. Recombinant mouse IL-4 (10 ng/ml; PeproTech)
11. Dendritic culture medium: RPMI 1640 supplemented with 2 mM L-glutamine, 100 U/ml penicillin, 100 mg of streptomycin, 50 μM 2-Mercaptoethanol, and 10% FBS (all from) supplemented with recombinant GM-CSF (10 ng/ml; PeproTech, Rocky Hill, NJ) and recombinant mouse IL-4 (10 ng/ml; PeproTech)
12. Plates: 24-well plate (BD Biosciences, Mississauga, Canada).
13. Ficoll-Paque (Amersham, Canada).

2.4. Buffers

1. 0.05 M HEPES, pH 7.0
2. 0.05 M Tris-HCl (pH 8.0)

3. 0.1 M glycine (pH 2.5)
4. 1 M Tris-HCl buffer (pH 9.0).
5. 250 mM EDTA
6. 0.15 M Na-borate/0.1 mM EDTA (pH 8.5)

2.5. RNA Isolation

1. Trizol Reagent (Invitrogen, Burlington, ON); store at 4°C.
2. Chroloform (Sigma, Oakville, ON); store at room temperature.
3. Isopropanol (Sigma, Oakville, ON); store at room temperature.
4. 70% ethanol, 70 ml 100% ethanol mix with 30 ml DEPC-treated water
5. DEPC-H_2O (Diethylpyrocarbonate)-treated water: add 1 ml of DEPC to 1,000 ml of distilled H_2O, mix and leave at room temperature of 1 h, autoclave and cool to room temperature prior to use.
6. 0.2 µm filter (Millipore, Billerica, MA)

2.6. cDNA Synthesis

1. Oligo dT (Invitrogen, Burlington, ON) 0.5 µg/µl; store at –20°C.
2. 0.1 M Dithiothreitol (DTT) (Invitrogen, Burlington, ON); store at –20°C.
3. 10 mM dNTP (Invitrogen, Burlington, ON); store at –20°C.
4. RNase inhibitor (Invitrogen, Burlington, ON); store at –20°C.
5. Superscript II Reverse Transcriptase (Invitrogen, Burlington, ON); store at –20°C.

2.7. PCR Primers

1. CD40: 5′-CCCTGCCCCTTACCCCTTCATTC-3′ (forward)
   5’-CGTACTTGTGCCCCTCCTTA TCTG-3’ (reverse);
2. GAPDH: 5′-TGATGACATCAAGAAG GTGGTGAA- 3′ (forward)
   5′-TGGGATGGAAATTGTGAGGGAGAT-3′ (reverse).

2.8. Real-Time PCR

1. Brilliant SYBR Green QPCR Master Mix (Stratgene, La Jolla, CA); store at –20°C. After the first thaw, the master mix is stable at 4°C for 1 month. Limit the number of freeze and thaw cycles.
2. Reference dye (Stratgene, La Jolla, CA).
3. Real-time machine: MX4000 (Stratagene).

2.9. Gene Transfection

1. Tranfection reagent: GenePorter (Gene Therapy Systems, San Diego, CA)
2. Antibodies: CD40 and MHC class II
3. Flow cytometry (FACScan; BD Biosciences, San Jose, CA)
4. Fluorescence microscope (BioRad Laboratories, Hercules, CA)

2.10. MLR

1. [^{3}H-labeled] thymidine (Amersham)
2. Wallac Betaplate liquid scintillation counter (Beckman, Fullerton, CA)

3. Methods

3.1. Preparation of Thiolated NLDC-145 mAb

3.1.1. Purification

1. Apply hybridoma culture supernatant to an affinity column containing sepharose CL-4B beads conjugated to recombinant streptococcal protein G.
2. Wash extensively with phosphate buffer saline (PBS).
3. Elute the bound antibodies by adding 0.1 M glycine (pH 2.5) in 1 ml fractions.
4. Immediately neutralize using 1 M Tris-HCl buffer (pH 9.0).
5. Measure the optical density at 280 nm (OD_{280}) of each eluted fraction using a Beckman Coulter DU800 spectrophotometer 6. Pool the eluted fractions that have an $OD_{280} > 0.1$.
6. Concentrate using Millipore Ultra-centrifugal Devices with a molecular weight cut off (MWCO) of 100 kDa, replacing buffer through extensive washing with PBS during concentration.
7. Measure the final antibody concentration (in mg/ml) using an extinction coefficient of 1.4 mg^{-1} ml cm^{-1} for IgG at 280 nm.
8. Add NaN_3 (0.01% v/v) to the purified antibody solution before sterilization through a 0.2 μm filter and store at 4°C.

3.1.2. Thiolation

1. Dissolve 1.5 mg of NLDC-145 in 0.15 Na-borate/ 0.1 EDTA (pH 8.5).
2. Thiolate for 1 h at room temperature using Traut's reagent (2-iminthiolate) in a 40:1 molar excess ratio.
3. Exchange buffer with 0.05 M HEPES/0.1 mM EDTA (pH 7.0) using a Millipore Ultra-centrifugal Device with a MWCO of 100 kDa (see Note 1).

3.2. Generating siIL

siIL structure is shown in Fig. 1.

3.2.1. Generating siRNA Liposome

1. Dissolve in a conical flask: POPC, DDAB, DSPE-PEG^{2000} and DSPE-PEG^{2000},-Mal in chloroform in molar ratios of 92:4:3:1 (for neutral liposomes), 91:5:3:1 (for 1 mole% positive liposomes), or 90:6:3:1 (for 2 mole% positive liposomes), respectively to the total of 20.2 μM (see Note 2).

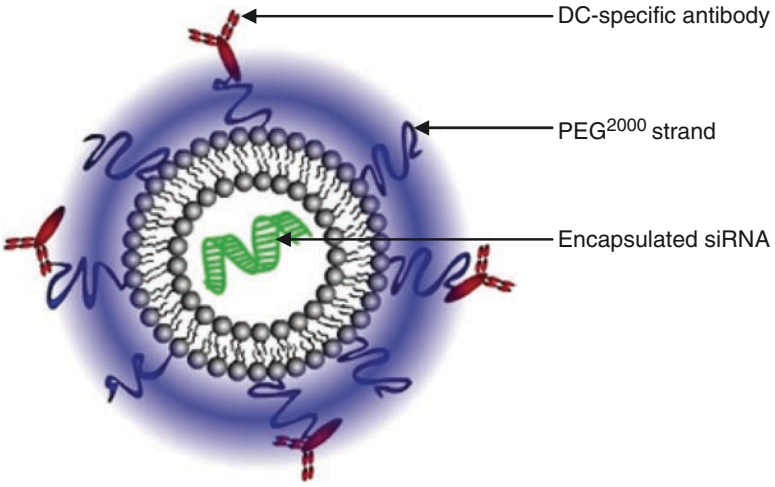

Fig. 1. The structure of silL. A schematic representation of siRNA-bearing immunoliposomes (silLs) showing siRNA incorporated within liposomes that are conjugated to a DC-specific mAb and endowed with molecular stealth by PEG2000 strands

2. Evaporate chloroform using nitrogen gas steam until a thin lipid film coating the flask walls is left.
3. Place lipid in a vacuum centrifuge for 90 min to remove residual chloroform.
4. Add 250 µg of Cy3-labeled siRNA, dissolved in 0.05 M Tris-HCl (pH 8.0) to a final volume of 0.2 ml, subsequently to the lipid film (see Note 3).
5. Vortex the dispersion for 5 min, and sonicate for 2 min using a bath sonicator (see Note 4).
6. Freeze by submerging in liquid N_2 and thaw at room temperature for 6 cycles.
7. Dilute liposomes by adding 3 ml of 0.05 HEPES (pH 7.0) to a concentration of 40 mM.
8. Extrude subsequently through 2 stacks of polycarbonate membranes of 400 nm-pore size.
9. Extrude again through 200 nm, then 100 nm, and then 50 nm-pore size polycarbonate membranes.
10. Add ShortCut RNase buffer (10% v/v), $MnCl_2$ (10% v/v), and 20 units of ShortCut RNase III to the liposome/RNA dispersion.

3.2.2. Conjugation of siRNA Liposome with NLDC-145 mAb

1. Mix prepared siRNA liposome (Subheading 3.2.1) with fresh thiolated NLDC-145 mAb.
2. Incubate overnight at room temperature.

3.2.3. Purification of silL

1. Fill Sepharose CL-4B gel matrix into a 1.5 × 10 cm Bio-Rad Econo chromatography column.
2. Balance the chromatography column with 0.05 mM PBS.
3. Load above-prepared siIL on Sepharose CL-4B column (see Note 5).
4. Elute the column with 0.05 mM PBS to separate siRNA-bearing immunoliposomes from digested siRNA fragments and non-conjugated antibody.
5. Collect the eluted using 1.5 ml eppendorf tube, each tube collects about 0.5 ml eluted.
6. Collect 0.5 ml each of eluted fractions 26–30.
7. Determine fluorescence (ex/em 550/570 and 650/668) of each eluted fraction using a Cary Eclipse mass spectrofluorometer.
8. Pool fractions corresponding to the first set of overlapping fluorescence peaks, which exhibit the co-migration of antibody and siRNA.
9. Concentrate pool using a Centricon device with a 100 kDa MWCO (see Note 6).
10. Measure siRNA fluorescence again, and determine the final concentration of encapsulated siRNA by comparing it with a standard.
11. Filter sterilized siILs using a 0.2 μm filter.
12. Measure the mean siIL diameter before and after conjugation of liposomes to mAb using a Zetasizer Nano particle sizer operated in the volume-weighed mode. The size of siIL is 86 nm (Fig. 2).

3.3. Generation of Bone Marrow-Derived DC

1. Flush bone marrow cells from femurs and tibias of C57BL/6 mice.
2. Wash and culture cells in 6-well plates (2 x 10^6 cells/ml) in 2 ml of DC complete medium (RPMI 1640 supplemented with 2 mM L-glutamine, 100 U/ml penicillin, 100 mg of streptomycin, 50 μM 2-Mercaptoethanol, and 10% FBS supplemented with recombinant GM-CSF (10 ng/ml) and recombinant mouse IL-4 (10 ng/ml)).
3. Incubate cultures at 37°C in 5% humidified CO_2.
4. Remove non-adherent granulocyte after 48 h of culture, and add fresh medium.
5. Measure the expression of DC-specific markers in day 7 DC by FACS.

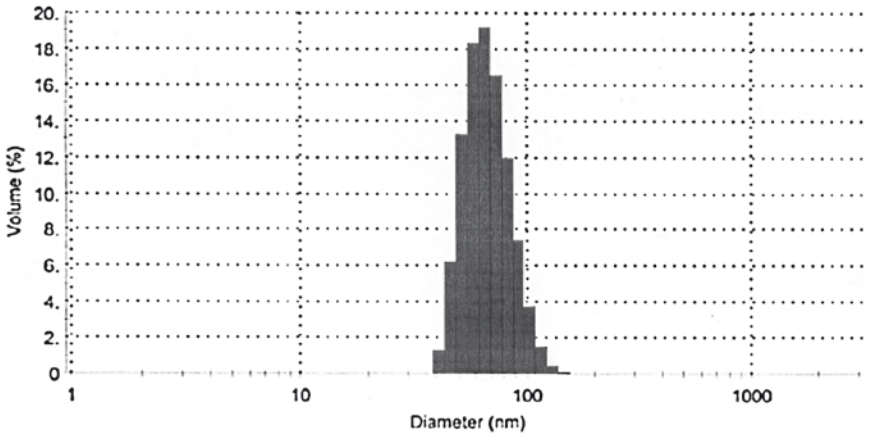

Fig. 2. Size of silL. Stealth liposomes encapsulating CD40 siRNA have a mean diameter of approximately 86 nm, as determined by dynamic light scattering

3.4. Transfecting DCs with GenePorter-Complexed or silL-Encapsulated siRNA

3.4.1. GenePorter Complexed Transfection

1. Collect day 6 BMDCs and suspend 1 x 10^6 cells in 200 µl of serum-free RPMI 1640.
2. Aliquot into a 24-well plate.
3. Separately, mix 1 µg of CD40 siRNA or negative control (non-specific) siRNA with 5 µl of GenePorter in a volume of 100 µl of serum-free RPMI 1640.
4. Incubate mixture at room temperature for 5 min.
5. Add siRNA mixture to the 200 µl of DC cell culture.
6. Transfect another batch of DC with 5 µl of GenePorter alone as negative control.
7. Incubate for 4 h at 37°C.
8. Add an equal volume of 20% FBC RPMI 1640 to the cells supplemented with LPS (10 ng/ml) for DC stimulation.
9. Incubate overnight at 37°C.
10. Add 1.6 ml of DC complete medium to the transfected DCs.
11. Measure CD40 expression by flow cytometry 48 h after transfection.

3.4.2. silL-Encapsulated siRNA Transfection

1. Collect day 6 BMDCs and suspend 1 x 10^6 cells in 200 µl of serum-free RPMI 1640.
2. Aliquot into a 24-well plate.
3. Separately, mix 0.7, 1.5, and 3.0 µg of siIL-encapsulated siRNA with 5 µl of GenePorter in a volume of 100 µl of serum-free RPMI 1640.
4. Incubate mixture at room temperature for 5 min.

5. Add siRNA mixture to the 200 µl of DC cell culture.
6. Transfect another batch of DC with equal volumes of PBS, equal amounts of siIL, or equal amounts of siIL-encapsulated negative control siRNA.
7. Add an equal volume of 20% FBC RPMI 1640 to the cells supplemented with LPS (10 ng/ml) for DC stimulation.
8. Incubate overnight at 37°C.
9. Add 1.6 ml of DC complete medium to the transfected DCs.
10. Measure CD40 expression by flow cytometry 48 h after transfection.

3.5. In Vitro DC-Specific Binding Assay

1. Collect 1 x 10^6 day 6 BMDCs.
2. Incubate for 30 min at 4°C with 3 µg of siIL-encapsulated CD40 siRNA.

3.5.1 BMDCs

3. Prepare control groups with an equal amount of CD40 siRNA liposomes or an equal volume of PBS, empty siILs, or CD40 siRNA mixed with GenePorter.
4. Wash cells with fresh RPMI medium.

3.5.2. L929

1. Seed the negative control L929 cells at a density of 2 x 10^5 in a 24-well plate overnight in complete medium (RPMI 1640 supplemented with 2 mM L-glutamine, 100 U/ml penicillin, 100 mg of streptomycin, 50 µM 2-Mercaptoethanol, and 10% FBS).
2. Remove the medium from cells.
3. Incubate cells with 3 µg of siIL-encapsulated CD40 siRNA for 30 min at 4°C.
4. Prepare control groups with an equal amount of CD40 siRNA liposomes or an equal volume of PBS, empty siILs, or CD40 siRNA mixed with GenePorter.
5. Wash cells with fresh RPMI medium.

3.5.3. Analyze DC-Specific Binding

Analyze the DC-specific binding of siIL to s and L929 cells by flow cytometry (FACScan) or by imaging using a fluorescence microscope (Fig. 3).

3.6. Flow Cytometry

1. Stain 1 x 10^6 BMDCs, splenocytes, or LN with FITC or PE-conjugated Ab or the appropriate isotype control Ab, at 4°C for 30 min.
2. Wash cells twice in 3 ml PBS with 1% BSA.
3. Suspend cells in 300 µl.
4. Analyze DC surface molecule expression of CD40, CD80, CD86, and MHC class II using FACScan apparatus.

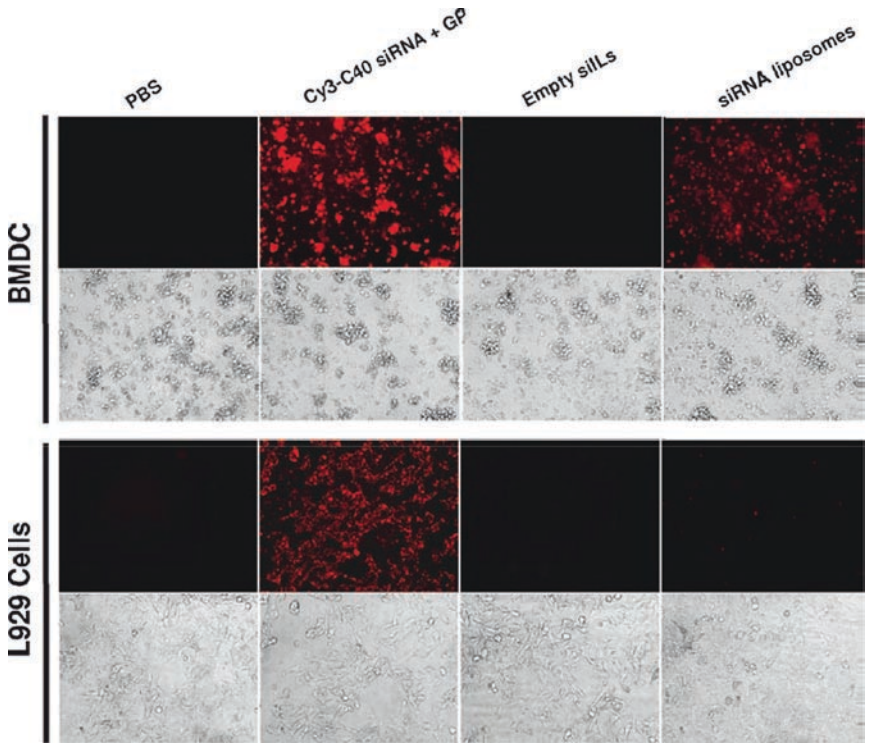

Fig. 3. silLs specifically target DCs in vitro. BMDCs were incubated for 30 min at 4°C with 1 mole% positive, DC-specific silLs containing Cy3-labeled CD40 siRNA. Cells were washed and imaged. Cy3-CD40 siRNA was complexed with Gene Porter (GP), a commercial transfection reagent, and used as a positive control treatment. silLs lacking Cy3-CD40 siRNA (Empty silLs) or the DC-targeting mAb (siRNA liposomes) were used as negative controls. A cell line (L929) that does not express DEC205 was also used as a negative control. The specificity of silL binding was determined by epifluorescence microscopy

3.7. Reverse Transcriptase Polymerase Chain Reaction (RT-PCR) and Quantitative Real-Time PCR

3.7.1. RNA Extraction

1. Collect cells and add 1 ml Trizol reagent. Leave the lysate at room temperature for 5 min.
2. Add 200 µl of chloroform and gently mix for 15 s. Centrifuge at 10,000×*g* for 15 min.
3. Collect the RNA solution (top layer solution).
4. Add 500 µl isopropanol and mix them completely. Centrifuge at 10,000×*g* for 10 min.
5. Discard the supernatant and suspend RNA pellet in 1 ml 75% ethanol.
6. Centrifuge it at 10,000×*g* for 5 min.
7. Dry the pellet in air.
8. Dissolve RNA in a certain amount of DEPC-treated distilled water. The amount of DEPC-H_2O depends on the size of the pellet.
9. Measure RNA concentration using spectrophotometry.

3.7.2. RT-PCR

Synthesize cDNA with oligo(dT) in a 20 µl volume.

3.7.2.1. cDNA Synthesis

1. Prepare the following RNA/oligo(dT) mixture in each tube: 1–3 µg Total RNA, 1 µl 0.5 µg/µl oligo(dT), DEPC H_2O to 12 µl.
2. Incubate the samples at 70°C for 10 min, and then on ice for 5 min.
3. Prepare reaction master mixture. For each reaction: 4 µl 5× 1st strand buffer, 2 µl 0.1 M DTT, 1 µl 10 mM dNTP.
4. Add the reaction mixture to the RNA/oligodT mixture, mix briefly, and incubate at 42°C for 2 min.
5. Add 0.5 µl (200 U/µl) of SuperScript II RT to each tube, mix and incubate at 42°C for 50 min.
6. Heat inactivate at 70°C for 15 min, and then chill on ice.
7. Store the 1st strand cDNA at –20°C until use for real-time PCR.

3.7.2.2. RT-PCR

1. Prepare PCR reaction mixture (below) on ice.

Reagents (per reaction)	Volume	Final conc.
10× Taq buffer	2.5 µl	1×
PCR forward primer (2 µM)	2.5 µl	0.2 µM
PCR reverse primer (2 µM)	2.5 µl	0.2 µM
10 mM dNTP	0.5 µl	200 nM
cDNA template	1 µl	
5 U/µl Taq DNA polymerase	0.2 µl	1 U
dH_2O	15.8 µl	
Total	25 µl	

2. Mix the mixture.
3. Centrifuge the reaction briefly.
4. Put sample into a theramal cycler.

   Set PCR program on theramal cycler: 95°C for 30 s, 58°C for 30 s, and then 72°C for 30 s (30 cycles).
5. Separate PCR products on 1.5% agarose gel, and visualize/stain gel with ethidium bromide.

3.7.3. Real-Time PCR

1. Prepare reactions buffer using SYBR Green PCR Master mix.
2. Add 100 nM of gene-specific forward and reverse primers with the same sequences used in the reverse transcriptase (RT)-PCR.

3. 3.The PCR reaction conditions: 95°C for 10 min, 95°C for 30 s, 58°C for 1 min and 72°C for 30 s (40 cycles).
4. Calculate gene expression using $2^{-\Delta\Delta(Ct)}$ (20), where Ct is cycle threshold, ΔΔ(Ct) = sample 1Δ (Ct) – sample 2Δ (Ct); Δ (Ct) = *GAPDH* (Ct) – testing gene (Ct).

3.8. In Vivo Gene Silencing

1. Prepare 50 μg KLH dissolved in 100 μl PBS.
2. Mix with an equal volume of complete Freund's adjuvant.
3. Inject KLH/CFA emulsion together with 17.5 μg of siIL-encapsulated CD40 siRNA, siIL-encapsulated negative control siRNA, naked CD40 siRNA or PBS subcutaneously at the base of the neck on day 0 of 7-week-old C57/B6 mice (see Note 5).
4. Inject the same siRNA treatment on day 1 intravenously.
5. Sacrifice on day 3 to assess the CD40 gene silencing capacity of CD40 siILs in the spleen and lymph nodes (LN).
6. Collect spleens and drain LN after sacrifice.
7. Collect LN cells and wash in fresh RPMI medium, whereas splenocytes are isolated by gradient centrifugation using Ficoll-Paque.
8. Stain cells with anti-mouse CD40 mAb, and measure the fluorescence from the cells by flow cytometry.

3.9. Immunohistochemistry

1. Inject mice with 17.5 μg of Cy3-labeled siRNA incorporated within DC- targeting immuoliposomes or with non targeting liposomes that lack the NLDC-145 mAB or with naked cy3 siRNA and PBS.
2. Dissect spleen, kidney, and liver at the time points of 20 min, 4 h, and 48 h following injection.
3. Flash freeze organs that are in OCT medium by submerging them in liquid N_2.
4. Section frozen tissues at the thickness of 10 μm.
5. Visualize and analyze fluorescence microscope and Northern Eclipse Software.

3.10. Mixed Lymphocyte Reaction

1. Collect day 6 BMDCs from C57/B6, and suspend 1×10^6 cells in 200 μl of serum-free RPMI 1640.
2. Aliquot into a 24-well plate.
3. Separately, mix 0.7, 1.5, and 3.0 μg of siIL-encapsulated siRNA with 5 μl of GenePorter in a volume of 100 μl of serum-free RPMI 1640.
4. Incubate mixture at room temperature for 5 min.

5. Add siRNA mixture to the 200 µl of DC cell culture.
6. Transfect another batch of DC with equal volumes of PBS or equal amounts of siIL-encapsulated negative control siRNA.
7. Add an equal volume of 20% FBC RPMI 1640 to the cells supplemented with LPS (10 ng/ml) for DC stimulation.
8. Incubate overnight at 37°C.
9. Add 1.6 ml of DC complete medium to the transfected DCs.
10. Irradiate activated DCs (3,000 rad), and seed in triplicate into a round-bottom 96-well plate as stimulators.
11. Isolate spleen T cells from BALB/c mice by gradient centrifugation using Ficoll-Paque.
12. Add the isolated spleen T cells as responders (2×10^5 cells/well).
13. Incubate the mixed lymphocyte culture at 37°C for 72 h in 200 µl RPMI 1640 supplemented with 10% FBS, 100 U/ml penicillin, and 100 µg/ml streptomycin.
14. Pulse the mixed lymphocyte culture with 1 µCi/well [^{3}H-labeled] thymidine for the last 16 hours of culture.
15. Harvest cells onto glass fiber filters.
16. Measure the radioactivity incorporated using a Wallac Betaplate liquid scintillation counter.

3.11. Antigen-Specific T Cell Proliferation Assays

1. Seed splenocytes or LN cells at 5×10^5/well into a 96-well flat-bottom micro-titer plate in triplicate.
2. Mix cells with KLH (10 µg/well).
3. Incubate for 72 h at 37°C.
4. Add 1 µCi [^{3}H] thymidine to each well for 16 h.
5. Harvest cells using cell harvester onto a glass microfiber filter.
6. Measure the incorporated radioactivity by a Wallac Betaplate liquid scintillation counter.

3.12. Statistical Analysis

siRNA encapsulation efficiency of different immunoliposome formulations containing 0, 1, and 2% DDAB was compared using a one-way analysis of variance (ANOVA), followed by the Newman–Keuls test. Data from real-time PCR, MLR, and KLH recall response assays were also analyzed using ANOVA. Differences for the value of $p < 0.05$ were considered significant.

4. Notes

1. Thiolated antibody should be used immediately. After storage, the antibody will lose its thiolation.
2. All lipids are dissolved in the chloroform and stored in glass containers.
3. siRNA should be dissolved in RNase-free water. Do not freeze and thaw siRNA more than 5 times; otherwise, siRNA will be degraded.
4. siRNA containing lipid mixture should be dissolved completely without any small particles at all. Otherwise, it will affect the siRNA incorporation and yield of siIL.
5. The column should be balanced very well before loading the sample, or it will affect the purity and yield of siIL.
6. Do not let the Centricon device dry. Set the speed of the centrifuge to ensure it does not surpass the limit of the Centricon device. Excessive speed will destroy the filter/membrane of the Centricon device.

References

1. Banchereau, J., Briere, F., Caux, C., Davoust, J., Lebecque, S., Liu, Y. J., Pulendran, B. and Palucka, K. (2000) Immunobiology of dendritic cells. *Annu. Rev. Immunol.* **18**:767.
2. Hill, J. A., Ichim, T. E., Kusznieruk, K. P., Li, M., Huang, X., Yan, X., et al. (2003) Immune modulation by silencing IL-12 production in dendritic cells using small interfering RNA. *J. Immunol.* **171**:691.
3. Li, M., Zhang, X., Zheng, X., Lian, D., Zhang, Z. X., Ge, W. et al. (2007) Immune modulation and tolerance induction by RelB-silenced dendritic cells through RNA interference. *J. Immunol.* **178**:5480.
4. Aigner, A. (2006) Delivery systems for the direct application of siRNAs to induce RNA interference (RNAi) in vivo. *J. Biomed. Biotechnol.* **4**:71659.
5. Hammond, S. M., Bernstein, E., Beach, D. and Hannon, G. J. (2000) An RNA-directed nuclease mediates post-transcriptional gene silencing in *Drosophila* cells. *Nature* **404**:293.
6. Nykanen, A., Haley, B. and Zamore, P. D. (2001) ATP requirements and small interfering RNA structure in the RNA interference pathway. *Cell* **107**:309.
7. Collins, R. E. and Cheng, X. (2005) Structural domains in RNAi. *FEBS Lett.* **579**:5841.
8. Miyagishi, M., Hayashi, M. and Taira, K. (2003) Comparison of the suppressive effects of antisense oligonucleotides and siRNAs directed against the same targets in mammalian cells. *Antisense Nucleic Acid Drug Dev.* **13**:1.
9. Kretschmer-Kazemi Far, R. and Sczakiel, G. (2003) The activity of siRNA in mammalian cells is related to structural target accessibility: a comparison with antisense oligonucleotides. *Nucleic Acids Res.* **31**:4417.
10. de Fougerolles, A., Vornlocher, H. P., Maraganore, J. and Lieberman, J. (2007) Interfering with disease: a progress report on siRNA-based therapeutics. *Nat. Rev. Drug Discov.* **6**:443.
11. Schwarz, D. S., Ding, H., Kennington, L., Moore, J. T., Schelter J., Burchard, J. et al. Designing siRNA that distinguish between genes that differ by a single nucleotide. *PLoS Genet.* **2**:e140.
12. Aagaard, L. and Rossi, J. J. (2007) RNAi therapeutics: principles, prospects and challenges. *Adv. Drug Deliv. Rev.* **59**:75.
13. Monnard, P. A., Oberholzer, T. and Luisi, P. (1997) Entrapment of nucleic acids in liposomes. *Biochim. Biophys. Acta.* **1329**:39.
14. Liu, Q. and Muruve, D. A. (2003) Molecular basis of the inflammatory response to adenovirus vectors. *Gene Ther.* **10**:935.

15. Donahue, R. E., Kessler, S. W., Bodine, D., McDonagh, K., Dunbar, C., Goodman, S. et al. (1992) Helper virus induced T cell lymphoma in nonhuman primates after retroviral mediated gene transfer. *J. Exp. Med.* **176**:1125.
16. Kawakami, S. and Hashida, M. (2007) Targeted delivery systems of small interfering RNA by systemic administration. *Drug Metab. Pharmacokinet.* **22**:142.
17. Morrissey, D. V., Lockridge, J. A., Shaw, L., Blanchard, K., Jensen, K., Breen, W. et al. (2005) Potent and persistent in vivo anti-HBV activity of chemically modified siRNAs. *Nat. Biotechnol.* **23**:1002.
18. Choung, S., Kim, Y. J., Kim, S., Park, H. O. and Choi, Y. C. (2006) Chemical modification of siRNAs to improve serum stability without loss of efficacy. *Biochem. Biophys. Res. Commun.* **342**:919.
19. Kraal, G., Breel, M., Janse, M. and Bruin, G. (1986) Langerhans' cells, veiled cells, and interdigitating cells in the mouse recognized by a monoclonal antibody. *J. Exp. Med.* **163**:981.
20. Pfaffl, M. W., Horgan, G. W. and Dempfle, L. (2002) Relative expression software tool (REST) for group-wise comparison and statistical analysis of relative expression results in real-time PCR. *Nucleic Acids Res.* **30**:e36.

Chapter 12

Hydrodynamic Delivery Protocols

Piotr G. Rychahou and B. Mark Evers

Abstract

RNA interference (RNAi) holds considerable promise as a novel therapeutic strategy to silence disease-causing genes not amenable to conventional therapeutics. Since it relies on small interfering RNAs (siRNAs), which are the mediators of RNAi-induced specific mRNA degradation, a major issue is the delivery of therapeutically active siRNAs into the target tissue. In vivo gene silencing with RNAi has been reported using both viral vector delivery and high-pressure, high-volume intravenous (i.v.) injection of synthetic siRNAs. For safety reasons, strategies based on viral vector delivery may be only of limited clinical use. The more desirable approach is to directly deliver active siRNAs. We describe the use of hydrodynamic administration as a technique to deliver naked siRNA constructs into experimental animals as a method of transient gene knockdown. This approach demonstrates that RNAi can be used to silence endogenous genes, involved in the cause of human diseases, with a clinically acceptable formulation and route of administration.

Key words: RNAi, siRNA, Hydrodynamics, Mice, In vivo siRNA delivery, Gene silencing, Drug delivery system

1. Introduction

RNAi holds great promise as a therapeutic tool (1–4). Substantial progress has been made in delivering siRNA in vivo through hydrodynamic methods and, more recently, through standard local and systemic administration (5–7). Hydrodynamic delivery involves rapid large-volume i.v. injection equivalent to the total blood volume. In the mouse, this involves injecting 2–3 ml over 10–15 s. The first report that this delivery method can be effective is from Budker et al. (8) who injected high volumes of either *lacZ* or luciferase reporter plasmids into the portal vein of mice. Using this approach, approximately 1% of all hepatocytes throughout the whole liver showed uptake of the plasmid. Because intraportal injection is not feasible in every laboratory, it was an

Wei-Ping Min and Thomas Ichim (eds.), *RNA Interference*, Methods in Molecular Biology, vol. 623,
DOI 10.1007/978-1-60761-588-0_12,

important discovery that injection of a high volume of plasmid DNA into the tail vein also leads to efficient uptake of DNA into the liver (9, 10). The first successful in vivo delivery of siRNA into cells using a hydrodynamic methodology was demonstrated in 2002 by McCaffrey et al. (11). Subsequent studies showed that the siRNA uptake into the liver after hydrodynamic tail vein delivery is more effective than plasmid DNA delivery (6).

To develop effective delivery systems of chemically synthesized siRNA, it is important to understand its biodistribution and pharmacokinetic properties at body-organ and cellular levels. siRNA duplexes are more stable than single-stranded RNAs, but they still degrade on incubation with serum, contributing to their short half-lives in vivo. For example, intravenous administration of naked siRNA in rats showed a half-life of 6 min and a clearance of 17.6 mL/min. The poor pharmacokinetic properties of siRNAs are related to their low in vivo stability, since they are degraded by endogenous RNases and quickly eliminated by kidney filtration because of their small molecular mass (~7 kDa) (12). siRNAs are widely distributed in the body after i.v. injection into mice, with preferential accumulation in the liver and kidney (13–16). Labeled siRNA is also distributed to the heart, spleen, and lung (14).

Improving the pharmacokinetic properties of siRNA duplexes is an important goal for developing siRNA-mediated gene silencing. Delivery can be enhanced either by improving siRNA attributes through chemical modifications of the duplex or by using different formulations such as cationic liposomes or polymers. Encapsulation of a stabilized siRNA within a liposomal nanoparticle greatly enhances serum half-life and bioavailability, and liposomal and polymeric nanoparticles coated with targeting ligands have been used for delivery in previous studies (17–20). Thus, a combination of these methods to generate stabilized siRNA-encapsulated nanoparticles may provide a method of choice to enhance delivery.

Developing and optimizing siRNA delivery in various types of animal disease models is a challenging process, but it will greatly accelerate drug discovery process and translate into clinically applicable administration methods for siRNA-based therapeutics to silence disease-causing genes.

2. Materials

2.1. Preparation for Hydrodynamic Tail Vein Injection in Rodents

1. Restraining device for mice or rats
2. Paper towels, alcohol prep pad, heating lamp, or warm water
3. Syringe with screw thread (3 ml; 22–30 gauge needle)
4. siRNA solution (1 mg/kg body weight)

2.2. Preparation for Portal Vein Injection in Rodents

1. Surgical instruments (scissors, tweezers, and retractors)
2. Betadine antiseptic solution or chlorhexidine solution
3. 24-gauge i.v. catheter
4. Gauze
5. Suture material 4–0
6. Fibrin/thrombin adhesive solution
7. Microvascular clamps
8. siRNA duplex (1 mg/kg body weight)

3. Methods

3.1. Hydrodynamic/ High Volume Tail Vein Injection in Rodents

Tail vein injection requires considerable skill in locating the vein and making sure that the needle is inserted into the vein. This procedure is suitable for all strains but is more difficult in black or pigmented rodents (see Note 1).

1. Weigh the rodent prior to the injection. The injection volume is determined by the weight of the animal and should be no more than 10% of the body weight.
2. This technique requires the animals to be warmed in order to dilate the blood vessels. The tail vein is dilated by application of warm water. Alternatively, some researchers dilate the tail vein by placing the whole animal under a heating lamp for 10 minutes. Rodents should be carefully monitored for signs of hyperthermia and dehydration (see Note 2).
3. Next, the animals are transferred into the barrel of the restrainer, which restrains the animal while allowing access to the tail vein. Insert the plunger and push it far enough to make sure that the animal cannot move. The lateral veins of the tail are the most frequently used veins (Fig. 1a). The lateral tail vein is identified (Fig. 1b) on either side, the injection site is disinfected, and the needle (27–30 gauge needle for mice and a 22–25 gauge needle for rats) is lined up, bevel side up, exactly in line with the vein.
4. Start midway between the tail tip and middle of the tail, moving toward the base of the tail if you need to inject the animal more than once (see Note 3). The needle should be as flat and parallel as possible to the tail. With the bevel of the needle facing upward and the needle almost parallel to the vein, slide the needle about 2 mm into the tail vein (Fig. 1c).
5. Confirm the location by gently pulling the plunger; if the needle is in the vein, you should see a flash of blood in the hub of the needle.

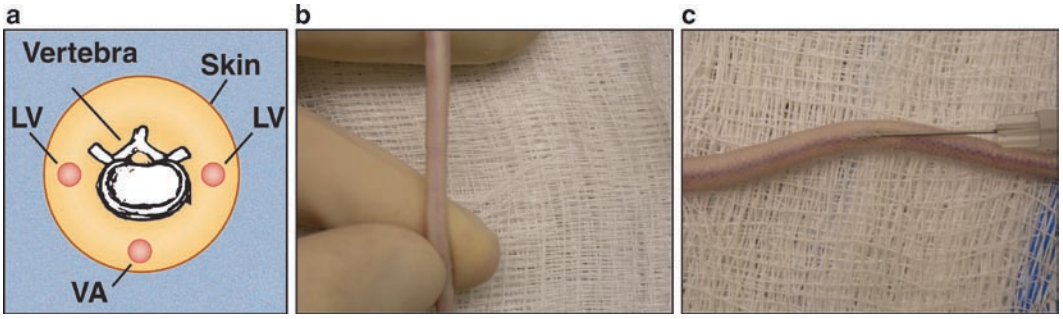

Fig. 1. (**a**) Diagram of a transverse sectional view of mouse tail showing the lateral veins (LV) and ventral artery (VA). (**b**) Example of a tail vein not ready for i.v. injection. Collapsed veins are a common reason for intravenous injection failure. (**c**) Example of tail vein ready for intravenous injection

6. After injecting a small test volume to ensure that the needle is safely placed in the vein, the whole volume is applied within 4–10 s (see Note 4). If the needle is in the vein, there will be no resistance; if the needle is not in the vein, the tissue near the injection site will change color, become swollen and the plunger will not move easily. In that case, halt the injection, wait 2–3 min and try again at a site closer to the tail base.
7. After removing the needle, hold the site with gauze to stop the bleeding before returning the animal to the cage (see Notes 5 and 6).

3.2. Intraportal Delivery of siRNA in Rodents

The hydrodynamic tail vein injection technique leads to high and reproducible siRNA uptake into the liver. It offers the possibility to investigate the effects of siRNA-mediated gene knockdown in the liver in different physiological and pathophysiological settings (see Notes 7–10). In humans, the portal vein can be reached without open surgery by puncturing the jugular vein and placing a catheter from the inferior vena cava through the liver. Thus, direct portal vein injection in the rodent can serve as a model for this procedure.

1. Animals are anesthetized with injectable anesthetics or gas-anesthesia (e.g., isoflurane). After anesthetizing the animal, the corneas should be protected with an ophthalmic lubricant. The following are suggested analgesics and anesthetics in rats and mice (remember to provide heat to anesthetized rodents):
   (a) Anesthetics:
   - Sodium Pentobarbital (Nembutal): mouse dose, 50–80 mg/kg IP; rat dose, 40–50 mg/kg IP

- Ketamine/xylazine solution: mouse dose, 100 mg/kg ketamine + 10 mg/kg xylazine IP; rat dose, 75 mg/kg ketamine + 10 mg/kg xylazine IP
- Inhalation anesthesia (e.g., isoflurane)

(b) Analgesic:

- Buprenorphine: mouse dose: 0.05–0.1 mg/kg SQ every 6–12 h; rat dose 0.05 mg/kg SQ every 8 h.

2. Once the animal is anesthetized, the fur is removed from the surgical site by shaving. This should be done in a location different from that used for performing the surgeries.
3. The surgical site is prepared with alternating scrubs of a betadine antiseptic solution or chlorhexidine and 70% alcohol. Cotton-tipped swabs or 2 × 2 gauze sponges may be used. It is important to avoid excessively wetting the animal, as this will lead to hypothermia and anesthetic complications.
4. Once prepped, the animal is placed on several 4 × 4 gauze sponges or a small heating pad (e.g., instant heat device, circulating hot water blanket) to provide warmth, and then relocated to the surgery station.
5. The animal is placed in a supine position and the ventral abdomen prepared for aseptic surgery. A ventral midline incision is made in the skin with a cranial terminus near the xiphoid process. A similar incision is made in the abdominal musculature. The bowels are wrapped in saline-soaked gauze and retracted laterally to obtain a good view of the portal vein (Fig. 2a, b). The portal vein is punctured with a 24-gauge intravenous catheter. After the plastic catheter is placed in a safe position, the needle is removed.

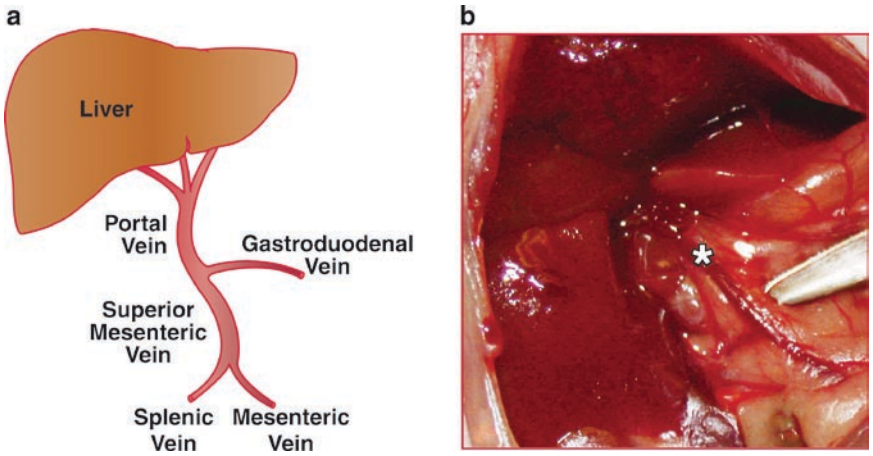

Fig. 2. (**a**) Diagrammatic representation of portal vein anatomy. (**b**) Asterisk identifies the portal vein as it courses cranially toward the liver

6. To avoid accidental movement of the catheter during injection, the portal vein is looped with a 4–0 ligature to tighten the catheter.
7. A total volume of up to 5% of animal body weight can be injected within 10 s. Before removing the needle, an adhesive solution of fibrin/thrombin is spread on the puncture site to prevent bleeding.
8. The abdominal cavity is closed with two separate layers of 4–0 suture material.

4. Notes

1. Tail vein injection requires considerable practice and skill.
2. Heat lamps and electrical heating pads are not recommended as they pose a higher risk of causing hyperthermia and burn-related injuries to the animals.
3. Absolutely no air can be injected, as this may cause an air embolus and result in animal death.
4. Using syringes without a screw thread will lead to disconnection during hydrodynamic injection.
5. Some animals will demonstrate heavy breathing and reduced activity after injection. These symptoms should not last longer than 30 min.
6. We prefer to perform standard hydrodynamic tail vein injection without anesthesia, as the combination of the high-volume injection together with anesthesia can lead to complications in some animals. If anesthesia is used, a gentle gas anesthesia (e.g., isoflurane) is preferred.
7. We recommend testing technical proficiency by using transgenic mice with reporter genes such as β-galactosidase (*lacZ*), firefly luciferase (Luc), or green fluorescent protein (GFP). Using this approach with established siRNA duplexes against *lacZ*, Luc or GFP, the efficiency of siRNA delivery into the liver can be monitored. Alternatively, Cy-3 or Cy-5 labeled siRNA can be injected.
8. Next, the efficiency of knockdown of a specific gene must be quantified by assaying mRNA and protein expression.
9. To rule out off-target effects of siRNA, two independent siRNAs against every target should be used.
10. For experiments that require sustained knockdown of the target gene, stability of the siRNA duplex in vivo must be tested individually. We prefer to use siRNA duplexes modified for extended stability and enhanced performance in nuclease-rich environments.

References

1. Leung, R. K. M., and Whittaker, P. A. (2005) RNA interference: From gene silencing to gene-specific therapeutics. *Pharmacol. Ther.* **107**, 222–239.
2. Lu, P. Y., Xie, F., and Woodle, M. C. (2005) In vivo application of RNA interference: from functional genomics to therapeutics. *Adv. Genet.* **54**, 117–142.
3. Paddison, P. J., Silva, J. M., Conklin, D. S., Schlabach, M., Li, M., Aruleba, S., et al. (2004) A resource for large-scale RNA-interference-based screens in mammals. *Nature* **428**, 427–431.
4. Berns, K., Hijmans, E. M., Mullenders, J., Brummelkamp, T. R., Velds, A., Heimerikx, M., et al. (2004) A large-scale RNAi screen in human cells identifies new components of the p53 pathway. *Nature* **428**, 431–437.
5. Zender, L., Hutker, S., Liedtke, C., Tillmann, H. L., Zender, S., Mundt, B., et al. (2003) Caspase 8 small interfering RNA prevents acute liver failure in mice. *Proc. Natl. Acad. Sci. U.S.A.* **100**, 7797–7802.
6. Song, E., Lee, S. K., Wang, J., Ince, N., Ouyang, N., Min, J., et al. (2003) RNA interference targeting Fas protects mice from fulminant hepatitis. *Nat. Med.* **9**, 347–351.
7. Ying, R. S., Zhu, C., Fan, X. G., Li, N., Tian, X. F., Liu, H. B., et al. (2007) Hepatitis B virus is inhibited by RNA interference in cell culture and in mice. *Antiviral Res.* **73**, 24–30.
8. Budker, V., Zhang, G., Knechtle, S., and Wolff, J. A. (1996) Naked DNA delivered intraportally expresses efficiently in hepatocytes. *Gene Ther.* **3**, 593–598.
9. Zhang, G., Budker, V., and Wolff, J. A. (1999) High levels of foreign gene expression in hepatocytes after tail vein injections of naked plasmid DNA. *Hum. Gene Ther.* **10**, 1735–1737.
10. Maruyama, H., Higuchi, N., Nishikawa, Y., Kameda, S., Iino, N., Kazama, J. J., et al. (2002) High-level expression of naked DNA delivered to rat liver via tail vein injection. *J. Gene Med.* **4**, 333–341.
11. McCaffrey, A. P., Meuse, L., Pham, T. T., Conklin, D. S., Hannon, G. J., and Kay, M. A. (2002) RNA interference in adult mice. *Nature* **418**, 38–39.
12. Soutschek, J., Akinc, A., Bramlage, B., Charisse, K., Constien, R., Donoghue, M., et al. (2004) Therapeutic silencing of an endogenous gene by systemic administration of modified siRNAs. *Nature* **432**, 173–178.
13. Jackson, L. N., Larson, S. D., Silva, S. R., Rychahou, P. G., Chen, L. A., Qiu, S., et al. (2008) PI3K/Akt activation is critical for early hepatic regeneration after partial hepatectomy. *Am. J. Physiol. Gastrointest. Liver Physiol.* **294**, G1401–G1410.
14. Larson, S. D., Jackson, L. N., Chen, L. A., Rychahou, P. G., and Evers, B. M. (2007) Effectiveness of siRNA uptake in target tissues by various delivery methods. *Surgery* **142**, 262–269.
15. Watanabe, H., Saito, H., Rychahou, P. G., Uchida, T., and Evers, B. M. (2005) Aging is associated with decreased pancreatic acinar cell regeneration and phosphatidylinositol 3-kinase/Akt activation. *Gastroenterology* **128**, 1391–1404.
16. Braasch, D. A., Paroo, Z., Constantinescu, A., Ren, G., Lk, O. K., Mason, R. P., et al. (2004) Biodistribution of phosphodiester and phosphorothioate siRNA. *Bioorg. Med. Chem. Lett.* **14**, 1139–1143.
17. Fenske, D. B., and Cullis, P. R. (2008) Liposomal nanomedicines. *Expert Opin. Drug Deliv.* **5**, 25–44.
18. Noble, C. O., Kirpotin, D. B., Hayes, M. E., Mamot, C., Hong, K., Park, J. W., et al. (2004) Development of ligand-targeted liposomes for cancer therapy. *Expert Opin. Ther. Targets* **8**, 335–353.
19. Zimmermann, T. S., Lee, A. C. H., Akinc, A., Bramlage, B., Bumcrot, D., Fedoruk, M. N., et al. (2006) RNAi-mediated gene silencing in non-human primates. *Nature* **441**, 111–114.
20. Hu-Lieskovan, S., Heidel, J. D., Bartlett, D. W., Davis, M. E., and Triche, T. J. (2005) Sequence-specific knockdown of EWS-FLI1 by targeted, nonviral delivery of small interfering RNA inhibits tumor growth in a murine model of metastatic Ewing's sarcoma. *Cancer Res.* **65**, 8984–8992.

Chapter 13

New Methods for Reverse Transfection with siRNA from a Solid Surface

Satoshi Fujita, Kota Takano, Eiji Ota, Takuma Sano, Tomohiro Yoshikawa, Masato Miyake, and Jun Miyake

Abstract

We describe two efficient and inexpensive methods for reverse transfection with siRNA from a solid surface. One method involves localized reverse transfection from spots on a glass slide, which is mainly useful for making "transfection microarrays" (TMAs). The other involves reverse transfection in multiple wells of microtiter plates. Conditions for cell culture, preparation of reagents, and details of reverse transfection have been determined for several lines of cells, but we focus here on experiments with HeLa cells. In particular, we evaluated the efficiency of transfection, the cytotoxic effects of reverse transfection, and the efficiency of gene "knockdown" by transfection. We also performed phenotypic screening for a functional gene, during which cell viability was evaluated in terms of fluorescence from Calcein-AM. Our methods for reverse transfection with siRNA should be powerful tools that are useful for high-throughput analysis of functional genes.

Key words: Reverse transfection, Solid surface, Transfection with siRNA, Transfection microarray (TMA), High-throughput phenotypic screening

1. Introduction

The development of methods for high-throughput screening for gene identification is important for the elucidation of the mechanisms of basic biological phenomena and disease processes. Such methods, based on reverse transfection from a solid surface, with plasmid DNA or siRNA attached to the surface of, for example, a glass slide or the surface of a culture dish for introduction into adherent cells, have been developed by several groups, including our own (1–6). These methods, which allow the comprehensive "knockdown" of genes by siRNAs, are very useful for assays of gene function that are based on cell phenotypes.

Wei-Ping Min and Thomas Ichim (eds.), *RNA Interference*, Methods in Molecular Biology, vol. 623,
DOI 10.1007/978-1-60761-588-0_13,

We have established two methods for reverse transfection with siRNA from a solid surface. One of these methods is used mainly for the preparation of cell microarrays; in this method, siRNAs, spotted on a slide, are reverse-transfected locally into adherent cells (4, 7). Several other methods are being developed (6, 8), and we have been testing these methods for their utility in the identification of functional genes (9–12). Our second method uses multiple wells of microtiter plates, and siRNAs that uniformly coat the surface of wells are reverse-transfected into adherent cells (13). These two methods have some common features that simplify procedures for high-throughput screening. Each method involves (1) one-step preparation of the surface for transfection of siRNAs and cell culture; (2) an attached transfection mixture that includes siRNA with long-term stability; and (3) a transfection procedure that is minimally stressful to cells and exhibits minimal toxicity.

We discuss, here, our two methods for reverse transfection with siRNA from a solid surface and provide an example of their use for screening of genes in HeLa cells.

2. Materials

2.1. Cell Culture

1. Dulbecco's modified Eagle's medium (DMEM; Nacalai Tesque, Kyoto, Japan), supplemented with 10% fetal bovine serum (FBS; ICN Pharmaceuticals, Costa Mesa, CA), 1% penicillin–streptomycin mix (Nacalai Tesque) and 1% kanamycin (Invitrogen, Carlsbad, CA). Store at 4°C.
2. 0.05%-Trypsin/0.53 mM-EDTA solution (Nacalai Tesque): a solution of trypsin (0.05%, w/v) and ethylenediamine tetraacetic acid (EDTA; 0.53 mM) in distilled water.
3. Dulbecco's phosphate-buffered saline (D-PBS[–] without calcium and magnesium, Nacalai Tesque).
4. HeLa cells (Riken Bioresource Center Cell Bank, Tsukuba, Ibaraki, Japan).

2.2. Localized Reverse Transfection on a Transfection Microarray (TMA)

1. Dulbecco's modified Eagle's medium (DMEM) without serum and phenol red (Invitrogen), stored in 1-ml aliquots in 1.5-ml tubes at 4°C.
2. Water (endotoxin-free; Sigma-Aldrich, St. Louis MO).
3. Solution of siRNA (20 μM). When freeze-dried samples are used, siRNA is dissolved at 20 μM in endotoxin-free water and stored in single-use aliquots at –80°C. We mainly use FlexiPlate siRNA (Qiagen, Valencia, CA) as the large siRNA

library for high-throughput screening, with Silence® Negative Control siRNA (Ambion, Austin, TX), Cy™3-labeled Negative Control #1 siRNA (Ambion), and AllStars RNAi Controls (Qiagen) as controls. Although siRNAs from other suppliers can be used, their conditions for use may be different because some components, such as salts, differ in preparations of freeze-dried siRNAs from different suppliers.

4. Lipofectamine™ 2000 Transfection Reagent (Invitrogen).
5. A solution of fibronectin (4 mg/ml): fibronectin (Life Laboratory Company, Yamagata, Japan; http://www.life-kenkyusho.co.jp/) is dissolved at 4 mg/ml in endotoxin-free water, and the solution is stored in 1-ml aliquots in 1.5-ml tubes at 4°C.
6. 0.1% (w/v) Gelatin: gelatin (Sigma-Aldrich) is dissolved in endotoxin-free water, and the solution is autoclaved before storage in 1-ml aliquots in 1.5-ml tubes at 4°C.
7. Poly L-lysine-coated glass slides (Matsunami Glass Ind., Osaka, Japan).
8. An ink-jet microarray printer (KCS-mini; Kubota Comps Corporation, Hyogo Japan).
9. Four-well dishes: non-treated, sterile, with lids (Plastic plates for glass slides) (Nalgene Nunc International, Rochester, NY).

2.3. Reverse Transfection in Multiple Wells of a Microtiter Plate

1. Dextran (MW 40,000; Wako Pure Chemical Industries, Osaka, Japan) is dissolved at 45 g/l in D-PBS(−), and the solution stored in 1-ml aliquots in 1.5-ml tubes at 4°C after filtration through a 0.22-μm filter (MILLEX®HV; Millipore, Billerica, MA).
2. 70% ethanol in endotoxin-free water. (Wako Pure Chemical Industries).
3. Solution of siRNA (20 μM), as described in detail in Subheading 2.2.
4. Lipofectamine™ 2000 Transfection Reagent (Invitrogen).
5. Poly(vinyl alcohol)500, completely hydrolyzed (PVA; Wako Pure Chemical Industries), is dissolved at 0.5% (v/v) in endotoxin-free water, and the 100 ml of solution in a glass bottle is autoclaved and stored at room temperature.

2.4. Confirmation of Transfection of Cells with siRNA

1. Solution of Cy3-labeled non-target siRNA (20 μM Cy™3-labeled Negative Control #1; Ambion) described in detail in Subheading 2.2.
2. Fluorescence microscope (IX 81; Olympus, Tokyo, Japan).

2.5. Analysis of Cytotoxicity of the Methods for Reverse Transfection

1. Solution of non-targeted (control) siRNA (20 μM), as described in detail in Subheading 2.2.
2. Dulbecco's phosphate-buffered saline (D-PBS[−]; Nacalai Tesque).
3. 70% methanol in endotoxin-free water (Wako Pure Chemical Industries).
4. A solution of ethidium homodimer-1 (Eth-D1) in DMSO (Invitrogen) is diluted to 5 μM with D-PBS(−) immediately before use.
5. Fluorescence microscope (IX 81; Olympus).

2.6. Analysis of the Efficiency of Gene Knockdown by Quantitation of mRNA by a Quantitative Version of the Polymerase Chain Reaction (QPCR)

1. Solution of non-targeted siRNA (20 μM AllStars RNAi Controls; Qiagen) and siRNA targeted against CDK2, (20 μM FlexiPlate siRNA; Qiagen), as described in detail in Subheading 2.2.
2. A TurboCapture mRNA kit (Qiagen).
3. One-Step SYBR PrimeScript RT-PCR Kit (Takara Bio Inc., Shiga, Japan).
4. Sequence-detection system (ABI PRISM 7700 system; Applied Biosystems, Foster City, CA).

2.7. Assessment of Cell Viability with Calcein-AM

1. Solution of non-targeted siRNA (20 μM AllStars RNAi Controls; Qiagen), apoptosis-inducing siRNA (20 μM AllStars Hs Cell Death Control siRNA; Qiagen), siRNA targeted against caspase 8 (20 μM FlexiPlate siRNA; Qiagen) as described in detail in Subheading 2.2.
2. Recombinant human TRAIL/Apo2L (TNF-related apoptosis-inducing ligand; PeproTech Inc., Rocky Hill, NJ). Store at −20°C.
3. A solution of Calcein-AM (2 μg/ml) is prepared by diluting Calcein-AM in anhydrous DMSO (1 μg/ml; Invitrogen) with DMEM immediately before use.
4. Microarray scanner (GenePix 4200A; Molecular Devices, Sunnyvale, CA).

3. Methods

We have developed two methods for reverse transfection with siRNA from a solid surface. Both methods are suitable for high-throughput analysis and screening for functional genes, and they are particularly useful for the identification of drug targets and the characterization of components in signal-transduction pathways.

Localized reverse transfection from spots of siRNA is mainly useful for exploitation of microarrays, which we call "transfection microarrays" (TMAs). In this method, siRNA enters adherent cells only as a result of contact between cells and the siRNA attached to the solid surface. Because the attached siRNA is localized as spots and does not diffuse, there is no cross-transfection among the siRNAs in the various spotted areas even though there are no raised physical barriers between the spots. Therefore, it is easy to prepare dense microarrays by concentrating each siRNA and miniaturizing each spot. Moreover, it is not necessary to control the number of cells that come into contact with each spot.

Reverse transfection in multiple wells of microtiter plates is no better than reverse transfection on TMAs in terms of miniaturization and concentration, but it does permit inclusion of soluble factors, such as humoral factors, drugs and ligands, in screenings. Moreover, because this second method was developed from conventional well-based assays, it can be used with conventional equipment for well-based analysis.

Prior to high-throughput analysis and screening for functional genes by both methods, it is very important to confirm (1) the efficiency of transfection with siRNA, (2) the efficiency and specificity of gene knockdown; and (3) the absence of cytotoxic effects of transfection with siRNA and the efficiency of such transfection.

3.1. Cell Culture

1. HeLa cells are cultured in DMEM supplemented with 10% fetal bovine serum in a humidified incubator at 37°C in an atmosphere of 5% CO_2 in air (see Note 1). In order to avoid bacterial contamination, addition of antibiotics to the culture medium is advisable. In a typical study, we add 1% penicillin–streptomycin mix and 1% kanamycin.
2. When approaching confluence, HeLa cells should be passaged to generate new maintenance cultures in 100-mm tissue culture dishes (see Note 2). Prepare a pre-warmed solution of 0.05% trypsin/EDTA, D-PBS(–) and DMEM supplemented with 10% fetal bovine serum at 37°C (see Note 3). Add 10 ml of D-PBS(–) to each 100-mm dish to wash cells, and then remove by aspiration. Add 2 ml of the pre-warmed solution of 0.05% trypsin/EDTA after aspiration of the D-PBS(–), and then incubate each dish at 37°C for 1 min. Add 2 ml of DMEM to interrupt the effects of trypsin and then transfer the entire contents of the dish to a 15-ml tube and centrifuge the tube at 800–1,200 rpm for 3 min. Remove the supernatant and add 10 ml of medium to the pelleted cells. After resuspension of cells by careful pipetting, transfer the suspension to a 100-mm tissue culture dish.

3.2. Localized Reverse Transfection on a Transfection Microarray (TMA)

1. Prepare DMEM without serum and phenol red; siRNA; Lipofectamine™ 2000 Transfection Reagent; a solution of fibronectin (4 mg/ml); and a 0.1% solution of gelatin. Put each reagent on ice.
2. Pipette 7.5 µl of DMEM and 7 µl of the 20 µM solution of siRNA into a 1.5-ml tube, centrifuge briefly, and tap the tube gently to mix the solutions (see Note 4).
3. Add 2 µl of Lipofectamine™ 2000 Transfection Reagent to the tube, centrifuge briefly, and tap the tube gently to mix the solutions.
4. Incubate each sample for 20 min at room temperature (15–25°C) to allow formation of the transfection complex.
5. Add 5 µl of fibronectin solution and 2.5 µl of the 0.1% solution of gelatin to the tube and spin them down. Mix the reagents by pipetting them up and down twice (see Note 5). The mixture is stable for two days at 4°C.
6. Spot samples on poly L-lysine-coated glass slides using an ink-jet printing device according to the supplier's manual (see Note 6). An ink-jet type of microarray printing device is available from various suppliers, for example, the MicroArray Printer KCS-mini (Kubota; see Notes 7 and 8). Spots of 15–25 nl per droplet, which are suitable for effective transfection, are air-dried immediately and spontaneously and form circular areas of 600–800 nm in diameter (see Notes 9 and 10). The amount of siRNA per spot is approximately 112 fmol.
7. Prepare a suspension of HeLa cells in culture medium (1.5×10^4 cells/ml) as described in Subheading 3.1. Put the glass slide with spots of siRNA in a plastic dish for glass slides. Pour 10 ml of the cell suspension very slowly (at a rate of less than 10 ml/min) onto the edge of the slide (see Note 11). Move the plastic plate from side to side to disperse cells uniformly over the slide (see Note 12).
8. Incubate the slide in the covered dish at 37°C for 24–48 h in a humidified atmosphere of 5% CO_2 in air to allow knock-down of gene expression by siRNA.

3.3. Reverse Transfection in Multiple Wells of a Microtiter Plate

1. Prepare the following reagents: a solution of dextran (4.5 g/l in D-PBS[−]); 70% ethanol; 20 µM siRNA; Lipofectamine™ 2000 Transfection Reagent; and 0.5% polyvinyl alcohol (PVA). Place PVA at room temperature and the others on ice.
2. Mix the solution of dextran and 70% ethanol at a ratio of 1:1 (v/v). Spot 10 µl or 40 µl of the mixture in the center of each well of a 96- or a 24-well microtiter plate and then dry the plate in a vacuum chamber for 1 h.

3. Add 7 µl of the 20 µM solution of siRNA and 16 µl of the dextran solution to a 1.5-ml tube (see Note 13), centrifuge the tube, and tap it gently to mix the solutions (see Note 14).
4. Add 2 µl of Lipofectamine™ 2000 Transfection Reagent to the tube (see Note 13), centrifuge the tube and tap it gently to mix the reagents.
5. Incubate the sample for 20 min at room temperature (15–25°C) to allow formation of the transfection complex.
6. Add 92 µl of the solution of PVA to the tube, centrifuge the tube and tap it gently to mix reagents.
7. Spot 4 µl or 22 µl of the mixture in the center of each dextran-coated well of the 96- or 24-well microtiter plate, and then dry the plate in a vacuum chamber for 1 h (see Note 15).
8. Prepare a suspension of HeLa cells in culture medium ($1–5 \times 10^4$ cells/well for 96-well microtitier plates and $0.4–2 \times 10^5$ cells/well for 24-well microtitier plates) according to the procedure described in Subheading 3.1. Place 100 µl or 400 µl, respectively, of the suspension of cells in each well of a 96- or a 24-well microtiter plate.
9. Incubate the plate at 37°C for 24–48 h in a humidified atmosphere of 5% CO_2 in air for adequate knockdown of gene expression by siRNA.

3.4. Confirmation of Transfection of Cells with siRNA

1. Transfect cells with Cy3-labeled non-target siRNA by each of the two methods for reverse transfection, as described in Subheadings 3.2 and 3.3 (see Note 16).
2. After incubation at 37°C for 24 h in a humidified atmosphere of 5% CO_2 in air, record phase-contrast and fluorescence images of cells with a fluorescence microscope (IX 81; Fig. 1).

3.5. Analysis of Cytotoxicity of the Methods for Reverse Transfection

1. Transfect cells with non-target siRNA by each of the two methods for reverse transfection, as described in Subheadings 3.2 and 3.3. The protocol that follows conforms to the analysis of HeLa cells in a 24-well microtiter plate. Changes in volume, for example, should be made when a different format is used, such as a 96-well microtiter plate or a glass slide.
2. Incubate cells after (or without) prior transfection at 37°C for 24 h in a humidified atmosphere of 5% CO_2 in air.
3. To prepare dead cells as a positive control, wash cells in each well once with 500 µl of D-PBS(−) and then add 500 µl of 70% methanol to each well and incubate the plate at room temperature for 30 min. Continue the incubation of transfected cells and of non-transfected cells as negative controls.

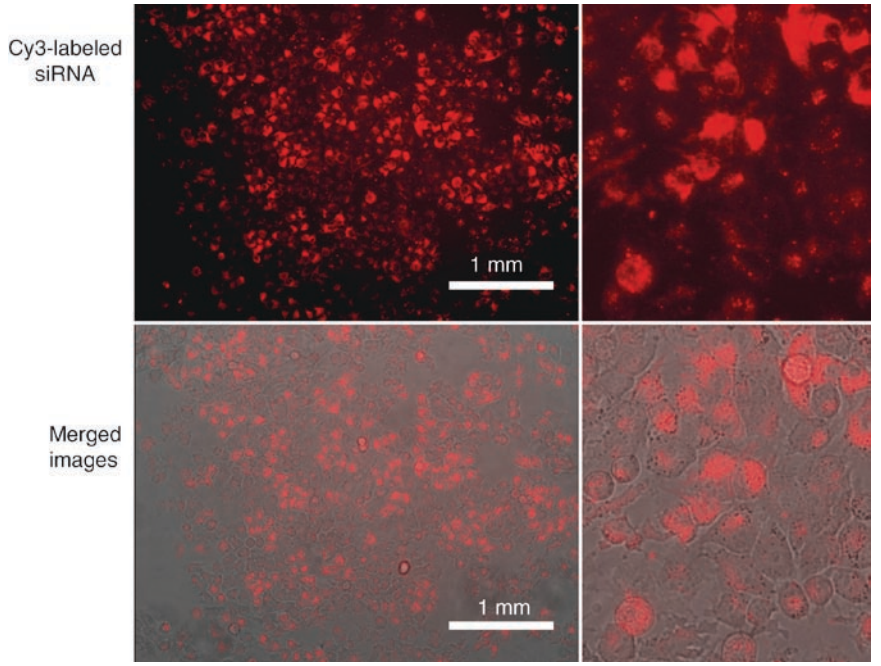

Fig. 1. Photographs of three typical lines of cells after reverse transfection with Cy3-labeled non-target siRNA in multiple wells of a microtiter plate. Left, HeLa cells; center, SK-BR-3 cells; right, MCF7 cells; upper images, phase-contrast; center images, fluorescence due to Cy3; lower images, merged phase-contrast and fluorescent images; left side of each rectangle, 4× lens; and right side of each rectangle, 20× lens. The figure was reprinted from (13). Scale bars, 1 mm or 200 μm

4. At the end of the experiment, wash cells in the various wells twice with 500 μl of D-PBS(−), place 500 μl of D-PBS(−) prepared with 5 μM ethidium homodimer-1 (EthD-1) in each well to stain dead cells selectively, and incubate plates at room temperature for 10 min.
5. After washing cells in the various wells once with 500 μl of D-PBS(−), record phase-contrast and fluorescence images of cells with a fluorescence microscope (IX 81; Fig. 2). Dead cells are stained with EthD-1; live cells remain unstained.

3.6. Analysis of the Efficiency of Gene Knockdown by Quantitation of mRNA by QPCR

1. Transfect cells with CDK2-specific siRNA or non-target siRNA, as a control, by reverse transfection in multiple wells of microtiter plates as described in Subheading 3.3. In a parallel control experiment, you should also transfect cells with these siRNAs by a conventional method (see Note 17).
2. Extract the mRNA from cells in each well with a TurboCapture mRNA kit (Qiagen) in accordance with the instructions from the manufacturer.
3. Perform QPCR using a One Step SYBR PrimeScript RT-PCR kit (Takara) and an ABI PRISM 7700 system (Applied Biosystems) in accordance with the instructions from the manufacturers (Fig. 3).

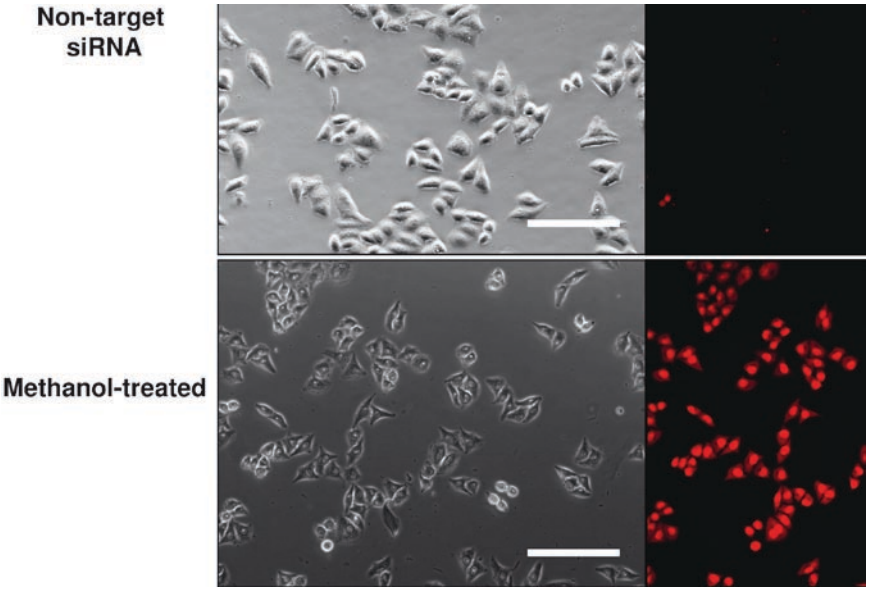

Fig. 2. Cytotoxic effects on three typical lines of cells (HeLa, SK-BR-3 and MCF7) of reverse transfection from a solid phase. Upper images, cells without transfection; center images, cells after transfection of non-target siRNA; lower images, methanol-treated cells without transfection; left side of each rectangle, phase-contrast image; and right side of each rectangle, fluorescence staining with ethidium homodimer (EthD-1). The figure was reprinted from (13). Scale bars, 200 μm

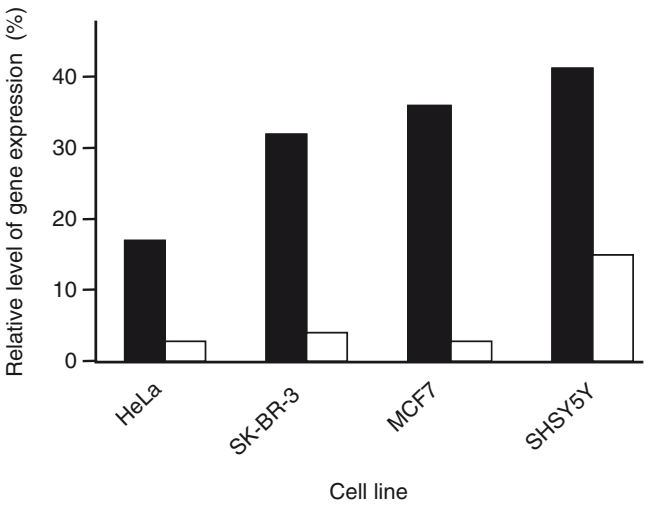

Fig. 3. Comparison of the gene-knockdown efficiency of a specific siRNA directed against CDK2 between well-based reverse transfection and conventional transfection methods. In all transfections, siRNA was introduced into cells in the presence of Lipofectamine™ 2000, as described in the text. The figure was reprinted from (13)

3.7. Assessment of Cell Viability with Calcein-AM

1. Transfect cells with caspase 8-specific siRNA, AllStars Hs Cell Death Control siRNA and non-target siRNA by the two methods for reverse transfection as described in Subheadings 3.2 and 3.3. The protocol that follows conforms

to the analysis of the induction of cell death in HeLa cells by TRAIL on a glass slide microarray.

2. Incubate HeLa cells (1.5×10^4 cells/ml) on a glass slide microarray of siRNAs in 10 ml of DMEM supplemented with 10% fetal bovine serum, 1% penicillin–streptomycin mix and 1% kanamycin at 37°C for 48 h in a humidified atmosphere of 5% CO_2 in air for knockdown of gene expression by siRNAs.
3. Replace the culture medium by DMEM supplemented with 1% fetal bovine serum, 1% penicillin–streptomycin mix, and 1% kanamycin (see Note 18).
4. Add 1 mg of TRAIL to the culture medium (to give a final concentration of 100 ng/ml).
5. Incubate the cells and microarray at 37°C for 24 h in a humidified atmosphere of 5% CO_2 in air.
6. Remove the medium and, after washing cells that have attached to the slide once with D-PBS(–), add 10 ml of a 2 μg/ml solution of Calcein-AM (see Note 18).
7. Incubate the slide with Calcein-AM at 37°C for 35 min in a humidified atmosphere of 5% CO_2 in air.

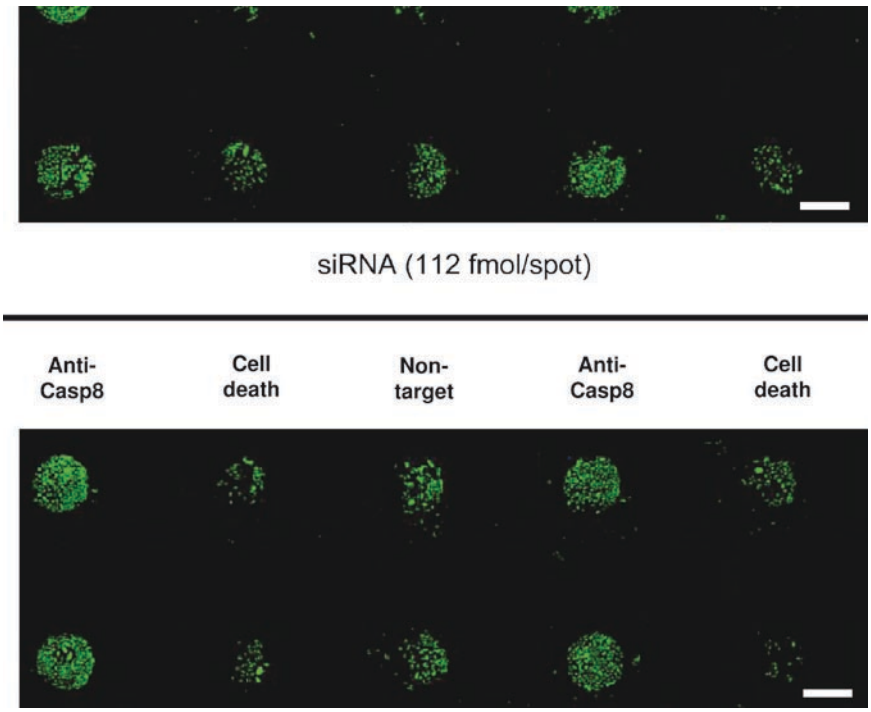

Fig. 4. Assessment of cell viability with Calcein-AM on a TMA slide. The amount of siRNA in each spot was varied, as indicated, by changing the volume of the drop, which ranged from 1 to 10.5 μl. The amount of siRNA in each spot ranged from 16 to 168 fmol. Anti-Casp8, siRNA directed against caspase 8; cell death, positive control siRNA; and Non-target, negative control. See text for details. Scale bars, 1 mm

8. Wash cells on the slide four times with 10 ml of D-PBS(−) (see Note 19), and then allow the slide with attached cells to dry in air at room temperature for 10 min.
9. Record the fluorescence from living cells on the slide with an image analyzer, such as GenePix 4200A (Fig. 4).

4. Notes

1. You should prepare stocks of frozen cells from the same batch because differences among batches can influence the results of high-throughput analysis and screening for functional genes by our methods.
2. The number of passages of cells should be controled because passaging influences the efficiency of transfection and the results of phenotypic analysis after reverse transfection from a solid surface.
3. Pre-warming is necessary because a cold solution might affect both cell viability after passaging and the results of phenotypic analysis. Maintenance of the temperature of the trypsin/EDTA solution at 37°C is useful for controling the activity of trypsin. The concentration of components in the trypsin/EDTA solution depends on the efficiency of adhesion of cells after passaging. A high concentration of trypsin, or treatment with trypsin for an extended period of time, can damage cells. Moreover, such damage to cells has a major effect on the efficiency of reverse transfection from a solid surface. Therefore, it is essential to identify suitable conditions for treatment of cells with trypsin.
4. Differences among strains and lines of cells and among target genes influence the efficiency of siRNA-mediated knockdown of gene expression. The appropriate volume of siRNA should be determined for each system. The volume of the solution of siRNA can vary between 1 and 10.5 μl, with DMEM accounting for up to 14.5 μl of the total volume.
5. The purity and stability of fibronectin influence the efficiency of transfection. Moreover, some preparations of fibronectin mediate cross-transfection among different spots. Addition of 0.1% gelatin helps to prevent such cross-transfections (1). However, we strongly recommend the fibronectin sold by Life Laboratory Company, Yamagata, Japan (http://www.life-kenkyusho.co.jp/).
6. You can prepare TMAs in 100-mm dishes, 35-mm dishes, and in 6-, 24-, 48-, and 96-well microtiter plates, confirming the reverse transfection of adherent cells on spots of siRNA.

7. An ink-jet type microarray printing device is preferable to a pin-type microarray device because droplets deposited by a pin-type microarray device yield torus-shaped spots when they dry.
8. If you do not have a printing device, you can make spots on a glass slide by hand. When you touch the tip of a micropipet with 2 µl of the solution of sample to the glass slide, a droplet will be deposited on the slide.
9. When printing many spots, you should take care that the solution of sample does not become concentrated as a result of evaporation.
10. A glass slide with spots of siRNA is stable in a vacuum-sealed plastic bag with silica gel at room temperature for more than 6 months.
11. In our study of HeLa cells, 1.5×10^5 cells (1.5×10^4 cells/ml in 10 ml of DMEM) were seeded on each glass slide. It is necessary to determine optimal conditions for each experiment.
12. For each strain of cells, there is a knack to spreading the cells. Therefore, practice is useful with each specific strain prior to each experiment.
13. Care should be taken to avoid bubbles. When applying the solution to wells of a 96-well microtiter plate, do not worry if the solution attaches to the walls of wells.
14. Differences among strains of cells and target genes influence the efficiency of gene knockdown by siRNA. The appropriate volume of solution of siRNA should be determined for each experiment. The volume of the solution of siRNA can vary from 1 to 10.5 µl, with the solution of dextran accounting for up to 23 µl of the total volume.
15. Spots on a microtiter plate in a vacuum-sealed plastic bag with silica gel are stable at room temperature for more than 6 months.
16. Cy3-labeled non-target siRNA is a very good reagent for confirming directly that siRNA has been introduced into the cytoplasm of cells.
17. It is difficult to quantify the mRNA in cells on individual spots of a TMA slide because of low cell number.
18. DMEM, D-PBS(–), and the solution of Calcein-AM should be warmed at 37°C before use.
19. Washing must be performed carefully in order to avoid dislodging cells from the surface of the glass slide.

Acknowledgments

This study was performed as part of "The Project for Development of Analytic Technology for Gene Functions with Cell Arrays", which was funded by the New Energy and Industrial Technology Development Organization (NEDO) of Japan.

References

1. Ziauddin, J., and Sabatini, D. M. (2001) Microarrays of cells expressing defined cDNAs. *Nature* **411**, 107–110.
2. Kumar, R., Conklin, D. S., and Mittal, V. (2003) High-throughput selection of effective RNAi probes for gene silencing. *Genome Res.* **13**, 2333–2340.
3. Mousses, S., Caplen, N. J., Cornelison, R., Weaver, D., Basik, M., Hautaniemi, S., et al. (2003) RNAi microarray analysis in cultured mammalian cells. *Genome Res.* **13**, 2341–2347.
4. Yoshikawa, T., Uchimura, E., Kishi, M., Funeriu, D. P., Miyake, M., and Miyake, J. (2004) Transfection microarray of human mesenchymal stem cells and on-chip siRNA gene knockdown. *J. Control. Release* **96**, 227–232.
5. Baghdoyan, S., Roupioz, Y., Pitaval, A., Castel, D., Khomyakova, E., Papine, A., Soussaline, F., and Gidrol, X. (2004) Quantitative analysis of highly parallel transfection in cell microarrays. *Nucleic Acids Res.* **32**, e77.
6. Uchimura, E., Yamada, S., Uebersax, L., Fujita, S., Miyake, M., and Miyake, J. (2007) A method for reverse transfection using gold colloid as a nano-scaffold. *J. Biosci. Bioeng.* **103**, 101–103.
7. Yamada, S., Uchimura, E., Ueda, T., Iguchi, F., Akiyama, Y., Fujita, S., Miyake, M., and Miyake, J. (2006) Area based analyzing technique at cell array experiment using neuronal cell line. *Nanobiotechnology* **2**, 95–100.
8. Uchimura, E., Yamada, S., Nomura, T., Matsumoto, K., Fujita, S., Miyake, M., and Miyake, J. (2007) Reverse transfection using antibodies against cell surface antigen in mammalian adherent cell lines. *J. Biosci. Bioeng.* **104**, 152–155.
9. Yamada, S., Nomura, T., Uebersax, L., Matsumoto, K., Fujita, S., Miyake, M., and Miyake, J. (2007) Retinoic acid induces functional c-Ret tyrosine kinase in human neuroblastoma. *Neuroreport* **18**, 359–363.
10. Yamada, S., Uchimura, E., Ueda, T., Nomura, T., Fujita, S., Matsumoto, K., et al. (2007) Identification of twinfilin-2 as a factor involved in neurite outgrowth by RNAi-based screen. *Biochem. Biophys. Res. Commun.* **363**, 926–930.
11. Yamada, S., Nomura, T., Takano, K., Fujita, S., Miyake, M., and Miyake, J. (2008) Expression of a chimeric CSF1R-LTK mediates ligand-dependent neurite outgrowth. *Neuroreport* **19**, 1733–1738.
12. Onuki-Nagasaki, R., Nagasaki, A., Hakamada, K., Uyeda, Q., P., T., Fujita, S., Miyake, M., and Miyake, J. (2008) On-chip screening method for cell-migration genes based on a transfection microarray. *Lab Chip* **8**, 1502–1506.
13. Fujita, S., Ota, E., Sasaki, C., Takano, K., Miyake, M., and Miyake, J. (2007) Highly efficient reverse transfection with siRNA in multiple wells of microtiter plates. *J. Biosci. Bioeng.* **104**, 329–333.

Chapter 14

Nonviral siRNA Delivery for Gene Silencing in Neurodegenerative Diseases

Satya Prakash, Meenakshi Malhotra, and Venkatesh Rengaswamy

Abstract

Linking genes with the underlying mechanisms of diseases is one of the biggest challenges of genomics-driven drug discovery research. Designing an inhibitor for any neurodegenerative disease that effectively halts the pathogenicity of the disease is yet to be achieved. The challenge lies in crossing the blood–brain barrier (BBB)/blood–cerebrospinal fluid barrier (BCSFB) to reach the catalytic pockets of the enzyme/protein involved in the molecular mechanism of the disease process. Designing siRNA with exquisite specificity may result in selective suppression of the disease-linked gene. Although siRNA is the most promising method, it loses its potency in downregulating the gene due to its inherent instability, off-target effects, and lack of on-target effective delivery systems. Viral as well as nonviral delivery methods have been effectively tested in vivo for silencing of molecular targets and have resulted in significant efficacy in animal models of Alzheimer's disease, amyotrophic lateral sclerosis (ALS), anxiety, depression, encephalitis, glioblastoma, Huntington's disease, neuropathic pain, and spinocerebellar ataxia. To realize the full therapeutic potential of siRNA for neurodegenerative diseases, we need to overcome many hurdles and challenges such as selecting suitable tissue-specific delivery vectors, minimizing the off-target effects, and achieving distribution in sufficient concentrations at the target tissue without any side effects. Cationic nanoparticle-mediated targeted siRNA delivery for therapeutic purposes has gained considerable clinical importance as a result of its promising efficacy.

Key words: Cationic nanoparticles, Targeted delivery, siRNA, Biotherapeutics, Gene silencing, Neurodegenerative diseases

1. Introduction

1.1. Target Selection and Efficient Therapeutic siRNA Design

The central nervous system is a sensitive physiological organization, which is highly vulnerable to any sort of minute changes that affect their molecular mechanism of regular function. The delivery of any small molecule drug or gene silencing RNA may thus have some short-term and long-term side effects. Two of

Wei-Ping Min and Thomas Ichim (eds.), *RNA Interference*, Methods in Molecular Biology, vol. 623,
DOI 10.1007/978-1-60761-588-0_14, © Springer Science+Business Media, LLC 2010

the major advantages of siRNA over small molecule drugs are that, first, sequences can be rapidly designed for highly specific inhibition of the target of interest and, second, targets can comprise any molecular class (1). However, the off-target effects of siRNA pose a major barrier for its success. Hence, it is important to design a specific and efficient siRNA sequence that will silence only the targeted gene without interfering with the functions of other genes. siRNA specificity, functionality, and efficacy are some of the major technical challenges in siRNA design. Algorithms have been designed to explore siRNAs with the highest efficacy and least amount of off-targets. Most of the available tools and algorithms are based on Tuschl's and Reynolds' rule sets along with rational design rule, followed with Basic Local Alignment Search Tool (BLAST) search to reduce the "off-target effect" for the effective siRNA design (2).

Standard or specialized algorithms can be applied to the target gene, in order to generate precise siRNA candidates that can recognize the target, either in a species-specific manner or across multiple species. BLAST analyses can be applied to assess off-target effects and specific emphasis can be placed on closely related genes. Using such analyses, highly selective siRNA sequences can be designed against a particular target for experimental evaluation (1). The various algorithms designed so far are not completely efficient as the percentage of false positives is much higher compared to true positives. Also, different design strategies used by different algorithms produce varied results for the same input sequence. Moreover, BLAST used for screening off-targets has limitations because it was not specifically designed to identify off-targets/similar target sequences for an siRNA to minimize cross-reactivity. BLAST searches often fail to detect off-target candidates as they initially look for contiguous matches that are at least seven nucleotide (7 nt) long. Also, the alternative splice variants used in datasets, such as Unigene and Refseq, lead to redundancy (see Notes 1–5).

Several empirical rule sets have been proposed to select the most specific and effective siRNA. Algorithms, based on these rule sets, apply additional rational design on siRNAs to make them more efficient and specific. To design a highly specific siRNA sequence, there are complex demands of fast and sensitive alignment algorithm for such short sequences. Apart from different rule sets, structural topology of the target site, approximate sequence matching, imperfect matches, positional effects, free energy, and thermodynamic characteristics can be taken into consideration to design an ideal siRNA. Although a number of empirical methods have been devised for the design of siRNAs, due to these limitations no algorithm gives 100% design accuracy. Hence, it is better to combine different algorithms and rule sets to make an integrated tool to scan a target gene for effective and potential siRNA sequences, as shown in Fig. 1. These sequences

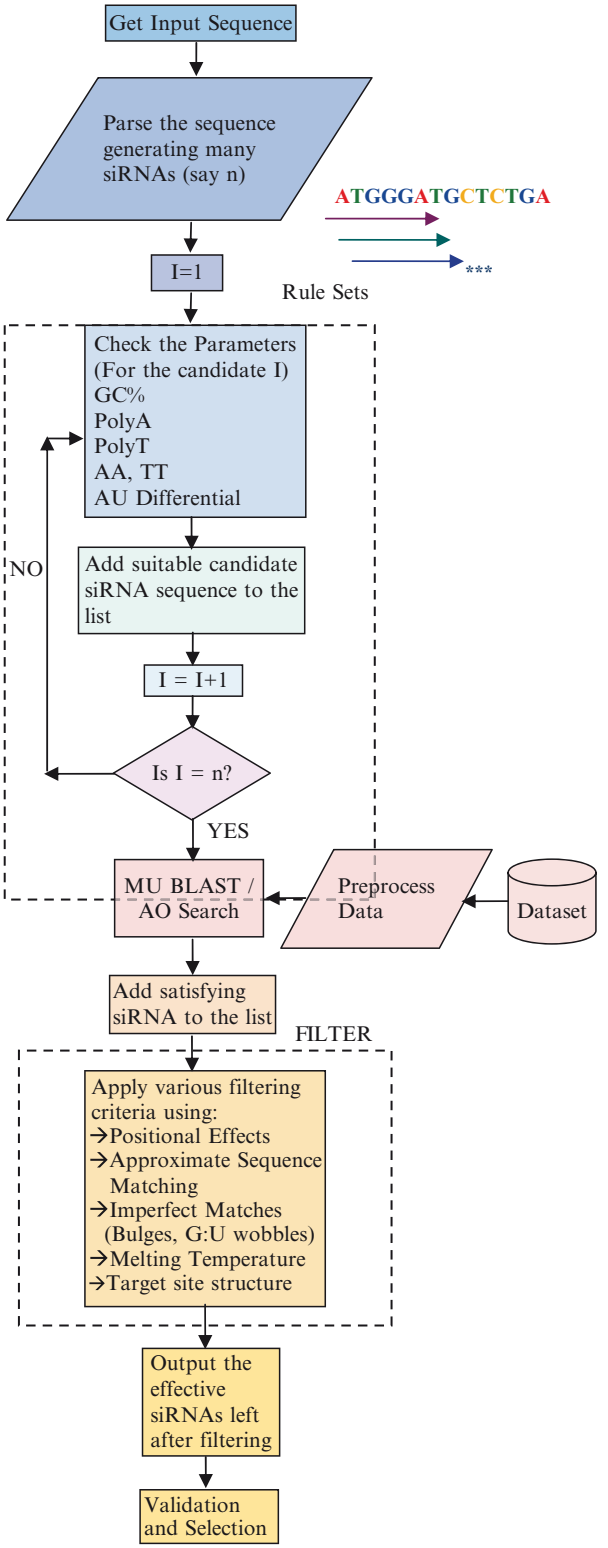

Fig. 1. Most algorithms designed for making specific and efficient siRNA with minimized/no off-target effects are not completely effective as they produce more false positives as compared to true positives. As a result, varied results are produced for the same input sequence. Hence, all the applicable factors related with the off-target activity have to be taken into the consideration for designing a better algorithm by combining the rules and checking all the responsible factors. This schematic explains the necessity and importance of each step to obtain an efficient siRNA

can be screened further to avoid cross-reactivity and maximize the silencing effect. The efficiency and performance can be validated by testing different siRNAs targeting the mouse transcriptome.

1.2. Therapeutic RNA Interference for Neurodegenerative Diseases

Neurodegenerative diseases are characterized by progressive, age-related loss of specific subsets of neural cells, which lead to diverse clinical phenotypes depending on the underlying anatomical involvement (3). The etiology of neurodegenerative diseases is most often multifactorial, likely a result of gene–environmental interaction (4). Tuschl and colleagues have demonstrated methods to manipulate the RNAi pathway in mammalian cells and refine the targets (5). Such targets have been identified for several inherited as well as sporadic neurodegenerative diseases. Altered gene expression due to mutations plays a major role in dysfunctional biological process. By modifying gene expression in vivo through siRNA-mediated gene silencing, we may restore normal function. Therapeutic targets that have been successfully inhibited with siRNA include ion channels (6), growth factors (7, 8), growth factor receptors (9, 10), neurotransmitters (11), and transcription factors (12, 13). RNA interference has been demonstrated clearly to be effective in vivo for reduction of pathological molecules in neurons, leading to significant efficacy in animal models of Alzheimer's disease, ALS, anxiety, depression, encephalitis, Huntington's disease, neuropathic pain, and spinocerebellar ataxia.

1.3. Off-Target Effects and Other siRNA-Induced Side Effects

Through siRNA it is possible to target unique areas of specific genes of interest, which are often considered nondrugable. However, as siRNAs are short sequences, they have similarities with other genes. Even a few nucleotide similarities can favor the silencing activity of unintended genes that is mediated by both the sense and antisense strands of siRNA, which can unintentionally knockdown many important genes. Different *in silico* prediction studies have shown that the probability for off-target effect in the human genome is quite significant (14). Despite our ability to rationally design effective and specific siRNAs that perfectly match the targeted mRNA, we may still find significant undesirable off-target effects. Introducing specific chemical modifications on the 5′ end of the siRNA and position-specific, sequence-independent chemical modifications have been formulated to virtually eliminate most of the off-target effects (15, 16) (see Note 6).

Interferon response is an important defense mechanism against viral infection, which can be activated by siRNA (as it exists in double-stranded RNA). This interferon response results in a signaling cascade that culminates with the activation of interferon responsive genes (IRG) and global translational repression (17). As neurons have endogenous RNA interference machinery, the brain expresses various miRNAs at different developmental stages (18).

Such pathways play a relevant role in the central nervous system. Disruption through exogenous siRNA may thus alter regular neuronal homeostasis. Introducing exogenous therapeutic siRNA constructs may deplete the resources of RNAi and saturate the endogenous RNAi machinery that is required for regular cell homeostasis.

1.4. Nonviral siRNA Delivery System

Naked siRNA delivery for therapeutic purposes is ineffective owing to the instability of siRNA, improper cellular distribution, low bioactivity, high dosage requirement of siRNA, and the necessity for continuous long-term infusion of siRNA. Yet another significant limitation with naked siRNA is its inability to cross the blood–brain barrier, and it is poorly taken up by neurons. Successful design and development of specific siRNAs as gene silencing therapeutics has been severely limited by inadequate drug delivery systems to the target sites. As of date, there have not been any reports of failure to inhibit a molecular target of interest with siRNA in vitro. However, siRNA therapeutics has been hindered by lack of efficient and safe delivery systems, variations in siRNA transfection efficiency, delivery-induced cytotoxicity, poor intracellular uptake, limited blood stability, poor intracellular compartment delivery, and off-target effects at high siRNA concentrations in vivo.

The application of siRNA as a novel therapeutic modality depends on the development of an efficient and clinically feasible means for siRNA delivery and administration. Although viral gene therapy vectors are the most efficient vectors available, concerns about their safety and immunogenicity have triggered investigations of nonviral delivery systems. Use of viral vectors in the nervous system is also known to trigger unwanted reactions, including cytotoxicity (19) and immunological complications (20). Nonviral delivery of siRNA to the nervous system has effectively normalized phenotype in animal models of pain (21), anxiety (22), depression (23), Huntington's disease (24), and encephalitis (25). Nonviral delivery of siRNA directly to the nervous system has been achieved with naked siRNAs and with siRNAs formulated with transfection reagent. The use of transfection reagents for delivery enables substantially lower doses of siRNA and potentially less frequent dosing to normalize the phenotype (24–26).

Cytotoxicity caused by transfection reagents is a major limitation, especially in the central nervous system. The challenges in vivo are to deliver a sufficient quantity of siRNA to the target tissue, and then to deliver a sufficient dose of siRNA to the intracellular compartment of the cell type of interest within the target tissue. Cationic biodegradable polymers, such as polyethyleneimine (PEI), are commonly used for siRNA transfection, providing a positively charged vehicle to carry the negatively charged

siRNA into the target cells (21). However, transfection frequency, cytotoxicity, serum stability, and active targeting are some of the major concerns related to nonviral mode of delivery. Self-assembled ligand-targeted nanoparticles made of cationic polymers, such as chitosan (27, 28), cyclodextrin polycations (29), poly-L-lysine (PLL) (30), and polyamidoamine dendrimers (31), are available to deliver the siRNA effectively and to overcome delivery limitations. These particles can be surface coated with polyethylene glycol (PEG) to eliminate phagocyte capture and nonspecific immune stimulation, which provides better stability and extended blood circulation with low toxicity (32, 33). Conjugating siRNA with cholesterol and transfection enhancers, such as penetratin1, provides substantial advantage for in vivo delivery and bioactivity of siRNA (15) (see Note 7).

2. Materials

2.1. siRNA Stock Preparation

1. 1× Phosphate Buffer Saline (PBS) solution: 8 g of NaCl, 0.2 g of KCl, 1.44 g of Na_2HPO_4 and 0.2 g of KH_2PO_4 to 800 ml of double distilled/deionized water, and adjust pH to 7.4 using HCl. Sterilize by autoclaving at 121°C for 15 min.
   OR
2. 1× 4-(2-hydroxyethyl)-1-piperazineethanesulfonic acid (HEPES) Buffer Saline solution: 10 mM HEPES, 151 mM NaCl, 4.7 mM KCl, 2 mM $CaCl_2$, 1.2 mM $MgCl_2$, and 7.8 mM glucose. Adjust the pH to 7.4 using 1 M NaOH. Sterilize by autoclaving at 121°C for 15 min.

2.2. Delivery of siRNA-Complex into Animal Model

1. Anesthetic for mice: Mix 5 ml of Ketamine (100 mg/ml), 2.5 ml of Xylazine (20 mg/ml) and 1 ml of Acepromazine (10 mg/ml). Add 1.5 ml of sterile saline to make the total volume 10 ml. Store it in dark; prepare fresh anesthetic every 2 weeks (see Note 8).
2. Restraining tube.
3. 27-gauge needle.
4. 1 ml syringe.
5. Clean gauze.

2.3. Blood Collection and Analysis

1. Microtainer® serum separator tubes (Becton, Dickinson).
2. Hitachi 911 automated Clinical Chemistry Blood analyzer machine (Roche Diagnostics).
3. Restraining tube.
4. 100% ethyl alcohol (anhydrous absolute alcohol).

5. Petroleum jelly (Vaseline).
6. 25-gauge and 23-gauge needles.
7. 3 ml and 1 ml syringes
8. Sterile razor
9. Clean gauze
10. 1.5 ml Eppendorf tubes

2.4. RNA Extraction from Tissue

1. Chloroform (without isoamyl alcohol), Diethylpyrocarbonate (DEPC) (Sigma).
2. 0.1% DEPC-treated water solution: add 1 ml of DEPC into 1,000 ml of water. Shake vigorously and let stand at room temperature for an hour, autoclave and let cool prior to use (see Note 9).
3. 4% paraformaldehyde (w/v) solution in PBS.
4. MiRNeasy Easy mini kit, RNeasy MinElute Kit (Qiagen).
5. RNAse-free Eppendorf tubes, RNase-free Buffer TE – pH8.0, RNAlater®, RNAseZAP® (RNase decontamination solution) (Ambion).
6. Homogenizer (PowerGen Model 125 Homogenizer) (Fisher).
7. Nanodrop Spectrophotometer (Fisher).
8. Agilent Bioanalyzer and Eukaryote total RNA nano chip setup.
9. TRIzol® Reagent, Glycogen (Invitrogen).
10. 70% Ethanol.
11. Mortar and pestle.
12. Spatulas.
13. Forceps.
14. Filter tips.
15. 50 ml polypropylene tubes.
16. Razor blades (Fisher).

2.5. Protein Extraction from Tissues

1. Radio Immuno Precipitation Assay (RIPA-Lysis) buffer (50 ml) is supplied in four vials of each 1× lysis buffer, phenylmethylsulfonyl fluoride (PMSF), protease inhibitor cocktail, and sodium orthovanadate (Santa-Cruz Biotechnology). As per the manufacturer's protocol, combine 10 µl of PMSF solution, 10 µl sodium orthovanadate solution, and 10–20 µl of protease inhibitor cocktail solution per ml of the 1× RIPA lysis buffer.
2. 1.7 ml Eppendorf/microcentrifuge tubes.

3. 50 ml polypropylene tubes.
4. Razor blades (Fisher).
5. PowerGen Model 125 Homogenizer (Fisher).

3. Methods

The specific siRNA can be designed based on the target. Various design algorithms filter ineffective candidates, and the resulting minimal set of siRNA may not meddle with any unintended gene target. The largest gene knockdown experiments performed to date have used multiple siRNAs that became very cumbersome, and the side effects based on off-target cannot be predicted easily. Major algorithms and tools have been devised, which not only discuss the effective sequence-specific design of siRNA but also the efficacy and performance of the sequence in terms of specificity and cross-reactivity. In order to minimize the unwanted side effects of siRNAs, the criteria used to design siRNAs must be more rigorously examined (see Notes 1–6).

3.1. siRNA Stock Preparation

1. The siRNA is received in a lyophilized powdered form and should be stored at –20°C or –70°C as received.
2. Prior to use, defrost the siRNA and weigh out the required amount to prepare a stock solution as per the required concentration. To prepare a stock solution, siRNA can be dissolved in standard buffers like PBS, HEPES, etc.
3. Prior to measuring the siRNA concentration, blank the UV spectrophotometer with a diluent (PBS, HEPES, etc.) and then read the siRNA absorbance at UV A260, to calculate the concentration of siRNA.
4. For example, to make up the volume to 1 mL, add 50 µL of resuspended siRNA to 950 µL of deionized or double distilled water. In this case, the dilution factor would be 1,000/50 = 20. Vortex or pipette up and down the diluted siRNA for 15 min and then take the absorbance at UV A260 (see Note 10).
5. The lyophilized siRNA is received with a detailed description stating its NCBI gene symbol, amount, form, purity, extinction coefficient, etc. and this is helpful in determining and calculating the concentration of siRNA (see Note 11).
6. The extinction coefficient mentions weight per OD of the siRNA in µg/Od units that is used to calculate the concentration in mg/ml, µg/ml, or µM.

7. Calculate the concentration of siRNA as: Concentration (μg/mL) = UV Reading (A260) × weight per OD (μg/Odu) × dilution factor (20 as per the above example).

3.2. Cationic Nanoparticle-Mediated siRNA Delivery

Scrambled siRNA can be used as a control during the in vivo experiments. It has the exact, but rearranged, sequence as the experimental siRNA. It can be considered as a negative control. Rearranged sequence does not interfere with any gene. However, sometimes (due to some reason) it might not work in the way it is expected. Control siRNAs need not be based on the experimental siRNAs. Any sequence that does not have homology to any genomic sequence will serve the purpose, provided the sequence has similar composition, size, and modification as the experimental siRNA. It is preferable to have 3' portion of siRNA completely scrambled as this end is important in target recognition.

1. Optimal conditions for reproducible transfection of cationic nanoparticle-mediated siRNA should be determined. The optimal conditions should ideally yield maximum transfection and minimum cytotoxicity.
2. Proper characterization and optimization of siRNA-loaded cationic nanoparticles should be performed to achieve efficient transfection in vitro.
3. The transfection efficiency depends on cell type and cell density (number of cells seeded per well) for in vitro studies.
4. Determine the optimal ratio of siRNA and cationic polymer (Chitosan/polyethylenimine(PEI)/cyclodextrin/poly-l-Lysine (PLL)/polyamidoamine dendrimers) used for transfection by testing different siRNA:Cationic polymer weight ratios on cell lines (see Note 12).
5. Determine size and surface charge of the formed nanoparticles of different weight ratios using a Particle sizer and zeta potential machine, respectively. For delivering cationic nanoparticles to the brain, it is required that the nanoparticles be <100 nm in size, have a neutral surface charge (zeta potential), and should be hydrophilic in nature. Hydrophilicity of cationic nanoparticles can be improved by surface coating them with hydrophilic molecules like PEG or surfactants like Polysorbate 80.
6. The siRNA loading efficiency can be analyzed via gel electrophoresis (qualitative) or by UV spectrophotometer (quantitatively) by ultracentrifuging the nanoparticles and determining the percentage of unbound siRNA in the supernatant of the ultra-centrifuged sample.

7. Serum stability of cationic nanoparticles carrying siRNA should also be analyzed to determine the half-life of the nanoparticles. In vitro determination of serum stability is important as it determines the potency of nanoparticles to deliver siRNA safely to the targeted site when administered intravenously.
8. The siRNA–nano complex can be made more target-specific by functionalizing them with target proteins (antibodies) or peptides, such as Arginine-Glycine-Aspartic acid (RGD) (34), rabies virus glycoprotein (RVG) (35), or Transferrin (36), which enhance transfection efficiency. Other ligands, such as aptamers and sugars (mannose, galactose), have been used to target siRNAs in vivo.

3.3. Delivery of siRNA–Nanocomplex into Animal Model

The systemic route is the most preferred, noninvasive route of administration for RNAi. However, successful systemic delivery can mostly be achieved if the target tissue be is liver. Therefore, the need for an efficient target tissue-specific siRNA delivery vehicle is evident. Liposomes have been widely used for in vivo RNAi applications but have not been very successful in targeting the brain. The nonviral approaches using polycationic polymers, like polyethyleneimine (PEI), have shown some success in vivo, but are extremely toxic (37). Other polymers that have been successfully used to deliver siRNA in vivo include Chitosan, Cyclodextrin, and poly(lactide-co-glycolide) PLGA (38). The most widely used technique for CNS delivery has been Intracerebroventricular Injection (ICVI)/Intrathecal (ITh) (6, 21, 23), wherein the medication is placed directly into the cerebrospinal fluid and surrounds the spinal cord. This method avoids the blood–brain barrier; although invasive, it requires a lower dosage when compared to intravenous delivery and it is more target-specific. The following protocol explains the intravenous mode of administration in mice.

1. The animal handling procedure should be in accordance with the approved animal use protocol (see Note 13).
2. Weigh the animals prior to injection and maintain their bodyweight record over the course of the complete animal trial experiment.
3. Sedate the animals mildly by injecting an anesthetic, Acepromazine (3 µl of the total stock prepared) into the outer side of their lower flank.
4. Prior to injection in the tail vein, warm up the vein to ~37°C by using a water bath or a heating lamp to dilate and better visualize the vein (see Note 14).
5. Place the animal in an approved restrainer that restrains the mouse yet gives access to its tail vein.

6. Disinfect the site of injection and slightly rotate the tail to better visualize the vein; insert the needle at a slight angle (see Note 15).
7. Inject at a rate of ~20 µl/s using a 27-gauge needle for mice, and constantly watch for clearing of the blood (see Note 16).
8. If resistance is encountered with a slight bulge in the tail vein, then the needle can be removed slowly and the process can be repeated proximal to the previous site.
9. After removing the needle, hold the site with clean gauze for approximately 30–45 s to stop the bleeding.

3.4. Blood Collection and Analysis

The following protocol collects blood through the sephanous vein, does not require anesthesia, and yields 150 µl of blood per mouse. Through this method, blood can be drawn every 3 weeks as per the Canadian Council on Animal Care (CCAC) guidelines. Many siRNA–nano complexes are expected to be cleared from the body via the liver where they may cause hepatotoxicity. Therefore, it is recommended to perform blood analysis for liver function test, which can be assessed using various enzymes such as albumin, alanine transaminase (ALT), aspartate transaminase (AST), alkaline phosphatase (ALP), and total bilirubin (TBIL), wherein ALT is more indicative of liver cell damage than AST. Levels of AST to ALT in blood (when compared to each other) are more indicative of the intensity of liver damage. It is expected to have increased levels of these enzymes, but it should be below tenfold at the highest dose of siRNA administered in mg/kg of the animal (mice).

1. Prior to blood collection, it is advised to warm up the animals by keeping a lamp over the animal cage for about 5 min.
2. Place the mouse in a restraining tube so that its head is covered and its hind legs are free.
3. Extend the hind leg by grasping the fold of the skin between the tail and thigh.
4. Remove hair from the outer area of lower hind leg with the help of a sharp razor.
5. Apply petroleum jelly on the shaved surface to ease blood collection.
6. Puncture the vein perpendicularly with a 25-gauge needle, and collect drops of blood in a Microtainer® serum separator collection tubes.
7. Apply pressure for approximately 30 s with the help of clean gauze to stop the bleeding.
8. The Microtainer® serum separator collection tubes containing blood are kept at room temperature for about 30 min, then centrifuged at 4°C for 20 min at 1,800×*g*.

9. The serum separates from the clot and is kept at −80°C in Eppendorf tubes.
10. Prior to analyzing serum in the blood analyzer machine (Hitachi 911), thaw the samples, again centrifuge at 1,800×*g* for 10 min, and pipette out 200 µl of each in the sample cups that are to be placed in the blood analyzer machine (see Note 17).
11. Completely anesthetize the animal and withdraw the blood by cardiac puncture using a 23-gauge needle in a 3-ml syringe.
12. Euthanize the animal at the end of the experiment.
13. Transfer the cardiac blood into serum separator tubes and allow it to clot prior to placement on ice.

3.5. RNA Extraction from Tissue

3.5.1. Tissue Harvesting

1. Remove the whole brain including the cerebellum and brainstem. Divide the cerebral hemispheres in two halves by cutting through the midline.
2. Fix half of the brain in cold 4% paraformaldehyde. It can be stored for several weeks.
3. From the other half of the brain, remove the brainstem and cerebellum by sectioning through the cerebral peduncles.
4. The dissection and sectioning should be done as quickly as possible on a parafilm overlying on a Petri dish filled with ice or on a freezing aluminium tray (aluminium foil over a block of dry ice, or aluminium foil over a stainless steel tray with pellets of dry ice).
5. Sectioned tissues are immediately stored in 15 ml polypropylene tubes, prelabelled and prechilled on dry ice containing 1.5 ml of RNAlater®, or they can be immediately snap-frozen in liquid nitrogen and then placed in −80°C freezer (see Note 18).

3.5.2. Tissue Homogenization, RNA Extraction, and Purification

1. Clean the homogenizer probe by running it at a maximum speed for 30 s in probe wash 50 ml polypropylene tubes sequentially containing RNAseZAP®, DEPC water, 100% Ethanol and, finally again, in DEPC water.
2. Prior to starting the experiment, prepare all the working solutions of buffer-like RPE (supplied as a concentrate along with Qiagen RNeasy Mini Kit) by adding 100% ethanol, as mentioned on the bottle.
3. Take the tissue samples from −80°C freezer and allow them to thaw, blot the excess RNAlater® from the tissue.
4. Place the tissue into a liquid N_2-cooled mortar and, using a sterile blade, cut it into small pieces and weigh the tissue.
5. Using a spatula put the tissue into the 50 ml sterile polypropylene tube containing TRIzol®.

6. Homogenize the sample for 90 s to 2 min at full speed (see Note 19).
7. Let the samples stand for 5 min at room temperature and allow cellular debris and foam to settle down (see Note 20).
8. Centrifuge the homogenate at 10,000×*g* for 15 min at 4°C and transfer 1 ml of the supernatant to fresh 1.7 ml RNAse-free Eppendorf tubes (see Note 21).
9. To each 1 ml aliquot of TRIzol® supernatant, add 1 µl of Glycogen (20 µg/µl stock).
10. Add 250 µl of chloroform and shake vigorously (see Note 22).
11. Let it stand for 10 min and again centrifuge at 10,000×*g* for 20 min at 4°C (see Note 23).
12. Transfer the top aqueous layer to fresh 1.7 ml RNAse-free Eppendorf tubes.
13. Add an equal volume of 70% ethanol to each tube, mix well by vortexing (see Note 24).
14. Pipette out 700 µl of the sample onto RNeasy Mini column including any precipitate that has formed and centrifuge at 10,000×*g* for 15–30 s (see Note 25).
15. Repeat step 13 to process all the samples you may have.
16. Remove the RNeasy Mini Column from the collection tube and put it aside. This spin column contains the total RNA.
17. With the flow through of the collection tube, add 450 µl of 100% ethanol and mix it by vortexing.
18. Add 700 µl of the above sample onto the RNeasy MinElute Column and again centrifuge at 10,000×*g* for 15–30 s.
19. Repeat step 17 until all samples have been processed.
20. Add 700 µl of buffer RWT (provided along with the RNeasy MinElute Kit) to the RNeasy MinElute spin column and again centrifuge at 10,000×*g* for 15–30 s.
21. Add 500 µl of buffer RPE (provided along with the RNeasy MinElute Kit) and centrifuge at 10,000×*g* for 15–30 s.
22. Add 500 µl of 80% ethanol and centrifuge at 10,000×*g* for 2 min.
23. Replace the RNeasy MinElute Column in a fresh collection tube and centrifuge again at 10,000×*g* for 5 min in order to dry the column.
24. Replace the RNeasy spin column into 1.5 ml Eppendorf tube, add 14 µl of RNAse-free water, and centrifuge it at 10,000×*g* for 1 min.
25. Combine all the samples from multiple columns and place them on ice. These samples have eluted and purified miRNA.

26. Obtain the RNeasy Mini Column from step 15 containing total RNA, place it in a fresh 2 ml collection tube and add 700 µl of buffer RWT.
27. Centrifuge at 10,000×*g* for 15–30 s.
28. Add 500 µl of buffer RPE and repeat step 26.
29. Place the RNeasy Mini Column in a fresh collection tube and centrifuge at 10,000×*g* for 2 min.
30. Place RNeasy Mini Column onto a fresh 1.5 ml Eppendorf tube, add 30 µl of RNAse-free water onto the column, and centrifuge at 10,000×*g* for 1 min.
31. Combine all samples from different multiple columns and keep on ice. These samples have eluted and purified total RNA.
32. Dilute 1 µl of the purified RNA in 19 µl of buffer TE (pH8.0) and make a 1:20 dilution.
33. Use the diluted RNA and quantify the miRNA and total RNA by taking the OD reading at OD230, OD260, and OD280 using Nano-drop spectrophotometer.
34. Agilent Bioanalyzer 2100 can be used to analyze the quality of the RNA.
35. mRNA Purification from total RNA can be performed using Oligotex mRNA purification kit from Qiagen.
36. In order to quantitate the amount of reduction in mRNA level, RT QPCR is recommended to analyze the expression as compared to control.

3.6. Protein Extraction from Tissues

1. Weigh tissue and dice into very small pieces using a clean razor blade. Frozen tissue should be sliced very thinly and thawed in RIPA buffer containing protease inhibitors, phosphatase inhibitors, and PMSF. Use 3 ml of ice-cold RIPA buffer per gram of tissue.
2. Further disrupt and homogenize tissue with a homogenizer or a sonicator, maintaining temperature at 4°C throughout all procedures. Incubate on ice for 30 min.
3. Transfer to microcentrifuge tubes, centrifuge at 10,000×*g* for 10 min at 4°C. Remove supernatant and centrifuge again. The supernatant fluid is the total cell lysate containing protein. A longer centrifugation may be necessary to obtain a clear lysate.
4. BIO-RAD protein assay can be performed by following the manufacturer's protocol to quantify the protein concentration.
5. SDS-PAGE should be performed for the protein obtained, followed by semi-dry blotting of the proteins onto the nitrocellulose membrane.

6. Use appropriate primary antibodies followed by an HRP-conjugated secondary antibodies for Chemiluminescence Western blot analysis using high quantum efficiency CCD camera.

4. Notes

1. siRNAs with 18–21 nucleotides have an effective silencing activity with low or no off-target cross-reactivity. Computational siRNA design provides revolutionary new capabilities, facilitating improvements in RNAi potency and specificity.
2. The efficient candidates of siRNA can be screened from the library using set cover optimization and further refinement can be done based on Reynolds's rule set, which helps to avoid any unintended gene targeting. Greedy algorithm can be used for determining the number of counts of siRNA against the potential variant targets to ensure the effective sequence-specific design of siRNA in terms of specificity and cross-reactivity. The off-targets can be further eliminated using AOSearch since BLAST has its own limitations.
3. siRNA information has to be combined with other factors to assist in effective target progression. Hence, keeping in mind the need to optimize the design of an efficient filtering algorithm for off-targets, a filter can be designed including such factors as approximate sequence matching, thermodynamic profile, G-U wobbles, bulges, positional effects, and free energy considerations.
4. After preprocessing the dataset through a suitable filter program, Khvorova's approach can be incorporated to mitigate off-target events and enhance specificity; for example, pooling functional siRNAs into a single potent reagent by exploiting sequence variations in a systematic way to provide a more varied pool of potential off-target candidates.
5. Apriori algorithm can be used to mine the pertinent features that serve as inputs for the support vector machine (SVM), where siRNA sequences represent vectors in a multidimensional feature space. They are subsequently classified with SVM into effective or ineffective siRNAs.
6. Genes that contain significant similarities with the siRNA should be monitored to verify that they are not being silenced. Sequences that provide better efficacy in screening experiments might cause unexpected toxicity in vivo.
7. Compared to naked siRNA and cationic lipids, these biodegradable nanopolyplexes display greater transfection efficiency and less toxicity in different cell lines. However, the transfection

efficiency varied based on cell types and density, type of nanopolyplexes, length of exposure of cells to polyplex–siRNA complexes, and the size and concentration of siRNAs.

8. Always remember to tap the bubbles out while loading the sample, anesthesia, or saline into the syringe.
9. DEPC is a carcinogen; therefore, care should be taken while handling it. Wear gloves and it should be opened only in the fume hood.
10. The diluted siRNA should be stored at 2–8°C for 3 days. It is always recommended to prepare fresh siRNA stock solution as per the study.
11. It is recommended to reserve a small sample of resuspended siRNA after each manipulation as a backup to meet any unexpected fault.
12. The siRNA:Cationic complexes should be prepared in serum-free and antibiotic-free media, as the negatively charged proteins in serum may compete with siRNA to bind to cationic polymer and antibiotic, which may cause unwanted toxicity if it goes inside the cell during transfection.
13. Animal handling training by the local facility should be important before carrying out animal trials.
14. A tail veiner can be bought from Braintree Scientific. This facilitates better visualization of the tail vein and thus guarantees success of injection.
15. The needle should be inserted just enough to get a bevel inserted into the tail vein. Care should be taken to keep the needle as parallel as possible to the tail.
16. With intravenous mode of delivery, do not inject more than 10% of the animal's body weight.
17. Avoid multiple freeze-thaw cycles, and also avoid hemolyzed or lipemic sera for the analysis. If required, user may filter out the centrifuged serum to avoid any clogging of the probe of blood analyzer machine.
18. Samples must be stored for a minimum of 12 h in RNAlater® at 4°C before the samples are processed. RNAlater® protects the tissue from RNAse activity.
19. During the RNA extraction process of brain, it is advisable to increase the amount of TRIzol® in general, as brain is rich in lipid content that creates lot of foam. For 50–100 mg of tissue use 1 ml of TRIzol®, for 100–150 mg of tissue use 1–2 ml of TRIzol®, and for 150–300 mg of tissue use 2–4 ml of TRIzol®.
20. If cellular debris do not accumulate, or TRIzol® does not turn muddy brown and instead stays pink in color, then skip steps 7 and 8.

21. After centrifuging, carefully observe the presence of any fatty/oily layer. If present over the supernatant, carefully pipette out the fatty layer before transferring the supernatant to fresh Eppendorf tubes.
22. Vigorous shaking is crucial as this step determines the RNA yield.
23. At this step, the sample separates into three phases: an upper colorless, aqueous phase containing RNA; a white opaque interphase containing denatured proteins and DNA; and a lower red, organic phase containing DNA and proteins. As the brain tissues are rich in fat, a clear phase may be visible below the red, organic phase.
24. Precipitates might form at this step after the addition of isopropanol; mix the precipitates well through pipetting or vigorous shaking.
25. For RNA concentration <45 µg, use Qiagen MinElute column; for >45 µg, use Qiagen RNEasy Mini Column.

Acknowledgments

We gratefully acknowledge the research grant received from Canadian Institute of Health Research (CIHR) to Dr. S. Prakash. We also acknowledge support of McGill Faculty of Medicine Internal Scholarship to M. Malhotra.

References

1. Sah, W. Y. (2006) Therapeutic potential of RNA interference for neurological disorders. *Life Sci.* **79**, 1773–1780.
2. Behlke, M. A. (2006) Progress towards *in-vivo* use of siRNAs. *Mol. Ther.* **13**, 644–670.
3. Gonzalez-Alegre, P. (2007) Therapeutic RNA interference for neurodegenerative diseases: from promise to progress. *Pharmacol. Ther.* **114**, 34–55.
4. Brown, R. C., Lockwood, A. H., and Sonawane, B. R. (2005) Neurodegenerative diseases: an overview of environmental risk factors. *Environ. Health Perspect.* **113**, 1250–1256.
5. Elbashir, S. M., Harborth, J., Lendeckel,W., Yalcin, A.,Weber, K., and Tuschl, T. (2001) Duplexes of 21-nucleotide RNA mediate RNA interference in cultured mammalian cells. *Nature* **411**, 494–498.
6. Dorn, G., Patel, S., Wotherspoon, G., Hemmings-Mieszczak, M., Barclay, J., Natt, F. J., et al. (2004) siRNA relieves chronic neuropathic pain. *Nucleic Acids Res.* **32**, e49.
7. Guan, H., Zhou, Z., Wang, H., Jia, S.F., Liu, W., and Kleinerman, E. S. (2005) A small interfering RNA targeting vascular endothelial growth factor inhibits Ewing's sarcoma growth in a xenograft mouse model. *Clin. Cancer Res.* **11**, 2662–2669.
8. Takei, Y., Kadomatsu, K., Yuzawa, Y., Matsuo, S., and Muramatsu, T. (2004) A small interfering RNA targeting vascular endothelial growth factor as cancer therapeutics. *Cancer Res.* **64**, 3365–3370.
9. Shen, J., Samul, R., Silva, R. L., Akiyama, H., Liu, H., Saishin, Y., et al. (2006) Suppression of ocular neovascularization with siRNA targeting VEGF receptor 1. *Gene Ther.* **13**, 225–234.
10. Zhang, Y., Zhang, Y. F., Bryant, J., Charles, A., Boado, R. J., and Pardridge, W. M. (2004) Intravenous RNA interference gene therapy

targeting the human epidermal growth factor receptor prolongs survival in intracranial brain cancer. *Clin. Cancer Res.* **10**, 3667–3677.

11. Luo, M., Ge, P., Hadwiger, P., Meyers, R., Sah, D. W. Y., Porreca, F., and Lai, J. (2005) RNAi of neuropeptide Y (NPY) for neuropathic pain. *Soc Neurosci Abstr.*
12. Bhoumik, A., Huang, T. G., Ivanov, V., Gangi, L., Qiao, R. F., Woo, S. L., Chen, S. H., and Ronai, Z. (2002) An ATF2-derived peptide sensitizes melanomas to apoptosis and inhibits their growth and metastasis. *J. Clin. Invest.* **110**, 643–650.
13. Gaudilliere, B., Shi, Y., and Bonni, A. (2002) RNA interference reveals a requirement for MEF2A in activity-dependent neuronal survival. *J. Biol. Chem.* **277**, 46442–46446.
14. Qiu, S., Adema, C. M., and Lane, T. (2005) A computational study of off-target effects of RNA interference. *Nucleic Acids Res.* **33**, 1834–1847.
15. Soutschek, J., Akinc, A., Bramlage, B., Charisse, K., Constien, R., Donoghue, M., et al. (2004) Therapeutic silencing of an endogenous gene by systemic administration of modified siRNAs. *Nature* **432**, 173–178.
16. Song, E., Lee, S. K., Wang, J., Ince, N., Ouyang, N., Min, J., et al. (2003) RNA interference targeting Fas protects mice from fulminant hepatitis. *Nat. Med.* **9**, 347–351.
17. Stark, G. R., Kerr, I. M., Williams, B. R., Silverman, R. H., and Schreiber, R. D. (1998) How cells respond to interferons. *Annu. Rev. Biochem.* **67**, 227–264.
18. Wheeler, G., Ntounia-Fousara, S., Granda, B., Rathjen, T., and Dalmay, T. (2006) Identification of new central nervous system specific mouse microRNA. *FEBS Lett.* **580**, 2195–2200.
19. Davis, M. E., Pun, S. H., Bellocq, N. C., Reineke, T. M., Popielarski, S. R., Mishra, S. Heidel, J. D. (2004) Self-assembling nucleic acid delivery vehicles via linear, water-soluble, cyclodextrin containing polymers. *Curr. Med. Chem.* **11**, 179–197.
20. Lu, P. Y., Xie, F. and Woodle, M. C. (2005) In vivo application of RNA interference: from functional genomics to therapeutics. *Adv. Genet.* **54**, 117–42.
21. Tan, P. H., Yang, L. C., Shih, H. C., Lan, K. C., and Cheng, J. T. (2005) Gene knockdown with intrathecal siRNA of NMDA receptor NR2B subunit reduces formalin-induced nociception in the rat. *Gene Ther.* **12**, 59–66.
22. Thakker, D. R., Hoyer, D., and Cryan, J. F. (2006) Interfering with the brain: use of RNA interference for understanding the pathophysiology of psychiatric and neurological disorders. *Pharmacol. Ther.* **109**, 413–438.
23. Thakker, D. R., Natt, F., Husken, D., van der Putten, H., Maier, R., Hoyer, D., and Cryan, J. F. (2005) siRNA-mediated knockdown of the serotonin transporter in the adult mouse brain. *Mol. Psychiatry* **10**, 782–789
24. Wang, Y. L., Liu, W., Wada, E., Murata, M., Wada, K., and Kanazawa, I. (2005) Clinicopathological rescue of a model mouse of Huntington's disease by siRNA. *Neurosci. Res.* **53**, 241–249.
25. Kumar, P., Lee, S. K., Shankar, P., and Manjunath, N. (2006) A single siRNA suppresses fatal encephalitis induced by two different flaviviruses. *PLoS Med.* **3**, e96.
26. Hassani, Z., Lemkine, G. F., Erbacher, P., Palmier, K., Alfama, G., Behr, C., and Demeneix, J.-P. (2005) Lipid-mediated siRNA delivery down-regulates exogenous gene expression in the mouse brain at picomolar levels. *J. Gene Med.* **7**, 198–207.
27. Katas, H., and Alpar, H.O. (2006) Development and characterisation of chitosan nanoparticles for siRNA delivery. *Mol. Ther.* **115**, 216–225.
28. Howard, K. A., Rahbek, U. L., Liu, X., Damgaard, C. K., Glud, S. Z., Andersen, M. Ø., et al. (2006) RNA interference *in-vitro* and *in-vivo* using a novel chitosan/siRNA nanoparticle system. *Mol. Ther.* **14**, 476–484.
29. Bartlett, D. W., Su, H., Hildebrandt, I. J., Weber, W. A., and Davis, M. E. (2007) Impact of tumor-specific targeting on the biodistribution and efficacy of siRNA nanoparticles measured by multimodality *in-vivo* imaging. *Proc. Natl. Acad. Sci. U.S.A.* **104**, 5549–5554.
30. Inoue, Y., Kurihara, R., Tsuchida, A., Hasegawa, M., Nagashima, T., Mori, T., et al. (2008) Efficient delivery of siRNA using dendritic poly(l-lysine) for loss-of-function analysis. *J. Control. Release* **126**, 59–66.
31. Patil, M. L., Zhang, M., Betigeri, S., Taratula, O., He, H., and Minko, T. (2008) Surface-modified and internally cationic polyamidoamine dendrimers for efficient siRNA delivery. *Bioconjug. Chem.* **19**, 1396–1403.
32. Park, Y., Kwok, K. Y., Boukarim, C., and Rice, K. G. (2002) Synthesis of sulfhydryl cross-linking poly(ethylene glycol)-peptides and glycopeptides as carriers for gene delivery. *Bioconjug. Chem.* **13**, 232–239.
33. Oupicky, D., Ogris, M., Howard, K. A. Dash, P. R., Ulbrich, K., and Seymour L. W. (2002) Importance of lateral and steric stabilization of polyelectrolyte gene delivery vectors for extended systemic circulation. *Mol. Ther.* **5**, 463–472.

34. Sun, Y. X., Zeng, X., Meng, Q. F., Zhang, X. Z., Cheng, S. X., and Zhuo, R. X. (2008) The influence of RGD addition on the gene transfer characteristics of disulfide-containing polyethyleneimine/DNA complexes. *Biomaterials* **29**, 4356–4365.
35. Kumar, P., Wu, H., McBride, J. L., Jung, K. E., Kim, M. H., Davidson, B.L., et al. (2007) Transvascular delivery of small interfering RNA to the central nervous system. *Nature* **448**, 39–43.
36. Pang, Z., Lu, W., Gao, H., Hu, K., Chen, J., Zhang, C., et al. (2008) Preparation and brain delivery property of biodegradable polymersomes conjugated with OX26. *J. Control. Release* **128**, 120–127.
37. Urban-Klein, B., Werth, S., Abuharbeid, S., Czubayko, F., Aigner, A. (2005) RNA-mediated gene-targeting through systemic application of polyethyleneimine (PEI)-complexes siRNA *in-vivo*. *Gene Ther.* **12**, 461–466.
38. Murata, N., Takashima, Y., Toyoshima, K., Yamamoto, M., and Okada, H. (2008) Antitumor effects of anti-VEGF siRNA encapsulated with PLGA microspheres in mice. *J. Control. Release* **126**, 246–254.

Chapter 15

Using siRNA to Uncover Novel Oncogenic Signaling Pathways

Jin-Mei Lai, Chi-Ying F. Huang, and Chang-Han Chen

Abstract

Tumor invasion and metastasis are the primary causes of cancer patient mortality, underscoring the need for identification of novel genes and signaling pathways that mediate these prognosis-determining phenomena. To identify and characterize novel lung adenocarcinoma genes associated with lung cancer progression, we created a bioinformatics-based approach that focuses on human cell-cycle-regulated genes that have evolved only in higher organisms but not in lower eukaryotic cells. In siRNA experiments in lung cancer cells, FLJ10540 was identified as one of several novel targets involved in cell migration and invasion. Here, we demonstrate that PI3K inhibition affects FLJ10540-mediated cell migration and invasion and further, that FLJ10540 knockdown ablates AKT-Ser^{473} phosphorylation. Taken together, these findings indicate that the FLJ10540/PI3K/AKT pathway may harbor new therapeutic targets for treating invasive lung adenocarcinoma.

Key words: FLJ10540, Migration, Invasion, PI3K/ AKT, VEGF-A

1. Introduction

With most cancer types, it is not the initial growth of tumor cells, but rather their ability to invade and metastasize to other tissues, that makes them life threatening. Tumor invasion and metastasis are increasingly recognized as complexly orchestrated pathological processes, with many genes and signaling pathways being aberrantly regulated in these events (1). For example, upregulation of epithelial-mesenchymal-transition (EMT)-associated genes enables tumor cells to detach and migrate away from primary tumor sites and increased expression of metalloproteinases is critical for tumor cell invasion. Overexpression and hyperactivation of PI3K/AKT have been detected in a wide range of human tumor types, are often linked with poor prognosis (2), and may

Wei-Ping Min and Thomas Ichim (eds.), *RNA Interference*, Methods in Molecular Biology, vol. 623,
DOI 10.1007/978-1-60761-588-0_15, © Springer Science+Business Media, LLC 2010

play a significant role in migration and invasion of several cancer cell types, including those of the lung (3).

Where more traditional methods have faltered, rapid advances in microarray technology have allowed for identification of numerous genes important to human cancer research. One of the enduring challenges to cancer-related microarray profiling, however, is sorting out how novel gene targets should be prioritized for further interrogation. Here, we use the poorly characterized cell-cycle-regulated FLJ10540 (or CEP55) gene, which is upregulated in human lung cancer microarray datasets (4), to demonstrate the efficacy of a bioinformatics-based approach in successful identification of novel targets crucial to cancer research (5). We next validate gene expression data using Q-RT-PCR and characterize FLJ10540 in a series of biochemical analyses. The results of these functional tests indicate that FLJ10540 expression results in a number of consequences common to oncogene activation, including anchorage-independent growth, enhanced cell growth at low serum levels, and induction of tumorigenesis in nude mice (6). Our findings demonstrate that microarray analysis used in combination with siRNA and other biochemical technologies can be used to rapidly identify and characterize novel cancer-related genes and signaling pathways.

2. Materials

2.1. Cell Culture and Reagents for MTT Assay

1. $CL_{1\text{-}0}$, A549, and H1299 cells are grown in Roswell Park Memorial Institute-1640 (RPMI-1640) (Invitrogen, Grand Island, NY) medium; all media are supplemented with 10% heat-inactivated fetal bovine serum (FBS) (Invitrogen), 100 unit/mL penicillin, and streptomycin (Invitrogen).
2. Solution of 10× trypsin-EDTA (Invitrogen).
3. 1 mg/mL solutions of vascular endothelial growth factor A (VEGF-A) (R&D systems, Minneapolis, MN) are prepared in dimethyl sulfoxide (DMSO) (Sigma, St. Louis, MO) and stored in single-use aliquots at −80°C. The working concentration of VEGF-A is 20 ng/ mL, prepared by dilution in 100 mg/mL BSA.
4. 100 mM solutions of p38 MAP kinase (SB202190, Sigma), MEK (PD98059, Sigma), and PI3K (LY294002, Sigma) inhibitors are prepared in DMSO, stored in aliquots at −80°C, and added to cell culture dishes as required. The working concentration of each inhibitor are SB202190 (20 μM), PD98059 (10 μM), and LY294002 (10 μM).
5. Cell lysis buffer: 20 mM 1,4-Piperazinediethanesulfonic acid (PIPES, Sigma); pH 7.2; 1 mM ethylenediaminetetraacetic

acid(EDTA,Sigma);10%sucrose;0.1%3-[(3-Cholamidopropyl) Dimethyl-Ammonio]-1-Propanesulfonate (CHAPS, Sigma); 100 mM sodium chloride (NaCl, Sigma); 1 mM dithiothreitol (DTT, Sigma); protease inhibitors (1 μg/mL Aprotinin, 1 μg/mL leupeptin, and 1 μg/mL pepstatin, Sigma; added before using); 1 mM phenylmethylsulfonyl fluorid (PMSF, Sigma; added before using); and 1 mM Sodium Vanadate (Na_3VO_4, Sigma; added before using). Aliquots are stored at –20°C.

6. Sample loading buffer (Laemmli loading dye) (3×): 240 mM Tris–HCl, pH 6.8; 6% sodium dodecyl sulfate (SDS, Sigma); 33% (w/v) glycerol (Sigma), 0.06% (w/v) Bromophenol Blue (Sigma); 16% β-mercaptoethanol (Sigma) (added before using). Aliquots are stored at 4°C.
7. MTT powder (3-(4,5-Dimethylthiazol-2-yl)-2,5-diphenyltetrazolium bromide, Sigma) is dissolved in PBS to make a 5 mg/mL solution, which is stored at –20°C.

2.2. Transient Transfection with siRNAs and Establishment of Stable Clones

1. Two double-stranded synthetic RNA oligomers, (5′-GGGA-GAAATTGCACACTTAtt-3′ and 5′-GGACTTTTAGCAA-AGATCTtt-3′), designed from human FLJ10540 sequence, and one *Silencer* negative control #4611G siRNA are purchased from Applied Biosystems (Austin, TX).
2. Transfections are performed with Lipofectamine™ (Invitrogen) according to the manufacturer's protocol.
3. A 100 mg/mL solution of G418 (Calbiochem) is prepared in PBS and stored in single- use aliquots at –80°C.
4. HA-tagged FLJ10540 stably expressing $CL_{1\text{-}0}$ cells are grown in RPMI-1640 and selected with 800 μg/mL G418.

2.3. Migration and Invasion Assay

1. For the migration assay performed in Costar Transwell supports (8-μm pore size polycarbonate membrane) (Corning, Lowell, MA), stable clones are suspended in 400 μl of RPMI-1640 containing 10% FBS and seeded (5×10^3) onto transwell inserts, while 600 μl of RPMI-1640 containing 10% FBS is added to the outer side of the insert.
2. For invasion assays, 80 μg/mL Matrigel (BD Bioscience, Bedford, MA) is added to the transwell inserts and allowed to gel at 37°C overnight. Cells (1×10^4) in 400 μl culture medium are seeded onto the transwell inserts, and 600 μl of culture medium is added to the outer side of the insert.

2.4. SDS-Polyacrylamide Gel Electrophoresis (SDS-PAGE)

1. This protocol is designed for western blotting with the Mini-PROTEAN 3 Electrophoresis System from Bio-Rad.
2. Separating buffer: 1.5 M Tris–HCl, pH 8.8, 0.4% SDS. Stored at room temperature.

3. Stacking buffer: 0.5 M Tris–HCl, pH 6.8, 0.4% SDS. Stored at room temperature.
4. Thirty percent Acrylamide/Bis Solution (29:1) (Bio-rad, Hercules, CA) (this is a neurotoxin when unpolymerized) and N,N,N,N′-Tetramethyl-ethylenediamine (TEMED, Sigma).
5. Ammonium persulfate: prepared as 10% solution in water, and immediately frozen at –20°C in single-use (100 µl) aliquots.
6. Running buffer: 25 mM Tris, 192 mM glycine, 0.1% (w/v) SDS. Stored at room temperature.
7. Prestained molecular weight markers: PageRuler prestained protein ladder (Fermentas, Life Science, Lithuania).

2.5. Western Blotting for Active AKT and Other Proteins

1. Transfer buffer: 48 mM Tris base (pH 8.3), 39 mM glycine, 20% (v/v) methanol.
2. PVDF membranes are purchased from Millipore (Bedford, MA) and 3MM chromatography paper is purchased from Whatman (Maidstone, UK).
3. Tris-buffered saline with Tween (TBST): 137 mM NaCl; 2.7 mM KCl; 25 mM Tris–HCl, pH 7.4; and 0.1% Tween-20.
4. Blocking buffer: 5% (w/v) nonfat dry milk (BD) in TBST.
5. Primary antibody dilution buffer: TBST supplemented with 5% (w/v) nonfat dry milk.
6. Antibodies specific for AKT or AKT-pSer^{473} (Cell Signaling Inc., Danvers, MA), anti-FLJ10540 (Abnova, Taipei, Taiwan), anti-HA (3F10, Roch Biochemicals, Indianapolis, IN, USA), and anti-βactin (Sigma).
7. Secondary antibody: Horse radish peroxidase-conjugated anti-mouse IgG or anti-rabbit IgG (Santa Cruz, CA).
8. Enhanced chemiluminescent (ECL) reagents are purchased from Millipore. (see Note 1).

3. Methods

To determine whether FLJ10540 participates in the process of cell transformation, NIH3T3 cells stably expressing pCDNA3 vector or HA-tagged FLJ10540 were established and added to soft agar. Our results show that FLJ10540 NIH3T3-stable transfectants grew better in soft agar than did vehicle-control clones, indicating FLJ10540 expression increases anchorage-independent NIH3T3 cell growth. Moreover, because oncogene-induced alterations in both growth properties and rates are often observed

in transformed cells, we used an siRNA approach to knockdown endogenous FLJ10540 expression in the human lung cancer cell line, A549, and then assayed transfected cells for proliferative, migration, and invasion potential. A549 cells were transfected with specific FLJ10540 siRNAs for 24 h, and successful knockdown was verified by western blot analysis with an antibody against FLJ10540. (see Note 2). We showed a dramatic reduction in FLJ10540 protein levels with both FLJ10540 siRNAs, and no significant reduction of FLJ10540 in negative siRNA-transfected controls (Fig. 1a). As determined by MTT assay (see Note 3), no significant growth difference was found between negative control and FLJ10540 siRNA-transfected cells over a 24-h period (Fig. 1b). Concurrently, negative and FLJ10540 siRNA-transfected A549

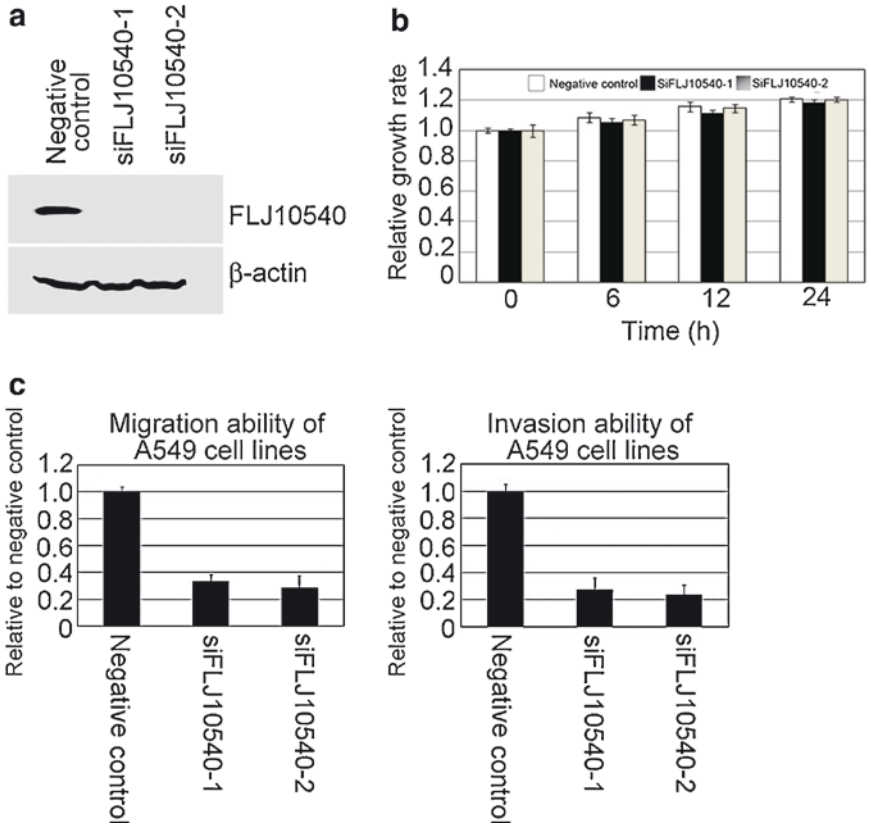

Fig. 1. FLJ10540 knockdown decreases the migration and invasion abilities of lung cancer cells. (**a**) One Silencer negative control siRNA and two different FLJ10540 siRNAs (siFLJ10540-1 and siFLJ10540-2) were transfected into A549 cells, respectively. 24 h posttransfection, a subset of these cells was harvested for FLJ10540 and β-actin detection by immunoblot. (**b**) To measure cell growth rates, 5×10^3 cells of each transfection from (**a**) were seeded into 96-well plates and an MTT assay was performed at the indicated time points. Data were expressed as the mean ± s.d. of three independent experiments. (**c**) The remaining cells were seeded with or without Matrigel onto transwell inserts for cell migration and invasion analysis. The relative migration and invasion abilities of cells were represented as the mean ± s.d. of three independent experiments

cells were seeded with or without Matrigel on Transwell inserts for invasion assays. After a 24-h incubation period, the motility and invasion potential of FLJ10540 knockdown cells was strongly inhibited compared to control siRNA-transfected cells (Fig. 1c, left and right). Together, these results strongly support the hypothesis that FLJ10540 plays a crucial role in cell migration and invasion in human lung cancer cells.

To elucidate the possible FLJ10540-influenced signaling pathway(s) involved in controlling transformation, a panel of phospho-antibodies directed against kinases commonly phosphorylated in activated signaling cascades was used for immunoblot analysis. Cell lysates from control NIH3T3 and FLJ10540-NIH3T3 stable transfectants were examined by western blotting with antibodies specific to the unphosphorylated or phosphorylated forms of ERK (p-Thr^{202}/Tyr^{204}), JNK (p-Thr^{183}), p38 (p-Thr^{180}), and AKT (p-Ser^{473}). Among the targets tested, only AKT-Ser^{473} phosphorylation was elevated in FLJ10540-NIH3T3 stable cells compared to control NIH3T3 cells (6), indicating the PI3K/AKT pathway may be involved in FLJ10540-induced cell transformation.

Accumulating evidence suggests a potential role for PI3K/AKT in migration and invasion of several cancer cell types, including those of the lung (7). To provide additional evidence for PI3K/AKT participation in FLJ10540-induced cell growth, we took the following approaches. First, we used an siRNA approach to inhibit endogenous expression of the catalytic subunit of PI3K, termed p110-α, and assayed activation of AKT in FLJ10540-transfected HEK293T cells. Our data indicate that AKT activity is inhibited by p110-α siRNA in FLJ10540-transfected cells (6). Second, we assessed whether exogenous FLJ10540 overexpression and endogenous FLJ10540 knockdown could influence PI3K/AKT activity in lung cancer cells. AKT-Ser^{473} phosphorylation was significantly reduced in FLJ10540-depleted cells (Fig. 2), whereas the total AKT levels in FLJ10540-siRNA-transfected lung cancer cells were similar as compared with parental and negative control cells. Next, we used three pharmacological inhibitors, including LY294002 (PI3K inhibitor, 10 μM), SB202190 (p38 inhibitor, 20 μM), and PD98059 (MEK inhibitor, 10 μM), to further test PI3K/AKT pathway involvement in FLJ10540-mediated cell migration and invasion. In addition, previous work in our lab has revealed that VEGF-A, a known PI3K/AKT activator (8, 9) and critical pro-angiogenic factor that regulates migration and invasion, can upregulate FLJ10540 protein expression (data not shown). Therefore, we also have included VEGF-A treatment in our migration and invasion assay. Our results indicated that AKT-Ser^{473} phosphorylation, migration, and invasion of FLJ10540-CL$_{1\text{-}0}$ stably expressing cells were diminished with the PI3K inhibitor LY294002, and to a much lesser extent, with

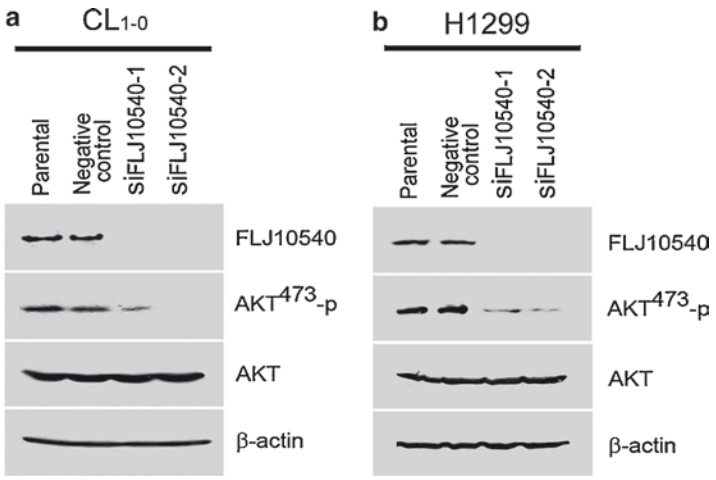

Fig. 2. FLJ10540 knockdown significantly decreases AKT activity. One *Silencer* negative control siRNA and two different FLJ10540 siRNAs (siFLJ10540-1 and siFLJ10540-2) were respectively transfected into CL_{1-0} (**a**) and H1299 (**b**) cells. 24 h posttransfection, cells were harvested for FLJ10540, AKT, phosphor-AKT (Ser^{473}) and β-actin detection by immunoblotting. β-actin was used as an internal loading control

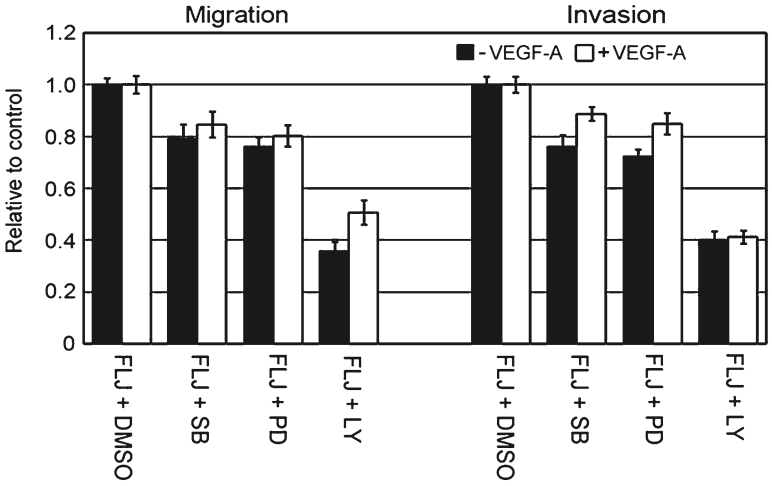

Fig. 3. Endogenous and VEGF-A-induced FLJ10540 expression promotes cell migration and invasion in a PI3K/AKT-dependent manner. Parental CL_{1-0} and FLJ10540-CL_{1-0} stable clones were seeded onto to Transwell inserts and serum-starved for 24 h. After serum starvation, cells were treated with or without SB202190 (20 μM), PD98059 (10 μM), and LY294002 (10 μM), and VEGF-A (20 ng/ mL) as indicated for 3 h. The migration and invasion ratios of vehicle-CL_{1-0} and FLJ10540-CL_{1-0} stable clones were determined and represented as the mean ± s.d. of three independent experiments

SB202190 and PD98059, independent of VEGF-A addition (Fig. 3). Together, our results from siRNA and chemical inhibitor studies indicate that FLJ10540 is required for proper VEGF-A-dependent signaling and contributes to PI3K/AKT-dependent cell migration and invasion.

3.1. Transient Transfection of siRNAs

1. One day before transfection, 2.5×10^5 cells are plated in 6-well cell culture plate with 5 mL growth medium, but without antibiotics, so as to be 50% confluent on the day of transfection.
2. The following day, a 50 nM siRNA solution by diluting stock siRNA in an eppendorf tube with 50 µl serum-free RPMI-1640 medium, mixed gently and incubated for 5 min at room temperature.
3. Following this incubation, 2 µl Lipofectamine™ is added to the 50 µl serum-free RPMI-1640 medium and incubated for an additional 5 min at room temperature.
4. The solution of diluted siRNA (step 2) and Lipofectamine™ (step 3) is then gently mixed by pipeting and incubated for an additional 20 min at room temperature.
5. Finally, 100 µl of the transfection mix (step 4) is added to each well containing lung cancer cells and 1 mL serum-free RPMI-1640 medium. The plate is mixed gently by rocking back and forth.
6. Five hours later, complexes with RPMI-1640 serum-free medium (step 5) are removed and fresh complete RPMI-1640 medium containing 10% FBS is added to the wells. Cells are incubated for 18–24 h at 37°C in a 5% CO_2-humidified incubator prior to testing for target gene expression.

3.2. Establishment of Stable Clones

1. The HA-tagged FLJ10540 expression plasmid is transiently transfected into $CL_{1\text{-}0}$ cells according to the notes listed in Subheading 3.1
2. For a 6-well plate, $CL_{1\text{-}0}$ cells are transfected with 1 µg plasmid DNA in 10 µl Lipofectamine™.
3. At 24 h posttransfection, $CL_{1\text{-}0}$ cells are selected with 800 µg/mL G418. After 2–3 weeks, individual clones are isolated and analyzed for exogenous FLJ10540 expression by Western blotting.

3.3. MTT Assay

1. 5×10^3 cells are seeded onto 96-well plates in RPMI-1640 medium containing 10% FBS and incubated overnight at 37°C in 5% CO_2-humidified atmosphere.
2. Twenty µl MTT reagent (2 mg/mL) is added to each well in the 96-well plate and then incubated at 37°C in 5% CO_2-humidified atmosphere for 3–5 h.
3. Absorbance values of wells are analyzed on a plate reader at a wavelength of 570 nm. Data are normalized to the background absorbance read at hour 0 for each control.

3.4. The Migration Assay

1. Each transwell insert is placed into 24-well plates. 5×10^3 cells are suspended in 400 µl growth medium and seeded onto transwell inserts, while 600 µl growth medium is added to the outer side of the chamber.

2. Plates are incubated at 37°C in a 5% CO_2-humidified incubator for 20–24 h.
3. Transwell inserts are removed from the well and put into a new 24-well plate. Medium in the chamber is discarded.
4. The transwell inserts are washed twice with 1× PBS buffer at room temperature.
5. Ice-cold methanol (−20°C) is added to each well to fix the cells, and plates are incubated for 15 min at room temperature.
6. The methanol in each plate insert is discarded. Each well is completely air dried without methanol for 2–3 h at room temperature.
7. A 1× Giemsa solution is prepared and 0.5 mL is added to each plate for 1 h at room temperature to stain the cells.
8. Next, the Giemsa solution is discarded, and inserts are washed twice with sterile water.
9. The membrane is removed from plate inserts with a razor and the underside of the membrane is placed on a glass slide. Cells from upper surface of the membrane (cells that did not migrate) are wiped with a cotton swab wet with sterile water.
10. The migratory cells are visualized and the number counted by light microscopy. The data represent the mean results from three to three independent experiments and migration is expressed as a difference relative to migration of vehicle- or negative-vector-control-treated cells.

3.5. The Invasion Assay

1. 80 μg/mL Matrigel is added to the transwell inserts and allowed to gel at 37°C overnight.
2. Each single transwell chamber is placed in a 24-well plate. 1×10^4 cells are suspended in 400 μl growth medium and seeded into the upper chamber, while 600 μl of growth medium is added to the outer side of the chamber.
3. The remaining procedures for invasion assessment are the same as those outlined in the migration assay.

3.6. SDS-PAGE Protocol

1. Assemble the glass plates, engage the spring-loaded lever, and place the gel cassette assembly on the gray casting stand gasket. The lever pushes the spacer plate down against the gray rubber gaskets.
2. Determine the volume of the gel mold. Prepare the appropriate volume of solution containing the desired concentration of acrylamide for the resolving gel. A 1.5-mm thick, 10% gel can be prepared by mixing: 3.3 mL acrylamide/Bis solution; 4 mL water, 2.5 mL separating buffer; 100 μl 10% SDS,

100 µl 10% ammonium persulfate; and 4 µl TEMED. Polymerization will begin as soon as the TEMED has been added. Without delay, swirl the mixture rapidly and pour the acrylamide solution into the gap between the glass plates, leaving space for a stacking gel. Using a Pasteur pipette carefully overlay the acrylamide solution with ethanol. The gel should polymerize in about 30 min.

3. Pour off the ethanol and prepare the stacking gel containing: 0.67 ml acrylamide/Bis solution; 2.7 mL water; 0.5 mL of stacking buffer; 40 µl 10% SDS; 40 µl 10% ammonium persulfate; and 4 µl TEMED. Polymerization will begin as soon as the TEMED has been added.
4. Pour the stacking gel solution directly onto the surface of the polymerized acrylamide resolving gel. Immediately insert a clean comb, being careful to avoid trapping air bubbles. Add more stacking gel solution to fill the spaces of the comb completely. The stacking gel should polymerize within 30 min.
5. Once the stacking gel has set, carefully remove the comb and wash the wells immediately with deionized water to remove any unpolymerized acrylamide.
6. Lower the inner chamber into the mini-tank and add the Tris–glycine electrophoresis buffer to the upper and lower chambers of the gel unit. Load each sample into the bottom of the wells. Include one well for prestained molecular weight markers. Load an equal volume of 1× SDS gel-loading buffer into any wells that are unused.
7. Attach the electrophoresis apparatus to an electric power supply. The gel can be run at 80 V through the stacking gel and 100 V through the resolving gel.

3.7. Western Blotting for Active AKT

1. The samples that have been separated by SDS-PAGE are transferred to PVDF membranes electrophoretically. A tray of setup buffer is prepared that is large enough to lay out a transfer cassette with its pieces of foam and with two sheets of 3 mm paper submerged on one side. A sheet of the PVDF cut just larger than the size of the separating gel is laid on the surface of a separate tray of methanol for 2–3 s to allow the membrane to wet by capillary action. Always wear gloves when handling membranes to prevent contamination.
2. Prepare chilled (4°C) transfer buffer and gel sandwich. First, place the cassette, with the gray side down, on a clean surface. Second, set up the transfer apparatus by placing the PVDF and gel on the gray side of the cassette in order as follows (from down to top): one prewetted fiber pad (3 mm paper); a sheet of filter paper; the equilibrated gel; the prewetted PVDF membrane; a piece of filter paper on the membrane;

and the last fiber pad. Removing air bubbles, that may have formed between the gel and membrane is very important for good results. Gently roll a glass tube over the last fiber pad to roll air bubbles out.

3. Close the cassette firmly, being careful not to move the gel and filter paper sandwich. Lock the cassette closed with the white latch and place the cassette in the module. The lid is put on the tank and the power supply activated. Transfers can be performed at either 50 V overnight or 400 mA for 2 h.
4. Upon completion of the run, disassemble the blotting sandwich. The PVDF is then incubated in 10 mL blocking buffer for 1 h at room temperature on a rocking platform.
5. The blocking buffer is discarded and the membrane quickly rinsed prior to addition of a 1:1,000 dilution of the anti-phosphorylated AKT antibody in TBST/5% nonfat dry milk, which is incubated with the membrane overnight at 4°C on a rocking platform.
6. The primary antibody is then removed (see Note 4) and the membrane is washed three times for 10 min each with TBST.
7. The secondary antibody is freshly prepared for each experiment as a 1:10,000-fold dilution in blocking buffer and added to the membrane for 2 h at room temperature on a rocking platform.
8. The secondary antibody is discarded and the membrane is washed three times for 10 min each with TBST.
9. The ECL reagents are mixed together and added to the blot, which is then rotated by hand to ensure even coverage. The blot is removed from the ECL reagents, and then placed between the leaves of an acetate sheet protector that has been cut to the size of an X-ray film cassette. (see Note 5).
10. The acetate containing the membrane is then placed in an X-ray film cassette with film for a suitable exposure time, typically a few minutes. An example of the results produced from this protocol is shown in Fig. 2.

4. Notes

1. Chemiluminescent reagents for X-ray development should be prepared in the dark room that so their activity is not lessened before film exposure. Furthermore, one should ensure that the signal, which exposes in the X-ray file, is not saturated.

2. The following approach, described here for FLJ10540, may be applied to investigate the effectiveness of specific siRNAs on endogenous protein target knockdown. An HA-tagged FLJ10540 expression construct can be co-transfected with three different siRNAs containing one *Silencer* negative control siRNA and two siRNAs specific for FLJ10540 (siFLJ10540-1 and siFLJ10540-2) into HEK293T cells, respectively. This experiment may seem redundant; however, this approach may also serve as a rapid screening assay to identify the most effective siRNA when antibodies against the endogenous target protein are not available.
3. To address whether FLJ10540 enhances cell proliferation, a cell viability assay, such as the MTT assay, should be performed. If the studied gene plays a role in cell proliferation, one should adjust the time period required for analyzing migrated cells.
4. The primary antibody can be saved for subsequent experiments by addition of 0.02% (final concentration) sodium azide (conveniently done by dilution from a 10% stock solution) and storage at 4°C. These primary antibodies can be used for up to five blots within one month. The only adjustment required is to increase length of exposure time in the film at the ECL step.
5. Backgrounds in this protocol are normally so clean that exact alignment of the subsequent film with the PVDF can be difficult. We apply a square of luminescent tape (Sigma, St. Louis, MO) to the edge of the acetate sheet to provide an alignment mark for the film and membrane and thus allow proper identification of the signals.

References

1. Friedl, P., and Wolf, K. (2003) Tumour-cell invasion and migration: diversity and escape mechanisms. *Nat. Rev. Cancer* **3,** 362-374.
2. Osaki, M., Oshimura, M., and Ito, H. (2004) PI3K-Akt pathway: its functions and alterations in human cancer. *Apoptosis* **9,** 667-676.
3. Ramesh, R., Ito, I., Gopalan, B., Saito, Y., Mhashilkar, A. M., and Chada, S. (2004) Ectopic production of MDA-7/IL-24 inhibits invasion and migration of human lung cancer cells. *Mol. Ther.* **9,** 510-518.
4. Su, L. J., Chang, C. W., Wu, Y. C., Chen, K. C., Lin, C. J., Liang, S. C., et al. (2007) Selection of DDX5 as a novel internal control for Q-RT-PCR from microarray data using a block bootstrap re-sampling scheme. *BMC Genomics* **8,** 140.
5. Chen, C. H., Lai, J. M., Chou, T. Y., Chen, C. Y., Su, L. J., Lee, Y. C., et al. (2009) VEGFA upregulates FLJ10540 and modulates migration and invasion of lung cancer via PI3K/AKT pathway. *PLoS ONE* **4,** e5052.
6. Chen, C. H., Lu, P. J., Chen, Y. C., Fu, S. L., Wu, K. J., Tsou, A. P., et al. (2007) FLJ10540-elicited cell transformation is through the activation of PI3-kinase/AKT pathway. *Oncogene* **26,** 4272-4283.
7. Cantley, L. C. (2002) The phosphoinositide 3-kinase pathway. *Science* **296,** 1655-1657.
8. Zachary, I. (2003) VEGF signalling: integration and multi-tasking in endothelial cell biology. *Biochem. Soc. Trans.* **31,** 1171-1177.
9. Laramée, M., Chabot, C., Cloutier, M., Stenne, R., Holgado-Madruga, M., Wong, A. J., and Royal, I. (2007) The scaffolding adapter Gab1 mediates vascular endothelial growth factor signaling and is required for endothelial cell migration and capillary formation. *J. Biol. Chem.* **282,** 7758-7769.

Chapter 16

Biodegradable Polymer-Mediated sh/siRNA Delivery for Cancer Studies

Dhananjay J. Jere and Chong-Su Cho

Abstract

Discovery of RNA interference (RNAi)-mediated specific gene silencing has raised hope for cancer therapy. Unfortunately, the execution of RNAi by delivering small-interfering RNA (siRNA) or small hairpin RNA (shRNA) remains a prime challenge. A methodical evaluation of cationic polymers in RNAi-based cancer studies may offer a promising solution to this problem. In this chapter, we report the methodologies for comprehensive characterization of a biodegradable polymeric system for sh/siRNA delivery in cancer studies. The chapter will describe synthesis, characterization, and optimization of biodegradable poly (β-amino ester) for sh/siRNA delivery. The protocols are provided for shRNA and siRNA complex preparation, stability and morphology study. Also, detailed methods are provided for the intracellular tracking and transfection of sh/siRNA using polymeric carrier. In addition, step-wise information is provided for the in vitro silencing of oncoprotein to study important cancer properties, including proliferation, malignancy, and metastasis of cancer cells.

Key words: siRNA, shRNA, Nonviral vector, Polymeric carrier, Gene delivery, siRNA delivery, Lung cancer, siRNA protocols, Cancer protocols

1. Introduction

RNA interference (RNAi)-mediated specific gene silencing has great potential in cancer gene therapy. Briefly, in the RNAi process, the cellular complex "Dicer" cleaves a double-stranded RNA (dsRNA) molecule to generate smaller dsRNA duplexes of 21–25 nucleotides in length. These small dsRNAs, also called short/small-interfering RNAs (siRNAs), guide the RNAi-induced silencing complex (RISC) to cleave target mRNAs that share sequence identity with the siRNA. In mammalian cells, RNAi can be induced via transfecting synthetic siRNA or DNA vectors capable of intracellularly expressing short hairpin RNA (shRNA).

Wei-Ping Min and Thomas Ichim (eds.), *RNA Interference*, Methods in Molecular Biology, vol. 623,
DOI 10.1007/978-1-60761-588-0_16,

But synthetic siRNAs yield a transient effect, while more durable knockdown is achieved using shRNA expressing vector (1–3).

RNAi, being highly target specific, has wide therapeutic potential in diseases, including cancer (4, 5). In cancer, RNAi machinery is intact, and can be utilized by delivering sh/siRNA to target oncoproteins whose overexpression is a prime cause of cancer. Knocking-down these oncoproteins (such as Akt1) using specific sh/siRNAs has demonstrated positive improvements in cancer by reducing tumorigenesis and limiting cancer cell migration, invasion and proliferation (6, 7) (Fig. 1). Hence, silencing Akt1, or any other oncoprotein, using specific sh/siRNAs has tremendous therapeutic interest. To accomplish effective silencing, there is a dire need for an efficient sh/siRNA delivery system, which is currently lacking, and this has emerged as a major bottleneck in using sh/siRNA in therapeutics. Current advances in polymeric carriers may offer a potential solution to this problem. Polymer chemistry is versatile and provides a scope for diverse modifications to embrace desirable properties in polymeric carriers for sh/siRNA delivery (8, 9). The most successful modification is the introduction of ester linkages in backbone for easy biodegradation. Poly (β-amino ester)s (PAE)s, the most commonly used biodegradable polyesters for gene delivery (10–13), may deliver sh/siRNA efficiently for cancer research (14), if designed and studied carefully. To assist developments in cancer research for ultimate therapeutic applications using polymeric carrier and sh/siRNAs, in this chapter we describe the step-by-step synthesis and characterization of biodegradable PAE carrier composed of low molecular weight polyethylenimine (PEI) and poly (ethylene glycol) (PEG), which is specifically formulated for transfection of pDNA and siRNA for cancer studies. Also, we detail the characterization of PAE–sh/siRNA polyplexes and cell transfection protocols. Importantly, the methods are provided for the silencing of reporter protein and oncoprotein using PAE carrier. Moreover, this chapter also describes protocols designed to study basic cancer properties, such as unrestricted proliferation, malignancy, and metastasis of cancer cells in vitro.

2. Materials

All apparatus, chemicals, and cell lines mentioned must be stored and maintained in the specified conditions. For high accuracy, highly pure chemicals and calibrated apparatus should be used throughout the experiments. All experiments should be performed without violating safety protocols to prevent personal accidents.

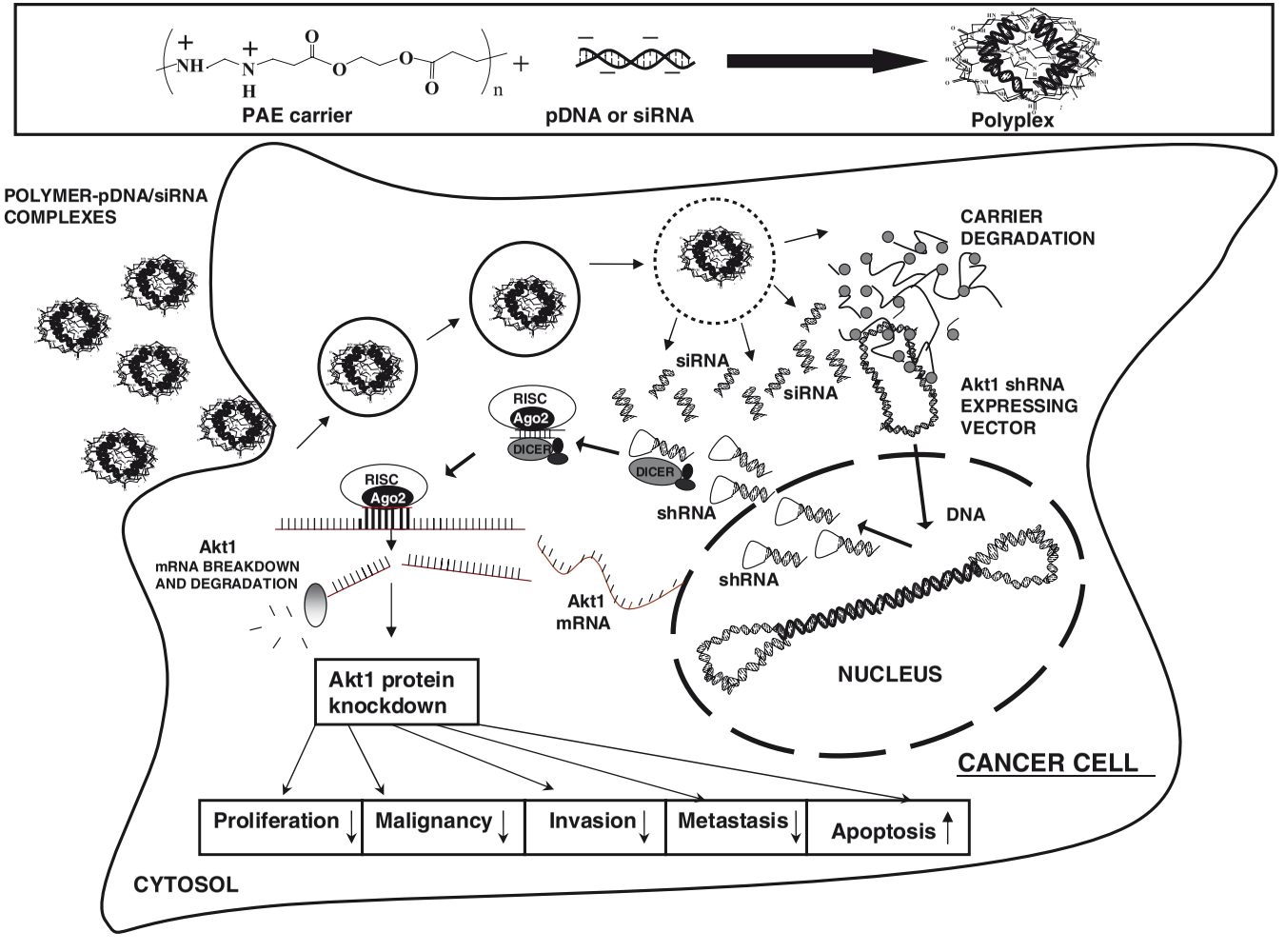

Fig. 1. Schematic representation of oncogene-targeted shRNA and siRNA delivery to cancer cell using degradable polymeric carrier and its consequences on cancer cells survival

2.1. Synthesis of Biodegradable Poly (β-Amino Ester) Carrier

1. Linear polyethylenimine (PEI) (M_n: 423 Da, purity: 97%) (Sigma-Aldrich, St. Louis, MO, USA). Store in a dry place. Always handle carefully with gloves as it is toxic (see Note 1).
2. Poly (ethylene glycol) diacrylate (PEGDA) (M_n: 258; 575; or 700 Da, purity 98%) (Sigma-Aldrich, St. Louis, MO, USA). Store in a dry place at 4°C (see Note 1).
3. Anhydrous dichloromethane (purity: 99.8%) (Sigma-Aldrich, St. Louis, MO, USA). Store in a cool place. Always handle carefully by wearing mask as it is highly volatile and inflammable solvent (see Note 1).
4. Very clean and dry reaction flask with wide mouth and flat bottom.
5. Multiangle incubator shaker with speed regulator.
6. Chemical fume hood.
7. Vacuum oven with vacuum assembly attached to it.
8. Cold (4°C) ultra-pure water.
9. Dialysis membrane with molecular weight cutoff 3,500 or 6,000 (Spectra/Por™).
10. Liquid nitrogen: store in a liquid nitrogen tank only, handle with care.
11. Freeze-dryer.
12. Deep freezer –20°C.
13. Deuterated water (D_2O) (Sigma-Aldrich, St. Louis, MO, USA).
14. ^{1}H-NMR tube.
15. ^{1}H-NMR spectroscopy (Advance™ 600 MHz, Bruker, Germany).

2.2. Preparation of PAE–sh/siRNA Polyplexes

1. Gel electrophoresis apparatus.
2. UV illumination chamber with camera.
3. Agarose powder.
4. Tris-acetate-EDTA (TAE) buffer (50×): 242 g Tris, 57.1 ml glacial acetic acid, 100 ml 0.5 M sodium EDTA (pH 8), water to make total volume of 1,000 ml.
5. Ethidium bromide (EtBr): 0.5 mg/ml. Highly toxic and carcinogenic; protect from light. Always handle with gloves and do not inhale.
6. Gel-loading dye.
7. DNA ladder.
8. 500 µl sterile and nuclease-free Eppendorf tubes.

9. Sodium acetate buffer: 25 mM, pH 5.8; sterile and nuclease free.
10. Sterile and nuclease-free ultra-pure water.
11. pDNA solution.
12. PAE stock solution.
13. siRNA solution (see Note 2).
14. Heparin (Sigma-Aldrich, USA).
15. Carbon-coated 400 mesh copper grids.
16. Phosphotungstic acid solution (2%) or uranil acetate solution (1%).

2.3. Transfection Method for Reporter Protein EGFP Silencing Using PAE–EGFP siRNA Polyplexes

1. Plasmid pEGFP-N2, with early CMV promoter and EGFP gene (pEGFP) (Clontech, Palo Alto, CA, USA).
2. Lipofectamine™ and Plus reagent (Invitrogen, California, USA).
3. RPMI medium with and without 10% fetal bovine serum (FBS) (Hyclone, South Logan, UT).
4. 12-well and 6-well cell culture plates (SPL Life Sciences).
5. *Silencer*™ GFP siRNA and scrambled siRNA (Ambion, Austin, TX, USA): Store at –20°C in defrost freezer. Always store in RNase-free condition, and divide in small aliquots to minimize freeze–thaw cycles.
6. Flow cytometry (BD FACS Calibur, Franklin Lakes, NJ, USA).
7. Sterile phosphate-buffered saline (PBS) (pH 7.4).
8. Flow cytometric cuvettes.
9. Confocal laser scanning microscopy (CLSM) (MRC 1024, Bio-Rad, UK).
10. Sterile cellulose-coated cell culture coverslips.

2.4. Transfection Method for Oncoprotein Akt1 Silencing Using PAE–Akt1 shRNA Polyplexes

1. The cassette of oligonucleotides encoding 19-mer hairpin sequences for the sense and antisense strands specific to the target sequence aaGAAGGAAGUCAUCGUGGCCaa of Akt1 mRNA (Mirus, USA) (Akt1 shRNA).
2. A scrambled shRNA with same nucleotide composition but lacking in sequence homology with genome was also synthesized (Mirus, WI, USA).
3. *Lable* IT Tracker™ CX-Rhodamine kit (Mirus, WI, USA).
4. 5 M sodium chloride solution.
5. 100% ethanol (Sigma-Aldrich, USA).

2.5. Quantification of Cancer Cell Survival After Oncoprotein Silencing

1. Cell Titre 96 Aqueous One Solution Reagent (Promega, USA): store at –20°C in dark. Always protect from light, and use in small aliquots to minimize freeze–thaw cycles.
2. 96-well cell culture plates (SPL Life Sciences).
3. ELISA plate reader (GLR 1000, Genelabs Diagnostics, Singapore).
4. Trypsin-EDTA solution.
5. Trypan blue solution: 0.4% (w/v) trypan blue in Hank's Balanced Salt Solution.
6. Neubauer chamber (Hemacytometer).
7. Annexin V-FITC and propidium iodide kit (Abcam, UK).

2.6. Measurement of Cancer Cell Malignancy After Oncoprotein Silencing

1. Noble agar, Difco (or low-melting agarose).
2. RPMI medium at double strength (see Note 3).
3. Sterile conical flask and bijoux bottles.
4. *p*-Iodonitrotetrazolium violet (Sigma-Aldrich, USA).

2.7. Measurement of Cancer Cell Metastasis After Oncoprotein Silencing

1. Sterile cell migration filter inserts for six-well plate (Transwell™ or Falcon™): pore size 8–12 µm.
2. Giemsa stain (Sigma, USA): make 1:25 dilution in PBS.
3. RPMI 1640 medium with 20% FBS.
4. Matrigel® (BD Bioscience, USA).
5. Cotton scraper.

3. Methods

All cell culture and transfection experiments should be performed using aseptic techniques in a Biological Safety Cabinet in nuclease-free conditions. Good Laboratory Practice (GLP) and other regulatory guidelines should be followed strictly to avoid any undesirable consequences. Chemicals used during the reaction, synthesis, and analysis must be disposed as per the environmental safety and regulatory guidelines.

As siRNA transfection studies, especially those using polymeric carrier, are very complex and sensitive, we strongly recommend validation of the steps in order to adjust particular experimental setup and personal skills. In this section, we provide step-wise methodologies for the evaluation of polymeric system in sh/siRNA delivery for cancer studies, although some modifications may be desirable depending on the nature of polymeric carrier or the study involved (see Note 4).

3.1. Synthesis of Biodegradable Poly (β-Amino Ester) Carrier

Poly β-amino esters (PAEs) are mainly synthesized by Michael addition reaction (see Note 5), particularly via the conjugate addition of either primary or secondary aliphatic amines to α, β-unsaturated carbonyl compounds to produce β-amino derivatives (15–17). PAEs, already known to be safe and efficient in gene delivery applications in vitro and in vivo, are a potential candidate for RNAi application (14). However, a number of parameters need to be studied carefully before establishing its success in sh/siRNA delivery in RNAi-based cancer studies. As a representative example, we have described the step-by-step synthesis of PAE composed of low molecular weight polyethylenimine (PEI) and poly (ethylene glycol) diacrylate (PEGDA)(18), and its evaluation in sh/siRNA-based lung cancer studies (6).

3.1.1. Procedure for the Synthesis of PAE by Michael Addition Reaction

Michael addition reaction between PEI and PEGDA is a rapid reaction, which can be carried out at a slightly elevated temperature in the presence of organic solvent. Although different molecular weights of PEGDA can be employed, the lowest molecular weight PEGDA at equimolar ratio gave the best results in our transfection studies (18).

1. Weigh accurately 2 g of PEI in a clean and dry 10 ml glass bottle. Add 3 ml of anhydrous dichloromethane (aDCM) in two portions into the bottle containing PEI, first add 2.5 ml and cap it tightly (see Note 6). Shake or stir the mixture gently to dissolve PEI completely. Final concentration of PEI solution is 0.788 mole.
2. Select the appropriate PEGDA with required molecular weight and calculate the exact amount of PEGDA required for the specific mole ratio. Add this PEGDA in a clean and dry glass bottle on a weight basis and add 3 ml of aDCM in two portions into the bottle containing PEGDA solution. First, add 2.5 ml and cap it tightly (see Note 6). Shake or stir the mixture gently to dissolve PEGDA completely.
3. To carry out Michael addition reaction, take a very clean and dry, wide mouth 50 ml reaction flask with flat bottom, and add a magnetic needle for stirring. At the same time, switch on incubator shaker and allow it to stabilize at temperature 45°C.
4. Transfer the PEI solution into the reaction flask, wash the bottle with remaining volume of 0.5 ml aDCM, and transfer the remaining volume into the reaction flask (see Note 6).
5. Add PEGDA solution drop-wise very slowly while stirring. Close the flask with solvent resistant cap. Allow the addition reaction to proceed at 45°C for 48 h in incubator shaker (see Note 7).

6. After 48 h reaction, remove the flask from the incubator shaker and cool to room temperature. The excess of aDCM should be removed at room temperature in the chemical fume hood for 24 h and then for 4 days in a vacuum oven at 30°C with negative pressure (see Note 8).
7. Once excess of aDCM is removed, cool the flask below 10°C and add 25 ml of cold (4°C) ultra-pure water to completely dissolve crude PAE. Then, transfer the solution into the pre-activated dialysis membrane (MWCO: 6,000–8,000) (Spectra/Por™), and seal the ends of the membrane tightly (see Note 9). Perform the dialysis for 24 h at 4°C using 5 l cold (4°C) ultra-pure water in dark. Replace the ultra-pure water with fresh, cold (4°C) ultra-pure water at least five times for complete removal of unreacted PEI and PEGDA (see Note 10).
8. After purification, immediately transfer the PAE solution into preweighed tubes and freeze the solution by placing the tubes in liquid nitrogen for 4–5 min. Then, subject the frozen solution to freeze–drying cycles until all water evaporates (see Note 11). After freeze–drying, calculate the percentage yield of PAE using the following formula:

   $$\%\text{Yield} = (\text{Practical yield}/\text{Theoretical yield}) \times 100$$

   where, Practical yield = weight of the purified product obtained after synthesis

   (i.e., weight of tube containing sample – weight of empty tube) and

   Theoretical yield = Total mass of the reactants added for the reaction.
9. Store PAE sample at –20°C in defrost deep freezer for further studies (see Note 12).

3.1.2. Confirmation of PAE Synthesis by ^{1}H-NMR Spectroscopy

1. Weigh accurately 7 mg of each PAE, PEI, and PEGDA samples, and dissolve in 1 ml of deuterated water (D_2O) separately (see Note 13).
2. Using pasture pipette, transfer these 1 ml PAE, PEI, and PEGDA solutions into three separate, clean and dry ^{1}H-NMR tubes carefully without forming bubbles, and immediately measure in 600 MHz ^{1}H-NMR spectroscopy (see Note 14).
3. Confirm the synthesis of PAE from the appearance of protons peaks for PEI, PEG and, ester linkages.
4. The composition of PEI and PEG in PAE can be measured from the integral values of the PEI and PEG proton peaks (see Note 15).

3.2. Preparation of PAE–sh/siRNA Polyplexes

The ability of PAE to complex and condense sh/siRNA is a critical determinant of its transfection efficiency. In an optimal polyplex delivery system, the electrostatic charge association between sh/siRNA and PAE must be strong enough to maintain the polyplex intact during the transit from extracellular to intracellular in target cell. Hence, optimization of amine moles in PAE (N) to phosphate moles (P) of sh/siRNA is essential for high transfection efficiency. Preparation of PAE–sh/siRNA polyplexes at a desired N:P ratio requires the following information:

1. M_w of sh/siRNA.
2. Number of phosphate groups in sh/siRNA (equal to 1 less than the number of base pairs).
3. M_w of PAE.
4. Number of amine groups per mole of PAE.

Also, see Note 16 for further information.

If the mole ratio of PEI to PEG is 1:1 in the synthesized PAE, then the concentration of PAE required for 1 µg of sh/siRNA at 1:1 N/P ratio is 1.03 µg/ml. Agarose gel electrophoresis is a potential method to study the complex formation and to optimize the N/P ratio of PAE to sh/siRNA. Also, it can be used to study complex stability at specific N/P ratio.

3.2.1. Complex Formation Study Between PAE and shRNA

1. Accurately prepare 10 mg/ml stock solution of PAE in cold nuclease-free ultra-pure water (see Note 17), and calculate the volumes of PAE required for different N/P ratios (for example, N/P ratio from 0.9 to 45) as described under Subheading 3.2.
2. Pipette out accurately 1 µl (0.1 µg) of shRNA from the shRNA stock solution (0.1 µg/µl) and add into the 500-µl Eppendorf tube containing PAE solutions (see Note 18).
3. Mix well and allow complex formation for 30 min at room temperature.
4. Adjust the volume to 13 µl with sterile and nuclease-free ultra-pure water, and add 2 µl of gel-loading dye. The complexes are ready for loading on agarose gel.
5. Weigh accurately 800 mg of agarose (0.8%) and add in 100 ml TAE buffer (1×).
6. Heat the solution until agarose dissolves in TAE (approximately 80–90°C for 2–3 min), and allow the temperature to reduce to 50°C.
7. Add 0.5 µl of EtBr solution and mix it efficiently. Transfer this solution into gel casting trays and insert comb for the formation of wells. Allow the melted agarose to settle into gel (15–30 min), and then remove the comb from the wells.

Now, transfer the gel into an electrophoresis tank, which is two-thirds filled with TAE buffer (1×).

8. Add DNA ladder (1,000 kb) and only shRNA in first and second wells, with polyplex solutions in all other wells. Run the gel at 100 V for 30–45 min.
9. After running, observe the gel under UV illumination and take picture immediately. Avoid longer UV exposure, as it may reduce the quality of bands in the picture.

3.2.2. Complex Formation Study Between PAE and siRNA

For successful siRNA delivery, the PAE carrier must form stable complexes with siRNAs. However, siRNAs are difficult to condense due to their limited anionic charge and relatively small, stiffer molecular topology. Nonoptimal condensation of siRNAs may reduce delivery efficiency as a result of leaching or exchange with anionic proteins. In this assay, we used polyanion-heparin exchange mechanism to study the PAE–siRNA polyplex stability.

1. Accurately prepare 10 mg/ml stock solution of PAE in cold nuclease-free ultra-pure water (see Note 17). Select best N/P ratio from the shRNA experiment and evaluate it at different siRNA concentrations. For example, accurately calculate the volumes of PAE required from the PAE stock for 45 N/P ratio at different siRNA concentrations as described under Subheading 3.2 (see Note 19).
2. Pipette out accurately 0.5, 1, 1.5, 2, 2.5, and 3 µl (25–150 pmol) of siRNA solutions from the siRNA stock (50 µmole/l) solution, and add into 500 µl nuclease-free sterile Eppendorf tubes containing polymer solutions in a sequence (see Note 20).
3. Mix well and allow complex formation for 30 min at room temperature.
4. For complex stability study, once complex is formed after 30 min incubation, the stability of the complexes can be challenged by incubating with heparin (10 and 20% v/v) for an additional 30 min.
5. Adjust the volume to 8 µl with sterile and nuclease-free ultra-pure water, and add 2 µl of gel-loading dye. The complexes are ready for loading on agarose gel.
6. Weigh accurately 3 g of agarose (3%) and add in 100 ml TAE buffer (1×).
7. Heat the solution until agarose dissolves in TAE (approximately 80–90°C for 2–3 min), and allow temperature to lower to 50°C.
8. Transfer this solution into gel casting trays and insert comb for the formation of wells. Allow gel formation (15–30 min) and then remove the comb from the wells. Now transfer the gel into an electrophoresis tank that is two-thirds filled with TAE buffer (1×).

9. Add DNA ladder (100 kb) and only siRNA in the first and second wells, respectively, with polymer–siRNA complex solutions in all other wells. Run the gel at 50 V for 20–30 min.
10. After running, soak the gel in 0.5% v/v EtBr solution in TAE buffer for 15–30 min, observe the gel under UV illumination, and take a picture immediately (see Note 21).

3.2.3. Complex Morphology Study Between PAE and siRNA

1. Prepare polyplex solutions as described under Subheading 3.2.2 except 100 pmol of siRNA should be used and the final volume should be 500 µl.
2. For examination by energy-filtering transmission electron microscopy (EF-TEM), deposit one drop (~30 µl) of polyplex solution on carbon-coated 400 mesh copper grids. Then, stain the grids with phosphotungstic acid solution (2%) or uranil acetate solution (1%) (see Note 22) for 2–3 min, and remove the excess of stain with filter paper. Allow the grids to dry for 20 min and examine with EF-TEM. An example of the result is shown in Fig. 2.

3.3. Transfection Method for Reporter Protein EGFP Silencing Using PAE–EGFP siRNA Polyplexes

Reporter protein (EGFP) silencing is a method of choice for the quantification of siRNA delivery efficiency. Two approaches are commonly used to accomplish this study in vitro. In the first, EGFP siRNA is delivered in the cells stably expressing EGFP protein. This stable cell line can be prepared by transfecting

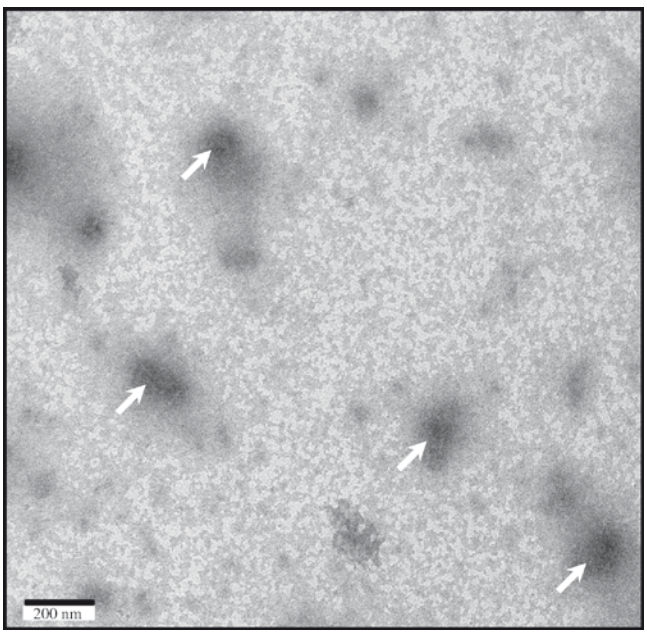

Fig. 2. Morphology of PAE–siRNA polyplexes by Energy-Filtering Transmission Electron Microscope (6). (Reproduced by permission with Elsevier)

plasmid EGFP (pEGFP), and then selecting EGFP-expressing cells using flow cytometer or antibiotic selection method. These selected cells are then recultivated into a stable cell line for prolonged EGFP expression. In the second approach, EGFP siRNA and pEGFP are co-transfected in cells and incubated. Although both methods have some advantages over the other, the second approach can be used for in vivo EGFP silencing studies. In this section, we provide step-wise procedures of the co-transfection method for in vitro silencing studies.

3.3.1. EGFP Expression

1. One day before transfection, in a 12-well tissue culture plate, seed A549 cells (ATCC) (2×10^5 cells/well) in 2 ml RPMI 1640 medium supplemented with 10% of serum and allow to attach overnight (see Note 23).
2. After reaching 70–80% confluence, cells become ready for transfection.
3. For a single transfection using Lipofectamine™ and Plus® reagents, dilute 2 µg of pEGFP in 100 µl of serum-free RPMI medium and mix gently.
4. Mix Plus® reagent before use, then add 12 µl of Plus® reagent to diluted pEGFP. Mix gently and incubate at room temperature for 15 min.
5. Mix Lipofectamine™ gently and dilute it in 100 µl of serum-free RPMI medium and mix gently.
6. Combine precomplexed DNA (step 4) and diluted Lipofectamine™ (step 5), mix and incubate for 15 min at room temperature.
7. Adjust the volume to 1 ml with serum-free RPMI medium and transfer it to the cells.
8. Incubate cells with Lipofectamine™–pEGFP complexes at 37°C in a 5% CO_2 incubator for 3 h, and then change the medium with RPMI medium containing 10% FBS. Incubate again for 6–11 h at 37°C in a 5% CO_2 incubator and proceed to Subheading 3.3.2 (see Note 24).

3.3.2. EGFP Silencing

1. For single silencing, PAE solutions are added in 100 µl of sterile nuclease-free sodium acetate buffer (25 mM; pH 5.2) in 2 ml sterile nuclease-free Eppendorf tube. EGFP siRNA solution is added at different siRNA concentrations (for example, 50–125 pmol) at a constant N/P ratio, as explained under Subheading 3.2.2. Mix gently and incubate for 30 min at room temperature (see Note 25). Similarly, complexes between scrambled siRNA and PAE are prepared.
2. Adjust the volume to 1 ml with serum-free RPMI 1640 medium.

3. Aspirate the medium from the cells transfected with pEGFP using Lipofectamine™, and transfer these polyplexes to the cells expressing EGFP protein.
4. Incubate polyplexes with cells for 12 h at 37°C in a 5% CO_2 incubator and change medium with RPMI 1640-containing serum.
5. After incubation, measure EGFP expression by flow cytometry and CLSM as described below.

3.3.3. Flow Cytometric Measurement

1. Forty-eight hours after transfection, collect cells by trypsinization and count using Neubauer chamber (Subheading 3.5.2, steps 2–8).
2. Suspend 1×10^5 cells in ice cold sterile PBS in flow cytometric cuvettes with minimal volume of 0.5 ml (see Note 26).
3. Untreated cell and mock polymer-treated cells can be employed for assigning gated region in flow cytometer with number of events 50,000. The number of cells expressing EGFP in scrambled siRNA, mock carrier, and EGFP siRNA-treated cells will provide percentage EGFP silencing.

3.3.4. Confocal Laser Scanning Microscopic Observation

1. Forty-eight hours after transfection, remove medium completely from the wells and wash twice with ice cold PBS. Fix the cells by using 10% formaldehyde (see Note 27). Remove coverslip carefully from the plate-well, and mount on glass slide by inversely placing it.
2. Observe untreated cells and remove auto-fluorescence from the cells, if any. Observe EGFP expression for scrambled siRNA, mock carrier, and EGFP siRNA-treated cells under CLSM with 488/509 nm excitation/emission wavelength and capture pictures.

3.4. Transfection Method for Oncoprotein Akt1 Silencing Using PAE–Akt1 shRNA Polyplexes

Akt1 (also known as Akt or protein kinase B) is a prime cell survival protein overexpressed in many cancers, including lung cancer. It is also responsible for cancer cell proliferation, malignancy, and metastasis. On silencing this key oncoprotein, cancer cell survival is significantly reduced (7). The reduction in cancer cell survival depends upon the extent of Akt1 silencing which, in turn, is governed by the delivery efficiency. In this section, we will study the delivery methodology for Akt1 shRNA using PAE carrier.

3.4.1. Visualization of Transfection of PAE-Rhodamine-Labeled Akt1 shRNA Polyplexes

1. Label Akt1 shRNA expression plasmid with rhodamine using *Label* IT Tracker™ CX-Rhodamine kit as described below.
2. Prepare 1 mg/ml stock solution of Akt1 shRNA in sterile, nuclease-free ultra-pure water.

3. Add 50 µl of tracker reconstitution solution to the pellet in the tube and mix well.
4. For labeling reaction, (1:1 v/w) ratio of *Label* IT® Tracker™ reagent to DNA can be used (the manufacturer has recommended a range of ratios from 0.25:1 to 1:1). Take 35 µl of sterile nuclease-free ultra-pure water in a sterile nuclease-free 500 µl Eppendorf tube and add 5 µl 10× labeling buffer A. To this solution, add 5 µl of Akt1 shRNA from the stock solution, followed by the addition of 5 µl *Label* IT® Tracker™ reagent.
5. Incubate reaction at 37°C for 1 h. Perform quick spin after 20 min to minimize the effect of evaporation. Then add 150 µl of sterile nuclease-free ultra-pure water.
6. Add 20 µl of 5 M sodium chloride and 400 µl of ice cold 100% ethanol to remove unreacted reagent from the labeled shAkt. Mix well and place at temperature below –20°C for at least 30 min.
7. Centrifuge at 4°C and 22,000 × *g* for 10 min to pellet labeled shRNA. Gently remove the ethanol with pipette without disturbing the pellet (see Note **28**).
8. Wash pellet once with 1 ml 70% ethanol and centrifuge again. Remove ethanol carefully and completely with pipette.
9. Immediately, resuspend the labeled Akt1 shRNA in 20 µl of sterile nuclease-free ultra-pure water.
10. Measure the concentration of labeled shRNA using UV spectrophotometer.
11. Store the purified labeled shRNA at –20°C (see Note 29).
12. For tracking study, repeat steps 1 and 2 described under Subheading 3.3.1 for CLSM measurement.
13. Prepare polyplex solutions (using a rhodamine-labeled Akt1 shRNA) as described under Subheading 3.3.2, except 4 µg of shRNA should be used. Adjust the volume to 1 ml with serum-free RPMI medium and transfer it to the cells. Incubate rhodamine-labeled polyplexes with cells for 4 h at 37°C in a 5% CO_2 incubator (see Note 30). After incubation, follow steps described under Subheading 3.3.4, and observe transfected cells for intracellular distribution of rhodamine-labeled Akt1 shRNA under high magnification at 597 nm wavelength (Fig. 3).

3.4.2. Transfection of PAE–Akt1 shRNA Polyplexes for Akt1 Oncoprotein Silencing

1. For transfection study, A549 cells (2×10^5 cells/well) are seeded in a six-well plate as described in steps 1 and 2 under Subheading 3.3.1.
2. Polyplexes of Akt1 shRNA and scrambled shRNA can be prepared as described in step 13 under Subheading 3.4.1, except 2 µg of Akt1 shRNA and scrambled shRNA should be used.
3. Adjust the volume to 2 ml with serum-free RPMI medium and transfer it to the cells. Incubate Akt1 shRNA/scrambled

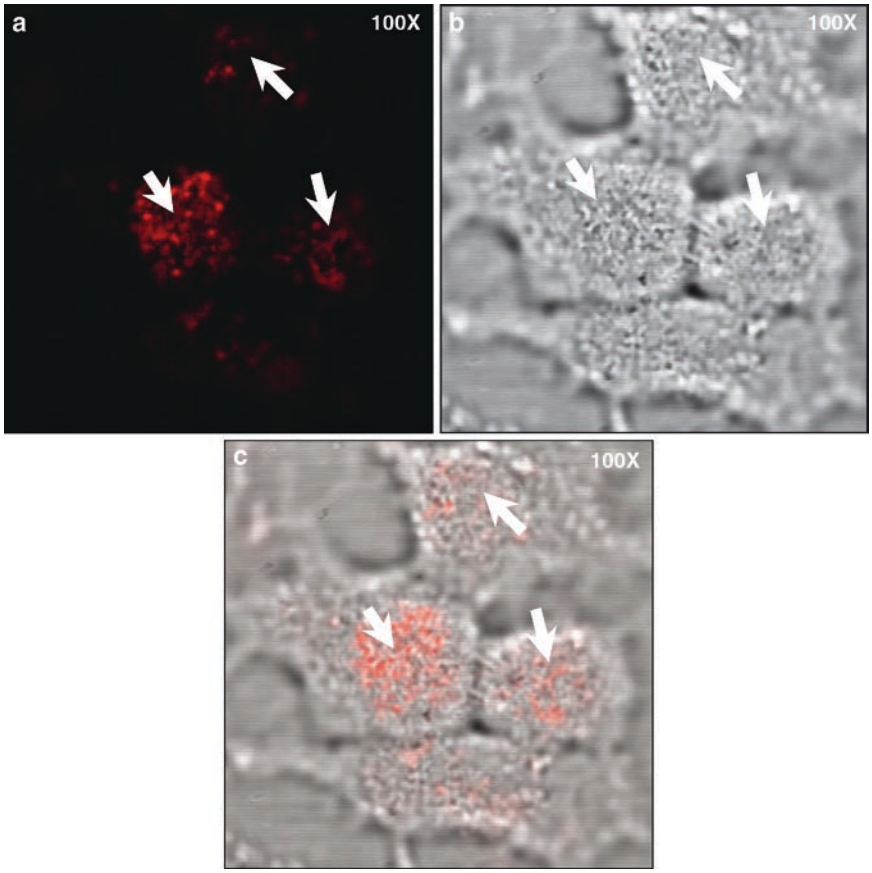

Fig. 3. Intracellular tracking of rhodamine-labeled PAE–Akt1 shRNA complexes by confocal laser scanning microscopy (magnification ×1,000): (**a**) dark field image (emission wavelength 597 nm), (**b**) phase contrast image, and (**c**) image obtained after overlapping dark field and phase contrast images (6). (Reproduced by permission with Elsevier)

shRNA polyplexes with cells for 12 h at 37°C in a 5% CO_2 incubator. Then change the medium with fresh medium containing serum, and incubate at 37°C and 5% CO_2 for 24, 48, or 72 h depending on the subsequent experiments. Control experiments should be performed with blank and mock carrier treatment. (Mock treatment uses only polymeric carrier at specific concentration, keeping other conditions the same.)

4. The Akt1 silencing can be confirmed by measuring Akt1 mRNA level and Akt1 protein level using semiquantitative RT-PCR and Western blot analysis, respectively.

3.5. Quantification of Cancer Cell Survival After Oncoprotein Silencing

Akt1 is a crucial cell survival protein that regulates the survival, proliferation, malignancy, and metastasis of cancer cells. Akt1 knockdown induces selective apoptosis in cancer cells and reduces malignant growth capacity. In this section, we provide a step-by-step procedure to study the alteration in cancer cell survival after oncoprotein silencing.

3.5.1. MTS Assay for Cell Viability

1. For this study, seed A549 cells (1×10^4 cells/well) in a 96-well plate in 200 µl RPMI 1640 (10% FBS) medium as described in steps 1 and 2 under Subdeading 3.3.1.
2. Polyplexes of Akt1 shRNA and scrambled shRNA can be prepared as described under Subheading 3.3.2, except 1 µg of each should be used and final volume should be 100 µl. Also, use mock carrier for the measurement of carrier toxicity. Untreated cells will serve as a positive control for cell viability.
3. Adjust the volume to 100 µl with serum-free RPMI medium and transfer it to the cells. Incubate polyplexes and mock polymer with cells for 24 h at 37°C in 5% CO_2 incubator.
4. After 24 h treatment, replace the medium with growth medium containing 20 µl of Cell Titre 96 Aqueous One Solution™ reagent. Also, add 20 µl of reagent in three empty wells as a reagent control.
5. Then incubate again at 37°C in 5% CO_2 incubator for 2 h, and measure absorbance at 540 nm using ELISA plate reader (see Note 31).
6. Calculate (%) cell viability using the following equation:

$$\text{Cell viability}\,(\%) = \frac{\text{OD}_{540(\text{sample})}}{\text{OD}_{540(\text{control})}} \times 100.$$

7. Consider the viability of untreated cell as 100% and plot the graph for the viability of treated cells.
8. The percent decrease in cancer cell survival following oncoprotein Akt1 knockdown can be calculated as:

   % reduction in oncoprotein specific survival = %cell $\text{survival}_{(\text{scrsiRNA})}$ – %cell $\text{survival}_{(\text{Akt1 shRNA})}$

3.5.2. Trypan Blue Dye Exclusion Assay for Cell Viability

Trypan blue is a dye that is used to determine the viability of a cell. Living cells exclude the dye, whereas dead cells will take up the blue dye. The blue stain is easily visible, and cells can be counted using a light microscope.

1. For this study, perform the steps 1–3 described under Subheading 3.4.2.
2. After incubation, remove the medium through aspiration and add 5 ml of PBS, swirl, and aspirate.
3. Add 500 µl of trypsin-EDTA and swirl to cover the monolayer of cells and incubate for few minutes (2–4 min) at 37°C.
4. Add 1 ml of RPMI 1640 medium (10% FBS) to neutralize the trypsin reaction.
5. Transfer the cell suspension to a sterile centrifuge tube. Centrifuge the cell suspension at 2,000 × *g* for 3–4 min to pellet the cells.

6. Remove the medium through aspiration and resuspend the cell pellet in an appropriate volume of PBS.
7. Place 10 µl on a hemacytometer (between the counting slide and the glass coverslip).
8. Count the cells under a microscope. There are grid markings on the hemacytometer that can be seen under magnification. Count the cells in all four outer quadrants of the grid. Divide this number by four to determine the average number of cells in one quadrant.
9. To calculate the number of cells, multiply the average number of cells per quadrant by the dilution factor. Multiply this number by 10^4 to calculate the number of cells in 1 ml of suspension. The equation is as follows:

   Number of cells/ml = average number of cells per quadrant × dilution factor × 10^4.
10. To calculate the total number of cells, multiply the number of cells/ml by the volume (ml) of the cell suspension.
11. To calculate the percentage of viable cells, combine 0.5 ml of trypan blue solution and 0.3 ml of sterile PBS (pH 7.4).
12. Add 0.1 ml of the cell suspension to the trypan blue mix, mix well, and incubate for 5 min at room temperature.
13. Count the number of unstained cells on the hemacytometer under a microscope as described above. (Dead cells will take up the trypan blue stain.)
14. Count the total number of cells, and determine the percentage of viable cells by dividing the number of unstained cells by the total number of cells and multiplying by 100. The equation is as follows:

$$(\%)\ \text{live cells} = \frac{\text{number of unstained cells}}{\text{total number of cells}} \times 100.$$

15. Consider the viability of untreated cell as 100% and plot the graph for the viability of treated cells.
16. The percent decrease in cancer cell survival after oncoprotein Akt1 knockdown can be calculated as:

   % reduction in oncoprotein specific survival = %live $\text{cells}_{(\text{scrsiRNA})}$ – % live $\text{cell}_{(\text{Akt1 shRNA})}$.

3.5.3. Annexin V-FITC and Propidium Iodide Assay for Apoptosis and Necrosis

Annexin V, a protein that selectively binds with cells undergoing program cell death or apoptosis, is commonly used for the measurement of early- and late-stage apoptosis. Propidium iodide (PI) labeling is nonspecific and provides the measurement of cells undergoing necrotic cell death.

1. For this study, perform the steps 1–3 explained under Subheading 3.4.2.

2. After 72 h incubation, collect the total number of cells and count as described under Subheading 3.5.2, steps 2–10.
3. Collect 1×10^5 from the total number of cells and resuspend cells in 500 µl of Annexin V binding buffer in flow cytometric cuvettes (see Note 32).
4. Label the transfected cells by adding 5 µl of Annexin V-FITC and 5 µl of PI. Incubate for 5 min at room temperature in dark.
5. Also, use untreated cells, only Annexin V-FITC-treated cells, only PI-treated cells, and Annexin V-FITC plus PI-treated cells as controls for flow cytometric settings.
6. Analyze cells by flow cytometry (Ex. = 488 nm; Em. = 530 nm) using FL1 channel for detecting Annexin V-FITC staining and FL2 channel for detecting PI staining.

3.5.4. Measurement of Cancer Cell Proliferation After Oncoprotein Silencing

1. Perform the steps 1–3 described under Subheading 3.4.2 in three different sets and measure at three different time intervals (24, 48, and 72 h).
2. After 24 h incubation, count the number of cells as per the procedure described in steps 2–10 under Subheading 3.5.2.
3. Calculate the relative proliferation by normalizing the number of cells at 0 time of transfection.
4. Use untreated cells and scrambled shRNA-treated cells as controls for measuring the reduction in proliferation of Akt1 shRNA-treated cells.
5. Repeat the procedure after 48 and 72 h, and calculate the relative decrease in cell proliferation on Akt1 shRNA treatment.

3.6. Measurement of Cancer Cell Malignancy After Oncoprotein Silencing

Cancer cells are distinguished from the normal body cells mainly due to their unique malignant growth capability. Normal cells, except hematopoietic cells, exhibit *anchorage-dependent* growth; in contrast, malignant cancer cells are capable of *anchorage-independent* growth. Soft agar assay is specially designed to study malignant growth characteristics of cancer cells where they grow on soft agar gel and form distinguishable floating colonies. This malignant growth capability is significantly reduced with oncoprotein Akt1 silencing. In this section, we provide a protocol for soft agar assay in order to measure malignant growth of cancer cells.

3.6.1. Soft Agar Assay for Measuring Malignancy of Cancer Cells

1. Transfect cells using Akt1 shRNA and scrambled shRNA, as described in the steps 1–3 under Subheading 3.4.2.
2. Perform soft agar assay 48 h after transfection as described below.
3. Prepare double strength (2×) RPMI 1640 medium containing 40% FBS, and place it in a 37 ± 1°C water bath.

4. Weigh accurately 1.2 g agar and dissolve it in 100 ml sterile ultra-pure water by boiling the solution for 2–3 min. Then keep the flask in a separate water bath maintained at 55 ± 2°C.
5. Take additional 100 ml sterile ultra-pure water in a sterile bottle and place it in 37 ± 1°C water bath.
6. As shown in Fig. 4a, prepare a 0.6% agar for underlay by combining an equal volume of 2× medium and 1.2 % agar, and keep it at 37°C. Add 1 ml of 0.6% agar medium to each well of six-well plate, mix, and ensure that it forms a uniform bottom layer. Allow to set and solidify at room temperature.
7. Now, as shown in Fig. 4b, prepare 0.3% agar medium by diluting 2× medium (37°C) with 1.2% agar (55°C) and sterile ultra-pure water (55°C) in the proportions 2:1:1, respectively.
8. Now, collect and count the Akt1 shRNA and scrambled shRNA-transfected cells as explained in steps 2–10 under Subheading 3.5.2. Also, use untreated cells as a control. Store some cells from the total samples for Western blot confirmation of Akt1 silencing.
9. Add 1×10^5 cells in 2 ml 0.3% agar medium at 37°C and overlay on the top of the solidified 0.6% agar layer (see Note 33).
10. Add 2 ml RPMI medium (10% FBS) above the 0.3% agar layer and incubate for 15 days at 37°C in a 5% CO_2 incubator.
11. Change the medium every alternate day.
12. After 15 days incubation, stain the colonies with *p*-iodonitrotetrazolium violet by incubating for 6–12 h.
13. Count the number of colonies in plates containing untreated cells, Akt1 shRNA and scrambled shRNA-treated cells and capture images (Fig. 4c).

3.7. Measurement of Cancer Cell Metastasis After Oncoprotein Silencing

Cancer cell invasion and metastasis is a highly complex process in which the cellular mechanism is not yet completely established. The acquired ability by tumor cells to invade, migrate and proliferate to the secondary site has a major role in cancer cell survival. Transwell cell culture insert assay is commonly used to measure the migratory tendency of cancer cells, and Matrigel coating provides an invasive capacity of the cancer cells. In this section, we provide a detailed procedure to measure migration and invasive-migration of cancer cells.

3.7.1. Transwell Assay for Measuring Migration of Cancer Cells

1. Transfect cells using Akt1 shRNA and scrambled shRNA, as described in the steps 1–3 under Subheading 3.4.2.
2. After 48 h expression, collect and count the Akt1 shRNA and scrambled shRNA-transfected cells as explained in steps 2–5

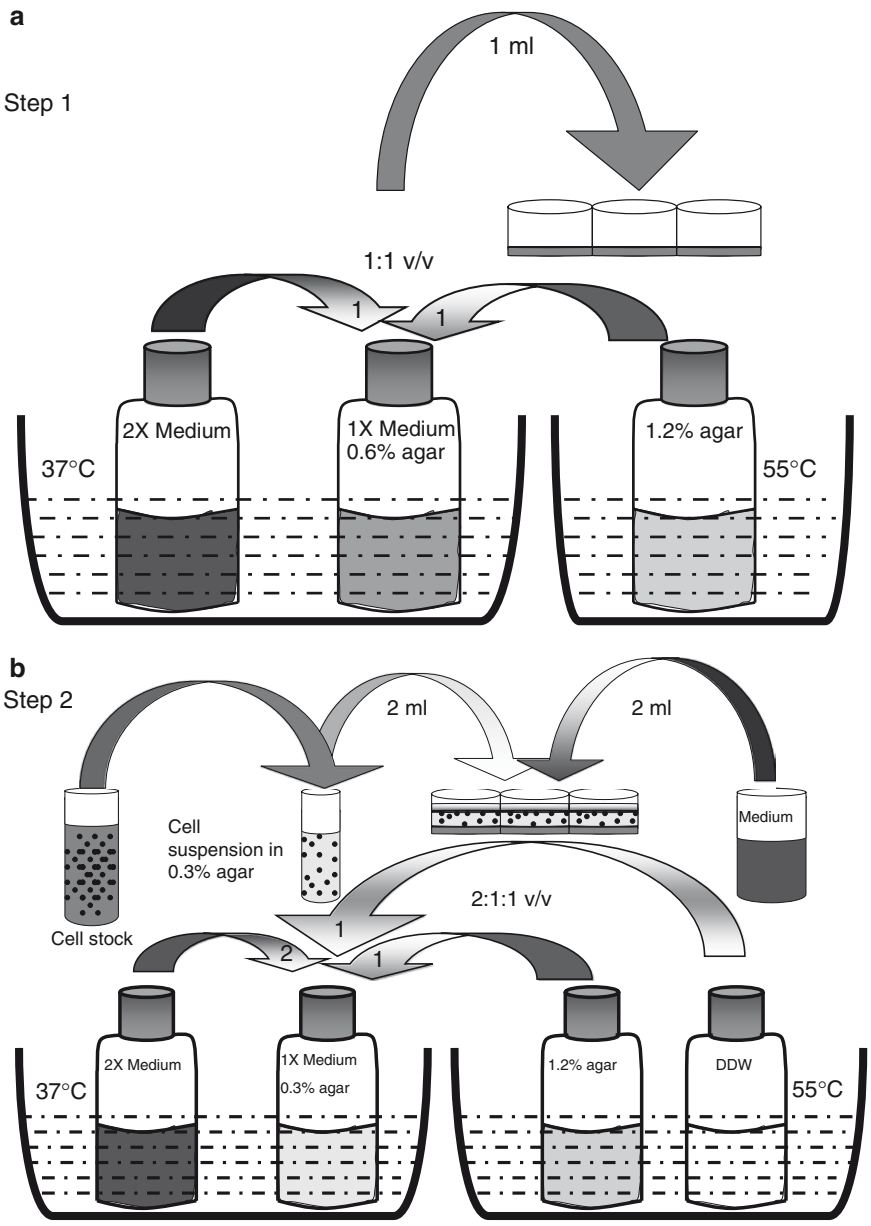

Fig. 4. Soft agar assay for the measurement of cancer cell malignancy: (**a**) step 1, preparation of agar underlay, (**b**) step 2, suspending cells in soft agar, and

under Subheading 3.5.2. Also, use untreated cells as a control. Store some cells from the total samples for Western blot confirmation of Akt1 silencing.

3. Prepare cell suspension in serum-free RPMI medium.
4. Add 2 ml prewarmed RPMI medium (20% FBS) as a chemoattractant to each well of a six-well plate (lower chamber).

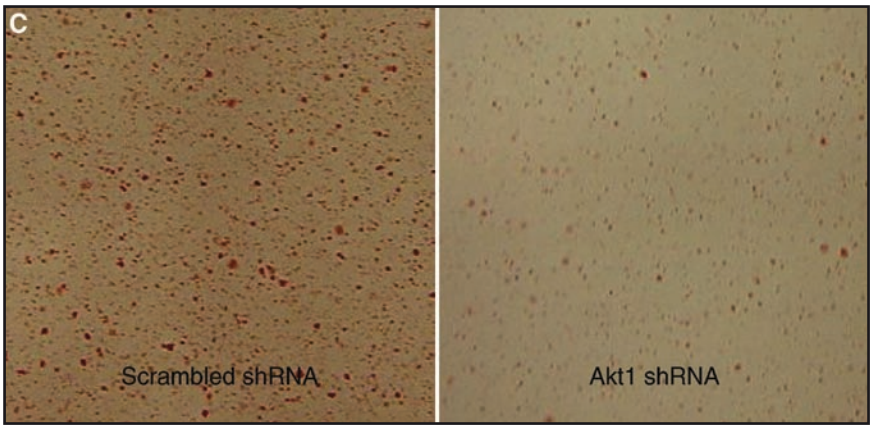

Fig. 4. (continued) (**c**) colony formation on soft agar gel (6). (Reproduced by permission with Elsevier)

5. Gently place cell culture insert into the well with sterile forceps. Avoid air trapping under the inset by tilting the insert while lowering it into the well.
6. Add 1×10^5 cells from the above cell suspension into the insert chamber (upper chamber) and move it gently for uniform distribution of the cells.
7. Incubate the assembly at 37°C in a 5% CO_2 incubator for 24 h.
8. After 24 h incubation, remove medium from the upper chamber using pasture pipette. (Do not use high pressure to remove medium as this might detach migrated cells.)
9. Remove cells on the topside (upper chamber side) of the filter by scrubbing twice with cotton tipped swab, moistened with serum-free medium or scrabber. (Do not use trypsin-EDTA to remove cells from the membrane.) Slightly raise the insert from the medium to prevent detachment of migrated cells (lower chamber) in medium.
10. Sequentially arrange four six-well plates filled with 100% ice cold methanol, PBS, Giemsa stain, and PBS again.
11. Transfer the inserts into these four 6-well plates by inserting lower chamber into these solutions. First insert into 100% methanol for 1 min, then wash with PBS and insert into Giemsa stain for 15 min. Again wash two to three times with PBS to remove excess of stain (Fig 5a).
12. Detach the membrane from the inserts by cutting with a sharp blade, and observe the lower portion under the microscope.
13. Count the number of migrated cells using Neubauer chamber in three different fields of observation (Fig. 5b).

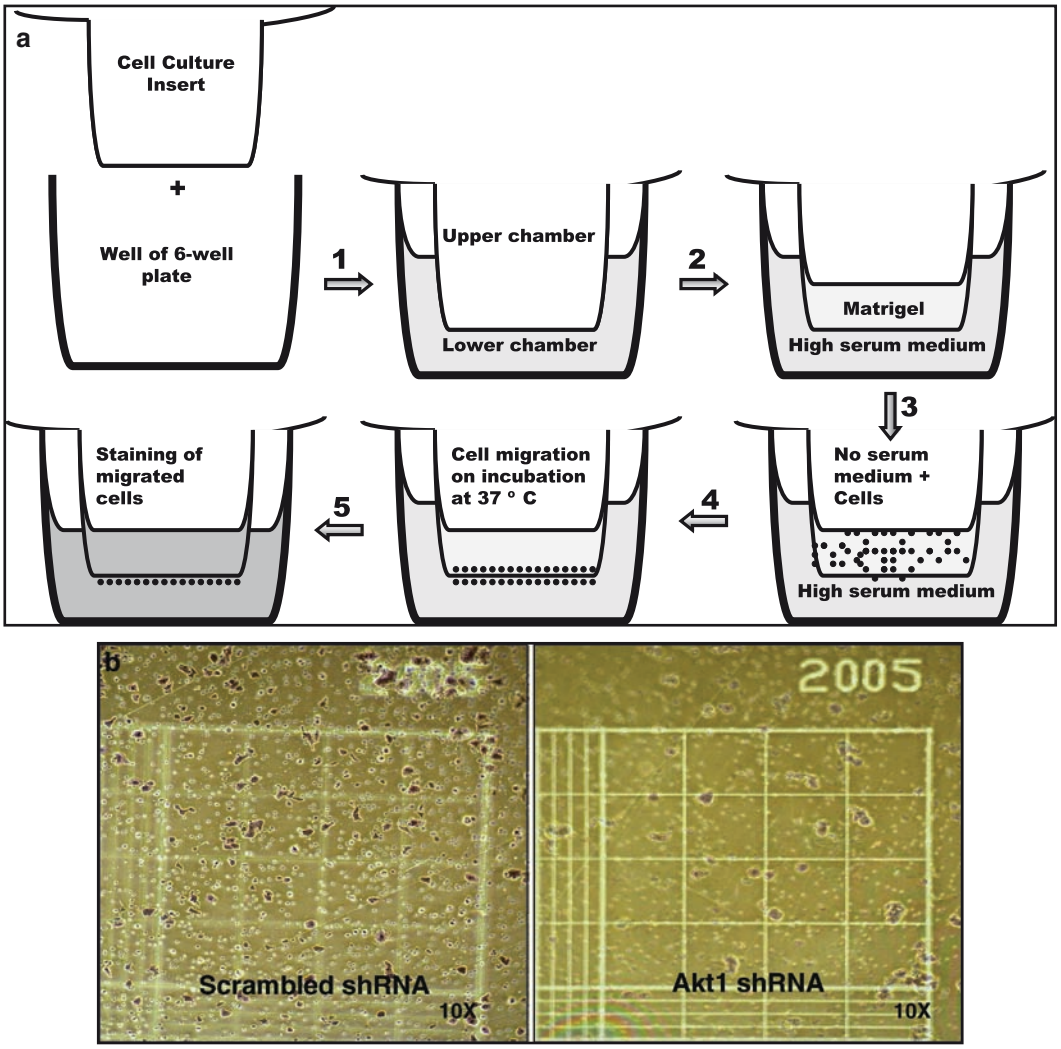

Fig. 5. Transwell cell culture insert assay for the measurement of cell invasion and migration: (**a**) schematic procedure for the assay (**b**) microscopic observation and counting of migrated cells (6). (Reproduced by permission with Elsevier)

14. Normalize the values with untreated cells and scrambled shRNA-treated cells in order to determine the percentage of cell migration.

3.7.2. Transwell-Matrigel Assay for Measuring Invasive Migration of Cancer Cells

1. Perform **steps 1–5** as described in above Subheading 3.7.1.
2. Thaw Matrigel at 4°C overnight.
3. Dilute Matrigel (5 to 1 mg/ml) in serum-free, cold RPMI 1640 medium.
4. Put 100–300 µl of the diluted Matrigel into upper chamber of the six-well cell culture insert, and spread immediately to form an uniform layer on the inner surface of the membrane.

5. Incubate the cell culture insert at 37°C for at least 4–5 h for gelling.
6. After gel formation, carry out steps 6–14 exactly the same way as described in above Subheading 3.7.1.

4. Notes

1. Minimize its exposure in atmosphere to prevent moisture absorption.
2. For all siRNA-based experiments, RNase-free conditions should be followed strictly. All apparatus, solutions, and pipettes are treated with di-methyl propyl carbonate (DMPC) to make them RNase free, while pipette tips, Eppendorf tubes and water can be purchased directly in RNase-free certified form from Ambion RNA Company Ltd.
3. Prepare the medium from 10× concentrate to half the recommended final volume, and add twice the normal concentration of serum.
4. As polymeric carriers vary in chemical composition, they differ in their pDNA/siRNA binding capacity. Different polymeric carriers will have different optimal N/P ratios, and need to be optimized before performing siRNA studies. Also, in the same carrier if composition varies with mole ratios or with reaction conditions, then a shift in optimal N/P ratio is commonly observed.
5. The Michael addition reaction employed in the synthesis of PAE is highly sensitive to the presence of moisture/water at room or elevated temperature. Hence, reaction should be performed in a dry (no moisture/water) condition (anhydrous chemicals, thoroughly dry apparatus, dry environmental conditions etc.).
6. Dichloromethane (aDCM) is highly volatile and the sample may leak from the pipette very quickly, so transfer should be done carefully. Also, aDCM evaporates very quickly at room temperature, so precautions should be taken to minimize its evaporation from the container.
7. The rate of adding the PEGDA solution to PEI solution should be controlled to get the linear polymer and to avoid excessive branching or cross-linking. Rapid addition may form excessively branched PAE with low molecular weight, which may exhibit low transfection efficiency. The color of reaction mixture will change from yellow to dark red, and a gel like crude PAE will form as the reaction proceeds.

8. aDCM is a highly volatile solvent. Its rapid evaporation under vacuum will flash the product out of the flask; moreover, it may damage the flask. Hence, slow but complete removal of aDCM is essential for high yield and superior quality of product. Moreover, the product is very viscous in nature which makes removal of aDCM very difficult. If done incorrectly, it may result in excess aDCM in the final product. After making PAE solution, if excess aDCM is observed on the surface of water, then it is an indication of poor aDCM removal from the sample. Hence, sufficient time must be provided for complete aDCM evaporation; otherwise, the final PAE will be of inferior quality.
9. The dialysis membrane with MWCO 3500 or 2000 can also be used for high yield, but higher retention of low molecular weight PAE fragments may reduce transfection efficiency.
10. To minimize hydrolytic breakdown of the synthesized PAE, it is very important to maintain the temperature of water below 4°C at all times. Also, the volume of water and number of replacements are very crucial for complete purification of PAE.
11. Complete removal of moisture is a necessity for high stability of the PAE samples. Even small traces of moisture will degrade PAE and reduce its efficiency. The final PAE after complete drying, if synthesized correctly, will form yellow fluffy powder. Inferior quality PAE will appear yellow and sticky.
12. PAE is sensitive to moisture, and care should be taken to prevent exposure to the atmospheric moisture. To minimize this type of PAE degradation during handling, it can be subdivided and stored at –20°C.
13. PAE, PEI, PEGDA, and D_2O are hygroscopic and, if not handled carefully, they may absorb atmospheric moisture to give water peak in 1H-NMR spectra, which may interfere in correct estimation.
14. Avoid lag time in ^{1}H-NMR measurement as PAE may degrade rapidly by hydrolysis before correct estimation.
15. The mole composition of PEI to PEG is very important for the accurate calculation of total nitrogen content and N/P ratio.
16. In the case of polyamines, the charge ratio is defined as the N/P ratio; that is, the ratio of number of nitrogen atoms from polycation to phosphate groups from DNA. In the case of PAE, exact N/P ratio can be calculated on the basis of PEI composition obtained from ^{1}H-NMR. We routinely use N/P ratio of 45 for this PAE carrier. We also have evaluated some lower and higher N/P ratios in different cell types and observed a variation in transfection efficiency. Although optimal

balance between transfection efficiency and safety was observed at N/P 45, this needs to be reevaluated more systematically for different cell types and conditions.

17. Do not vortex vigorously to dissolve PAE. Also, do not keep solution at room temperature to minimize hydrolytic degradation.
18. The sequence of addition is very important for efficient complex formation. Always add pDNA solution into the cationic polymer solution. Also, addition of 1–3 µl of sterile nuclease-free sodium acetate buffer (25 mM; pH 5.2) is recommended for efficient complex formation.
19. In case of siRNA, the concentration of siRNA retained in complex with polymeric carrier at particular charge ratio is a critical factor. At higher concentrations of siRNA, leaching from the complexes or exchange with anionic proteins is a commonly observed phenomenon.
20. The sequence of addition is very important, so add siRNA solutions into the cationic polymer solution. Also, addition of 1–3 µl of sterile nuclease-free sodium acetate buffer (25 mM; pH 5.2) is recommended for efficient complex formation. The volume differences in Eppendorf tubes should be equalized using sterile nuclease-free ultra-pure water.
21. If polymer–siRNA complexes are very strong, then EtBr bands may not be clearly visible; however, success of the experiment can be confirmed from the bands of free siRNA and ladder. If band quality is weak or poorly visible, then increase either EtBr percentage or incubation time. Also, protect EtBr solution and gel from light. Longer UV exposure may reduce the quality of bands in picture.
22. If particle morphologies are not clearly visible due to the high polyplex concentration, then dilute the solution and observe again. For EF-TEM staining, another stain other than the specified one may be used on the basis of personal expertise.
23. For CLSM measurement, the cells should be seeded on a sterile, cellulose-coated cell culture coverslips instead of plate-wells for clear observation under microscope. A549 cells can attach and grow efficiently on the surface of uncoated glass cell culture coverslips; however, cellulose coating is necessary for most of the cell lines.
24. Although a few researchers prefer to perform Subheadings 3.3.1 and 3.3.2 together for co-transfection, at our experimental setup the silencing was superior when the gap between two transfections was high. The selection of optimum time gap is necessary to reduce cytotoxicity and to obtain maximum silencing.

25. Do not vortex vigorously; it might reduce transfection efficiency by complex aggregation.
26. If cells are not fixed, then immediate EGFP measurement should be done to minimize the transfected cell apoptosis.
27. Without fixing the cell samples, expression will be bright but samples need to be observed immediately and cannot be stored for long. Also, very delicate and careful handling is necessary.
28. Small DNA pellet is difficult to observe; hence, orient the precipitate containing tubes in the microcentrifuge in such a way that it is known where the pellet forms.
29. At all times (during and after preparation), protect labeled shRNA from the light, and perform all the operations by inserting Eppendorf tube in ice.
30. The rhodamine-labeled shRNA should not be used at a concentration less than 4 μg/ml as it will be difficult to visualize. Also, measurements at different time intervals (0.5–5 h) are recommended for best results.
31. The color of the medium will start changing slowly from yellow to brown on incubation. The rate of color change will be proportional to cell viability. If the color becomes very dark brown, then the values will exceed detection limit and will give misleading results. For accurate results, optimize the incubation time by observing at different time intervals like 0.5, 1, 1.5, 2, 2.5 h and select the optimum incubation time. Also, measurements can be done at 620 and 490 nm but values should not be over or under the detection limit.
32. If cells are not fixed, then immediate measurement should be done to minimize the cell death due to stress.
33. Always make sure that the agar medium for the top layer has adequate time to cool to 37°C before adding the cells to it.

References

1. Amarzguioui, M., Rossi, J.J. and Kim, D. (2005) Approaches for chemically synthesized siRNA and vector-mediated RNAi. *FEBS Lett.* **579,** 5974–5981.
2. Dykxhoorn, D.M. and Lieberman, J. (2006) Knocking down disease with siRNAs. *Cell* **126,** 231-235.
3. Engelke, D.R. and Rossi, J.J. (eds.) (2005) *RNA interference*. Elsevier, San Diego, California, USA.
4. Devi, G.R. (2006) siRNA-based approaches in cancer therapy. *Cancer Gene Ther.* **13,** 819-829.
5. Pai, S.I., Lin, Y.Y., Macaes, B., Meneshian, A., Hung, C.F. and Wu, T.C. (2006) Prospects of RNA interference therapy for cancer. *Gene Ther.* **13,** 464-477.
6. Jere, D., Xu, C.X., Arote, R., Yun, C.H., Cho, M.H. and Cho, C.S. (2008) Poly(beta-amino ester) as a carrier for si/shRNA delivery in lung cancer cells. *Biomaterials* **29,** 2535-2547.
7. Xu, C.X., Jere, D., Jin, H., Chang, S.H., Chung, Y.S., Shin, J.Y., *et al.* (2008) Poly(ester amine)-mediated, aerosol-delivered Akt1 small interfering RNA suppresses lung tumorigenesis. *Am. J. Respir. Crit. Care Med.,* **178,** 60-73.
8. Kim, T.H., Jiang, H.L., Jere, D., Park, I.K. and Cho, C.S. (2007) Chemical modification of chitosan as a gene carrier in vitro and in vivo. *Prog. Polym. Sci.* **32,** 726-753.

9. Gary, D.J., Puri, N. and Won, Y.Y. (2007) Polymer-based siRNA delivery: perspectives on the fundamental and phenomenological distinctions from polymer-based DNA delivery. *J. Control Release,* **121,** 64-73.
10. Jere, D., Yoo, M.K., Arote, R., Kim, T.H., Cho, M.H., Nah, J.W., Choi, Y.J. and Cho, C.S. (2007) Poly (amino ester) composed of poly (ethylene glycol) and aminosilane prepared by combinatorial chemistry as a gene carrier. *Pharm. Res.,* **25**, 875-885.
11. Jere, D., Kim, T.H., Arote, R., Jiang, H.L., Cho, M.H., Nah, J.W. and Cho, C.S. (2007) A Poly(β-amino ester) of spermine and poly(ethylene glycol) diacrylate as a gene carrier. *Key Eng. Mater.* **342-343**, 425-428.
12. Arote, R.B., Hwang, S.K., Yoo, M.K., Jere, D., Jiang, H.L., Kim, Y.K., et al. (2008) Biodegradable poly(ester amine) based on glycerol dimethacrylate and polyethylenimine as a gene carrier. *J. Gene Med.*, **10**, 1223-1235.
13. Arote, R., Kim, T.H., Kim, Y.K., Hwang, S.K., Jiang, H.L., Song, H.H., et al. (2007) A biodegradable poly(ester amine) based on polycaprolactone and polyethylenimine as a gene carrier. *Biomaterials* **28**, 735-744.
14. Jere, D., Arote, R., Cho, M.H. and Cho, C.S. (2008) *Biodegradable poly(B-amino ester) derivatives for gene and siRNA delivery.* NOVA, New York.
15. Mather, B.D., Vishwanathan, K., Miller, K.M. and Long T.E., (2006) Michael addition reactions in macromolecular design for emerging technologies. *Prog. Polym. Sci.* **31**, 487-531.
16. Akinc, A., Anderson, D.G., Lynn, D.M. and Langer, R. (2003) Synthesis of poly(beta-amino ester)s optimized for highly effective gene delivery. *Bioconjug. Chem.* **14,** 979-988.
17. Anderson, D.G., Lynn, D.M. and Langer, R. (2003) Semi-automated synthesis and screening of a large library of degradable cationic polymers for gene delivery. *Angew. Chem. Int. Ed. Engl.* **42,** 3153-3158.
18. Park, M.R., Han, K.O., Han, I.K., Cho, M.H., Nah, J.W., Choi, Y.J. and Cho, C.S. (2005) Degradable polyethylenimine-alt-poly(ethylene glycol) copolymers as novel gene carriers. *J. Control Release* **105,** 367-380.

Chapter 17

Cellular siRNA Delivery Using TatU1A and Photo-Induced RNA Interference

Tamaki Endoh and Takashi Ohtsuki

Abstract

RNA interference (RNAi)-mediated silencing of specific genes represents a powerful tool for analyzing protein function. It also has profound biotechnological applications for cellular engineering and therapeutics. However, it is necessary to have a method that controls RNAi in response to artificially regulated stimulation. We designed a fluorescently labeled carrier protein to deliver short hairpin RNA (shRNA) with activity that could be regulated via photostimulation. We constructed a cell-permeable RNA-binding protein (RBP) by fusing the U1A RBP and a HIV-1 Tat peptide, which was labeled with an Alexa Fluor 546 fluorophore (TatU1A-Alexa). TatU1A-Alexa bound specifically to shRNA, which contains a U1A-binding sequence. The TatU1A-Alexa/shRNA complex was then internalized into cells via an endocytotic pathway and redistributed from endosomes to the cytosol by photostimulation, which induced RNAi-mediated gene silencing. This successive strategy was termed CLIP-RNAi (*C*PP-*l*inked RBP-mediated RNA *i*nternalization and *p*hotoinduced *RNAi*).

Key words: siRNA, shRNA, TatU1A, CPP-RBP, RNA-binding protein, CLIP-RNAi

1. Introduction

In mammals, RNAi-mediated gene silencing can be induced by the cytosolic delivery of short double-stranded RNAs, termed small-interfering RNAs (siRNAs), or short hairpin RNAs (shRNAs) (1, 2). A wide variety of synthetic cationic carriers, such as lipids, polymers, and dendrimers, has been developed to deliver these RNAs (3), which can effect gene silencing in all cells within a culture dish. In this report, we describe a photoinducible RNAi method (4) that enables artificial control of timing, position, and strength of gene silencing.

We have devised a sequence-specific RNA carrier molecule (4), namely TatU1A-Alexa that contains three main parts:

Wei-Ping Min and Thomas Ichim (eds.), *RNA Interference*, Methods in Molecular Biology, vol. 623,
DOI 10.1007/978-1-60761-588-0_17,

(1) the HIV-1 Tat-peptide (–YGRKKRRQRRR–), which is one of the most well-characterized cell-penetrating peptides (CPPs); (2) a U1A RNA-binding protein; and (3) Alexa Fluor 546, which is attached to the Tat-U1A (TatU1A) fusion protein via a C-terminal Cys. Together with fused or conjugated biologically active macromolecules, the Tat-peptide internalizes into cells via an endocytotic pathway (5–7). Like many CPP-conjugated macromolecules that become trapped in endocytotic compartments after cellular internalization (8–10), TatU1A/shRNA complex molecules are also entrapped in endosomes. Fluorescently labeled CPPs entrapped in endosomes can be redistributed into the cytosol by photostimulation (11, 12). We attached Alexa Fluor 546 to TatU1A and found that the internalized TatU1A-Alexa/shRNA complex was redistributed from endosomes to the cytosol by photostimulation and that it caused RNAi-mediated gene silencing within the areas of photostimulation (4). A schematic diagram is shown in Fig. 1.

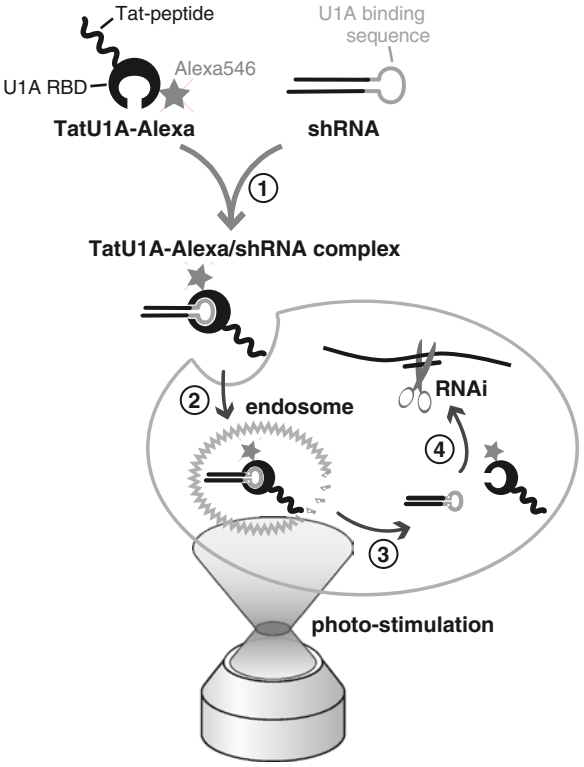

Fig. 1. Principle of TatU1A-Alexa-mediated RNA delivery and photoinducible RNAi. *1* TatU1A-Alexa forms a protein/RNA complex with shRNA, which contains a U1A binding sequence in its loop region. *t* Protein/RNA complex internalization and passage into the endocytotic pathway is mediated by the cell permeable Tat-peptide. *3* Internalized complex becomes trapped in cellular endosomes, but is redistributed into the cytosol by photostimulation, which excites the Alexa Fluor 546 fluorophore. *4* Redistributed shRNA causes RNAi-mediated silencing of specific genes

2. Materials

2.1. Expression and Purification of TatU1A

1. Plasmid pET-TatU1A-C is used for expression of the carrier protein TatU1A (4).
2. *Escherichia coli* BL21(DE3) competent cells (Novagen, US; Merck, Germany).
3. LB medium: 1% tryptone, 0.5% yeast extract and 1% NaCl. Kanamycin solution (final concentration 50 μg/mL; Sigma, US) is added following autoclave sterilization.
4. LB agar plate: LB medium with 1.5% Bacto agar. Kanamycin solution (final concentration 50 μg/mL) is added following autoclave sterilization, and then the medium is dispensed to sterilized petri dish.
5. Isopropyl β-D-1-thiogalactopyranoside (1 M; Nacalai Tesque, Japan) is dissolved in H_2O and stored in aliquots at −20°C.
6. SOC medium: 2% Bacto tryptone, 0.5% Bacto yeast extract, 10 mM NaCl, 2.5 mM KCl, 10 mM $MgSO_4$, 10 mM $MgCl_2$ and 20 mM glucose. The medium is prepared and autoclaved without $MgSO_4$ or glucose, which are filter sterilized and added subsequently.
7. Poly-Prep chromatography column (Bio-Rad, US).
8. Ni-NTA agarose (Qiagen, US) (see Note 1). Buffer solutions for protein purification (see Note 2):
9. Buffer A for sonication: 50 mM HEPES-KOH (pH 7.5), 150 mM $(NH_4)_2SO_4$, 7 mM $MgCl_2$, 20% glycerol, 7 mM β-mercaptoethanol, 100 μM phenylmethylsulfonyl fluoride (PMSF). Store at 4°C. β-mercaptoethanol and PMSF are added to the solution immediately prior to use.
10. Buffer B for wash: 50 mM HEPES-KOH (pH 7.5), 1 M NH_4Cl, 40 mM imidazole, 20% glycerol. Store at 4°C.
11. Buffer C for elution: 50 mM HEPES-KOH (pH 7.5), 100 mM $(NH_4)_2SO_4$, 150 mM imidazole, 20% glycerol. Store at 4°C.

2.2. Preparation of Alexa546-Labeled TatU1A

1. Alexa Fluor 546 C5 maleimide (10 mM; Molecular Probes, US) is dissolved in dimethyl sulfoxide (DMSO) and stored in aliquots at −20°C.
2. Transduction buffer (Buffer-T): 20 mM HEPES-KOH (pH 7.4), 115 mM NaCl, 5.4 mM KCl, 1.8 mM $CaCl_2$, 0.8 mM $MgCl_2$, 13.8 mM glucose. Prepare a 10× stock and dilute 5 mL with 45 mL sterile water for use. Store at 4°C.
3. Centri-Sep spin column (Princeton Separations, US).
4. Protein Assay Kit (Bio-Rad, US).

5. Bovine serum albumin (BSA) protein standard (2 mg/mL; Pierce, US). Store at 4°C. Dilute 5 μL with 45 μL sterile water for use (0.2 mg/mL standard BSA).

2.3. Cell Culture and RNA Delivery

1. Synthetic shRNA containing the U1A-binding sequence in its loop region (see Note 3). Dissolve the RNA in RNase-free water, denature at 90°C for 1 min, and then anneal by slow cooling (1°C/min) until 30°C (see Note 4). Store at –80°C.
2. Ham's F-12 medium (Sigma) supplemented with 10% fetal bovine serum (Biowest), 100 units/mL penicillin and 100 μg/mL streptomycin (Gibco, Invitrogen, US). Store at 4°C.
3. Hygromycin B solution (50 mg/mL; Roche, Switzerland) is stored at –20°C. Dissolve in cell culture medium at 100–500 μg/mL for use (see Note 5).
4. Trypsin solution (0.25 %) and ethylenediamine tetraacetic acid (EDTA; 1 mM; Gibco, Invitrogen). Store at 4°C.
5. 96-well cell culture plate with clear bottom and black wall (see Note 6).
6. RNase A solution (34 mg/mL) (Sigma) is stored at –20°C. Dissolve in cell culture medium at 34 μg/mL for use (see Note 7).

2.4. Photostimulation and Induction of RNAi

1. Inverted fluorescence microscope system to irradiate cells for excitation (IX51/IX2-FL-1/MP5Mc/OL-2; Olympus, Japan) (see Note 8).
   (a) 100-W halogen lamp (USH-1030L; Olympus) is used as a light source.
   (b) Various percentage neutral-density filters (ND filters; Olympus) are used to adjust the excitation intensity.
   (c) U-WIG mirror unit (Olympus) is used to irradiate cells with light at 540 ± 10 nm, the excitation wavelength for Alexa Fluor 546.
2. Cell Counting Kit-8 (Dojindo, Japan).

3. Methods

3.1. Expression and Purification of TatU1A

TatU1A is a recombinant fusion protein containing the cell-penetrating peptide Tat (YGRKKRRQRRR) and the minimal RNA-binding domain of U1 small nuclear ribonucleoprotein A (U1A). It is recommended that the purification procedure be performed at a low temperature (4°C) as this protein tends to aggregate at higher temperatures.

1. *E. coli* BL21(DE3) competent cells (50 μL) are mixed with pET-TatU1A-C (1–10 ng) and incubated on ice for 30 min.
2. The cells are transformed with pET-TatU1A-C by 1 min heat-shock at 42°C and subsequent 2 min incubation on ice.
3. SOC medium (300 μL) is added, and the cells are incubated at 37°C for 60 min.
4. Transformed cells are spread onto LB agar plate containing 50 μg/mL kanamycin and incubated at 37°C over night.
5. After 12–16 h, a single colony is transferred to 200 mL LB medium and incubated with shaking at 37°C until the A_{600} reaches 0.8–1.0.
6. After 30-min incubation at 25°C, protein expression is induced by addition of 1 mM IPTG, and the culture is incubated at 25°C with shaking for 16–20 h.
7. Cells are harvested by centrifugation (2,750×*g*, 10 min, 4°C) and suspended in 10 mL of buffer A (see Note 9).
8. Cells are sonicated for 15 min on ice, and soluble lysate is obtained by centrifugation (12,000×*g*, 30 min, 4°C) (see Note 10).
9. During centrifugation, 500 μL Ni-NTA agarose slurry (250 μL bed volume) is added to a chromatography column and initialized with buffer A.
10. The supernatant (soluble lysate) is applied to the Ni-NTA agarose and the top and bottom outlets of the column are capped immediately.
11. The column is rotated gently at 4°C for 20–60 min.
12. The caps are removed from the column allowing the lysate to flow out.
13. The column bed is washed with buffer A (10 mL) and then with buffer B (10 mL) (see Note 11).
14. TatU1A protein is eluted with buffer C (5 mL) and the eluates are collected in several tubes (1 mL each) (see Note 12).

3.2. Preparation of Alexa546-Labeled TatU1A (TatU1A-Alexa)

1. Alexa Fluor 546 C5 maleimide (100 μM final concentration) is added to the purified TatU1A and then incubated at 25°C for 1 h in the dark (see Note 13).
2. During the incubation, a Centri-Sep spin column is initialized for 30 min with 800 μL buffer-T. The column is then centrifuged (750×*g*, 2 min, 4°C), after which buffer-T (400 μL) is reapplied and the column is centrifuged again (750×*g*, 2 min, 4°C).
3. TatU1A-Alexa reaction mixture is loaded onto the Centri-Sep spin column.
4. Centrifugation (750×*g*, 2 min, 4°C) of the Centri-Sep spin column is used to replace the labeling reaction buffer

containing TatU1A-Alexa, with buffer-T (see Note 14). Protein concentration is quantified using a 0.2 mg/mL standard BSA solution and Protein Assay Kit.

5 Absorbance at 556 nm is used to quantify labeled TatU1A and determine labeling efficiency (see Note 15).

3.3. RNA Delivery and Induction of RNAi by Photostimulation

Medium or buffer replacement is required at several points during the experimental procedure, and it is important to pipette carefully in order to ensure that cells are not lost. To obtain reliable results, it is important to prepare replicate wells (at least in duplicate), as well as to run controls (see Note 16).

1. One day prior to the experiment, Chinese hamster ovary (CHO) cells expressing EGFP (see Note 5) are seeded into a 96-well culture plate and grown to 70% confluence.
2. TatU1A-Alexa (2 μM) and 200 nM shRNA, containing the U1A-binding sequence, are mixed in 50 μL buffer-T and then incubated at 37°C for 10 min for formation of the TatU1A-Alexa/shRNA complex (see Note 17).
3. During the 10 min incubation, cells are washed once with buffer-T (200 μL).
4. Following replacement of the buffer with the preincubated complex, the cells are incubated at 37°C for 3 h.
5. To remove extracellularly bound RNAs, cells are washed twice (30 min × 2) at 37°C with Ham's F-12 medium containing 34 μg/mL RNase A.
6. The RNase-containing medium is then replaced with normal Ham's F-12 medium (200 μL).
7. Cells are irradiated at 540 ± 10 nm (U-WIG mirror unit) using a 4× or 40× objective lens, which causes the redistribution of the TatU1A-Alexa/shRNA complex from the endosome to cytosol (see Notes 18, 19).
8. Cells are incubated at 37°C until gene silencing appears to have reached a maximum (see Note 20).
9. After incubation for 22 h, the culture medium is replaced with medium containing substrate for the Cell Counting Kit-8 (10 μL/well). After a 1 h incubation with the cell-counting substrate at 37°C (see Note 21), the A_{450} of each well is measured by a microwell plate reader.
10. At 24 h after photostimulation, cells are washed twice with buffer-T, and then, buffer-T (100 μL) is added to each well.
11. Cellular fluorescence (EGFP) signals are measured directly without cell lysis using a fluorescence microwell plate reader (480 nm excitation and 540 nm emission filter set), after which gene silencing is evaluated (see Note 22).
12. Cellular fluorescence signals are then imaged by fluorescence microscopy (see Note 23).

4. Notes

1. There are many commercially supplied affinity reagents for purification of His-tagged proteins. We confirmed that Ni-NTA agarose performed well.
2. β-mercaptoethanol is added to buffer A as reductant to cleave disulfide bonds. However, it should not be added to buffer C because it reacts with the Alexa Fluor 546 C5 maleimide.
3. shGFP*U1A* is an shRNA that targets EGFP mRNA. Its sequence is 5′- GGCUACGUCCAGGAGCGCACAUUGCACUCCGUGCGCUCCUGGACGUAGCCUU-3′. The underlined sequence represents a U1A-binding sequence, inserted into the shRNA loop region. Other parts of the sequence generate a double-stranded 19-mer and a 3′ UU overhang. The double-stranded region can be replaced, depending upon the target mRNA sequence. We purchased synthetic RNAs from Japan Bio Services Co., Ltd.
4. When the shRNA is dissolved in water, both intra- and intermolecular double strands are formed. Thus, the shRNA should be denatured and cooled slowly, in order to enhance intramolecular annealing.
5. CHO cells expressing destabilized EGFP (dEGFP-CHO cells) were prepared using a Flp-In-recombination system containing Flp-In-CHO cell line (Invitrogen) (4]. To maintain EGFP expression, cells are cultured in medium containing 100–500 μg/mL of hygromycin B. However, hygromycin B is not added to the culture medium when cells are seeded into the 96-well culture plate.
6. A 96-well plate with a clear bottom and black wall provides a better background for evaluation of cellular fluorescence intensity than an entirely clear plate.
7. RNase A is a stable, strong nuclease and thus, it is important that it does not contaminate samples or stock solutions.
8. Microscopy could be performed using general fluorescence microscopy and mirror units that emit light around 540 nm. The intensity of excitation light will affect the optimum con ditions for photostimulation (see Note 19).
9. Harvested cell pellets can be stored at −80°C for later use.
10. Sonication times and power depend upon the instrument. The cell suspension becomes somewhat transparent after cell wall disruption.
11. Buffers A and B flow out via gravity. However, if the flow rate is particularly slow, we pump buffers out under pressure.
12. Eluted proteins are analyzed by 15% SDS-PAGE and stained with Coomassie Brilliant Blue (CBB), in order to estimate

their purity and concentration. Sufficiently purified fractions are collected in one tube and then aliquotted for the next labeling step. It is preferable that the protein concentration does not exceed 0.5 mg/mL because Alexa546-labeled TatU1A easily aggregates at high concentrations (see Note 14). Proteins are stored at −80°C.

13. Under the protein concentrations of 10–20× molar excess of Alexa Fluor 546 C5 maleimide, we were unable to obtain sufficient amounts of labeled TatU1A, due to aggregation. We suggest 100 μM of Alexa Fluor 546 C5 maleimide, which represents approximately 5× the protein concentration. In addition, a 1 h reaction time is sufficient for labeling protein as extended reactions result in aggregation.
14. The maximum volume that can be processed per column is 100 μL. If the reaction volume is greater than 100 μL, several columns should be utilized.
15. At 556 nm, the molar absorbance coefficient of Alexa 546 is 104,000 L/mol cm. Labeling efficiency is given as $((A_{556}/104{,}000)/\text{Protein concentration})$. We usually obtain a labeling efficiency 0.6–0.8. It is recommended that the labeling efficiency be adjusted using separately dialyzed TatU1A, in order to obtain reproducible results (see Note 19).
16. The required controls are: (1) cells treated with buffer-T alone and no TatU1A-Alexa or shRNA; and (2) wells without any cells (see Notes 21, 22).
17. For efficient delivery of RNA and RNAi, a 10× molar concentration of TatU1A-Alexa is required for shRNA.
18. In the culture well, cells were irradiated completely using a 4× objective lens, with a focal point of 7 mm (diameter). In contrast, local irradiation was performed using a 40× objective lens, with a focal point of 0.7 mm.
19. Optimum conditions for photostimulation are affected by the labeling efficiency of TatU1A-Alexa and light intensity at the focal point. In cases of low-labeling efficiency and weak light intensity, longer irradiation times are required for efficient downregulation of gene expression. However, excessive photostimulation impairs cellular proliferation, and causes cells to assume a more rounded shape. Optimization of irradiation conditions, such as irradiation length and type of ND filters, is recommended.
20. Incubation time depends upon the target mRNA. With respect to destabilized EGFP, gene silencing appears 20–30 h after photostimulation.
21. Incubation time depends upon cell line and cell number. Too short incubation causes too weak absorbance, and too long

incubation makes the absorbance saturated. It is recommended to measure A_{450} of each well after 30 min, 1 h and 2 h, and use the results of appropriate incubation time. Measured values are normalized by subtracting those of wells without cells. Relative cell proliferation is evaluated from these values. Values for cells incubated with buffer-T without TatU1A-Alexa and RNA during the 3 h before photostimulation are considered to have 100% proliferation.

22. Cellular fluorescence intensity is normalized by subtracting the fluorescence of wells without cells. Relative fluorescence intensity is determined against cell number, providing an indication of relative gene expression, and it is calculated after cell counting. Values for cells incubated with buffer-T alone during the 3 h before photostimulation are considered to be 100%.
23. In the case of local stimulation via a 40× objective lens, evaluation of cell proliferation is not necessary. Position-specific RNAi is evaluated by imaging cellular fluorescence signals around the stimulated position at 24 h after the photostimulation.

    Figs. 2 and 3 represent examples of RNAi-mediated EGFP silencing using 4× and 40× objective lenses, respectively.

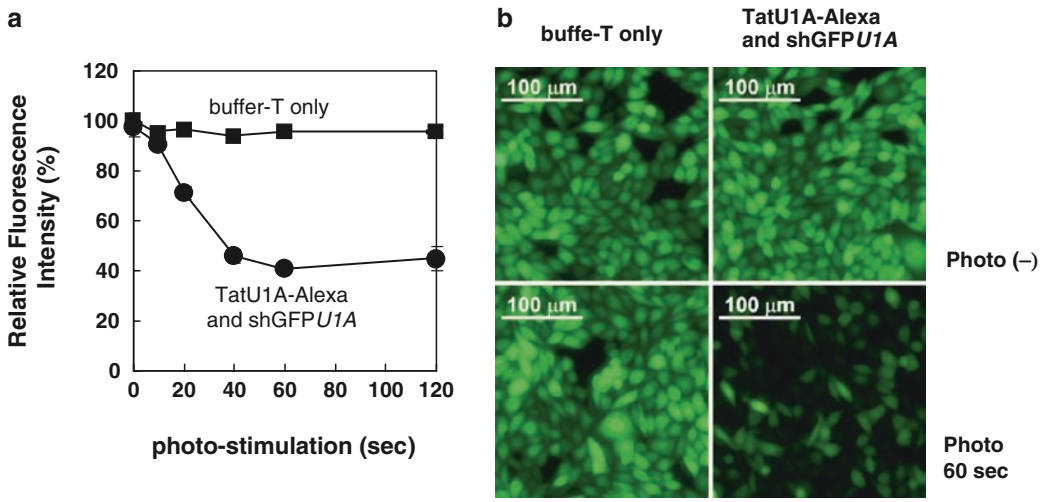

Fig. 2. Induction of RNAi-mediated EGFP silencing via photostimulation. dEGFP-CHO cells were treated with a complex of TatU1A-Alexa (2 μM) and shGFP*U1A* (200 nM). Cells in a 96-well plate were irradiated (540 ± 10 nm) completely using a 4× objective lens. Relative EGFP intensity was evaluated after 24-h incubation. (**a**) EGFP silencing is dependent upon photostimulation time. Fluorescence decreased with length of photostimulation from 0–60 s. (**b**) Cellular fluorescence images with (60 s) or without photostimulation. EGFP silencing was not observed in the absence of photostimulation due to complete endosomal entrapment of the TatU1A-Alexa/shRNA complex

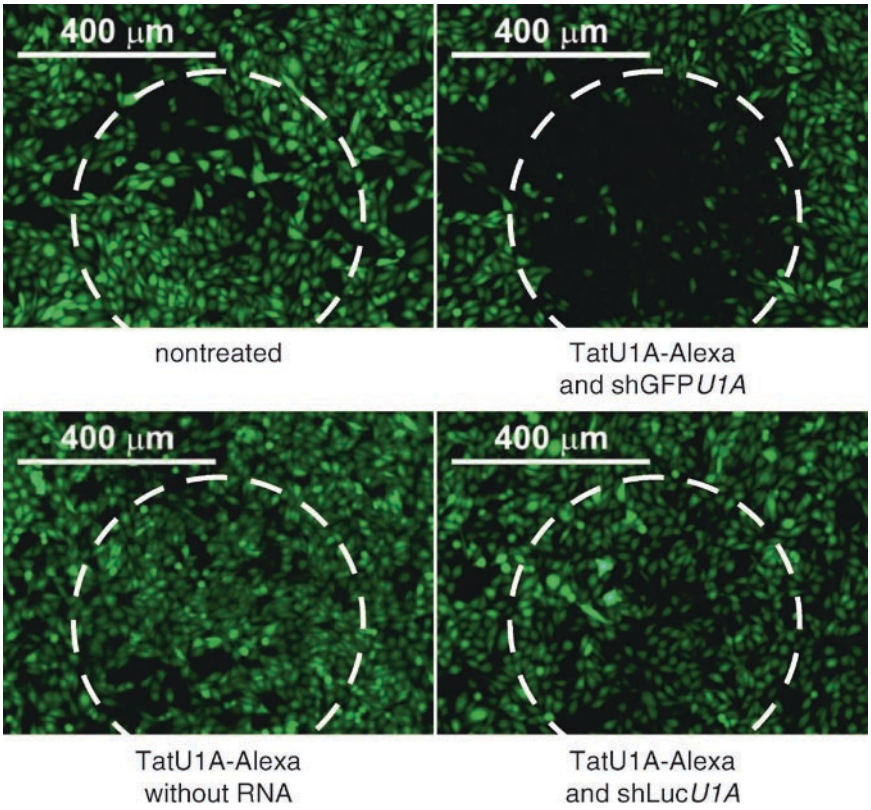

Fig. 3. Position-specific EGFP silencing using local photostimulation. dEGFP-CHO cells were treated with a complex of TatU1A-Alexa (2 μM) and shGFP*U1A* (200 nM). The cells were photostimulated (5 s) locally using a 40× objective lens. Light from the halogen lamp was reduced to 12% using an ND filter. Cellular fluorescence signals around the stimulated area were imaged after 20 h incubation. Stimulated areas are located inside the circle. EGFP silencing was observed only in the sample treated with TatU1A-Alexa/shGFP*U1A* complex and was limited to the stimulated area

Acknowledgments

We thank Prof. M. Sisido (Okayama University) for valuable discussions. This work was supported by a grant from the New Energy and Industrial Technology Development Organization (NEDO) (05A02707a).

References

1. Caplen, N. J., Parrish, S., Imani, F., Fire, A., and Morgan, R. A. (2001) Specific inhibition of gene expression by small double-stranded RNAs in invertebrate and vertebrate systems. *Proc. Natl. Acad. Sci. USA*. **98**, 9742–9747.

2. Elbashir, S. M., Harborth, J., Lendeckel, W., Yalcin, A., Weber, K., and Tuschl, T. (2001) Duplexes of 21-nucleotide RNAs mediate RNA interference in cultured mammalian cells. *Nature* **411**, 494–498.

3. Zhang, S., Zhao, B., Jiang, H., Wang, B., and Ma, B. (2007) Cationic lipids and polymers mediated vectors for delivery of siRNA. *J. Control Release* **123**, 1–10.
4. Endoh, T., Sisido, M., and Ohtsuki, T. (2008) Cellular siRNA delivery mediated by a cell-permeant RNA-binding protein and photoinduced RNA interference. *Bioconjug. Chem.* **19**, 1017–1024.
5. Murriel, C. L., and Dowdy, S. F. (2006) Influence of protein transduction domains on intracellular delivery of macromolecules. *Expert Opin. Drug Deliv.* **3**,739–746.
6. Wadia, J. S., and Dowdy, S. F. (2002) Protein transduction technology. *Curr. Opin. Biotechnol.* **13**, 52–56.
7. Brooks, H., Lebleu, B., and Vives, E. (2005) Tat peptide-mediated cellular delivery: back to basics. *Adv. Drug Deliv. Rev.* **57**, 559–577.
8. Wadia, J. S., Stan, R. V., and Dowdy, S. F. (2004) Transducible TAT-HA fusogenic peptide enhances escape of TAT-fusion proteins after lipid raft macropinocytosis. *Nat. Med.* **10**, 310–315.
9. Abes, S., Williams, D., Prevot, P., Thierry, A., Gait, M. J., and Lebleu, B. (2006) Endosome trapping limits the efficiency of splicing correction by PNA-oligolysine conjugates. *J. Control Release* **110**, 595–604.
10. Michiue, H., Tomizawa, K., Wei, F. Y., Matsushita, M., Lu, Y. F., Ichikawa, T., et al. (2005) The NH2 terminus of influenza virus hemagglutinin-2 subunit peptides enhances the antitumor potency of polyarginine-mediated p53 protein transduction. *J. Biol. Chem.* **280**, 8285–8289.
11. Maiolo, J. R., 3rd, Ottinger, E. A., and Ferrer, M. (2004) Specific redistribution of cell-penetrating peptides from endosomes to the cytoplasm and nucleus upon laser illumination. *J. Am. Chem. Soc.* **126**, 15376–15377.
12. Matsushita, M., Noguchi, H., Lu, Y. F., Tomizawa, K., Michiue, H., Li, S. T., et al. (2004) Photo-acceleration of protein release from endosome in the protein transduction system. *FEBS Lett.* **572**, 221–226.

Chapter 18

Polyethylenimine (PEI)/siRNA-Mediated Gene Knockdown In Vitro and In Vivo

Sabrina Höbel and Achim Aigner

Abstract

Since its discovery about 10 years ago, RNA interference (RNAi) has become an almost standard method for the knockdown of any target gene of interest. It is mediated by small interfering RNAs (siRNAs), which trigger a catalytic mechanism for mRNA degradation. Consequently, the delivery of intact siRNA is of critical importance for the induction of RNAi. Due to the physicochemical and biological properties of siRNAs, resulting in high instability and poor cellular uptake, siRNA modifications and pharmaceutical formulations have been used to enhance RNAi efficacy. This is particularly relevant for the in vivo delivery of siRNAs, which still poses a major hurdle for the experimental or therapeutic application of RNAi.

Polyethylenimines (PEIs) are water-soluble, linear, or branched synthetic polymers of variable length with protonable amino groups in every third position. We have shown that certain PEIs are able to form noncovalent complexes with siRNAs, which mediate their protection against nucleolytic degradation as well as enhance their cellular uptake and intracellular release. In this chapter, the preparation and use of PEI/siRNA complexes for various in vitro and in vivo applications are described. Examples for conducting gene targeting experiments and the analysis of knockdown efficacies are given.

Key words: RNA interference, Small interfering RNA, Polyethylenimine, In vivo siRNA delivery, Gene knockdown, RNAi, siRNA, PEI

1. Introduction

Since its discovery in the late 1990s (1), RNA interference (RNAi) has emerged as a naturally occurring, powerful method for the knockdown of any target gene of interest. While this provides a powerful tool for the functional analysis of a given gene product, it may also lead to the therapeutic inhibition of pathologically relevant target genes, which are upregulated in a given pathology. RNAi is mediated by small interfering RNAs (siRNAs), which

Wei-Ping Min and Thomas Ichim (eds.), *RNA Interference,* Methods in Molecular Biology, vol. 623,
DOI 10.1007/978-1-60761-588-0_18,

exert a catalytic, sequence-specific mechanism for the degradation of their target mRNA (see (2) for review). Since all other components of the RNAi machinery are provided by the target cells, the siRNA delivery is of critical importance and rate-limiting for the induction of RNAi. Beyond the selection of optimal siRNA sequences (3), the choice of a strategy that (i) protects siRNAs against degradation, (ii) mediates their cellular uptake, (iii) allows their escape from endosomes/lysosomes, and (iv) results in their correct intracellular localization will determine the success for the induction of RNAi especially in vivo (see (2, 4) for review). Additional aspects include favourable pharmacokinetic parameters, high biocompatibility/low toxicity as well as the absence of unwanted side effects.

Polyethylenimines (PEIs) are synthetic branched or linear polymers, which are available at various different molecular weights (5–8). Based on the partial protonation of the amino groups in every third position, they possess a high cationic charge density already at physiological pH and are thus able to form noncovalent complexes with negatively charged siRNAs. This leads to the siRNA compaction ("condensation") and the shielding of their negative charges and allows the endocytosis of the nanometer size complexes. While siRNA complexation occurs with all PEIs, only certain PEIs are suitable for siRNA delivery (see Note 1). These include the commercially available, linear, ~22 kD jetPEI (9, 10) as well as the branched ~10 kD PEI F25-LMW, which is purified from 25 kD PEI through size exclusion chromatography (8). Both PEIs display high efficacies as well as low cytotoxicity in vitro and in vivo ((8); Höbel et al., under review).

2. Materials

2.1. Preparation of PEI/siRNA Complexes

1. Complexation Buffer: 0.15 M NaCl, 0.01 M HEPES, pH 7.4 is prepared with nuclease-free water, and pH is adjusted with HCl. Sterile filtered 50 mL aliquots are stored at –20°C or, once thawed, at 4°C.
2. Predesigned siRNAs (e.g., luciferase siRNAs GL2 and GL3 from MWG, Ebersberg, Germany) or custom-made siRNAs (e.g., from Ambion, Foster City, CA, USA or Dharmacon, Lafayette, CO, USA) are dissolved according to the manufacturer's instructions in buffer or nuclease-free water. Aliquots of a 100 µM stock solution are stored at –80°C. A 20 µM dilution is used as working solution, which is stored at –20°C to –80°C.
3. jetPEI is from Polyplus (Illkirch, France). Note that "jetPEI" is used for in vivo experiments when working with siRNAs (not "in vivo jetPEI"). PEI F25-LMW is prepared from the commercially available branched 25 kD polyethylenimine

(Sigma-Aldrich, St. Louis, MO, USA) by gel filtration as described (8). It is filter sterilized through a 0.2 µm filter and stored at 4°C (see Note 2).

2.2. Transfection of Cells in Tissue Culture

1. Dulbecco's PBS without Ca and Mg is stored at 4°C. 0.5 mg/mL Trypsin/0.22 mg/mL EDTA (PAA, Pasching, Austria) is stored at –20°C or, for shorter time periods, at 4°C.
2. Iscove's Modified DMEM (IMDM) (PAA, Pasching, Austria) supplemented with 10% fetal calf serum (FCS) (Invitrogen, Carlsbad, CA, USA) is stored at 4°C.
3. Normocin 50 mg/mL (InvivoGen, San Diego, CA, USA), an antibiotic against mycoplasma, bacteria and fungi, is stored at –20°C. 1 mL Normocin is diluted in 500 mL cell culture medium (see Note 3).

2.3. Determination of Targeting Efficacies: Quantitative RT-PCR (qRT-PCR)

1. peqGOLD TriFast™ (PEQLAB, Erlangen, Germany) is stored at 4°C, protected from the light. This reagent contains phenol and guanidinium thiocyanate. Work under a hood and avoid skin contact.
2. Revert Aid™ H Minus M-MuLV Reverse Transcriptase, 200 u/µL supplied in 50 mM Tris–HCl (pH 8.3), 0.1 M NaCl, 1 mM EDTA, 5 mM DTT, 0.1% (v/v) Triton X-100, 50% (v/v) glycerol and 5× Reaction Buffer: 250 mM Tris–HCl (pH 8.3), 250 mM KCl, 20 mM $MgCl_2$, 50 mM DTT (Fermentas, St. Leon-Rot, Germany) are stored at –20°C.
3. 20× Random Hexamer Primer, a 100 µM mixture of single-stranded random hexanucleotides with 5′- and 3′-hydroxyl ends, 10 mM dNTP Mix and RiboLock™ RNase Inhibitor, 40 u/µL (Fermentas, St. Leon-Rot, Germany) are stored at –20°C.
4. The QuantiTect™ SYBR® Green PCR Kit (Qiagen, Hilden, Germany) consists of 2× QuantiTect™ SYBR® Green PCR Master Mix and RNase-free water and is stored at –20°C, protected from the light. 2× QuantiTect™ SYBR® Green PCR Master Mix contains HotStarTaq® DNA Polymerase, QuantiTect™ SYBR® Green PCR Buffer (Tris–HCl, KCl, $(NH_4)_2SO_4$, 5 mM $MgCl_2$, pH 8.7), dNTP mix including dUTP, SYBR® Green I, ROX (passive reference dye), 5 mM $MgCl_2$.
5. Actin forward (5′-CCA ACC GCG AGA AGA TGA-3′) and actin reverse (5′-CCA GAG GCG TAC AGG GAT AG-3′) primers as well as qRT-PCR primers specific for the gene of interest (MWG, Ebersberg, Germany, or any other provider of DNA oligonucleotides) are dissolved in nuclease-free water. A 100 µM stock solution and 5 µM aliquots of a mix of forward and reverse primers ("specific primers" and "loading control primers") are stored at –20°C.
6. 6× DNA loading dye and GeneRuler™ 1 kb DNA Ladder (Fermentas, St. Leon-Rot, Germany) are stored at 4°C.

2.4. Determination of Targeting Efficacies: Luciferase Assay

1. The Luciferase Assay System (Promega, Madison, WI, USA) consisting of Luciferase Cell Culture Lysis Reagent 5×: 125 mM Tris–phosphate (pH 7.8), 10 mM DTT, 10 mM 1,2-diaminocyclohexane-*N,N,N′,N′*-tetraacetic acid, 50% (v/v) glycerol, 5% (v/v) Triton® X-100, Luciferase Assay Buffer and Luciferase Assay Substrate are stored at –20°C. The reconstituted Luciferase Assay Reagent, i.e., Luciferase Assay Substrate dissolved in Luciferase Assay Buffer, can be stored in aliquots at –20°C for up to 1 month or at –70°C for up to 1 year. Protect from light (see Note 4).

2.5. In Vivo Gene Targeting Through Systemic or Local Administration of PEI/siRNA Complexes in Mouse Tumor Xenograft Models

1. Athymic Nude Mice – Hsd:Athymic Nude-Foxn1^{nu} (Harlan, Indianapolis, IN, USA) are used for experiments with tumor xenografts (see Note 5). For other applications, immunocompetent mice or other transgenic/mutant mice may be employed as well.
2. Isoflurane (Baxter, Unterschleissheim, Germany), an inhalation anesthetic. Store at 4°C, avoid exposure.
3. Steril single-use syringes and needles (26 gauge × ½″ for subcutaneous cell injection and i.p. complex injection, 30 gauge × ½″ for i.v. complex injection).
4. Microvette® CB 300, system for capillary blood collection (Sarstedt, Nümbrecht, Germany).

2.6. Determination of siRNA Biodistribution Through Anaylsis of [^{32}P]-Labeled siRNAs

1. [γ-^{32}P]-ATP (6,000 Ci/mmol, 20 mCi/mL EasyTide Lead; PerkinElmer, Waltham, MA, USA) is stored at 4°C.
2. T4 Polynucleotide Kinase and 10× Reaction Buffer A for T4 Polynucleotide Kinase: 500 mM Tris–HCl, pH 7.6, 100 mM $MgCl_2$, 50 mM DTT, 1 mM spermidine and 1 mM EDTA (Fermentas, St. Leon-Rot, Germany) are stored at –20°C.
3. 0.5 M EDTA, pH 8.0 is stored at room temperature.
4. Micro Bio-Spin® 6 Chromatography Columns (Bio-Rad, Hercules, CA, USA) are stored at 4°C.
5. Agarose NEEO (Carl Roth, Karlsruhe, Germany).
6. MOPS buffer (10×): 0.4 M MOPS (3-(N-morpholino) propanesulfonic acid), pH 7.0, 0.1 M Na-acetate, 0.01 M EDTA are dissolved in 1 L DEPC-treated, autoclaved water. After filtration, the buffer should be stored at room temperature, protected from light.
7. SSC buffer (20×): 3 M NaCl and 0.3 M Na_3-citrate × $2H_2O$ are dissolved in 1 L ddH_2O and autoclaved. Store at room temperature.
8. Loading dye (10×): 0,1% (w/v) xylenecyanol, 0,1% (w/v) bromphenol blue, 50% (v/v) glycerol, 50% (v/v) ddH_2O. Store at room temperature or at 4°C.

9. Nylon membrane Hybond™-N (GE Healthcare, Chalfont St. Giles, UK).
10. Chromatography Paper 3MM CHR (Whatman, Maidstone, UK).

3. Methods (see Note 6)

Critical parameters for PEI-mediated siRNA delivery are the size, net charge and stability of the complexes as well as complexation efficacy and biocompatibility/toxicity. These properties are influenced by the PEI molecular weight and degree of branching, the ratio between PEI and nucleic acids (the so-called N/P ratio referring to the nitrogen atoms of PEI and the nucleic acid phosphates), the buffer conditions employed during complexation, and the molecular weight of the nucleic acid. Additionally, covalent coupling of the PEI to other polymers like polyethyleneglycol (=PEGylated PEIs, PEG–PEIs) can lead to markedly altered complex properties due to shielding of the net complex charge, which is still under investigation.

For the in vitro delivery of siRNAs, several transfection reagents are commercially available with PEI being one example. In vivo, however, only a very limited set of reagents or strategies exist for the direct application of siRNAs to induce RNAi for analytical or therapeutic purposes. The two low-molecular weight PEIs described here have been shown to efficiently deliver siRNAs while displaying low cytotoxicity: the commercially available linear ~22 kD jetPEI and the branched ~10 kD PEI F25-LMW (see Note 1).

3.1. Preparation of PEI/siRNA Complexes

1. Complexation protocol for transfection of cells seeded in 24-well plates with PEI/siRNA-complexes: For each well of a 24-well plate, dilute 60 pmol (0.8 µg) siRNA in 50 µL Complexation Buffer. Mix the solution by vortexing or vigorous shaking, and incubate for 5–10 min at room temperature. In parallel, prepare one of the following PEI solutions.
   (a) jetPEI: dilute 3.2 µL jetPEI or 0.8 µL 4× jetPEI in 50 µL Complexation Buffer (N/P 10), mix and incubate at room temperature for 5–10 min.
   (b) PEI F25-LMW: dilute 4 µg (N/P 38.5) to 8 µg (N/P 77) PEI F25-LMW in Complexation Buffer ad 50 µL, mix and incubate at room temperature for 5 min.

   The PEI solution is then added to the siRNA solution and mixed by vortexing. Incubate the complexes for 30–60 min at room temperature. Then, vortex again since complexes may

precipitate, and add the solution dropwise to the cell culture medium (see Subheading 3.2).

2. Complexation protocol for in vivo applications (amounts for one i.p. injection into a mouse):

   Dilute 750 pmol (10 µg) siRNA in 50 µL Complexation Buffer, mix as described above and incubate for 5–10 min. In parallel, prepare one of the PEI solutions.

   (a) jetPEI: dilute 40 µL jetPEI or 10 µL 4× jetPEI in 50 µL Complexation Buffer, mix and incubate at room temperature for 10 min.

   (b) PEI F25-LMW: dilute 50 µg (N/P 38.5) to 100 µg (N/P 77) PEI F25-LMW in Complexation Buffer ad 50 µL, mix and incubate at room temperature for 10 min.

   The PEI solution is then added to the siRNA solution and mixed by vortexing. Incubate the complexes for 60 min at room temperature, vortex again and use for one injection within 30 min (see Subheading 3.5).

3. To control for nonspecific effects of the transfection or the carrier influencing gene expression in vitro, the PEI complexation of a nonspecific siRNA or a scrambled siRNA should be performed in parallel. Upon transfection, these wells will serve as a negative control in addition to untransfected cells.

4. For the optimization of complexation conditions, the targeting of a reporter gene like luciferase (see below) can be performed. In this case, stable luciferase-expressing cells can be employed, or cells can be transiently transfected with a DNA expression vector 24 h prior to siRNA transfection, using any commercially available transfection reagent.

3.2. Transfection of Cells in Tissue Culture

1. For transfection in 24-well plates, seed ~40,000 cells in 1 mL medium/well on the day of, or one day prior to, transfection. Transfection can be performed in cell suspension or after attachment of the cells at the bottom of the well, and in the presence or absence of 10% FCS. Efficacies and optimal conditions will be dependent on the cell line. For accurate results, it is important that cell numbers are identical in each well at the time point of transfection.

2. If larger cell numbers are required, e.g., for analytical purposes, transfection may be upscaled. Typically, ~200,000 cells/well are seeded in 2 mL medium into 6-well plates and transfected with the 2.5-fold amounts of the above complexes.

3. Most PEI complexes, as well as other transfection mixes for DNA, need to be freshly prepared. However, in the case of PEI F25-LMW, it is possible to store the complexes at –20° to –80°C for several months without loss of bioactivity (11).

This allows the preparation of larger amounts that can then be stored, aliquotted and, prior to use, only need thawing, brief mixing and incubation for ~30 min.

3.3. Variations in Complexation and Transfection Conditions for Optimal Gene Knockdown

1. Best complexation and transfection conditions may vary dependent on the cell line and should be optimized with regard to N/P ratios and amounts of the complexes, incubation time, medium change and medium conditions. Desired results are high gene knockdown efficacies and the absence of cytotoxic effects (see Note 10). Due to simple measurement techniques, reporter genes like luciferase provide an easy readout for gene targeting, and thus, cells transfected with a reporter gene, stably or transiently 1 d prior to siRNA transfection, may provide a less laborious approach for initial optimization experiments in a given cell line than the probably somewhat more tedious analysis of the endogenous gene of interest.
2. The optimal N/P ratio appears to be among the most important parameters and can be addressed by varying PEI/siRNA mixing ratios by a factor ~0.5–2. Likewise, in initial experiments various amounts of PEI/siRNA complexes should be tested. Larger complex amounts may translate into higher knockdown efficacies, but can also lead to cytotoxic effects (see Note 10). Another parameter affecting transfection efficacy is complexation time. For most cell lines, the optimal time for complexation is about 60 min. Exceeding the complexation time will eventually result in decreased transfection efficacies due to PEI/siRNA complex aggregation.
3. Because the cellular uptake of PEI/siRNA complexes is determined by the diffusion of the complexes to the cell surface and their subsequent cellular uptake, the transfection should be performed for at least 6 h. If cytotoxicity is not a problem, the transfection medium can remain on the cells for several days; otherwise, a medium change can be performed. Special care needs to be taken when working with antibiotics as they may affect transfection efficacies.

3.4. Determination of Targeting Efficacies

1. For the simple and accurate analysis of gene targeting efficacies, the determination of luciferase activity can be performed either in stable luciferase-expressing cells (if available) or in wild-type cells, upon prior transient transfection with a luciferase expression vector. Luciferase knockdown after siRNA transfection usually reaches maximum values at 72–96 h after siRNA transfection. The activity of the luciferase enzyme is measured in a luminometer and expressed in relative light units (RLU). Using the luciferase quantitation kit from Promega, we employed the following, slightly modified protocol: Prepare

the 1× Lysis buffer by adding 4 volumes of water to 1 volume of 5× Lysis buffer. After removing the growth medium from adherent cells, or in the case of cells in suspension after spinning them down at 800×g and aspirating the medium, ad 100 µL/well (24-well plate) Lysis Buffer to the cells and incubate on a rocking platform for 10 min at room temperature, prior to checking for complete cell lysis under the microscope. For the measurement of the luciferase activity in the luminometer, dispense 25 µL of the Luciferase Assay Reagent into a luminometer tube, ad 10 µL of the cell lysate, mix both components by carefully tapping against the tube and measure immediately. To avoid background signals, no gloves should be worn when handling the luminometer tubes.

2. The ultimate goal is the knockdown of any target gene of interest in a given project. Knockdown efficacies are often determined on mRNA level by Northern blotting or, being more accurate and relying on smaller RNA amounts, by quantitative RT-PCR (qRT-PCR). RNA isolation can be performed using the commercially available TriFast™ solution, which contains phenol and guanidinium thiocyanate. Cells grown in wells of a 6-well plate are lysed by addition of 1 mL Trifast™ ~ 72–96 h after siRNA transfection. The solution is incubated for 5 min at room temperature, and the cell lysate is pipetted up and down several times prior to transfer into a 1.5 mL vial. Add 0.2 mL chloroform to each mL of Trifast™ and shake vigorously for 15 s. Incubate at room temperature for 3–10 min. Centrifuge at 12,000×g. Transfer the aqueous upper phase containing the RNA into a new tube. Add 0.5 mL isopropanol per 1 mL of TriFast™ and incubate 5–15 min on ice for RNA precipitation. Centrifuge at 12,000×g for 10 min. Remove the supernatant and wash the RNA pellet with 75% ethanol. Centrifuge again at 7,500×g for 5–10 min at 4°C. Air-dry the RNA pellet and resuspend the RNA in nuclease-free water. It is very important that excess ethanol is evaporated completely before resuspending the RNA in 10–50 µL RNAse-free water. Freezing and incubating the solution for 5 min at 65°C will aid the dissolving of the RNA.
3. In vivo knockdown efficacies in target tissues taken from animals can be determined by qRT-PCR as well. For the preparation of RNA from tumor xenografts or other tissues/organs, 100–400 mg tissue is homogenized in liquid nitrogen using a mortar. (Special precautions need to be taken when working with liquid nitrogen!) The homogenized tissue is then resuspended in at least 1.5 mL TriFast™ and further processed as described above, with all other components being upscaled according to the volume of TriFast™.

4. For Northern blotting, RNA pellets can be dissolved in RNA loading buffer directly and further processed according to Northern blot protocols.
5. For qRT-PCR, cDNA can be generated using the RevertAid™ H Minus M-MuLV Reverse Transcriptase from Fermentas. In a PCR tube, 1 µg total RNA is mixed with 1 µL Random Hexamer Primer, and DEPC-treated water is added to a final volume of 12.5 µL. The mix of RNA and primers is incubated for 5 min at 65°C and chilled on ice. After spinning down the solution by short centrifugation, 4 µL 5× reaction buffer, 0.5 µL RiboLock™ RNase Inhibitor, 2 µL 10 mM dNTP Mix and 1 µL RevertAid™ H Minus M-MuLV Reverse Transcriptase are added. All components are mixed, the solution is spun down by brief centrifugation and the tubes are placed into a Thermo Cycler. The initial incubation is at 25°C for 10 min, followed by the elongation step at 42°C for 60 min, and an enzyme inactivating step at 70°C for 10 min. The cDNA is cooled down to 4°C and used directly for PCR or stored at –20°C.
6. To perform quantitative PCR using a Light Cycler (Roche), the cDNA is diluted 1:10 in DEPC-treated water. For duplicates, 2.2 µL 5 µM Primer-Mix (containing appropriate primers to amplify the gene of interest or, as a loading control, a housekeeping gene) and 10 µL SYBR Green are added to 8.8 µL cDNA. The components are mixed thoroughly by pipetting the solution up and down for at least ten times, and 10 µL of the reaction mixture are transferred into a LightCycler capillary. In the LightCycler, the reaction is preincubated at 95°C for 15 min to activate the HotStarTaq® DNA Polymerase. Then, 55 cycles are performed consisting of a 15-s denaturation step at 94°C, a 30-s annealing step at 55°C, and a 30-s extension step at 72°C, prior to cooling down to 4°C. The annealing temperature may vary depending on the primers used and may require optimization. PCR reactions with target gene-specific and, for normalization, with housekeeping gene-specific primer sets (e.g., actin) are run in parallel for each sample, and expression levels of the gene of interest are determined by the formula $2^{CP(\text{target gene})}/2^{CP(\text{actin})}$ with CP = cycle number at the crossing point (0.3).
7. Knockdown efficacies are determined by the comparison of expression levels of the target gene in cells treated with the specific PEI/siRNA complexes vs. cells treated with PEI/non-specific siRNA complexes, and are expressed in "% remaining expression over control" or in "% knockdown compared to control".

8. Along with determining mRNA levels by Northern blotting or qRT-PCR, other methods for measuring expression levels can also be employed. These include, but are not limited to, protein quantitation by ELISA, FACS or Western blotting as well as various tests for protein or enzyme activity, and will strongly depend on the protein of interest.
9. The most reliable documentation of gene knockdown relies on the parallel determination of targeting efficacies on both mRNA and protein levels, and is often required by referees when submitting articles to peer-reviewed journals.

3.5. In Vivo Gene Targeting Through Systemic or Local Administration of PEI/siRNA Complexes in Mouse Tumor Xenograft Models

While several siRNA delivery reagents have been introduced for in vitro use, the in vivo situation is considerably more complex. Among others, the following additional requirements have to be met: protection of siRNA molecules against degradation (e.g., in serum, transfer through several biological membranes), favourable pharmacokinetic properties (for example, with regard to serum half-life and biodistribution), efficient delivery to and uptake into the target organ as well as high biocompatibility and the absence of other unwanted effects. PEI/siRNA complexes based on jetPEI and PEI F25-LMW have been successfully used for systemic or local application of siRNAs.

1. Systemic administration of PEI F25-LMW/siRNA complexes can be performed through intraperitoneal or intravenous injection (see Notes 7 and 8). For i.p. injections in mice, a rather broad range of injection volumes has been described; however, the maximum volume is ~ 50 mL/kg, i.e., 1.5 mL for a mouse with 30 g body weight. For i.v. injections, a maximum volume of 5 mL/kg, i.e., 150 µL for a 30 g mouse, should not be exceeded and the injection should be performed slowly. Typically, we use 150 µL for i.p. and 100 µL for i.v. injections in our experiments.
2. Prior to in vivo applications, toxicity studies may be performed to determine maximum amounts of PEI/siRNA complexes, which allow repeated application without visible adverse effects. In mice, repeated injections of 10–30 µg (i.p.) or 10 µg (i.v.) PEI-complexed siRNA is well tolerated.
3. Local application of PEI/siRNA complexes can be performed as well. Among others, this includes intrathecal injections into the brain or instillation into the lung. Special care needs to be taken not to exceed maximum volumes with these modes of administration, which in mice are ~ 2 µL or ~ 50 µL, respectively. If the volume is a limiting factor, complexation conditions (see Subheading 3.1) can be modified by reducing volumes of HEPES/NaCl buffer to achieve higher complex concentrations.

3.6. Determination of siRNA Biodistribution Through Anaylsis of [^{32}P]-Labeled siRNAs

For the induction of RNAi in vivo, the delivery of intact siRNAs is of critical importance. Thus, prior to a large therapeutic experiment involving several treatment groups, it may be advantageous to test for siRNA delivery into the target tissue/organ of interest. Likewise, when observing therapeutic effects, the method described below demonstrates that these are indeed based on the in vivo delivery of siRNA molecules, thus validating the results with regard to specificity. In contrast to other methods relying on the in situ detection of labeled siRNAs, this protocol tests exclusively for intact siRNA molecules since degradation products are purified off. Please note, however, that this method relies on radioactive labelling (see Note 9).

1. 5′-labelling of siRNAs: In a 1.5 mL reaction tube, mix 7.5 µg siRNA with 10 µL (γ-^{32}P]ATP, 5 µL 10× reaction buffer A (Fermentas), 2 µL T4 Polynucleotide Kinase and water ad 50 µL. Incubate the mixture for 30 min at 37°C. Stop the reaction by adding 2 µL 0.5 M EDTA, pH 8.0 and purify labeled siRNAs from free nucleotides by gel filtration. For example, use Micro Bio-Spin® 6 Chromatography Columns according to the manufacturer's protocol for purifying labeled siRNA molecules: resuspend the resin, place the column into a 2.0 mL tube and remove the cap of the tube. Wait until the packing buffer has drained and empty the 2.0 mL tube. Centrifuge the column for 2 min at 1,000×g and place it into a new 1.5 mL tube. Apply the labelling reaction mix onto the resin and centrifuge the column for 4 min at 1,000×g. The flow-through contains the labeled, purified siRNAs.
2. siRNA biodistribution: Prepare PEI/siRNA complexes as described in Subheading 3.1 with a maximum of 3 µg radioactively labeled siRNA/injection per mouse (fill up with unlabeled siRNAs to reach desired siRNA amounts, if applicable). Inject the complex solution into the mouse and wait 1–3 min prior to collecting blood from the tail vein using a capillary tube like Microvette® CB 300. At the time point(s) of interest, typically after 30 min to 8 h, sacrifice the mice by exposing to an overdose of isoflurane, immediately take blood by puncturing the heart and remove organs to be analysed, e.g., lung, liver, kidney, spleen, skeletal muscle, tumor xenografts, brain. For most accurate results regarding the efficacy of siRNA delivery, analyse the whole organ/tissue if possible. Rinse tissues in PBS to remove excess blood and determine the exact weight. Freeze the tissues in liquid nitrogen or proceed immediately with the homogenization of the tissue.
3. RNA preparation from tissue samples: Put the tissue sample into a mortar and, if frozen, wait until the tissue starts to thaw. Flatten the sample with a pestle and add some liquid nitrogen. Grind the tissue by pushing the pestle and by adding

more liquid nitrogen, if necessary, until you get a fine powder. Add 0.75 mL TriFast™ and transfer the suspension into a 2.0 mL reaction tube. With another 0.75 mL TriFast™, rinse the mortar to collect residual tissue pieces and combine with the ground sample. Proceed with the preparation of RNA as described in Subheading 3.4. Resuspend the RNA pellet in 50 µL 1× loading dye.

4. Gel electrophoresis: Prepare a 10% agarose gel by dissolving 2 g agarose in 175 mL boiling water. Let the solution cool down to 55–60°C prior to adding 20 mL 10× MOPS buffer and 5 mL 37% formaldehyde (work under a hood!) and pouring the gel in an appropriate gel electrophoresis device. Load equal amounts of the samples and run the gel at 80 V for ~90 min.
5. Capillary transfer: Fill a wide container with 20× SSC buffer and place a glass plate on its top. Place a sheet of Whatman 3MM chromatography paper on the glass plate with its ends reaching into the buffer. Soak the whole paper in buffer prior to placing the gel upside down onto the paper. Presoak a gel-size nylon membrane and four gel-size chromatography sheets in 20× SSC buffer and put them, nylon membrane first, onto the gel. Carefully remove any bubbles from the sandwich, overlay with a ~10 cm layer of dry paper towels, put a ~1 kg weight on top and allow the capillary transfer to proceed overnight.
6. Autoradiography: The nylon membrane, wrapped in plastic, can be directly exposed to an X-ray film or a phosphoimager screen. Scan the film or screen and determine signal intensities using any appropriate software.

3.7. Application Example: Antitumor Treatment and Determination of Targeting Efficacies In Vivo in s.c. Tumor Xenografts in Mice

1. For any therapeutic treatment experiment, at least two negative controls, i.e., one group of mice treated with PEI-complexed, nonspecific siRNA and one group of mice left untreated, need to be included to control for nonspecific effects.
2. To establish subcutaneous tumors in athymic nude mice, $3–6 \times 10^6$ tumor cells in 150 µL PBS are subcutaneously injected into both flanks of 6- to 8-week-old nude mice (see Note 5). When the fluid is reabsorbed, i.e. 3–5 days after injection, tumors are measured regularly every 2–3 days, and tumor sizes are estimated from the product of the perpendicular diameters of the tumors. Depending on the cell line, the establishment of tumors and start of tumor growth takes 1–3 weeks.
3. For treatment of s.c. tumor xenografts, PEI/siRNA complexes are typically injected i.p. three times per week. The growth rate of the tumors, their appearance and animal welfare determine the duration of the experiment.

4. Upon termination of the experiment, mice are sacrificed by exposure to an overdose of isoflurane, and tissues of interest are taken out. It is useful to divide the tissue samples into three parts for RNA preparation, protein detection and immunohistochemical analysis, if applicable. The samples for RNA and protein analysis are frozen in liquid nitrogen and stored at –80°C, while tissues for immunohistochemical analysis are transferred into 10% formalin for paraffin embedding.

4. Notes

1. PEI-mediated delivery of nucleic acids can also be employed for shRNA-encoding DNA plasmids. In this case, shRNAs are transcribed in the cell and further processed to siRNAs, which then induce RNAi. The PEIs and protocols described here are also suitable for DNA complexation and delivery.
2. If not protected from light, PEI F25-LMW solutions can change to a yellow or light brown color. To our knowledge, this does not impair its transfection performance.
3. In tissue culture experiments, we recommend regular treatment of cells with an antibiotic against mycoplasma infection. Seemingly poor transfection efficacies may be due to mycoplasma contamination of the cells.
4. In some cases, low detected light units may be due to old Luciferase Assay Reagent. One can try to recover Luciferase Assay Reagent by adding 2-mercaptoethanol because reductive conditions are needed for the luciferase reaction.
5. Mice need to be kept and handled according to the appropriate laboratory animal guidelines. For the successful establishment of s.c. tumors, cells should be injected directly under the skin while avoiding injection into deeper regions.
6. Experiments described here may include work with potentially hazardous or genetically modified material. Please consult the safety guidelines in your lab for proper handling.
7. In mice, the tail veins are located on the left and right side of the tail whereas the arteries are located on the dorsal and ventral side of the tail. For i.v. injection, the mice should be transferred to a restraining device to avoid movement. Warming the tail with an infrared lamp or warm water will enlarge the veins. Alternatively, a disinfectant solution can be sprayed onto the skin of the tail for vein enlargement. For injection, we suggest using a 30-gauge needle.

8. To facilitate the penetration of the needle during i.p. injection, hold the mouse tightly. It may happen that organs in the abdomen and pelvis, e.g., colon or bladder, are accidentally punctured. To avoid this, the lower left part of the abdomen is proposed as site of injection.
9. Special care needs to be taken when working with (^{32}P)-labeled material. Consult your lab safety manuals and radiation safety personnel.
10. Dependent on the cell line, cytotoxic effects may be observed in vitro upon treatment with PEI complexes. To accurately determine threshold concentrations of PEI concentrations, commercially available tests for the assessment of viable cells (MTT assay, WST-1 assay) or cell death (LDH release assay) can be performed. The same tests may be used for monitoring specific effects upon gene targeting, i.e., if antiproliferative or apoptotic effects are anticipated after knockdown of the gene of interest.

Acknowledgments

The authors' work was supported by grants from the German Cancer Aid (Deutsche Krebshilfe) and the German Research Foundation (Deutsche Forschungsgemeinschaft; AI 24/6-1 and Research Group 627 "Nanohale").

References

1. Fire, A., Xu, S., Montgomery, M. K., Kostas, S. A., Driver, S. E., and Mello, C. C. (1998) Potent and specific genetic interference by double-stranded RNA in Caenorhabditis elegans. *Nature* **391**, 806–811.
2. Aigner, A. (2007) Applications of RNA interference: current state and prospects for siRNA-based strategies in vivo. *Appl. Microbiol. Biotechnol.* **76**, 9–21.
3. Mittal, V. (2004) Improving the efficiency of RNA interference in mammals. *Nat. Rev. Genet.* **5**, 355–365.
4. de Fougerolles, A., Vornlocher, H. P., Maraganore, J., and Lieberman, J. (2007) Interfering with disease: a progress report on siRNA-based therapeutics. *Nat. Rev. Drug Discov.* **6**, 443–453.
5. Boussif, O., Lezoualc'h, F., Zanta, M. A., Mergny, M. D., Scherman, D., Demeneix, B., and Behr, J. P. (1995) A versatile vector for gene and oligonucleotide transfer into cells in culture and in vivo: polyethylenimine. *Proc. Natl. Acad. Sci. U.S.A.* **92**, 7297–7301.
6. Tang, M. X. and Szoka, F. C. (1997) The influence of polymer structure on the interactions of cationic polymers with DNA and morphology of the resulting complexes. *Gene Ther.* **4**, 823–832.
7. Godbey, W. T., Wu, K. K., and Mikos, A. G. (1999) Size matters: molecular weight affects the efficiency of poly(ethylenimine) as a gene delivery vehicle. *J. Biomed. Mater. Res.* **45**, 268–275.
8. Werth, S., Urban-Klein, B., Dai, L., Hobel, S., Grzelinski, M., Bakowsky, U., Czubayko, F., and Aigner, A. (2006) A low molecular weight fraction of polyethylenimine (PEI) displays increased transfection efficiency of DNA and siRNA in fresh or lyophilized complexes. *J. Control. Release* **112**, 257–270.

9. Urban-Klein, B., Werth, S., Abuharbeid, S., Czubayko, F., and Aigner, A. (2005) RNAi-mediated gene-targeting through systemic application of polyethylenimine (PEI)-complexed siRNA in vivo. *Gene Ther.* **12**, 461–466.
10. Grzelinski, M., Urban-Klein, B., Martens, T., Lamszus, K., Bakowsky, U., Hobel, S., Czubayko, F., and Aigner, A. (2006) RNA interference-mediated gene silencing of pleiotrophin through polyethylenimine-complexed small interfering RNAs in vivo exerts antitumoral effects in glioblastoma xenografts. *Hum. Gene Ther.* **17**, 751–766.
11. Hobel, S., Prinz, R., Malek, A., Urban-Klein, B., Sitterberg, J., Bakowsky, U., Czubayko, F., and Aigner, A. (2008) Polyethylenimine PEI F25-LMW allows the long-term storage of frozen complexes as fully active reagents in siRNA-mediated gene targeting and DNA delivery. *Eur. J. Pharm. Biopharm.* **70**, 29–41.

Chapter 19

Transfection of siRNAs in Multiple Myeloma Cell Lines

Jose L.R. Brito, Nicola Brown, and Gareth J. Morgan

Abstract

RNA interference (RNAi), a valuable tool to specifically silence gene expression, is becoming an indispensable weapon in the arsenal of functional genomics, target validation and gene-specific therapeutic research. We have shown that Streptolysin-O (SLO) reversible permeabilization is an efficient method to deliver small interfering RNAs (siRNAs) to hard-to-transfect human myeloma cell lines. In addition, we have shown that transfection of siRNAs, using the SLO reversible permeabilization, specifically and efficiently induces gene silencing in myeloma cell lines.

Key words: Myeloma, Streptolysin-O, SLO, Transfection, siRNA, Knockdown, Silencing, RNAi

1. Introduction

The use of RNA interference (RNAi) has been shown to be an effective tool in functional genomics, target validation and gene-specific therapeutic research through the induction of gene silencing (1–4). Gene silencing, induced by RNAi, is mediated by microRNAs (mirRNA) and small interfering RNA (siRNA) forming Watson–Crick base pairing to a target mRNA, subsequently leading to its sequence-specific cleavage (2).

The use of RNAi technology in multiple myeloma to understand its molecular pathobiology has been hampered by the lack of an efficient and easy-to-use method to deliver siRNAs (5–7). We have shown that Streptolysin-O can be used to make myeloma cells permeable to siRNAs (8), effectively leading to the knockdown of their target mRNA transcripts. The use of Streptolysin-O to make myeloma cells amenable to siRNAs depends on the activation of the Streptolysin-O. Flow activated cell sorting (FACS), real-time PCR and/or Western blotting allow confirmation of the transfection efficiency and siRNA target specificity.

Wei-Ping Min and Thomas Ichim (eds.), *RNA Interference,* Methods in Molecular Biology, vol. 623,
DOI 10.1007/978-1-60761-588-0_19, © Springer Science+Business Media, LLC 2010

2. Materials

2.1. Cell Culture and Lysis

1. RPMI 1640 Medium supplemented with 10% (v/v) fetal bovine serum (Invitrogen Life Technologies, Paisley, UK).
2. Phosphate buffered saline (PBS) (Invitrogen Life Technologies, Paisley, UK).
3. Lysis buffer: 50 mM Tris–HCl, pH 7.5, 150 mM NaCl, 1% (v/v) Triton X-100 + 0.5% (w/v) Na-Deoxycholate, 1 mM EDTA, 1 mM PMSF and a cocktail of protease inhibitors (Roche Applied Science, UK).
4. Modified 2× Laemmli buffer for cell lysis: 125 mM Tris–HCl, pH 6.8, 4% (v/v) SDS, 20% (v/v) glycerol, 0.006% (w/v) bromophenol blue and 350 mM β-mercaptoethanol (see Note 1).
5. Bicinchoninic acid assay (BCA assay) (Perbio Science UK).

2.2. Trypan Blue Dye Exclusion

1. Trypan Blue Stain (Invitrogen Life Technologies, Paisley, UK).
2. Bright-Line Haemocytometer (Sigma Aldrich, Poole, UK).

2.3. Activation of Streptolysin-O

1. Streptolysin-O from Streptococcus pyogenes (Sigma Aldrich, Poole, UK).
2. Bovine Serum Albumin (Sigma Aldrich, Poole, UK).
3. DL-Dithiothreitol (Sigma Aldrich, Poole, UK).
4. 50 mL polypropylene Falcon tube (BD Biosciences, Oxford, UK).

2.4. Transfection of Myeloma Cell Lines

1. RPMI 1640 without fetal bovine serum (Invitrogen Life Technologies, Paisley, UK).
2. Flat bottom 96-well plate (BD Biosciences, Oxford UK).
3. 6-well plates (BD Biosciences, Oxford, UK).
4. Alexa Fluor 488 conjugated negative control siRNA: sense 5′UUCUCCGAA CGUGUCACGUdTdT 3′ (Qiagen, Crawley, UK).
5. ERK2 siRNA: sense 5′UGCUGACUCCAAAGCUCUGdTdT 3′ (QIAGEN, Crawley, UK). Both siRNA duplexes are resuspended in RNase-free water at 100 µM stock solution and stored in aliquots at −20°C or lower.
6. RNaseZap® (Applied Biosystems/Ambion, UK).

2.5. Flow Activated Cell Sorting (FACS) of Myeloma Cells

1. LSR II flow cytometer equipped with FACSDIVA software (BD Biosciences, Oxford, UK).
2. 5 mL polystyrene round-bottom tube (BD Biosciences, Oxford, UK).

2.6. SDS-Polyacrylamide Gel Electrophoresis (SDS-PAGE)

1. Mini-PROTEAN Electrophoresis System.
2. PageR Gold precast gels 4–20% (Cambrex, UK).
3. Running buffer (5×): 125 mM Tris–HCL, 960 mM glycine, 0.5% (w/v) SDS. Store at room temperature.
4. Pre-stained molecular weight markers (Bio-Rad Laboratories, UK).

2.7. Western Blotting for Knockdown ERK2

1. Transfer buffer: 25 mM Tris (do not adjust pH), 190 mM glycine, 10% (v/v) methanol. Store the Transfer buffer at 4°C (with cooling when in use, see Note 2).
2. PVDF membrane (Bio-Rad Laboratories, UK), and 3 MM Chromatography paper (Watman, Maidstone, UK).
3. Mini Trans-Blot cell system.
4. Tris-Buffered saline with Tween (TBS-T): 10× stock with 1.37 M NaCl, 27 mM KCl, 250 mM Tris–HCl, pH 7.4, 1% (v/v) Tween-20. Dilute 100 mL with 900 mL water for use.
5. Blocking buffer: 5% (w/v) nonfat dry milk in TBS-T.
6. Anti-ERK2 and anti-GAPDH antibodies (Santa Cruz Biotechnology, Heidelberg, Germany) diluted in Blocking buffer (see Note 3).
7. Secondary antibody: anti-mouse IgG conjugated to horseradish peroxidase (Santa Cruz Biotechnology, Heidelberg, Germany) diluted in Blocking buffer.
8. Enhanced chemiluminescence (ECL-Plus) reagents (GE Health care, UK) and BioMAX ML film (Sigma Aldrich, Poole, UK).
9. Saran Wrap (Dow Chemical Company, UK)

2.8. Stripping and Reprobing Blots for GAPDH

1. Stripping buffer: 62.5 mM Tris–HCl, pH 6.8, 2% (w/v) SDS. Store at room temperature. Warm to working temperature of 70°C, and add 100 mM β-mercaptoethanol.
2. Washing buffer: 0.1% (w/v) BSA in TBS-T.
3. Primary antibody: anti-GAPDH (Santa Cruz Biotechnology, Heidelberg, Germany).

3. Methods

The delivery of siRNA duplexes into MM cells is of utmost importance to enable the use of RNAi technology in functional genomics in such cells. To efficiently induce gene-specific knockdown, it is important to use a reliable, reproducible and easy-to-use siRNA duplex delivery method. The method of choice for

myeloma cell lines is the Streptolysin-O reversible permeabilization. The latter consists of initially activating the Streptolysin-O and optimizing the number of Streptolysin-O units required to efficiently induce pore formation on the MM cell plasma membrane whilst minimizing cell death. Ultimately, it is important to determine whether the siRNA duplex is efficiently delivered into MM cells where it can specifically bind to its target mRNA and induce its degradation. This is accomplished through flow activated cytometry sorting (FACS). FACS confirms whether the cells have taken up the siRNA duplex. In addition, it helps to exclude false positive results; that is, to discriminate between cells that have siRNA duplex bound to the outer side of the plasma membrane compared to those that have taken the siRNA duplexes intracellularly. Finally, the efficiency of the siRNA duplex to specifically reduce the protein level of the targeted mRNA needs to be confirmed. This is performed by Western blotting analysis using an antibody against the relevant protein.

3.1. Activation of Streptolysin-O

1. Lyophilized Streptolysin-O (25,000 Units) is resuspended in 5 mL of PBS supplemented with 0.05% (w/v) BSA. The mixture is mixed by pipetting and vortexing. The dissolved Streptolysin-O is then transferred to a 50 mL Falcon tube.
2. To the 5 mL dissolved Streptolysin-O, 20 mL of PBS is added giving rise to 1,000 Units of Streptolysin-O per mL.
3. The activation of Streptolysin-O is achieved by adding 125 µl of 1 M DTT, then mixing and incubating at 37°C in a water bath for 2 h.
4. Activated Streptolysin-O is then aliquoted and stored at –20°C (see Note 4).

3.2. Transfection of Myeloma Cells

1. Human MM cell lines are passaged when approaching confluence to 6–7 × 10^5/mL in T75 cm culture flasks. On the day before transfection, cells are plated at 2 × 10^5/mL cell density; 24 h later, the cells are ready for the Streptolysin-O reversible permeabilization.
2. All materials required for the Streptolysin-O reversible permeabilization are prepared: the activated Streptolysin-O is thawed and kept on ice, the RPMI 1640 (with and without 10% (v/v) fetal bovine serum) is pre-warmed to 37°C, and 15 mL polypropylene tubes and 96-well plates are labelled.
3. The cell density and cell viability are estimated using Trypan Blue dye exclusion and a haemocytometer. 1 × 10^6 cells are taken per experimental condition and washed twice in pre-warmed serum-free RPMI 1640 medium to remove any residual fetal bovine serum that may inhibit Streptolysin-O pore formation. The 1 × 10^6 cells are then resuspended in 50 µl of in pre-warmed serum-free RPMI 1640 medium (see Note 5).

4. At this stage all equipment, including tips boxes, pipettors, flasks, 96-well plates and bench are cleaned with a paper towel soaked with RNaseZap® to remove any RNases (see Note 6).
5. The siRNA, Streptolysin-O and cells are added as follows to a 96-well plate: 2.5 µl of 100 µM stock of siRNA duplex followed by several Units of activated Streptolysin-O (i.e. 2, 4, 6, 8, 10, and 12 Units), followed by 50 µl of cells (i.e. 1×10^6 cells) in serum-free RPMI 1640 medium (see Note 7).
6. The cells, siRNA and activated Streptolysin-O are mixed twice (approximately 10 s each) at low speed on a vortex during the incubation period of 10 min at 37°C.
7. To reverse pore formation on the membrane of cells caused by the Streptolysin-O, 250 µl of pre-warmed RPMI 1640 medium supplemented with 10% (v/v) fetal bovine serum is added to the mixture. Cells are then incubated at 37°C for another 30 min.
8. Cells are transferred to a 6-well plate in a total volume of 2.5 mL of pre-warmed RPMI 1640 medium supplemented with 10% (v/v) fetal bovine serum and incubated for 48 h at 37°C (see Note 8).

3.3. FACS Analysis to Determine SiRNA Duplex Delivery Efficiency

1. Transfection efficiency can be assessed by using Alexa Fluor 488 labelled siRNA duplex or other fluorochromes by FACS 24 h after the Streptolysin-O reversible permeabilization procedure.
2. The cells should be washed in ice-cold PBS once to remove any culture residuals and resuspended in PBS supplemented with 1% (v/v) fetal bovine serum at approximately 5×10^5 cells/mL, then transferred to a FACS tube.
3. Run control samples, followed by the samples in which the cells have been incubated with activated Streptolysin-O in the presence of the fluorescently-labelled siRNA duplex in a FACScan cytometer (i.e. LSR II flow cytometer). Alexa 488 is excited by an argon laser at 488 nm emission, and is detected by using a 530 ± 30 nm band pass filter. Transfection efficiency is assessed by comparing cells + siRNA and cells + siRNA + activated Streptolysin-O. Examples of the expected results with good transfection efficiency are shown in Figs. 1 and 2.

3.4. Preparation of Samples to Assess Knockdown by Western Blotting

1. The human myeloma cells are passaged when approaching confluence to allow the culture to grow in its exponential phase at the time that protein lysates are prepared to assess the knockdown by Western blotting. The cells are usually passaged into 6-well plates as the reversible Streptolysin-O permeabilization procedure starts with only 1×10^6 cells per experimental condition (see Note 9).

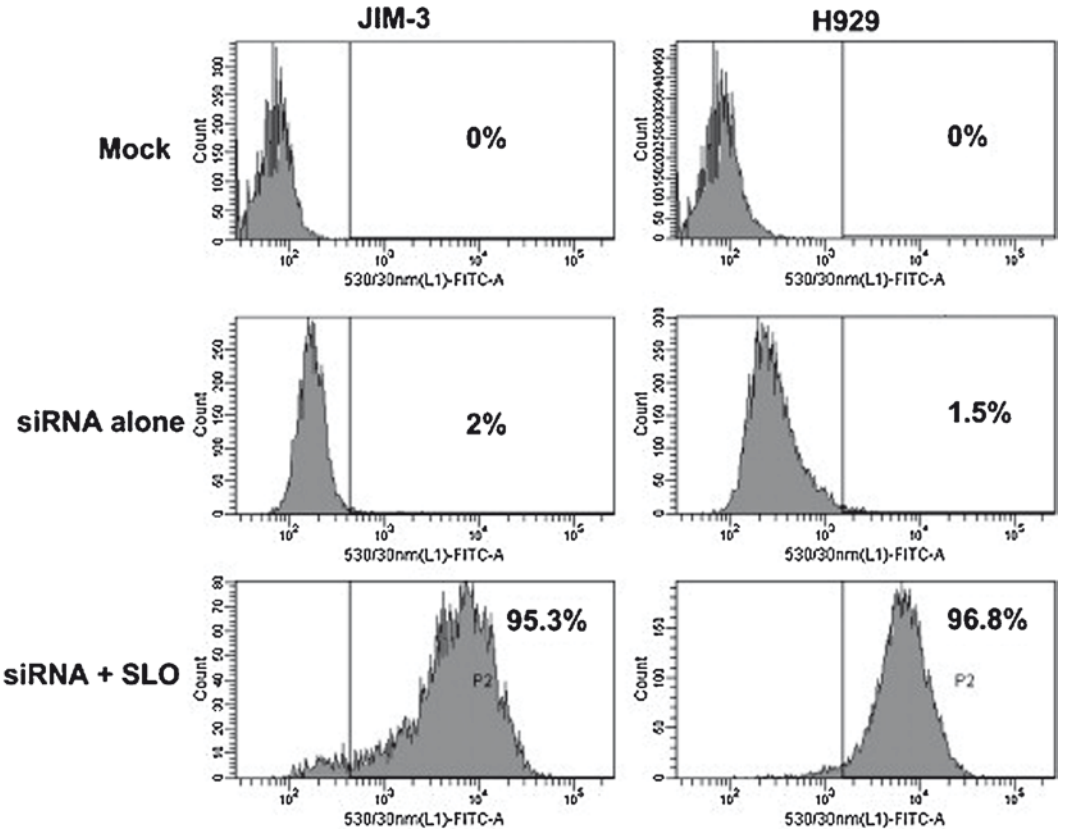

Fig. 1. Negative control Alexa 488-labelled siRNA transfection into myeloma cell lines using the Streptolysin-O reversible permeabilization method. JIM-3 and H929 cells were treated with 6 and 8 Units of activated Streptolysin-O, respectively. Transfection was performed in the presence of 5 μM of siRNA duplex. Transfection efficiency was assessed 24 h later using FACS. The use of activated Streptolysin-O induced a substantial uptake of the siRNA duplex by the myeloma cells above 95%. (Reproduced from ref. 8 with permission from Elsevier Science)

2. The human myeloma cells are washed once in 1 mL of ice-cold PBS, and the cell pellet is resuspended in Lysis buffer and incubated on ice for 30 min with occasional vortexing. The protein lysates are cleared by centrifuging for 10 min at 16,000×g. The protein concentration is estimated using BCA assay.
3. Protein lysates are mixed 1:1 in Modified 2× Laemmli buffer and boiled for 5 min. After cooling to room temperature, the samples are now ready for SDS-PAGE.

3.5. SDS-PAGE

1. The Mini-Protean electrophoresis system is used with the precast 4–20% gels. It is important to remove the excess buffer with water where the precast gel has been stored. Assemble the tank according to the manufacturer's instructions.
2. Prepare the Running buffer by diluting 100 mL of the 5× Running buffer with 400 mL of water in a measuring cylinder. Cover with parafilm and invert to mix.

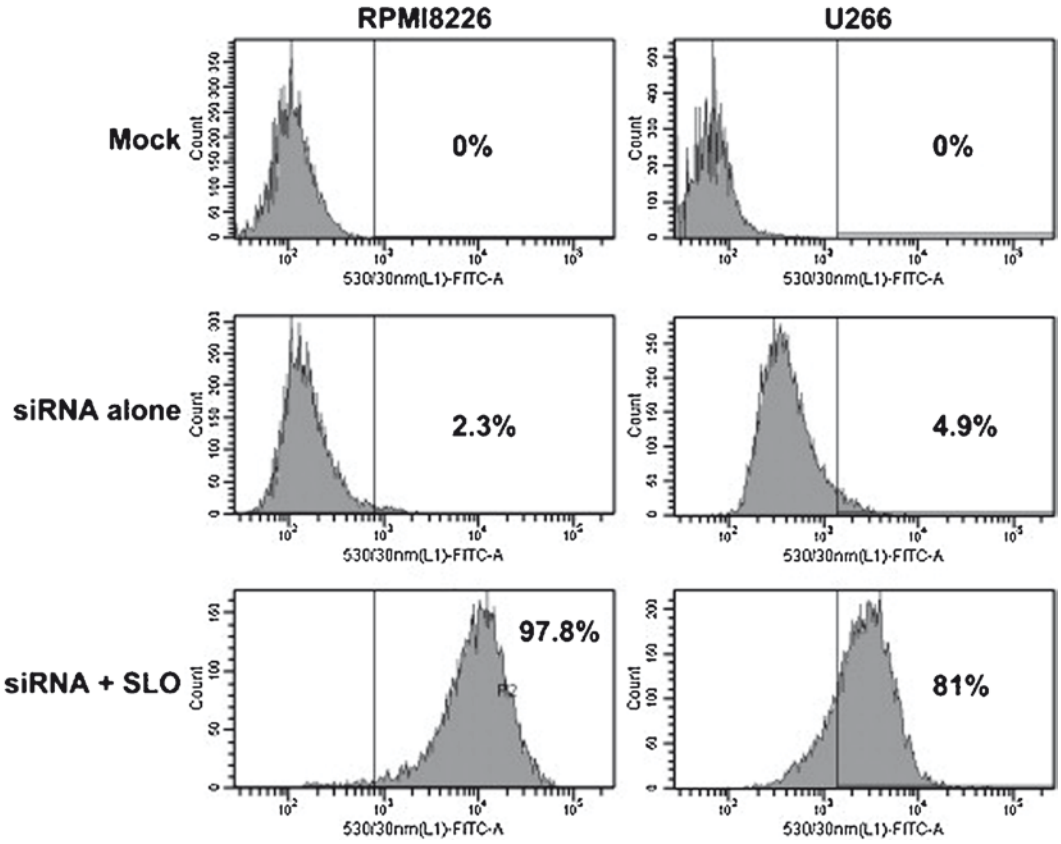

Fig. 2 Negative control Alexa 488-labelled siRNA transfection into myeloma cell lines using the Streptolysin-O reversible permeabilization method. RPMI8226 and U266 cells were treated with 8 and 10 Units of activated Streptolysin-O, respectively. Transfection was performed in the presence of 5 μM of siRNA duplex. Transfection efficiency was assessed 24 h later using FACS. The use of activated Streptolysin-O induced a substantial uptake of the siRNA duplex by the myeloma cells above 80%. (Reproduced from ref. 8 with permission from Elsevier Science)

3. Add the Running buffer to the middle chamber of the unit and load 20–50 μg of total protein per well from the lysate samples. Include one well for pre-stained molecular weight markers.
4. Complete the assembly of the gel unit and connect to the power supply. The gel is run at 140 V for about 1–2 h at room temperature. When the dye is about to run off the gel end, stop the SDS-PAGE.

3.6. Western Blotting for ERK2

Here is an example in which ERK2 is targeted by a siRNA using Streptolysin-O reversible permeabilization method. The same procedure can be applied to other siRNA targets.

1. The sample(s), when they have been separated by SDS-PAGE, are transferred to supported PVDF membranes electrophoretically. These directions assume the use of a Mini Trans-Blot cell system. The PVDF membrane is pre-wetted

in 100% methanol followed by two washes of 5 min each in transfer buffer. The gel and the PVDF membrane are sandwiched between two sheets of 3 MM paper followed by two pieces of foam and locked, taking care that there are no air bubbles between the gel and the PVDF membrane. The membrane is then submerged in the Transfer buffer in the transfer tank.

2. The lid is put on the tank and the power supply is activated. Transfers can be achieved at either 30 V overnight or 70 V for 2 h.
3. Once the transfer is complete, the cassette is taken out of the tank and carefully disassembled, with top foam and sheets of 3 MM paper removed. The PVDF membrane is then carefully removed. The protein markers should be clearly visible on the membrane.
4. The PVDF membrane is then incubated in 50 mL Blocking buffer for 1 h at room temperature on a rocking platform.
5. The Blocking buffer is discarded and the membrane is incubated with 1:1,000 dilution of the ERK2 antibody in Blocking buffer for 1 h at room temperature on a rocking platform.
6. The primary antibody is then removed, and the membrane is washed 3 times for 5 min each with 40 mL of Blocking buffer.
7. The secondary antibody is prepared as 1:2,000 dilution in Blocking buffer, and added to the membrane for 30 min at room temperature on a rocking platform.
8. The secondary antibody is discarded, and the membrane is washed 3 times for 5 min with TBS-T.
9. During the last wash, the ECL Plus Western blotting Detection reagent is prepared by mixing the solutions in the kit. Once the final wash is removed from the blot, the prepared ECL Plus Western blotting Detection reagent is then immediately added to the blot and incubated for 5 min at room temperature.
10. The blot is then removed from the ECL Plus Western blotting Detection reagent, blotted with KIM-Wipes, placed between Saran Wrap sheets, and then placed in an X-ray film cassette with film for a suitable exposure time. An example of the results produced is shown in Fig. 3.

3.7. Stripping and Reprobing Blots for GAPDH

1. Once the satisfactory exposure for the result of the knockdown of ERK2 is obtained, the membrane is stripped of the signal and then reprobed with an antibody that recognizes GAPDH. This will determine if equal amounts of protein samples were loaded to the gel at the beginning of the SDS-PAGE.
2. The blot is incubated in stripping buffer for 2–3 min with gentle mixing by rocking.

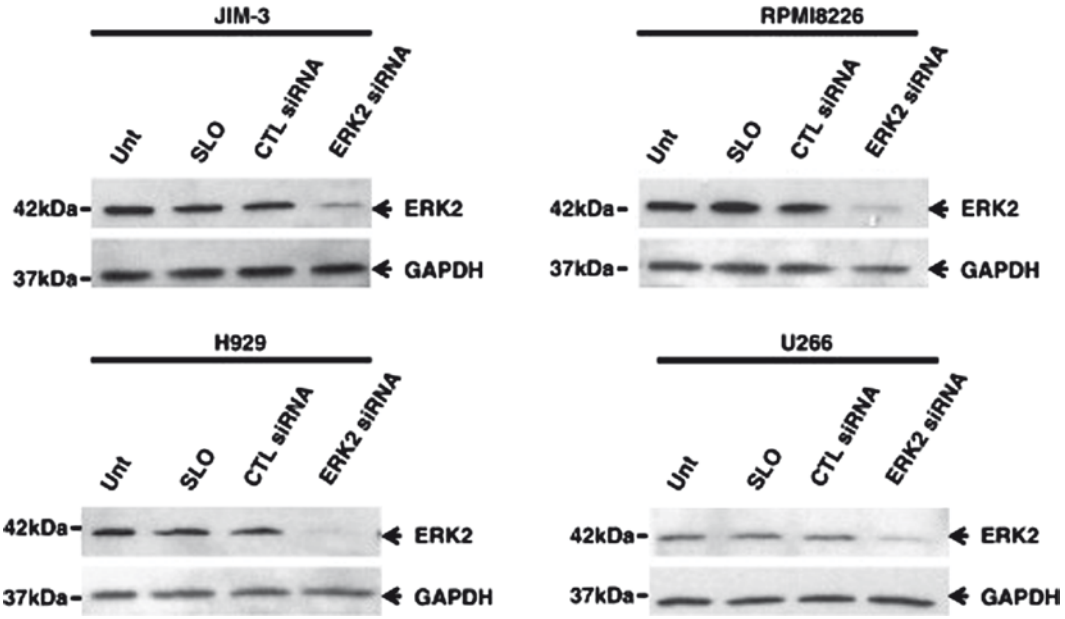

Fig. 3. ERK2 siRNA mediated knockdown in myeloma cell lines using the Streptolysin-O reversible permeabilization method. Myeloma cell lines (JIM-3, H929, RPMI8226 and U266) were incubated with 5 μM of ERK2 or negative control siRNA duplex in the presence/absence of activated Streptolysin-O. The knockdown was assessed 48 h after transfection by Western blotting analysis, the equal loading was monitored by stripping the membrane and reprobe for GAPDH. The use of activated Streptolysin-O combined with siRNA duplex induces a substantial reduction of the ERK2 protein level. (Reproduced from ref. 8 with permission from Elsevier Science)

3. Once the blot is stripped, it is washed twice in water 2 min each, followed by a final wash with TBS-T. The blot is then blocked again with Blocking buffer.
4. The membrane is then ready to be reprobed with anti-GAPDH (1:1,000 dilution) in Blocking buffer followed by washed, secondary antibody and ECL Plus detection as described above. An example of the expected result is shown in Fig. 3.

4. Notes

1. Unless stated otherwise, all solutions should be prepared in water that has a resistivity of 18.2 M Ω cm and total organic content of less than five parts per billion. This standard is referred to as "water" in this text.
2. The Transfer buffer can be used for up to two transfers. It is important to keep the Transfer buffer cooled when in use to prevent head-induced damage of the apparatus and prevent

protein denaturation. To keep the Transfer buffer cooled, plastic sockets with ice can be used.

3. The antibodies described herein can be replaced by other antibodies supplied by other numerous suppliers.
4. Activation of Streptolysin-O and transfection must be performed under aseptic conditions to prevent contaminating the cell lines to be transfected.
5. The number of cells that are needed for the transfection has to take into consideration that the same number of cells used to test a specific siRNA duplex will be needed for each control. Several controls should be used when performing a transfection, these include: (a) cells only, (b) cells + siRNA, and (c) cells + Streptolysin-O.
6. If not using a hood specifically designated for RNA work, all plastic ware and bench need to be wiped with a paper towel soaked in RNaseZap® to prevent degradation of the siRNA.
7. The siRNA duplex and cells have to be pipetted at the opposite sides of each well in the 96-well plate. This will prevent potential siRNA degradation from the RNases present in the medium in which the cells are resuspended.
8. The incubation period varies, depending on several factors, i.e. transfection efficiency, half-life of the target transcript and efficiency of the siRNA. In addition, if real-time PCR is used to assess the transcript knockdown, the incubation period might be shorter. Conversely, if the knockdown is being assessed at the protein level by Western blotting, then the half-life of the mRNA protein product needs to be taken into consideration.
9. Cells can also be grown in flasks/petri dishes with a higher surface area than 6-well plates. The factors dictating the latter are the cell line doubling time and maintenance of cells in the exponential phase of their growth.

Acknowledgments

The authors would like to thank Dr. Julie Irving and Prof. Andy Hall for their encouragement to perform this study. This work was supported by the Kay Kendall Leukaemia Fund.

References

1. Fire, A. (1999) RNA-triggered gene silencing. *Trends Genet.* **15(9)**,358–363.
2. Sandy, P., Ventura, A. and Jacks, T. (2005) Mammalian RNAi: a practical guide. *Biotechniques* **39(2)**,215–224.
3. Tuschl, T. (2002) Expanding small RNA interference. *Nat. Biotechnol.* **20(5)**, 446–448.
4. Tuschl, T. and Borkhardt, A. (2002) Small interfering RNAs: a revolutionary tool for the analysis of gene function and gene therapy. *Mol. Interv.* **2(3)**,158–167.
5. Croonquist, P.A. and Van Ness, B. (2005) The polycomb group protein enhancer of zeste homolog 2 (EZH 2) is an oncogene that influences myeloma cell growth and the mutant ras phenotype. *Oncogene* **24(41)**, 6269–6280.
6. Gomez-Benito, M., Balsas, P., Carvajal-Vergara, X., Pandiella A., Anel A., Marzo I., et al. (2007) Mechanism of apoptosis induced by IFN-alpha in human myeloma cells: role of Jak1 and Bim and potentiation by rapamycin. *Cell. Signal.* **19(4)**,844–854.
7. Hurt, E.M., Wiestner, A., Rosenwald, A., Shaffer A., Campo E., Grogan T., et al. (2004) Overexpression of c-maf is a frequent oncogenic event in multiple myeloma that promotes proliferation and pathological interactions with bone marrow stroma. *Cancer Cell* **5(2)**,191–199.
8. Brito, J.L., Davies, F.E., Gonzalez, D. and Morgan, G.J. (2008) Streptolysin-O reversible permeabilisation is an effective method to transfect siRNAs into myeloma cells. *J. Immunol. Methods* **333(1–2)**,147–155.

Part III

Clinical Implementation

Chapter 20

A New Approach for Therapeutic Use by RNA Interference in the Brain

Yukio Akaneya

Abstract

RNA interference (RNAi) is a gene silencing phenomenon that is induced by ribonucleoprotein complexes containing 21–28 nucleotides (nt) of double-stranded RNA (si/miRNA). Although this phenomenon occurs in an inherent manner, it can also be induced in an artificially manipulated manner. Recently, the understanding of RNAi mechanisms has progressed from that in plants to that in mammals. As RNAi is a highly efficient and readily available procedure to knockdown specific targets, it can possibly be used as a new technique providing many researchers and clinicians with opportunities for its experimental use and prospective clinical application. Consequently, there has been a rush of elucidation of the effective sequences of siRNAs used for the knockdown of the targets in many fields, including neuroscience and experiments for neurological disorders. However, in many cases, it is difficult to effectively introduce si/miRNA into cells without causing injury to the recipient cells. Apart from the off-target effects and the pathogenic property of si/miRNA per se, which are designed and produced, the possibility and intensity of cell injury by RNAi depends on the method employed for the introduction of si/miRNA. Possible methods include si/miRNA delivery systems using liposome, polyethylenimine (PEI), electroporation, and viral infection. Currently, various methods for delivering si/miRNA into cells have been developed and challenged. Here, I review the advantages, disadvantages, and perspective of employing the RNAi procedure in the brain. Given that the disadvantages of RNAi can be overcome, the clinical application of RNAi technologies may be useful in realizing the elimination of pathogenic genes not only in the brain, but also in the other organs in the near future.

Key words: RNA interference, Brain, Electroporation, si/miRNA, Specific region, Knockdown, Clinical trial, Protein, Disease

1. Introduction

A valuable strategy to treat hereditary and acquired genetic human diseases is the removal of the deleterious genes. Various methods for this type of therapy have been developed experimentally and,

Wei-Ping Min and Thomas Ichim (eds.), *RNA Interference,* Methods in Molecular Biology, vol. 623,
DOI 10.1007/978-1-60761-588-0_20, © Springer Science+Business Media, LLC 2010

some of them, actually used in clinical trials. However, all of them have flaws and are considered insufficient to accomplish the goal of therapy. It has been reported that double-stranded RNA has a potential effect on silencing the gene in *Caenorhabditis elegans* (1).

RNA interference (RNAi) is a potential tool to knockdown the target gene because of its high specificity and efficiency. Importantly, this effect cannot be achieved until small interfering RNA (siRNA) has entered the cell. Viral infection is limited to introducing the siRNA, for reasons of safety in vivo. Another important factor to determine the efficacy of RNAi is the stability of siRNA, because the effectiveness of RNAi is transient. Generally, siRNA introduced into cells is active for approximately 1 week, after which it is degraded. For clinical applications, however, it is necessary to maintain the effect of RNAi.

Since the discovery of a small RNA, lin-4, in *Caenorhabditis elegans* (2, 3), hundreds of microRNAs (miRNAs) have been identified in a broad spectrum of species, including mammals. The miRNAs are a group of small RNA molecules that attenuate gene activity post-transcriptionally by suppressing translation or destabilizing messenger RNAs (mRNAs) in a similar way to the siRNAs (4, 5). Recently, the functions of miRNAs have been uncovered, not only in the fate of neuronal cells and maintenance of tissue identity, but also in the genetic etiology of neurological and psychiatric diseases. RNAi has been a major breakthrough in understanding the molecular mechanisms and therapy for these diseases. It is obviously important to establish reliable and safe animal models of the disease before trials in patients are conducted (6). To facilitate the preclinical and clinical use of RNAi, greater understanding of the mechanisms of RNAi regarding the role of miRNAs in diseases, as well as the development of new methods for delivery of siRNAs, is needed.

2. Mechanisms of RNAi

RNAi was first discovered in plants in the 1980s (7, 8), but its mechanisms remained unknown even in the 1990s. The phenomenon of RNAi, conserved in organisms such as protozoa, plants, *C. fingi*, and animals, is not only a normal defense against viruses and the mobilization of transposable genetic elements called transposons (9–11), but it also helps regulate gene expression and normal cell development (4).

There are mainly two pathways for RNAi, one involving extracellular siRNAs and the other involving miRNAs, which are respectively initiated by extracellular transfection and endogenous generation in the nucleus. Long dsRNAs are transported into the cytoplasm via viral infections, transposons,

liposomes, electroporations, etc. In the cytoplasm, the RNase III enzyme Dicer generates siRNAs, which are ~21 to 25-nucleotide (nt)-long dsRNA with 5′ phosphorylated ends and 3′ 2-nt overhangs on each end (12, 13). These siRNAs are then incorporated into the multiprotein RNA-induced silencing complex (RISC/RITS), which in turn unwinds the duplex (14, 15). In an alternative pathway, in the nucleus RNA polymerase transcribes the DNA genome, producing long RNAs termed primary miRNA (pri-RNA), which in turn are processed into an approximately 70-nt stem–loop precursor miRNA (pre-miRNA) by Drosha (16, 17). The pre-miRNAs are then exported into the cytoplasm by Exportin-5, which binds the pre-miRNA (18–20). In the cytoplasm, the pre-miRNAs are cleaved into mature 21-nt dsRNAs by Dicer, similar to the production of siRNAs (21). These single-stranded miRNA duplexes preferentially enter ribonucleoprotein complexes, miRNP, which are analogous to RISC (22). Each siRNA/miRNA strand incorporating RISC/RITS/miRNAP is then presented to the cytoplasmic mRNA pool, where either of the two strands independently associates with its complementary target mRNA strand (23). RISC starts the endonucleotic cleavage or translational arrest of the target mRNA (13, 24–26), and it may also affect the modification of chromatin to induce gene silencing at the transcriptional level (27–30). The effect of RNAi depends on the sequence complementarity of the guiding siRNA strand with that of the target mRNA.

3. Design and Synthesis of siRNA

How should one design and synthesize an siRNA for clinical use? Considering that the effectiveness of RNAi depends on the sequence conformity between the siRNA and the target mRNA, it is important to design competent siRNA sequences for animal experiments and clinical trials in the future. Although intensive studies have developed algorithms to design siRNAs for the target genes, the effects of knockdown on the level of the same target genes are dependent on the algorithm employed (31–34). Although there has been no perfect method for predicting the siRNA sequence for a particular target knockdown to date, there are indications of improvement in the scenario. Moreover, a device for the construction of siRNAs has to be engineered that will prolong its half-life in vivo because of RNase activity in the circulation.

Recent reports indicate that 5′-antisense ends of siRNAs are favorable in obtaining effective RNAi compared with the 5′-sense ends (35). If the 5′-antisense end of the siRNA duplex is easier to unwind by the helicase in RISC, the antisense strand of the siRNA duplex will be passed on the RISC, and the sense strand

will be degraded by the RNase. Thus, intrinsic thermodynamic properties should be considered for designing siRNA sequences (33). Although most studies have used synthetic 21-mer dsRNAs with 19-base central double-stranded domains with 2-base overhangs at 3′, recent successes in RNAi have been reported with other designs of siRNA; for example, blunt 19-mer duplexes with various internal 2′-*O*-methyl modifications (36) and 25-mer duplexes with sense strand 2′-*O*-methyl modifications (37), which may be efficacious and resistant to nucleases. Moreover, it has been reported that synthetic asymmetric 27-mer duplexes as the substrate of Dicer are more potent than 21-mer duplexes, which neither induce interferon (IFN) nor activate protein kinase R (PKR) (38).

Used in single-stranded antisense oligonucleotides, phosphorothioate or boranophosphate modification can be applied in the synthesis of modified siRNAs. It has been reported that not only dsRNA, but also single-stranded RNA with boranophosphate modification have highly effective silencing activity with more potent resistance to nuclease activity (39, 40).

The accessibility of the target RNA by the siRNA depends on the local secondary structure of the target RNA (41–43). In general, high-GC stretches of the target are avoided (31, 33, 34, 44). Moreover, GU-rich sequences in the siRNA design should be avoided because of the possibility of inducing IFN and inflammatory cytokines (45).

4. Delivery System of siRNA

The rate-limiting step for gene silencing is the delivery and introduction of siRNA into the target cells. The efficacy of knockdown, which depends on the sequence of the siRNA, can be predicted by preliminary experiments before therapeutic use. Owing to chemical instability and membrane impermeability of siRNA, chemical modifications of the siRNAs are required for protection from degradation by nuclease activity and plasma clearance (36, 46).

Prior to in vivo experiments, in vitro experiments using established systems such as cell cultures, should be carried out to determine the optimal conditions for RNAi, such as the sequences of the siRNAs, chemical modifications, and shRNAs. Both off-target effects and IFN responses should be checked as well as the efficacy of the knockdown. It is preferable to determine several sequences for the siRNA during in vitro experiments before undertaking in vivo experiments.

For in vivo application, there are two methods of siRNAs administration – systemic and focal. The choice of the method

depends on the purpose of the experiment and the tissue and cell types targeted. For systemic administration, the siRNAs are generally applied intravenously or intraperitoneally, or rarely subcutaneously, and are delivered to the target organs via the peripheral circulation. Although systemic administration is suitable for the therapy of systemic diseases such as leukemia and systemic viral or bacterial infection, it also induces silencing of the target in organs, such as the lung, liver, and spleen, where circulation is high (47). Systemic administration has several shortcomings: (1) rapid degradation of siRNAs by extracellular and intracellular nucleases before, during, and after arrival at the target organ; (2) ineffectiveness of the siRNA injected systemically due to their dilution in the entire body; (3) loss of siRNAs from the body via urine; (4) toxicity to organs other than the target, which may be promoted by overdose of siRNAs due to (2) and (3); and (5) insufficient penetration rate of siRNAs into the cells unless they are forced to use liposome transfection or electroporation.

To overcome these deficits and increase the stability of siRNAs in vivo, chemically-modified synthetic siRNAs and carriers of siRNAs have been tried, and these were successful in a number of experiments (48). Compared with viral carriers, non-viral carriers have an advantage – although viral and plasmid carriers must enter the nucleus to exhibit their function, non-viral carriers do not have to, which is preferable because the active site of RNAi is the cytoplasm. As non-viral siRNA carriers, cationic lipids and polymers, both positively charged, can bind to the negatively charged siRNAs, forming a complex. Polyethylenimines (PEIs) have been used successfully with DNA, as they allow complexation with siRNAs that are covered with PEIs (49). These complexes are taken up by endocytosis, and are protected against nucleolytic degradation by RNase and serum nucleases. Moreover, intraperitoneal (i.p.) injection of a complex of siRNA and lipoplex, a cationic liposome, was successful in silencing the expression of tumor necrosis factor-α (TNF-α) in mice (47). Recently, it was found that highly branched histidine–lysine (HK) polymer can be an effective carrier of siRNAs, which significantly inhibited Raf-1 expression in MDA-MB-435 xenografts by intratumoral injection of a complex of Raf-1 siRNA and HK polymer (50). These non-viral siRNA delivery systems do not induce an immune response, and are safe and effective for the in vivo administration of siRNAs.

Local administration of siRNAs is applicable for treating diseases with focal lesions in the clinical setting and for establishing animal models, in which the effects of knockdown on non-target regions are undesirable during trials. For application in the brain, however, systemic administration of siRNAs is likely to have disadvantages. First, siRNAs that are injected intravenously or intraperitoneally must pass through the blood–neural barrier (BNB) to reach the target cells. The BNB, including the blood–brain

barrier (BBB) and blood–retinal barrier, is an endothelial barrier comprising an extensive network of endothelial cells, astrocytes, and neurons that have an important role in maintaining a precisely regulated microenvironment for reliable neuronal activity (51). In vivo administration of siRNAs via the peripheral circulation seems to pose difficulties for RNAi in the brain. Second, the diversity of the properties of the brain regions, for example, the hippocampus, midbrain, and cerebellum, may lead to differences in the effectiveness of knockdown against the target genes.

After experiments with in vitro RNAi in neurons and glial cells, a number of studies of in vivo RNAi in the brain have been tried, with local injection to sub-regions such as the hypothalamic nuclei (52) and brainstems (53). In these studies, however, the effectiveness of transfection of siRNAs administered intravenously was relatively low.

It has been reported that, when administered by stereotaxic intra-cerebroventricular injection, cationic vectors with PEI or a mixture of lipids show nearly 80% knockdown of the exogenously expressed target gene (54). Because of the high susceptibility of neurons to liposomal toxicity or impaired metabolism (55), however, this cationic lipid-based reagent may be restricted.

Recently, we have established a new method for in vivo RNAi using local electroporation at the target brain regions (56, 57) (Fig. 1). In this method, first, siRNAs are stereotaxically introduced into the brain region via a microinjection pump; the injected siRNAs are then allowed to expand in the target region. Bipolar electrodes are inserted at the borders of the target region, and electric pulses comprising alternating high-voltage, short-duration pulses (driving pulse) and low-voltage, long-duration pulses (poring pulse) are applied to the target tissues, which should contain the siRNAs. Previous methods for introducing small molecules, such as siRNAs, have used strong electric pulses of high voltage and long duration, which may damage the target tissues; however, our method avoids this possibility. The poring pulse forms pores in the target cell membranes, while the driving pulse introduces the siRNAs into the cytoplasm. The membrane pores remain open for a few seconds, so the extracellular siRNAs can easily be introduced even by low voltage. A long-duration driving pulse is preferred to introduce the siRNAs effectively. We have not observed side effects, such as off-target effects, activation of IFN response genes, or pathogenic changes in the target tissues such as apoptosis, and have been able to use the knockdown animals for experiments in electrophysiology, biochemistry, and immunohistology. With one injection of the siRNAs, however, the effect of knockdown is transient – one week at the longest. Repeated injections at intervals will be necessary to prolong the knockdown effect. Thus, this method can overcome problems, such as difficulties in delivering the siRNAs due to the

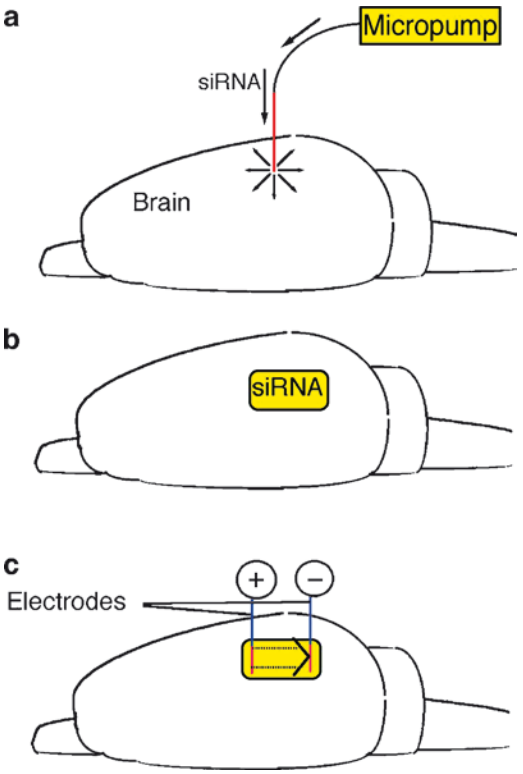

Fig. 1. In vivo RNAi with local electroporation in the target brain region. (**a**) After anesthesia, animals such as rat or mouse are stereotaxically fixed. Then, three holes (one in the center for injection of siRNAs, and two on the sides for electroporation electrodes) are made in the skull with a hand drill. A thin needle, connected to a Hamilton syringe containing siRNAs is inserted into the target region of the brain via the central pore, followed by slow injection of the siRNAs with a mini-pump. (**b**) After allowing the administered siRNAs to expand throughout the target region, two electrodes are inserted around the borders of the target region via the bilateral side pores. Poring pulses and driving pulses (**c**) are then applied to the target region through the positive and negative poles of the electrodes

BBB and the diversity of properties in a set of brain cells, and will be available for in vivo RNAi targeting of tissues and organs such as muscle, liver, and kidney.

Another method of delivering siRNAs into the brain uses an osmotic mini-pump implanted in the body that slowly releases the siRNAs to the target region by body heat. Because this method introduces the siRNAs over a longer period of time, the knockdown effect can be maintained for a longer period, although it is temporary (58, 59).

The effect of the synthesized double-stranded siRNAs are transient in mammals because of the apparent lack of RNAi-amplifying mechanisms, unlike in plants, worms, and *Drosophila* (60–62). Efforts to prolong the effect of knockdown involve designing the plasmid, viral, and non-viral vectors that can achieve the long-lasting effects of the siRNAs. Using vectors expressing

shRNAs, in vivo delivery into the brain was carried out recently and found to be successful. In a study of liposomal transfection, a vector expressing shRNAs was successful in downregulating Agouti Related Protein (AGRP), but the effect was transient (52). Therefore, it remains undetermined whether liposomal transfection achieves a long-lasting in vivo RNAi response. However, electroporation using several paradigms of single or repeated rectangle electric pulses of the same strength have been performed with vectors expressing shRNAs in vivo in brain regions, such as the neocortex (63) and cerebellum (64). Surprisingly, knockdown was observed even in adults in the former study, although it was investigated only in developmental stages in the latter.

Several viral vectors have been engineered to express shRNAs for a long period of time (65). In vivo lentivirus vectors can easily infect not only dividing cells, but also non-dividing/post-mitotic cells, including neurons (66, 67). Human immunodeficiency virus type 1 (HIV-1) and equine infectious anemia virus-based virus vectors have been successful in achieving a long-lasting RNAi effect in the brain and spinal cord in vivo, producing a model for familial amyotrophic lateral sclerosis (ALS) by targeting human Cu/Zn superoxide dismutase (*SOD1*) (68, 69). However, there is a possibility that these lentivirus vectors may induce mutagenesis such as leukemia by integrating into the host genome. Therefore, the use of lentivirus vectors for therapy is critical.

Unlike the lentivirus vectors, adenoviruses do not integrate into the host genome (70). However, the use of adenoviruses for RNAi in vivo has a major disadvantage because of the potential induction of immune responses. Recombinant adeno-associated viruses (AAVs) characteristically induce a limited immune response unlike adenoviruses, and integrate into the host genome at low frequencies (71, 72). They have the ability of stable transduction into both dividing and non-dividing/post-mitotic cells such as neurons (73). A number of attempts to attain long-lasting effects of RNAi using AAVs have succeeded in the target brain regions, resulting in generating models of some genetic neurological diseases. It has been reported that a single injection of AAV-expressing vascular endothelial growth factor (VEGF) into the hippocampus induced the inhibition of environmental induction of VEGF and subsequent neurogenesis of hippocampal neurons, an effect that was maintained for five weeks (74). Direct injection of AAV-expressing tyrosine hydroxylase-targeted shRNA into the midbrain produced a significant reduction in TH mRNA levels in dopaminergic neurons (75). This knockdown animal model represents a potential treatment model for Parkinson's disease in which dopaminergic neurons are impaired.

In another study, non-viral vectors that could be taken up into the cells after intravenous administration were engineered to access a target brain region across the BNB (76). DNA vectors expressing

shRNAs were encapsulated within liposomes that were externally conjugated to polyethylene glycol (PEG) at the liposome surface. Liposome encapsulation protects the vectors from degradation by endonucleases, while PEG alleviates reticuloendothelial uptake of the liposomes, resulting in a prolonged liposome lifespan. Moreover, the PEG molecules are tethered with a receptor-specific monoclonal antibody, which facilitates target-specific delivery of the vectors.

5. Therapeutic Use

RNAi therapy has an advantage in that it is independent of the host's immunological function, unlike vaccines. Thus, for example, patients who have HIV or cancer as well as the elderly and infants with impaired immune systems can receive RNAi therapy.

In addition to the above-mentioned models, reports of preclinical models for neurological and psychiatric diseases have increased recently. In a model of familial ALS with mutant *SOD1* (*SOD1*^{G93A}), intramuscular injections of AAV that retrogradely transported *SOD1*-targeting shRNA to the motor neurons in the spinal cord, improved the motor performance of the mutant mice for about five weeks. For polyglutamine disorders, such as Huntington's disease and spinocerebellar ataxia type 1, injections of AAV expressing the shRNAs targeting disease-related genes improved the behavioral impairments for several months (77).

Evidence of the involvement of miRNAs in neurological disorders has been expanding recently (78). Considering the possible severe side effects to the non-target organs and brain regions on systemic administration of siRNAs, it seems that focal administration is preferable for clinical use. Indeed, a first clinical trial in patients with age-related macular degeneration has been initiated by direct injection into the eye with VEGF-specific siRNAs that were previously shown to reduce VEGF-dependent vascular invasion of the eye in mice (79). Although there may be some uncertainties, a number of clinical trials of RNAi, including neurological diseases and cancers, have been projected.

References

1. Fire, A., Xu, S., Montgomery, M. K., Kostas. S. A., Driver, S. E., and Mello, C. C. (1998) Potent and specific genetic interference by double-stranded RNA in *Caenorhabditis elegans*. *Nature* **391,** 806–811.
2. Lee, R. C., Feinbaum, R. L., Ambros, V. (1993) The *C. elegans* heterochronic gene lin-4 encodes small RNAs with antisense complementarity to lin-14. *Cell* **75,** 843–854.
3. Wightman, B., Ha, I., and Ruvkun, G. (1993) Posttranscriptional regulation of the heterochronic gene lin-14 by lin-4 mediates temporal pattern formation in *C. elegans*. *Cell* **75,** 855–862.

4. Ambros, V. (2004) The functions of animal microRNAs. *Nature* **431,** 350–355.
5. Bartel, D. P. (2004) MicroRNAs: genomics, biogenesis, mechanism, and function. *Cell* **116,** 281–297
6. Fjose, A., and Drivenes, O. (2006) RNAi and microRNAs: from animal models to disease therapy. *Birth Defects Res. C Embryo Today* **78,** 150–171.
7. Napoli, C., Lemieux, C., and Jorgensen, R. (1990) Introduction of a Chimeric Chalcone Synthase Gene into Petunia Results in Reversible Co-Suppression of Homologous Genes in trans. *Plant Cell* **2,** 279–289.
8. van der Krol, A. R., Mur, L. A., Beld, M., Mol, J. N., and Stuitje, A. R. (1990) Flavonoid genes in petunia: addition of a limited number of gene copies may lead to a suppression of gene expression. *Plant Cell* **2,** 291–299.
9. Tijsterman, M., Pothof, J., and Plasterk, R. H. (2002) Frequent germline mutations and somatic repeat instability in DNA mismatch-repair-deficient Caenorhabditis elegans. *Genetics* **161,** 651–660.
10. Bender, J. (2004) Chromatin-based silencing mechanisms. *Curr. Opin. Plant Biol.* **7,** 521–526.
11. Lippman, Z., and Martienssen, R. (2004) The role of RNA interference in heterochromatic silencing. *Nature* **431,** 364–370.
12. Bernstein, E., Caudy, A. A., Hammond, S. M., and Hannon, G. J. (2001) Role for a bidentate ribonuclease in the initiation step of RNA interference. *Nature* **409,** 363–366.
13. Elbashir, S. M., Harborth, J., Lendeckel, W., Yalcin, A., Weber, K., and Tuschl, T. (2001) Duplexes of 21-nucleotide RNAs mediate RNA interference in cultured mammalian cells. *Nature* **411,** 494–498.
14. Hammond, S. M., Bernstein, E., Beach, D., and Hannon, G. J. (2000) An RNA-directed nuclease mediates post-transcriptional gene silencing in Drosophila cells. *Nature* **404,** 293–296.
15. Kisielow, M., Kleiner, S., Nagasawa, M., Faisal, A., and Nagamine, Y. (2002) Isoform-specific knockdown and expression of adaptor protein ShcA using small interfering RNA. *Biochem. J.* **363**, 1–5.
16. Reinhart, B. J., and Bartel, D. P. (2002) Small RNAs correspond to centromere heterochromatic repeats. *Science* **297,** 1831.
17. Lee, Y., Ahn, C., Han, J., Choi, H, Kim, J., Yim, J., et al. (2003) The nuclear RNase III Drosha initiates microRNA processing. *Nature* **425,** 415–419.
18. Yi, R., Qin, Y., Macara, I. G., and Cullen, B. R. (2003) Exportin-5 mediates the nuclear export of pre-microRNAs and short hairpin RNAs. *Genes Dev.* **17,** 3011–3016.
19. Gregory, R. I., Yan, K. P., Amuthan, G., Chendrimada, T., Doratotaj, B., Cooch, N., et al. (2004) The Microprocessor complex mediates the genesis of microRNAs. *Nature* **432,** 235–240.
20. Lund, E., Güttinger, S., Calado, A., Dahlberg, J. E., and Kutay, U. (2004) Nuclear export of microRNA precursors. *Science* **303,** 95–98.
21. Meister, G., and Tuschl, T. (2004) Mechanisms of gene silencing by double-stranded RNA. *Nature* **431,** 343–349.
22. Mourelatos, Z., Dostie, J., Paushkin, S., Sharma, A., Charroux, B., Abel, L., et al. miRNPs: a novel class of ribonucleoproteins containing numerous microRNAs. *Genes Dev.* **16,** 720–728.
23. Martinez, J., Patkaniowska, A., Urlaub, H., Lührmann, R., and Tuschl, T. (2002) Single-stranded antisense siRNAs guide target RNA cleavage in RNAi. *Cell* **110,** 563–574.
24. Doench, J. G., Petersen, C. P., and Sharp, P. A. (2003) siRNAs can function as miRNAs. *Genes Dev.* **17,** 438–442.
25. Saxena, S., Jónsson, Z. O., and Dutta, A. (2003) Small RNAs with imperfect match to endogenous mRNA repress translation. Implications for off-target activity of small inhibitory RNA in mammalian cells. *J. Biol. Chem.* **278,** 44312–44319.
26. Davidson, T. J., Harel, S., Arboleda, V. A., Prunell, G. F., Shelanski, M. L., Greene, L. A., et al. (2004) Highly efficient small interfering RNA delivery to primary mammalian neurons induces MicroRNA-like effects before mRNA degradation. *J Neurosci.* **24,** 10040–10046.
27. Mette, M. F., Aufsatz, W., van der Winden, J., Matzke, M. A., and Matzke, A. J. (2000) Transcriptional silencing and promoter methylation triggered by double-stranded RNA. *EMBO J.* **19,** 5194–5201.
28. Volpe, A. M., Horowitz, H., Grafer, C. M., Jackson, S. M., and Berg, C. A. (2001) Drosophila rhino encodes a female-specific chromo-domain protein that affects chromosome structure and egg polarity. *Genetics* **159,** 1117–1134.
29. Pal-Bhadra, M., Leibovitch, B. A., Gandhi, S. G., Rao, M., Bhadra, U., Birchler, J. A., et al. (2004) Heterochromatic silencing and HP1 localization in Drosophila are dependent on the RNAi machinery. *Science* **303,** 669–672
30. Verdel, A., Jia, S., Gerber, S., Sugiyama, T., Gygi, S., Grewal, S. I., et al. (2004) RNAi-mediated targeting of heterochromatin by the RITS complex. *Science* **303,** 672–676.

31. Heale, B. S., Soifer, H. S., Bowers, C., and Rossi JJ. (2005) siRNA target site secondary structure predictions using local stable substructures. *Nucleic Acids Res.* **33,** e30.
32. Amarzguioui, M., Lundberg, P., Cantin, E., Hagstrom, J., Behlke, M. A., and Rossi, J. J. (2006) Rational design and in vitro and in vivo delivery of Dicer substrate siRNA. *Nat. Protoc.* **1,** 508–517.
33. Gong, D., and Ferrell, J. E. Jr. (2004) Picking a winner: new mechanistic insights into the design of effective siRNAs. *Trends Biotechnol.* **22,** 451–454.
34. Reynolds, A., Leake, D., Boese, Q., Scaringe, S., Marshall, W. S., and Khvorova, A. Rational siRNA design for RNA interference. *Nat. Biotechnol.* **22,** 326–330.
35. Khvorova, A., Reynolds, A., and Jayasena, S. D. (2003) Functional siRNAs and miRNAs exhibit strand bias. *Cell* **115,** 209–216.
36. Czauderna, F., Fechtner, M., Dames, S., Aygün, H., Klippel, A., Pronk, G. J., et al. (2003) Structural variations and stabilising modifications of synthetic siRNAs in mammalian cells. *Nucleic Acids Res.* **31,** 2705–2716.
37. Yu, B., Yang, Z., Li, J., Minakhina, S., Yang, M., Padgett, R. W., et al. Methylation as a crucial step in plant microRNA biogenesis. *Science* **307,** 932–935.
38. Kim, D. H., Behlke, M. A., Rose, S. D., Chang, M. S., Choi, S., and Rossi, J. J. (2005) Synthetic dsRNA Dicer substrates enhance RNAi potency and efficacy. *Nat. Biotechnol.* **23,** 222–226.
39. Hall, A. H., Wan, J., Spesock, A., Sergueeva, Z., Shaw, B. R., and Alexander, K. A. (2006) High potency silencing by single-stranded boranophosphate siRNA. *Nucleic Acids Res.* **34,** 2773–2781.
40. Hall, A. H., Wan, J., Shaughnessy, E. E., Ramsay Shaw, B., and Alexander, K. A. (2004) RNA interference using boranophosphate siRNAs: structure-activity relationships. *Nucleic Acids Res.* **32,** 5991–6000.
41. Holen, T., Amarzguioui, M., Wiiger, M. T., Babaie, E., and Prydz, H. (2002) Positional effects of short interfering RNAs targeting the human coagulation trigger Tissue Factor. *Nucleic Acids Res.* **30,** 1757–1766.
42. Vickers, T. A., Koo, S., Bennett, C. F., Crooke, S. T., Dean, N. M., and Baker, B. F. (2003) Efficient reduction of target RNAs by small interfering RNA and RNase H-dependent antisense agents. A comparative analysis. *J. Biol. Chem.* **278,** 7108–7118.
43. Kretschmer-Kazemi Far, R., and Sczakiel, G. (2003) The activity of siRNA in mammalian cells is related to structural target accessibility: a comparison with antisense oligonucleotides. *Nucleic Acids Res.* **31,** 4417–4424.
44. Amarzguioui, M., and Prydz, H. (2004) An algorithm for selection of functional siRNA sequences. *Biochem. Biophys. Res. Commun.* **316,** 1050–1058.
45. Sledz, C. A., Holko, M., de Veer, M. J., Silverman, R. H., and Williams, B. R. (2003) Activation of the interferon system by short-interfering RNAs. *Nat. Cell Biol.* **5,** 834–839.
46. Braasch, D. A., Jensen, S., Liu, Y., Kaur, K., Arar, K., White, M. A., et al. (2003) RNA interference in mammalian cells by chemically-modified RNA. *Biochemistry* **42,** 7967–7975.
47. Sørensen, D. R., Leirdal, M., and Sioud, M. (2003) Gene silencing by systemic delivery of synthetic siRNAs in adult mice. *J. Mol. Biol.* **327,** 761–766.
48. Aigner, A. (2006) Delivery systems for the direct application of siRNAs to induce RNA interference (RNAi) in vivo. *J. Biomed. Biotechnol.* **71,** 659.
49. Urban-Klein, B., Werth, S., Abuharbeid, S., Czubayko, F., and Aigner, A. (2005) RNAi-mediated gene-targeting through systemic application of polyethylenimine (PEI)-complexed siRNA in vivo. *Gene Ther.* **12,** 461–466.
50. Leng, Q., and Mixson, A. J. (2005) Small interfering RNA targeting Raf-1 inhibits tumor growth in vitro and in vivo. *Cancer Gene Ther.* **12**, 682–690.
51. Kim, J. H., Kim, J. H., Park, J. A., Lee, S. W., Kim, W. J., Yu, Y. S., et al. Blood-neural barrier: intercellular communication at glio-vascular interface. *J. Biochem. Mol. Biol.* **39,** 339–345.
52. Makimura, H., Mizuno, T. M., Mastaitis, J. W., Agami, R., and Mobbs, C. V. (2002) Reducing hypothalamic AGRP by RNA interference increases metabolic rate and decreases body weight without influencing food intake. *BMC Neurosci.* **3,** 18.
53. Shishkina, G. T., Kalinina, T. S., and Dygalo, N. N. (2004) Attenuation of alpha2A-adrenergic receptor expression in neonatal rat brain by RNA interference or antisense oligonucleotide reduced anxiety in adulthood. *Neuroscience* **129,** 521–528.
54. Hassani, Z., Lemkine, G. F., Erbacher, P., Palmier, K., Alfama, G., Giovannangeli, C., et al. (2005) Lipid-mediated siRNA delivery down-regulates exogenous gene expression in the mouse brain at picomolar levels. *J. Gene Med.* **7,** 198–207.
55. Lingor, P., Schöll, U., Bähr, M., and Kügler, S. (2005) Functional applications of novel Semliki Forest virus vectors are limited by vector toxicity in cultures of primary neurons

in vitro and in the substantia nigra in vivo. *J. Neurophysiol.* **93,** 594–602.

56. Akaneya, Y., Jiang, B., and Tsumoto, T. (2005) RNAi-induced gene silencing by local electroporation in targeting brain region. *J. Neurophysiol.* **93,** 594–602.
57. Akaneya, Y., and Tsumoto, T. (2006) Bidirectional trafficking of prostaglandin E2 receptors involved in long-term potentiation in visual cortex. *J. Neurosci.* **26,** 10209–10221.
58. Thakker, D. R., Natt, F., Hüsken, D., Maier, R., Müller, M., van der Putten, H., et al. Neurochemical and behavioral consequences of widespread gene knockdown in the adult mouse brain by using nonviral RNA interference. *Proc. Natl. Acad. Sci. U S A* **101,** 17270–17275.
59. Thakker, D. R., Natt, F., Hüsken, D., van der Putten, H., Maier, R., Hoyer, D., et al. (2005) siRNA-mediated knockdown of the serotonin transporter in the adult mouse brain. *Mol. Psychiatry* **10,** 782–789.
60. Dalmay, T., Hamilton, A., Rudd, S., Angell, S., and Baulcombe, D. C. An RNA-dependent RNA polymerase gene in Arabidopsis is required for posttranscriptional gene silencing mediated by a transgene but not by a virus. *Cell* **101,** 543–553.
61. Sijen, T., Fleenor, J., Simmer, F., Thijssen, K. L., Parrish, S., Timmons, L., et al. (2001) On the role of RNA amplification in dsRNA-triggered gene silencing. *Cell* **107,** 465–476.
62. Lipardi, C., Wei, Q., and Paterson, B. M. (2001) RNAi as random degradative PCR: siRNA primers convert mRNA into dsRNAs that are degraded to generate new siRNAs. *Cell* **107,** 297–307.
63. Bai, J., Ramos, R. L., Ackman, J. B., Thomas, A. M., Lee, R. V., and LoTurco, J. J. (2003) RNAi reveals doublecortin is required for radial migration in rat neocortex. *Nat. Neurosci.* **6,** 1277–1283.
64. Konishi, Y., Stegmüller, J., Matsuda, T., Bonni, S., and Bonni, A. (2004) Cdh1-APC controls axonal growth and patterning in the mammalian brain. *Science* **303,** 1026–1030.
65. Davidson, B. L., and Harper, S. Q. (2005) Viral delivery of recombinant short hairpin RNAs. *Methods Enzymol.* **392,** 145–173.
66. Naldini, L., Blömer, U., Gallay, P., Ory, D., Mulligan, R., Gage, F. H., et al. In vivo gene delivery and stable transduction of nondividing cells by a lentiviral vector. *Science* **272,** 263–267.
67. Blömer, U., Naldini, L., Kafri, T., Trono, D., Verma, I. M., and Gage, F. H. (1997) Highly efficient and sustained gene transfer in adult neurons with a lentivirus vector. *J. Virol.* **71,** 6641–6649.
68. Raoul, C., Abbas-Terki, T., Bensadoun, J. C., Guillot, S., Haase, G., Szulc, J., et al. (2005) Lentiviral-mediated silencing of SOD1 through RNA interference retards disease onset and progression in a mouse model of ALS. *Nat. Med.* **11,** 423–428.
69. Ralph, G. S., Radcliffe, P. A., Day, D. M., Carthy, J. M., Leroux, M. A., Lee, D. C., et al. (2005) Silencing mutant SOD1 using RNAi protects against neurodegeneration and extends survival in an ALS model. *Nat. Med.* **11,** 429–433.
70. Walther, W., and Stein, U. (2000) Viral vectors for gene transfer: a review of their use in the treatment of human diseases. *Drugs* **60,** 249–271.
71. Nakai, H., Yant, S. R., Storm, T. A., Fuess, S., Meuse, L., and Kay, M. A. (2001) Extrachromosomal recombinant adeno-associated virus vector genomes are primarily responsible for stable liver transduction in vivo. *J. Virol.* **75,** 6969–6976.
72. Thomas, C. E., Ehrhardt, A., and Kay, M. A. (2003) Progress and problems with the use of viral vectors for gene therapy. *Nat. Rev. Genet.* **4,** 346–358.
73. Peel, A. L., and Klein, R. L. (2000) Adeno-associated virus vectors: activity and applications in the CNS. *J. Neurosci. Methods* **98,** 95–104.
74. Cao, L., Jiao, X., Zuzga, D. S., Liu, Y., Fong, D. M., Young, D., et al. (2004) VEGF links hippocampal activity with neurogenesis, learning and memory. *Nat. Genet.* **36,** 827–835.
75. Hommel, J. D., Sears, R. M., Georgescu, D., Simmons, D. L., and DiLeone, R. J. Local gene knockdown in the brain using viral-mediated RNA interference. *Nat. Med.* **9,** 1539–1544.
76. Zhang, X., Xie, J., Li, S., Wang, X., and Hou, X. (2003) The study on brain targeting of the amphotericin B liposomes. *J. Drug Target* **11,** 117–122.
77. Harper, S. Q., Staber, P. D., He, X., Eliason, S. L., Martins, I. H., Mao, Q., et al. RNA interference improves motor and neuropathological abnormalities in a Huntington's disease mouse model. *Proc. Natl. Acad. Sci. USA* **102,** 5820–5825.
78. Rogelj, B., and Giese, K. P. (2004) Expression and function of brain specific small RNAs. *Rev. Neurosci.* **15,** 185–198.
79. Check, E. (2005) A crucial test. *Nat. Med.* **11,** 243–244.

Chapter 21

Inhibitory RNA Molecules in Immunotherapy for Cancer

Chih-Ping Mao and T.-C. Wu

Abstract

Over the past few decades, our expanding knowledge of the mammalian immune system – how it is developed, activated, and regulated – has fostered hope that it may be harnessed in the future to successfully treat human cancer. The immune system activated by cancer vaccines may have the unique ability to selectively eradicate tumor cells at multiple sites in the body without inflicting damage on normal tissue. However, progress in the development of cancer vaccines that effectively capitalize on this ability has been limited and slow. The immune system is restrained by complex, negative feedback mechanisms that evolved to protect the host against autoimmunity and may also prevent antitumor immunity. In addition, tumor cells exploit a plethora of strategies to evade detection and elimination by the immune system. For these reasons, the field of cancer immunotherapy has suffered considerable setbacks in the past and faces great challenges at the present time. Some of these challenges may be overcome through the use of RNA interference, a process by which gene expression can be efficiently and specifically "knocked down" in cells. This chapter focuses on the current status and future prospects in the application of small interfering RNA and microRNA, two main forms of RNA interference, to treat cancer by curtailing mechanisms that attenuate the host immune response.

Key words: RNA interference (RNAi), Small interfering RNA (siRNA), MicroRNA (miRNA), Cancer, Tumor, Immunotherapy, Vaccine, Dendritic cell, T cell

1. Introduction

1.1. The Promises and Pitfalls of Cancer Immunotherapy

Despite decades of persistent and intense research effort, the treatment of late-stage cancer in the clinic has achieved limited success and remains elusive. Standard chemotherapeutic regimens frequently fail to control the growth of large, disseminated tumors without causing severe side effects in patients. In addition, surgical and radiological methods are unable to eradicate metastatic or minimal residual disease, and the recurrence of malignancy after treatment by these approaches continues to be a virtually insurmountable

Wei-Ping Min and Thomas Ichim (eds.), *RNA Interference*, Methods in Molecular Biology, vol. 623,
DOI 10.1007/978-1-60761-588-0_21, © Springer Science+Business Media, LLC 2010

obstacle. As a result, the current survival periods for late-stage cancer patients are dismal and in urgent need of improvement.

The generation of tumor-specific $CD4^+$ and $CD8^+$ T cell-mediated immunities by cancer vaccines represents a potentially promising route to the successful control of advanced cancer. Type 1-helper $CD4^+$ T (Th1) cells are able to efficiently stimulate and maintain the effector function of cytotoxic $CD8^+$ T cells. Together, these two arms of the adaptive immune system have the specificity and potency to kill cancerous cells at multiple sites in the body without inflicting significant damage on normal tissue. Furthermore, the establishment of immunological memory after the tumor has been cleared may provide complete and long-term protection against disease relapse. Over the past decade, vaccination with defined antigens has emerged as one of the most attractive approaches to generate antigen-specific $CD4^+$ and $CD8^+$ T cell-mediated immunities and therefore provides an attractive alternative strategy to cancer treatment. However, these vaccines have limited effectiveness, and thus, their promise has not yet been realized in the clinic.

1.2. The Process of RNA Interference

As part of the homeostasis of the host, the immune system is constantly held in check by mechanisms that limit the duration and magnitude of an acute inflammatory response or maintain peripheral tolerance to self-antigen. Furthermore, the tumor microenvironment is rich in immunosuppressive molecules that inhibit the survival, activation, and function of infiltrating T cells either directly or through the recruitment of regulatory immune cells. RNA interference (RNAi) – a remarkable phenomenon first observed in the late 1980s that later evolved into a technology with immense biomedical applications – provides the unique and unparalleled ability to specifically silence expression of target genes (for reviews, see (1–3)). RNAi has thus recently emerged as a powerful addition to the arsenal of cancer immunotherapy that could overcome many of the obstacles it currently faces.

RNAi can be mediated either by small interfering RNA (siRNA) or microRNA (miRNA) molecules. Figure 1 illustrates the molecular steps involved in the RNAi process. In siRNA-mediated gene silencing, cytoplasmic double-stranded RNA (dsRNA) is first cleaved into 21–28 nucleotide duplexes by the RNase-III enzyme Dicer. These duplexes are incorporated into the multiprotein RNA-inducing silencing complex (RISC) and serve as a template that binds to complementary target mRNA, which is degraded by the RISC enzyme Slicer. Multiple types of dsRNA have been delivered into a wide variety of cells and organisms, demonstrating broadly that siRNA is an effective tool for specific gene knockdown (for review, see (4)).

In the early 1990s, it was discovered that multiple aspects of cellular function are influenced by endogenous miRNA, a diverse

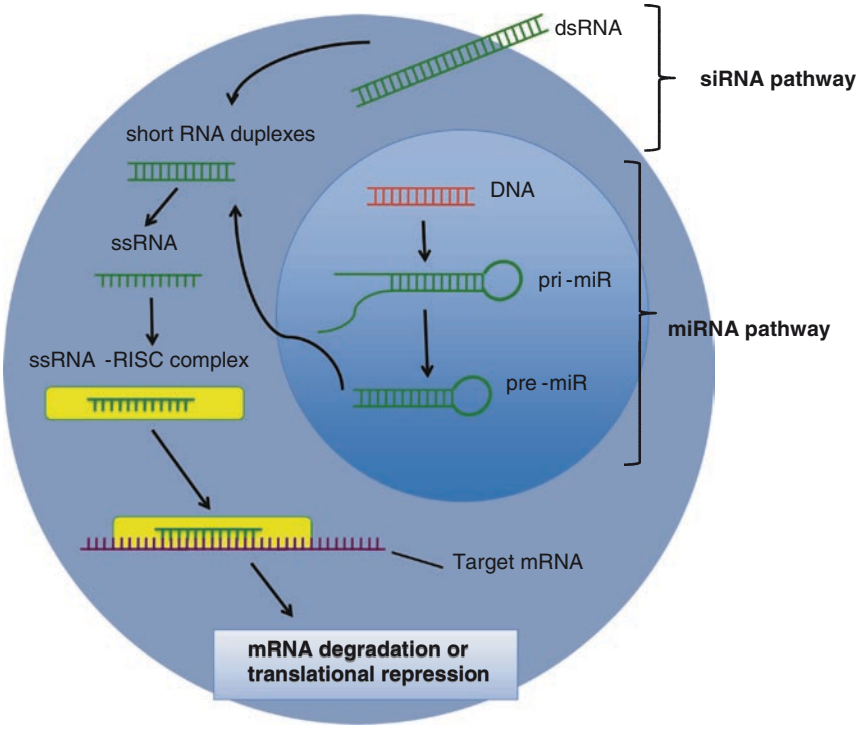

Fig. 1. The processes of siRNA and miRNA-mediated gene silencing. In the miRNA pathway, primary RNA transcripts (pri-miR) are processed by the enzyme Drosha into 60 base pair precursors (pre-miR) in the nucleus. Following export into the cytoplasm, the pre-miR is cleaved into single-stranded 22 nucleotide sequences by the enzyme Dicer and then incorporated into the RISC. The mature miRNA guides the RISC to target mRNA sequences, where it induces either degradation or translational inhibition. The siRNA pathway is similar to the miRNA pathway, with the exception that long, exogenous double-stranded RNA is the initial agent that is processed into a silencing complex

class of small (~22 nucleotide) and copious RNA species that, similar to siRNA, knocks down a vast array of genes at the post-transcriptional stage. Collectively, these molecules are predicted by computer algorithms to modulate the expression of as much as 90% of human genes. miRNA is initially produced as a ~60 nucleotide precursor with a defined stem-loop structure. Following nuclear export, it is processed by the enzyme Dicer into a ~22 nucleotide duplex, and a single strand is then preferentially incorporated into RISC. The miRNA–RISC binds to partially complementary sites in the 5′ or 3′ untranslated regions of target mRNA molecules, where it induces either translational repression or mRNA degradation (for review, see (5)).

1.3. Applications of RNA Interference to Cancer Immunotherapy

In this chapter, we summarize the current progress and future prospects for the application of siRNA and miRNA in cancer immunotherapy. In this context, the use of these molecules to target specific genes in dendritic cells (DCs) and T cells – essential players in adaptive immunity – will be discussed. Specifically, we will examine how RNAi can be employed to empower the immune

system, to abolish intrinsic inhibitory pathways that restrict its function, and to render it insensitive to the suppressive nature of the tumor microenvironment. The majority of experiments on this topic have been conducted in cell culture and animal models, with few studies translated into the clinic. Undeniably, several obstacles – including targeted delivery, incomplete gene silencing, non-specific immune responses, and off-target effects – must be overcome before RNAi can be successfully delivered into humans. Some of these obstacles are outlined together with potential solutions. Altogether, we hope to show that siRNA and miRNA, while small in size, are large in medical significance. These molecules are powerful and emerging additions to the clinical toolkit, which may one day propel immunotherapy to the forefront of remedies for cancer and transform the way it is delivered to patients.

2. RNA Interference in Dendritic Cells

Among all the professional antigen-presenting cells (APCs), mature DCs unquestionably have the strongest capacity to present antigen to and prime either naïve $CD8^+$ or $CD4^+$ T cells. Therefore, the delivery of tumor-associated antigen (TAA) to DCs is a cornerstone of cancer immunotherapy. In the major histocompatibility complex (MHC) class I-restricted pathway for antigen presentation, cytoplasmic antigen is processed by proteasomes and loaded onto MHC class I molecules in the endoplasmic reticulum, where it is eventually shuttled to the DC surface and can interact with the T cell receptor (TCR) on cognate $CD8^+$ T cells. In comparison, in the MHC class II-restricted pathway, extracellular antigen is taken up into DCs by endocytosis into endosomes, where the acidic environment and the presence of proteases degrade the antigen for loading onto membrane-bound MHC class II molecules, which are transported to the cell surface where they interact with the TCR of $CD4^+$ T cells. Efficient T cell activation requires binding between antigen-MHC complexes and the cognate TCR, as well as engagement of costimulatory molecules on DCs.

Mature DCs have high numbers of MHC and costimulatory molecules and are capable of migrating into secondary lymphoid organs, making them excellent activators of naïve T cells and, consequently, ideal instigators of tumor-specific immune responses. Many vaccination strategies developed thus far have focused on engineering DCs with molecules that would enhance the immunostimulatory capacity of these cells. However, the functions of DCs are also negatively regulated by feedback mechanisms, which prevent hyperactivation of the adaptive immune system. These mechanisms are currently being unraveled at a swift pace, and

their inhibition offers a new and potentially effective approach to unleash the unbridled antigen presentation ability of DCs. RNAi technology, as delivered through siRNA or miRNA, provides an ideal way to achieve this purpose. Specifically, it may be of interest to use this technology to suppress the major immunosuppressive pathways, to bias $CD4^+$ T cell differentiation towards a Th1 response, and to prolong the lifespan of DCs.

2.1. Suppression of Immunosuppressive Pathways in Dendritic Cells

DCs express a variety of molecules that may suppress antigen presentation or T cell activation and function. Two such important molecules are A20 and suppressor of cytokine signaling 1 (SOCS1). A20 is an ubiquitin ligase involved in the attenuation of T cell-mediated responses (6, 7). SOCS1 is a broadly immunosuppressive protein that inhibits signaling through the interferon (IFN)-γ, interleukin (IL)-2, IL-6, IL-7, IL-12, and IL-15 pathways, all of which contribute to T cell expansion (8). In addition, SOCS1 can directly suppress antigen presentation to T cells (9). Studies have shown that antigen-loaded DCs, silenced for either A20 (10) or SOCS1 (8, 11, 12) by siRNA, are able to activate large numbers of effector T cells, which correlates with inhibition of tumor growth in mice. Therefore, knockdown of both of these molecules by RNAi represents an effective strategy for cancer immunotherapy.

Recent studies have shown that the upregulation of SOCS1 in DCs is at least in part due to signaling through the Tyro3/Axl/Mer (TAM) family of receptor tyrosine kinases (13). These molecules signal through the STAT1 pathway to induce expression of SOCS1 (13). Notably, transgenic mice that lack the TAM receptors develop profound, broad-spectrum autoimmune disease, suggesting that these receptors play a critical role in controlling the magnitude of the immune response (14). It was recently demonstrated that the TAM component Mer blocks the NF-κB pathway and is required for apoptotic cell-induced T cell tolerance (15). Therefore, RNAi-mediated silencing of TAM, and in particular Mer, represents a potentially effective strategy for therapeutic vaccination against cancer. We have recently found that in vivo knockdown of Mer in epidermal DCs by shRNA dramatically enhances the number of T cells specific for the E7 oncoprotein of human papillomavirus type-16, generated by an E7 DNA vaccine (Mao et al., personal communication). In the future, it will be of interest to explore the suppression of each of the TAM receptors in DCs individually as well as in combination with one another.

In addition to the molecules mentioned above, which suppress antigen presentation, DCs also secrete a variety of proteins that directly inhibit the activation, survival, and function of cognate T cells. For instance, the tryptophan-degrading enzyme indoleamine-2,3-dioxygenase (IDO) is secreted abundantly by plasmacytoid

DCs and depletes tryptophan availability in tumor-draining lymph nodes (16). This induces profound anergy in T cells, as they rely heavily on tryptophan for proliferation and function (17). Therefore, reduction of IDO expression by RNAi may improve the overall cytotoxic activity of T cells in the tumor microenvironment.

Molecules expressed on the surface of DCs also have direct suppressive effects on T cells and represent excellent targets for cancer immunotherapy. For example, the surface proteins programmed death-1 ligand (PD-L1) and PD-L2 – members of the B7 family – recognize and bind to the PD-1 receptor on T cells. Signaling through PD-1 inhibits T cell activation through suppression of the IL-2 and IFN-γ pathways (18) and through induction of cell cycle arrest (19). Antibody blockade of PD-L1 and PD-L2 on DCs has been shown to improve proliferation of and cytokine production by $CD4^+$ T cells (20), leading to improved control of ovarian carcinoma in a preclinical model (21). This finding suggests that siRNA-mediated knockdown of PD-L1 might achieve a similar immunostimulatory effect. In addition, the surface molecules immunoglobulin receptor 2 (DIgR2) (22) and Notch ligands (Delta1, Jagged1, Jagged2) (23–25) expressed by DCs have all been shown to deliver suppressive signals to T cells. Importantly, vaccination of mice with tumor antigen-loaded DCs transfected with DIgR2 siRNA, compared to control siRNA, generated higher levels of tumor-specific $CD4^+$ and $CD8^+$ T cells as well as protective immunity against tumor challenge (22). Furthermore, $CD4^+$ T cells, incubated with allogeneic DCs transfected with siRNA targeting the Notch ligands, displayed higher levels of IFN-γ production (26). These studies indicate that DIgR2 and Notch ligands play a suppressive role in DC biology, and that the downregulation of these molecules is an attractive approach for generating therapeutic immunity against cancer.

DCs have unparalleled capacity to present antigen to and to prime naïve T cells, but express abundant amounts of the proapoptotic surface molecule Fas ligand (FasL) (27). Interactions between FasL and the Fas death receptor on the membrane of T cells may curb the magnitude of the adaptive immune response. Therefore, knockdown of FasL in DCs by RNAi might prevent activation-induced T cell apoptosis upon vaccination and thus bolster antitumor immunity. Huang et al. have previously developed an in vivo gene delivery system using gene gun that could efficiently deliver DNA-encoding siRNA to silence the expression of specific molecules on DCs (27). With this system, they demonstrated that a short hairpin RNA construct targeting FasL was able to significantly enhance the potency of a DNA vaccine against the E7 oncoprotein of human papillomavirus type-16, a model cervical cancer antigen (27). These immunological effects correlated with the eradication of subcutaneously implanted E7-expressing tumors in mice (27).

DCs also secrete factors that attract regulatory T (T_{reg}) cells to the site of antigen presentation in order to tame the immune response. Iellem et al. showed that DCs recruit these cells principally by secreting the chemokines CCL17 and CCL22, which bind to the CCR4 and CCR8 receptors on T_{reg} cells, respectively (28). In this context, it is conceivable that the silencing of CCL17 and CCL22 by RNAi would be a possible way to reduce T_{reg} cell migration to the lymphoid compartments and thereby prevent the suppression of T cell activation.

Finally, it has been revealed that miRNA molecules have an important role in control of the immune system (29). It has been shown that mice deficient in Bic, the gene that codes for miR-155, have poorly functional immune systems characterized by reduced cytokine and antibody production as well as heightened susceptibility to bacterial challenge (30, 31). We have recently found that in DCs, miR-155 appears to have a suppressive role (Mao et al., personal communication). We showed in a mouse model that miR-155 is induced in bone marrow-derived DCs upon stimulation with Toll-like receptor agonists. In addition, in vivo biolistic transfection of mice with DNA-encoding miR-155 via gene gun suppressed antigen-specific T cell-mediated immunity, whereas transfection with a partially antisense inhibitor of the miRNA reversed this effect. Our current findings suggest that miR-155 plays a suppressive role in DC biology, likely through post-transcriptional silencing of critical mediators of the NF-κB pathway such as IKKε. A miRNA that may have a similar function in DCs is miR-146a, an activation-induced molecule shown to silence TRAF6 and IRAK1, key components of the Toll-like receptor pathway (32). Thus, introduction of an inhibitor of miR-155 or miR-146a into DCs may represent an effective way to enhance the antigen presentation ability of these cells and augment tumor-specific immunity.

2.2. Induction of Th1-Polarizing Pathways in Dendritic Cells

It is now clear that, in addition to cytotoxic $CD8^+$ T cells, helper $CD4^+$ T cells are also critical in the development of robust antitumor immunity. During antigen presentation, cytokines secreted by DCs profoundly influence the developmental fate of naïve $CD4^+$ T cells. Based on our current understanding, T cells are programmed through this interaction to adopt the Th1, Th2, Th17, or T_{reg} lineages, each of which is distinguished by a characteristic cytokine secretion profile and has a distinct role in the immune response against cancer. It has been shown that cytokines produced by Th1 cells, including IFN-γ and TNF-α, promote the proliferation and function of activated $CD8^+$ T cells. In this respect, Th1 cells are important for the generation of optimal tumor-specific immunity. Thus, strategies that improve the Th1-polarizing ability of DCs may represent a promising direction in cancer vaccine design.

A delicate balance between exposure to the DC-secreted cytokines, IL-10 and IL-12, determines naïve CD4+ T cell fate: IL-12 induces Th1 differentiation while IL-10 inhibits it. Therefore, decreasing the amount of IL-10 relative to IL-12 in DCs provides a potential method for promoting Th1 responses. Liu et al. have shown that transfection with siRNA targeting IL-10 reduces levels of this cytokine and elevates production of IL-12 in DCs (33). Furthermore, these DCs preferentially induced the development of naïve CD4+ T cells into the Th1 phenotype (33). In addition, it has been found that IL-6 stimulates Th2 differentiation at the expense of the Th1 response (for review, see (34)). Therefore, silencing of IL-6 by siRNA, either alone or in combination with IL-10 knockdown, may further augment Th1-mediated immunity. It will be important to explore the therapeutic efficacy of these approaches in animal as well as clinical models of cancer in the future.

2.3. Attenuation of Apoptotic Pathways in Dendritic Cells

When CD8+ T cells are activated following antigen presentation, they secrete cytotoxic granules that induce apoptosis in neighboring DCs (35), a process which is thought to be an important immunoregulatory mechanism. The amount of the antiapoptotic protein Bcl-2 present in DCs determines the longevity of these cells in response to the death stimuli (36, 37). As a result, raising the amount of Bcl-2 in DCs provides a way to prolong their lifespan and hence sustain antigen presentation. Kim et al. have previously shown that in vivo transfection of DCs with Bcl-2 together with DNA encoding the E7 oncoprotein of human papillomavirus type-16 could increase DC survival, which correlated with an enhanced frequency of E7-specific CD8+ T cells as well as improved therapeutic effects against E7-expressing tumors (38). Because Bcl-2 functions through inhibition of the proapoptotic proteins Bax and Bak, the silencing of these two molecules in DCs by RNAi may directly increase the duration of antigen presentation in the context of a vaccine (39, 40). The delivery of RNAi would circumvent concerns of oncogenicity associated with administration of DNA plasmids. It was shown that siRNA targeting Bax/Bak could be efficiently delivered to silence expression of these molecules in vivo, and co-administration of this siRNA with E7 DNA elicited strong E7-specific T cell-mediated immunity and antitumor effects in a preclinical model (40).

Collectively, these studies demonstrate that RNAi technology directed against proapoptotic molecules can be incorporated into vaccines to produce potent therapeutic immune responses against cancer.

3. Cancer Immunotherapy by Genetic Modification of T Cells

Even the most potent degree of antigen presentation by DCs would not generate significant control of cancer if activated T cells do not efficiently home to, proliferate, and function in the tumor microenvironment. In this regard, the genetic modification of antigen-specific T cells provides a direct and effective route to generate antitumor immunity. For example, the biology of T cells could be altered such that they exhibit rapid and high frequency accumulation in tumors, enhanced clonal expansion, as well as improved helper and cytotoxic function. While development of the technology for the in vitro and in vivo transfection of naïve or activated T cells is still in its infancy, there are many areas in which RNAi may be used to modulate the properties of these cells for therapeutic purpose. In this section, we review one of these areas: suppression of immunosuppressive pathways.

3.1. Suppression of Immunosuppressive Pathways in T Cells

Just as the antigen processing and presentation functions of DCs are regulated by a variety of immunosuppressive pathways, the helper and cytolytic functions of T cells are subject to many negative feedback mechanisms as well. The attenuation of these mechanisms through RNAi technology thus represents a way to unleash the full functional capacity of these T cells, as they are primed to recognize and eliminate cancers. Here, we discuss three such relevant and classical mechanisms: the TGF-β, CTLA-4, and PD-1 signaling pathways.

Many cancers, such as neuroblastoma and Hodgkin Reed–Sternberg tumors, secrete abundant amounts of the immunosuppressive cytokine TGF-β (41–43). When TGF-β binds to and signals through the TGF-β receptor (TGF-βR) on T cells, the phosphorylation and nuclear translocation of the transcription factors Smad 2 and 3 is triggered (44, 45), resulting in growth arrest, terminal differentiation (46, 47), and induction of tolerance (48, 49). This signaling cascade is a major route through which tumors routinely escape immunological surveillance and therefore provides an excellent molecular target for clinical intervention. The use of siRNA to silence the expression of TGF-β receptor in tumor-specific T cells could protect them from tumor-mediated tolerance and thus generate a highly functional therapeutic immune response.

In addition to the TGF-β pathway, the cytotoxic T lymphocyte-associated antigen 4 (CTLA-4) pathway also imposes strong inhibitory control over T cells. CTLA-4 is expressed highly on T cells following antigen exposure and activation. It is a homolog

of the CD28, the major receptor for the costimulatory protein B7. However, CTLA-4 binds to B7 with several thousand times the affinity of CD28 and, as a result, has an overwhelmingly negative influence on T cell priming. CTLA-4 signaling also suppresses IL-2 synthesis and release by T cells, thereby inhibiting their proliferation. It has been shown that blockade of CTLA-4 on T cells with monoclonal antibodies could lead to successful rejection of tumors as well as protection from subsequent challenge (50). Therefore, knockdown of CTLA-4 with siRNA in T cells may be a potentially promising avenue for exploration as a cancer immunotherapy.

PD-1 is another member of the CD28 receptor family and, like CTLA-4, strongly inhibits T cell proliferation and cytokine secretion. The pathway of this molecule is described above. It has been shown in mouse models that blockade of PD-1 signaling improved the accumulation of effector T cells in the tumor, enhanced the cytolytic function of these cells, and inhibited the spread of both B16 melanoma and CT26 colon cancer cells (51). Thus, siRNA-mediated silencing of PD-1 in T cells may also represent a fruitful strategy for cancer immunotherapy.

As the role of effector T cells in the antitumor immune response becomes increasingly apparent, it has too become clear that an effective response would require the presence of functional T cells. Thus, the genetic modification of T cells in this regard has emerged as a distinctly attractive strategy for cancer immunotherapy. Hopefully, as more becomes understood about the molecular pathways governing T cell activation and tolerance, RNAi technology can be exploited for this purpose.

4. Translation of RNAi Technology into the Clinic as a Form of Immunotherapy

Recent advances in our understanding of the RNAi process, as well as how the immune system is regulated, have created great opportunities in the field of cancer immunotherapy. The development of synthetic siRNA over the past few years has made it feasible to apply this technology for clinical purposes. However, the efficient in vivo delivery of RNAi remains a significant challenge.

The efficacy of in vivo siRNA-mediated gene silencing is limited by the transient nature of RNAi as well as the inherent instability of the RNA molecule. It has been shown that on average dsRNA is degraded about 36–48 h after introduction into cells (for review, see (52)). Furthermore, the efficiency of gene knockdown varies by tissue depending on the readiness with which siRNA is uptaken into cells. Although the effects of RNAi may persist for several weeks in terminally differentiated or senescent cells, they typically disappear within one week in rapidly proliferating cells.

To overcome the issues associated with siRNA half-life, investigators have created chemically modified, synthetic dsRNAs that have increased stability and resist degradation in blood or tissue. In addition, the dsRNAs can be designed to be protected from serum RNase, linked with fusogenic peptides, encased in lipid complexes, or conjugated to membrane protein-specific antibodies for cell-specific delivery (for review, see (3)). To enhance this specificity, conditionally replicating viral vectors harboring the siRNA have been developed (53). The incorporation of tissue-specific RNA polymerase II promoters to drive expression of the siRNA (54), or conjugation to nanocomplexes (55), has been exploited as a strategy to further enhance preferential uptake of the molecules into a particular type of tissue. With these novel developments, it is likely that delivery of siRNA will become much more practical in the clinic in the near future.

To achieve potency in addition to specificity, siRNA may be incorporated into viral vectors, which have the ability to integrate into the host genome and thereby induce long-term gene silencing. Previous studies have investigated this approach using lentiviral (56–58), retroviral (58–60), or adenoviral vectors (57, 61, 62). However, in general, these vectors lack tissue specificity and raise concerns of toxicity associated with the viral structural proteins.

Although much progress has been made in the enhancement of RNAi administration, numerous hurdles remain. Intracellular stability, tissue-specific delivery, and sustained gene silencing are issues that must be addressed before this technology can become widely applicable in the clinic. Additionally, questions related to the so-called non-specific or "off-target" effects, as well as cellular resistance to siRNA or miRNA, must be answered before the therapeutic use of RNAi technology may be considered.

Nonetheless, as scientists continue to unravel the complexities of the RNAi machinery, optimism is generated that what originated as the discovery of a remarkable cellular phenomenon at the turn of the century may soon evolve into a technology that is safe and effective to administer in humans. At this point, it would be possible to use this technology to augment the potency of conventional vaccines against cancer. Specifically, the down-regulation of immunosuppressive molecules in DCs and T cells (Fig. 2), key components of the immune system, are promising strategies that could abrogate the ability of tumors to escape immunological control. At the rapid pace of our understanding of the intricate regulation of the innate and adaptive immune systems, it is hopeful that the use of RNAi in cancer immunotherapy may soon become a reality that saves the lives of many people worldwide.

Immunosuppressive molecular targets in dendritic cells

Molecule	Function	References
A20	Suppression of TNF and TLR signaling	6, 7, 10
SOCS1	Suppression of cytokine pathways	8, 11, 12
Tyro3/Axl/Mer	Suppression of TLR signaling; induction of apoptotic cell-mediated tolerance	13-15
IDO	Inhibition of T cell proliferation and function	16, 17
PD-L1	Induction of growth arrest and inhibition of IL-2 and IFN- γ synthesis by T cells	18-21
DIgR2	Suppression of T cell activation	22
Notch ligands	Suppression of T cell activation	23-26
FasL	Induction of T cell apoptosis	27
CCL17, CCL22	Recruitment of T_{reg} cells	28
miR-155	Inhibition of NF-κB pathway	63
miR-146a	Suppression of TLR and cytokine receptor pathways	32

Fig. 2. Immunosuppressive molecules expressed by DCs that can be targeted by RNAi for cancer immunotherapy. A20, SOCS1, and Tyro3/Axl/Mer suppress the antigen presentation and T cell activation capacity of DCs. IDO, PD-L1, DIgR2, Notch ligands, and FasL directly inhibit T cell proliferation, function, or survival. CCL17 and CCL22 mediate the recruitment of T_{reg} cells to the tumor. miR-155 and miR-146a are predicted to be suppressive miRNAs which inhibit DC function

Acknowledgments

This review is not intended to be an encyclopedic one, and we apologize to any authors not cited. We would like to thank Ms. Archana Monie for help with preparation of the manuscript and Ms. Lucy Wangaruro for excellent secretarial support. This work is funded by the National Cancer Institute SPORE (P50CA098252) and the NCDDG program (U19 CA113341).

References

1. Caplen, N.J. (2004) Gene therapy progress and prospects. Downregulating gene expression: the impact of RNA interference. *Gene Ther.* **11**, 1241–1248.
2. Leung, R.K. and Whittaker, P.A. (2005) RNA interference: from gene silencing to gene-specific therapeutics. *Pharmacol. Ther.* **107**, 222–239.
3. Shankar, P., Manjunath, N. and Lieberman, J. (2005) The prospect of silencing disease using RNA interference. *JAMA* **293**, 1367–1373.
4. Pai, S.I., Lin, Y.Y., Macaes, B., Meneshian, A., Hung, C.F. and Wu, T.C. (2006) Prospects of RNA interference therapy for cancer. *Gene Ther.* **13**, 464–477.
5. Bartel, D.P. (2004) MicroRNAs: genomics, biogenesis, mechanism, and function. *Cell* **116**, 281–297.
6. Lee, E.G., Boone, D.L., Chai, S., Libby, S.L., Chien, M., Lodolce, J.P. et al. (2000) Failure to regulate TNF-induced NF-kappaB and cell death responses in A20-deficient mice. *Science* **289**, 2350–2354.
7. Boone, D.L., Turer, E.E., Lee, E.G, Ahmad, R.C., Wheeler, M.T., Tsui, C. et al. (2004)

The ubiquitin-modifying enzyme A20 is required for termination of Toll-like receptor responses. *Nat. Immunol.* **5**, 1052–1060.

8. Shen, L., Evel-Kabler, K., Strube, R. and Chen, S.Y. (2004) Silencing of SOCS1 enhances antigen presentation by dendritic cells and antigen-specific anti-tumor immunity. *Nat. Biotechnol.* **22**, 1546–1553.
9. Kubo, M., Hanada, T. and Yoshimura, A. (2003) Suppressors of cytokine signaling and immunity. *Nat. Immunol.* **4**, 1169–7116.
10. Song, X.T., Evel-Kabler, K., Shen, L., Rollins, L., Huang, X.F. and Chen, S.Y. (2008) A20 is an antigen presentation attenuator, and its inhibition overcomes regulatory T cell-mediated suppression. *Nat. Med.* **14**, 258–265.
11. Zhou, H., Zhang, D., Wang, Y., Dai, M., Zhang, L., Liu, W. et al. (2006) Induction of CML28-specific cytotoxic T cell responses using co-transfected dendritic cells with CML28 DNA vaccine and SOCS1 small interfering RNA expression vector. *Biochem. Biophys. Res. Commun.* **347**, 200–207.
12. Yang, R., Yang, X., Zhang, Z., Zhang, Y., Wang, S., Cai, Z. et al. (2006) Single-walled carbon nanotubes-mediated in vivo and in vitro delivery of siRNA into antigen-presenting cells. *Gene Ther.* **13**, 1714–1723.
13. Rothlin, C.V., Ghosh, S., Zuniga, E.I., Oldstone, M.B. and Lemke, G. (2007) TAM receptors are pleiotropic inhibitors of the innate immune response. *Cell* **131**, 1124–1136.
14. Lu, Q. and Lemke, G. (2001) Homeostatic regulation of the immune system by receptor tyrosine kinases of the Tyro 3 family. *Science* **293**, 306–311.
15. Wallet, M.A., Sen, P., Flores, R.R., Wang, Y., Yi, Z., Huang, Y. et al. (2008) MerTK is required for apoptotic cell-induced T cell tolerance. *J. Exp. Med.* **205**, 219–232.
16. Munn, D.H., Sharma, M.D., Lee, J.R., Jhaver, K.G., Johnson, T.S., Keskin, D.B. et al. (2002) Potential regulatory function of human dendritic cells expressing indoleamine 2,3-dioxygenase. *Science* **297**, 1867–1870.
17. Munn, D.H., Sharma, M.D., Hou, D., Baban, B., Lee, J.R., Antonia, S.J. et al. (2004) Expression of indoleamine 2,3-dioxygenase by plasmacytoid dendritic cells in tumor-draining lymph nodes. *J. Clin. Invest.* **114**, 280–290.
18. Carter, L., Fouser, L.A., Jussif, J., Fitz, L., Deng, B., Wood, C.R. et al. (2002) PD-1:PD-L inhibitory pathway affects both CD4(+) and CD8(+) T cells and is overcome by IL-2. *Eur. J. Immunol.* **32**, 634–643.
19. Latchman, Y., Wood, C.R., Chernova, T., Chaudhary, D., Borde, M., Chernova, I. et al. (2001) PD-L2 is a second ligand for PD-1 and inhibits T cell activation. *Nat. Immunol.* **2**, 261–268.
20. Brown, J.A., Dorfman, D.M., Ma, F.R., Sullivan, E.L., Munoz, O., Wood, C.R. et al. (2003) Blockade of programmed death-1 ligands on dendritic cells enhances T cell activation and cytokine production. *J. Immunol.* **170**, 1257–1266.
21. Curiel, T.J., Wei, S., Dong, H., Alvarez, X., Cheng, P., Mottram, P. et al. (2003) Blockade of B7-H1 improves myeloid dendritic cell-mediated antitumor immunity. *Nat. Med.* **9**, 562–567.
22. Shi, L., Luo, K., Xia, D., Chen, T., Chen, G., Jiang, Y. et al. (2006) DIgR2, dendritic cell-derived immunoglobulin receptor 2, is one representative of a family of IgSF inhibitory receptors and mediates negative regulation of dendritic cell-initiated antigen-specific T-cell responses. *Blood* **108**, 2678–2686.
23. Hoyne, G.F., Le Roux, I., Corsin-Jimenez, M., Tan, K., Dunne, J., Forsyth, L.M. et al. (2000) Serrate1-induced notch signalling regulates the decision between immunity and tolerance made by peripheral CD4(+) T cells. *Int. Immunol.* **12**, 177–185.
24. Wong, K.K., Carpenter, M.J., Young, L.L., Walker, S.J., McKenzie, G., Rust, A.J. et al. (2003) Notch ligation by Delta1 inhibits peripheral immune responses to transplantation antigens by a CD8+ cell-dependent mechanism. *J. Clin. Invest.* **112**, 1741–1750.
25. Amsen, D., Blander, J.M., Lee, G.R., Tanigaki, K., Honjo, T. and Flavell, R.A. (2004) Instruction of distinct CD4 T helper cell fates by different notch ligands on antigen-presenting cells. *Cell* **117**, 515–526.
26. Stallwood, Y., Briend, E., Ray, K.M., Ward, G.A., Smith, B.J., Nye, E. et al. (2006) Small interfering RNA-mediated knockdown of notch ligands in primary CD4+ T cells and dendritic cells enhances cytokine production. *J. Immunol.* **177**, 885–895.
27. Huang, B., Mao, C.P., Peng, S., Hung, C.F. and Wu, T.C. (2008) RNA interference-mediated in vivo silencing of fas ligand as a strategy for the enhancement of DNA vaccine potency. *Hum. Gene Ther.* **19**, 763–773.
28. Iellem, A., Mariani, M., Lang, R., Recalde, H., Panina-Bordignon, P., Sinigaglia, F. et al. (2001) Unique chemotactic response profile and specific expression of chemokine receptors CCR4 and CCR8 by CD4(+)CD25(+)

regulatory T cells. *J. Exp. Med.* **194**, 847–853.

29. Baltimore, D., Boldin, M.P., O'Connell, R.M., Rao, D.S. and Taganov, K.D. (2008) MicroRNAs: new regulators of immune cell development and function. *Nat. Immunol.* **9**, 839–845.
30. Rodriguez, A., Vigorito, E., Clare, S., Warren, M.V., Couttet, P., Soond, D.R. et al. (2007) Requirement of bic/microRNA-155 for normal immune function. *Science* **316**, 608–611.
31. Thai, T.H., Calado, D.P., Casola, S., Ansel, K.M., Xiao, C., Xue, Y. et al. (2007) Regulation of the germinal center response by microRNA-155. *Science* **316**, 604–608.
32. Taganov, K.D., Boldin, M.P., Chang, K.J. and Baltimore, D. (2006) NF-kappaB-dependent induction of microRNA miR-146, an inhibitor targeted to signaling proteins of innate immune responses. *Proc. Natl. Acad. Sci. U.S.A.* **103**, 12481–12486.
33. Liu, G., Ng, H., Akasaki, Y., Yuan, X., Ehtesham, M., Yin, D. et al. (2004) Small interference RNA modulation of IL-10 in human monocyte-derived dendritic cells enhances the Th1 response. Eur. J. Immunol. **34**, 1680–1687.
34. Diehl, S. and Rincon, M. (2002) The two faces of IL-6 on Th1/Th2 differentiation. *Mol. Immunol.* **39**, 531–536.
35. Ingulli, E., Mondino, A., Khoruts, A. and Jenkins, M.K. (1997) In vivo detection of dendritic cell antigen presentation to CD4(+) T cells. *J. Exp. Med.* **185**, 2133–2141.
36. Hou, W.S. and Van Parijs, L. (2004) A Bcl-2-dependent molecular timer regulates the lifespan and immunogenicity of dendritic cells. *Nat. Immunol.* **5**, 583–589.
37. Nopora, A. and Brocker, T. (2002) Bcl-2 controls dendritic cell longevity in vivo. *J. Immunol.* **169**, 3006–3014.
38. Kim, T.W., Hung, C.F., Ling, M., Juang, J., He, L., Hardwick, J.M. et al. (2003) Enhancing DNA vaccine potency by coadministration of DNA encoding antiapoptotic proteins. *J. Clin. Invest.* **112**, 109–117.
39. Peng, S., Kim, T.W., Lee, J.H., Yang, M., He, L., Hung, C.F. et al. (2005) Vaccination with dendritic cells transfected with BAK and BAX siRNA enhances antigen-specific immune responses by prolonging dendritic cell life. *Hum. Gene Ther.* **16**, 584–593.
40. Kim, T.W., Lee, J.H., He, L., Boyd, D.A., Hardwick, J.M., Hung, C.F. et al. (2005) Modification of professional antigen-presenting cells with small interfering RNA in vivo to enhance cancer vaccine potency. *Cancer Res.* **65**, 309–316.
41. Hsieh, C.L., Chen, D.S. and Hwang, L.H. (2000) Tumor-induced immunosuppression: a barrier to immunotherapy of large tumors by cytokine-secreting tumor vaccine. *Hum. Gene Ther.* **11**, 681–692.
42. Poppema, S., Potters, M., Visser, L. and van den Berg, A.M. (1998) Immune escape mechanisms in Hodgkin's disease. *Ann. Oncol.* **9 Suppl 5**, S21–S24.
43. Scarpa, S., Coppa, A., Ragano-Caracciolo, M., Mincione, G., Giuffrida, A., Modesti, A. et al. (1996) Transforming growth factor beta regulates differentiation and proliferation of human neuroblastoma. *Exp. Cell Res.* **229**, 147–154.
44. Jayaraman, L. and Massague, J. (2000) Distinct oligomeric states of SMAD proteins in the transforming growth factor-beta pathway. *J. Biol. Chem.* **275**, 40710–40717.
45. Massague, J. (1998) TGF-beta signal transduction. *Annu. Rev. Biochem.* **67**, 753–791.
46. Depoortere, F., Pirson, I., Bartek, J., Dumont, J.E. and Roger, P.P. (2000) Transforming growth factor beta(1) selectively inhibits the cyclic AMP-dependent proliferation of primary thyroid epithelial cells by preventing the association of cyclin D3-cdk4 with nuclear p27(kip1). *Mol. Biol. Cell* **11**, 1061–1076.
47. Sandhu, C., Garbe, J., Bhattacharya, N., Bhattacharya, N., Daksis, J., Pan, C.H. et al. (1997) Transforming growth factor beta stabilizes p15INK4B protein, increases p15INK4B-cdk4 complexes, and inhibits cyclin D1-cdk4 association in human mammary epithelial cells. *Mol. Cell Biol.* **17**, 2458–2467.
48. Fargeas, C., Wu, C.Y., Nakajima, T., Cox, D., Nutman, T. and Delespesse, G. (1992) Differential effect of transforming growth factor beta on the synthesis of Th1- and Th2-like lymphokines by human T lymphocytes. *Eur. J. Immunol.* **22**, 2173–2176.
49. Palladino, M.A., Morris, R.E., Starnes, H.F. and Levinson, A.D. (1990) The transforming growth factor-betas. A new family of immunoregulatory molecules. *Ann. N.Y. Acad. Sci.* **593**, 181–187.
50. Leach, D.R., Krummel, M.F. and Allison, J.P. (1996) Enhancement of antitumor immunity by CTLA-4 blockade. *Science* **271**, 1734–1736.
51. Iwai, Y., Terawaki, S. and Honjo, T. (2005) PD-1 blockade inhibits hematogenous spread of poorly immunogenic tumor cells by enhanced recruitment of effector T cells. *Int. Immunol.* **17**, 133–144.

52. Ryther, R.C., Flynt, A.S., Phillips, J.A., 3rd and Patton, J.G. (2005) siRNA therapeutics: big potential from small RNAs. *Gene Ther.* **12**, 5–11.
53. Carette, J.E., Overmeer, R.M., Schagen, F.H., Alemany, R., Barski, O.A., Gerritsen, W.R. et al. (2004) Conditionally replicating adenoviruses expressing short hairpin RNAs silence the expression of a target gene in cancer cells. *Cancer Res.* **64**, 2663–2667.
54. Song, J., Pang, S., Lu, Y., Yokoyama, K.K., Zheng, J.Y. and Chiu, R. (2004) Gene silencing in androgen-responsive prostate cancer cells from the tissue-specific prostate-specific antigen promoter. *Cancer Res.* **64**, 7661–7663.
55. Schiffelers, R.M., Ansari, A., Xu, J., Zhou, Q., Tang, Q., Storm, G. et al. (2004) Cancer siRNA therapy by tumor selective delivery with ligand-targeted sterically stabilized nanoparticle. *Nucleic Acids Res.* **32**, e149.
56. Sumimoto, H., Miyagishi, M., Miyoshi, H., Yamagata, S., Shimizu, A., Taira, K. et al. (2004) Inhibition of growth and invasive ability of melanoma by inactivation of mutated BRAF with lentivirus-mediated RNA interference. *Oncogene* **23**, 6031–6039.
57. Sumimoto, H., Yamagata, S., Shimizu, A., Miyoshi, H., Mizuguchi, H., Hayakawa, T. et al. (2005) Gene therapy for human small-cell lung carcinoma by inactivation of Skp-2 with virally mediated RNA interference. *Gene Ther.* **12**, 95–100.
58. Duxbury, M.S., Ito, H., Benoit, E., Zinner, M.J., Ashley, S.W. and Whang, E.E. (2004) Retrovirally mediated RNA interference targeting the M2 subunit of ribonucleotide reductase: A novel therapeutic strategy in pancreatic cancer. *Surgery* **136**, 261–269.
59. Brummelkamp, T.R., Bernards, R. and Agami, R. (2002) Stable suppression of tumorigenicity by virus-mediated RNA interference. *Cancer Cell* **2**, 243–247.
60. Chen, J., Wall, N.R., Kocher, K., Duclos, N., Fabbro, D., Neuberg, D. et al. (2004) Stable expression of small interfering RNA sensitizes TEL-PDGFbetaR to inhibition with imatinib or rapamycin. *J. Clin. Invest.* **113**, 1784–1791.
61. Chen, L.M., Le, H.Y., Qin, R.Y., Kumar, M., Du, Z.Y., Xia, R.J. et al. (2005) Reversal of the phenotype by K-rasval12 silencing mediated by adenovirus-delivered siRNA in human pancreatic cancer cell line Panc-1. *World J. Gastroenterol.* **11**, 831–838.
62. Uchida, H., Tanaka, T., Sasaki, K., Kato, K., Dehari, H., Ito, Y. et al. (2004) Adenovirus-mediated transfer of siRNA against survivin induced apoptosis and attenuated tumor cell growth in vitro and in vivo. *Mol. Ther.* **10**, 162–171.

Chapter 22

Preventing Tissue Injury Using siRNA

Zhu-Xu Zhang, Marianne E. Beduhn, Xiufen Zheng, Wei-Ping Min, and Anthony M. Jevnikar

Abstract

RNA interference (RNAi) is a process through which double-stranded RNA induces the activation of endogenous cellular pathways of RNA degradation, resulting in selective and potent silencing of genes that have homology to the double strand. Much of the excitement surrounding small interfering RNA (siRNA)-mediated therapeutics arises from the fact that this approach overcomes many of the shortcomings previously experienced with alternative approaches to selective blocking that use antibodies, antisense oligonucleotides or pharmacological inhibitors. Induction of RNAi through administration of siRNA has been successfully applied to the treatment of hepatitis, viral infections, and cancer. Increased success in addressing issues of siRNA delivery and efficiency will permit this approach to evolve as a new paradigm in clinical therapeutics. In this chapter, we present applications of RNAi in tissue injury, and the possibilities of using this highly promising approach in the context of transplantation.

Key words: RNAi, siRNA, Ischemia reperfusion injury, Gene silencing, Kidney, Heart, Liver, Delayed graft function, Inflammation, Transplantation

1. Introduction

Ischemia reperfusion (I/R) injury occurs invariably in organ transplantation and other medical settings, and causes characteristic and often severe injury to organs and tissues. I/R injury induces a perturbence of endothelial cell signaling pathways and the expression of a family of molecules that promote injury in the attempt to facilitate repair. Many toxic metabolic products accumulate during I/R injury in tissues, resulting in organ dysfunction and many life-threatening conditions and diseases. The intracellular and molecular mechanisms involved in the development of I/R injury are complex and not yet fully understood (1). A lack of

Wei-Ping Min and Thomas Ichim (eds.), *RNA Interference*, Methods in Molecular Biology, vol. 623,
DOI 10.1007/978-1-60761-588-0_22, © Springer Science+Business Media, LLC 2010

therapeutic approaches has resulted in a lack of specific or effective treatments for I/R injury.

Methods for manipulating biological systems have included pharmacological drugs, antisense oligonucleotides (AO), ribozymes, and antibodies. In transplantation, all of these approaches have been applied with varying degrees of success. The revolutionary discovery that the endogenous cellular process of RNA interference (RNAi) can be artificially manipulated to induce gene-specific silencing, using synthesized small interfering RNA (siRNA), has led to an explosion of interest in this technique. The attractiveness of RNAi, in contrast to other methods of manipulation, arises from its extremely high inhibitory activity, its specific inhibition, and the ease with which various methods of inducing RNAi can be applied. The process of tissue injury modulation offers a plethora of molecular targets for siRNA silencing such as: (1) genes associated with ischemia/reperfusion damage and genes causing apoptosis of cells within transplanted organs; (2) biological response modifiers such as cytokines; (3) molecules associated with lymphocyte extravasation and homing; and (4) effector molecules of immunity such as complement, perforin, and granzymes. The following describes our approaches and methodologies in siRNA as a therapeutic potential in solid organ transplantation.

2. Materials

2.1. Mice

CD1 mice were purchased from the Jackson Laboratory (Bar Harbor, ME). The mice were maintained under strict pathogen-free conditions. All mice were males of 6–10 weeks in age, and were housed in filter-top cages (4 mice per cage) at the Animal Facility, University of Western Ontario according to Canadian Council for Animal Guidelines. Mice were fed food and water, and were allowed to settle for 2 weeks before the initiation of experimentation, which had ethical approval from the university board.

2.2. Antibodies and Cell Line

All antibodies were purchased as indicated in each section. The L929 cell line was obtained from ATCC.

2.3. Target Gene siRNA Design

Complement 3 (C3) siRNA: Select the target sequences 5′-CTGTGCAAGACTTCCTAAAGA-3′ specific to C3. The oligonucleotides containing sense and antisense of the target sequences and loop sequence should be synthesized.

Caspase 3 siRNA: The oligonucleotides contain target-specific sequences and restriction enzyme sites at the end of the strands: 5′GATCCC*AACTACTGTCCAGATAGATCC*TTCAAGAGA *GGATCTATCTGGACAGTAGTT*TTTTTTCCAAA-3′ (sense),

5′-AGCTTTTGGAAAAAA *AACTACTGTCCAGATAGATCC*TC
TCTTGAA*GGATCTATCTGGACAGTA GTT* GG-3′ (antisense).

2.4. Cell Culture and Lysis

1. RPMI-1640 medium (Invitrogen, Burlington, Ontario, Canada) supplemented with 2 mM L-glutamine (Life Technologies, Burlington, Ontario, Canada), 100 U/ml penicillin (Life Technologies), 100 mg of streptomycin, (Life Technologies), 50 μM 2-Mercaptoethanol (Life Technologies), and 10% FBS (heat-inactivated) (Life Technologies). Store at 4°C.
2. Buffer: 75 mM Tris-HCl, pH 6.8, 1.5% (w/v) sodium dodecyl sulfate (SDS), 7.5% (w/v) glycerol, 200 mM β-mercaptoethanol, 0.03% (w/v) bromophenol blue, 0.003% (w/v) pyronin-Y. Store in aliquots at –20°C.
3. Teflon cell scrapers (Fisher).

2.5. PRNATU6.1 Vector Preparation

1. pRNATU6.1 plasmid (Genescript), stored at –20°C.
2. Restrict enzymes: *Bam*HI, *Hin*dIII and *Eco*RV (Biolabs).
3. Competent *E. coli* (DH5a) (Invitrogen), stored at –80°C.
4. T4 DNA ligase (Biolabs), stored at –20°C.
5. Agar plates (BD Falcon), stored at 4°C.
6. LB broth (Invitrogen), stored at 4°C.
7. Qiagen plasmid Mini kit.
8. Qiagen plasmid Midi kit.
9. Ampicillin (Bioshop), stored at –20°C.

2.6. PCR

1. Deionized distilled water; 18.2μΩ water was collected and sterilized.
2. PCR and RT-PCR were performed using kits from Invitrogen.
3. Real-time PCR SYBR Green kits were from Stratagene, stored at –20°C.

2.7. Transfection

1. Lipofectin (Gibco RBL), stored at 4°C.
2. PBS, PH = 7, 0.1 M, stored at 4°C (Sigma).
3. L929 cell line (ATCC).

2.8. In Vivo Silencing

1. 1× PBS stored at 4°C.
2. Occlusion clamp (microvascular clamp, Roboz Surgical Instrument, Washington D.C.).
3. 30 gauge needle (BD Biosciences).
4. Decalcifier I solution. (SurgiPath, Richmond, IL, USA)
5. Deoxynucleotidyl transferase (TdT)-DNA FragEL™ detection kit (Calbiochem, San Diego, CA. USA).

2.9. Immunochemistry

1. OCT compound (Sakura, Finefeck, Torrance, CA).
2. Blocking buffer: 10% normal horse serum in PBS, stored at 4°C.
3. EnVision+ Rabbit-HRP (Dako, Carpinteria, CA), stored at 4°C.
4. Chromogenic substrate (DAB); sections counterstained with hematoxylin, stored at 4°C.
5. Ready-to-useperoxidase-blockingsolution(DakoCytomation, Carpinteria, CA), stored at 4°C.

3. Methods

Two important pathways that contribute significantly to the pathogenesis of renal I/R injury are inflammation and apoptosis. Mechanisms leading to increased gene expression and biosynthesis of proinflammatory and apoptotic mediators have been investigated extensively in recent years. C3 and C5a as well as apoptosis-related genes, such as Fas, Caspase 3, or Caspase 8, are reportedly involved in murine renal ischemia (2). These molecules are candidates for siRNA targeting to prevent kidney I/R injury.

Nuclear factor κB (NF-κB) is a rapid-response transcription factor, which is critical to both the regulation of apoptosis and the increased expression of many proinflammatory mediators (3, 4). Inhibition of NF-κB by IκB super-repressor gene transfer or NF-κB decoy oligodeoxynucleotides has been shown to ameliorate I/R injury in an experimental lung transplant model (5) and in a rat renal I/R injury model (6). In mammals, the NF-κB family consists of five members that form homodimeric and heterodimeric complexes: RelA, RelB, c-Rel, NF-κB1, and NF-κB2 (7, 8). These complexes can directly regulate gene expression. Therefore, NF-κB is a therapeutic target that may be of clinical relevance (9).

3.1. PRNATU6.1 Vector Backbone Preparation (see Note 1)

1. Digest 5–10 μg of pRNATU6.1 plasmid DNA with 10 Units of *Bam*HI and *Hin*dIII in 30–40 μl of reaction volume for 2 h at 37°C. Heat the digestion to 65°C for 10 min to inactivate the enzyme.
2. Load the digestion solution onto 0.8% agarose gel and run for 30–40 min at 60 V electrophoresis. The length of time necessary depends on how well the undigested and digested DNA separates. The digested DNA will be linear and therefore move more slowly in the gel than the undigested circular DNA. Load undigested DNA as a control and use a ladder to the separate wells.
3. Cut the digested bands visualized under UV light and extract DNA from the gel cut using Qiagen gel extraction kit.
4. Measure the DNA concentration at OD260. DNA concentration in μg/ml = Dilution factor × OD260 × 50 μg/ml.

3.2. Annealing of shRNA Oligo DNA

1. Dissolve shRNA oligos in deionized and distilled (DD)-water at the concentration of 10 μg/μl.
2. Dilute 1 μl of the oligos to 1 μg/μl.
3. Assemble the 50 μl annealing mixture as follows:

Component	Amount
Sense shRNA encoding oligos	2 μl
Antisense shRNA encoding oligos	2 μl
1× DNA annealing solution	46 μl

4. Heat the mixture to 90°C for 3 min.
5. Cool to 37°C and incubate for 1 h. The annealed siRNA insert can either be ligated into a vector or stored at −20°C for future ligation.

3.3. Ligation

1. Set up two 10 μl ligation reactions. Use a plus-insert ligation as a positive control, and a minus-insert for the negative control.
2. To each tube, add the following reagents:

Insert (annealed oligs)	Minus-insert (backbone alone)	Component
1 μl		Annealed insert oligos
	1 μl	1× DNA annealing solution
6 μl	6 μl	DD-water
1 μl	1 μl	10× T4 DNA ligase buffer
1 μl	1 μl	Backbone (8–10 ng/ml)
1 μl	1 μl	T4 DNA ligase (5 U/μl)

3. Incubate the ligation reaction for 1–16 h at room temperature or 37°C. The fully constructed vector is displayed in Fig. 1.

3.4. Transformation of E. coli with the Ligation Products

1. Combine 20–40 μl of transformation competent *E. coli* (DH5a) with 5 μl of the ligation products.
2. Leave the *E. coli* on ice for 5 min.
3. Heat at 42°C for 38 s.
4. Put on ice for 2 min.
5. Add 200–300 μl of prewarmed LB, and put in air-shaker for 30 min at 37°C using a speed of 20 g.
6. Transfer to LB agar plates containing antibiotic and incubate for 18 h at 37°C.

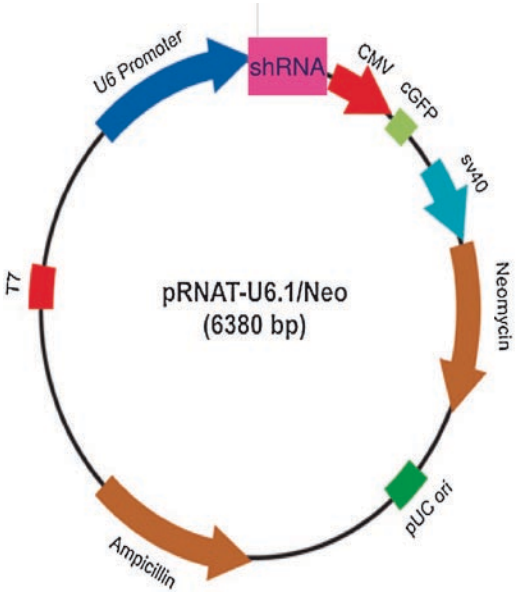

Fig. 1. Construct of pRNATU6.1 vector. pRNATU6.1 vector is used to generate shRNA. pRNATU6.1 contains a U6.1 promoter, unique restrict *Bam*HI and *Hin*d III cutting site, cGFP reporter gene sequence, and Neomycin selective marker. Encoding sequence of shRNA is inserted between *Bam*HI and *Hin*dIII site. cGFP reporter gene allows monitoring of gene transfection efficacy. Neomycin selective marker is used to select transfected cell and get stable cell lines

3.5. Identifying Clones

1. Pick 2–3 colonies (number of colonies that should be picked depends on how many colonies are present on the negative plate).
2. Put colony into 5 ml of LB medium containing the same antibiotic as the plate, and grow overnight at 37°C.
3. Collect the *E. coli*, and purify shRNA expression plasmid with Qiagen mini-prep kit.
4. Sequence the sample to confirm the insertion.

3.6. In Vitro Silencing of the C3, C5a, Caspase 3, Caspase 8, or RelB Genes via Gene Transfection

1. Culture L929 cells in RPMI 1640 or DMEM with 10% FBS.
2. Seed the cells into 24-well plates (1×10^5 cells per well) and grow overnight in order to reach 90% confluence.
3. Mix 2 μg of plasmid DNA with 2 μl of Lipofectin suspended in 100 μl of PBS at room temperature for 45 min in 1 ml of serum-free medium. Alternatively, add to dissociated NPIC or dog pancreatic islets supplemented with 0.5 ml of serum-free medium in a 48-well plate.

4. After 4 h of incubation at 37°C with 5% CO_2, wash and culture the cells in RPMI 1640 or DMEM with 10% FBS for 48 h or indicated time. Use supernatants and cell lysates to detect gene expression as described below.

3.7. RNA Isolation (see Note 2)

Collect cells for RNA isolation and pellet by centrifugation. Lyse cells in TRIzol reagent ($5–10 \times 10^6$ animal or plant cells, or 1×10^7 bacterial cells/1 ml reagent). For adherent cells, aspirate the culture medium, wash with PBS, and then add 0.5 ml TRIzol directly to the cells.

1. Transfer the sample to a 1.5 ml Eppendorf tube.
2. Incubate the samples for 5 min at 15–30°C.
3. Add 0.2 ml of chloroform per 1 ml of TRIzol reagent, shake/invert the tubes by hand for 15–30 s, and incubate for 2–3 min at 15–30°C (or room temperature).
4. Centrifuge 12,000×*g* for 15 min at 2–8°C.
5. Transfer the supernatant (aqueous phase) to a fresh tube, add 0.5 ml isopropyl alcohol (isopropanol) /(1 ml TRIzol reagent), incubate 10 min at 15–30°C.
6. Centrifuge 12,000×*g* for 10 min at 2–8°C.
7. Remove the supernatant, wash pellets using 75% ethanol (100% ethanol mixed with DEPC water) 1 ml/1 ml TRIzol reagent. Tapping the tube by hand, let the pellets suspend in 75% ethanol, centrifuge 7,500×*g* for 5 min at 2–8°C.
8. Air dry the RNA pellet.
9. Add RNase-free (DEPC) water and incubate 55–60°C for 10 min. The volume of the water depends on the size of the pellets, and the RNA can be used for cDNA.

3.8. Measurement of Messenger RNA Levels by Reverse Transcriptase, Quantitative Polymerase Chain Reaction (PCR), and Quantitative Real-Time PCR

First strand cDNA was synthesized using an RNA PCR kit with the oligo $(dT)_{16}$ primer. Complete cDNA synthesis with olgdT in 20 µl volume as described below:

3 µg total RNA
0.9 µl (0.5 µg/µl) olgdT → total 12.75 µl
DEPC-DD water

1. Incubate at 70°C for 10 min.
2. Chill on ice for 5 min.
3. Spin the tube and then add

5× 1st strand buffer	4 µl
0.1 M DTT	2 µl
10 mM dNTP	1 µl
RNase inhibitor	0.25 µl

4. Leave at 42°C for 2 min before adding 0.5 µl (200 U/µl) Reverse Transcriptase.
5. Incubate at 42°C for 50 min, followed by 70°C for 15 min (hold at 4°C once completed). The cDNA is now ready for PCR.

PCR is used to detect target gene expression. The total volume is 25 µl. The primers for real-time PCR are listed in Subheading 3.8, step 4.

cDNA	1 µl	
10× PCR buffer	2.5 µl	
2 µM Primer (forward + reverse)	2.5 µl	200 nM
10 mM dNTP	0.5 µl	200 µM
50 mM $MgCl_2$	0.75 µl	1.5 mM
Taq polymerase (5 U/µl)	0.2 µl	1 U
DD-water	17.55 µl	

1. Put samples in the PCR machine. Use the primers for glyceraldehyde-3-phosphate dehydrogenase (GAPDH) as a control reference gene. RT-PCR and PCR are performed with an Eppendorf Cycler (Mastercycler gradient).

   PCR conditions: 95°C for 30 s, 58°C for 30 s, and then 72°C for 30 s (30 cycles). The detection of siRNA target gene expression is shown in Fig. 2.
2. Real-time PCR reactions should be performed to examine gene expression in the Stratagene MX 4000 multiplex quantitative PCR system. Use the SYBR Green PCR Master mix and 100 nM of gene-specific forward and reverse primers. Primers used for the amplification of target genes and house keeper gene GAPDH are as follows:

   GAPDH 5′-TGATGACAT CAAGAAGGTGGTGAA-3′ (forward) and 5′-TGGGATGGAAATTGTGAGGGAGAT-3′ (reverse).
   C3: 5′-CCCTGCCCCTTACCCCTTCATTC-3′ (forward), and 5′-CGTACTTGTGCCCCTCCTTA TCTG-3′ (reverse).

   PCR should be performed under the following conditions: 95°C for 30 s, 58°C for 30 s, and then 72°C for 30 s (40 cycles).

   Caspase 3, 5′-CGGGGTACGGAGCTGGACTGT-3′ (forward) and 5′-AATTCCGTTGCCACCTTCCTGTT-3′ (reverse),

   Perform PCR under the following conditions: 95°C for 30 s, 58°C for 30 s, and then 72°C for 30 s (40 cycles).
   Samples are normalized using the housekeeping gene GAPDH, and a comparative C_T method is used for the analysis.

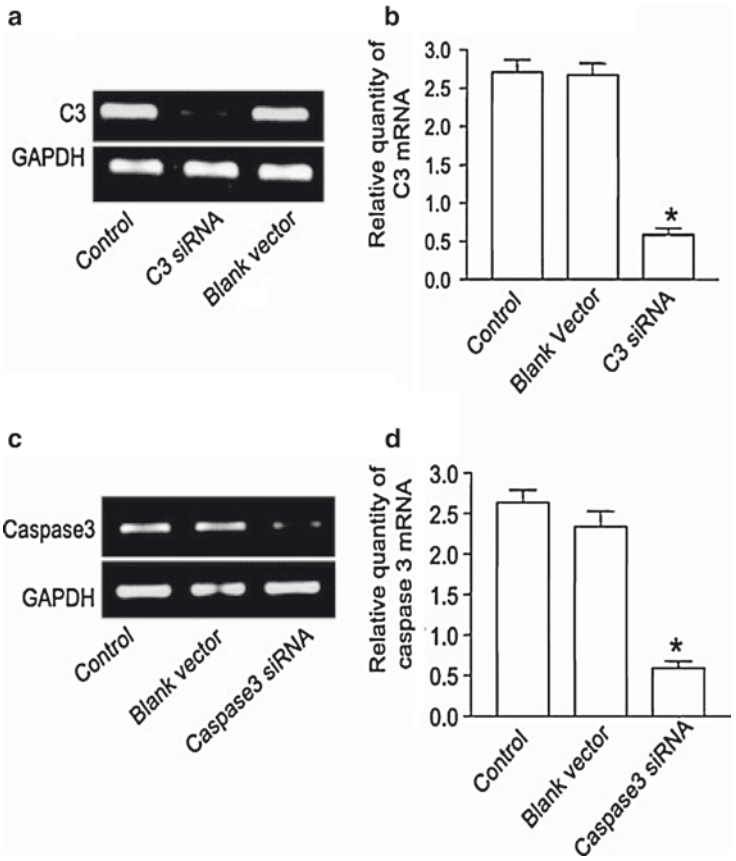

Fig. 2. In vitro gene silencing. (**a** and **b**) Silencing C3 gene. L929 cell lines are transfected with C3 cDNA vectors using Lipofectamine 2000 and co-transfected with C3 siRNA, empty vectors, or non-siRNA (control). Then 24 h after transfection, cells are harvested to extract total RNA. Transcripts of C3 and GAPDH are determined using RT-PCR (**a**) and quantitative PCR (**b**). (**c** and **d**) Silencing caspase 3 gene. L929 cells are transfected with caspase 3 siRNA, empty vectors, or non-siRNA (control). Then 24 h after transfection, expression of caspase 3 is detected using RT-PCR (**c**) and quantitative PCR (**d**). Data (**a** and **c**) are representative of four independent experiments. Data (**b** and **d**) are expressed as mean ± SEM. Statistical significance as compared with siRNA vs. vector (*$p < 0.05$)

3.9. Renal I/R Injury Model (see Notes 3 and 4)

1. Mice (25–30 g) are anesthetized with an intraperitoneal injection of ketamine (100 mg/kg) and xylazine (10 mg/kg) combined with inhalation of enflurane. Keep the body temperature of the mice constant by placing a warm pad (37°C) beneath the animal.
2. Following abdominal incisions, renal pedicles should be bluntly dissected. Place a microvascular clampon the left renal pedicle for 35 min. During this procedure, keep the animals

well hydrated with warm saline (0.8 ml) and at a constant temperature (37°C). The time of ischemia is chosen to obtain a reversible model of ischemic acute renal failure with a minimum amount of vascular thrombosis, and to avoid animal mortality.

3. After removal of the clamp, observe the left kidney for an additional 1 min to see the color change that is indicative of blood reperfusion; then, resect the right kidney. For the survival observance experiment, perform surgery in an identical fashion, except use 35 min for the time of ischemia (clamping).
4. Suture the incisions, and allow the animals to recover with free access to food and water.
5. Blood creatinine levels should be analyzed 24 h after reperfusion. Harvest the left kidney for analysis after 24 h reperfusion.

3.10. In Vivo Silencing of Target Gene

1. For systemic injection, shRNAs (in 0.8–1 ml PBS) should be rapidly injected (within 10 s) into one of the tail side veins or the penis vein. To dilate the tail veins, immerse the tail in warm water (50–55°C), while the mouse is under ether narcosis for 5 ± 1 s.
2. For local injection, first visualize the left renal pedicle from a median laparotomy. Do minimal preparation above the renal vessels on the left side of the aorta to insert an occlusion clamp.
3. Then clip the aorta and the vena cava, and puncture the renal vein with a 30-gauge needle to inject 0.1 ml of PBS containing siRNA.
4. Keep the needle in place for 5 s, then remove slowly while applying compression to the renal vein for 30 s with Avitene® held with forceps. Leave the Avitene® in place thereafter.
5. Remove the aorta and vena cava clamp immediately after the left renal pedicle is occluded for ischemia.

3.11. Measurement of Renal Target Gene mRNA Levels by Quantitative Real-Time PCR

1. RNA should be extracted from kidneys using TRIzol and reverse-transcribed using the oligo-(dT) primer and reverse transcriptase as described in Subheading 3.7.
2. Perform real-time PCR reactions to examine gene expression using the MX 4000 multiplex quantitative PCR system and the SYBR Green PCR Master mix. Normalize gene expression using the housekeeping gene GAPDH, and a comparative C_T method for the analysis (Fig. 3).

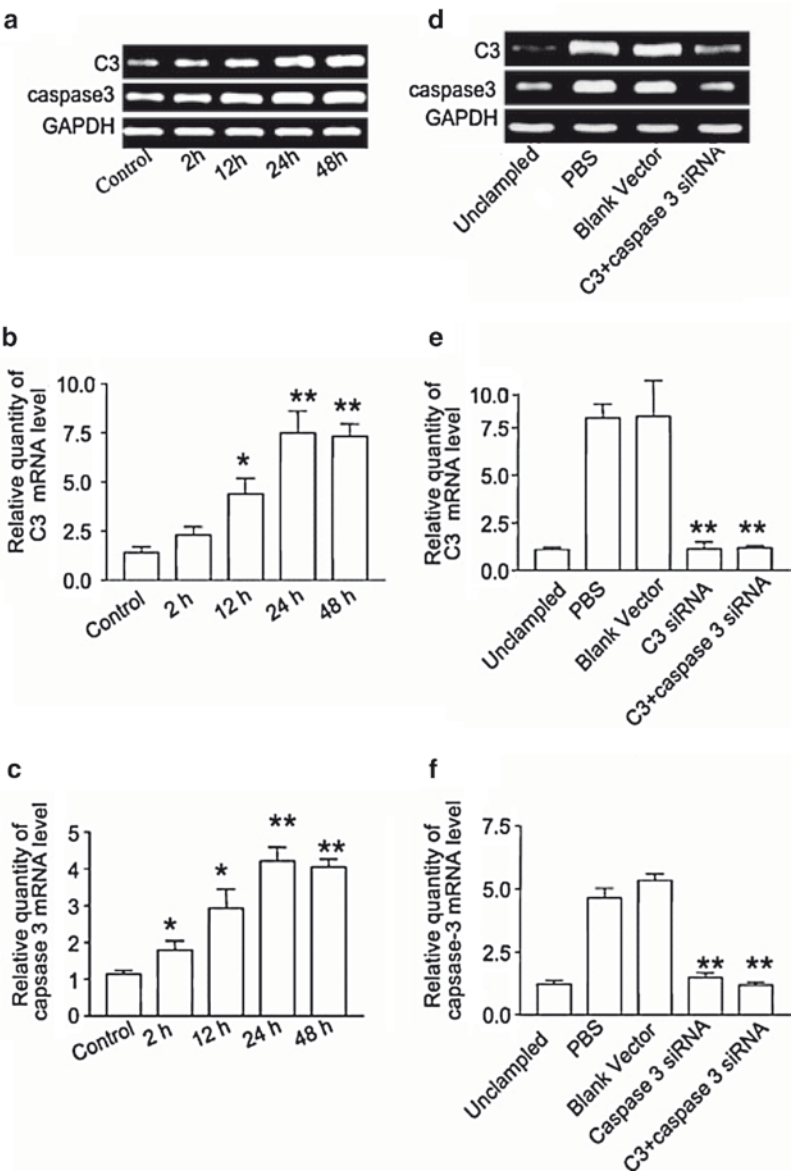

Fig. 3. Upregulated gene expression by I/R and gene silencing in vivo. (**a**–**c**) Upregulated expression of C3 and caspase 3 genes in the kidney after I/R injury. Left kidneys of mice ($n=4$) are subjected to clamping for 25 min as described in Methods (*see* Subheading 3.9). Kidneys are harvested at indicated time points after clamping. The expression of C3 (**a** and **b**) and caspase 3 (**a** and **c**) is detected by RT-PCR (**a**) and real-time PCR (**b** and **c**). (**d**–**f**) C3 and caspase 3 gene silencing in vivo. Mice ($n=8$ each group) are pre-treated with 50 μg of C3 siRNA and caspase 3 siRNA, or empty vectors for 48 h followed by I/R experiments. Kidneys are harvested 24 h after I/R for determination of C3 (**d** and **e**) and caspase 3 (**d** and **f**) gene expression using RT-PCR (**d**) and real-time PCR (**e** and **f**). Data (**a** and **d**) are representative of four independent experiments. Data (**b**, **c**, **e**, and **f**) are expressed as mean ± SEM. Statistical significance as compared with different time point vs. control in data (**b** and **c**), siRNA treatment vs. PBS or blank vector (*$p<0.05$; **$p<0.001$)

3.12. Assessment of Renal Function

Blood samples should be obtained from the inferior vena cava 24 h post ischemia for measuring serum BUN and creatinine levels (Fig. 4).

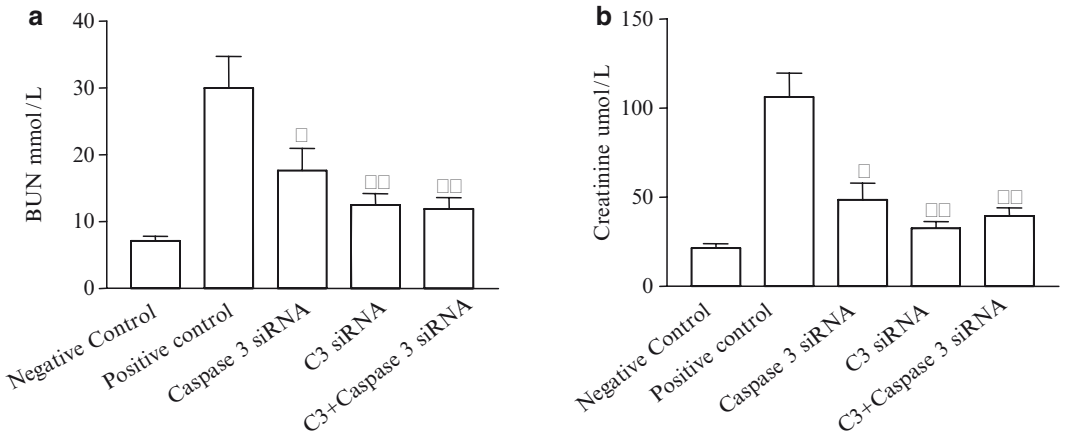

Fig. 4. siRNA prevents kidney from ischemic injury. Renal pedicles are clamped for 25 min. Blood is collected before clamping (0 h) and 24 h after reperfusion to determine levels of BUN (**a**) and serum creatinine (**b**). Data shown are mean ± SEM (siRNA treated versus untreated and sham mice, $*p < 0.05$; $**p < 0.001$)

3.13. Assessment of Renal Morphological Changes

1. 24 h post ischemia, dissect kidneys from mice and fix tissue slices in 10% formalin buffer. Decalcify by immersing in Decalcifier I solution overnight, then rinse tissues in running water.
2. Paraffin sections should be made by routine procedure. Cut 5-μm paraffin sections and heat at 60°C for 30 min.
3. Hydration should be done by transferring the sections through the following solutions: triple to xylene for 6 min, and then for 2 min to 100% ethanol twice, 95% ethanol, 70% ethanol.
4. Stain sections with hematoxylin and eosin (H&E) and mount (Fig. 5).
5. Examine the sections in a double-blinded fashion by a pathologist. The percentage of histology changes in the cortex and medulla should be scored using a semiquantitative scale designed to evaluate the degree of infarction, tubular vacuolization, and cast formation on a 5-point scale, based on the injury area of involvement, as follows: 0, normal kidney; 0.5, <10%; 1, 10–25%; 2, 25–50%; 3, 50–75%; and 4, 75–100%.

3.14. Apoptosis Assay

The TUNEL assay can detect cellular apoptosis using the terminal deoxynucleotidyl transferase (TdT)-DNA FragEL™ detection kit.

1. Permeabilize paraffin sections of the kidneys in situ and inactivate using endogenous peroxidase, followed by DNA fragment labeling, termination and detection of labeled DNA according to the manufacturer's instructions.

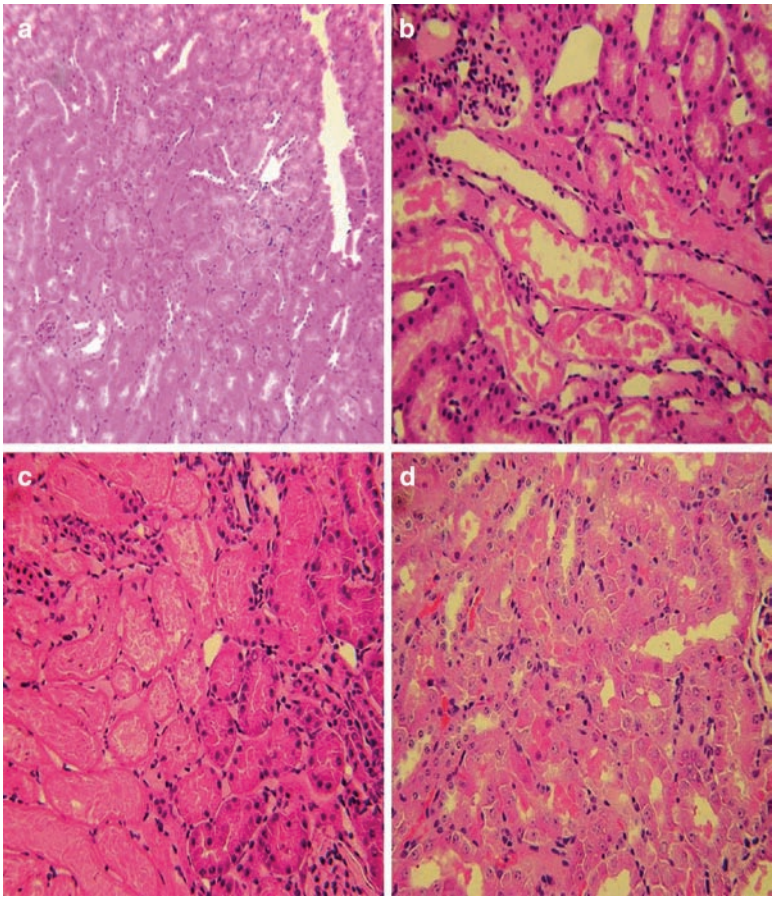

Fig. 5. Histological changes in I/R injuried kidneys. Mice are treated with siRNA, and I/R injury experiments are performed as described in Fig. 2b. Then 24 h after I/R, kidney tissues are harvested and sectioned, then stained with H&E. Tissue injury is determined and necrosis of tubule and glomerulus is assessed under high power (400×) over five fields. (**a**) Normal unclamped kidney. (**b**) PBS-treated I/R kidney. (**c**) Empty vectors-treated I/R kidney. (**d**) C3 siRNA and caspase 3 siRNA-treated I/R kidney

2. Evaluate cell apoptosis by counting 5,000 random cells from each section at 400× magnification in 4–6 pituitary slides from each mouse.

3.15. Immunohistochemistry

1. Kidneys in OCT compound should be snap-frozen in liquid nitrogen and stored at −80°C.
2. Use cryostat to cut 5 μm frozen sections, then fix in cold acetone for 10 min and allow to air dry.
3. Then the sections should be blocked with 10% normal horse serum in PBS.
4. Antibody Rabbit anti-mouse C3, anti-caspase 3, or caspase 8 antibodies should be used as the primary antibody for 1 h at

room temperature, followed by incubation with EnVision+ Rabbit-HRP. After incubating with the chromogenic substrate (DAB), counterstain the sections with H&E. Then, examine the slides under a light microscope.

5. Rinse the sections with PBS and treat with a ready-to-use peroxidase-blocking solution.
6. After washing with PBS, incubate the slides with rabbit EnVison+ HRP for 30 min.
7. Wash and develop the sections with ready-to-use DAB for 1–3 min and counter-stain with H&E. For negative controls, use isotype sera and omit primary antibody.

3.16. Immunohistochemical Staining for MPO

1. Evaluate kidney MPO activity by immunohistochemistry. Paraffin sections should be deparaffinized and rehydrated as described earlier.
2. Perform the microwave antigen retrieval procedure (10 μm citrate buffer, pH 6.0) and incubate the samples in a ready-to-use peroxidase blocking solution to inhibit endogenous peroxidase. To block nonspecific background staining, the sections should be incubated with 10% horse serum.
3. Then, incubate the sections with rabbit anti-human MPO antibody 1:100, followed by incubation with EnVision+ Rabbit-HRP. After incubating with the chromogenic substrate (DAB), counterstain the sections with H&E.
4. Finally, examine the slides under a light microscope at 400× magnification. Evaluate the staining of cytoplasmic MPO in the neutrophils, and express the results as an average percentage of neutrophils cytoplasmically stained positive for MPO in 10 fields in the same section.

3.17. Statistical Analysis

Data are expressed as mean ± SEM. A one-way ANOVA is used for statistical comparisons among groups, followed by the Newman-Keuls Test method and log-rank test for survival statistical analyses. The threshold for statistical significance is $p < 0.05$.

4. Notes

1. PRNATU6.1 vector backbone preparation

   To successfully obtain a positive clone, the preparation of completely digested and purified vector backbone is important. Run agarose gel as long as needed to totally separate digested and undigested plasmid bands, in order to avoid contamination from the partial digested or undigested plasmid.

2. Measurement of renal target gene mRNA levels by quantitative real-time PCR.

   RNA is easily degraded because RNase exists widely in living cells. Extracting RNA from kidney tissues is more difficult than from cultured cells. Great care should be taken during the extraction procedure.

3. Ischemia-reperfusion model

   Many factors, including anesthesia, air temperature, and ischemic time, can affect I/R injury. Before anesthetizing the mice, weighing them is necessary. Try to use mice with a similar body weight for all experiments. Keep room temperature constant during the operation. The temperature can affect the severity of injury; therefore, it can be lowered to limit injury.

4. Mouse strain and IRI

   There is a strain difference in mice for IRI and this should be considered in experiments. Optimizing the conditions for IRI should be conducted when using different mouse strains.

References

1. Chatterjee, P.K. (2007) Novel pharmacological approaches to the treatment of renal ischemia-reperfusion injury: a comprehensive review. *Naunyn Schmiedebergs Arch. Pharmacol.* **376**, 1–43.
2. Zhang, X., Zheng, X., Sun, H., Feng, B., Li, M., Chen, G., et al. (2006) Prevention of renal ischemic injury by silencing the expression of renal caspase 3 and caspase 8. *Transplantation* **82**, 1728–1732.
3. Barkett, M. and Gilmore, T.D. (1999) Control of apoptosis by Rel/NF-kappaB transcription factors. *Oncogene* **18**, 6910–6924.
4. Daemen, M.A., de Vries, B. and Buurman, W.A. (2002) Apoptosis and inflammation in renal reperfusion injury. *Transplantation* **73**, 1693–1700.
5. Ishiyama, T., Dharmarajan, S., Hayama, M., Moriya, H., Grapperhaus, K. and Patterson, G.A. (2005) Inhibition of nuclear factor kappaB by IkappaB superrepressor gene transfer ameliorates ischemia-reperfusion injury after experimental lung transplantation. *J. Thorac. Cardiovasc. Surg.* **130**, 194–201.
6. Cao, C.C., Ding, X.Q., Ou, Z.L., Liu, C.F., Li. P., Wang, L., et al. (2004) In vivo transfection of NF-kappaB decoy oligodeoxynucleotides attenuate renal ischemia/reperfusion injury in rats. *Kidney Int.* **65**, 834–845.
7. Ghosh, S., May, M.J. and Kopp, E.B. (1998) NF-kappa B and Rel proteins: evolutionarily conserved mediators of immune responses. *Annu. Rev. Immunol.* **16**, 225–260.
8. Siebenlist, U., Franzoso, G. and Brown, K. (1994) Structure, regulation and function of NF-kappa B. *Annu. Rev. Cell Biol.* **10**, 405–455.
9. Lee, J.I. and Burckart, G.J. (1998) Nuclear factor kappa B: important transcription factor and therapeutic target. *J. Clin. Pharmacol.* **38**, 981–993.

Chapter 23

Preventing Immune Rejection Through Gene Silencing

Xusheng Zhang, Mu Li, and Wei-Ping Min

Abstract

Dendritic cells (DCs) comprise a family of professional antigen-presenting cells responsible for the induction of primary immune responses. DCs are also important for the induction of immunological tolerance. Recent research has revealed that DC maturation is associated with activation of the NF-kB pathway. RelB, one of the five families of Rel proteins involved in the NF-kB pathway, plays a critical role in coordinating the terminal stages of DC maturation and has the ability to induce optimal Th1 T cell responses. DCs generated from mouse bone marrow can be silenced using siRNA specific for the target gene. Silencing RelB in DCs will result in the generation of immunoregulatory dendritic cells that inhibit allogenic T cell responses. The KLH-specific T cell response should also be inhibited after the RelB siRNA treatment. Furthermore, silencing the RelB gene in DCs can generate regulatory T cells. Administering donor-derived RelB-silencing DCs can prevent allograft rejection in murine heart transplantation.

Key words: Dendritic cells, RelB, siRNA, T regulatory cells, Antigen-specific response, Heart transplantation

1. Introduction

Dendritic cells (DCs) are the most potent antigen-presenting cells, having a role in both priming the adaptive immune response and inducing immunological tolerance (1, 2). It has been demonstrated that properties of DCs depend on maturation status, phenotype and source of origin, and that DCs can be either immunostimulatory or immunoregulatory. In general, mature DCs express high levels of CD11C, major histocompatibility complex class II (MHC II) and the costimulatory molecules CD40 and CD86. DCs that inhibit immune responses have been described as immature (imDC), having plasmacytoid morphology,

Wei-Ping Min and Thomas Ichim (eds.), *RNA Interference*, Methods in Molecular Biology, vol. 623,
DOI 10.1007/978-1-60761-588-0_23, © Springer Science+Business Media, LLC 2010

or being alternatively activated. Collectively, suppressive DCs have been termed "tolerogenic DCs." Previous studies have demonstrated that donor-specific, allogeneic tolerogenic DCs can enhance survival of transplanted grafts (3, 4).

Recent research has revealed that DC maturation is associated with activation of the NF-κB pathway (5, 6). Inhibitors of NF-κB activation have been shown to block the maturation of DCs, resulting in reduced expression of T cell stimulatory molecules, such as MHC class II, CD80 and CD86 molecules (6, 7). It is also evident that NF-κB activity is essential for the development of Th1 responses. There are five proteins in the mammalian NF-κB family including c-Rel, RelA, RelB, NF-κB1, and NF-κB2. In contrast to other NF-κB family members, such as RelA which chiefly contributes to cell survival, RelB is required for DC development and differentiation (8, 9). RelB plays a critical role in regulating the maturation and function of DCs and has the ability to induce optimal Th1 T cell responses. Direct evidence for a relationship between RelB and DCs has been shown in studies in which the RelB gene was disrupted via either mutation or gene knockout, resulting in a dramatic reduction of NF-κB activity with impaired DC function (10–12). Therefore, we hypothesize that RelB is a potential target for generating tolerogenic DCs.

RNA interference (RNAi) is a newly discovered process in which the introduction of double-stranded RNA (dsRNA) into cells results in sequence-specific gene silencing (13). When long dsRNA enters the cytoplasm, it is recognized and cleaved into 21–23 bp fragments by Dicer, an RNase III enzyme. These cleaved components of dsRNA, termed small interfering RNA (siRNA), are incorporated into a ribonucleoprotein complex called RISC (RNA-induced silencing complex), which can then mediate the silencing of endogenous genes. Exogenous administration of siRNA is capable of blocking gene expression in mammalian cells without triggering the nonspecific panic response (14). Gene silencing using siRNA is a potent, selective, and easily inducible method for specifically blocking expression of desired genes (15). The use of siRNA, shown to have therapeutic benefits in animal models of various diseases, is currently in clinical trials (16).

Generating DCs from mouse bone marrow and silencing the RelB gene with RelB siRNA should theoretically produce tolerogenic DCs. These RelB-silenced DCs are immunoregulatory, and therefore can inhibit T cell responses in an antigen-specific manner and generate regulatory T (Treg) cells. Administering donor-derived RelB-silenced DCs should significantly prevent allograft rejection in murine heart transplantation.

2. Materials

2.1. Generation of Dendritic Cells from Mouse Bone Marrow

1. 6–8 week-old C57BL/6 male mice (Jackson Laboratory, Bar Harbor, Maine) (see Note 1).
2. Complete RPMI 1640 culture medium: RPMI 1640 medium (Sigma, Oakville, ON) supplemented with 10% fetal bovine serum(FBS,Gibco,Burlington,ON),100U/mlpenicillin,100μg/ml streptomycin, 2 mM glutamine and 2-mercaptoethanol (Gibco, Burlington, ON) . Store at 4°C.
3. Dendritic cell culture medium: Complete RPMI 1640 culture medium,addmouserecombinantGM-CSFandIL-4cytokineat final concentration 10 ng/ml. Make fresh every time when used.
4. ACK Lysing buffer (Lonza, Walkersville, MD).
5. Recombinant Murine Granulocyte/Macrophage Colony-Stimulating Factor (GM-CSF) and Recombinant Interleukin-4 (IL-4) (PeproTech, Rocky Hill,NJ). Store at –20°C.
6. LPS, Lipopolysaccharide (Sigma, Oakville, ON): add tissue culture medium, dilute to concentration of 1 mg/ml. Reconstituted LPS may be further diluted to working concentration of 10μg/ml, and store at –20°C.

2.2. DC Transfected with RelB siRNA Using Genesilencer Reagent

1. Four sequences specific to the RelB gene are selected: target 1 (UGGAAAUCAU CGACGAAUAUU), target 2 (GCUACGGUGUGGACAAGAAUU), target 3 (GAAGAU CCAGCUGGGAAUUUU), and target 4 (GGGAAAGAC-UGCACGGACGUU). siRNA is synthesized and annealed by the manufacturer (Darmacon, Chicago, IL). A pool consisting of four targeting siRNA is used to silence DCs. Store the pooled siRNA at –20°C.
2. Genesilencer siRNA Transfection Reagent (Genlantis, San Diego, CA). Store at 4°C.

2.3. Gene Silencing Efficiency Test Using Real-Time PCR

2.3.1. RNA Isolation

1. TRIzol Reagent (Invitrogen, Burlington, ON), store at 4°C.
2. Chroloform (Sigma, Oakville, ON), store at room temperature.
3. Isopropanol (Sigma, Oakville, ON), store at room temperature.
4. 75% ethanol, 75 ml 100% ethanol mix with 25 ml DEPC-treated water.
5. Diethylpyrocarbonate (DEPC)-treated water: add 1 ml of DEPC to 1,000 ml of distilled H_2O. Mix and leave at room temperature for 12 h, autoclave and cool to room temperature prior to use.

2.3.2. cDNA Synthesis

1. Oligo dT 0.5 µg/µl (Invitrogen, Burlington, ON), store at –20°C.
2. 0.1 M Dithiothreitol (DTT) (Invitrogen, Burlington, ON), store at –20°C.
3. 10 mM dNTP (Invitrogen, Burlington, ON), store at –20°C.
4. RNase inhibitor (Invitrogen, Burlington, ON), store at –20°C.
5. Superscript II Reverse Transcriptase (Invitrogen, Burlington, ON), store at –20°C.

2.3.3. Real-Time PCR

1. Brilliant SYBR Green QPCR Master Mix (Stratgene, La Jolla, CA). Store master mix at –20°C; after first thaw, the master mix can be stable at 4°C for 1 month. Limit the number of freeze/thaw cycles.
2. Reference dye (Stratgene, La Jolla, CA).
3. Sequence of GAPDH Primer, forward: TGATGACATCAAGAAGGTGGTGAA, Reverse: TCCTTGGAGGCCATGTAGGCCAT.
4. Sequence of RelB Primer, forward: CCCCTACAATGCTGGCTCCCTGAA, Reverse: CACGGCCCGCTCTCCTTGTTGATT.

2.4. Phenotypical Analysis by Flow Cytometry

1. Day 7 LPS-stimulated mouse dendritic cells.
2. Fluorochrome-conjugated antibodies: FITC-labelled anti-mouse MHCII CD86, PE-labelled anti-mouse CD40 antibody, and isotype control antibody (eBioscience, San Diego, CA). Store at 4°C.
3. FACS buffer: 1X Dulbecco's PBS, Ca^{2+} and Mg^{2+} free (Sigma, Oakville, ON) with 2% FBS and 0.1% sodium azide. Store at 4°C.
4. Fixed buffer: 2% formaldehyde-PBS pH 7.4, freshly prepared. 2 g paraformaldehyde (Sigma, Oakville, ON), 100 ml PBS adjust pH to 7.2. Store protected from light ≤1 month at 4°C. To dissolve paraformaldehyde, heat solution to 70°C in a fume hood for 1 h. Cool to room temperature before adjusting pH. Do not heat the solution above 70°C.
5. 12 × 75 mm round-bottom tubes (BD Falcon, Mississauga, ON).

2.5. RelB siRNA-Silenced DCs Inhibit Allogeneic Lymphocyte Reaction

1. Freshly removed spleen from mouse (6–8 weeks old BALB/c).
2. 60 × 15 mm culture dishes (Sarstedt, Montreal, Quebec).
3. 40 µm Nylon cell strainer (BD Falcon, Mississauga, ON).
4. High-density solution: Ficoll-Paque (GE Healthcare, Baie d'Urfe, Quebec).
5. Tritium Thymidine (MP Biomedical, Solon, OH).

2.6. RelB siRNA-Silenced DCs Inhibit Antigen-Specific Response

1. KLH, keyhole limpet hemocyanin (Sigma, Oakville, ON): dilute with deionized water at concentration of 5 mg/ml, and store at –20°C for a maximum of 2 months.
2. OVA, (Ovalbumin) Albumin from chicken egg white (Sigma, Oakville, ON), store at 4°C.

2.7. RelB siRNA-Silenced DCs Generate T Regulatory Cells

1. FITC anti-mouse/rat Foxp3 Staining Set (eBioscience, San Diego, CA). Components:
   (a) Fixation/Permeabilization Concentrate, store at 4°C.
   (b) Fixation/Permeabilization Diluent, store at 4°C. Dilute 1 part Fixation/Permeabilization Concentrate with 3 parts Fixation/Permeabilization Diluent to make the Fixation/Permeabilization working solution. This buffer should not be stored for more than 1 day.
   (c) Permeabilization Buffer (10×), store at 4°C. Dilute to 1× with deionized/distilled water and store at 4°C. The 1× permeabilization buffer should be made fresh before each experiment.
2. Anti-mouse/rat Foxp3 (FJK-16s), store at 4°C.
3. PE-Cy5-labelled anti-mouse CD4 (eBioscience, San Diego, CA), store at 4°C.
4. PE-labelled anti-mouse CD25 (eBioscience, San Diego, CA), store at 4°C.

2.8. Prevent Immune Rejection Through Gene Silencing

1. 8–12-week-old C57BL/6 male mice (Jackson Laboratory, Bar Harbor, Maine) used as donors.
2. 8–12-week-old BALB/c male mice (Jackson Laboratory, Bar Harbor, Maine) used as recipients.
3. Bone marrow DCs cultured from 6 to 8-week-old C57BL/6 male mice.
4. RelB siRNA (Darmacon, Chicago, IL). Store at –20°C.
5. Genesilencer siRNA Transfection Reagent (Genlantis, San Diego, CA), store at 4°C.

3. Methods

3.1. Generation of Dendritic Cells from Mouse Bone Marrow

1. Remove femurs and tibias from mice and remove the muscles from the bones. Spray the bones with 70% ethanol, and keep in RPMI 1640 medium until all the bones have been prepared.
2. Prepare three 60 × 15 mm culture dishes. One for 70% ethanol, one for wash buffer, another one for RPMI 1640. Immerse the bones for 1 min in a culture dish containing 70% ethanol, and then wash the bones in dish full of washing buffer.

3. Cut off both ends of each bone with scissors and place in a separate culture dish. Obtain the marrow by flushing out each of the shafts with RPMI 1640 using a 3 ml syringe for 2–3 times on each side of the bone.
4. Resuspend the bone marrow plug from the bones, and break up the clumps with Pasteur pipettes. Transfer the suspension to a 50 ml tube.
5. Lyses red blood cells by adding 5 ml ACK buffer. Wash the marrow cells twice with RPMI 1640, each time by centrifuging 5 min at 400 g at room temperature.
6. Count viable cells and adjust cell concentration to 1×10^6 cells/ml in fresh DC culture medium. Plate cell suspension at 4 ml/well in a 6-well plate. Incubate the plate at 37°C in 5% humidified CO_2.
7. At day 2, gently swirl the plate and remove the old culture medium. Add 4 ml fresh DC culture medium (see Note 2).
8. Change the culture medium every 2 days: remove 2 ml old medium, then add 2 ml fresh DC culture medium .
9. On day 7, add LPS 100 ng/ml to stimulate DCs to mature.

3.2. Transfect Dendritic Cells with RelB siRNA Using Genesilencer Reagent

1. Keep cultured DCs from mouse bone marrow on day 6.
2. Prepare the Genesilencer reagent by diluting in serum-free medium (5 µl Genesilencer reagent + 25 µl serum-free medium).
3. Prepare the siRNA dilution by first mixing siRNA Diluent and serum-free medium (15 µl siRNA Diluent + 25 µl serum-free medium). Use the Diluent/serum-free medium mix to dilute 0.5 µg RelB siRNA and negative-control siRNA. Mix well by pipetting up and down several times. Incubate at room temperature for 5 min. It is important that you do not vortex the diluted siRNA mixture.
4. Add the siRNA dilution for step 3 to the diluted Genesilencer solution in step 2. Incubate at room temperature for 5 min to allow the siRNA/lipid complex to form (see Note 3).
5. While the siRNA/Genesilencer complexes are forming, collect the DCs and resuspend them in 2.5×10^6/ml of serum-free medium.
6. Transfer 400 µl/well (equal to 1×10^6 DCs) cell suspension to the 24-well plate.
7. Add the siRNA/Genesilencer mix to the cells. Gently mix the cells by pipetting up and down several times (see Note 4).
8. Four hours post transfection, add 400 µl 20% FBS and 20 ng/ml GM-CSF and IL-4 cytokine dendritic cell culture medium; incubate overnight.
9. Next morning post transfection, add 800 µl fresh dendritic cell culture medium. Assay can be done 24–48 h after transfection.

3.3. Gene Silencing Efficiency Test Using Real-Time PCR

3.3.1. RNA Isolation

1. Pallet post-transfected dendritic cells by centrifuge at 400×g for 5 min, lyses cells in 0.5 ml TRIzol Reagent.
2. Transfer the sample to a 1.5 ml eppendorf tube.
3. Incubate the samples for 5 min at room temperature.
4. Add 0.1 ml of chloroform, shake/invert the tubes by hand for 15–30 s, and incubate for 2–3 min at room temperature.
5. Centrifuge 12,000×g for 15 min at 2–8°C.
6. Transfer the supernatant (aqueous phase) to a fresh tube, add 0.25 ml isopropanol and incubate 10 min at 15–30°C.
7. Centrifuge 12,000×g for 10 min at 2–8°C.
8. Remove the supernatant, wash pellets using 0.5 ml 75% ethanol (100% ethanol mixed with DEPC water); tapping the tube by hand, let the pellets suspend in 75% ethanol, and centrifuge 7,500×g for 5 min at 2–8°C.
9. Discard the supernatant, air-dry the RNA pellets.
10. Add DEPC-treated water. The volume of the water depends on the size of the pellets, incubate 55–60°C for 10 min, the total RNA can be used for cDNA.

3.3.2. First-Stranded cDNA Synthesis Using SuperScript II RT

cDNA synthesis with oligo(dT) in 20 µl volume

1. Prepare the following RNA/oligo(dT) mixture in each tube:

Total RNA	3 µg
0.9 µl (0.5 µg/µl) oligo(dT)	0.9 µl
DEPC H_2O	to 12.25 µl

2. Incubate the samples at 70°C for 10 min and then on ice for 5 min.
3. Prepare reaction master mixture. For each reaction:

5× 1st-strand buffer	4 µl
0.1 M DTT	2 µl
10 mM dNTP	1 µl
RNase inhibitor	0.25 µl

4. Add the reaction mixture to the RNA/oligo(dT) mixture, mix briefly, and incubate at 42°C for 2 min.
5. Add 0.5 µl of SuperScript II RT (200 u/µl) to each tube, mix and incubate at 42°C for 50 min.
6. Heat inactivate at 70°C for 15 min, and then chill on ice.
7. Store the 1st-strand cDNA at –20°C until use for real-time PCR.

3.3.3. Real-Time PCR Using Brilliant SYBR Green QPCR Master Mix

1. Prepare PCR reaction mixture (below) on ice.

Reagents (per reaction)	Volume	Final concentration
SYBR Master Mix (2×)	12.5 µl	1×
PCR Forward primer (2 µM)	1.25 µl	0.1 µM
PCR Reverse primer (2 µM)	1.25 µl	0.1 µM
Diluted reference dye	0.375 µl	30 nM
cDNA template	1 µl	
dH_2O	8.625 µl	
Total	25 µl	

2. Gently mix the reactions without creating bubbles (do not vortex) (see Note 5).
3. Centrifuge the reaction briefly.
4. Place the reactions in the instrument MX4000P (STRATAGENE) and run the PCR program below.

Cycles	Duration of cycle	Temperature
1	10 min	95°C
40	30 s	95°C
	1 min	58°C
	1 min	72°C

5. Analyze the result using MX4000 software (Fig. 1).

3.4. Phenotypical Analysis by Flow Cytometry

1. Collect Day 7 LPS-stimulated bone marrow dendritic cells, centrifuge cell suspension for 5 min at 400×g, 4°C, and discard supernatant. Resuspend cell pellet to 1×10^7 cells/ml in FACS buffer, 4°C.
2. Add 100 µl cell suspension (10^6 cells) to 12 × 75-mm round-bottom test tubes.
3. Add 1 µl PE- or FITC-labelled anti-mouse CD40, CD86, MHCII antibody or isotype control antibody to each tube containing cells and mix gently. Incubate 30 min at 4°C in the dark (see Note 6).
4. Wash cells by adding 3 ml FACS buffer, 4°C.
5. Centrifuge cell suspension for 5 min at 400×g, 4°C. Carefully pour or pipette off the supernatant fluid.
6. Repeat wash steps 4 and 5 one time.
7. Resuspend stained cell pellets in 300 µl of 4°C FACS buffer or fixed buffer. Keep the cell suspension at 4°C in the dark until analysis by flow cytometry (Fig. 2) (see Note 7).

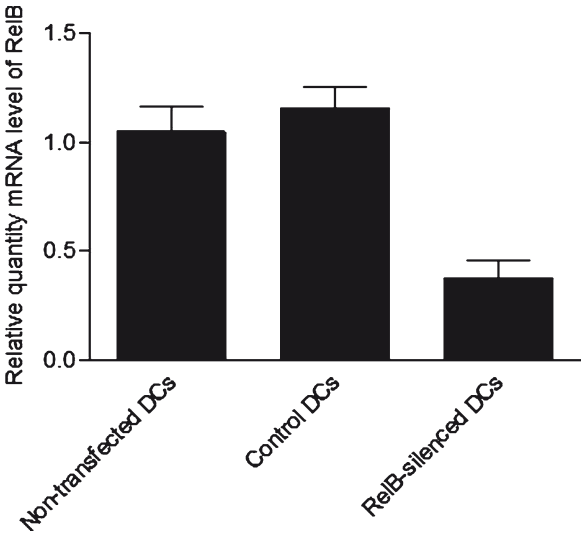

Fig. 1. RelB-silenced DCs using RelB siRNA. RelB expression is determined by real-time PCR. At day 6, cultured DCs are transfected with control siRNA or RelB siRNA in vitro. 48 h after gene silencing, total RNAs are extracted from transfected DCs. Real-time quantitative PCR is performed as described in Subheading 3.3

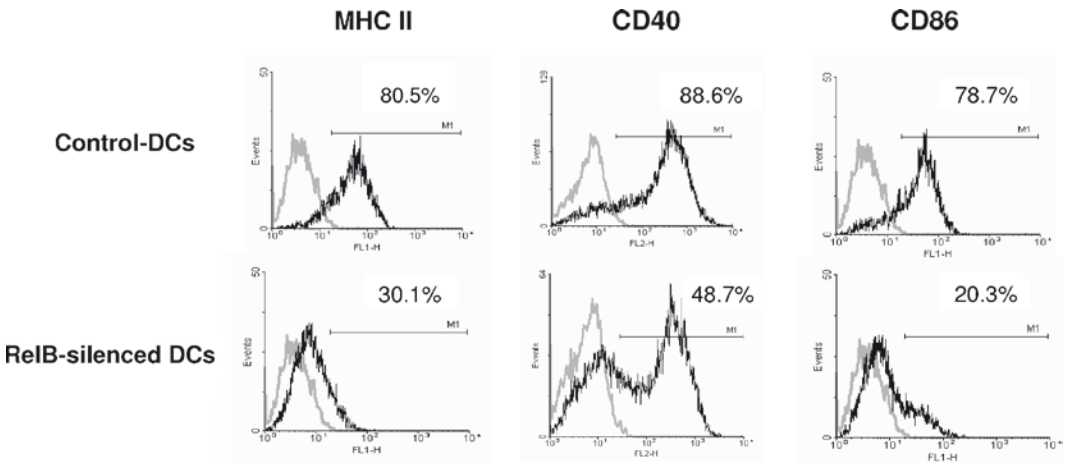

Fig. 2. Phenotypic analysis of DCs after silencing RelB. Bone marrow-derived DCs (1×10^6) are transfected with 0.5 μg RelB siRNA (RelB-silenced DCs) or negative-control siRNA (Control-DCs) on day 6. Subsequently, transfected DCs are activated for 24 h with 100 ng/ml LPS. Maturation is assessed in terms of expression of MHC II, CD80, and CD86 by flow cytometry using FITC- or PE-conjugated antibodies (*dark line*) and isotype controls (*grey line*)

3.5. RelB siRNA-Silenced DCs Inhibit Allogeneic Lymphocyte Reaction

1. Sacrifice the BALB/c mouse and take the spleen. Put spleen in 3 ml RPMI 1640 medium in a 15 ml tube.
2. Prepare three 60×15 mm culture dishes. One for 70% ethanol, one for RPMI 1640 medium and the other for RPMI 1640 complete medium. Place freshly removed spleen in the dish

with 70% ethanol, rinse for 30 s, then wash the spleen in dish with RPMI 1640 medium for 1 min.

3. Put a 40 μm Nylon cell strainer in the tissue dishes containing 10 ml complete RPMI 1640 medium. Place the spleen into the strainer and squeeze the spleen through the cell strainer with the rubber end of a plunger from a 1 ml syringe.
4. Put 4 ml of room temperature Ficoll-Paque solution in 15 ml polypropylene tube, slowly loading spleen suspension on the top surface of Ficoll-Paque solution (see Note 8).
5. Centrifuge at 900×g for 25 min at room temperature. Use rapid acceleration and slow deceleration (no brake) to get the best separation result (see Note 9).
6. Isolate spleen lymphocyte cells floating on top of the Ficoll-Paque solution by slowly moving tip of pipette over surface of high-density layer and drawing cells up in a 3.5-ml pipette (try to collect as little high-density solution as possible). Transfer spleen lymphocyte cells to another 15 ml tube.
7. Add 10 ml complete RPMI 1640 medium, wash and centrifuge for 5 min at 400×g.
8. Resuspend the spleen lymphocytes in 2×10^6/ml with complete RPMI 1640 medium.
9. Use spleen lymphocytes from naïve BALB/c mouse as responder cells. Stimulator cells are C57BL/6 mouse bone marrow DCs transfected with either RelB siRNA or negative-control siRNA, after these DCs have been irradiated (2,000 rad).
10. To a 96-well microtiter plate, add 2×10^5 responder cells in 0.1 ml to each well. For each experimental group, use three replicate wells.
11. Prepare irradiated stimulator DCs. Use the ratios of 2:1, 5:1, and 20:1 for responder cells: stimulator cells.
12. Place microtiter plates in a humidified 37°C, 5% CO2 incubator for 72 h.
13. At the last 18 h, add 1 μci[^{3}H]thymidine to each well. Return the plates to CO2 incubator to pulse for 18 h. Harvest cells using a harvester, and measure cpm in scintillation counter (Fig. 3).

3.6. RelB siRNA-Silenced DCs Inhibit Antigen-specific Response

1. Culture mouse bone marrow DCs on day 6.
2. Immunize C57BL/6 mice with 10 μg OVA by s.c. injection.
3. Transfect mouse bone marrow DCs with RelB siRNA or negative-control siRNA using Genesilencer reagent according to Subheading 3.2.
4. 24 h after transfection, pulse DCs with keyhole limpet hemocyanin (KLH; Sigma-Aldrich) at a final concentration of 50 μg/ml.

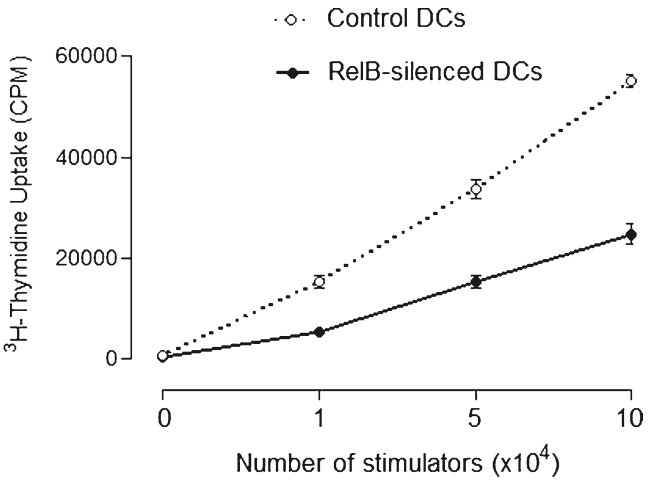

Fig. 3. RelB siRNA transfection inhibits DCs allostimulatory ability. C57BL/6-derived DCs are transfected with negative control siRNA (Control DCs) or RelB siRNA (RelB-silenced DCs) for 24 h. Allogeneic (BALB/c) spleen lymphocytes (2×10^5) are incubated with siRNA-silenced DCs at the indicated concentration for 72 h. Proliferation is determined using [^{3}H] thymidine incorporation. *$p < 0.05$

5. After being pulsed for 24 h, stimulate DCs for another 24 h with LPS at a concentration of 100 ng/ml.
6. Collect cells and resuspend in DPBS, inject 1×10^6 cells into the OVA-immunized C57BL/6 mice by s.c. injection.
7. After 10 days, sacrifice mice and take the draining lymph nodes.
8. Place the lymph nodes into a 40 μm nylon cell strainer, put the strainer in a 60 × 15 mm cell culture dish containing 10 ml PRMI 1640 complete medium, and squeeze the lymph nodes through the cell strainer with the rubber end of a plunger from a 1 ml syringe.
9. Transfer the cell suspension to a 15 ml tube, and pipette up and down to make a single cell suspension.
10. Count the cells and dilute in RPMI 1640 complete medium at a concentration of 4×10^6/ml.
11. To a 96-well microtiter plate, add 4×10^5 lymph node cells in 0.1 ml to each well. For each experimental group, set up three replicate wells.
12. Add different concentrations of antigen KLH or OVA (5 μg/ml, 10 μg/ml, and 50 μg/ml) to make the total volume in each well 200 μl.
13. Place microtiter plates in a humidified 37°C, 5% CO2 incubator for 72 h.

14. At the last 18 h, add 1 μci[^{3}H]thymidine to each well. Return the plates to CO_2 incubator to pulse for 18 h. Harvest cells using a harvester and measure cpm in scintillation counter.

3.7. RelB siRNA-Silenced DCs Generate T Regulatory Cells

1. Culture C57BL/6 mouse bone marrow DCs on day 6.
2. Transfect mouse bone marrow DCs with RelB siRNA or negative-control siRNA, using Genesilencer reagent according to Subheading 3.2.
3. 24 h after transfection, stimulate mouse DCs with LPS at concentration of 100 ng/ml.
4. After 24 hours, collect DCs, resuspend the cells at a concentration of 4×10^5/ml.
5. Place 4×10^5 transfected DCs in 12-well plate.
6. Isolate BALB/c mouse spleen lymphocytes according to Subheading 3.5, resuspend spleen lymphocyte in RPMI 1640 complete medium at a concentration of 2×10^6/ml.
7. Add 4×10^6 BALB/c spleen lympnocyte to the 12-well plate, co-culture with transfected C57BL/6 mouse DCs for 7 days.
8. After co-culturing for 7 days, collect the cells, wash with RPMI 1640 medium and centrifuge at 400×g for 5 min.
9. Resuspend the cells using FACS buffer at the concentration of 1×10^7/ml, add 100 μl of prepared cells to the 12 × 75 mm round-bottom tube.
10. Add 1 μl PE-labelled anti-mouse CD25 and PE-Cy5-labelled anti-mouse CD4 antibody to each sample tube and put at 4°C in the dark for 30 min.
11. Wash cells by adding 3 ml FACS buffer, 4°C.
12. Centrifuge cell suspension 5 min at 400×g, 4°C. Carefully pour or pipette off supernatant fluid.
13. Resuspend cell pellet with 1 ml of freshly prepared Fixation/Permeabilization working solution to each sample tube and pulse vortex.
14. Incubate at 4°C for 30 min in the dark.
15. Add 2 ml 1× Permeabilization wash buffer, centrifuge at 400×g for 5 min and discard supernatant.
16. Repeat step 15 again, then add 100 μl 1× permeabilization buffer to each sample tube.
17. Add 1 μl fluorochrome conjugated anti-Foxp3 antibody or isotype control to each sample tube, mix and incubate at 4°C for at least 30 min in the dark.
18. Wash cells with 2 ml 1× Permeabilization buffer. Centrifuge at 400×g for 5 min and discard the supernatant.

19. Repeat wash step 18.
20. Resuspend the cells in 300 µl FACS buffer and analyze on cytometer.

3.8. Prevent Immune Rejection Through Gene Silencing

1. Culture bone marrow DCs from 6 to 8-week-old C57BL/6 mice on day 6.
2. Transfect mouse bone marrow DC with RelB siRNA or negative-control siRNA, using Genesilencer reagent according to Subheading 3.2.
3. 48 h after transfection, collect DCs and resuspend in 10×10^6/ml in PBS. Inject 5×10^6 DCs to BALB/C recipient mice by tail vein.
4. 3 days after DC injection, heterotopic heart transplantation is performed. Donor organs are from C57BL/6 mice and BALB/c mice are used as recipients. Untreated mice or mice treated with negative control siRNA-transfected DCs are used as negative control.
5. Pulsation of heart grafts is monitored daily by two independent observers who are blinded to the treatment protocol. Direct abdominal palpation is used to assess graft viability, and the degree of pulsation should be scored as: A, beating strongly; B, noticeable decline in the intensity of pulsation; or C, complete cessation of pulsation.
6. Monitor graft survival to make a survival curve chart (Fig. 4).

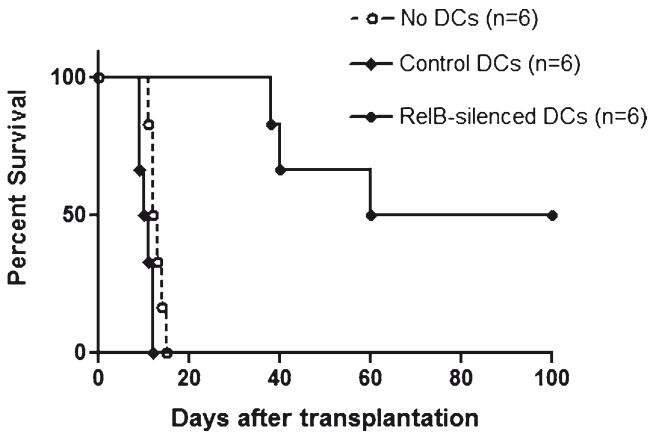

Fig. 4. Induction of tolerance in allogeneic heart transplantation by RelB-silenced DCs. 6-day cultured donor (C57BL/6)-derived DCs are transfected with RelB siRNA (RelB-silenced DCs) or negative control siRNA (Control DCs). Subsequently, cells are injected intravenously (5×10^6 cells/mouse) into recipient (BALB/c) mice. 3 days after DC treatment, allogeneic (C57/BL6 to BALB/c) heart transplantation is performed. Data demonstrate survival rate of grafts after transplantation

4. Notes

1. Male mice are preferred because they have bigger bones and can yield larger numbers of progenitor cells.
2. On day 2, gently swirl the plate and discard the old culture medium, as this medium will contain granulocytes, which are developing often as nonadherent round cells. By discarding the medium, you will get an almost pure culture of DCs. On day 4, you will start to see the growing of DCs, attached to the adherent stroma. On day 6, the wells will have many immature DCs.
3. You can incubate the complex for longer than 5 min, but make sure it is no longer than 30 min in order to maintain maximum siRNA transfection efficiency.
4. This step is important to avoid cell clumping.
5. Bubbles interfere with fluorescence detection.
6. All antibody concentrations here are only recommendations. You should titrate the antibody concentrations for your specific cell populations. Low temperature and presence of sodium azide assist in preventing capping and shedding or internalizing the antibody–antigen complex after the antibodies bind to the receptors, which can produce a loss of fluorescence intensity.
7. Stained cells resuspended in FACS buffer at 4°C can be used within 4 hours; in fixed buffer, they can be used in 48 h. If using fixed buffer, vortex and loosen cell pellet with the residual wash buffer otherwise, the cells will become fixed into a solid mass that cannot pass through the flow cytometer.
8. The densities of Ficoll-Paque and Lympholyte-M are temperature dependent. This protocol and the commercially available high-density solutions are designed for use at room temperature. Care should therefore be taken to bring cell suspensions, centrifuge, and high-density solutions to room temperature. Failure to do so will result in loss of live cells from the interface – instead of floating to the top of the high-density layer, they will collect at the bottom of the tube.
9. The efficacy of the separation procedures is dependent on the interface diameter; therefore, 50-ml tubes are used when separation of higher numbers of cells is desired, while 15-ml tubes can be used for lower cell numbers. For minimal cell loss due to adherence, polypropylene tubes are recommended over polystyrene tubes.

References

1. Banchereau, J., Briere, F., Caux, C., Davoust, J., Lebecque, S.and Liu, Y.J. et al. (2000) Immunobiology of dendritic cells. *Annu. Rev. Immunol.* **18**, 767–811.
2. Reis e Sousa, C. (2006) Dendritic cells in a mature age. *Nat. Rev. Immunol.* **6(6)**, 476–483.
3. Xu, D.L., Liu, Y., Tan, J.M., Li, B., Zhong, C.P. and Zhang, X.H. et al. (2004) Marked prolongation of murine cardiac allograft survival using recipient immature dendritic cells loaded with donor-derived apoptotic cells. *Scand. J. Immunol.* **59(6)**, 536–544.
4. Wang, Q., Zhang, M., Ding, G., Liu, Y., Sun, Y., Wang, J. et al. (2003) Anti-ICAM-1 antibody and CTLA-4Ig synergistically enhance immature dendritic cells to induce donor-specific immune tolerance in vivo. *Immunol. Lett.* **90(1)**, 33–42.
5. Rescigno, M., Martino, M., Sutherland, C.L., Gold, M.R. and Ricciardi-Castagnoli P. (1998) Dendritic cell survival and maturation are regulated by different signaling pathways. *J. Exp. Med.* **188(11)**, 2175–2180.
6. Ardeshna, K.M., Pizzey, A.R., Devereux, S. and Khwaja, A. (2000) The PI3 kinase, p38 SAP kinase, and NF-kappaB signal transduction pathways are involved in the survival and maturation of lipopolysaccharide-stimulated human monocyte-derived dendritic cells. *Blood* **96(3)**, 1039–1046.
7. Caamano, J. and Hunter, C.A. (2002) NF-kappaB family of transcription factors: central regulators of innate and adaptive immune functions. *Clin. Microbiol. Rev.* **15(3)**, 414–429.
8. Wu, L., D'Amico, A., Winkel, K.D., Suter, M., Lo, D. and Shortman, K. (1998) RelB is essential for the development of myeloid-related CD8alpha– dendritic cells but not of lymphoid-related CD8alpha+ dendritic cells. *Immunity* **9(6)**, 839–847.
9. Cejas, P.J., Carlson, L.M., Kolonias, D., Zhang, J., Lindner, I. and Billadeau, D.D. et al. (2005) Regulation of RelB expression during the initiation of dendritic cell differentiation. *Mol. Cell. Biol.* **25(17)**, 7900–7916.
10. Burkly, L., Hession, C., Ogata, L., Reilly, C., Marconi, L.A. and Olson, D. et al. (1995) Expression of relB is required for the development of thymic medulla and dendritic cells. *Nature* **373(6514)**, 531–536.
11. Weih, F., Carrasco, D., Durham, S.K., Barton, D.S., Rizzo, C.A. and Ryseck, R.P. et al. (1995) Multiorgan inflammation and hematopoietic abnormalities in mice with a targeted disruption of RelB, a member of the NF-kappa B/Rel family. *Cell* **80(2)**, 331–340.
12. Zanetti, M., Castiglioni, P., Schoenberger, S. and Gerloni, M. (2003) The role of relB in regulating the adaptive immune response. *Ann. N. Y. Acad. Sci.* **987**, 249–257.
13. Fire, A., Xu, S., Montgomery, M.K., Kostas, S.A., Driver, S.E. and Mello, C.C. (1998) Potent and specific genetic interference by double-stranded RNA in *Caenorhabditis elegans. Nature* **391(6669)**, 806–811.
14. Elbashir, S.M., Harborth, J., Lendeckel, W., Yalcin, A., Weber, K. and Tuschl, T. (2001) Duplexes of 21-nucleotide RNAs mediate RNA interference in cultured mammalian cells. *Nature* **411(6836)**, 494–498.
15. Hill, J.A., Ichim, T.E., Kusznieruk, K.P., Li, M., Huang, X. and Yan, X. et al. (2003) Immune modulation by silencing IL-12 production in dendritic cells using small interfering RNA. *J. Immunol.* **171(2)**, 691–696.
16. de Fougerolles, A., Vornlocher, H.P., Maraganore, J. and Lieberman, J. (2007) Interfering with disease: a progress report on siRNA-based therapeutics. Nat. Rev. Drug Discov. **6(6)**, 443–453.

Chapter 24

Topical Application of siRNA Targeting Cutaneous Dendritic Cells in Allergic Skin Disease

Miyuki Azuma, Patcharee Ritprajak, and Masaaki Hashiguchi

Abstract

RNA interference is a promising method for silencing specific genes and has great potential for therapeutic applications. However, the major hurdle for therapeutic application is the limited stability of double-strand RNA (dsRNA) and the absence of a reliable delivery method to target cells. Skin appears to be a favorable target for small interfering RNA (siRNA) therapy. Dendritic cells (DCs) exist in the skin and mucosae on the front lines of defense; these cells capture antigens and play a crucial role in inducing immunity and tolerance.

In our recent work, we have shown a successful treatment using CD86 siRNA targeting cutaneous DCs. A costimulatory molecule, CD86, is induced on DCs in situ after antigen uptake, and CD86-expressing DCs migrate to the regional lymph nodes to present antigens to T cells. Topical application of cream-emulsified CD86 siRNA ameliorated the clinical manifestations in murine contact hypersensitivity (CH) and atopic dermatitis (AD)-like disease. Our method may be advantageous for the treatment of allergic skin diseases.

Key words: Dendritic cells, siRNA, Topical application, CD86, Costimulatory molecules, Skin allergic disease

1. Introduction

Engagement of the B7 family of molecules on antigen-presenting cells (APCs) with their T cell-associated cosignal receptors, such as CD28 and CD152 (CTLA-4), provides pivotal positive and negative costimulatory signals for T-cell activation and tolerance (1). The lack of costimulation after the engagement of the T-cell receptor by antigen, results in a state of antigen-specific unresponsiveness, termed anergy. Manipulation of the CD28/B7 pathway becomes a potential strategy for achieving therapeutic immunosuppression or tolerance. CTLA4-Ig (abatacept)

Wei-Ping Min and Thomas Ichim (eds.), *RNA Interference*, Methods in Molecular Biology, vol. 623,
DOI 10.1007/978-1-60761-588-0_24, © Springer Science+Business Media, LLC 2010

–a recombinant protein fused with the extracellular region of the CTLA-4 and the constant region of the heavy chain of IgG1 that can bind to CD28 ligand with a higher affinity than CD28 – and LEA29Y (belatacept) – a two amino acid, substituted CTLA4-Ig to improve the binding avidity for CD80 and CD86– have already been shown to have beneficial therapeutic effects in patients with rheumatoid arthritis and renal transplantation (2). These new immunosuppressive agents have been systemically administered and are thought to bind both CD80 and CD86 efficiently, competing against the CD28 expressed on T cells.

Dendritic cells (DCs) are a highly specialized population of immune cells involved in both the process of inducing immunity and tolerance as a conductor of the immune system (3). DCs, located at body surfaces, capture pathogens (antigens) at the front lines of defense, and migrate to regional lymph nodes to interact with T cells. Manipulation of the various functional molecules targeting DCs, greatly affects their immunoregulatory capacity (3, 4). CD86 is one of the crucial costimulatory ligands induced on DCs, and blockade of the CD86 pathway efficiently interferes with antigen-specific T-cell responses in murine Th2-mediated allergic disease models (5). Preferential induction and functional contribution of CD86 induced on DCs have been reported in skin inflammatory allergic diseases in both humans (6, 7) and mice (8–10).

We have successfully developed a small interfering RNA (siRNA)-based therapeutic application for murine allergic skin disease that targets the CD86 costimulatory molecule expressed on cutaneous DCs (11). The cream lotion, mixed with siRNA against CD86, has been topically applied to healthy or atopic skin. The treatment with CD86 siRNA cream lotion provided efficient amelioration in contact hypersensitivity reactions and skin allergic atopic dermatitis lesions (11). For siRNA-based clinical application, the targeting of cutaneous DCs may be a promising strategy in the treatment of allergic skin disease. This strategy can be expanded to include the genes for additional costimulatory molecules or cytokines as well as such target tissues as the nasal, oral, alveolar, and gastrointestinal mucosae.

2. Materials

2.1. Dilution of siRNA Duplex

1. Lyophilized siRNA (20 nmol) (designed and synthesized by Qiagen 2-for-silencing siRNA duplexes, Qiagen, Valencia, CA).
2. siRNA suspension buffer: 100 mM potassium acetate, 30 mM HEPES-KOH (PH 7.4), and 2 mM magnesium acetate.

2.2. Selection of Efficient siRNA

1. Cultured 293T cells.
2. Complete Dulbecco's modified Eagle's medium (DMEM): DMEM High Glucose with L-Glutamine and Phenol Red (Wako, Osaka, Japan) supplemented with 10% fetal bovine serum (FBS, Invitrogen, St.Louis, MO) and gentamycin (Sigma, Steinheim, Germany).
3. A set of 24-well flat-bottom plates (Iwaki, Tokyo, Japan).
4. The full-length mouse CD86 expression vector (pcDNA3/mCD86).
5. Lipofectamine 2000 (Invitrogen).
6. Opti-MEM (Invitrogen).
7. Appropriate fluorochrome-conjugated anti-mouse CD86 mAb or isotype control Ig (eBioscience, San Diego, CA).
8. FACSCalibur and CellQuest software (BD Biosciences, San Jose, CA).

2.3. Preparation of Cream-Emulsified siRNA

1. 20 μM siRNA duplex stock solutions. (After thawing, the tubes are spun briefly to bring the contents to the bottom of the tubes).
2. Cream-based ointment (Johnson's baby lotion, no fragrance; Johnson & Johnson, New Brunswick, NJ) is sterilized by autoclave to avoid RNase contamination (see Note 1).
3. End-cut tips (The ends from 200 μL pipette tips cut at a length of 1 cm. All the end-cut pipette tips should be sterilized by autoclave.) (see Note 2).
4. A set of 1.5 mL microtubes sterilized by autoclave.

2.4. Murine Contact Hypersensitivity (CH) Model

1. Female 6-week-old BALB/c specific pathogen-free mice (Japan SLC, Hamamatsu, Japan).
2. An electric shaver (Hitachi, Japan).
3. (a) Haptens, 2,4-dinitro-1-fluorobenzene (DNFB, Sigma) or fluorescein isothiocyanate (FITC, Wako, Osaka, Japan) (see Note 3).
   (b) DNFB-induced CH: 0.5% DNFB dissolved in acetone:olive oil (4:1 v/v) for sensitization and 0.2% DNFB dissolved in acetone:olive oil (4:1 v/v) for challenge.
   (c) FITC-induced CH: 0.5% FITC dissolved in dibutyl phthalate:acetone (1:1 v/v) for sensitization and challenge.
4. A dial thickness gauge (Peacock, Ozaki, Tokyo, Japan).

2.5. Murine Atopic Dermatitis (AD) Model

1. Female 6-week-old NC/Nga mice (12, 13) (Japan SLC, Hamamatsu, Japan). The mice should be maintained under conventional conditions (see Note 4).

2. An electric shaver (Hitachi, Japan).
3. A cream-based hair remover (Kracie, Tokyo, Japan) (see Note 5).
4. Sterile cotton.
5. Sterilized MilliQ water.
6. Mite antigen (Mite Extract *Dermatophagoides farinae* (Df); LSL, Tokyo, Japan) dissolved in 1× PBS.

3. Methods

At first, several sequences of siRNA duplexes should be designed, and the silencing effect of each siRNA should be tested by cotransfection with each respective siRNA and expression vector into suitable cells that provide high transfection efficiency. In this protocol, a 293T cell line (human embryonic kidney cell line) is used. For suitable evaluation of the silencing effect by siRNA, the transfected cells should provide more than 70% expression of the targeted gene. The efficiency of siRNA delivery into the cells can be evaluated using fluorochrome (e.g. Alexa 488)-conjugated siRNA by flow cytometry. After confirmation of the silencing effects of siRNA in vitro, siRNA should be applied to in vivo treatment.

3.1. Dilution and Stock of Lyophilized siRNA (see Note 6)

1. Add 1 mL of the siRNA suspension buffer to the lyophilized siRNA (20 nmol) to obtain a 20 μM solution.
2. Heat the tubes to 90°C for 1 min.
3. Incubate at 37°C for 60 min.
4. Perform your experiment or store aliquots at –20°C.

3.2. Selection of Efficient siRNA by the Evaluation of In Vitro Silencing Effects Using a 293T Transfection System

1. The 293T cells, cultured in complete DMEM (high-glucose DMEM supplemented with 10% fetal bovine serum and gentamycin), are plated into 24-well plates (2×10^5/well) 1 day before transfection.
2. The cells are co-transfected with 0.2 μg of the pcDNA3/CD86 expression vector and 40 pmol of either nonsilencing control or CD86 siRNA duplexes with Lipofectamine 2000 diluted in Opti-MEM, according to the manufacturer's instructions. To verify the transfection efficiency of the CD86 gene, make additional wells with or without pcDNA3/CD86 vector alone, in the absence of any siRNA.
3. If required, change the medium at 24 h and culture another 24 h with DMEM. Beware of cells that detach from the culture plate.

4. Harvest cells from each well at 24 or 48 h after transfection.
5. Stain cells with fluorochrome-conjugated anti-CD86 mAbs or appropriate control reagents, and analyze by flow cytometry.
6. Select the best siRNA sequence that provides the greatest silencing effect for the in vivo treatment.

3.3. Preparation of Cream-Emulsified siRNA

1. Add sterile cream and either nonsilencing or CD86 siRNA duplex into an autoclaved 1.5 ml microtube, and mix homogeneously. If required, vortex for 30 s. For the control with the cream alone, prepare the cream-based ointment mixed with autoclaved water instead of the siRNA duplex. For CH treatment, mix 7.5 μL of cream and 12.5 μL of 20 μM siRNA duplex (0.25 nmol). For AD treatment, mix 15 μL of cream and 25 μL of 20 μM siRNA duplex (0.5 nmol) (see Note 7).
2. Keep all prepared solutions at 4°C or on ice until use.

3.4. Induction of CH and Treatment with siRNA

1. Maintain BALB/c mice under specific pathogen-free conditions for at least 1 week in your animal facility after transfer.
2. Shave the abdominal area using an electric shaver.
3. For DNFB sensitization, paint 20 μL of 0.5% DNFB onto the shaved abdominal skin using a 20 μL-tip on days 0 and 1. For FITC sensitization, paint 400 μL of 0.5% FITC onto the shaved abdominal skin using a 200 μL-tip on day 0 once.
4. On day 5, 1 h before challenge, apply 10 μL each (total 20 μL) of the siRNA-cream mixture prepared in Subheading 3.3 onto the ventral and dorsal sides of ear skin (see Note 8).
5. For challenge, apply 10 μL each (total 20 μL) of either 0.2% DNFB or 0.5% FITC onto the ventral and dorsal sides of the ear on day 5.
6. Measure the ear thickness before challenge and 24, 48, and 72 h after challenge using a dial thickness gauge. The ear swelling value is shown as the mean difference between the pre-and post-challenge values.

3.5. Induction of AD and Treatment with siRNA

1. Maintain NC/Nga mice under conventional conditions (This is important!) (see Note 4).
2. Shave the upper back area of NC/Nga mice roughly using an electric shaver.
3. Apply the cream-based hair remover onto the shaved area for 5 min, and remove the cream using sterile cotton swabs.

4. Wipe out the residual cream with wet cotton swabs or tissue paper, and let the skin dry naturally.
5. Apply 20 μg of mite antigen, diluted in 100 μL PBS, onto the shaved upper back skin and dorsal ears of the mice three times per week (14) (see Note 9).
6. Have two persons who are unaware of each mouse's treatment status score the skin lesions weekly, according to the following criteria (Table 1).
7. To see therapeutic effects, start treatment after all the mice develop the skin lesions. In this scoring method, we start the treatment 2 weeks after the initial application of mite antigen when the skin scores in all mice reach over five. Apply a total volume of 40 μL of the cream-emulsified siRNA onto the upper back skin and dorsal ears every day (see Notes 8 and 10).
8. Monitor the skin score of individuals weekly and, if required, collect blood sera every 2 weeks for the measurement of Df-specific and/or total immunoglobulin (e.g., IgG1, IgE).

Table 1
Scoring of skin lesions

Features	None (0)	Mild (1)	Moderate (2)	Severe (3)
Dorsal ear skin				
Erythema/ Hemorrhage	–	Ery; over half in one side or Hem; point	Ery; over half in one side or Hem; over half in both side	Hem; over half in both side
Excoriation/ Erosion	–	Exc; one side or Ero; none	Exc; both side or Ero; one side	Ero; both side
Scaling/Dryness	–	Less than half in one side	Less than half in both side or over half in one side	Over half in both side
Upper back skin				
Erythema/ Hemorrhage	–	Ery; ≤5 mm^2 and Hem (–)	Ery; <5 mm^2 and Hem; point or Ery; >5 mm^2 and Hem (–)	Ery; >5 mm^2 and Hem (+)
Excoriation/ Erosion	–	Exc; <3 mm^2 and Ero (–)	Exc; 3 mm^2 and Ero (+) or Exc; >3 mm^2 and Ero (–)	Exo; >3 mm^2 and Ero (+)
Scaling/Dryness	–	≤1/3	1/3–2/3	≥2/3

The areas of dorsal ear and upper back skin are separately scored. The lesions are observed by three categories
The sum of scores is defined as total skin score (range from 0 to 18). *Ery* Erythema, *Hem* Hemorrhage, *Exo* Exoriation, *Ero* Erosion

4. Notes

1. You may use the following formula instead of Johnson's baby lotion:

   Low-substituted hydroxypropylcellulose (L-HPC) 1%

   High-substituted hydroxypropylcellulose (H-HPC) 1%

   Methylparapen 0.2%

   Propylene glycol 5% (This is essential!)

   Water 92.8%

2. Use the end-cut pipette tips to transfer the cream into the tubes because the cream has high viscosity. If required, measure the weight of the cream in advance and adjust the correct volume of the cream by balance.
3. Hapten solution should be prepared just before use. For the DNFB solution, prepare the olive oil and acetone mixture in a glass tube first. Measure the approximate amount of DNFB in a glass tube or polypropylene centrifuge tube. Then, add the suitable volume of the olive oil and acetone mixture and mix well. For the FITC solution, measure the approximate amount of FITC in a glass or polypropylene centrifuge tube, add the suitable volume of dibutyl phthalate and vortex well. Then add the same volume of acetone into the tube.
4. NC/Nga mice need to be maintained in an air-uncontrolled conventional room. The incidence and severity of dermatitis are greatly affected by the housing conditions (the humidity, temperature, and cleanliness in the room).
5. The selection of cream-based hair remover is important. Because you need to treat with hair remover often, after the development of dermatitis, the treatment itself sometimes induces an exacerbation of the dermatitis.
6. The incubation steps only need to be carried out the first time you use the siRNA. The procedure will disrupt aggregates, which may have formed during the lyophilization process, and is necessary to maximize the siRNA silencing potential. Repeated freeze-thaw cycles will not interfere with the siRNA sample as long as RNAse-free conditions are strictly maintained.
7. It has been shown that dsRNA can induce the production of type I interferon by triggering TLR signaling (15). To avoid the IFN effects of siRNA treatment in vivo, the lowest amount of siRNA that can provide the sufficient effect should be considered (16). In our experiments, 0.25 nmol (2.5 μg) per ear and 0.5 nmol (5 μg) per mouse were the optimal doses for CH and AD treatments, respectively.

8. The pipette tips for topical painting should be changed individually.
9. The amount of mite antigen for the induction of AD may need to be adjusted, depending on the housing conditions.
10. The induction of AD accelerates the hair growth due to the inflammation. The growing hair may interfere with the absorption of antigen as well as cream-emulsified siRNA. Thus, hair removal is often required. The treatment with hair remover induces bleeding after the development of AD. The scoring should be performed at least two days after the hair treatment.

Acknowledgments

This work was supported by a Grant-in-Aid from the Ministry of Education, Culture, Sports, Science and Technology of Japan.

References

1. Sharpe, A.H. and Freeman, G.J. (2002) The B7-CD28 superfamily. *Nat. Rev. Immunol.* **2**, 116–126.
2. Vincenti, F. (2008) Costimulation blockade in autoimmunity and transplantation. *J. Allergy Clin. Immunol.* **21,** 299–306.
3. Banchereau, J., Briere, F., Caux, C., Davoust, J., Lebecque, S., Liu, Y. J. et al. (2000) Immunobiology of dendritic cells. *Annu. Rev. Immunol.* **18,** 767–811.
4. Steinman, R.M. and Banchereau, J. (2007) Taking dendritic cells into medicine. *Nature* **449,** 419–426.
5. Jen, K.Y., Jain, V.V., Makani, S. and Finn, P.W. (2006) Immunomodulation of allergic responses by targeting costimulatory molecules. *Curr. Opin. Allergy Clin. Immunol.* **6,** 489–494.
6. Ohki, O., Yokozeki, H., Katayama, I., Umeda, T., Azuma, M., Okumura, K. et al. (1997) Functional CD86 (B7-2/B70) is predominantly expressed on Langerhans cells in atopic dermatitis. *Br. J. Dermatol.* **136,** 838–845.
7. Yokozeki, H., Katayama, I., Ohki, O., Arimura, M., Takayama, K., Matsunaga, T. et al. (1997) Interferon-gamma differentially regulates CD80 (B7-1) and CD86 (B7-2/B70) expression on human Langerhans cells. *Br J Dermatol.* **136,** 831–837.
8. Nuriya, S., Yagita, H., Okumura, K. and Azuma, M. (1996) The differential role of CD86 and CD80 co-stimulatory molecules in the induction and the effector phases of contact hypersensitivity. *Int. Immunol.* **8,** 917–926.
9. Katayama, I., Matsunaga, T., Yokozeki, H. and Nishioka, K. (1997) Blockade of costimulatory molecules B7-1 (CD80) and B7-2 (CD86) down-regulates induction of contact sensitivity by haptenated epidermal cells. *Br. J. Dermatol.* **136,** 846–852.
10. Santa, K., Watanabe, K., Nakada, T., Kato, H., Habu, S. and Kubota, S. (2003) Enhanced expression of B7.2 (CD86) by percutaneous sensitization with house dust mite antigen. *Immunol. Lett.* **85,** 5–12.
11. Ritprajak, P., Hashiguchi, M. and Azuma, M. (2008) Topical application of cream-emulsified CD86 siRNA ameliorates allergic skin disease by targeting cutaneous dendritic cells. *Mol. Ther.* **16,** 1323–1330.
12. Suto, H., Matsuda, H., Mitsuishi, K., Hira, K., Uchida, T., Unno, T. et al. (1999) NC/Nga mice: a mouse model for atopic dermatitis. *Int. Arch. Allergy Immunol.* **120** Suppl 1, 70–75.
13. Matsuda, H., Watanabe, N., Geba, G.P., Sperl, J., Tsudzuki, M., Hiroi, J. et al. (1997)

Development of atopic dermatitis-like skin lesion with IgE hyperproduction in NC/Nga mice. *Int. Immunol.* **9,** 461–466.

14. Inoue, R., Nishio, A., Fukushima, Y. and Ushida, K. (2007) Oral treatment with probiotic Lactobacillus johnsonii NCC533 (La1) for a specific part of the weaning period prevents the development of atopic dermatitis induced after maturation in model mice, NC/Nga. Br. *J. Dermatol.***156,** 499–509.
15. Takeda, K., Kaisho, T. and Akira, S. (2003) Toll-like receptors. *Annu. Rev. Immunol.* **21,** 335–376.
16. Cullen, B.R. (2006) Enhancing and confirming the specificity of RNAi experiments. *Nat. Methods.* **3,** 677–681.

Chapter 25

Direct Application of siRNA for In Vivo Pain Research

Philippe Sarret, Louis Doré-Savard, and Nicolas Beaudet

Abstract

Pain is the new burden of the twenty-first century, raising enormous socio-economic costs to developed and underdeveloped countries. Chronic pain is a central nervous system (CNS) pathology, affecting a large proportion of the population. Morphine and its derivatives are still the golden clinical standards for treating pain although they induce severe side effects. To this day, we still have poor understanding of nociceptive pain and its underlying complex mechanisms; furthermore, novelty in clinical analgesics is lacking.

RNA interference technologies are promising both for pain research and treatment. This genetic approach will likely provide new insights into pain mechanisms and eventually offer nonpharmacological therapeutic approaches. In vivo research is thus crucial to reach this goal. Preclinical studies on rodents are necessary to validate small interfering RNA (siRNA) candidates and to target precise physiological pain modulators. Aiming treatment at the CNS is delicate work, and here we will describe how to perform adequate pain research using siRNA, including siRNA preparation and injection, animal behavioral models, and CNS tissue collection.

Key words: Pain, Analgesia, GPCR, Silencing, siRNA, In vivo, Rodents, Behavior

1. Introduction

Translation of RNA interference (RNAi) technologies to in vivo models is a key step to expose pathology-related mechanisms that cannot be studied in vitro. Moreover, in vivo potency of such technologies is of interest, taking into account pathologies for which pharmacological treatments are lacking or have reached their limit of effectiveness.

Research domains of pain and analgesia have now reached those borders. Existing pharmacopoeia is effective for only 60% of chronic pain-coping patients, leaving an important subset of the population dependent on research breakthrough in this field. Moreover, clinical opioid derivatives, which primarily target the

Wei-Ping Min and Thomas Ichim (eds.), *RNA Interference*, Methods in Molecular Biology, vol. 623,
DOI 10.1007/978-1-60761-588-0_25, © Springer Science+Business Media, LLC 2010

mu opioid receptor, present severe side effects such as constipation, nausea, respiratory depression, dependence, and tolerance, impairing long-term, pain-easing treatments.

Unfortunately, cellular studies confine our understanding of pain's highly complex mechanisms to subcellular interactions occuring between receptors and channels involved in nociception transmission. The necessity of studying pain paradigms in vivo is thus indispensable to evaluate the full potency of novel therapeutic approaches and to consider all the neurophysiolgical mechanisms and levels of modulation that affect the integrated response to pain.

Obviously, prior in vitro validation is required for future RNAi experiments to be translated into in vivo research. Once functional, the assay can be prompted in vivo; however, at this level, many hurdles are encountered. Degradation by nucleases, rapid blood clearance, poor delivery, toxicity, and inflammation are among the major drawbacks that occur in such studies (1). When focusing on central nervous system (CNS) pathologies, we are also confronted with volume limitations due to CNS point structures and the selective blood-brain barrier.

Using a new generation of siRNA, referred to as Dicer-substrate siRNA (DsiRNA), we describe how it can be used in vivo to evaluate changes in reaction to painful stimuli. DsiRNA are modified 27 nucleotides sequences, capable of incorporating the DICER unit for cleavage into 21 nt siRNA. This processing step enables them to be favorably loaded in the RISC complex in order to induce potent silencing toward the target RNA at low dose (for review, (2, 3)). This concept of low dose is critical in the CNS to avoid adverse effects and inflammation while ensuring sustained knockdown (4).

The method, herein, describes the application of RNAi technology in pain research at the spinal level. The present protocol outlines the steps and provides important hints for successful efficient silencing using DsiRNA, aiming at a target involved in the pain paradigm. We describe formulation and injection procedures, and further present appropriate models for the screening of RNAi compounds as well as the study of pain in rodents. Finally, we explain how to collect CNS tissues, an important step for further molecular analyses that can support and validate the potency of siRNA for in vivo research.

2. Materials

2.1. DsiRNA Preparation

2.1.1. Resuspension of RNA

1. Sterile injectable solution of sodium chloride (0.9%) (Hospira Healthcare Solutions, Montreal, QC).
2. Lyophilised Dicer substrate siRNA (40 nmol).
3. Electrical vortex.

2.1.2. DsiRNA Formulation

1. Sterile injectable solution of sodium chloride (0.9%) (Hospira Healthcare Solutions, Montreal, QC).
2. Stock solution of Dicer substrate siRNA (200 μM; Integrated DNA Technologies Inc., Coralville, IA).
3. iFect transfection reagent solution (Neuromics, Minneapolis, MN).

2.2. Animals and Injections

1. Male Sprague-Dawley rats (200–225 g; Charles River Laboratories, St-Constant, QC). Ensure approval with local animal care and ethics committee in compliance to International Association for the Study of Pain guidelines.
2. Tec-3 Isoflurane vaporizer (Dispomed, Joliette, QC) + Small Rodent induction chamber.
3. Isoflurane (99.9%) (Abbott Laboratories Limited, Montreal, QC).
4. Oxygen or medical air line or portable tank input.
5. Formulated Dicer substrate siRNA (target). Keep on ice.
6. Formulated Dicer substrate siRNA (negative control). Keep on ice.
7. Formulated Texas Red labelled Dicer substrate siRNA. Keep on ice.
8. 10 μl Hamilton Syringe (Hamilton Company, Reno, NV).
9. 27 gauge needles (length: 0.5 inch; Becton Dickinson Company, Franklin Lakes, NJ).
10. 1.5 × 4 inch rubber tube.

2.3. Behavioral Tests

2.3.1. Tail Flick Test

1. Automatic tail flick water bath (IITC Life Sciences, Woodland Hills, CA).
2. Hand towels.
3. Timer (optional).
4. Thermometer (optional).

2.3.2. Formalin Test

1. Solution of 37% formaldehyde (Fisher Scientific, Ottawa, ON). Store at room temperature.
2. Sterile injectable solution of sodium chloride (0.9% ; Hospira Healthcare Solutions, Montreal, QC).
3. Clear plastic enclosures (2); size: 30 × 30 × 30 cm. Positioned over a 45° angled mirror in order to allow an unobstructed view of the paws.
4. 50 μl Hamilton syringe (Hamilton Company, Reno, NV).
5. 27 gauge needles (length: 0.5 inch; Becton Dickinson Company, Franklin Lakes, NJ).
6. Hand towels for restraining.
7. Laptop computer equipped with ANY-Maze video-tracking software (Stoelting, Wood Dale, IL).

2.4. Validation of RNAi and Effective Knockdown

2.4.1. Cerebrospinal Fluid Collection for Inflammation Evaluation

1. Dry ice.
2. Scalpel (handle #3) equipped with the appropriate surgical blade (blade #10, or according to experimenter's preference).
3. Surgery and microsurgery instruments (Fine Science Tools Inc., North Vancouver, BC). Recommended: spring scissors (No. 15000-00), fine scissors (No. 14088-10), bone trimmers (No. 16109-14), Friedman rongeur (No. 16000-14) and Dumont forceps (No. 11253-25).
4. Sterile Q-tips.
5. 18 gauge needle (Becton Dickinson Company, Franklin Lakes, NJ).
6. 27 gauge winged needle linked to 12 inch catheter tubing (length: 0.5 inch; ref# 387312, Becton Dickinson Company, Franklin Lakes, NJ).
7. Stereotaxic frame.

2.4.2. Fresh Nervous Tissue Removal for Protein and RNA Analyses

1. Dry ice.
2. Rodent guillotine.
3. Surgery and microsurgery instruments (Fine Science Tools Inc., North Vancouver, BC). Recommended: spring scissors (No. 15000-00), fine scissors (No. 14088-10), bone trimmers (No. 16109-14), Friedman rongeur (No. 16000-14) and Dumont forceps (No. 11253-25).

2.4.3. Transaortic Perfusion

1. Ketamine/Xylazine (87 mg/kg – 13 mg/kg; C.D.M.V., St-Hyacinthe, QC) Authorization from your respective Governmental Health Division could be required for ketamine, which is now a controlled substance in Canada.
2. Distilled water.
3. Paraformaldehyde EM grade (Polyscience, Warrington, PA).
4. Aqueous NaOH (4%).
5. Phosphate buffer (0.2 M; pH = 7.2)
6. Heating plate.
7. Thermometer.
8. 20 gauge (length: 1 inch) gavage feeding needle (Fine Science Tools Inc., North Vancouver, BC).
9. Surgical instruments (Fine Science Tools Inc., North Vancouver, BC). Recommended: Halsted-Mosquito Hemostats (No.13008-12), standard forceps, Hardened Fine Iris Scissors (No. 14090-09), ToughCut Sharp/Blunt Scissors (No. 14054-13).
10. Vera peristaltic pump plus (Manostat, Barrington, IL).
11. Plastic container.

2.4.4. Nervous Tissue Removal

1. Surgery and microsurgery instruments (Fine Science Tools Inc., North Vancouver, BC). Recommended: spring scissors (No. 15000-00), fine scissors (No. 14088-10), bone trimmers (No. 16109-14), Friedman rongeur (No. 16000-14) and Dumont forceps (No. 11253-25).
2. Sucrose solution (30%).

3. Methods

3.1. DsiRNA Preparation for Injection in Rat Central Nervous System

Pain research involves the study of G protein coupled receptors (GPCRs) in order to broaden our understanding of pain mechanisms and accelerate the development of new classes of analgesics. The present example of RNAi relates to the knockdown of NTS2 mRNA with specific NTS2-targeted DsiRNA to reach these purposes. The selected transfection agent is the cationic lipid i-Fect.

1. Dehydrated DsiRNAs must be kept at 4°C until resuspended. Resuspension is performed with sterile saline. The appropriate volume to reach a concentration of 200 µM is added to the DsiRNA, and the solution is vortexed for 15 s to ensure proper dissolution. For example, 40 nmol of DsiRNA (MW≈16,600 g/mol) are dissolved in 200 µl of saline. Store on ice for immediate use, or store in 10 µl aliquots at –80°C for future use.
2. Formulation of DsiRNA to i-Fect transfection reagent is performed no more than 30 min before injection (or according to manufacturer's specific transfection reagent protocol). A 5:1 ratio of i-Fect transfection reagent to DsiRNA solution is used for efficient cell penetration. For a 10 µl injection volume (see Note 1), mix 8.3 µl of i-Fect with 0.3 µl of DsiRNA 200 µM solution and 1.4 µl of sterile saline. Let stand for 5 min and proceed to injection. Formulate as many doses as can be injected within 30 min (see Note 2).

3.2. Intrathecal Injection of DsiRNA

To this day, siRNA molecules cannot cross the blood-brain barrier. Thus, direct site injections into the CNS are required. For pain research in supraspinal (i.e. brain) structures, stereotaxic injections can be performed in the periaqueductal gray matter or rostro ventral medulla. At the spinal level, we recommend intrathecal infusion or punctual injections to study nociceptive modulations of noxious stimuli. The lumbar spinal level is often the preferred site of injection because of its low marrow puncture risk and the presence of afferent nerves from the lower limbs and tail, frequently targeted in pain models. The latter is the method we chose to describe.

1. Place one rat at a time in the induction box.
2. Submit to anesthesia under a flux of 2 L per minute of oxygen and 5% of isoflurane.
3. Meanwhile, load a 10 µl Hamilton syringe with formulated DsiRNA solution from Subheading 3.1. Make sure the rat is properly anesthetized before injection by pinching a hind paw. If no reaction is observed, you can proceed.
4. Place the nozzle of the animal in a mask connected to a corrugated tube to maintain anesthesia.
5. Place the animal in ventral decubitus over a 1.5 inch rubber tube, adjusted under the hips, to arch the rodent's back and expand the space between L5 and L6 vertebrae.
6. By tactile exploration, situate the L5–L6 gap (see Note 3).
7. Insert the 27 gauge needle, forming a 90° angle with the animal's back, through skin to reach the intrathecal space.
8. Penetration of the needle through the dura should be accompanied by a quick twitch of the tail (flick), indicative of adequate needle positioning in between the "cauda equina" projections (see Note 4).
9. Slowly inject the solution (over approximately 2 s) and remove needle. Normally, no blood should be observed (see Note 5). Let rats recover from anesthesia using 2 L per minute of oxygen.
10. Injection is repeated after 24 h, or according to the chosen experimental pattern (see Note 6).

3.3. Behavioral Validation of siRNA Knockdown

In pain paradigms, either pharmacological or genetic, a research or therapeutic approach requires nociceptive behavioral validation. In a study by Doré-Savard and colleagues (4), NTS2 GPCR activation leads to analgesia. Thus, the silencing of this target RNA by interference techniques results in lost efficacy of its specific agonists. Before being used in chronic pain models, a screening of siRNA efficacy is performed in "acute" and "tonic" pain models. These models are various, either aimed at the hindlimb paws or at the tail, and they evaluate thermal, mechnical or chemical nociceptive stimuli. Here, we described two frequently used tests for such purpose.

3.3.1. Acute Tail Flick Test

1. The tail flick test is a rapid method to assess the modification of basal acute pain perception or to evaluate the analgesic response to pharmacological compounds or genetic approaches.
2. Acclimatization to environment and habituation to manipulations is performed daily starting 2 days prior to testing. This can be done right after DsiRNA injection since an intrathecal injection will also be performed on experimental days. Here is a suggested habituation schedule: Wrap the head and body

of the animal in a small towel and practice your restraining manipulation for 30 s–1 min (see Note 7). Hold the animal over the apparatus and press the timer pedal twice, just like when a real value is taken. Repeat at least three times for each animal. The DsiRNA intrathecal injection, as described in Subheading 3.2, should be done before the restraining habituation because it will be performed in this order on the day of the behavioral testing.

3. Rats should always be transferred to the experimental room at least 60 min before each habituation and testing day (see Note 8).
4. Prior to tail flick test, the temperature of the bath is adjusted to 52°C (see Note 9).
5. Intrathecal drug injections, if applicable, are performed at least 15 min (see Note 10) before the first measure to avoid interference from anesthesia.
6. Wrap the animal in a towel and dip a length (6 cm) of tail in the water.
7. Press the pedal to start the timer exactly at the time the tail enters the water.
8. When the rat flicks its tail, press the pedal to stop the timer and note the latency time.
9. Repeat the procedure three times at 10 min intervals.

3.3.2. Tonic Formalin Test

1. Prepare formalin solution (5%) by adding 2.5 μl of formalin (100%) to 47.5 μl of saline per dose. Prepare fresh and keep at room temperature.
2. Wrap the head and body of the animal in a small towel, pull the right hind paw to be injected and hold it firmly without impairing blood flow (see Note 11).
3. Inject the formalin (50 μl) over a 2-second period in the plantar surface of the hind paw (see Note 12).
4. Place the animal in a clear Plexiglas™ enclosure and immediately start to record behaviors for 60 min.

Formalin injection in the hind paw induces pain behaviors that can be classified in four different stages:

0: No difference between the injected paw before and after the injection.

1: Weight borne on the injected paw is decreased, but the paw remains in partial contact with the surface.

2: Injected paw is guarded, off the surface.

3: Injected paw is bitten, licked or shaken.

Typically, two distinct phases are observed. The acute phase I is short and intense, lasting for the first 9 min of the test. Inflammatory phase II lasts from the 21st minute until the end of

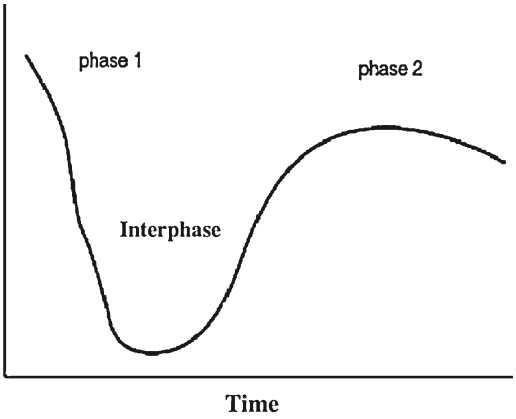

Fig. 1. Two distinct phases are observed during the tonic formalin test. Acute phase I and inflammatory phase II are separated by an inhibition phase

the test, and pain behaviors are sustained with a slight decrease during the late half of that phase. There is also an interphase between phase 1 and 2, known as an active inhibition phase as shown in Fig. 1 (5).

3.4. Silencing Validation of DsiRNA

Molecular validation of siRNA silencing in vivo is a crucial step, which can be performed at different stages of the testing schedule. One needs to prepare appropriate groups to perform point euthanasia and then proceed to fluid and CNS tissue collection to evaluate the duration and evolution of the knockdown. We recommend the collection of cerebrospinal fluid (CSF) for the evaluation of collateral inflammation due to potential siRNA or transfection reagent toxicity. Also, fresh tissues should be collected for real-time PCR analysis of targeted RNA decrease and for Western blot analysis of the protein, subsequent to cellular content diminution. Finally, perfusion of CNS tissues is important if you choose the option of a fluorescently-tagged siRNA to perform slice preparation for cellular evaluation uptake.

3.4.1. Cerebrospinal Fluid Collection

1. The animal is anesthetized with ketamine/xylazine injected intramuscularly. Wait for the deepest state of anesthesia.
2. Place the rat into the stereotaxic frame. No movement of the head should be possible.
3. Perform a 3 cm longitudinal incision of the scalp to expose the skull bone.
4. Find the junction of the sutures at the back of the skull, corresponding to the posterior end of the sagittal suture. Move the needle of the stereotaxic frame 3 mm backward from that junction.
5. With the tip of an 18 gauge needle, bore a small hole in the skull bone to access the brain. Remove any blood or fluid that

may leak from the hole or the skin with a sterile, cotton-tipped applicator.

6. Insert in the hole the 27 gauge winged needle, linked to a catheter to which a 1 ml syringe is attached, and slowly progress according to a 45° angle (needle pointing down and toward the experimenter), through the cerebellum to reach the cisterna magna.
7. Retrieve a small amount of liquid to make sure the needle is properly located in the cisterna. If no liquid is coming, insert the needle again at a more appropriate angle.
8. Obtain as much CSF as possible (100–200 µl) by slowly pulling the piston of the syringe. Ensure there is no negative pressure in the syringe when retrieving the needle to avoid contamination with blood (see Note 13).
9. Transfer the CSF into a sterile 0.6 ml eppendorf tube and quick-spin to eliminate all blood contamination. Transfer the supernatant in a new tube and immediately store on dry ice.
10. Transfer CSF to –80°C freezer (see Note 14).

3.4.2. Fresh CNS Tissue Removal

1. This step is recommended in addition to CSF collection.
2. Always under anesthesia, proceed to decapitation using the guillotine.
3. Immediately open the spine, collect lumbar spinal cord and dorsal root ganglia (DRG) and store on dry ice. Transfer tissues in –80°C freezer (see Note 14).

3.4.3. Fixed CNS Tissue Removal

1. The animal is anesthetized with ketamine/xylazine (87 mg/kg – 13 mg/kg), injected intramuscularly. Wait for deep anesthesia.
2. Stabilize the animal on the cap of a plastic container by taping each of the animal's paws in extension with medical or standard masking tape.
3. Pinch the skin at the distal part of the sternum with tweezers. Proceed to an incision with scissors through the skin and muscles.
4. Make an incision through the diaphragm to induce respiratory depression and to access the heart. Cut the ribs on both sides of the heart. This should create a V-shape wound. Clip the tip of the skin/muscle layer and the rib cage with a hemostat, and settle it on the head to clear the thoracic cavity (see Note 15).
5. Expose the heart muscle by removing the pericardia membrane and the thymus. Aorta should be visible.
6. Cut the apex of the heart to access the left ventricle. Push the gavage feeding needle, linked to a peristaltic pump, along the left

wall of the ventricle until the aorta is entered by 3 mm. Using another hemostat, clip the aorta in which the gavage needle is now inserted. Once firmly clipped in place, start the peristaltic pump at 25 ml/min and incise the right atria to enable circulation, and evacuate fluids from the animal body. Avoid circulating bubbles.

7. Perfuse 500 ml of buffered paraformaldehyde. Complete fixation can be confirmed by the hard and white appearance of the liver and lungs (see Note 16).
8. Immediately open the spine, collect lumbar spinal cord and DRG and transfer on ice in sucrose 30% at 4°C for 48 h. Store tissues at −80°C for further use (see Note 17).

4. Notes

1. One should inject the minimal volume that is suitable for an optimal N/P ratio and efficient experiment in order to avoid side effects induced by CSF hypervolemia and minimize costs associated with transfection reagents. The injected volume in the intrathecal space of the rat should not exceed 10% of the total CSF volume (rat = approx. 250 µl). Consequently, a maximum of 25 µl can be administered to the rat in the intrathecal space. Moreover, in our case, a volume of 10 µl was chosen for the previously cited reasons and for the DsiRNAs to be efficiently formulated with the transfection reagent without any precipitation at a dose of 1 µg. A different volume can be used if the formulation demands it, or if the RNA concentration required is higher with, for example, standard 21-mer siRNAs.
2. The efficient formulation of the RNAi sequence has been fixed at 30 min after mixing, according to i-Fect manufacturer's validation. Beyond this point, the stability of the lipoplexes is unknown and not guaranteed. If you have several rats to inject, prepare two different tubes, one containing an adequate amount of saline and i-Fect and the other containing the resuspended RNAi compound. Keep on ice and formulate when the time is appropriate, either once you are set at the animal facility or beginning your second cohort of animals to inject.
3. To identify the L5–L6 space, situate the iliac crests with your thumbs. From these anatomical reference points, displace one of your thumbs in coronal toward the center of the two crests until you reach the vertebral column. From there, proceed with point-by-point tactile exploration of the spinous processes in direction of the head. The L6 vertebrae will rapidly

be detected, its spinous process is sharp and evident to palpation in comparison to surrounding processes, which have a more flattened structural conformation. Moving upward from there, you should immediately feel a gap before the palpation of L5 spinous process. This gap is where you need to insert your needle.

4. At the lumbar level (between L5 and L6 vertebrae), there is virtually no risk of damaging the spinal structures as, at this level, your needle will be overlooking the cauda equina projections in the vertebral canal. It is very unlikely to observe paralytic or ataxic effects caused by the injection procedure. If these effects occur, this could be an indication of either a temporary side effect of a newly tested transfection reagent or a link to the novel analgesic drug you are testing. If the substances you inject are known and have no record of intrathecal side effects, this could indicate injection occurred at a level higher than the L2 vertebrae, signalling a puncture of the spinal cord. The animal should thus be discarded from the testing group.
5. Blood-return from the intrathecal site of injection is not frequent but, at the same time, not a sign of poor injection technique. Indeed, small capillaries under the surface of the skin may have ruptured without any damage to the nervous structures. If bleeding occurs, press the site with the finger or gauze for 5 s, and proceed with the habitual schedule of testing.
6. The experimental pattern was chosen by considering high potency and efficacy of DsiRNAs. Indeed, two injections were shown to induce a sustained effect over 3 days (4). However, classic siRNAs could necessitate up to 4 injections as described earlier (6) or continuous infusion could be required. Therefore, dose and window of injection have to be adapted according to the RNAi technology selected.
7. Rats are wrapped, and thus restrained, in a small towel for the different manipulations because they feel more comfortable in a dark and restricted environment. Pain and stress being highly related, we try to minimize stressful manipulations by making the animal as habituated and comfortable as possible.
8. In continuity with note 7, rats should be habituated to any modification in temperature, luminosity, humidity, and noise level between housing and experimental rooms. This will minimize stress and, consequently, uncontrollable variables affecting modulation of pain response.
9. Even though the bath is electronically adjusted to 52°C, temperature can be unequal within the depth of water. The experimenter should stir the water with a thermometer to ensure no thermal layer has formed, and counter-verify the temperature

with the thermometer used to stir. This step is crucial taking into consideration that nociceptor neurons expressing heat-sensitive channels display different thresholds, and are stimulated according to the temperature of the water. At 52°C, all the nociceptive neurons should be activated (7).

10. Peak of action of our tested compounds (neurotensin analogs) is between 15 and 30 min. Use of a different pharmacological compound can necessitate later measurements. However, no measurement should be taken before 15 min as the pain response could be modified by the volatile anesthetic. Since animals are not exposed to anesthesia for a long period (2–5 min), we have observed rapid cognitive recuperation with no apparent side effects at 15 min.
11. Holding the hind paw too tightly before the injection can (1) provoke pain in the animal; (2) induce stress; (3) impair blood flow causing a brief loss of sensation in the paw. Since the pain response to intraplantar injection of formalin begins immediately after the injection, this could significantly change the pain response during the first minutes of the test. This technique is highly recommended to be performed by two experimenters. The contention can be better performed by lightly pressing the lower back of the animal and pushing the tail aside with fingers. With the other hand, seize the hind paw and immobilize it at the knee joint between the index finger and the thumb. The second experimenter can then inject the paw.
12. If the injection is well realized between the second and third finger pads of the hind paw, a bubble should be obvious in the plantar surface and remain there. If it diffuses, you have achieved subcutaneous injection rather than intradermal injection. The pain response will not be the same. A partial intravenous injection can also occur if a blood return is detectable in the needle, often accompanied by a purple coloration under the plantar surface. In this case, the rat needs to be discarded from the group.
13. Hemolysis within the CSF sample can affect subsequent immunological analysis. Blood contamination should be kept to a minimum, and blood should be removed as quickly as possible. Centrifuge the CSF even if it seems that no contamination occurred.
14. CSF can be used for ELISA assays or Luminex analysis of proinflammatory cytokine titres. Frozen or freshly-collected tissues are used for protein and mRNA quantification by Western blot and quantitative real-time PCR, respectively (not described).
15. The plastic lid on which the rat is taped can be a large Tupperware. We recommend that you drill holes 1 inch from the edge.

When the apex is incised, blood loss will occur and persist for the whole perfusion procedure. All the fluids should flow through the holes of the lid in the Tupperware. This way, the procedure area remains clean and you can easily discard the biological fluids.

16. Central nervous system structures are the last to be reached by the fixative agent. If blood can still be observed within the liver, lungs or paw tips of the animals, there is a strong probability that the CNS is not fixed appropriately. Degradation of the tissue can then occur with time, and further quality of sliced structures and immunochemistry will be poor.
17. Fixed tissues are stable for a long period of time (when cryoprotected in sucrose), and are most often cut on a microtome or cryostat for microscopic visualization (not described). Cryoprotection takes 24 h–48 h depending on the tissue. When ready, the tissue will sink to the bottom of the tube.

References

1. Behlke, M.A. (2006) Progress towards in vivo use of siRNAs. *Mol.Ther.* **13,** 644.
2. Amarzguioui, M., Lundberg, P., Cantin, E., Hagstrom, J., Behlke, M.A. and Rossi, J.J. (2006) Rational design and in vitro and in vivo delivery of Dicer substrate siRNA. *Nat. Protoc.* **1,** 508.
3. Kim, D.H., Behlke, M.A., Rose, S.D., Chang, M.S., Choi, S. and Rossi, J.J. (2005) Synthetic dsRNA Dicer substrates enhance RNAi potency and efficacy. *Nat. Biotechnol.* **23,** 222.
4. Dore-Savard, L., Roussy, G., Dansereau, M.A., Collingwood, M.A., Lennox, K.A, Rose, S.D., et al. (2008) Central delivery of Dicer-substrate siRNA: a direct application for pain research. *Mol. Ther.* **16,** 1331–9.
5. Henry, J.L., Yashpal, K., Pitcher, G.M. and Coderre ,T.J. (1999) Physiological evidence that the 'interphase' in the formalin test is due to active inhibition. *Pain* **82,** 57–63.
6. Luo, M.C., Zhang, D.Q., Ma, S.W., Huang, Y.Y., Shuster, S.J., Porreca, F. and Lai, J. (2005) An efficient intrathecal delivery of small interfering RNA to the spinal cord and peripheral neurons. *Mol. Pain* **1,** 29.
7. Tominaga, M. and Caterina, M.J. (2004) Thermosensation and pain. *J. Neurobiol.* **61,** 3–12.

Chapter 26

A Potential Therapeutic for Pandemic Influenza Using RNA Interference

Shaguna Seth, Michael V. Templin, Gregory Severson, and Oleksandr Baturevych

Abstract

RNA interference (RNAi) involves sequence-specific downregulation of target genes, leading to gene silencing in vitro and in vivo. Synthetic small interfering RNAs (siRNAs), formulated with appropriate delivery agents, can serve as effective tools for RNAi-based therapeutics. The potential of siRNA to provide antiviral activity has been studied extensively in many respiratory viruses, including influenza virus, wherein specific siRNAs target highly-conserved regions of influenza viral genome, leading to potent inhibition of viral RNA replication. Despite various delivery strategies, such as polycations and liposomes that have been employed to formulate siRNAs, effective delivery modalities are still needed. Although current strategies can provide significant biodistribution and delivery into lungs allowing gene silencing, complete protection and prolonged survival rates against multiple strains of influenza virus still remains a key challenge. Here, we describe methods and procedures pertaining to screening and selection of highly effective influenza-specific siRNAs in cell culture, in mice, and in the ferret model. This will be potentially useful to evaluate RNAi as a therapeutic modality for future clinical application.

Key words: RNA interference, Small interfering RNA (siRNA), In vitro and in vivo screening, Liposomes, Dual luciferase assay, $TCID_{50}$ and Plaque assay, Influenza virus infection, Intranasal dosing, Cytokine assay

1. Introduction

Influenza virus, known to cause one of the most widespread respiratory virus infections in humans, is considered a major public health concern worldwide. Influenza virus infection is relatively quick, with peak viral titers achieved within 1–3 days post initial exposure. The virus polymerase is particularly error prone, causing a great deal of sequence variability and re-assortment of avian and human viruses that often leads to antigenic shift and antigenic drift. Strains isolated from ducks, horses, swine, and

Wei-Ping Min and Thomas Ichim (eds.), *RNA Interference*, Methods in Molecular Biology, vol. 623,
DOI 10.1007/978-1-60761-588-0_26, © Springer Science+Business Media, LLC 2010

turkey have shown remarkable similarities with those infecting humans, suggesting persistence of a vast reservoir of multiple subtypes and strains of influenza virus that can potentially "jump" the species barrier and infect humans (1, 2). Vaccine and antiviral drugs, which are currently available against influenza, seem to be highly effective against seasonal strains of influenza, but could prove ineffective against a H5N1 pandemic. RNA interference (RNAi) offers a potential solution as a new antiviral approach targeting highly-conserved regions of influenza viral genome. RNAi involves the use of small interfering RNAs (siRNAs) to enable sequence-specific degradation of targeted mRNA sequence against multiple strains of seasonal and highly pathogenic influenza virus (3–6).

A number of published studies have shown the great promise of siRNAs or shRNAs (short hairpin RNA) against influenza virus. SiRNAs that target nucleocapsid (NP), matrix (M), or polymerase subunits (PB1, PB2, and PA genes) have shown significant inhibition of viral replication, both in vitro and in vivo (7–12). Administration of siRNAs before and after viral infection has demonstrated better efficacy than strictly therapeutic dosing of siRNAs. However, siRNA therapeutic is unlikely to provide substantial treatment benefit over the normal immune response to the viral infection as the influenza virus replicates rapidly within the first 48 h of infection (2). Cytokine response against double-stranded siRNA (dsRNA) duplexes should also be carefully monitored during the viral infection, and specific siRNA modifications (such as 2′-*O*-methyl at the 2′ position of the ribose sugar) should be utilized to avoid interference in the therapeutic potential of RNAi (13–15). Here, we review some commonly used reagents and methods in the design and screening of highly effective and potent influenza-specific siRNAs, both in vitro and in vivo in the mouse and ferret model systems.

2. Materials

2.1. General

1. Tissue culture-related instruments and equipments: Laminar flow hood, incubators, shakers (VWR, Westchester, PA)
2. Sterile pipettes and tips (Rainin, Oakland, CA)
3. Tissue culture flasks with filter lid, T150 and T225 (BD Falcon, Franklin Lakes, NJ)
4. V-bottomed 96-well tissue culture plates (Sigma-Aldrich, St. Louis, MO)
5. 6-well, 12-well, 24-well, and 96-well tissue culture plates (BD Falcon, Franklin Lakes, NJ)
6. 96-well sterile block, 0.5 mL (VWR, Westchester, PA)

7. 2 mL Whatman Uniplate (Fisher Scientific, Pittsburg, PA)
8. Reagent Reservoir: 25–100 mL (VWR, Westchester, PA)
9. Cell culture medium, buffers, and supplements: Dulbecco's modified Eagle medium with high glucose (DMEM), OptiMEM, Dulbecco's phosphate buffered saline, HEPES buffer (100×), l-Glutamine (Gibco-Invitrogen, Carlsbad, CA), MEM Non-essential amino acids (Media Tech, Manassas, VA)
10. Heat-inactivated fetal bovine serum (Gibco-Invitrogen, Carlsbad, CA)
11. 2.5% Trypsin and 0.25% Trypsin-EDTA (Invitrogen, Carlsbad, CA)
12. Penicillin-streptomycin (100 units/mL) (Invitrogen, Carlsbad, CA)
13. Oxoid purified agar (Remel, Lenexa, KS)
14. 35% Bovine serum albumin (BSA) (Sigma-Aldrich, St. Louis, MO)
15. Lipofectamine™ RNAiMAX 2000 (Invitrogen, Carlsbad, CA)
16. Tissue homogenizers (Fast prep, MP Biomedicals, Solon, OH)
17. Animal dissecting tools
18. Light and inverted phase contrast microscope (Olympus, Center Valley, PA)

2.2. Dual Luciferase Assay

1. A549 lung epithelial cell line (ATCC, Manassas, VA)
2. 12-channel wand with 20-gauge needles, 13 mm long (V&P Scientific Inc., San Diego, CA)
3. Sterile eppendorf tubes and 15 mL conical tubes (VWR, Westchester, PA)
4. Pipettes and multi-channel pipettes
5. siRNA suspension buffer (Dharmacon, Lafayette, CO)
6. siRNA and influenza target gene(s) cloned in a pSiCheck plasmid construct
7. Dual-Glo luciferase reporter assay system (Promega, Madison, WI)
8. Microlite Luminescence Microtiter 96-well plates (Thermo Labsystems, Franklin, MA)
9. Flat-bottom 96-well plate (VWR, Westchester, PA)
10. LMax II Luminometer (Molecular Device, Sunnyvale, CA)

2.3. Influenza Infection, Plaque Assay, and $TCID_{50}$ Assay

1. MDCK cell line (ATCC, Manassas, VA).
2. Influenza A/PR/8/34 virus stock (ATCC, Manassas, VA).
3. PBS/BSA with antibiotics is prepared by combining 4.3 mL of 35% BSA, 5 mL of 100× penicillin/streptomycin stock solution, and 490.7 mL of PBS. Store at 4°C.

4. Prepare cell growth medium by mixing 440 mL of Dulbecco's Modified Eagles Medium (DMEM) with 50 mL of FBS (10% v/v), 5 mL of 1 M HEPES (Invitrogen, Carlsbad, CA) and 5 mL of penicillin/streptomycin (PS), 100 units/mL.
5. Infection medium is prepared by mixing 485 mL of DMEM with 5 mL of 1 M HEPES, 5 mL of penicillin/streptomycin, 100 units/mL, 4.3 mL of 35% BSA and 80 μL of 2.5% trypsin.
6. Prepare 2× DMEM medium for agar overlay by combining 26.96 g of DMEM powder in 700 mL of sterile water. Add 98.8 mL of 7.5% sodium bicarbonate ($NaHCO_3$) solution (Invitrogen, Carlsbad, CA), 10 mL of 100× penicillin/streptomycin and 10 mL of 1 M HEPES. Adjust pH to 7.1 with 10% HCl solution then add up to 1 L water. Prepare 1.5% purified Oxoid Agar (Remel, Lenexa, KS) with 1.5 g purified Oxoid Agar in 100 mL of distilled water, autoclave and store at room temperature. Melt 1.5–2% oxoid agar and bring to about 40°C in a water bath. Prepare 250 mL of 2× DMEM medium by combining 221 mL of 2× DMEM, 10 mL of DEAE- Dextran (Sigma, St. Louis, MO) and 8.5 mL of 35% BSA and 10 mL of L-Glutamine (final concentration ~0.2 M) with 50 μL of 2.5% trypsin solution. Sterile filter and store at 4°C. Equilibrate at 37°C when ready to pour onto the infected plates by adding 250 mL of melted agar.
7. Prepare fixing solution: To 990 mL of DPBS, add 10 mL of 50% Gluteraldehyde (Ted Pella, Redding, CA) to make 0.5% Gluteraldehyde solution.
8. Dissolve 10 g of crystal violet (Sigma, St. Louis, MO) in 300 mL water and 700 mL methanol for preparation of crystal violet stain. Store at room temperature.

2.4. In Vivo Screening of siRNAs in Mice

1. BALB/c mice, 5–12 weeks old, female (Charles River Laboratories, Wilmington, MA)
2. Clean mouse cage
3. Ketamine/Xylazine hydrochloride solution (Sigma, St. Louis, MO)
4. 28-gauge single use needles (VWR, Westchester, PA)
5. Lysing matrix (MP Biomedicals, Solon, OH)
6. FastPrep-24 homogenizer (MP Biomedicals, Solon, OH)
7. Chicken red blood cells (Lampire biologicals, Pipersville, PA)

2.5. Quantitative Real-Time PCR Assay

1. DEPC-treated RNase-free water (Invitrogen, Carlsbad, CA)
2. 95–100% Ethanol (Sigma-Aldrich, St. Louis, MO).
3. RNase *AWAY*® Reagent (Invitrogen, Carlsbad, CA).

4. Invitrogen PURELink 96 RNA Isolation Kit (Invitrogen, Carlsbad, CA). Make 200 mL of 1× wash buffer II and 8 mL of freshly prepared DNase I solution for each 96-well plate. Prepare 10× DNase I buffer using RNase-free water to yield the final concentration of 200 mM Tris–HCl, pH 8.4, 20 mM $MgCl_2$ and 500 mM KCl. For DNase I digestion, add 10× DNase I Buffer 0.8 mL, DNase I (3,200 units) and RNase-free water making up the volume to 8 mL in a sterile RNase-free tube. Add 10 μL 14.3 M β-mercaptoethanol to 1 mL of RNA lysis solution for cell lysis. Addition of β-mercaptoethanol (β-ME) (Invitrogen, Carlsbad, CA) will improve the lysis of the cell. You will need 100 mL of RNA lysis solution for each 96-well plate.
5. SuperScript III First-Strand Synthesis System (Invitrogen, Carlsbad, CA)
6. TaqMan Universal PCR Master Mix without AmpErase UNG (Applied Biosystem, Foster City, CA).
7. SYBR Green FastMix, ROX (Quanta Biosciences Inc., Gaithersburg, MD)
8. Multichannel pipettes
9. RNase-free ART aerosol resistant pipette tips (Molecular BioProducts, San Diego, CA)
10. Vacuum manifold and vacuum supply
11. FastPrep-24 (Sample preparation system; MP Biomedicals, Solon, OH)
12. Nanodrop spectrophotometer, ND-1000 (Thermo Scientific, Wilmington, DE)
13. Bioanalyzer 2100 (Agilent Technologies, Santa Clara, CA)
14. 7900 Real Time PCR System (Applied Biosystems, Foster City, CA)
15. ABI PRISM 96 well Optical Reaction Plates with Barcode and ABI PRISM Optical Adhesive Covers (Applied Biosystem, Foster City, CA)
16. RNA 6000 Nano LabChip® (Agilent Technologies, Santa Clara, CA)
17. Lysing Matrix 2 mL tubes (MP Biomedicals, Solon, OH)

2.6. RACE Assay

1. RACE assay kit (Invitrogen, Carlsbad, CA)
2. Trizol reagent (Invitrogen, Carlsbad, CA)
3. Thermocycler (Eppendorf, Westbury, NY)
4. Custom GSP1, nest GSP2, and nest GSP3 primers
5. TE, pH 8.0 buffer (Invitrogen, Carlsbad, CA)
6. Taq DNA polymerase (Invitrogen, Carlsbad, CA)

7. SeaKem® LE Agarose (Teknova, Hollister, CA)
8. Electrophoresis apparatus (BioRad Laboratories, Hercules, CA)

2.7. In Vivo Screening of siRNAs in Ferrets

1. 6–8 month old, influenza-naïve ferrets (FFF, Sayre, PA)
2. Stainless steel cages (Shor-line, Kansas City, KS)
3. 96- well cell culture plates (VWR, Westchester, PA)
4. Turkey red blood cells (Lampire biologicals, Pipersville, PA)
5. 10-day embryonated eggs (S&G Poultry, Clanton, AL)
6. Ketamine, xylazine and atropine (Sigma, St. Louis, MO)
7. Temperature transponder (Biomedic Data Systems, Seaford, DE)
8. Implantable microidentification device (IPTT-300 Chip, Biomedic Data Systems, Seaford, DE)
9. Gentamicin solution (Invitrogen, Carlsbad, CA)
10. SAS software (SAS/STAT software, SAS Institute, Inc., Cary NC)

2.8. In Vitro Cytokine Detection

1. Bleach
2. PBS (Invitrogen, Carlsbad, CA)
3. Ficoll-Hypaque (Amersham Biosciences, Piscataway, NJ)
4. Iscove's modified DMEM (IMDM) (Mediatech Inc., Manassas, VA)
5. Non-essential amino acids (NEAA) (Invitrogen, Carlsbad, CA)
6. Glutamine (Invitrogen, Carlsbad, CA)
7. Lipofectamine™ RNAiMAX Transfection Reagent (Invitrogen, Carlsbad, CA)
8. OptiMEM reduced serum medium (Invitrogen, Carlsbad, CA)
9. 50 mL Conical tubes (VWR, Westchester, PA)
10. Collected human peripheral blood (Golden West Biological, Temecula, CA)
11. Human Interferon ELISA kit (PBL Biomedical Laboratories, Piscataway, NJ)

2.9. In Vivo Cytokine Detection

1. 6–8 week old BALB/c mice (Charles River Laboratories, Wilmington, MA)
2. 28-gauge single use needles (VWR, Westchester, PA)
3. Ketamine/xylazine mouse anesthesia (Sigma, St. Louis, MO)
4. Suture (~4-0 silk braided suture), cut into 4-inch pieces
5. 20-gauge Luer hub adapters (VWR, Westchester, PA)
6. 1 mL slip-tip syringes (VWR, Westchester, PA)
7. 0.3% BSA solution in PBS and 1% penicillin-streptomycin, stored at 4°C (freshly prepared)

8. Eppendorf tubes, 1.8 mL
9. Mouse Interferon ELISA kit (PBL Biomedical Laboratories, Piscataway, NJ)
10. Procarta™ custom 10-plex cytokine profiling kit
11. Luminex 100 IS System (Bio-Rad Life Sciences, Hercules, CA)
12. Surgical tools: micro dissecting scissors; micro dissecting spring scissors or other very small, fine-tipped scissors; two pairs of forceps (at least one pair fine-tipped and angled).

3. Methods

3.1. In Vitro Screening of siRNAs

Influenza-specific siRNAs, designed against viral gene targets, are first evaluated for inhibition of target mRNAs and viral replication in vitro. This can be achieved by (a) co-transfecting siRNAs with a plasmid construct carrying the viral gene in a luciferase expression-based system in A549 lung epithelial cell line, or (b) transfecting siRNAs and subsequently infecting with influenza virus using the Vero and MDCK cell transfection-infection method. The potency of selected siRNAs can then be assessed by titrating siRNAs in a concentration range from 10 pM to 10 nM to establish the IC_{50} and maximal inhibition for each siRNA.

The appropriate design of influenza-specific siRNAs requires careful inspection of highly-conserved sites using existing design algorithms. These involve base compositions, preferences, low RNA secondary structures, choice of a Dicer substrate, and RISC substrate or short hairpin RNA (shRNA) expressed from a plasmid vector that can provide maximal siRNA efficacy across multiple strains of influenza virus (2). Off-target effects and immune activation can be minimized by using optimal chemical modifications (avoiding RISC cleavage sites, positions 9 and 10 on the sense strand) such as 2′-*O*-methyl, 2′-Fluoro, and ribothymidine in place of uracil; this would restore activity and improve chemical and nuclease stability of siRNAs (16–18). A plethora of published reports describe algorithms for identification and selection of siRNA target sites by setting forth multiple design criteria for highly active siRNAs (19–24).

3.1.1. Dual Luciferase Assay

1. Seed log phase growing A549 (or substitute with HeLa cells) as 1.2×10^4 cells per well in a 96-well flat-bottom plate a day before the transfection.
2. On the day of transfection, when cells are 70–80% confluent, thaw the DNA and prepare cocktails for co-transfection. Keep the stocks on ice.
3. Mix plasmid DNA (100 ng/well) and siRNA in OptiMEM. Mix Lipofectamine™ RNAiMAX (0.2 μL/well of a 96-well

plate) in OptiMEM, and incubate for 5 min at room temperature.

4. Mix the lipofectamine-complex in OptiMEM with plasmid DNA-siRNA cocktail. Incubate for 30 min at room temperature.
5. Include controls with plasmid DNA alone or untransfected controls (in triplicates).
6. The cocktail can be prepared in a V-bottom 96-well plate. Cover the plate to prevent evaporation during the incubation period.
7. Add 25 μL per well and incubate for 4–5 h at 37°C. Aspirate the supernatant from each well after transfection and add 75 μL of DMEM medium with 10% FBS into each well. Incubate at 37°C for 24 h.
8. Measure the luciferase activity using Dual-Glo luciferase reporter assay system. (mentioned in Materials Subheading 2.2).

3.1.1.1. Measuring Firefly Luciferase Activity (Based on Promega's Instructions)

1. Transfer the contents of one bottle of Dual-Glo Luciferase Buffer to one bottle of Dual-Glo Luciferase substrate (Dual-Glo luciferase reporter assay kit as mentioned in Materials Subheading 2.2) to form the "working" Dual-Glo Luciferase Reagent. Mix by inversion until the substrate is thoroughly dissolved. Aliquot and store at −20°C.
2. Allow an aliquot of pre-made "working" Dual-Glo Luciferase Reagent to equilibrate to room temperature before use.
3. Allow the transfection plate to reach room temperature.
4. Add 75 μL of room temperature "working" Dual-Glo Luciferase Reagent into each well of the plate containing the cells and 75 μL of culture medium.
5. After ~3 min, mix reactions (150 μL per well) and transfer the reactions from the culture plate to a black OptiPlate-96. Seal the plate with a foil cover, and incubate at room temperature for at least 10 min but no longer than 2 h.
6. Measure the luminescence using a luminometer.

3.1.1.2. Measuring *Renilla* Luciferase Activity

1. Dilute the Dual-Glo Stop and Glo Substrate 1:100 into an appropriate volume of Dual-Glo Stop and Glo Buffer in a new container.
2. Add 75 μL of Dual-Glo Stop and Glo Reagent to each well (equal to the original culture medium volume).
3. Mix thoroughly (225 μL per well). Seal the plate with a foil cover, and incubate at room temperature for at least 10 min and no longer than 2 h.
4. Measure the luminescence using a luminometer.

5. Calculate the ratio of dual luciferase activity using the following formula: Average Renilla activity from triplicates/Average firefly activity from triplicates. The percentage of Renilla activity reduction is equal to 100 × (1 – siRNA positive dual activity/siRNA negative dual activity).

3.1.2. Influenza Infection and Co-transfection Assay

1. Vero cells are seeded at 1.5×10^4 cells per well in a 96-well plate in 100 µL of DMEM with 10% FBS medium per well, one day prior to transfection.
2. At 24 h post seeding, various concentrations of influenza-specific siRNAs or non-targeting control siRNA are complexed with 0.2 µL of Lipofectamine™ RNAiMAX (1 mg/mL stock) per well, and incubated in 25 µL OptiMEM for 20 min at room temperature.
3. Upon removal of supernatant, the cells are supplemented with 75 µL of 10% FBS containing DMEM.
4. A 25 µL of siRNA and Lipofectamine™ RNAiMAX complex is then added to each well. It is important to include untreated, virus-infected cells as a control to compare the treatment effect with siRNAs.
5. At 3 h post transfection, supernatants are removed and cells are washed with 150 µL of 1× PBS containing 0.3% BSA in 10 mM HEPES/PS.
6. Cells are infected with the influenza virus at the desired multiplicity of infection (MOI) and further incubated for 1 h at 37°C.
7. Discard innoculum and wash off the unbound virus using PBS. Add 200 µL of infection medium into each well (Mentioned in Materials Subheading 2.3).
8. Incubate for 48 h at 37°C for virus propagation.
9. Check for viral growth by observing cytopathic effects (CPE) at 24 and 48 h post infection.
10. At the end of incubation (48 h post infection), harvest supernatants and perform Plaque assay (see Subheading "Plaque Assay") or $TCID_{50}$ assay (see Subheading "Tissue Culture Infective Dose 50 (TCID50) and Hemagglutination Assay" for viral quantification. Inhibition of viral RNA in treated cells can also be measured by quantitative RT-PCR assay using RNA isolated from the infected cells (see Subheading 3.2.2). Store residual supernatants at –80°C.

3.1.2.1. Plaque Assay

1. Seed MDCK cells at a density of 3.0×10^5–7.0×10^5 cells per well. Seed density will depend on cell growth rate. Incubate overnight at 37°C at 5% CO_2 to get a confluent monolayer.

2. On day one, prepare ten-fold serial dilutions of the viral supernatants, by taking 50 μL of the virus and diluting in 450 μL of infection medium.
3. Perform ten-fold serial dilutions 10^{-1} to 10^{-8} (based on viral titer stock).
4. Wash cells twice with the infection medium to remove serum-containing medium. Do not remove the wash until you are ready to add the virus dilutions.
5. Add 200 μL of diluted virus to duplicate wells. Proceed from higher dilution to lower dilution and incubate for 1 h at 37°C.
6. During viral incubation, melt the 1.5% agar in a microwave and incubate in 45°C water bath until equilibrated. Prepare DMEM solution and 1.5% agar separately, as shown in the Materials Subheading 2.3.
7. Remove the plates after 1 h of incubation and aspirate the innoculum from the cells. Working quickly, mix the DMEM solution with the melted 1.5% agar and add 1.5–2.0 mL of overlay per well.
8. Allow about 5–10 min for the agar to solidify at room temperature before incubation (in hood with lid ajar). Incubate for 48–72 h at 37°C with 5% CO_2 for viral propagation.
9. On day four, fix infected cells with 0.5% Gluteraldehyde in PBS for 30–45 min. Remove agar using a spatula by peeling up one edge of the agar from the wells.
10. Stain fixed cells with 1 mL crystal violet and incubate at room temperature for 10 min. Rinse carefully with water and let dry at room temperature.
11. Count plaques at the dilution with approximately 10–50 well separated plaques. Use this number to calculate plaque-forming units (pfu/mL).
12. Calculate the fold change in viral titers of the treated samples as compared to the untreated infected samples.

3.1.2.2. Tissue Culture Infective Dose 50 ($TCID_{50}$) and Hemagglutination Assay

1. Each 96-well plate that is prepared will accommodate the dilution of three samples.
2. One day prior to transfection, prepare MDCK cell suspension at 2.0×10^4 cells per well in growth medium (96-well plate). Incubate at 37°C with 5% CO_2 overnight.
3. On the day of infection, add 450 μL of infection medium to each well of dilution Block (0.5 mL).
4. Remove medium containing FBS from assay plate, and wash with infection medium. Do not remove the wash until you are ready to add the virus dilutions.
5. Add 50 μL virus to the 1st row of wells in the dilution block, and mix well by pipetting up and down.

6. Using a 12-channel pipette, remove 50 μL suspension from the first row of wells and add to the 2nd row of wells, mix well.
7. Perform tenfold serial dilution up to 10^{-10} (dependent on the stock viral titer).
8. Remove the wash medium from assay plates. Transfer using 8-channel pipette, 100 μL of diluted virus from the dilution block to the appropriate wells. Incubate the virus dilutions at 37°C with 5% CO_2 for 1 h.
9. Remove the viral innoculum and add 200 μL of fresh infection medium to each well.
10. Incubate for 48 h at 37°C with 5% CO_2 for viral propagation.
11. Harvest supernatants for hemagglutination assay or observe infected cells for cytopathic effects under the phase contrast microscope.
12. Set up ice buckets with sufficient area to incubate HA plates. Prepare 0.5% chicken red blood cells in PBS (5 mL per plate).
13. Test each sample in duplicate. Transfer 100 μL aliquots of culture supernatant from each treated and untreated sample to two wells in the first row of the 96-well V-bottom plate. Change tips between samples. The plate should be oriented where eight tests will fit onto each plate. Each test will have 12 serial dilutions. Use a multi-channel pipette to add 50 μL PBS per well to the rest of the plate, except the first row that received viral supernatant. Use a multi-channel pipette to aspirate 50 μL of the culture supernatant from the first row, and then mix with the 50 μL PBS in the second row. Pipette up and down three times. Use a multi-channel pipette to aspirate 50 μL diluted sample from the second row and mix with the 50 μL PBS in the third row. Pipette up and down three times. Repeat steps 5 and 6 until reaching the last row. Discard 50 μL of the final dilution.
14. Add 50 μL 0.5% chicken red blood cells (RBCs) into each well. Prepare 0.5% of chicken RBCs by diluting 10 mL of 5% washed chicken RBCs to 90 mL of DPBS. It is not necessary to change tips if the well wall is not touched. Incubate the plates on ice for 1 h. Read the HA results. Positive HA yields a uniform, opaque, rust-colored mat evenly distributed in the V-bottom well. Negative HA yields a dark, red colored drop in the center of the V-bottom well with the surrounding well relatively clear. Mark wells as positive or negative. Based on the above observations, calculate the $TCID_{50}$ using the Reed and Muench method (25). The HA dishes may be stored at 4°C for later observation.
15. Calculate the fold decrease in viral titers of the treated samples over the untreated, infected control samples.

3.2. In Vivo Screening of siRNAs

One of the challenges for siRNA-based antiviral drugs is to deliver siRNAs at the site of influenza infection. Significant progress has been made in RNAi-related therapeutics to enable efficient delivery, allowing efficient cell uptake and cytosol localization to nasal and lung epithelium (26–28). A number of approaches are available to deliver influenza-specific siRNAs to the lungs that include local (such as direct nasal or pulmonary instillation, intra-tracheal) and systemic (via intravenous mode of administration) delivery methods. Liposomes containing cationic lipids, such as DOTMA and DOTAP, along with neutral co-lipids, such as cholesterol and/or DOPE, have shown potential in local and systemic delivery of siRNAs to various tissues (29–31). Systemic delivery with polycations, such as polyethylenimine (PEI), polylysine (PLL), polyarginine, and chitosans, has also been previously studied (11, 32–34). Here, we describe siRNA instillation using the intranasal mode of administration.

3.2.1. Intranasal Delivery of siRNAs in the Mouse Model

On days −2, −1, and 0 (with reference to influenza infection), 6–8 week old BALB/c female mice (ten mice per group) are anesthetized with ketamine/xylazine intraperitoneally (200 μL dose/mouse, 80 mg/kg ketamine/12 mg/kg xylazine). Animals are then dosed with 50 μL of siRNA, formulated in any polymer or lipid-based delivery system, by intranasal mode of administration. Using the left hand to immobilize the head, hold the left portion of the mouse neck to keep it erect and instill slowly making sure every drop is breathed into the nostril. Hold the mouse for an additional few seconds before placing back into the cage.

1. Mice can be dosed once daily for three consecutive days in a prophylactic dosing regimen or three times post infection, to study the therapeutic potential of the siRNA in the presence or absence of a delivery vehicle. The optimal siRNA dose required to cause viral inhibition can be determined by titrating from 0.5 mg/kg to 5 mg/kg dose in the presence of a delivery agent. Unformulated siRNAs require a much higher siRNA dose of 10 mg/kg to provide therapeutic benefit (see Note 1).
2. On day 0, at 4 h post final siRNA dose period, animals are anesthetized with ketamine/xylazine intraperitoneally again, and infected intranasally with mouse minimum infectious dose 50 (MID_{50}) of mouse-adapted A/PR/8/34 virus in 50 μL 1× PBS/0.3% BSA/1× PenStrep solution.
3. Body weight and clinical signs of infection are assessed daily following infection.
4. Day 2 post infection, the whole lung [right and left lobes] is harvested from each mouse and suspended in a Lysing Matrix

2 mL tube containing 1 mL 1× PBS/0.3% BSA/1× PenStrep. Tubes, containing each lung, are frozen immediately on dry ice and stored at −80°C for preparation of lung homogenate.

Tissues are thawed quickly at 37°C, homogenized using FastPrep-24 (Sample preparation system) for 45 s to 1 min, and frozen at −80°C until viral titer estimation by $TCID_{50}$ (see Subheading "Tissue Culture Infective Dose 50 (TCID50) and Hemagglutination Assay" or Quantitative RT-PCR assay to determine mRNA inhibition is performed as described in Subheading 3.2.2. Identification of RISC-specific cleavage of mRNA target site can be achieved by rapid amplification of cDNA ends (RACE) assay (see Subheading 3.2.3).

3.2.2. Assessment of Viral mRNA Inhibition using Quantitative Real-Time PCR Assay

Total RNA is extracted from tissue samples stored in RNAlater solution after harvesting lungs from treated and untreated animals. The isolation of total RNA is done using the Invitrogen PURELink 96 RNA Isolation Kit, according to the manufacturer's protocol for RNA isolation from mammalian tissue (as listed in Materials Subheading 2.5) (see Notes 2 and 3).

1. Add 1 mL RNA lysis solution to the lysing matrix 2 mL tubes. Place ~10 mg of lung tissue sample in each tube. Homogenize the tissue using FastPrep 24 for 45 s at 6.5 m/s speed one time, keeping the samples on ice and homogenize again. Transfer 500 μL supernatant to the 2 mL 96-well block, and add 500 μL of RNA lysis solution. Add 1 mL of 70% ethanol, and mix. Proceed to isolating RNA using 1,000 μL of the tissue lysate per well of the RNA filter plate.
2. Place the RNA filter plate on the vacuum manifold. Transfer 1,000 μL of the tissue lysate per well to the RNA filter plate. Apply vacuum for 2 min at room temperature. Release vacuum. Add 500 μL of wash buffer I to each well of the RNA Filter Plate. Apply vacuum for 2 min at room temperature. To remove genomic DNA from the samples, add 80 μL of DNase I solution into each well of the RNA Filter Plate and apply vacuum briefly to allow the solution to soak into the filter matrix. Incubate the plate at room temperature for 15 min.
3. Add 500 μL of wash buffer I to each well of the RNA Filter Plate. Incubate for 5 min at room temperature. Apply vacuum for 2 min at room temperature. Release vacuum.
4. Add 1 mL of 1× wash buffer II to the RNA filter plate and apply vacuum for 2 min at room temperature. Repeat the wash step twice. After releasing vacuum, place the filter plate with the filter side down on a stack of paper towels and firmly pat dry the plate. Place the RNA filter plate on the vacuum manifold, and apply vacuum for 5–10 min at room temperature.

5. Place the receiver plate in the vacuum manifold (in place of the waste collection tray), and place the RNA filter plate on top of the receiver plate. Add 170 µL of RNase-free water to each well of the RNA filter plate. Incubate for 5 min at room temperature. Centrifuge at 1,500 × *g* for 5 min at room temperature. The RNA is eluted into the receiver plate. Store RNA at –80°C for further use.
6. Total RNA is quantified by measuring OD_{260} in RNase-free 10 mM Tris, pH 8.0 buffer (1:100 dilution). To ensure superior RNA quality, the ratio of A_{260}:A_{280} should be greater than 2.0 and A_{260}:A_{230} ratio should be greater than 1.7. Alternatively, nanodrop spectrophotometer can also be used for undiluted RNA quantification. Turn on the NanoDrop software by selecting "Nucleic Acid" analysis tool and initiate the software program. Before making measurements, a blank should be measured by placing 1 µL of water on the pedestal. Add 1 µL RNA sample to the tip. Measure the RNA concentration.
7. Determine the integrity of isolated RNA by using Agilent Bioanalyzer 2100 system. Electrophorese a fraction of each RNA sample on a denaturing agarose gel or on an Agilent BioAnalyzer® using an RNA 6000 Nano LabChip®, and verify that there is a sharp distinction at the small side of both the 18 S and 28 S ribosomal RNA (rRNA) bands or peaks. Any smearing or shoulder to the rRNA bands or peaks indicates that there is RNA degradation.
8. Total RNA normalized to 100–400 ng is reverse transcribed into cDNA using the SuperScript III First-Strand Synthesis System. Combine total RNA (up to 500 ng), 1 µL of 50 µM Primer oligo $(dT)_{20}$ or 50 ng/µL random hexamer, 1 µL of 10 mM dNTP mix, and make up the volume to 10 µL with DEPC-treated water. Incubate at 65°C for 5 min, then place on ice for at least 1 min. Prepare the cDNA synthesis mix by adding 2 µL of 10× RT buffer, 4 µL of 25 mM $MgCl_2$, 2 µL of 0.1 M DTT, 1 µL of RNaseOUT (40 U/µL), and 1 µL of SuperScript III RT (200 U/µL). Add 10 µL of cDNA synthesis mix to each RNA/primer mixture, mix gently, and collect by brief centrifugation. Incubate Oligo $(dT)_{20}$ for 50 min at 50°C or Random hexamer for 10 min at 25°C, followed by 50 min at 50°C. Terminate the reaction at 85°C for 5 min and allow it to chill on ice. Add 1 µL of RNase H to each tube, and incubate for 20 min at 37°C. The cDNA is then rechecked for concentration using the Nanodrop and then diluted 1:10 for qRT-PCR analysis.

9. TaqMan® primer and probe sets or SYBR Green primers can be designed using the primer express software, version 2.0. Mouse-specific primers for housekeeping genes, Glyceraldehyde 3-phosphate dehydrogenase (GAPDH), Peptidylprolyl isomerase A (PPIA), and β-Actin are commonly used housekeeping genes for subsequent normalization. The design of influenza-specific primers is dependent on the choice of the siRNA target genes, such as nucleocapsid (NP), polymerase (PB1, PB2 or PA), and matrix (M) genes.
10. Plan out 384-well PCR reaction on the template. Thaw SYBR Green Fastmix in the dark. Prepare the master mix in an eppendorf tube with total volume of 10 μL per reaction, multiplied by the number of samples that will be processed for PCR. Combine 5 μL of 2× SYBR green PCR Fastmix, 1 μL of 20× forward and reverse primer mix at a final concentration of 200 nM and 2 μL water. Keep the master mix on ice.
11. Put the 384-well optical reaction plate on ice block. Add 8 μL of reaction cocktail into the bottom of each well. Add 2 μL of cDNA into well that contains reaction cocktail. Put the optical adhesive cover on the plate. Centrifuge briefly to collect components at the bottom of the plate wells (see Note 4).
12. Turn on the Real-Time PCR System. Start the Absolute Quantification software. Follow the menu to choose the right SYBR Green primers to set up plate map and sample numbers and save the document. Place the plate in the plate holder. Make sure A1 position is pointing to the upper left corner and the plate is flat.
13. The samples are run on the Applied Biosystems 7900HT platform using fast cycling conditions. Data is then exported from the SDS 2.3 software using a threshold value of 0.2. These are then formatted for $\Delta\Delta$ C_T analysis using qBASE relative quantification software to calculate the fold decrease in mRNA levels of the treated samples as compared to the untreated, PBS-infected samples.

3.2.3. Rapid Amplification of cDNA Ends (RACE) Assay

To ascertain that siRNA-induced viral gene inhibition is mediated by specific cleavage of target mRNA at the RISC cleavage site, amplification and sequencing of the 5′ end of the cleavage product, exactly ten nucleotides from the 5′ end of the antisense strand, is performed by 5′ RACE assay (Invitrogen) based on manufacturer's instructions.

1. Isolate RNA using Trizol method of total RNA isolation. Homogenize 50–100 mg tissue in 1 mL of Trizol reagent. Use a glass Teflon or a power homogenizer. Sample volume should not exceed 10% of the Trizol volume. Incubate the homogenized samples for 5 min at room temperature (15–30°C).

2. Add 0.2 mL of chloroform per 1 mL of Trizol reagent. Shake the tubes vigorously for 15 s and incubate for 3 min at room temperature.
3. Centrifuge samples at no more than 12,000×*g* for 10 min at 2–8°C.
4. Following the centrifugation, the mixture separates into a lower red phenol-chloroform phase, an interphase, and a colorless upper aqueous phase containing the RNA. The aqueous phase is about 60% of the Trizol volume. Remove the aqueous phase and transfer to another tube.
5. Add 500 μL of isopropanol per 1 mL of Trizol reagent. Centrifuge RNA at 12,000×*g* for 10 min at 2–8°C. Remove the supernatant and wash the RNA pellet extensively with 70% ethanol, then vortex. Centrifuge samples at 7,500×*g* for 5 min at 2–8°C. Allow the RNA pellet to air dry for 5 min and redissolve in 50–100 μL of DEPC-treated water. A DNase treatment is performed following steps 3 and 6 from Subheading 3.2.2.
6. Prepare 1× wash buffer for column purification of cDNA by mixing 1 mL of the wash buffer concentrate with 18 mL of distilled water and 21 mL of absolute ethanol into a 50 mL graduated cylinder. Also prepare 70% ethanol wash by adding 35 mL of absolute ethanol to 15 mL of distilled water. Store in sterile bottle at 4°C.
7. Perform first strand synthesis reaction. To a 0.5 mL thin-walled PCR tube, add 2.5 pmoles (~10–25 ng) gene-specific primer 1 (GSP1) that is homologous to the target gene site about 700–800 nucleotides upstream of the RISC cleavage site, 1–5 μg of total RNA and make up the volume to 15.5 μL. Incubate the mixture at 70°C to denature RNA. Chill for 1 min on ice.
8. To the above mixture, add 2.5 μL of 10× PCR buffer, 2.5 μL of 25 mM $MgCl_2$, and 1 μL of 10 mM dNTP mix. Mix gently, spin down quickly, and incubate for 1 min at 42°C. Add 1 μL of SuperScript II RT enzyme. Mix gently and incubate for another 50 min at 42°C. Incubate at 70°C for 15 min to terminate the reaction. Centrifuge 10–20 s, then place the reaction at 37°C. Add 1 μL of RNase mix, mix gently but thoroughly, and incubate at 37°C. Collect the reaction by brief centrifugation and place on ice.
9. To purify cDNA by S.N.A.P. column purification, equilibrate the binding solution to room temperature. Add 120 μL of binding solution (6 M NaI) to the first-strand reaction. Transfer the cDNA/NaI solution to the S.N.A.P. column. Centrifuge at 13,000×*g* for 20 s. Remove the cartridge insert from the tube and transfer the flow through to a fresh tube.

10. Add 0.4 mL of cold 1× wash buffer to the spin cartridge. Centrifuge at 13,000×*g* for 20 s. Discard the flow through. Repeat this wash step thrice. Wash the cartridge two times with 400 µL of cold 70% ethanol, then spin down at 13,000×*g* for 20 s, and discard flow through. Centrifuge at 13,000×*g* for 1 min. Transfer the spin cartridge insert into a fresh sample recovery tube. Add 50 µL of water preheated to 65°C to the spin cartridge. Centrifuge at 13,000×*g* for 20 s to elute the cDNA.
11. Perform TdT tailing of the cDNA ends by adding 5 µL of 5× tailing buffer, 2.5 µL of 2 mM dCTP to 10 µL of S.N.A.P. purified cDNA sample, and make up the volume to 24 µL with water. Incubate for 2 or 3 min at 94°C. Chill on ice and spin down the tube, to collect the contents at the bottom.
12. Add 1 µL of TdT, mix gently, and incubate for 10 min at 37°C. Inactivate TdT using heat for 10 min at 65°C. Spin down the tube to collect the contents at the bottom and place on ice.
13. Perform PCR amplification of the dC-tailed cDNA in 0.5 mL thin-walled PCR tube by mixing 5 µL of 10× PCR buffer (200 mM Tris–HCl, pH 8.4 and 500 mM KCL), 3 µL of 25 mM $MgCl_2$, 1 µL of 10 mM dNTP mix, 2 µL nested GSP2 primer (prepared as a 10 µM solution), 2 µL of Abridged anchor primer (10 µM) and 5 µL of dC-tailed cDNA, and make up the volume to 49 µL. Lastly, add 0.5 µL of Taq DNA polymerase (5 units/mL) to the above mix. The thermocycler conditions include initial denaturation at 94°C for 1–2 min, followed by 30–35 cycles of denaturation step at 94°C for 1 min, annealing at 55°C for 0.5–1 min, and extension at 72°C for 1–2 min. This is followed by final extension at 72°C for 5–7 min.
14. A single PCR of 25–35 cycles will not generate enough PCR product to be detectable by ethidium bromide staining. To get around this, perform another nested PCR reaction using the AUAP or UAP available in the kit and the custom-nested GSP3 primer.
15. Dilute a 5 µL aliquot of the primary PCR into 495 µL of TE buffer (10 mM Tris–HCl, pH 8.0 and 1 mM EDTA), and perform a second nested PCR reaction using the conditions described for the first PCR reaction. Analyze 5 µL–20 µL of the amplified PCR product using agarose gel electrophoresis. Perform sequencing reaction to confirm the predicted cleavage site on the target mRNA.

3.2.4. Intranasal Delivery of siRNAs in Ferret Model

Influenza virus in humans is an upper respiratory tract virus with respiratory symptoms along with fever, myalgia, and malaise. Ferrets can be infected with human clinical isolates directly

without passages, and are known to produce symptoms and immune responses analogous to humans. Ferrets are considered a more predictive model than mice for human influenza infection.

1. On days –2, –1, 0 (prior to viral challenge), 1 and 2 (post viral challenge), six- to eight- month old ferrets are anesthetized by intramuscular route of administration with ketamine/xylazine/atropine mixture. The mixture is formulated to provide dose levels of 25 mg/kg ketamine, 1.7 mg/kg xylazine, and 0.05 mg/kg of atropine to each animal. Ferrets are then dosed intranasally with 0.5 mL/nostril of the appropriate siRNA or control in the presence or absence of delivery vehicles. The dosing regimen of treatments should be empirically determined for siRNAs based on their efficacy and potency evaluations in the presence or absence of delivery vehicles (see Notes 5, 6 and 7).
2. On day 0, at 4 h post treatment, each ferret is challenged with 0.5 mL/nostril of 10^3–10^5 FID_{50} (Ferret minimum infectious dose 50) for the influenza viral strain, tested previously using the ferret model system (see Note 8). Ferrets are placed on their backs and held by the nape of the neck to allow dosing in a continuous manner. This will also provide minimal sneezing occurrences at the time of intranasal instillation.
3. Ferrets are monitored daily for clinical signs of influenza infection, such as weight loss, reduced activity, nasal discharge, sneezing, coughing, ocular discharge, diarrhea, and inappetance. Body temperatures are recorded twice daily. Temperatures should be measured at approximately the same time throughout the study period post challenge. A scoring system based on Reuman et al. (35) can be used to assess the activity levels in treated and untreated, infected animals: 0, alert and playful; 1, alert but playful only when stimulated; 2, alert but not playful when stimulated.
4. Nasal washes are collected in tubes at days –3, 1, 3, 5, 7, 9, and 11, placed on dry ice and subsequently stored at –80°C for further use. Ferrets are sedated with ketamine (25 mg/kg); then a mixture of 0.5 mL sterile PBS containing 1% bovine serum albumin and penicillin (100 U/mL), streptomycin (100 μg/mL), and gentamicin (50 μg/mL) is injected into each nostril and collected by allowing the animals to sneeze into a petri dish. The collected volume is resuspended in PBS and antibiotics up to 1 mL and clarified by centrifugation.
5. The supernatants are serially diluted (ten-fold dilution) in PBS-antibiotics and inoculated into 10-day-old embryonated chicken eggs in triplicate using 100 μL/egg. The infected eggs are incubated for 24 h at 33°C without CO_2.

6. Viral titers are estimated by determination of HA titers of the allantoic fluid collected from the infected eggs using 0.5% of turkey erythrocytes (RBCs). The 50% endpoint is calculated using the Reed and Muench method (25) from egg dilutions testing positive for HA activity.
7. At day 11, post nasal wash collection, animals are euthanized by intracardiac injection of Euthanasia V solution (1 mL/kg of body weight). When studying the treatment effect of siRNAs against H5N1 virus, infection is typically followed up to day 14 post infection – on days 1, 3, 5, 7, and 14, about three animals are euthanized and tissues from nasal turbinates, lungs, spleen, brain, and other major organs can be collected and frozen on dry ice for viral titer estimation and histopathological analyses.
8. To establish statistical significance for the data, differences in viral titers and weights are processed through Student's *t*-test. General linear remodeling on temperatures collected during the infection period can be evaluated using the SAS software (as mentioned in Materials Subheading 2.7).
9. The resulting decrease in viral replication from the siRNA-treated animals can be assessed by calculating the fold change in viral titers over the untreated, PBS-infected control during the course of viral infection between days 1–11.

3.3. Assessment of Cytokine Response

3.3.1. In Vitro Cytokine Detection

Double-stranded RNA (dsRNA) molecules, shown to be highly immuno-stimulatory, promote inflammatory cytokine production including interferons (IFN-α). To assess whether siRNA induces IFN-α and other cytokine production in vitro, human peripheral mononuclear cells are transfected with siRNAs and assayed for cytokine levels at 24 h post transfection.

3.3.1.1. Isolation and Transfection of Human Peripheral Blood Mononuclear Cells (PBMCs)

Isolation of PBMCs using a Ficoll-HyPaque method involves density-gradient centrifugation to separate lymphocytes from other elements in the blood. The sample is layered onto a Ficoll-sodium metrizoate gradient of specific density; following centrifugation, lymphocytes are collected from the plasma-Ficoll interface.

1. Warm PBS and IMDM medium in 37°C water bath for 15 min.
2. Prepare 10% bleach with tap water.
3. Transfer 50 mL of human blood into T75 flask with 100 mL PBS (without Ca^{+2}, Mg^{+2}) and mix. Set up five 50 mL conical tubes with 15 mL Ficoll per tube.
4. Gently layer the blood-PBS mix (30 mL) on top of Ficoll in a 50 mL tube (use 10 mL pipette; hold tube at an angle when layering blood over the Ficoll to avoid direct mixing of blood with Ficoll).

5. Centrifuge at 800×*g* for 30 min at room temperature without brakes.
6. Collect buffy coat (white thin layer right below the plasma) into two 50 mL conical tubes.
7. Fill each tube to 50 mL with PBS to dilute and wash. Centrifuge at 800×*g* for 10 min at room temperature.
8. After second wash, add 30 mL of Iscove's DMEM (IMDM) with 10% FBS and 1× NEAA.
9. Count cells using a hemacytometer, and seed isolated PBMCs one day prior to the transfection assay.
10. Bleach all Ficoll tubes in 10% bleach for 30 min and dispose accordingly.
11. Cells are plated in triplicate at a density of 200,000 cells per well of flat-bottom 96-well plate in IMDM with 10 % FBS in 100 μL (IMDM Complete Medium also contained 2 mM Glutamine, 100 U/mL penicillin and 100 μg/mL streptomycin and NEAA in addition to 10% FBS).
12. On the following day, cells are transfected by adding 20 μL of complexes (outlined below) directly into the 100 μL of complete DMEM medium on the cells. In all cases, water is placed in outer wells and only inner wells are used for plating cells.
13. Prepare siRNA at 12× concentration in OptiMEM, (10 μL/reaction) for 120 μL final volume for transfection mix (100 μL cells in medium + 10 μL siRNA diluted in OptiMEM + 10 μL RNAiMAX diluted in OptiMEM). Add 0.25 μL/well of RNAiMAX, diluted in 10 μL OptiMEM. Incubate for 5 min at room temperature, prior to adding siRNAs to RNAiMAX. The siRNA/RNAiMAX mixture is incubated for additional 20 min at room temperature prior to adding to cells. 20 μL is then added to each well. After 3 h incubation at 37°C, cells are further supplemented with 100 μL/well of 10% FBS/IMDM for 24 h at 37°C.
14. Harvest the supernatants into a V-bottom 96-well plate and centrifuge at 1,000×*g* for 10 min at room temperature to pellet any debris and cells. Spun supernatants are collected onto a new plate and then frozen at −80°C until ELISA is performed. ELISA is performed using PBL Biomedical Human Interferon-α kit (as mentioned in Materials subheading 2.8) according to manufacturer's instructions.

3.3.1.2. Detection of Human Interferon-α (IFN-α) using ELISA

The human interferon-α assay quantifies human interferon alpha component in the medium using a multiple antibody sandwich immunoassay. Interferon is captured by an antibody bound to the precoated microtiter plate wells. A secondary antibody binds specifically to the bound interferon-α in the samples.

An anti-secondary antibody, conjugated to horseradish peroxidase (HRP) in the presence of tetramethyl benzidine (TMB), allows for a peroxidase-catalyzed colorimetric assay.

1. Prepare wash buffer by diluting 50 mL of the wash solution concentrate to a final volume of 1,000 mL with distilled or deionized water. Mix thoroughly before use. The diluted wash buffer can be stored at 2–25°C.
2. Prepare human IFN-alpha solution by diluting the human interferon-alpha standard in dilution buffer provided at a concentration of 10,000 pg/mL. Construct a high sensitivity standard curve ranging from 12.5–500 pg/mL or extended range standard curve ranging from 156–5,000 pg/mL.
3. Prepare test samples of unknown interferon concentration to be tested using dilution buffer as required. Measurements in duplicate are recommended. Refrigerate until use.
4. Dilute antibody concentrate with dilution buffer. Refer to the lot-specific Certificate of Analysis (COA) for the correct amounts of antibody solution to prepare. Refrigerate until use.
5. Dilute HRP conjugate concentrate with HRP conjugate diluent. Refer to the lot-specific COA for the correct amounts of HRP Solution to prepare. Refrigerate until further use.
6. All incubations should be performed in a closed chamber at 24°C. During all wash steps, remove contents of plate by inverting and blotting the plate on lint-free absorbent paper; tap the plate dry.
7. Add 100 μL per well of the samples, interferon standards, and blanks. Cover and incubate for 1 h at room temperature. Following incubation, empty the contents of the plate by inverting and blotting the plate on lint-free absorbent paper, and wash the wells once with 200 μL of diluted wash buffer.
8. Add 100 μL of diluted anti-interferon-α secondary antibody solution to all wells. Cover and incubate for 1 h. After 1 h, empty the contents of the plate and wash the wells three times with diluted wash buffer.
9. Add 100 μL of diluted HRP conjugated anti-secondary interferon-α antibody solution to all wells. Cover and incubate for 1 h. During this incubation period, warm the TMB substrate solution to room temperature (22–25°C). Empty the contents of the plate and wash the wells four times with diluted wash buffer.
10. Add 100 μL of the TMB substrate solution to each well. Incubate in the dark for 15 min. Do not use a plate sealer during the incubation. After the 15 min incubation of TMB, add 100 μL of stop solution to each well.

11. Using a microplate reader, determine the absorbance at 450 nm within 5 min after the addition of the stop solution. The interferon titers can be determined by plotting the optical densities (OD) using a 4-parameter fit for the standard curve. Blank OD should be subtracted from the standards and sample OD to eliminate background. As the interferon samples are titrated against the international standard, the values from the curves can be determined in units/mL as well as pg/mL. The conversion factor of about 3–5 pg/unit is applicable for human interferon alpha.

3.3.2. In Vivo Cytokine Detection

RNA interference against most of the respiratory viruses has been shown to be influenced by immuno-stimulation, mediated by induction of innate immunity that is triggered by siRNAs. Proinflammatory cytokines with influenza-specific siRNAs are studied in the mouse bronchoalveolar lavage and lungs at various time intervals following intranasal administration of siRNAs.

3.3.2.1. Brochoalveolar Lavage (BAL) Collection

1. Six- to eight-week-old BALB/c mice are administered naked (e.g., PBS formulated) and liposomal-encapsulated siRNAs by intranasal mode of administration in a 50 μL dose volume. Mice are anesthetized using ketamine and xylazine solution via intraperitoneal injection prior to intranasal dosing.
2. At various time points (6 h, 12 h, 24 h, and 48 h) after single siRNA dose, mice are exsanguinated and the thoracic cavity is exposed. The glandular tissue, stylohyoid, and omohyoid muscles are gently resected to expose roughly 5 mm of the trachea.
3. A silk ligature is placed around the upper trachea to prevent the lavage reflux.
4. Use the spring scissors or other very fine-tipped scissor to snip a tiny hole in the trachea, then place luer hub adapter into hole in trachea (in direction to allow flow into lungs) and securely tie off suture around the adapter to keep it in the trachea during the lavage process.
5. The lower part of trachea between the ligature and the lungs is then entered via a 20-gauge, 0.5-inch needle attached to a syringe containing PBS-BSA solution. Slowly fill the lungs with PBS-BSA solution, and then the infusate is aspirated back and deposited into a sterile, ice-cold culture tube. The procedure is repeated until 3–5 mL of lavage fluid is obtained. Lungs could also be harvested at this point for cytokine profiling and stored immediately at -80°C.
6. Lavage fluid should be spun down slowly (500×*g*) for 5–10 min, and supernatant is collected into another tube. Supernatants should be stored frozen at –70°C until further

analysis using ELISA, similar to human interferon ELISA as described in Subheading "Detection of Human Interferon-α (IFN-α) using ELISA" and Procarta™ custom 10-plex cytokine panel, including IL-2, IL-6, IL-10, IL12 p40, IL12 p70, IL-13, IL-1β, TNFα and IFNγ, to enable detection of cytokines in the BAL fluid described in step 2 of Subheading "Detection of Human Interferon-α (IFN-α) using ELISA."

3.3.2.2. Procarta™ Cytokine Profiling Assay

Upregulation of proinflammatory cytokines, T_H1 and T_H2, polarizing response in BAL can be assessed using Procarta's cytokine profile kit, which uses xMAP® technology (multi-analyte profiling beads) to detect multiple cytokines in a 96-well format. The xMAP system combines a flow cytometer, fluorescent-dyed microspheres (beads), lasers and digital signal processing to multiplex proteins within a single sample.

1. Prepare 1× wash buffer by mixing 20 mL of the 10× wash buffer with 180 mL of deionized water. Reconstitute the premixed standard in 250 μL of buffer. Vortex gently for 10 s and incubate on ice for 5 min. Prepare serial dilutions of the premixed standard ranging from 2 pg/mL to 20 ng/mL.
2. Mark the standard and sample wells prior to use. Pre-wet the filter plate on the filter plate holder. Add 150 μL of reading buffer to each non-sealed well. Incubate for 5 min at room temperature and discard with vacuum filtration.
3. Vortex the premixed antibody beads for 30 s at room temperature. Add 50 μL of antibody beads to each unsealed well. Remove buffer with vacuum filtration.
4. Wash beads with 150 μL/well of 1× wash buffer and remove with vacuum filtration. Blot the bottom of the Filter Plate thoroughly with paper towels to remove residual buffer.
5. Add 25 μL/well of standards and samples to the appropriate wells with 25 μL of assay buffer. Seal the plate gently, and incubate with shaking for 30 min on a plate shaker at room temperature.
6. Use a multi-channel pipette and a plastic reservoir that is large enough for washing the plate three times.
7. Add 25 μL/well of the detection antibody. Seal the Filter Plate with a new Plate Seal. Shake for another 30 min on the plate shaker at room temperature. Wash the plate again three times.
8. Add 50 μL/well of streptavidin-PE and seal the plate. Incubate with shaking for 30 min on the plate shaker at room temperature. Remove the solution with vacuum filtration and wash the plate. Add 120 μL/well of the reading buffer. Shake for additional 5 min at room temperature before

analyzing on the Luminex instrument that has been calibrated appropriately. Standard curves of known concentration of all cytokines are then computed, and data from the unknown samples with the ten cytokines can be displayed in graphic or tabular format.

9. The cytokine induction can be assessed by calculating a fold change in the cytokine levels in BAL fluid of siRNA-treated animals over cytokines in BAL fluid of the untreated, PBS-control group.

4. Notes

1. Excessive administration of liquids during intranasal mode of instillation can cause severe damage to the mouse lungs and subsequently death. Volumes should be restricted between 50 and 100 μL.
2. General handling of RNA to prevent RNase contamination requires the use of disposable, individually wrapped, sterile plastic ware and only sterile, new pipette tips and micro centrifuge tubes. Wear gloves while handling reagents and RNA samples to prevent RNase contamination from the surface of the skin. Always use proper microbiological aseptic techniques when working with RNA. Use RNase *AWAY*® Reagent (as mentioned in Materials section 2.5) to remove RNase contamination from work surfaces.
3. Complete RNA procedure once started. Do not store the lysate in RNA lysis solution at −80°C, as it will adversely affect the quality of RNA.
4. After dispensing the sample mix into a 384-well plate for real-time PCR, centrifuge the plate at 600 g for 5 min to get rid of air bubbles.
5. Acclimatization of ferrets into ABSL-2 (animal biosafety level 2) should be done three to four days prior to the initiation of the study.
6. Ensure the ferrets that are used in influenza challenge experiments are serologically negative by performing hemagglutination inhibition assay for currently circulating seasonal influenza A or B viruses. Ferrets with hemagglutination inhibition titers (HAI) of >10 should be removed from the experimental analysis.
7. For ferret temperature measurements, either temperature monitors can be implanted subcutaneously into the animals or rectal thermometers can be used.

8. The ferret infectious dose 50 (FID_{50}) for each virus can be determined by intranasal infection of three ferrets each with 10^4, 10^3, and 10^2 and 10^1 EID_{50} (Egg Infectious Dose 50) of virus. Nasal washes are collected on day 3 post infection, and titrated in eggs to detect the infectious virus associated with the viral dose. Animals with nasal wash titers of $\geq 10^2$ EID_{50}/mL are considered positive for virus. The FID_{50} is then calculated by using the Reed and Muench method (25).
9. Measuring the fold change decrease in viral replication in ferrets during the peak viral titer days (days 3 to 5 post infection) provides significant information on the treatment potential of siRNAs in the presence or absence of a delivery vehicle.

References

1. Zeitlin, G. A., and Maslow, M. J. (2006) Avian influenza. *Curr. Allergy Asthma Rep.* **6**, 163–170.
2. McSwiggen, J. A., and Seth, S. (2008) A potential treatment for pandemic influenza using siRNAs targeting conserved regions of influenza A. *Expert Opin. Biol. Ther.* **8**, 299–313.
3. Hannon, G. J., and Rossi, J. J. (2004) Unlocking the potential of the human genome with RNA interference. *Nature* **431**, 371–378.
4. Mello, C. C., and Conte, D. (2004) Revealing the world of RNA interference. *Nature* **431**, 338–342.
5. Meister, G., and Tuschl, T. (2004) Mechanisms of gene silencing by double-stranded RNA. *Nature* **431**, 343–349.
6. Filipowicz, W., Jaskiewicz, L., Kolb, F. A., and Pillai, R. S. (2005) Post-transcriptional gene silencing by siRNAs and miRNAs. *Curr. Opin. Struct. Biol.* **15**, 331–341.
7. Ge, Q., McManus, M. T., Nguyen, T., Shen, C. H., Sharp, P. A., Eisen, H. N., and Chen, J. (2003) RNA interference of influenza virus production by directly targeting mRNA for degradation and indirectly inhibiting all viral RNA transcription. *Proc. Natl. Acad. Sci. U. S. A.* **100**, 2718–2723.
8. Ge, Q., Filip, L., Bai, A., Nguyen, T., Eisen, H. N., and Chen, J. (2004) Inhibition of influenza virus production in virus-infected mice by RNA interference. *Proc. Natl. Acad. Sci. U. S. A.* **101**, 8676–8681.
9. Ge, Q., Eisen, H. N., and Chen, J. (2004) Use of siRNAs to prevent and treat influenza virus infection. *Virus Res.* **102**, 37–42.
10. Tompkins, S. M., Lo, C.-Y., Tumpey, T. M., and Epstein, S. L. (2004) Protection against lethal influenza virus challenge by RNA interference in vivo. *Proc. Natl. Acad. Sci. U. S. A.* **101**, 8682–8686.
11. Thomas, M., Ge, Q., Lu, J. J., Klibanov, A. M., and Chen, J. (2005) Polycation-mediated delivery of siRNAs for prophylaxis and treatment of influenza virus infection. *Expert Opin. Biol. Ther.* **5**, 495–505.
12. Zhou, H., Jin, M., Yu, Z., Xu, X., Peng, Y., Wu, H., et al. (2007) Effective small interfering RNAs targeting matrix and nucleocapsid protein gene inhibit influenza A virus replication in cells and mice. *Antiviral Res.* **76**, 186–193.
13. Reynolds, A., Anderson, E. M., Vermeulen, A., Fedorov, Y., Robinson, K., Leake, D., Karpilow, J., Marshall, W. S., and Khvorova, A. (2006) Induction of the interferon response by siRNA is cell type- and duplex length-dependent. *RNA* **12**, 988–993.
14. Judge, A. D., Sood, V., Shaw, J. R., Fang, D., McClintock, K., and MacLachlan, I. (2005) Sequence-dependent stimulation of the mammalian innate immune response by synthetic siRNA. *Nat. Biotechnol.* **23**, 457–462.
15. Judge, A., and MacLachlan, I. (2008) Overcoming the innate immune response to small interfering RNA. *Hum. Gene Ther.* **19**, 111–124.
16. Chiu, Y. L., and Rana, T. M. (2003) siRNA function in RNAi: a chemical modification analysis. *RNA* **9**, 1034–1048.
17. Czauderna, F., Fechtner, M., Dames, S., Aygun, H., Klippel, A., Pronk, G. J., Giese, K., and Kaufmann, J. (2003) Structural variations and stabilising modifications of synthetic

siRNAs in mammalian cells. *Nucleic Acids Res.* **31**, 2705–2716.

18. Amarzguioui, M., Holen, T., Babaie, E., and Prydz, H. (2003) Tolerance for mutations and chemical modifications in a siRNA. *Nucleic Acids Res.* **31**, 589–595.
19. Khvorova, A., Reynolds, A., and Jayasena, S. D. (2003) Functional siRNAs and miRNAs exhibit strand bias. [Erratum to document cited in CA139:376163]. *Cell (Cambridge, MA, United States)* **115**, 505.
20. Reynolds, A., Leake, D., Boese, Q., Scaringe, S., Marshall, W. S., and Khvorova, A. (2004) Rational siRNA design for RNA interference. *Nat. Biotechnol.* **22**, 326–330.
21. Ladunga, I. (2007) More complete gene silencing by fewer siRNAs: transparent optimized design and biophysical signature. *Nucleic Acids Res.* **35**, 433–440.
22. Katoh, T., and Suzuki, T. (2007) Specific residues at every third position of siRNA shape its efficient RNAi activity. *Nucleic Acids Res.* **35**, e27.
23. Pei, Y., and Tuschl, T. (2006) On the art of identifying effective and specific siRNAs. *Nat. Methods* **3**, 670–676.
24. Ui-Tei, K., Naito, Y., and Saigo, K. (2006) Essential Notes Regarding the Design of Functional siRNAs for Efficient Mammalian RNAi. *J.Biomed. Biotechnol.* **2006**, 65052.
25. Reed, L. J., and Muench, H. (1938) A simple method of estimating fifty percent endpoints. *Am. J. Hyg.* **27**, 493–497.
26. Behlke, M. A. (2006) Progress towards in Vivo Use of siRNAs. *Mol. Ther.* **13**, 644–670.
27. Li, W., and Szoka, F. C., Jr. (2007) Lipid-based Nanoparticles for Nucleic Acid Delivery. *Pharm. Res.* **24**, 438–449.
28. Aigner, A. (2006) Delivery systems for the direct application of siRNAs to induce RNA interference (RNAi) in vivo. *J. Biomed. Biotechnol.* **2006**, 71659.
29. Ren, T., Song, Y. K., Zhang, G., and Liu, D. (2000) Structural basis of DOTMA for its high intravenous transfection activity in mouse. *Gene Ther.* **7**, 764–768.
30. Spagnou, S., Miller, A. D., and Keller, M. (2004) Lipidic carriers of siRNA: differences in the formulation, cellular uptake, and delivery with plasmid DNA. *Biochemistry (Mosc.)* **43**, 13348–13356.
31. Templeton, N. S., Lasic, D. D., Frederik, P. M., Strey, H. H., Roberts, D. D., and Pavlakis, G. N. (1997) Improved DNA: liposome complexes for increased systemic delivery and gene expression. *Nat. Biotechnol.* **15**, 647-652.
32. Thomas, M., Lu, J. J., Ge, Q., Zhang, C., Chen, J., and Klibanov, A. M. (2005) Full deacylation of polyethylenimine dramatically boosts its gene delivery efficiency and specificity to mouse lung. *Proc. Natl. Acad. Sci. U. S. A.* **102**, 5679–5684.
33. Kichler, A., Chillon, M., Leborgne, C., Danos, O., and Frisch, B. (2002) Intranasal gene delivery with a polyethylenimine-PEG conjugate. *J. Control Release* **81**, 379–388.
34. Howard, K. A., Rahbek, U. L., Liu, X., Damgaard, C. K., Glud, S. Z., Andersen, M. O., et al. (2006) RNA interference in vitro and in vivo using a novel chitosan/siRNA nanoparticle system. *Mol. Ther.* **14**, 476–484.
35. Reuman, P. D., Keely, S., and Schiff, G. M. (1989) Assessment of signs of influenza illness in the ferret model. *J. Virol. Methods* **24**, 27–34.

Chapter 27

Evaluation of Targets for Ovarian Cancer Gene Silencing Therapy: In Vitro and In Vivo Approaches

Anastasia Malek and Oleg Tchernitsa

Abstract

Ovarian cancer is the most lethal neoplasm of the female genital tract. Despite progress with chemotherapy, surgery and supportive care, the death rate remains extremely high. Gene silencing therapy represents a possible opportunity to advance the management of ovarian cancer patients. The concept of gene silencing therapy, which is based on RNA interference (RNAi) phenomenon, requires selection of targeted genes and development of a strategy for genetic drug development. Recently, plenty of research studies in ovarian cancer genetics have been published. Although they can be analyzed regarding candidate gene selection, the therapeutic effect of particular gene silencing can only be evaluated experimentally at this time. Obviously, the correct choice and application of a genetic drug delivery system determines the efficacy of gene silencing. Complexation of therapeutic nucleic acids with cationic polymers, cationic lipids, or their combination, represents a main strategy of non-virus-mediated delivery of genetic drug. Owing to a tendency of ovarian cancer to spread through the abdominal cavity, a delivery system should allow intraperitoneal mode of administration. Therefore, clinical application of RNAi may rely on a combination of biosciences and nanotechnology: in particular, identifying optimal small interfering RNAs (siRNAs) against optimal target genes and developing an efficient system for siRNA delivery into the cancer cells.

Key words: Ovarian cancer, Gene silencing therapy, RNA interference, Polymer-based siRNA delivery, Intraperitoneal drug administration

1. Introduction

Epithelial ovarian cancer is one of the leading causes of cancer deaths in women due to difficulties in both diagnostics and therapy (2). The molecular mechanisms that are responsible for the initiation and progression of the sporadic malignant transformation in ovarian surface epithelium remain elusive. It makes the search of potential targets for gene silencing therapy in part empirical. The genes, which can be considered as a therapeutic target, share sev-

Wei-Ping Min and Thomas Ichim (eds.), *RNA Interference*, Methods in Molecular Biology, vol. 623,
DOI 10.1007/978-1-60761-588-0_27, © Springer Science+Business Media, LLC 2010

eral characteristics. They should be upregulated in cancer cells in comparison to normal counterparts. Their expression should be able to maintain the malignant phenotype and/or ensure tumor cell survival. Importantly, the role of optimal targets should not be essential for the functionality of normal cells. Ideally, the mechanism behind the biological effect of the therapeutic gene targeting should be known. Potential targets can be pre-selected on the basis of published data analysis, and then they must be evaluated experimentally. Established ovarian cancer cell lines, as well as primary cell lines, can serve as a model for this approach.

As the phenomenon of RNAi is still under investigation, the selection of an optimal-targeted site in messenger RNA (mRNA) molecules and the design of an efficient siRNA duplex are again partially experiential (1). Various web-available software and some common rules (3) can be used to select siRNAs that are most likely efficient. Some companies guarantee the efficiency of pre-designed siRNAs or even offer siRNAs with validated silencing efficiency. However, the efficiency of gene-specific knockdown must be verified for any duplex after transient transfection of specific cells, and the optimal siRNA sequence can be selected for further experiments. A cocktail of various siRNA duplexes, or so-called esi RNA, targeting together a large region of mRNA molecules, can serve as a robust positive control of gene knockdown efficacy; however, such a mixture cannot guarantee the absence of off-target effects. Usually, a direct comparison of gene-silencing efficacy among three or four siRNA duplexes allows selection of the optimal one. Finally, the specific character of selected siRNA action must be confirmed by control transfection using scrambled duplex. Since optimal siRNA sequence and the effect of transient gene silencing are validated, hairpin-based, knockdown constructs can be designed on the basis of the selected sequence, and then used for stable silencing. The design of hairpin can be done according to published recommendations (4, 5). Subsequent transfection, selection of stably transfected cell population, control of knockdown efficiency and specificity represent well established procedures. Finally, cell proliferation assays, cell cycle analysis or estimation of apoptosis rate can be applied to validate the effect of targeted gene silencing.

In vivo application of RNAi-based gene silencing technique requires development of a xenograft model of ovarian cancer that is distributed intraperitoneally (i.p.). Since this procedure is not trivial, a pilot experiment for i.p. tumor cell implantation is recommended prior to starting the main study. Some established ovarian cancer cell lines are capable of growing and disseminating in the abdominal cavity of nude mice. Other less aggressive cell lines might require using mice with strongly affected immunity or adding a supplemented substance to facilitate implantation. The regimen and duration of treatment by gene targeting construct is determined by dynamics of tumor progression and toxicity rate of the transfection

reagent. Therapeutic effect is reflected by i.p. tumor mass and ascites volume, whereas gene silencing efficacy can be validated by the assessment of specific mRNA level in tumor tissue.

2. Materials

2.1. Cell Cultures

1. Dulbecco's Modified Eagle's Medium (Cambrex, Walkersville, MD) supplemented with 10% fetal calf serum, 2 mM glutamine and antibiotics (for ovarian carcinoma cell lines Skov-3, A27/80, Ovcar-3, CAOV-3, OAW-42).
2. Mixture 1:1 of medium 199 (Sigma, Deisenhofen, Germany) and MCDB105 (Life Technologies, Karlsruhe, Germany) supplemented with 10% fetal calf serum, 2 mM glutamine and antibiotics (for human ovarian surface epithelial cells HOSE).
3. Phosphate-buffered saline PBS (×10): 2.3 g NaH_2PO_4, 11.5 g Na_2HPO_4, 87.5 g NaCl, water up to 1 L. Store at room temperature.

2.2. RT-PCR

1. Trizol Reagent (Invitrogen GmbH, Karlsruhe, Germany).
2. One-Step Reverse Transcription-PCR System (Roche Diagnostics GmbH, Mannheim, Germany).
3. *HMGA2* specific primers for conventional RT-PCR: 5′-TGGGAGGAGCGAAATCTAAA-3′ and 5′-AAGCACC-TTGGTCAACCATC-3′.
4. *beta-actin* specific primers for conventional RT-PCR: 5′-TGAAGATCAAGATCATTGCTCC-3′ and 5′-GCCATG-CCAATCTCATCTTG-3′.
5. Reverse Transcriptase AMV (Roche Applied Science GmbH, Mannheim, Germany).
6. Real-Time SYBR Green PCR system (Qiagen GmbH, Hilden, Germany).
7. *HMGA2* specific primers for real-time PCR: 5′-TCCCTCTAAA-GCAGCTCAAAA-3′ and 5′-ACTTGTTGTGGCCATTTCCT-3′.
8. *beta-actin* specific primers for real-time PCR: 5′-TCCCTCTAAA-GCAGCTCAAAA-3′ and 5′-CCAACCGCGAGAAGATGA-3′

"3" and "4" are primers for conventional PCR, whereas "7" and "8" are primers for quantitative real-time PCR, designed with help of UniversalProbeLibrary software from Roche (www.roche-applied-scince .com) so that forward and reverse primers are annealed on both side of mRNA splicing site and length of amplicon is about 90-120 b.p.

2.3. Western Blot

1. Lysis buffer: 10 mM Hepes (pH 7.9), 400 mM NaCl, 0.1 mM EGTA, 5% glycerol, 0.5 mM DTT, 0.5 mM PMSF. Perform fresh.
2. SDS-Polyacrylamide accumulative gel: 4% Acrylamid (29/1), 0.125 M Tris–HCl (pH 6.8), 0.5% SDS, 0.25% APS, 0.01% TEMED.
3. SDS-Polyacrylamide separating gel: 15% Acrylamid (29/1), 0.375 M Tris–HCl (pH 8.8), 0.5% SDS, 0.25% APS, 0.01% TEMED.
4. Running buffer (5×): 15.1 g Tris-base, 72 g Glycin , 25 ml 20% SDS water up to 1 L. Store at room temperature.
5. Blotting buffer (2.5×): 14.525 g Tris-base, 7.325 g Glycin, 4.65 ml 20% SDS, 500 ml Methanol, water up to 1 L. Store at room temperature.
6. TBST buffer: 8.8 g NaCl, 0.2 g KCl, 3 g Tris-base, 500 µl Tween-20, water up to 1 L, pH 7.4. Store at room temperature.
7. Polyclonal mice antibody against human *HMGA2* (Eurogentec, Seraing, Belgium).
8. Polyclonal mice antibody against human *beta-actin* (Chemicon, Temecula, CA, USA).
9. Horseradish peroxidase (HRP) conjugated anti-mouse antibody (eBioscience, San Diego, USA).
10. Blots development ECL system (AmershamPharmacia, Buckingshamshire, UK).
11. Western Blot recycling kit (Alpha Diagnostics, San Antonio, TX, USA).

2.4. Transient HMGA2 Gene Silencing In Vitro

1. siRNA1: 5′-GGCACTTTCAATCTCAATC-3′, siRNA2: 5′-CAGGAAGCAGCAGCAAGAA-3′, siRNA3: 5′-CGCCAA-CGTTCGATTTCTA-3′ and siRNA4: 5′-GATGGTTGACC-AAGGTGCT-3′, SiRNA3 scrambled duplexes 5′-CGCCA (tgca)TC(ttag)TCTA-3′. Sense sequences are shown.
2. Silencer™ siRNA Construction Kit (Ambion Inc, Austin, USA).
3. X-tremeGENE si RNA Dicer Kit (Roche Diagnostics GmbH, Mannheim, Germany).
4. Oligofectamine Reagent (Invitrogen GmbH, Karlsruhe, Germany).
5. Serum-free OptiMEM (Invitrogen GmbH, Karlsruhe, Germany).

2.5. Stable HMGA2 Gene Silencing In Vitro

1. Sh-insert sequence (sense): 5′-GAATTCGCTGTTGACA-GTGAGCG (GCGTCAACGTTCGATTTCTGCC) TAGT-GAAGCCACAGATGTA (GGTAGAAATCGAACGTTGGCGC) TGCCTACTGCCTCGGAGAATTC-3′. Scrambled Sh-insert sequence: 5′-GAATTCGCTGTTGACAGTGAGCG (GCGTCA

(tgca)TC(ttag)TCTGCC)TAGTGAAGCCACAGATGTA (GGTAGA(ctaa)GA(tgca)TGGCGC)TGCCTACTGCCTC-GGAGAATTC-3′. Gene targeting sequences are in parenthesis, EcoRI restriction sites are underlined.

2. pSM2 expression vector (Open Biosystems, Huntsville, USA).
3. PirPlus™ competent cells (Open Biosystems, Huntsville, USA).
4. Bacterial selection markers: 25 μg/ml chloramphenicol, 25 μg/ml kanamycin.
5. Arrest-In transfection reagent (Open Biosystems, Huntsville, USA).
6. Mammalian selectable marker: Puromycin 2.5 μg/ml.
7. QIAfilter Plasmid Kits (QIAGEN GmbH, Hilden, Germany).

2.6. Estimation of HMGA2 Silencing Effect In Vivo

1. Sodium 3′ (1-(phenyl-amino-carbonyl)-3,4-tetrazolium)-bis (4-methoxy-6-nitro)-benzenesulfonic acid hydrate (XTT)-based colorimetric assay (Roche Diagnostics GmbH, Mannheim, Germany).
2. Plates that are preliminarily coated with poly-2-hydroxyethyl methacrylate (Poly-HEMA) (Sigma, Deisenhofen, Germany). Poly-HEMA is dissolved in 96% ethanol (5 mg/ml) overnight at room temperature, pipetted 100 μl/well into 96-well plates and dried during 3 days at 37°C. Prepared plates can be stored up to 3 months at sterile conditions.
3. Phosphate-buffered saline (PBS 1×), 70% ethanol, DNase-free RNase A (Roche Diagnostics GmbH, Mannheim, Germany),
4. Propidium iodide (PI) (Sigma, Deisenhofen, Germany).
5. Incubation buffer: 10 mM Hepes/NaOH, pH 7.4, 140 mM NaCl, 5 mM CaCl2.
6. Annexin-V-Fluos (Roche Diagnostics GmbH, Mannheim, Germany).

2.7. Estimation of HMGA2 Silencing Effect In Vivo

1. Crl:CD-1 –Foxn1^{NU} mice (Charles River Laboratory, Sulzfeld, Germany).
2. Jet-PEI in vivo (Polyplus-transfection SA, Illkirch, France).

3. Methods

Recently, a number of gene-profiling studies of ovarian cancer have been done, and a huge amount of data is available for the analysis and selection of potential candidates for gene silencing therapy. In our previous work, we have discovered the over-expression of gene coding nuclear factor, *HMGA2,* as a result of Ras-induced

transformation of rat ovarian surface epithelial cells (6). Later, genome-wide investigations revealed upregulation of *HMGA2* gene in primary human ovarian cancer (7, 8). The *HMGA2* gene is not detectable in adult human tissues where it is probably completely silenced (9, 10). Re-expression of *HMGA2* gene can be observed in many human malignancies, such as breast cancer (11), non-small lung cancer (12), pancreatic carcinoma (13), retinoblastoma (14), squamous cell carcinoma (15) as well as myeloproliferative disorders (16). Although the precise role of *HMGA2* in malignant transformation is still not fully understood, it has been shown to be essential for cancer progression in several studies (17, 18). On the basis of this data, *HMGA2* gene has been selected as a potential target for gene silencing therapy in ovarian cancer. In order to confirm this suggestion, we had to select an appropriate ovarian cancer cell line, develop a method for stable, efficient and specific silencing of *HMGA2* gene, estimate the effect of *HMGA2* gene silencing on cancer cell growth in vitro and, finally, validate the therapeutic outcome in a xenograft model of advanced ovarian cancer.

3.1. Analysis of Initial Activity of Target-Gene in Ovarian Cancer and Immortalized Ovarian Surface Epithelial Cell Lines

1. Cells are seeded in a 6-well plate and grown to 80% confluence.
2. In order to estimate the level of *HMGA2* gene expression, cells are washed twice with cool PBS, total RNA is isolated by Trizol-based method, and One-Step Reverse Transcription-PCR is performed according to the manufacturer's protocol. PCR products can be visualized by electrophoresis in Et.Br containing 1% agarose gel (see Note 1). Considerably, different levels of *HMGA2* gene expression in different types of ovarian cancer cell lines can be evaluated. The level of *HMGA2* gene expression in HOSE cell line is undetectable (Fig. 1a).
3. In order to estimate the level of *HMGA2* protein expression, cells are washed with PBS, twice frozen/thawed (−80°/+4°C)

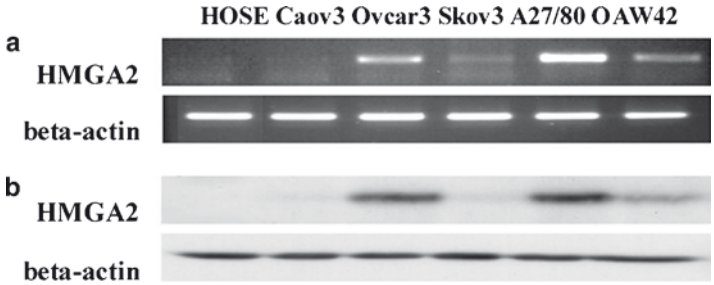

Fig. 1. *HMGA2* gene/protein expression in ovarian cancer and HOSE cell lines. (**a**) RT-PCR; control of RNA amount is performed in parallel reaction with beta actin specific primers. (**b**) Western blot analysis; loading control is performed with actin specific antibodies. Reprinted from ref. 19

and, afterwards, treated with lysis buffer for 5–10 min at 4°C (see Note 2). Protein extracts are separated by electrophoresis in SDS-PAAG, and transferred into the polyvinyl membrane. The membrane should be blocked for 1 h in 5% non-fat dry milk in TBST buffer and incubated overnight at 4°C with anti-*HMGA2* antibody (diluted in fresh TBST 1:1,000). Then, the membrane is washed again in TBST (20 min, thrice) and incubated with secondary anti-mouse antibodies for 1 h (diluted in fresh TBST 1:10,000). After a brief wash in fresh TBST buffer (5 min, twice), results can be estimated with blot development ECL system (see Note 3). Once the level of *HMGA2* protein expression is evaluated, blots are stripped and re-probed with anti-beta actin antibodies to confirm equal protein loading. The difference in *HMGA2* protein expression between tested cell lines confirms the results of RT-PCR assay (Fig. 1b).

3.2. Selection of Optimal siRNA Duplex and Validation of Temporal Silencing Efficiency

1. Sequences of *HMGA2*-targeting siRNAs are designed with the help of "siRNA target finder" software available on Applied Biosystems Website (see Note 4). Finally, four duplexes for targeting *HMGA2* mRNA in the following sites: siRNA1 (233–251), siRNA2 (709–725), siRNA3 (1146–1164), and siRNA4 (2298–2316) are produced by in vitro transcription and purified according to the kit producer's manual.
2. For the design of *HMGA2*-targeting esiRNA (RZPDp-3000D027D), a freely available tool from RZPD (Deutsches Ressourcenzentrum für Genomforschung GmbH, Berlin, Germany) web site is used. Double-stranded DNA 311 b.p., complemented to 3754–4064 region of human *HMGA2* mRNA and tailed by strong T7 promoters at either end, is used for in vitro transcription of dsRNA, following generation and purification of diced esiRNA duplexes according to the manufacturer's manual.
3. Ovarian cancer cell line over-expressing *HMGA2* gene (Ovcar-3) is seeded in a 6-well plate and grown to 30% confluence. Transfection by single duplex or mix of diced siRNA is carried out in serum-free OptiMEM medium using Oligofectamine Reagent, according to the manufacturer. The final concentration of siRNA is 0.1 μM, time of transfection is 4 h; after that, FCS is added into the medium to a final concentration of 10%. Cells treated in parallel with any scramble duplex can be used as negative control (see Note 5). 72 h after transfection, cells are harvested and the level of *HMGA2* mRNA is evaluated. This experiment reveals the optimal sequence of *HMGA2*-targeting duplexes: siRNA3 (Fig. 2a).
4. To evaluate the temporal profile of gene silencing, transient transfection with optimal duplex and cell harvesting (24, 48,

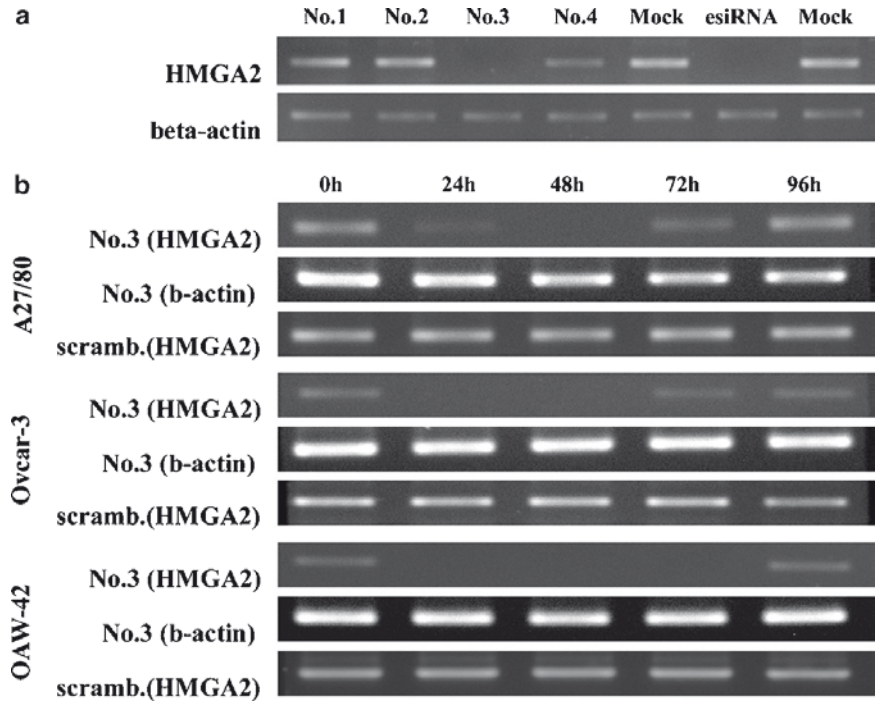

Fig. 2. Transient silencing of *HMGA2* gene. (**a**) RT-PCR analysis of silencing efficiency in Ovcar-3 cells 72 h after transfection by duplexes: siRNA1, siRNA2, siRNA3, siRNA4, and cocktail of different 21–23-base esiRNA (esiRNA) duplexes. Control RT-PCR is performed for cells treated by transfection reagents alone (Mock), for mono-duplex as well as for poly-duplex transfection, respectively. Parallel RT-PCR reactions are performed with beta-actin specific primers. (**b**) RT-PCR analysis of transient silencing of *HMGA2* using siRNA3 in A27/80, Ovcar-3 and OAW-42 cell lines at 0, 24, 49, 72, and 96 h after transfection. Level of beta-actin mRNA expression in transfected cells is controlled in parallel reactions. Transfection with scrambled duplex does not change the level of *HMGA2* mRNA expression. Reprinted from ref. 19

72, and 96 h after transfection) are carried out. Estimation of *HMGA2* mRNA level at these time points reveals a period of optimal gene knockdown: 24–72 h after transfection for all studied cells (Fig. 2b). Transfection with a scrambled duplex confirms the specific character of gene silencing. Effect of *HMGA2* gene silencing on the proliferation of ovarian cancer cells can be validated by treating with optimal duplex (siRNA3) and performing cell proliferation assay during the period of maximal gene silencing. Cells are grown in a 6-well plate until they reach 60–70% confluence, then transfected with siRNA3 as described above. After 24 h, they are split again and seeded into 96-well plates (1,000 cell/well). A parallel experiment with scrambled duplex should be performed to control transfection specificity. For evaluation of the anchorage-independent cell proliferation, 96-well plates should be preliminarily coated with Poly-HEMA. Cell proliferation is monitored semi-quantitatively using

XTT-based colorimetric assay 48 h after transfection (see Note 6). The growth-suppression effect of transient *HMGA2* gene silencing is observed in tested cell lines to various extents, which correlated with the initial level of targeted gene expression (not shown) (19).

3.3. Stable HMGA2 Gene Silencing In Vitro

1. The short hairpin RNA (shRNA) has to be designed to target the same site as the siRNA3 duplex of mRNA molecule. The sequence of insert includes sense and antisense siRNA strands on opposite direction, separated by loop sequence and tailed by mir-30 structures and EcoRI restriction sites. After synthesis, annealing, and purification, 108 b.p. double-strand fragment is cloned into the pSM2 expression vector under control of Pol III U6 promoter (see Note 7). Efficiently-transfected clones are selected for kanamycin//25 mg/ml + chloramphenocol//25 mg/ml resistance in PirPlus™ chemically competent *E. coli*, and cloning correctness is evaluated by conventional sequencing.
2. Selected clone of PirPlus™ *E. coli* is propagated, and a sufficient amount of plasmid DNA is purified by any appropriate kit. Aliquots of bacterial culture have to be quickly frozen in liquid nitrogen in the presence of 7% DMSO and saved for next experiments.
3. Cells are seeded in a 6-well plate and grown to 50% confluence. Transfection by shRNA expression plasmid is carried out in serum-free OptiMEM using Arrest-In transfection reagent. Preparation of transfection mix is done according to producer's manual, and the transfection procedure is described above. Stable transfectants are selected for puromycin// 2.5 mg/ml resistance.
4. Gene silencing efficacy has to be confirmed on the mRNA and protein level, as described above.
5. The effect of stable, specific gene silencing in ovarian cancer cell lines can be evaluated by cell proliferation (XTT) assay as described above. Cell cycle analysis and apoptosis rate estimation can be performed according to conventional techniques. Annexin-V staining and PI incorporation are measured using a logarithmic amplification in the FL1-H channel for Fluorescein detection (515 nm) and FL3-H channel for PI fluorescence detection (623 nm). Stable silencing of the *HMGA2* gene results in the inhibition of cancer cell growth, G1 arrest, reduction in cell number in the S-phase of cell cycle, and an increase in the apoptosis rate (not shown) (19).

3.4. Stable HMGA2 Gene Silencing In Vivo

1. To validate *HMGA2* gene knockdown efficiency in vivo, subcutaneous tumor xenografts in athymic nude mice must be generated: Ovcar-3 ovarian carcinoma cells (3 million cells in 150 µl of PBS) are injected subcutaneously into both flanks. Usually, two weeks after injection, mice bear solid growing tumors about 5–7 mm in diameter (see Note 8).
2. In order to validate the therapeutic effect of *HMGA2* gene silencing, an intraperitoneal xenograft model is generated by i.p. injection of Ovcar-3 cells (10 million cells in 500 µl of PBS).
3. Transformed and frozen previously, PirPlus™ Competent *E. coli* are used to produce a sufficient amount of sh-RNA3-expressiong vector. Plasmid DNA purification can be performed by QIA filter Plasmid Kits.
4. Mice bearing s.c. tumors can be treated with shRNA expression plasmid or control plasmid at a dose ranging from 30 to 100 µg, formulated with jet-PEI and injected intraperitoneally. Using two doses is recommended to reveal a correlation between an applied dose and gene silencing efficacy and/or therapeutic effects. Mice, bearing i.p. tumors can be treated with low dose (30 µg per injection) because intraperitoneal mode of drug delivery (which can be considered local) requires a decreased amount of drug (see Note 9).
5. Treatment (in both s.c. and i.p. models) begins 2 weeks after tumor cell inoculation. Plasmid DNA (sh-RNA3-expression vector) is complexed *ex tempore* with low molecular weight polyethylenimine jet-PEI, according to the manufacturer's protocol. Complex formation is carried out at N/P ratio 10 (on the basis of PEI Nitrogen: 43.1 Da/Nitrogen per nucleic acid Phosphate: 340 Da/Phosphate). Amount of polymers can be calculated in relation to DNA dose. DNA and PEI are diluted separately, mixed and allowed to equilibrate 1 h at room temperature. The mixture is injected intraperitoneally as a bolus of 600 µl once per week for 1 month (4 injections).
6. Animals bearing s.c. tumors can be harvested when the difference in tumor size becomes considerable between the treated and control groups. Tumor tissues are collected, total RNA is extracted, reverse transcribed and used for the estimation of gene silencing efficacy by conventional real-time PCR. The level of *HMGA2* mRNA is shown to decrease to 60% in tumors of treated mice compared to control mice. This result allows consideration of *HMGA2* gene silencing as a causal factor of observed s.c. tumor growth suppression (Fig. 3).
7. Animals bearing i.p. tumors are harvested when abdominal volumes of control mice increase considerably. Tumor tissues are collected, weighed and, if possible, also used for estimating gene knockdown efficiency. A significant decrease of abdominal tumor mass, as well as efficient *HMGA2* gene silencing, was observed as a result of treatment (Fig. 4).

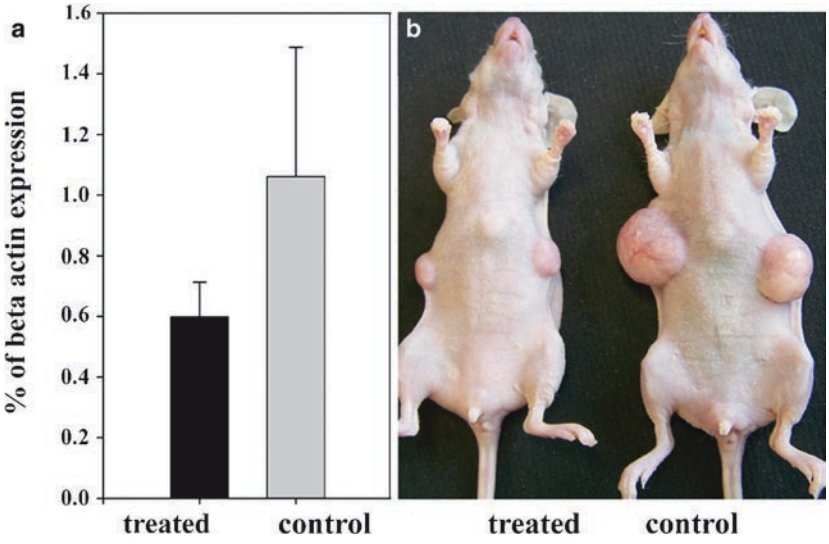

Fig. 3. Inhibition of s.c. tumor growth due to *HMGA2* gene targeting. Animals are sacrificed one week after the last injection, and tumor tissues are removed for analysis. Effect of *HMGA2* gene silencing is analyzed by real-time PCR (**a**). Level of *HMGA2* gene expression is calculated as % of beta actin expression and shown as mean ± SD of five animals. Right panel (**b**) shows a representative example of s.c. tumors in animals treated with a low dose (35 µg DNA per injection) and control animals. Reprinted from ref. 19

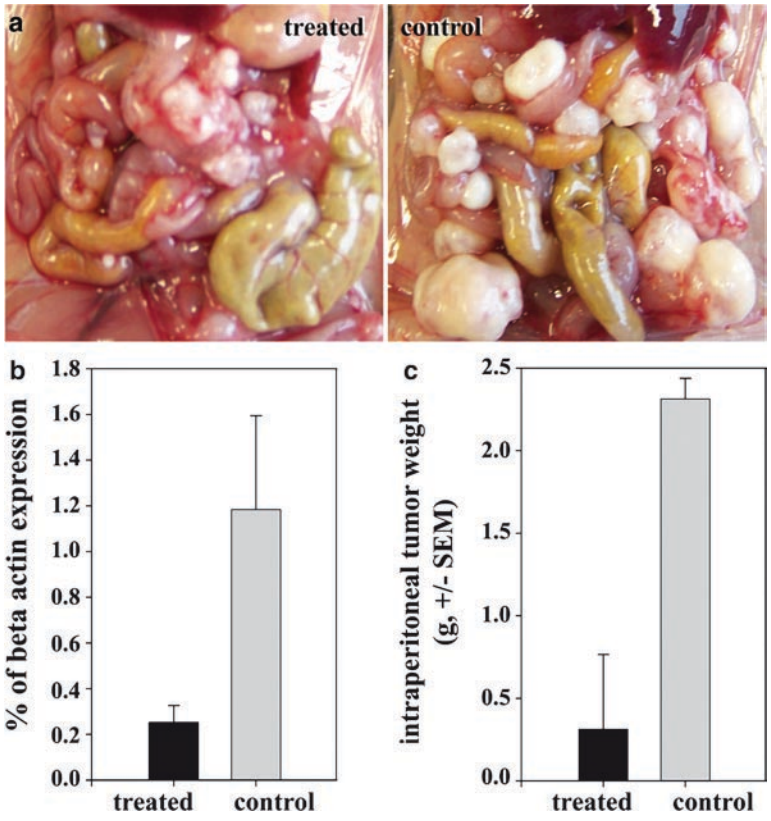

Fig. 4. Inhibition of i.p. tumor growth due to *HMGA2* gene targeting. Amount and size of intraperitoneal tumor nodules are found to be much less in the treated group compared to control (**a**). The effect of *HMGA2* gene silencing is analyzed by real-time PCR (**b**), results are shown as % of beta actin expression ± SD of five animals. The panel (**c**) shows differences in i.p. tumor burden between treated and control groups at the end of the experiment. Reprinted from ref. 19

4. Notes

1. The number of PCR cycles, appropriate for clear comparison of gene expression level in different cell lines or in different conditions of the same cell line, requires experimental adjustment regardless of the gene. A preliminary experiment can be done to estimate the number of PCR cycles needed for the PCR product to reach the plateau. The quantity of cycles used in the main experiment can be 4–6 or fewer. However, real-time PCR technique is widely accepted and can be used as well. Results obtained by real-time PCR are easy to quantify, though this approach requires specific primer design, separate reaction of reverse transcription, and accurate normalization of tested RNA amount. Optimally, both techniques can be used to confirm each other.
2. Freezing/thawing procedure can increase the yield of DNA-binding proteins due to damage of DNA-protein association. There is a reason to do this for the DNA-bound protein extraction only.
3. Parameters, such as blocking conditions, working concentration of antibodies, and stringency of membrane washing, are defined mostly by the quality and specificity of primary antibodies, and they have to be adjusted.
4. In order to optimize design of siRNA, we recommend using several freely-available search tools simultaneously. Most of them are well reviewed on the web site of Rockefeller University: http://www.rockefeller.edu/labheads/tuschl/sirna.html. Then, a BLAST search for unwanted partial homologies of any selected siRNA should be performed to avoid the unintended shutdown of genes other than the target gene. It is also desirable if the structure of siRNA is in agreement with known key requirements (20–24). Additional prediction of siRNA activity on the basis of its biophysical characteristics can be done on the web server of University of Nebraska-Lincoln: http://optirna.unl.edu.
5. As mentioned in the introduction, optimal control of silencing specificity is transfected with scramble duplex, bearing four-base-pair overturns in the middle of sequence compared to tested duplex. However, at the stage of preliminary testing of several siRNAs, we would recommend you to use any that does not match human transcriptome duplex. One possible option is GL3 siRNA targeting firefly luciferase mRNA (Sense sequence: 5′-CUUACGCUGAGUACUUCGATT-3′). Another well accepted, so-called “mock” control can be applied carefully, while free negatively charged transfection reagent can be toxic for the cells and can induce unpredictable transcriptional changes.

6. Even both the high initial expression and efficient silencing of certain genes cannot guarantee growth suppression of cancer cells. Because conduction of stable silencing is quite a time-consuming procedure, we recommend estimating the preliminary growth-suppressive effect of temporal gene silencing before beginning the stable silencing experiment.
7. In case you are familiar with cloning procedures, and in order to reduce time, you can purchase 108 b.p. single-stranded DNA oligos (sense and antisense), then perform annealing and use double-stranded DNA directly for cloning. However, if you need to adjust condition of cloning, we recommend that you synthesize and purify a sufficient amount of DNA insert.
8. Intraperitoneal, disseminated tumor obviously represents a more adequate model of ovarian cancer than s.c. tumors. Nevertheless, we recommend using s.c. xenograft beforehand, or in parallel reaction with the i.p. model, because it can be easily established and easily monitored. In case of obvious effect of applied therapy, you may be able to stop the experiment in time to retain enough tumor tissue material for RNA extraction and analysis. In the case of a paltry therapeutic effect, you still have an option of switching to an intratumoral mode of drug administration, which is less relevant to clinical application but is considerably more efficient.
9. The amount of plasmid DNA or siRNA needed to treat i.p. tumors is still being debated. Proper free nucleic acids are not toxic, especially when injected intraperitoneally. However, an increased amount of applied DNA or RNA requires an appropriate increase in the quantity of transfection reagent, which is definitely more or less toxic. Therefore, we recommend that you refer to toxicological data concerning the reagent being used, and not to exceed an amount of 150–200 μg/injection when using cationic polymers.

References

1. Elbashir, S.M., Harborth, J., Lendeckel, W., Yalcin, A., Weber, K., and Tuschl, T. (2001) Duplexes of 21-nucleotide RNAs mediate RNA interference in cultured mammalian cells. *Nature* **411**, 494–498.
2. Omura, G.A. (2008) Progress in gynecologic cancer research: the gynecologic oncology group experience. *Semin. Oncol.* **35**, 507–521.
3. Aigner, A. (2007) Applications of RNA interference: current state and prospects for siRNA-based strategies in vivo. *Appl. Microbiol. Biotechnol.* **76**, 9–21.
4. Paddison, P.J., Caudy, A.A., Sachidanandam, R. and Hannon, G.J. (2004) Short hairpin activated gene silencing in mammalian cells. *Methods Mol. Biol.* **265**, 85–100.
5. Hannon, G.J. and Conklin, D.S. (2004) RNA interference by short hairpin RNAs expressed in vertebrate cells. *Methods Mol. Biol.* **257**, 255–266.
6. Tchernitsa, O.I., Sers, C., Zuber, J., Hinzmann, B., Grips, M., Schramme, A., et al. (2004) Transcriptional basis of KRAS oncogene-mediated cellular transformation in ovarian epithelial cells. *Oncogene* **23**, 4536–4555.

7. Welsh, J.B., Zarrinkar, P.P., Sapinoso, L.M., Kern, S.G., Behling, C.A., Monk, B.J., et al. (2001) Analysis of gene expression profiles in normal and neoplastic ovarian tissue samples identifies candidate molecular markers of epithelial ovarian cancer. *Proc. Natl. Acad. Sci. U.S.A.* **98**, 1176–1181.
8. Adib, T.R., Henderson, S., Perrett, C., Hewitt, D., Bourmpoulia, D., Ledermann, J., and Boshoff, C. (2004) Predicting biomarkers for ovarian cancer using gene-expression microarrays. *Br. J. Cancer* **90**, 686–692.
9. Rogalla, P., Drechsler, K., Frey, G., Hennig, Y., Helmke, B., Bonk, U., and Bullerdiek, J. (1996) HMGI-C expression patterns in human tissues: Implications for the genesis of frequent mesenchymal tumors. *Am. J. Pathol.* **149**, 775–779.
10. Gattas, G.J., Quade, B.J., Nowak, R.A., and Morton, C.C. (1999) HMGIC expression in human adult and fetal tissues and in uterine leiomyomata. *Genes Chromosomes Cancer* **25**, 316–322.
11. Rogalla, P., Drechsler, K., Kazmierczak, B., Rippe, V., Bonk, U., and Bullerdiek, J. (1997) Expression of HMGI-C, a member of the high mobility group protein family, in a subset of breast cancers: relationship to histologic grade. *Mol. Carcinog.* **19**, 153–156.
12. Meyer, B., Loeschke, S., Schultze, A., Weigel, T., Sandkamp, M., Goldmann, T., et al. (2007) *HMGA2 overexpression in non-small cell lung cancer. Mol. Carcinog.* **46**, 503–511.
13. Abe, N., Watanabe, T., Suzuki, Y., Matsumoto, N., Masaki, T., Mori, T., et al. (2003) An increased high-mobility group A2 expression level is associated with malignant phenotype in pancreatic exocrine tissue. *Br. J. Cancer* **89**, 2104–2109.
14. Chau, K.Y., Manfioletti, G., Cheung-Chau, K.W., Fusco, A., Dhomen, N., Sowden, J.C., et al. (2003) Derepression of HMGA2 gene expression in retinoblastoma is associated with cell proliferation. *Mol. Med.* **9**, 154–165.
15. Miyazawa, J., Mitoro, A., Kawashiri, S., Chada, K.K., and Imai, K. (2004) Expression of mesenchyme-specific gene HMGA2 in squamous cell carcinomas of the oral cavity. *Cancer Res.* **64**, 2024–2029.
16. Andrieux, J., Demory, J.L., Dupriez, B., Quief, S., Plantier, I., Roumier, C. et al. (2004) Dysregulation and overexpression of HMGA2 in myelofibrosis with myeloid metaplasia. *Genes Chromosomes Cancer* **39**, 82–87.
17. Berlingieri, M.T., Manfioletti, G., Santoro, M., Bandiera, A., Visconti, R., Giancotti, V., and Fusco, A. (1995) Inhibition of HMGI-C protein synthesis suppresses retrovirally induced neoplastic transformation of rat thyroid cells. *Mol. Cell Biol.* **15**, 1545–1553.
18. Pentimalli, F., Dentice, M., Fedele, M., Pierantoni, G.M., Cito, L., Pallante, P., et al. (2003) Suppression of HMGA2 protein synthesis could be a tool for the therapy of well differentiated liposarcomas overexpressing HMGA2. *Cancer Res.* **63**, 7423–7427.
19. Malek, A., Bakhidze, E., Noske, A., Sers, C., Aigner, A., Schafer, R., and Tchernitsa, O. (2008) HMGA2 gene is a promising target for ovarian cancer silencing therapy. *Int. J. Cancer* **123**, 348–356.
20. Elbashir, S.M., Martinez, J., Patkaniowska, A., Lendeckel, W., and Tuschl, T. (2001) Functional anatomy of siRNAs for mediating efficient RNAi in *Drosophila melanogaster* embryo lysate. *EMBO J.* 20, 6877–6888.
21. Yuan, B., Latek, R., Hossbach, M., Tuschl, T., and Lewitter, F. (2004) siRNA Selection Server: an automated siRNA oligonucleotide prediction server. *Nucleic Acids Res.* 32(Web Server issue), W130–W134.
22. Ui-Tei, K., Naito, Y., Takahashi, F., Haraguchi, T., Ohki-Hamazaki, H., Juni, A., et al. (2004) Guidelines for the selection of highly effective siRNA sequences for mammalian and chick RNA interference. *Nucleic Acids Res.* **32**, 936–948.
23. Amarzguioui, M. and Prydz, H. (2004) An algorithm for selection of functional siRNA sequences. *Biochem. Biophys. Res. Commun.* **316**, 1050–1058.
24. Khvorova, A., Reynolds, A., and Jayasena, S.D. (2003) Functional siRNAs and miRNAs exhibit strand bias. *Cell* **115**, 209–216.

INDEX

A

B

C

D

E

F

G

H

I

J

K

L

M

N

O

P

Q

R

S

T

U

V

W

X

Z